Polynuclear Nickel and Cobalt Complexes of Pyridonate Ligands

by

Euan K. Brechin

Thesis Presented for the Degree of Doctor of Philosophy

The University of Edinburgh

1997

Declaration

I declare that this thesis has been entirely composed by myself and that the work described herein is my own except where clearly stated in reference or text.

Abstract

This thesis presents routes to several high nuclearity nickel and cobalt complexes of pyridonate ligands. Solution reactions of simple metal salts and the sodium salts of 6-methyl-, 6-bromo- and 6-chloro-2-pyridone produced compounds whose nuclearities range from three to twenty four. Among these is $[Co_{24}(OH)_{18}(OMe)_2(Cl)_6(mhp)_{22}]$, the highest nuclearity complex containing cobalt, which consists of cubic-close packed planes of hydroxide, methoxide and chloride anions bridging cobalt centres. Preliminary magnetic studies indicate the presence of a high spin ground state and the possibility of superparamagnetic behaviour. Thermolysis reactions of protonated pyridones produced the first nickel and cobalt complexes which contain M_4O_6 adamantane units. They are also the first examples of vertex- and face-sharing adamantanes.

Introduction of rigid linking carboxylate ligands to the reactions of 6-methyl-2-pyridone produced a family of deca- to dodecanuclear nickel and cobalt complexes whose structures are based on centred-tricapped-trigonal prisms which contain either zero, one or two additional caps on the 'upper' and 'lower' triangular faces. The nuclearity and structure of these complexes can be controlled through variation of pyridonate, carboxylate and solvent. Similar reactions involving 6-chloro-2-pyridone produced, amongst others, a series of trimers of general formula $[M_3(O_2CR)_2(xhp)_4(R'OH)_6]$ and a dodecanuclear cobalt metallocycle. Replacement of binucleating with tetranucleating carboxylates led to the synthesis of two large polymetallic complexes : a cobalt tridecamer and a nickel-sodium supracage. The supracage assembly in which four nickel cubanes are linked through a sodium octahedron appears to be unprecedented. The synthetic procedures used to produce homometallic species have been expanded to give a number of bimetallic 3d-3d and 3d-4f complexes.

Acknowledgements

University.

Richard Winpenny - my supervisor.

The people of labs 244/247/85 in particular, Craig Grant, Greg Solan, Fokke Dijksma, Steve Harris, Mark Murrie, Dave Nation, Steve Archibald and the boy Pace.

The crystallography team : Simon Parsons, Steve Harris, Bob Gould and Fokke Dijksma

Magnetic measurements : Gavin Whittaker and Cristiano Benelli.

CHN and Atomic Absorption : Lorna Eades.

Financial support : EPSRC.

Personal.

The old dears - nae a bad hotel. Nice one.

Gogs and Al - The Bald Boys. The ugly ducklings. The dirty-orange glory-hunter and schemey Leith scrubber. Fatman and Robin. The rock and the sponge. Top drinking partners. Not bad lads.

Cammy-all-grown-up, Spoon-get-well-soon, Mouri-the-pot-bellied-psychopath, wee-Steve-coos-lick, Bobby-beach-shorts, Karen-frankenspice, spare-Clare-geeza-fag and their I'm-always-skint girlie crew.

The boozer.

The leej.

The mighty Longniddry Villa. The rocks gone now boys.

The not-so-mighty-AFC. One win would do.

Contents

Chapter 1. Introduction.

Chapter 2. Polymetallic nickel and cobalt complexes of 6-chloro-, 6-bromo- and 6-methyl-2-pyridone.

Chapter 5. Heterometallic complexes of pyridonate ligands : high nuclearity cobalt-copper and nickel-copper coordination complexes and a series of nickel- and cobalt-lanthanide compounds.

List of crystal structures.

Chapter 2.

$[Ni_4(OMe)_4(xhp)_4(MeOH)_7]$. MeOH xhp = chp **1**, bhp **2**.

$[Ni_2Na_2(chp)_6(MeCN)_4(H_2O)]$ **3**.

$[Ni_2Na_2(chp)_6(MeCN)_4(H_2O)_2]$ **4**.

$[Ni_2Na_2(chp)_6(H_2O)]_n$ **5**.

$[Ni_4Na_4(mhp)_{12}(Hmhp)_2]$ **6**.

$[Co_4(OMe)_4(chp)_4(MeOH)_7]$. MeOH **7**.

$[Co_{12}(chp)_{18}(OH)_4(Cl)_2(Hchp)_2(MeOH)_2]$ **8**.

$[Co_{10}(OH)_4(chp)_{16}(MeCN)_2]$ **9**.

$[Co_2Na_2(chp)_6(H_2O)]_n$ **10**.

$[Co_2Na_2(chp)_6]_n$ **11**.

$[Co_{24}(OH)_{14}(OMe)_2(Cl)_6(mhp)_{22}]$ **14**.

$[Ni_7(chp)_{12}(MeOH)_6(Cl)_2]$ **15**.

$[Ni_7(OH)_2(chp)_{12}(MeOH)_6]$ **16**.

$[Ni_9(OH)_2(chp)_{16}(MeCN)_2]$ **17**.

$[Co_9(chp)_{18}]$ **18**.

$[Ni_{11}(OH)_6(mhp)_{15}(Hmhp)(Cl)(H_2O)_2]$ **19**.

Chapter 3.

$[Ni_{12}(OH)_6(mhp)_{12}(O_2CCH_2Cl)_6]$ **21**.

$[Ni_{11}(OH)_6(chp)_9(O_2CPh)_6(EtOH)_3]^+[Ni(chp)_3]^-$ **22**.

$[Ni_{11}(OH)_6(mhp)_9(O_2CMe)_6(H_2O)_3]_2[CO_3]$ **23**.

$[Ni_{11}(OH)_6(mhp)_9(O_2CMe)_7(Hmhp)_2]$ **24**.

$[Co_{10}(OH)_6(mhp)_6(O_2CPh)_7Cl(Hmhp)_3(MeCN)]$ **25**.

$[Ni_{10}(OH)_4(mhp)_{10}(O_2CCMe_3)_6(MeOH)_2]$ **26**.

$[Ni_6(mhp)_6(PhCOO)6(PhCOOH)_4(H_2O)_6]$. Hmhp **29**.

Chapter 4.

$[Ni_3(O_2CCMe_3)_2(chp)_4(MeOH)_6]$ **30**.

$[Ni_3(PhCH_2CO_2)_2(chp)_4(MeOH)_6]$. 2MeOH **31**.

$[Co_{12}(O_2CMe)_{12}(chp)_{12}(H_2O)_6(THF)_6]$ **32**.

$[Co_7(OH)_2(chp)_8(PhCOO)_4(MeCN)]$ **33**.

$[Co_7(OH)_2(chp)_8(O_2CCMe_3)_4(Hchp)_{0.69}(MeCN)_{0.31}]$ **34**.

$[Ni_{12}Na_4(OH)_2(O_2CCH_2Cl)_8(chp)_8(MeCN)_2]$ **35**.

$[Co_{13}(OH)_2(chp)_{20}(phth)_2]$ **36**.

$[Ni_{16}Na_6(chp)_4(phth)_{10}(Hphth)_2(OMe)_{10}(OH)_2(MeOH)_{20}]$ **37**.

$[NEt_4]_2[Ni_4(OMe)_2(chp)_4(PhCOO)_4(H_2O)_6]$ **38**.

$[NEt_4]_2[Ni_6(OH)_2(chp)_8(CF_3COO)_4(H_2O)_2]$ **39**.

$[Co_2Na_2(pic)_4(chp)_2(MeOH)]$. 2MeOH **40**.

Chapter 5.

$[Co_7Cu_2(OH)_2(chp)_{10}(O_2CMe)_6]$ **41**.

$[M_6Cu_2(OH)_4(mhp)_2(O_2CPh)_{10}(Hmhp)_4(H_2O)_2]$ M = Co **42**, Ni **43**.

$[Ni_2Er_2(chp)_6(NO_3)_4(MeCN)_2]$ **44**.

$[NEt_4]_2[Co(chp)_4]$ **45**.

$[NEt_4]_2[Co_2Yb_2(OH)(chp)_6(NO_3)_5]$ **46**.

$[NEt_4]_2[Co_2Dy_2(OH)(chp)_6(NO_3)_5]$ **47**.

$[NEt_4]_2[Co_2Gd_2(OH)(chp)_6(NO_3)_5]$ **48**.

$[NEt_4]_2[CoNd_2(chp)_5(NO_3)_5]$ **49**.

$[NEt_4]_2[CoSm_2(chp)_5(NO_3)_5]$ **50**.

List of Figures.

Chapter 1.

Chapter 2.

Chapter 3

Chapter 4.

Chapter 5.

Chapter 6.

List of Tables.

Chapter 2.

Chapter 3.

Chapter 4.

Chapter 5.

Abbreviations.

Me methyl

Et ethyl

Ph phenyl

Hxhp 6-substituted-2-pyridone

xhp 6-substituted-2-pyridonate

X general substituent

Hchp 6-chloro-2-pyridone

Hbhp 6-bromo-2-pyridone

Hmhp 6-methyl--pyridone

M metal

Ln lanthanide

FAB-MS fast atom bombardment mass spectrometry

Å Angstrom (10^{-10}m)

χ_m molar magnetic susceptibility

T temperature

S spin quantum number

L orbital quantum number

μ magnetic moment

g g-factor

n integer or infinity

J exchange parameter (cm^{-1})

EPR electron paramagnetic resonance

CHAPTER 1

INTRODUCTION

1.0. An introduction to magnetism.

Magnetic susceptibility measurements provide a means of studying the oxidation states, electronic configurations and metal...metal interactions of transition metal ions. The magnetic moment (μ) of any isolated metal ion is a result of the movement of its electrons both about their own axes (spin moment, S) and around the nucleus (orbital moment, L). The total magnetic moment is therefore a combination of these two factors and is given by the expression :

$$\mu = g\sqrt{J(J+1)} \qquad (1)$$

where J (the total moment) = S + L, and g is the g-factor (a constant) for the particular metal. For first row transition metals in general the orbital contribution is quenched and the spin contribution dominates. The value of S is simply given by half the number of unpaired electrons (n) that the metal contains (i.e. S = 1/2(n) since each electron has S = 1/2). Thus for a Ni^{2+} ion in an octahedral environment, which has two unpaired electrons, S = 1 and for a high spin Co^{2+} ion in an octahedral environment S = 3/2. For each value of S, m_s (the spin magnetic quantum number) varies from +S to -S in integer steps and in the absence of a magnetic field these m_s states are in theory degenerate. Magnetic moments however are not directly measureable but can be calculated from the molar magnetic susceptibility (χ_m). When a molecule is placed in a magnetic field (H) it acquires a molar magnetisation (M) related to this applied field by :

$$\chi = dM/dH \qquad (2)$$

if the field is weak enough the susceptibilty becomes independent of field and so :

$$M = \chi H \qquad (3)$$

The molar magnetic susceptibility can be related to the magnetic moment through the

expression :

$$\mu = \sqrt{8\chi T} \qquad (4)$$

Therefore the relationship betwen the product $\chi_m T$ and S can be written as :

$$\chi_m T = g^2/8 \{S(S+1)\} \qquad (5)$$

Within this text $\chi_m T$ will be used in preference to magnetic moment for two reasons. Firstly, magnetic moment is only a valid concept if the Curie Law is obeyed, which is not the case for systems where metal ions are interacting. Secondly, for multi-centre systems $\chi_m T$ is a little more easily calculated than moment. If n centres are present equation (5) becomes :

$$\chi_m T = g^2/8 \, n \{S(S+1)\} \qquad (6)$$

Equally where non-equivalent spin centres are present, as is the case for some compounds in this thesis,

$$\chi_m T = g_a^2/8 \, n_a \{S_a(S_a+1)\} + g_b^2/8 \, n_b \{S_b(S_b+1)\} \qquad (7)$$

where g_a, n_a, S_a and g_b, n_b, S_b are the g-values, number of centres and spin of each centre for metals a and b.

Thus the theoretical value of $\chi_m T$ for any number of non-interacting metal centres can be calculated and any observed variation in the value of $\chi_m T$ with tempearture will then indicate the presence and type of magnetic interaction that exists between the metal centres. If at room temperature, the metal centres are not interacting then the observed value of $\chi_m T$ will be equal to the theoretical value. If, as the temperature drops the spins allign antiparallel to each other then the value of $\chi_m T$ will drop. This type of behaviour is termed antiferromagnetic exchange. Conversely if the spins allign themselves parallel to each other the value of $\chi_m T$ will increase. This is termed ferromagnetic exchange. These two types of behaviour are therefore clearly distinguishable if the product $\chi_m T$ is plotted against temperature. The observed minimum or maximum in $\chi_m T$ also allows an estimation of the spin ground state of the molecule.

1.1. The magnetic properties of large inorganic clusters.

Molecular magnetism has become an area of intensive research in recent years [1-3]. Magnetic materials of mesoscopic dimensions may exhibit novel and useful properties which in principle could have future applications in information storage and magnetic memories, and from a fundamental point of view may provide examples of manifestation of quantum effects in large objects. The main synthetic driving force behind molecular magnetism has been the search for molecular ferromagnets that order at or above room temperature, and to this end a number of groups ranging from physicists to solid state scientists to chemists have tried a variety of synthetic approaches to such compounds.

For example, Miller and Epstein [4-6] have prepared organometallic ferromagnets based on electron transfer salts in which metallocene or metallomacrocyclic cations and organic anions interact in a donor-acceptor fashion. Magnets have also been prepared where fullerenes act as the acceptor atoms [7]. Kahn has designed ferromagnetic chain compounds based on bimetallic manganese (II) and copper (II) building blocks [1, 8-12]. Verdaguer and Mallah have reported a number of heterometallic complexes which belong to the Prussian blue family of compounds in which hexacyanometallates, acting as Lewis bases, are combined with Lewis acids to produce 1D, 2D and 3D-networks of cyano-bridged transition metals [13-19]. Another successful approach, employed by Gatteschi, has been to couple organic radicals with transition metal ions [20].

3d-transition metal clusters were initially synthesised as a means of studying naturally occuring phenomena : thus large iron oxo hydroxo complexes were synthesised to provide an understanding of the hydrolytic processess involved in mineral formation and in iron biomineralisation, and to provide model compounds for iron-oxide type materials found in

biological systems such as ferritin - the iron storage protein. Similarly manganese clusters have been synthesised in order to model the polymetallic core in Photosystem II. Recently additional interest in such polynuclear clusters has stemmed from molecular magnetism. 3d-transition metals generally exist in moderate oxidation states and hence are paramagnetic. Therefore the clusters they form may themselves exhibit unusual magnetic properties or act as molecular building blocks to magnetic materials and thus allow the study of the transition from molecular to bulk magnetic behaviour.

The magnetic properties which are peculiar to large molecular clusters are those giving rise to high spin ground states, long relaxation times and superparamagnetism, tunnelling and the coexistence of quantum and classical effects and sensitivity to external fields. What follows is a brief overview of some high nuclearity clusters of 3d-metals which have displayed some of these properties.

1.1. Manganese clusters.

Perhaps the most interesting magnetic property displayed by any polynuclear manganese compound is that of slow relaxation of the magnetisation - a phenomenon associated with superparamagnetism. A series of dodecanuclear manganese complexes has recently been synthesised following the formation of the 'parent' compound $[Mn_{12}O_{12}(O_2C\text{-}Me)_{16}(H_2O)_4]$. $2CH_3COOH$. $4H_2O$ in 1980 [21]. Magnetic studies of this compound suggest that it possesses a high spin ground state and unusual relaxation effects [22, 23]. The structure of this Mn_{12} cluster [Figure 1.1] consists of four manganese (IV) ions in a $[Mn_4O_4]^{8+}$ cubane within a non-planar ring of eight manganese (III) ions. The structure is held together internally through twelve oxide bridges and externally by sixteen acetates. At low temperature the cluster

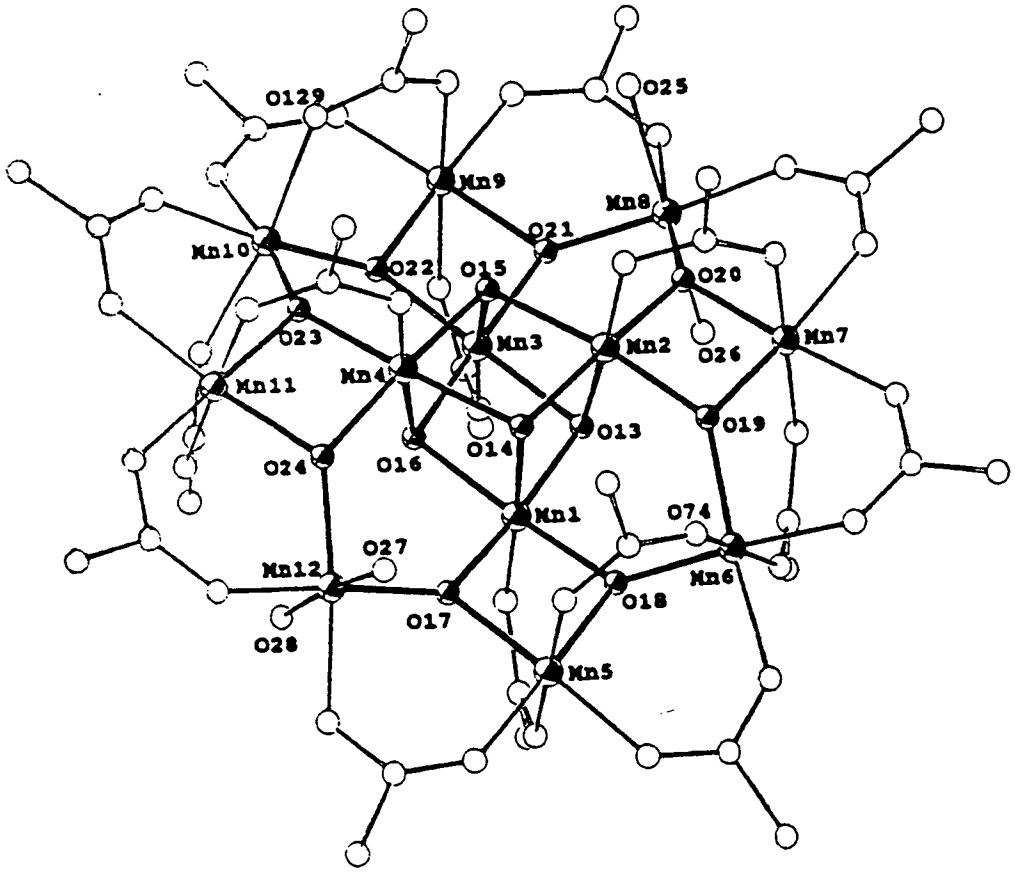

Figure 1.1. The crystal structure of $[Mn_{12}O_{12}(O_2CMe)_{16}(H_2O)_4]$

displays a high spin ground state of S = 10 which is consistent with all of the Mn(III) spins (8 x S = 2) pointing up and all of the Mn(IV) spins (4 x S = 3/2) pointing down. The compound undergoes very slow relaxation of the magnetisation below 10 K. The S = 10 ground state has zero-field splitting determined by the Mn(III) ions (the S = 2 spins are parallel to each other) which are Jahn Teller distorted, leaving the $m_s = \pm 10$ components lowest in energy and the $m_s = 0$ component highest in energy. This produces an anisotropy barrier [Figure 1.2] which must be overcome if the magnetisation is to be inversed. At low temperature only the $m_s = \pm 10$ level is populated and so reversing the magnetisation corresponds to passing from $m_s = -10$ to $m_s = -9$ to $m_s = -8$ and so on up to $m_s = 0$, and then from $m_s = 0$ down to $m_s = -10$. This anisotropy barrier is large and at low temperature the relaxation is slow. The compound also shows a hysteresis loop at 2.5 K [Figure 1.3] which results from the field dependence of the relaxation : the application of a magnetic field in the

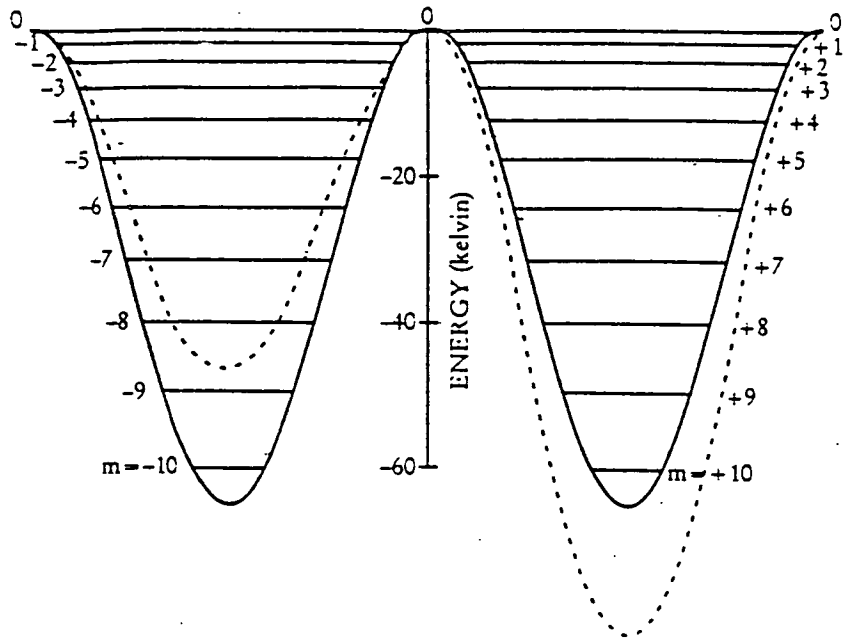

Figure 1.2. The anisotropy barrier in Mn_{12}.

opposite direction to the magnetisation of the sample reduces the size of the anisotropy barrier and thus increases the rate of relaxation. The spins are first aligned by the application of a field, but when the field is removed (or sufficiently decreased) the spins become 'frozen' and remain in the magnetised state until a magnetic field is reached which is large enough to overcome the barrier, and hence reverse the magnetisation. This behaviour is consistant with that of a superparamagnet. It has also been suggested that the reversal of the magnetic moment can be achieved by tunnelling through the energy barrier [24, 25]. Tunnelling between the two sides of this barrier occurs when the two potential wells are degenerate [i.e. when there is no applied field the energy level of $m_s = +10$ is equal to the energy level of $m_s = -10$ and so on] and also when an applied field raises one potential well high enough above the other so that the energy levels again coincide but for different values of m_s [i.e. so that the energy level of $m_s = -10$ in one potential well, for instance, is equal to the energy level of $m_s = +9$ in the other well]. This allows lots of spins to escape from one well to the other, reducing the

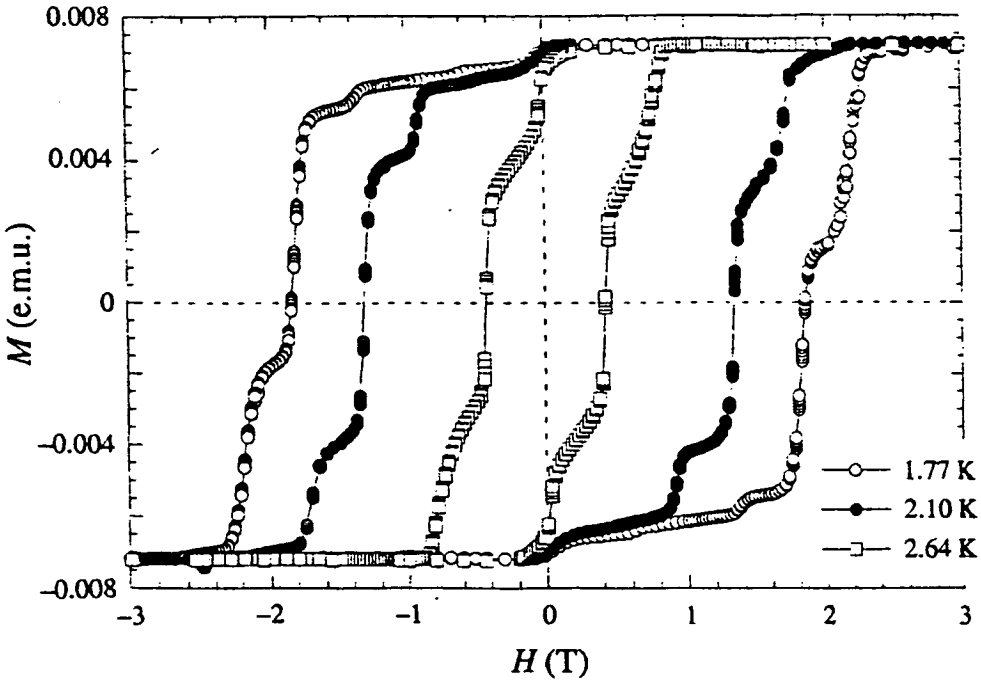

Figure 1.3. The hysteresis loop displayed by Mn_{12}.

magnetisation. Thus if the applied field is continually increased one well will sink lower and lower with the m_s levels coming into resonance in a series of steps [meaning therefore that the change in magnetisation also occurs in a series of steps] until all the spins rest at the bottom of the second well and the samples magnetisation is reversed. To what extent this tunnelling phenomenon is aided or enhanced by temperature is still a little unclear. However inorganic clusters like the Mn_{12} species appear ideal candidates to study such behaviour given that each molecule is the same size, has the same spin and the same anisotropy - all of which are known or calculable parameters. Complexes which display tunnelling effects have potential applications in magnetic memory devices and quantum computing. However, above a few Kelvin the tunnelling effects are not observed and hence are so far impractical. Complexes which exhibit the same characteristics as the Mn_{12} cluster but at higher temperatures are thus the subject of keen research.

As a result of the properties displayed by the Mn_{12} cluster a series of similar

compounds in which the carboxylate ligand or counter ion have been changed, have been synthesised and studied. $[Mn_{12}O_{12}(O_2CEt)_{16}(H_2O)_3]$, $[Mn_{12}O_{12}(O_2CPh)_{16}(H_2O)_4]$ [26, 27] and $[Mn_{12}O_{12}(O_2CMe)_4(O_2CEt)_{12}(H_2O)_4]$ [28] all have essentially the same structure as the Mn_{12} parent compound with a core of four Mn(IV) ions surrounded by eight Mn(III) ions. All have been reported to have S = 9 ground states and again display similar superparamagnetic-like behaviour. A fifth dodecanuclear manganese complex $[PPh_4][Mn_{12}O_{12}(O_2CEt)_{16}(H_2O)_4]$ [29] was synthesised by the reduction of $[Mn_{12}O_{12}(O_2CEt)_{16}(H_2O)_3]$ and contains the valence trapped $[Mn^{(II)}Mn^{(III)}{}_7Mn^{(IV)}{}_4]$ anion. It has an S = 19/2 ground state and again displays similar magnetic relaxation effects - the first anionic species to do so.

Recently two decanuclear manganese complexes $[Me_4N]_4[Mn^{(II)}{}_6Mn^{(III)}{}_4O_4(biphen)_4X_2]$ (biphen = 2, 2'-biphenoxide; X = Br, Cl) were synthesised which were initially reported to contain $12 \leq S \geq 14$ ground states [30, 31]. More recently HF-EPR experiments have confirmed that the ground states of the two compounds are in fact S = 12 [32]- the largest yet reported for any manganese compound, and amongst the highest known for any molecular species. The compounds were formed by the reaction of manganese bromide (or chloride) with 2, 2'-biphenoxide in ethanol. Its structure [Figure 1.4] consists of an inner octahedron of four Mn(III) ions and two Mn(II) ions with each face of the octahedron capped by a Mn(II) ion. It is a rare example of a polynuclear manganese complex which is not held together by carboxylate ligands. Although a number of models have been proposed the high spin ground state is thought to result from antiferromagnetic exchange between the two Mn(II) (S = 5/2) and the four Mn(III) (S = 2) sites in the central octahedron mediated by the bridging oxo ligands. Also reported in the same paper was the species $[Et_3NH]_2[Mn(CH_3CN)_4(H_2O)_2]$ $[Mn_{10}O_4(biphen)_4Br_{12}]$. This Mn_{10} complex is isostructural to the two compounds above and magnetic studies on this decamer also gave an S = 12 ground state. Zero-field splitting within this ground state was confirmed by EPR measurements, and presumably arose from the

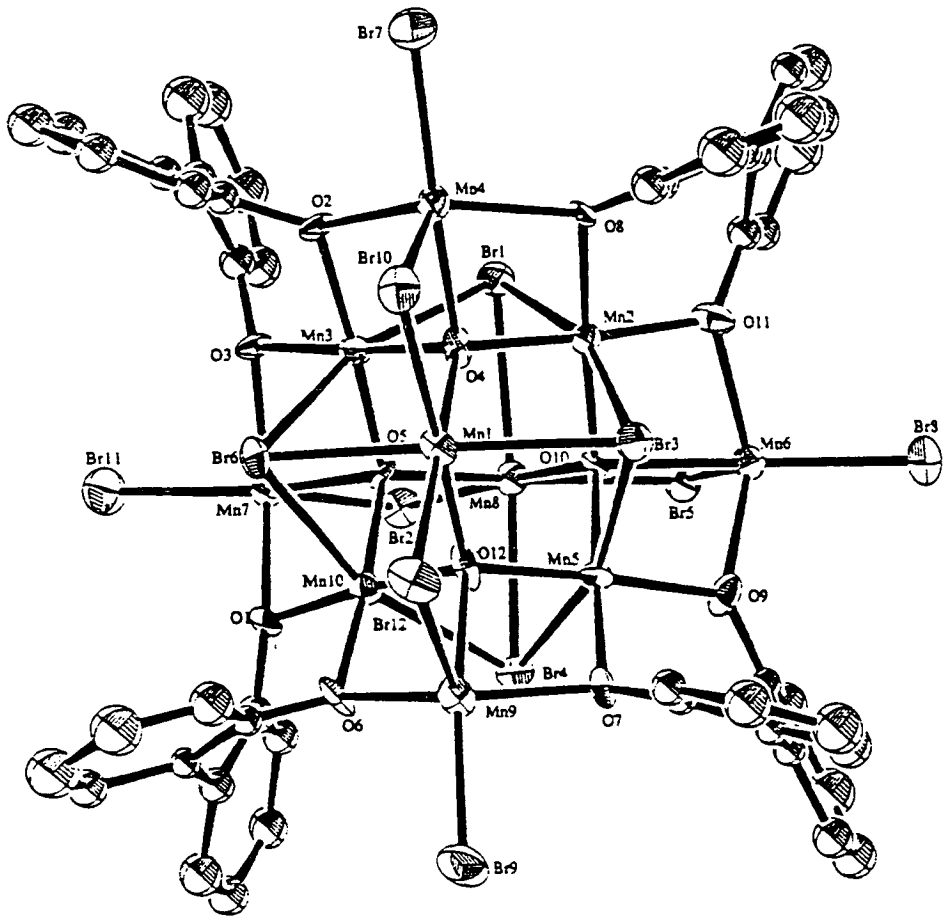

Figure 1.4. The crystal structure of $[Me_4N]_4[Mn_{10}O_4(biphen)_4Br_{12}]$

anisotropy of the Mn(III) ions. However the same slow relaxation phenomenon observed for the Mn_{12} species is not seen here. In the Mn_{10} complex there are only four Mn(III) S = 2 spin centres present while in the Mn_{12} compounds there are eight Mn(III) centres, thus the overall anisotropy is reduced in comparison, the energy barrier falls and the relaxation is fast.

Another example of a manganese cluster which exhibits a high spin ground state is the hexanuclear metallocycle $[Mn(hfac)_2NITPh]_6$[33] (hfac = hexafluoroacetyl acetonate) in which manganese ions and nitronyl nitroxide radicals alternate. The coupling between the Mn(II) (6 x S = 5/2) centres and the radicals (6 x S = 1/2) is antiferromagnetic and leads to a ground S = 12 state. No unusual relaxation properties have been reported for this cluster which is unsurprising as only isotropic Mn(III) centres are present.

1.2. Iron clusters.

In general the magnetic interactions in iron clusters have been dominated by antiferromagnetic exchange between iron (III) centres mediated by bridging oxo or hydroxo ligands. The strength of the interaction is dependent upon the nature of the ligand [oxo bridges promote stronger interaction than hydroxo bridges [34]] and on the bridging angle between the two metals [the more obtuse the angle the stronger the exchange [35]].

The highest spin ground state yet reported for any molecular species is that of a system containing two different iron clusters in the same cell, one of which consists of seventeen iron (III) ions $[Fe_{17}O_4(OH)_{16}(heidi)_8(H_2O)_{12}]^{3+}$ and the other nineteen iron (III) ions $[Fe_{19}O_6(OH)_{14}(heidi)_{10}(H_2O)_{12}]^{+}$ ($H_3heidi = N(CH_2COOH)_2(CH_2CH_2OH)$) [36, 37]. The complexes were formed by the addition of H_3heidi / pyridine to an aqueous solution of iron (III) nitrate at pH = 2.6. The structure of the Fe_{17} cluster is given in Figure 1.5. Both complexes have very similar structures containing $[Fe_3(OH)_4]^{5+}$ cubes surrounded by a mixture of iron-heidi units and water molecules. They are essentially planar with central $[Fe_7(\mu_3\text{-}OH)_6(\mu_2\text{-}OH)_4\{(\mu_3\text{-}O)Fe\}_2]^{13+}$ core unit which can be described as a portion of an $[Fe(OH)_2]_n^{n+}$ lattice consisting of hexagonal close-packed hydroxides with the irons in the octahedral holes.

Magnetic studies indicate ferrimagnetic exchange between the iron centres with a high spin ground state of at least S = 33/2. The minimum value of the product χT occurs at room temperature showing significant antiferromagnetic exchange between the irons with the maximum value of χT at low temperature. The exchange between the metal centres is described through a series of triangular interactions which leads to spin frustration effects which stabilise the high spin ground state. The presence of two discrete molecules in the same cell makes analysis of the data difficult, but the maximum χT at low temperature means that

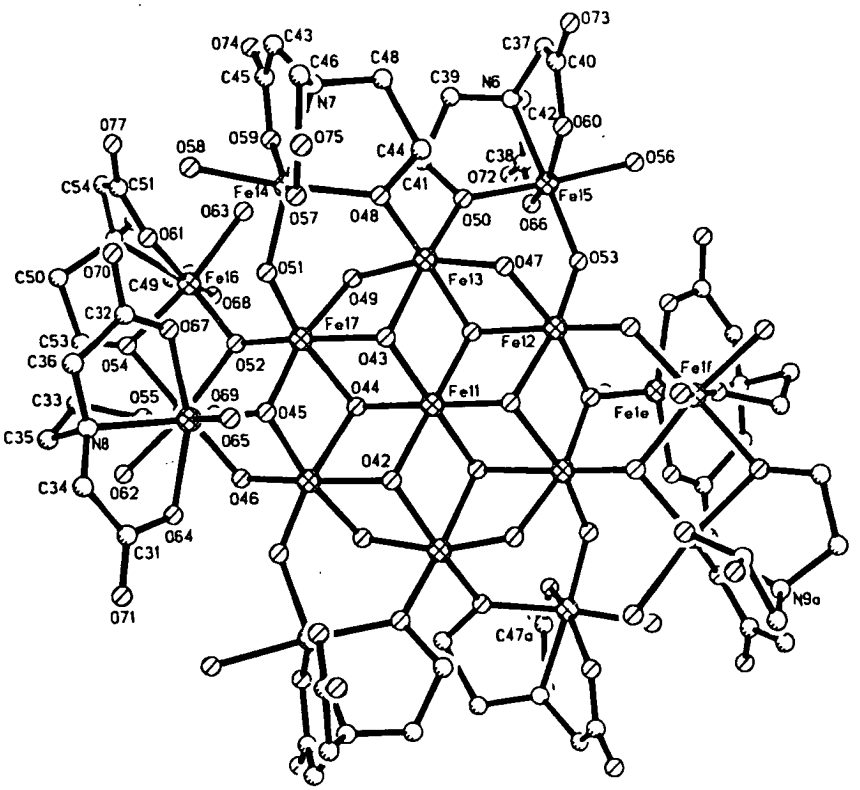

Figure 1.5. The crystal structure of $[Fe_{17}O_4(OH)_6(heidi)_8(H_2O)_{12}]^{3+}$.

either one or both of the clusters displays the high spin state. Similar spin frustration effects are also thought to be responsible for the S = 11 or 23/2 ground state in the complex $[Fe_{10}Na_2(\mu_4\text{-}O)_2(\mu_3\text{-}O)_4(\mu_3\text{-}OH)_4(O_2CPh)_{10}(chp)_6(H_2O)_2(Me_2CO)_2]$ (Hchp = 6-chloro-2-hydroxypyridone) [38]. Its structure consists of a cage of ten iron (III) ions bridged predominantly by oxo groups. The minimum value of χT at room temperature indicates the presence of antiferromagnetic interactions with the maximum value at low temperature consistant with ferrimagnetic exchange. The S = 11 ground state cannot be a result of simple antiferromagnetic exchange between the S = 5/2 spins.

Superparamagnetic behaviour, similar to that observed for the dodecanuclear manganese clusters, has been exhibited by an octanuclear iron complex $[Fe_8O_2(OH)_{12}(tacn)_6Br_7(H_2O)]Br$ (tacn = 1, 4, 7-triazacyclononane) first reported by Wieghardt et al [39, 40]. The complex [Figure 1.6] contains eight iron (III) ions which are coupled together *via* twelve μ_2-hydroxide and two μ_3-oxo bridges with the four irons connected by the oxo groups defining a

central 'butterfly' type arrangement. The structure could also be described as a piece of an oxo-hydroxo iron layer. Magnetic studies show the maximum value of χT occuring at low temperature and corresponding to an S = 10 ground state. However this high spin state is not a result of spin frustration effects. At room temperature strong antiferromagnetic coupling is observed - the value of χT is below that expected for eight uncoupled S = 5/2 spins. As the temperature is lowered the value of χT increases indicating that the number of spins up is different from the number of spins down, showing that the cluster exhibits ferrimagnetic behaviour. The four iron atoms in the central 'butterfly' are aligned antiparallel to each other [i.e. two up, two down, (S = 0)] with the four remaining iron atoms at the exterior of the molecule aligned parallel to each other [i.e. all pointing up giving S = 10]. More recent magnetic studies coupled with EPR and Mössbauer experiments have shown that zero-field

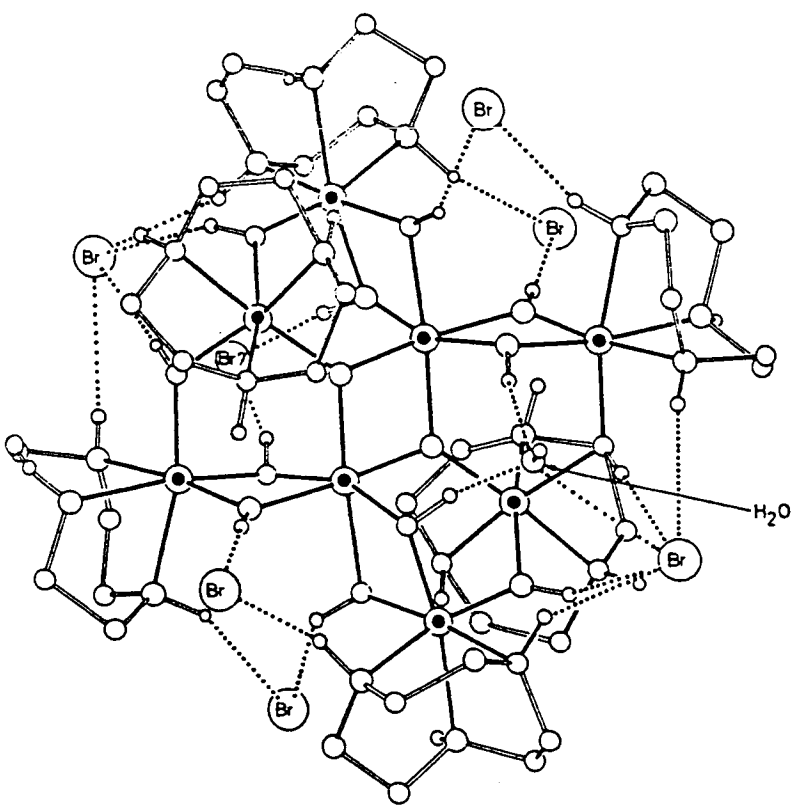

Figure 1.6. The crystal structure of $[Fe_8O_2(OH)_{12}(tacn)_6Br_7(H_2O)]^+$.

splitting exists within the ground state and that the $m_s = \pm 10$ component lies lowest in energy. As a result the system becomes anisotropic at low temperature which means that the reorientation of the magnetisation becomes a slow process : behaviour analogous to superparamagnets and to the Mn_{12} compounds. Similar results have also been reported for the mixed valent polyiron oxo complex $[Fe^{(III)}_4Fe^{(II)}_8O_2(OMe)_{18}(O_2CMe)_6(MeOH)_{4.67}]$ [41, 42] and the mixed metal iron species $[Fe_{16}MO_{10}(OH)_{10}(O_2CPh)_{20}]$ where M =Mn, Fe, Co [43, 44].

Another type of unusual magnetic behaviour - that of sensitivity to external fields - is exhibited by two cyclic iron structures, the ferric wheel $[Fe(OMe)_2(O_2CCH_2Cl)]_{10}$ [45, 46] and a hexanuclear compound $[Fe_6Na(OMe)_{12}(dbm)_6]Br$ (dbm = dibenzoylmethane)[47] reported by Lippard et al. Cyclic structures are in general good examples of compounds which can be used to study the magnetic properties of linear chains. The ferric wheel [Figure 1.7] was formed by allowing the monochloroacetate analogue of basic iron acetate $[Fe_3O(O_2CCH_2Cl)_6(H_2O)_3][NO_3]$ to react with iron nitrate in methanol. The complex consists of ten ferric ions which are arranged in a near perfect circle with two molecules of methoxide and one molecule of chloroacetate bridging each pair of Fe(III) ions.

Magnetic studies of the ferric wheel showed that the compound is strongly antiferromagnetically coupled with a diamagnetic ground state. More interestingly however is the observation that at 0.6 K the magnetisation of the sample increases in a stepwise fashion as the field increases. At zero-field S = 0 and therefore $m_s = 0$ is lowest in energy and the magnetisation of the sample is zero. As the field is increased the S = 1 level becomes populated and the magnetisation of the sample increases sharply. When the field is increased again [by the same magnitude] the S = 2 level becomes populated and the magnetisation rises. This pattern is repeated continually. These steps originate from crossovers of spin, which means that as the field is increased the S = 1 state drops in energy (below the S = 0 state) and becomes the ground state. In the same manner when the field reaches a certain magnitude the

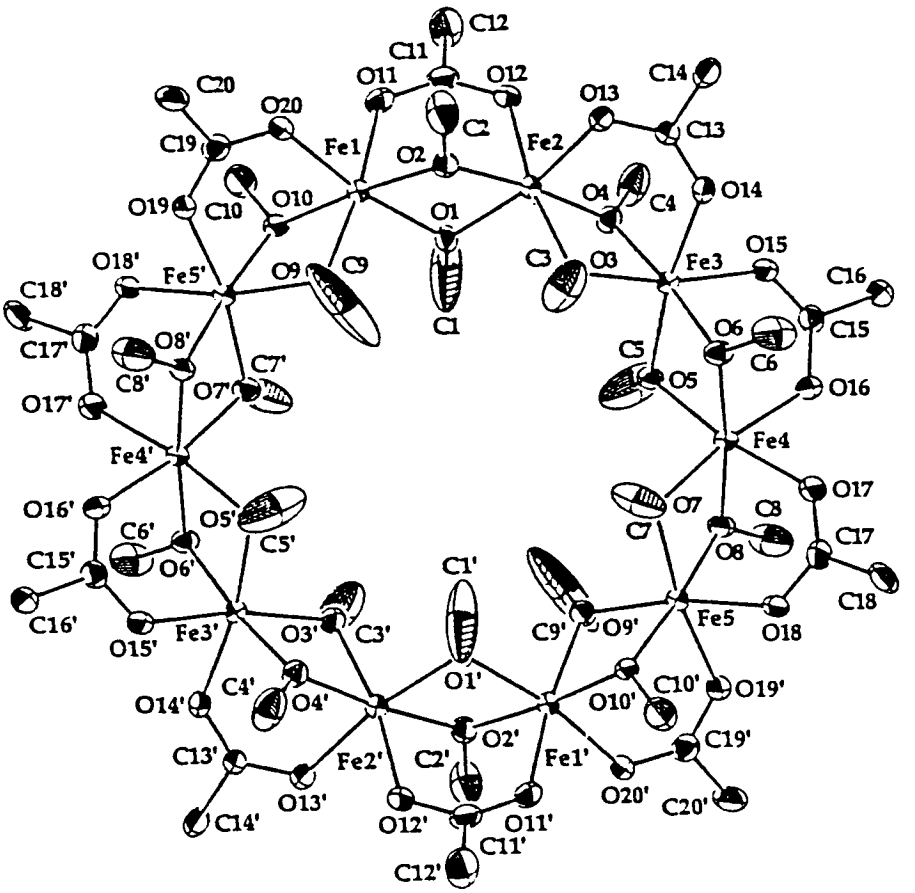

Figure 1.7. The crystal structure of $[Fe(OMe)_2(O_2CCH_2Cl)]_{10}$.

S = 2 level falls below the S = 1 level and so on. The crossover transitions are observed at 0.6 K because at this temperature only the lowest spin state is initially populated. By using continually larger fields crossover transitions for spin states up to S = 9 can be established. This is most clearly observed in a differential magnetisation study which showed the change in magnetisation with respect to the field as the field varied. This is shown in Figure 1.8. Similar behaviour has also been reported for $[Fe_6Na(OMe)_{12}(dbm)_6]Br$, which also has a cyclic structure. The magnetisation of the Fe_6 ring (at 0.65 K) at low field is zero, but on increasing field several steps are seen where the magnetisation increases rapidly. The steps are again regularly spaced in field and observed up to S = 3.

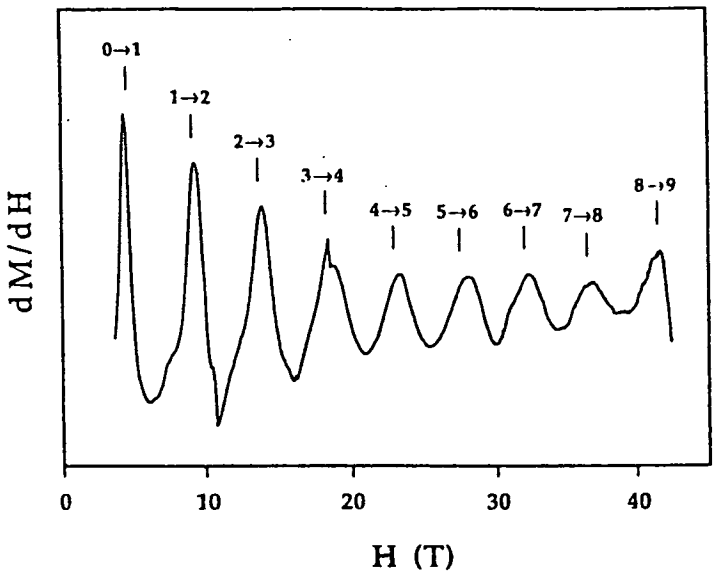

Figure 1.8. Differential magnetisation for the ferric wheel indicating the spin crossovers at increasing field.

Magnetic properties such as high spin ground states, slow relaxation effects and sensitivity to external fields have rarely been observed for polynuclear 3d-metal clusters outwith manganese and iron. One exception is the nickel metallocycle $[Ni_{12}(O_2CMe)_{12}(chp)_{12}(THF)_6(H_2O)_6]$ in which ferromagnetic exchange between the Ni(II) centres stabilises an S = 12 ground state. The compound was synthesised in this group and is related to new complexes reported in this thesis and will therefore be discussed in detail within this text.

1.4. Aims.

The aims of this thesis are :

1) To synthesise and characterise a number of new polynuclear nickel (II) and cobalt (II) complexes.

2) To try to understand the synthetic procedures required to make such compounds, including the role of metal, ligand and solvent.

3) To investigate the magnetic properties they display.

1.5. Pyridone ligand systems.

The ligands used in this thesis are derivatives of 2-pyridone : they are 6-chloro-2-pyridone (Hchp), 6-bromo-2-pyridone (Hbhp) and 6-methyl-2-pyridone (Hmhp).

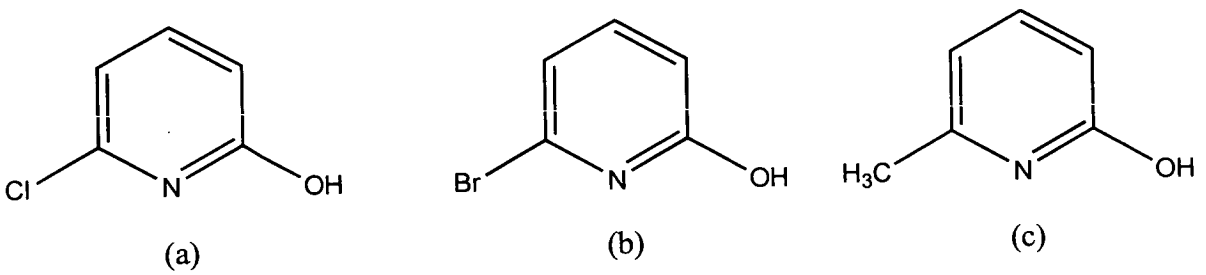

(a) (b) (c)

Figure 1.9. (a) Hchp (b) Hbhp (c) Hmhp.

These ligands have two potential donor atoms; the ring nitrogen and the exocyclic oxygen atom. 6-substituted pyridones have been chosen specifically for two main reasons. Firstly the substituent provides a steric block to polymerisation and secondly the choice of substituent alters the tautomeric equilibrium [48, 49], such that electron-withdrawing groups [for example chlorine] favour the enol form and electron-donating groups [for example methyl] favour the keto form. Thus the presence ot two possible donor atoms means that the pyridone ligands offer a variety of possible binding modes.

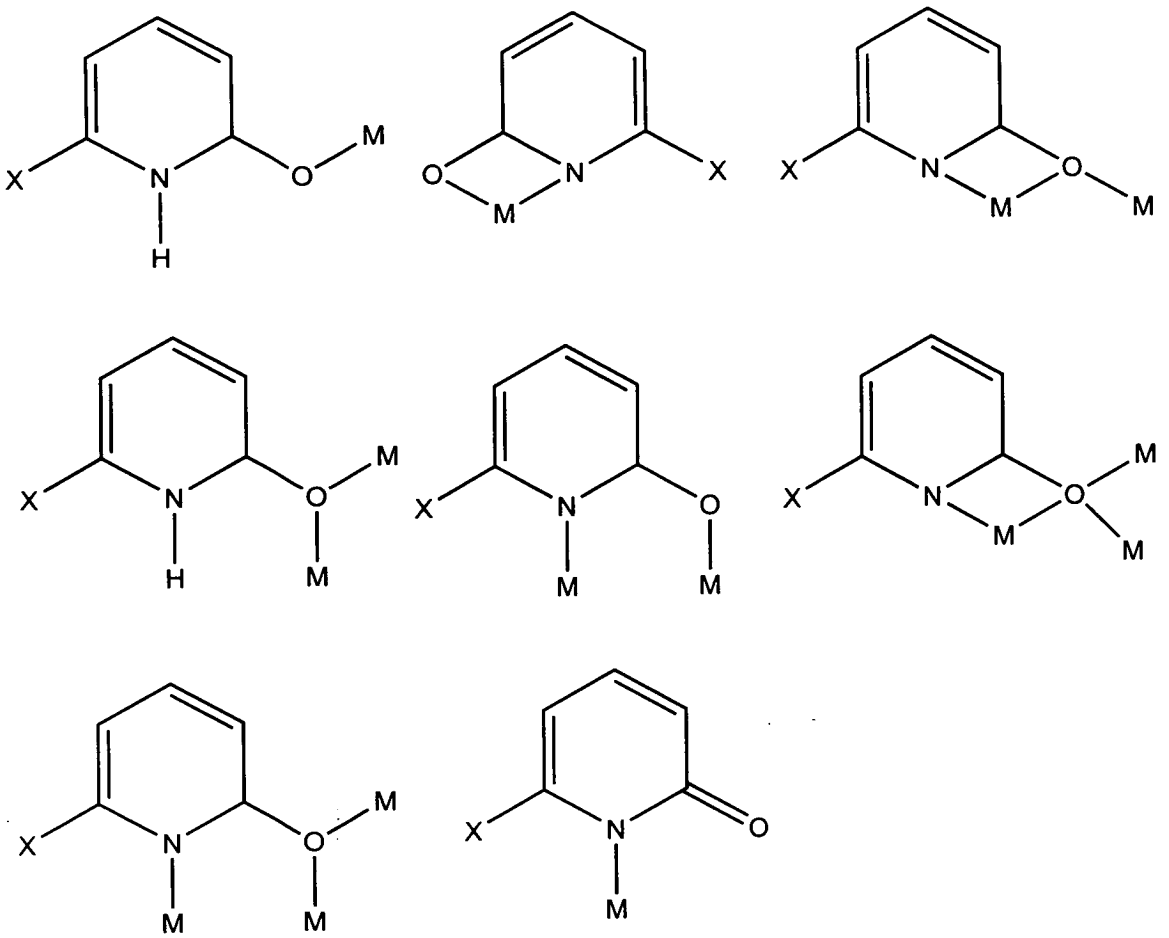

Figure 1.10. Possible binding modes for the pyridone ligands.

1.6. Methodology.

The reactions described in this thesis involve the use of all / or a combination of metal salts, pyridonate ligands, carboxylate ligands and solvent. Thus there are up to four reactants which can be altered in any one reaction. The methodology employed in this work is to systematically vary one of these reactants at any one time continually repeating reactions until all of the possible combinations of that reactant have been examined. The reason for adopting such a methodical approach is to try to establish the exact role of each reactant in determining the nature of the final product.

1.7. Previous work with pyridone ligands.

There are many previous examples of transition metal compounds of 2-pyridone and its derivatives and this chemistry has been reviewed [50]. The bulk of these compounds contain transition metals from the 2nd and 3rd rows and in general, with the possible exception of chromium and copper, compounds of the 1st row have been largely neglected. For example only one compound, $[V_2O_2Cl_4(Hmhp)_3]$, of a metal from groups 3, 4 or 5 has ever been reported.

There were no known polynuclear nickel-pyridonate compounds until very recently when work carried out in this group produced a family of trimers and a dodecanuclear metallocycle. These will be discussed in more detail within this text.There are however a few more examples of cobalt compounds in the literature. The trimeric species $[Co_3(chp)_6(IPA)_6]$ and the two dimers $[Co(bhp)(O_2CMe)(Me_2\text{-bpy})]_2$ and $[Co_2(fhp)_4(Me_2\text{-bpy})]$ (IPA = isopropyl alcohol; Me_2-bpy = 4, 4'-dimethyl-2, 2'-bipyridine; Hbhp = 6-bromo-2-pyridone; Hfhp = 6-fluoro-2-pyridone) all contain linear arrangements of metal ions bridged by a mixture of pyridonate and carboxylate ligands [51]. Three heterobimetallic species of cobalt and sodium have also been reported : two unusual polymers $[Co_2Na_2(mhp)_6(Hmhp)(H_2O)]_n$ and $[Co_4Na_{16}(O_2CMe)_{23}(NO_3)(MeOH)_{15}]$ [52]; and a hexanuclear metallocrown $[Na\{Co(mhp)_2\}_6][O_2CMe]$ in which six $[Co(mhp)_2]$ units encapsulate a sodium atom [53]. The most interesting cobalt-pyridonate complex yet reported is the dodecanuclear compound $[Co_{12}(OH)_6(O_2CMe)_6(mhp)_{12}]$ [54]. Its structure is based on a pentacapped-trigonal prism and is related to a number of new complexes reported in this thesis. It will therefore be discussed in detail later.

CHAPTER 2

POLYMETALLIC NICKEL AND COBALT COMPLEXES OF 6-CHLORO-, 6-BROMO- AND 6-METHYL-2-PYRIDONE THAT CONTAIN NO CARBOXYLATES.

2.1. Introduction

This chapter outlines the synthesis of a number of novel polynuclear nickel and cobalt compounds from only two simple starting materials: namely a metal salt and the ligand of choice in either protonated [Hxhp,where xhp= chp, or mhp] or deprotonated [Na(xhp)] form, where xhp= chp, bhp or mhp) form. The diversity of the compounds produced illustrates the huge influence that a change of metal, ligand or solvent exerts on the structure of the final product.

Reactions of the sodium salts of 6-chloro-, 6-bromo- and 6-methyl-2-pyridone produce, amongst others, isostructural nickel and cobalt cubanes, a dodecanuclear "chain of cubes" and a series of related heterobimetallic nickel/cobalt- sodium structures. Also reported is a cubic-close packed tetraicosanuclear cobalt compound, the highest known nuclearity complex containing cobalt. Magnetic studies of this compound indicate the presence of a high spin ground state and the possibility of superparamagnetic behaviour. Thermolysis reactions of 6-chloro-(Hchp) and 6-methyl-2-pyridone (Hmhp) produce the first examples of nickel and cobalt complexes which contain M_4O_6 adamantane units, which are also the first examples of vertex- and face-sharing adamantanes.

2.2. Nickel (II) Pyridonates

The reaction between nickel chloride and Na(xhp) was investigated using both hydrated and anhydrous nickel (II) chloride and the sodium salts of 6-chloro-, 6-bromo- and 6-methyl-2-pyridone. The general reaction scheme is similar for all the compounds produced : a two-fold equivalent of the ligand [Na(xhp)] is stirred in a methanolic solution of nickel (II) chloride for a set period of time, prior to being filtered and dried to a paste. Crystallisation of this paste from various solvents leads to a number of products whose structures are wholly dependant upon the ligand used [chp, bhp or mhp] and upon the crystallistion solvent.

2.2.1. Synthesis and structure of $[Ni_4(\mu_3\text{-}OMe)_4(\eta\text{-}xhp)(xhp)_3(MeOH)_7].MeOH$, where xhp= chp 1, bhp 2.

Nickel chloride and two equivalents of Na(chp) were stirred in a methanolic solution for 24 hours before being filtered and the solvent removed producing an uncharacterised green paste. Crystallisation of this paste from fresh methanol produced green crystals of $[Ni_4(OMe)_4(\eta\text{-}chp)(chp)_3(MeOH)_7]$. MeOH **1** [Figure 2.1] in 80% yield after 24 hours [55].

1 consists of a $[Ni_4O_4]^{2+}$ cube with metal and oxygen atoms (derived from the μ_3-methoxides) occupying the alternate corners of a distorted cubane. Each nickel atom is six coordinate with its coordination sphere completed by methanol or chp ligands. One of the four chp units is chelating [to Ni1] whilst the remaining chps are monodentate, binding through their exocyclic oxygen atom only - one to each of the three remaining nickels.

The Ni-O(μ_3-OMe) bond lengths range from 2.023 - 2.074(3) Å, the Ni-O(chp) bonds fall between 2.067 - 2.094(3) Å with the Ni-O(MeOH) bonds being 2.068- 2.115(3) Å in length. The chelating pyridones small bite angle [N2R-Ni1-O2R, 62.6(2)°] has the effect of

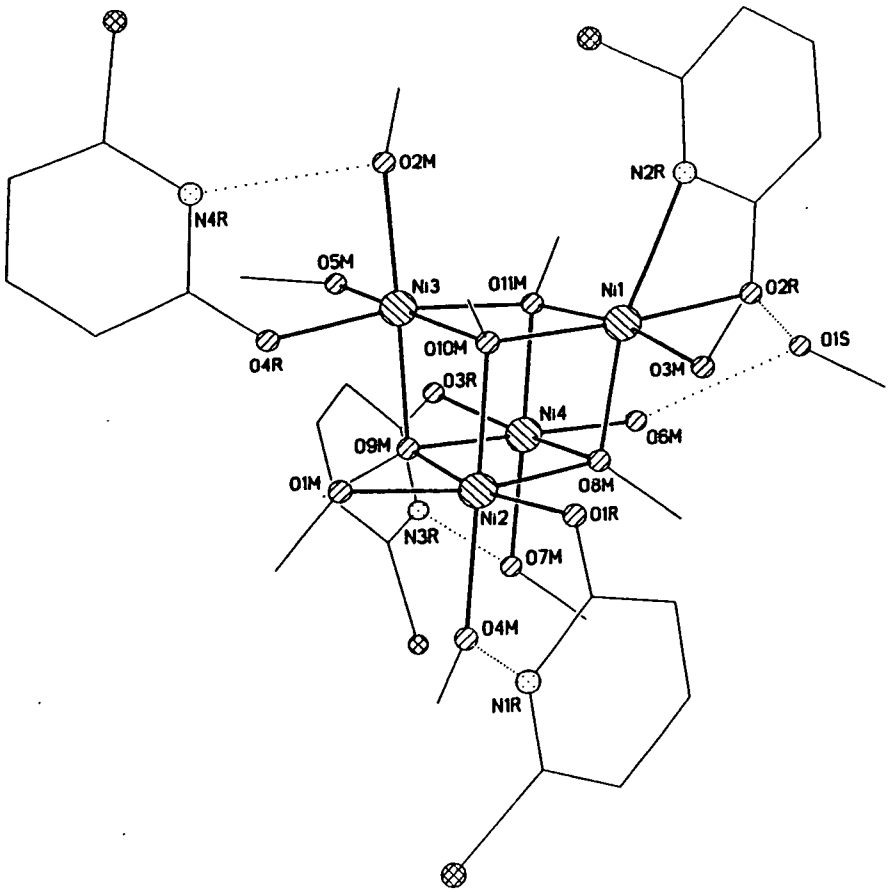

Figure 2.1. The structure of **1** in the crystal

producing a more distorted octahedral geometry around Ni1 in comparison to the three other nickel sites. For Ni1, the *cis* angles are in the range 62.6 -113.4(2)° with the *trans* angles 161.9 - 175.6(2)°. For all the other nickel sites the *cis* angles are 80.4 -100.1(2)°, and the *trans* angles 167.2 - 178.4(2)°. The angles within the cubane unit itself range from 94.8-99.7(2)° for the Ni-O(μ_3-OMe)-Ni angles and 80.7-84.3(2)° for the O(μ_3-OMe)-Ni-O(μ_3-OMe) angles, as a result of the four methoxides being pushed in toward the centre of the cubane.

There is extensive hydrogen bonding in **1** between the terminal methanol molecules and the ring nitrogens of the chp ligands, with the O...N distances in the range 2.614-2.660(3) Å, and between the solvent methanol molecule and the oxygen of the chelating chp ligand [O1S...O2R, 2.585(3) Å] and the terminal methanol on Ni4 [O1S...O6M, 2.629(3) Å]. The Ni...Ni contacts in **1** vary between 3.036(4) Å [Ni1-Ni2] to 3.127(4) Å [Ni1-Ni4].

$[Ni_4(\mu_3\text{-}OMe)_4(\eta\text{-}bhp)(bhp)_3(MeOH)_7]$. MeOH **2** was synthesised in an identical manner to **1** replacing Na(chp) with Na(bhp). **2** is isostructural with **1**. Selected bond lengths and angles for both **1** and **2** are given in Table 2.1. These nickel cubanes can be synthesised in a number of ways [experimental section 2.6.1 and 2.6.2] though the method described above produces the highest percentage yield of product. There are many examples of nickel cubanes in the literature [55-65].

2.2.2. Magnetochemistry of 1.

The magnetic behaviour of **1** was studied in the temperature range 300 - 1.8 K in an applied field of 1000 G. The variation of the product $\chi_m T$ (where χ_m is the molar magnetic susceptibility) with temperature is illustrated in Figure 2.2.

The room temperature value of $\chi_m T$ is approximately 7 emu K mol^{-1} which is consistent with four non-interacting S = 1 Ni(II) centres [$\chi_m T$ = 5.7 emu K mol^{-1}, g = 2.4]. There is a steady increase in $\chi_m T$ to 100 K at which point there is a sharp increase in the value to 9.25 emu K mol^{-1}, indicative of ferromagnetic exchange between the nickel centres. Below 10 K $\chi_m T$ drops sharply presumably due to intermolecular antiferromagnetic exchange. The 10 K value corresponds to an approximately S = 3 state. This type of behaviour has been observed for similar $[Ni_4O_4]^{2+}$ cubanes before [56-66, 63-65].

Table 2.1 Seleced bond lengths (Å) and angles (°) for **1**, **2**.

	1	2		1	2
Ni1-O10M	2.023(3)	2.021(3)	O8M-Ni1-O2R	99.69(9)	99.62(10)
Ni1-O8M	2.051(2)	2.053(3)	O11M-Ni1-O2R	96.97(10)	96.72(10)
Ni1-O11M	2.057(3)	2.047(3)	O10M-Ni1-O3M	90.65(9)	90.54(10)
Ni1-O2R	2.065(3)	2.055(3)	O8M-Ni1-O3M	90.83(9)	90.59(9)
Ni1-O3M	2.093(3)	2.089(3)	O11M-Ni1-O3M	169.14(9)	168.44(9)
Ni1-N2R	2.211(3)	2.240(3)	O2R-Ni1-O3M	91.34(11)	91.80(10)
Ni2-O9M	2.037(3)	2.067(3)	O10M-Ni1-N2R	113.49(9)	114.4(2)
Ni2-O1R	2.062(3)	2.080(3)	O8M-Ni1-N2R	161.99(9)	161.5(2)
Ni2-O10M	2.062(3)	2.028(3)	O11M-Ni1-N2R	97.70(9)	98.42(12)
Ni2-O8M	2.069(3)	2.060(3)	O2R-Ni1-N2R	62.52(10)	62.05(9)
Ni2-O4M	2.076(3)	2.080(3)	O3M-Ni1-N2R	92.33(11)	91.89(9)
Ni2-O1M	2.085(3)	2.081(3)	O9M-Ni2-O1R	169.74(9)	168.54(9)
Ni3-O10M	2.030(3)	2.042(2)	O9MNi2-O10M	81.99(10)	82.2(1)
Ni3-O9M	2.072(2)	2.068(3)	O1R-Ni2-O10M	90.66(10)	89.9(1)
Ni3-O11M	2.074(2)	2.058(2)	O9M-Ni2-O8M	80.53(10)	81.12(10)
Ni3-O5M	2.073(3)	2.072(3)	O1R-Ni2-O8M	91.49(10)	91.60(9)
Ni3O4R	2.075(3)	2.070(3)	O10M-Ni2-O8M	82.77(9)	82.34(10)
Ni3-O2M	2.087(3)	2.079(3)	O9M-Ni2-O4M	98.11(11)	91.52(10)
Ni4-O9M	2.044(3)	2.042(2)	O1R-Ni2-O4M	89.45(10)	89.92(10)
Ni4-O8M	2.052(3)	2.073(3)	O10M-Ni2-O4M	178.30(9)	176.92(9)
Ni4-O11M	2.067(3)	2.061(3)	O8M-Ni2-O4M	98.93(13)	100.0(2)
Ni4-O6M	2.068(3)	2.066(3)	O9M-Ni2-O1M	91.97(9)	92.73(10)
Ni4-O3R	2.091(3)	2.099(3)	O1R-Ni2-O1M	94.76(12)	96.10(9)
Ni4-O7M	2.115(3)	2.115(3)	O10M-Ni2-O1M	86.72(10)	87.61(10)
O10M-Ni1-O8M	84.18(9)	83.93(10)	O8M-Ni2-O1M	167.83(9)	168.26(9)
O10M-Ni1-O11M	81.56(10)	81.42(10)	O4M-Ni2-O1M	91.58(9)	89.45(10)
O8M-Ni1-O11M	80.91(10)	81.26(10)	O10M-Ni3-O9M	81.93(10)	81.82(10)

Table 2.1 continued

	1	2		1	2
O10M-Ni3-O11M	81.01(10)	81.20(9)	O9M-Ni4-O3R	89.50(10)	89.45(9)
O9M-Ni3-O11M	82.02(10)	81.55(10)	O8M-Ni4-O3R	167.16(9)	166.64(9)
O10M-Ni3-O5M	168.74(9)	169.11(10)	O11M-Ni4-O3R	89.89(9)	89.40(9)
O9M-Ni3-O5M	92.79(9)	92.29(10)	O6M-Ni4-O3R	92.42(9)	92.80(10)
O11M-Ni3-O5M	88.43(10)	88.60(9)	O9M-Ni4-O7M	95.23(9)	96.93(9)
O10MNi3-O4R	91.08(11)	91.81(9)	O8M-Ni4-O7M	99.14(9)	99.18(9)
O9M-Ni3-O4R	87.98(9)	88.20(11)	O11M-Ni4-O7M	178.07(8)	177.23(9)
O11M-Ni3-O4R	168.00(9)	167.80(11)	O6M-Ni4-O7M	85.47(10)	85.83(10)
O5M-Ni3-O4R	98.70(11)	97.88(10)	O3R-Ni4-O7M	90.01(10)	90.70(10)
O10M-Ni3-O2M	96.59(11)	96.30(11)	Ni4-O8M-Ni1	99.26(10)	98.69(10)
O9M-Ni3-O2M	177.26(9)	176.92(11)	Ni4-O8M-Ni2	98.37(10)	96.31(10)
O11M-Ni3-O2M	100.06(9)	100.81(9)	Ni1-O8M-Ni2	94.96(10)	95.62(9))
O5M-Ni3-O2M	89.06(9)	89.00(12)	Ni2-O9M-Ni4	99.64(10)	97.15(10)
O4R-Ni3-O2M	89.74(9)	89.55(10)	Ni2-O9M-Ni3	97.20(9)	97.37(9)
O9M-Ni4-O8M	80.76(10)	80.49(9)	Ni4-O9M-Ni3	96.99(9)	98.93(10)
O9M-Ni4-O11M	82.84(9)	82.60(12)	Ni1-O10M-Ni3	99.65(10)	96.13(9)
O8M-Ni4-O11M	80.67(9)	80.44(11)	Ni1-O10M-Ni2	96.00(9)	99.50(9)
O9M-Ni4-O6M	177.96(9)	178.10(9)	Ni3-O10M-Ni2	97.72(11)	97.74(9)
O8M-Ni4-O6M	97.24(10)	96.93(11)	Ni1-O11M-Ni4	98.55(10)	99.20(10)
O11M-Ni4-O6M	96.46(10)	96.90(110	Ni1-O11M-Ni3	97.13(11)	97.48(10)

The magnetic interaction between the Ni(II) centres in the cube is propagated by the bridging methoxides.The nature of this interaction (ferro- or antiferromagnetic) is dependent on the Ni-O(μ_3-OMe)-Ni bridging angle with, in general, angles <99° (i.e. toward 90°) producing a ferromagnetic interaction and angles >99° (i.e. toward 180°) producing an antiferromagnetic interaction [56]. Direct metal-metal interactions should not occur given that

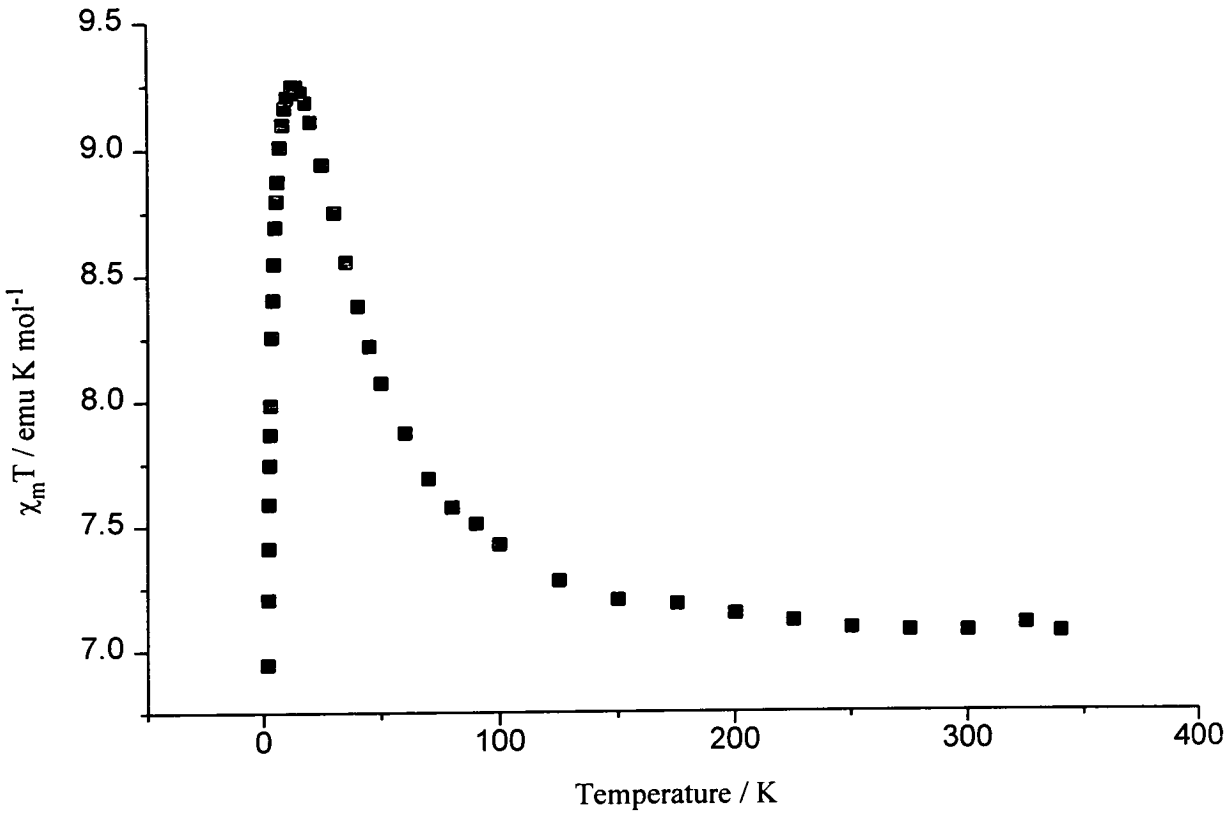

Figure 2.2. The variation of the product $\chi_m T$ vs temperature for **1**.

the closest Ni...Ni contact is over 3 Å. The Ni...Ni distance in nickel metal is 2.44 Å.

There are several theoretical models which have been used to describe the magnetic interaction between the metal centres of a $[Ni_4O_4]^{2+}$ cubane [56, 59, 64, 65]. The four nickel atoms can be regarded as being at the corners of a tetrahedron, with the exchange between any two metal centres described by an exchange parameter, J [Figure 2.3]. For example the exchange between Ni1 and Ni4 is J_{14}. Thus there are a total of six possible exchange parameters, with the total number of different J values depending on the symmetry of the molecule. A high level of symmetry in the molecule reduces the number of different exchange parameters. **1** has effectively no symmetry and therefore would require six J values. Although such a model could be developed there would inevitably be correlation between J values.

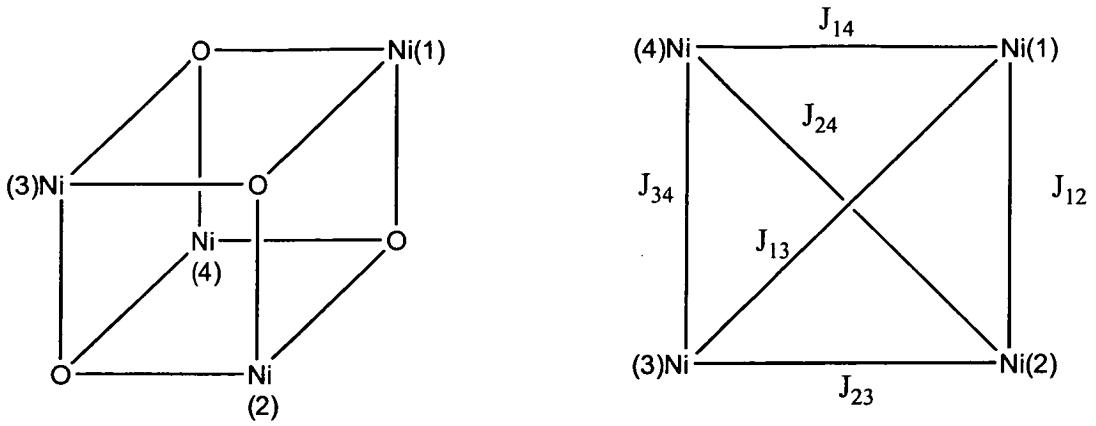

Figure 2.3. The magnetic exchange between the four Ni(II) centres in a cube.

2.2.3. Synthesis and structure of $[Ni_2Na_2(chp)_6(MeCN)_4(H_2O)]$ 3 and $[Ni_2Na_2(chp)_6(MeCN)_4(H_2O)_2]$ 4.

Nickel chloride was stirred for 24 hours in a methanolic solution that contained two equivalents of Na(chp), producing a paste after filtration and solvent removal. Crystallisation of this paste from acetonitrile produced the tetrametallic species $[Ni_2Na_2(chp)_6(MeCN)_4(H_2O)]$ **3** [Figure 2.4] after one day [66]. **3** crystallises about a two fold rotation axis. The molecule contains $[Ni(chp)_3]^-$ "complex ligands" linked to a central sodium core. Each nickel is surrounded by three chelating chp ligands, two of which further bridge to one sodium [either Na1 or Na1A] through the exocyclic oxygen atom. The third pyridonate is purely chelating with the exocyclic oxygen atom [O1R or O1RA] bound only to the nickel.

The nickels have a distorted octahedral geometry due to the small bite angle of the chp ligands [average NXR-Ni-OXR, 63.91(13)°].The *cis* angles of the nickel range from 63.80-106.80(20)°, with the *trans* angles varying between 151.75-161.52(10)°.The sodium is five coordinate being bound to two chp oxygen donors , a μ_2-water molecule (which bridges the

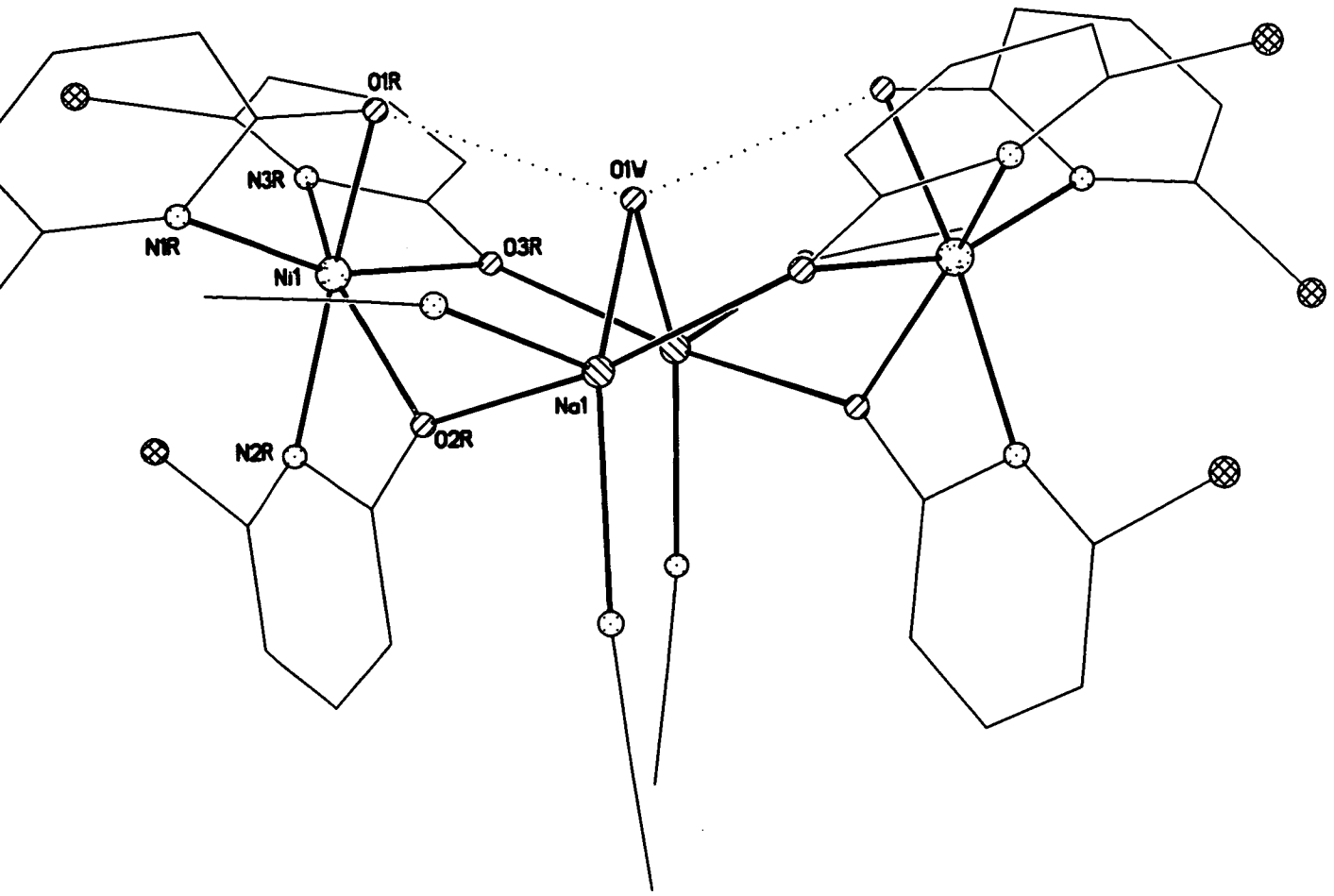

Figure 2.4. The structure of **3** in the crystal.

two sodium centres) and two acetonitrile molecules. The bridging water molecule is strongly hydrogen bonded to the non-bridging oxygen atoms of the chp ligands [O1R, O1RA.....OW, 2.705(3) Å].The Na...Na distance is 3.348(4) Å, with the Ni..Ni contact being over 6 Å.

The packing of **3** in the crystal is shown in Figure 2.5. The molecules are packed in "rows and columns", i.e. stacked directly side by side, with the chlorine atoms of the chp ligands approximately 3.4 Å apart, and directly one on top of another with the aromatic rings stacked "graphitically".The rows are staggered with one row being directly in line with the row two above.

If a similar reaction to that which produced **3** is repeated in the presence of sodium phenylacetate **3** is reproduced but co-crystallised with another tetranuclear species $[Ni_2Na_2(chp)_6(MeCN)_4(H_2O)_2]$ **4** [Figure 2.6]. There is obviously a close similarity between **3**

and **4**, the significant difference being that the two sodium centres in **4** are bridged by two μ_2-water molecules. Each bridging water forms only one strong hydrogen bond [O2W...O4R, 2.641(6) Å] whereas the bridging water in **3** formed two. The nickel coordination spheres are identical in the two complexes but the sodium coordination environment in **4** is six coordinate, bound to two bridging water molecules, two acetonitrile ligands and two μ_2-oxygen donors from chp ligands .

The Na...Na contact is slightly longer in **4** at 3.565(3) Å with the Ni...Ni distance almost reaching 7 Å. An interesting feature of both **3** and **4** is the *fac* coordination of the chp ligands in the $[Ni(chp)_3]^-$ units. Selected bond lengths and angles for **3** and **4** are given in Table 2.2 and Table 2.3 respectively.

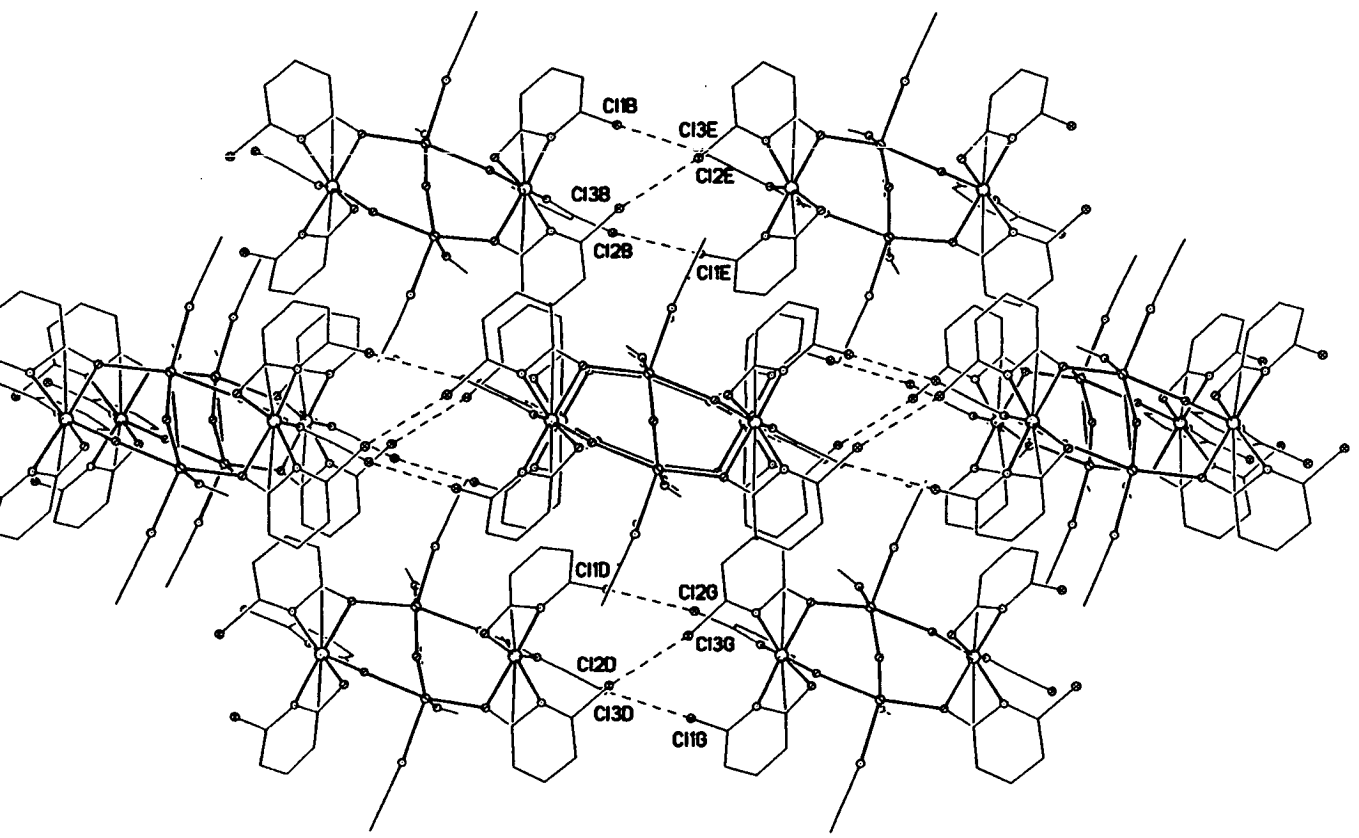

Figure 2.5. The packing of **3** in the crystal.

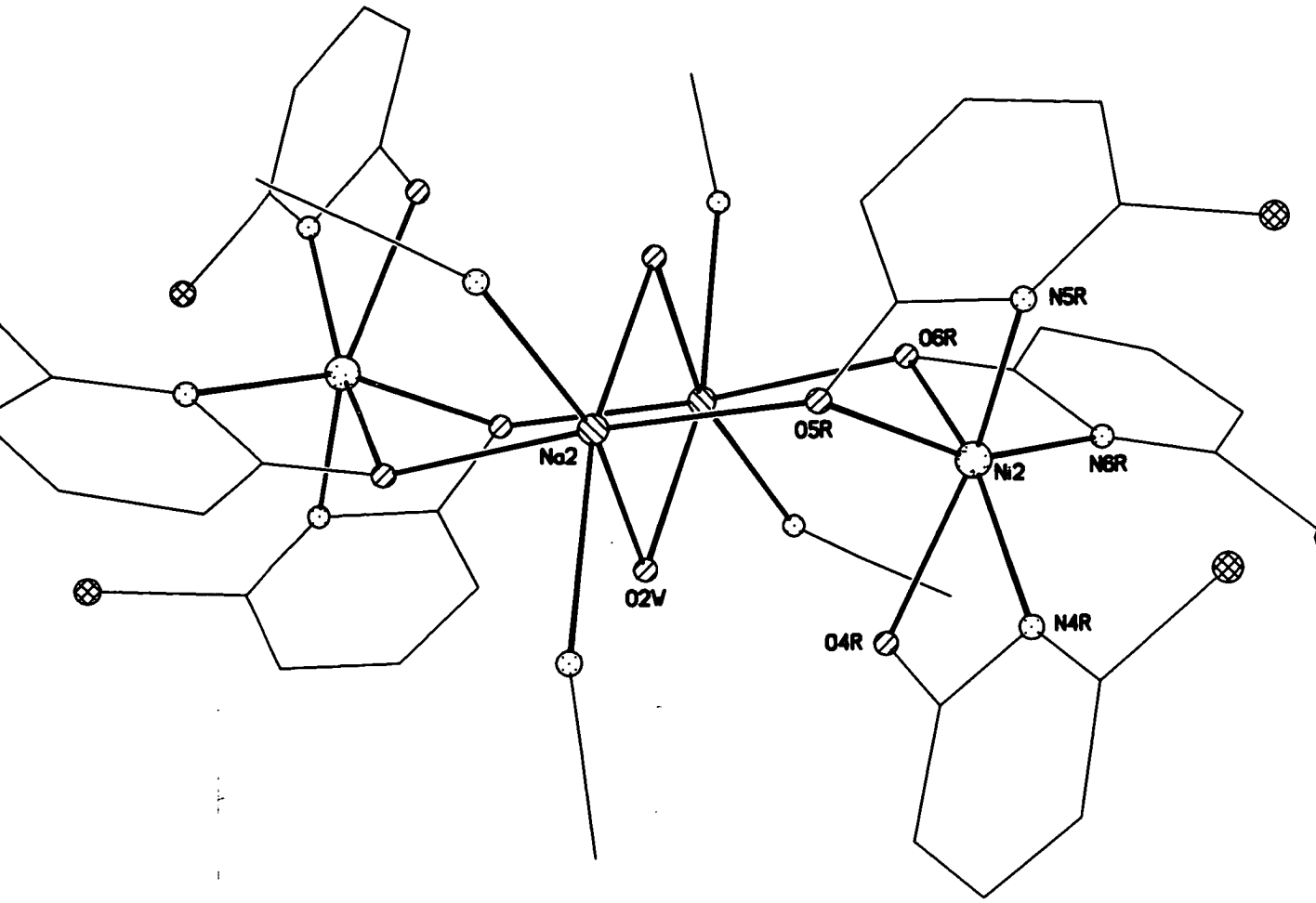

Figure 2.6. The structure of 4 in the crystal.

Table 2.2. Selected bond lengths (Å) and angles (°) for **3**.

Ni1-O1R	2.123(4)	N2R-Ni1-N3R	102.692)
Ni1-O2R	2.139(4)	N1R-Ni1-N3R	105.3(3)
Ni1-O3R	2.108(3)	N2R-Ni1-O3R	91.892)
Ni1-N1R	2.059(4)	N1R-Ni1-O3R	160.8(2)
Ni1N2R	2.046(4)	N3R-Ni1-O3R	64.23(15)
Ni1-N3R	2.066(4)	N2R-Ni1-O1R	158.4(2)
Na1-O1W	2.328(4)	N1R-Ni1-O1R	64.17(15)
Na1-O2R	2.479(4)	N3R-Ni1-O1R	98.8(2)
Na1-O3RA	2.347(4)	O3R-Ni1-O1R	100.33(14)
Na1-N1A	2.438(6)	N2R-Ni1-O2R	63.8(2)
Na1-N1B	2.468(6)	N1R-Ni1-O2R	100.4(2)
N2R-Ni1-N1R	106.5(2)	N3R-Ni1-O2R	153.7(2)

Table 2.2 continued

O3R-Ni1-O2R	92.65(15)	O1W-Ni1-O2R	79.66(12)
O1R-Ni1-O2R	97.65(14)	O3RA-Ni1-O2R	161.9(12)
O1W-Ni1-O3RA	82.68(12)	N1A-Na1-O2R	97.3(2)
O1W-Ni1-N1A	112.8(2)	N1B-Na1-O2R	88.1(2)
O3R-Ni1-N1A	93.2(2)	Na1-O1W-Na1A	92.0(2)
O1W-Ni1-N1B	148.6(2)	Ni1-O2R-Na1	120.6(2)
O3R-Ni1-N1B	105.2(2)	Ni1-O3R-Na1A	109.4(2)
N1A-Ni1-N1B	97.4(2)		

Table 2.3. Selected bond lengths (Å) and angles (°) for **4**.

Ni2-O4R	2.144(4)	N4R-Ni2-O5R	93.18(15)
Ni2-O5R	2.121(3)	N5R-Ni2-O5R	63.44(15)
Ni2-O6R	2.100(4)	N6R-Ni2-O5R	156.6(2)
Ni2-N4R	2.058(4)	O6R-Ni2-O5R	97.76(14)
Ni2-N5R	2.069(4)	N4R-Ni2-O4R	63.60(15)
Ni2-N6R	2.078(3)	N5R-Ni2-O4R	155.4(2)
Na2-O2W	2.425(4)	N6R-Ni2-O4R	100.3(2)
Na2-O2WA	2.404(5)	O6R-Ni2-O4R	97.00(14)
Na2-O5R	2.294(4)	O5R-Ni2-O4R	96.56(14)
Na2-O6RA	2.414(4)	O5R-Na2-O2WA	81.9(2)
Na2-N1C	2.631(7)	O5R-Na2-O6RA	169.21(15)
Na2-N1D	2.428(4)	O2WA-Na2-O6RA	94.51(15)
N4R-Ni2-N5R	101.3(2)	O5R-Na2-O2W	94.74(14)
N4R-Ni2-N6R	108.8(2)	O2WA-Na2-O2W	84.8(2)
N5R-Ni2-N6R	103.2(2)	O6RA-Na2-O2W	74.75(14)
N4R-Ni2-O6R	158.79(15)	O5R-Na2-N1D	99.0(2)
N5R-Ni2-O6R	99.8(2)	O2WA-Na2-N1D	96.8(2)
N6R-Ni2-O6R	64.28(15)	O6RA-Na2-N1D	91.6(2)

Table 2.3 continued.

O2W-Na2-N1D	166.3(2)	N1D-Na2-N1C	95.4(2)
O5R-Na2-N1C	91.1(2)	O5R-Na2-Na2A	87.76(12)
O2WA-Na2-N1C	166.7(2)	Na2-O2W-Na2A	95.2(2)
O6RA-Na2-N1C	90.3(2)	Ni2-O5R-Na2	121.6(2)
O2W-Na2-N1C	84.5(2)	Ni2-O6R-Na2A	119.7(2)

2.2.4. Synthesis and structure of $[Ni_2Na_2(chp)_6(H_2O)]_n$ 5.

Two equivalents of Na(chp) were added to a methanolic solution of nickel chloride and stirred over a period of 24 hours. The paste produced from the removal of the solvent, once dried, was crystallised from ethyl acetate to give the polymeric species $[Ni_2Na_2(chp)_6(H_2O)]_n$ **5** [Figure 2.7] [66] in moderate yield after two days.

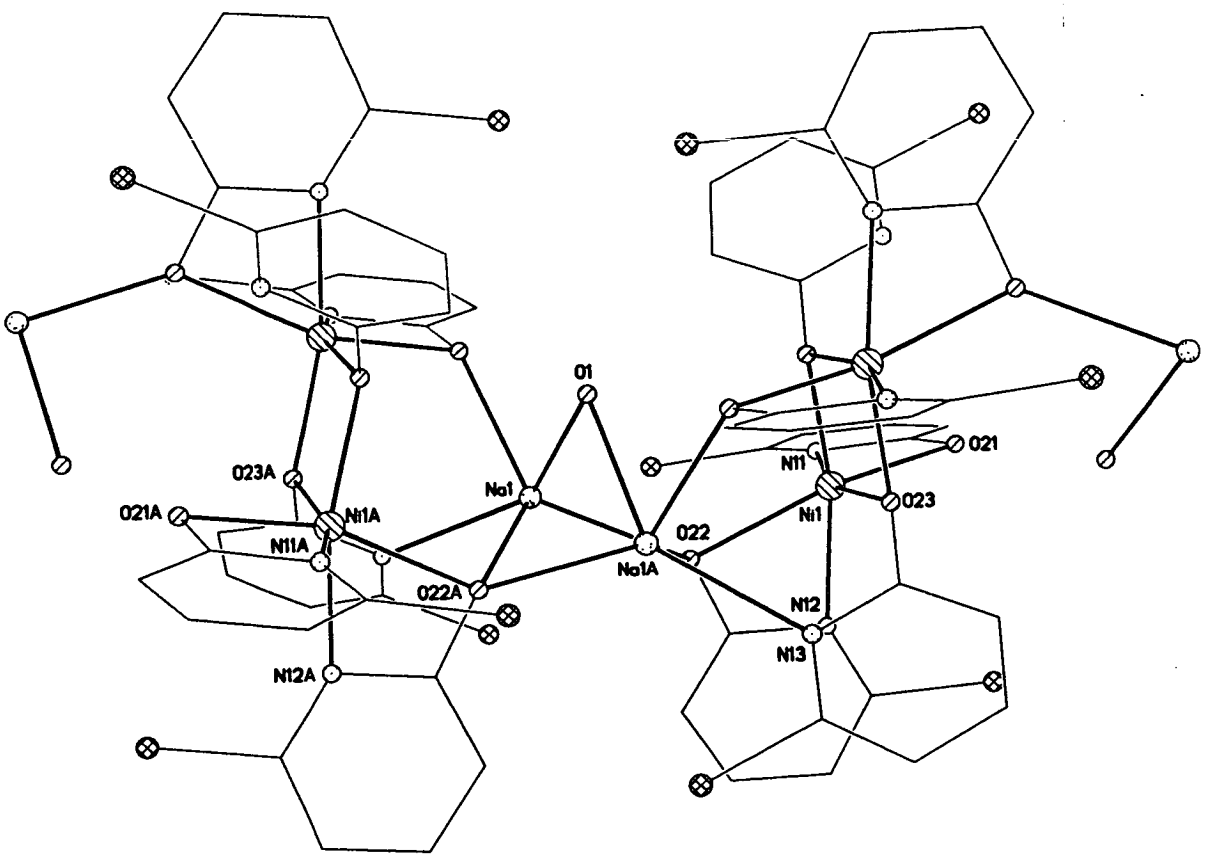

Figure 2.7. The structure of **5** in the crystal.

In **5** the nickel site is six coordinate, but there are only two chelating chp ligands bound to the metal, as opposed to **3** and **4** which contained $[Ni(chp)_3]^-$ units. The remaining two sites are occupied by two μ_2-oxygen donors [O23 and symmetry equivalent] from trinucleating chp ligands. The nickel site therefore has two nitrogen and four oxygen donors coordinated, rather than the three nitrogen and three oxygen donors in **3** and **4**.

The crystallographically unique sodium site is quite different to those found in **3** and **4**. It is five-coordinate, bound to one nitrogen and four oxygen atoms. The nitrogen donor [N13] is derived from the chp ligand which provides the oxygen donor [O23] which bridges Ni1 and Ni1A, while the four oxygen donors are derived from a variety of ligands. O1 is a μ_2-bridging water , similar to those found in **3** and **4**, and bonds to two sodium centres. A further oxygen [O21] is μ_2-bridging between a nickel and sodium site and is derived from a chelating chp. The final two oxygen donors are derived from chelating chp ligands, but also bridge between two sodium sites and are thus μ_3-bridging. The result is that the two neighbouring sodium sites are bridged by three oxygen atoms and within the polymer there are alternating dinuclear nickel and sodium fragments. **5** can therefore be regarded as consisting of $[Ni_2(chp)_6]^{2-}$ units ligating $[Na_2(H_2O)]^{2+}$ units in comparison to **3** and **4** where there are two $[Ni(chp)_3]^-$ units ligating a $[Na_2(H_2O)_{1,2}(MeCN)_4]^{2+}$ core.

Again the nickels have distorted octahedral geometries with the *cis* angles ranging from 63.3 -103.9(2)° and the *trans* angles varying between 155.6-165.6(2)°. The Ni1...Ni1A distance is 3.161(4) Å with the bridging angle between the two *via* O23 (and symmetry equivalent) being 101.3(2)°. The Na1...Na1A distance is 3.126(3) Å with the closest Ni...Na contact being 3.583(3) Å between Ni1...Na1A. A summary of bond lengths and angles for **5** is given in Table 2.4.

Table 2.4. Selected bond lengths (Å) and angles (°) for **5**.

Ni1-O23B	2.035(5)	O21-Ni1-N11	63.4(2)
Ni1-O23	2.052(4)	O23B-Ni1-O22	103.9(2)
Ni1-N12	2.052(4)	O23-Ni1-O22	101.6(2)
Ni1-O21	2.117(4)	N12-Ni1-O22	63.4(2)
Ni1-N11	2.118(4)	O21-Ni1-O22	155.7(2)
Ni1-O22	2.182(4)	N11-Ni1-O22	97.1(2)
Na1-Na1A	3.583(4)	O1-Na1-O21C	72.1(2)
Na1-O1	2.365(4)	O1-Na1-O22	79.3392)
Na1-O21C	2.366(5)	O21B-Na1-O22	137.5(2)
Na1-O22	2.380(5)	O1-Na1-O22A	78.80(15)
Na1-O22A	2.407(4)	O21C-Na1-O22A	116.9(2)
Na1-N13A	2.491(5)	O22-Na1-O22A	86.5(2)
O23B-Ni1-O23	78.7(2)	O1-Na1-N13A	141.1(2)
O23B-Ni1-N12	165.6(2)	O21C-Na1-N13A	83.5(2)
O23-Ni1-N12	96.7(2)	O22-Na1-N13A	135.7(2)
O23B-Ni1-O21	93.6(2)	O22A-Na1-N13A	86.2(2)
O23-Ni1-O21	98.4(2)	Na1-O1-Na1A	82.7(2)
N12-Ni1-O21	100.6(2)	Ni1-O22-Na1	129.7(2)
O23B-Ni1-N11	97.7(2)	Ni1-O22-Na1A	102.6(2)
O23-Ni1-N11	161.3(2)	Na1-O22-Na1A	81.6(2)
N12-Ni1-N11	90.9(2)	Ni1-O23-Ni1B	101.3(2)

2.2.5 Magnetochemistry of 5.

The magnetic behaviour of **5** was studied in the temperature range 300 - 1.8 K in an applied field of 1000 G. The variation of $\chi_m T$ with temperature is shown in Figure 2.8. The room temperature value of $\chi_m T$ is approximately 3.2 emu K mol^{-1} which is consistant with two non-interacting S = 1 Ni(II) centres [$\chi_m T$ = 2.88 emu K mol^{-1}, g= 2.4]. The value remains

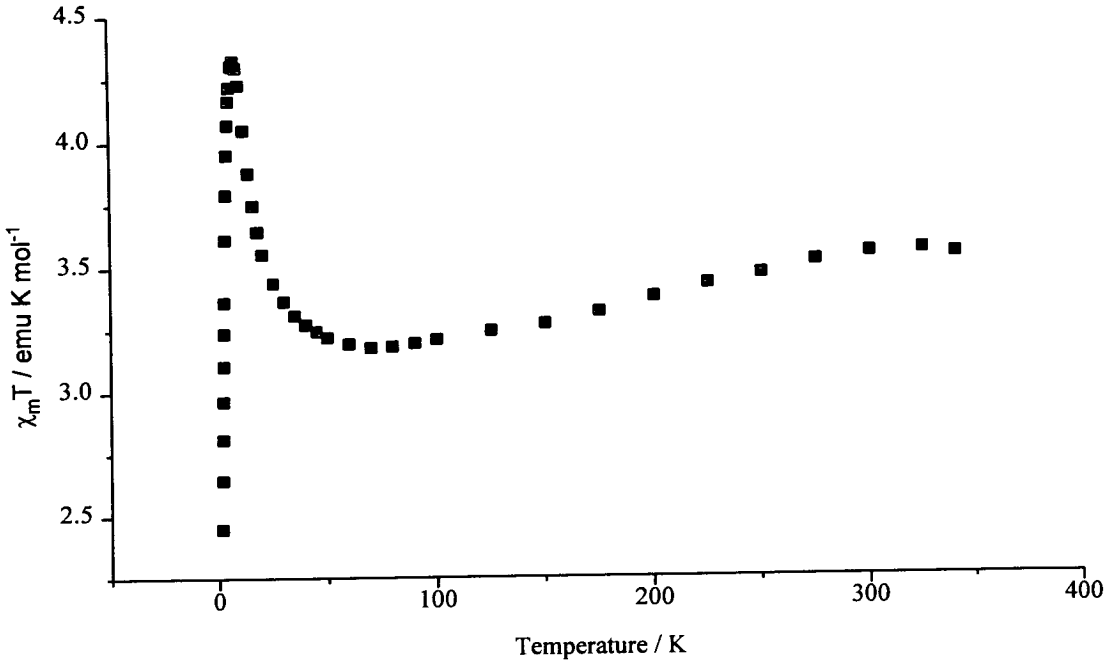

Figure 2.8. The variation of $\chi_m T$ with temperature for **5**.

fairly constant as the temperature drops, until at approximately 50 K where the value of $\chi_m T$ rises to a maximum of 4.4 emu K mol^{-1} at 10 K. Below 10 K the value drops sharply to a minimum of 2.5 emu K mol^{-1} at 1.8 K. The 10 K value corresponds to an approximately S = 2 ground state and indicates ferromagnetic exchange between the metal centres.

2.2.6. Synthesis and structure of $[Ni_4Na_4(mhp)_{12}(Hmhp)_2]$ 6.

Reaction of nickel chloride with two equialents of Na(mhp) in methanol over 24 hours leads, after crystallisation from either acetonitrile or ethyl acetate, to the complex $[Ni_4Na_4(mhp)_{12}(Hmhp)_2]$ **6** [Figure 2.9] in high yield [66]. **6** is a centrosymmetric structure which contains four identical $[Ni(mhp)_3]^-$ units surrounding a central sodium chair. These $[Ni(mhp)_3]^-$ units are similar to those observed ligating the sodium centres in **3** and **4.** Each nickel is coordinated to three chelating mhp ligands , two of which further bind to one sodium through their exocyclic oxygen atoms and are thus μ_2-bridging.The oxygen atom of the third chelating mhp binds to two further sodiums and is thus μ_3-bridging. Two Hmhp ligands are also found

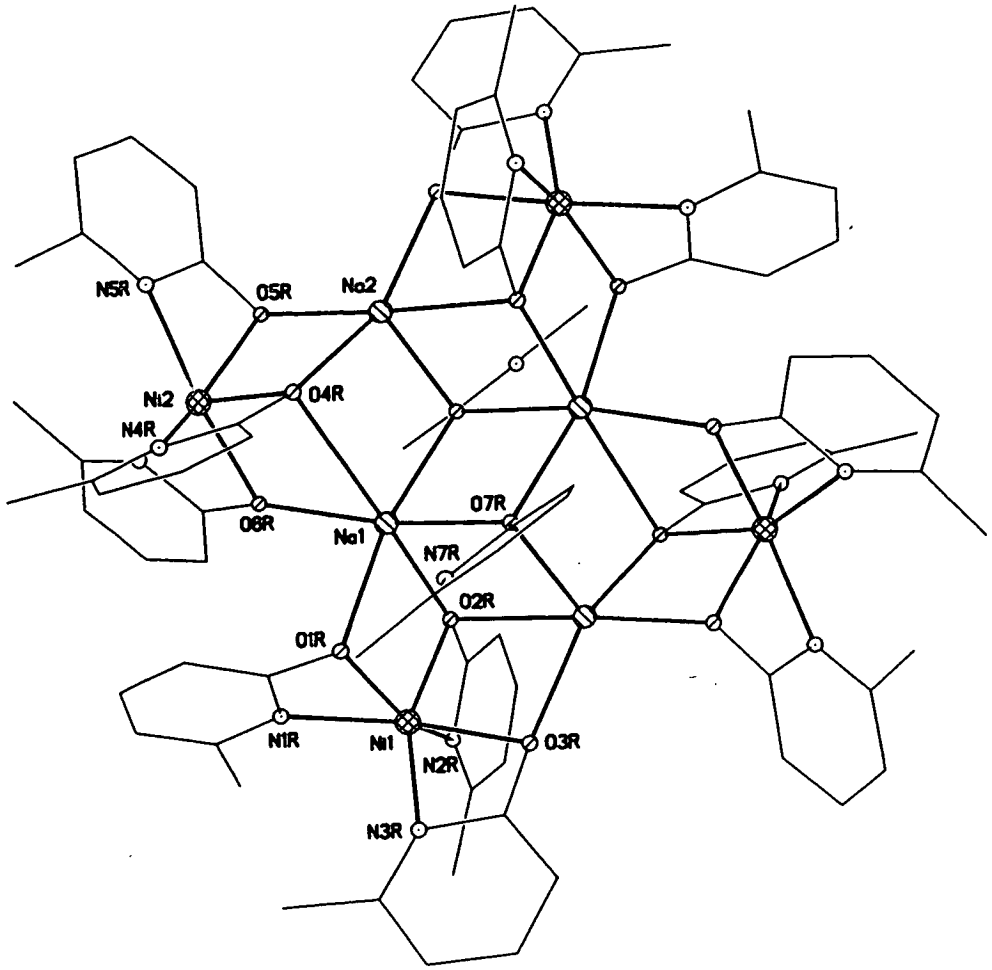

Figure 2.9. The structure of **6** in the crystal

in the structure and show a novel binding mode, each bridging three sodium atoms through the exocyclic oxygen atom alone. This mode of bonding has never been reported either for Hxhp or xhp ligands and represents bridging by the keto-tautomer of the pyridonate ligand as the ring nitrogen atom is protonated. Thus a ketone oxygen is bridging three metal centres.

The nickel centres in **6** have distorted octahedral coordination geometries as a result of the small bite angles of the chelating mhp ligands [for example:N1R-Ni1-O1R, 63.73(12)°]. The *cis* angles range from 63.73-109.91(12)° and the *trans* angles from 152.94-161.27(13)°. Each nickel has three oxygen and three nitrogen donors as with **3** and **4**, with the Ni-N bond lengths slightly shorter than the Ni-O bonds, although the two bond length ranges overlap. A summary of the bond lengths and angles is given in Table 2.5.

The two crystallographically unique sodium sites [Na1, Na2] show distinct geometries.

Na1 has five contacts to oxygen donors between 2.230-2.487(3) Å with one longer contact of 3.008(2) Å to O4R. Na2 has five contacts to oxygen donors which fall in the range 2.269-2.541(2) Å but no further long contacts. For both sodium sites the coordination geometries are extremely irregular. There is no difference between the Na-O bonds to the mhp or Hmhp ligands which is surprising. The Na-O(Hmhp) bonds average 2.35(3) Å which is extremely short for a Na-O(ketone) distance. This is still more surprising considering that this ketone oxygen is bridging three sodium sites, and is therefore formally five-valent. Only four previous examples have been reported of μ_3-oxygen bridges where the oxygen donor is derived from a ketone[67-70]. The metal polyhedron [Figure 2.10] can be described as four linked cubes with each cube missing a vertex; for example the cube comprising Na1, O7R, Na2A, O3R, Ni1, O1R and O2R. Each cube contains one nickel, two sodiums and four oxygen atoms and is linked to two others , sharing an edge [Na2, O7R or symmetry equivalents] with one, and a vertex [Na1, Na1A] with a second. The average Na...Na contact is 3.499(4) Å with the closest Ni...Ni contact being over 6 Å.

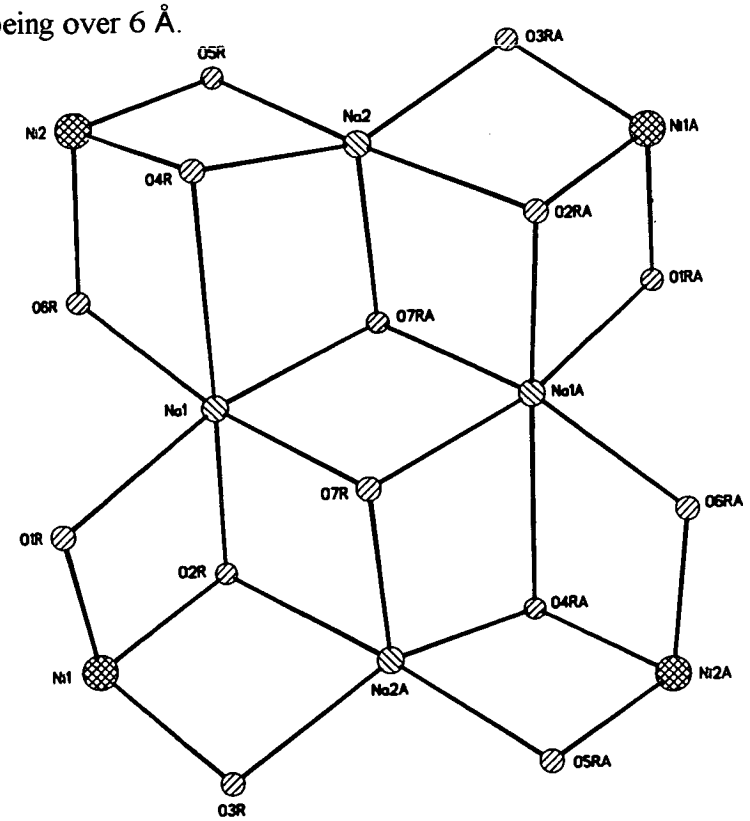

Figure 2.10. The metal polyhedron of **6**.

Table 2.5. Selected bond lengths (Å) and angles (°) for **6**.

Ni1-N1R	2.043(3)	N3R-Ni1-O3R	64.01(12)
Ni1-N2R	2.096(3)	N2R-Ni1-O3R	91.30(12)
Ni1-N3R	2.061(3)	O2R-Ni1-O3R	92.30(12)
Ni1-O1R	2.144(3)	N1R-Ni1-O1R	63.73(12)
Ni1-O2R	2.107(7)	N3R-Ni-O1R	96.78(12)
Ni1-O3R	2.114(3)	N2R-Ni1-O1R	152.95(12)
Ni2-N4R	2.067(3)	O2R-Ni1-O1R	93.25(11)
Ni2-N5R	2.074(3)	O3R-Ni1-O1R	104.77(11)
Ni2-N6R	2.088(3)	N4R-Ni2-N5R	101.93(14)
Ni2-O4R	2.149(3)	N4R-Ni2-N6R	112.80(14)
Ni2-O5R	2.117(3)	N5R-Ni2-N6R	103.59(13)
Ni2-O6R	2.108(3)	N4R-Ni2-O6R	100.83(13)
Na1-O6R	2.230(3)	N5R-Ni2-O6R	156.99(12)
Na1-O2R	2.325(3)	N6R-Ni2-O6R	64.03(12)
Na1-O7R	2.352(3)	N4R-Ni2-O5R	150.31(12)
Na1-O7RA	2.367(3)	N5R-Ni2-O5R	64.06(12)
Na1-O1R	2.487(3)	N6R-Ni2-O5R	96.35(12)
Na2-O3RA	2.269(3)	O6R-Ni2-O5R	96.84(11)
Na2-O4R	2.302(3)	N4R-Ni2-O4R	63.89(12)
Na2-O7RA	2.327(3)	N5R-Ni2-O4R	102.73(12)
Na2-O5R	2.357(3)	N6R-Ni2-O4R	153.52(12)
Na2-O2RA	2.542(3)	O6R-Ni2-O4R	90.22(12)
N1R-Ni1-N3R	101.33(13)	O5R-Ni2-O4R	92.56(11)
N1R-Ni1-N2R	105.25(13)	O6R-Na1-O2R	109.58(12)
N3R-Ni1-N2R	109.91(13)	O6R-Na1-O7R	162.87(12)
N1R-Ni1-O2R	102.72(13)	O2R-Na1-O7R	87.14(11)
N3R-Ni1-O2R	155.94(13)	O6R-Na1-O7RA	99.38(11)
N2R-Ni1-O2R	64.00(13)	O2R-Na1-O7RA	97.08(11)
N1R-Ni1-O3R	16.27(13)	O7R-Na1-O7RA	81.58(10)

Table 2.5 continued

O6R-Na1-O1R	93.20(11)	O5R-Na2-O2RA	176.72(11)
O2R-Na1-O1R	79.85(11)	Ni1-O1R-Na1	90.66(11)
O7R-Na1-O1R	85.98(10)	Ni1-O2R-Na1	96.22(11)
O7RA-Na1-O1R	167.34(11)	Ni1-O2R-Na2A	89.21(10)
O3RA-Na2-O4R	151.37(13)	Na1-O2R-Na2A	92.49(10)
O3RA-Na2-O7RA	105.42(11)	Ni1-O3R-Na2A	96.79(11)
O4R-Na2-O7RA	102.47(12)	Ni2-O4R-Na2	91.93(11)
O3RA-Na2-O5R	98.73(12)	Ni2-O5R-Na2	91.22(12)
O4R-Na2-O5R	82.84(11)	Ni2-O6R-Na1	112.71(13)
O7RA-Na2-O5R	99.39(11)	Na2A-O7R-Na1	97.51(11)
O3RA-Na2-O2RA	78.29(10)	Na2A-O7R-Na1A	94.32(11)
O4RNa2-O2RA	99.12(12)	Na1-O7R-Na1A	98.42(10)
O7RA-Na2-O2RA	82.79(10)		

2.3. Cobalt (II) Pyridonates.

The reactions between cobalt salts and the pyridonate ligands were investigated, using both anhydrous and hydrated cobalt chloride, cobalt acetate and both the deprotonated and protonated forms of 6-chloro- and 6-methyl-2-pyridone.

There are two general reaction schemes: the first is similar to that used in the synthesis of the previous nickel compounds- a solution of the cobalt salt is stirred with two equivalents of the sodium salt of the ligand in a solvent for a fixed period of time. Removal of the solvent then produces a paste which can be crystallised from a number of solvents. The second is a thermolysis reaction wherein a cobalt precursor [for example a cobalt carboxylate] is mixed with the protonated form of the ligand [Hxhp] and heated to the melting point of the ligand, producing a "melt" from which gas [i.e. the carboxylic acid and water] is removed under vacuum and unreacted Hxhp sublimed to a cold finger.The "melt" product is then crystallised from a variety of solvents.

2.3.1 Synthesis and structure of $[Co_4(\mu_3\text{-}OMe)_4(\eta\text{-}chp)(chp)_3(MeOH)_7].MeOH$ 7

Cobalt acetate was heated to 140°C with two equivalents of Hchp under nitrogen in a Schlenk tube for two hours. The acetic acid and water produced during the reaction was pumped off to a cold trap and the product dissolved in methanol which contained sodium methoxide. Red crystals of $[Co_4(\mu_3\text{-}OMe)_4(\eta\text{-}chp)(chp)_3(MeOH)_7].MeOH$ **7** [Figure 2.11] were produced after 24 hours in high yield [71].

7 is isostructural with the nickel cubanes **1** and **2**. The complex is again held together by μ_3-methoxides producing a cobalt-oxygen cubane with the distorted octahedral geometries of the cobalts completed by chp ligands and terminal solvent molecules. The cubane core

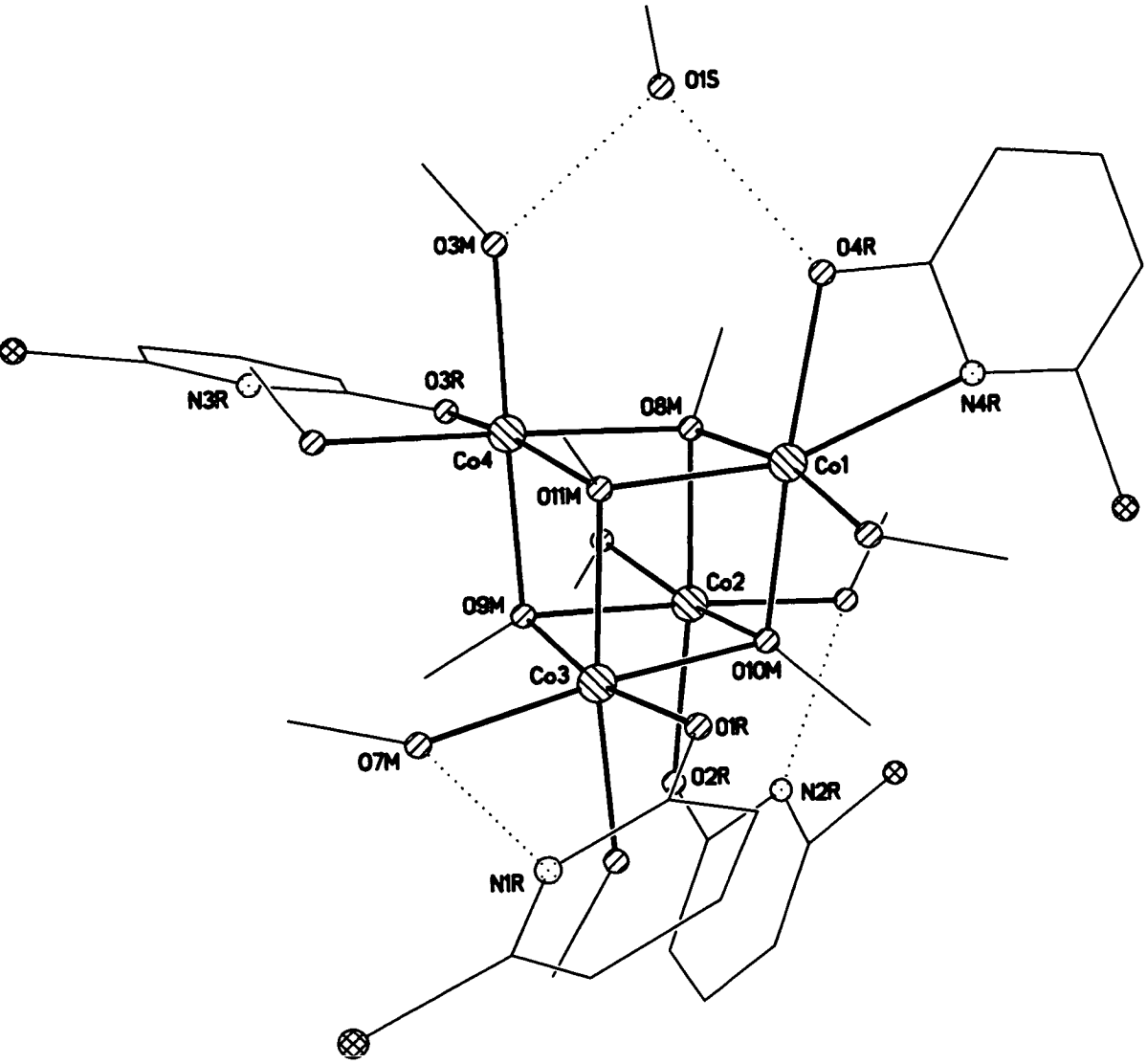

Figure 2.11. The crystal structure of **7**.

of the complex is similar to that in **1** and **2** with the Co-O(OMe)-Co angles varying between 80.30 and 84.22(10)° and the O(OMe)-Co-O(OMe) angles between 94.69 and 100.20(11)°. A summary of the bond lengths and angles for **7** is given in Table 2.6.

The presence of terminal solvent molecules suggests that desolvation might cause oligomerisation of the cubes by forcing the xhp ligands to bridge, thus filling the coordination sites vacated by the displaced methanol. However the coupling of smaller fragments into larger units has, with the exception of a tetranuclear manganese compound [72], rarely been reported.

7 can be synthesised in a number of ways [experimental section 2.6.7] including the

addition of Na(chp) to a methanolic solution of cobalt chloride as in the synthesis of **1** and **2** This however produces **7** in extremely low yields [ca. 10%] in comparison to the thermolysis reaction which can produce yields of up to 90%.

Table 2.6. Selected bond lengths (Å) and angles (°) for **7**.

Co1-O1	2.110(3)	Co4-N4R	2.259(3)
Co1-O2	2.057(3)	O2-Co1-O3M	177.97(10)
Co1-O4	2.100(3)	O2-Co1-O4	80.58(10)
Co1-O3M	2.090(3)	O3M-Co1-O4	97.51(11)
Co1-O5M	2.160(3)	O2-Co1-O1	83.23(10)
Co1-O3R	2.132(3)	O3M-Co1-O1	95.81(11)
Co2-O2	2.078(3)	O4-Co1-O1	80.73(10)
Co2-O4	2.091(3)	O2-Co1-O3R	89.04(11)
Co2-O1R	2.094(3)	O3M-Co1-O3R	92.76(11)
Co2-O7M	2.112(3)	O4-Co1-O3R	167.11(10)
Co2-O2M	2.112(3)	O1-Co1-O3R	90.52(10)
Co2-O10M	2.114(3)	O2-Co1-O5M	95.87(11)
Co3-O1	2.111(3)	O3M-Co1-O5M	85.11(11)
Co3-O2	2.117(3)	O4-Co1-O5M	99.77(10)
Co3-O3	2.052(3)	O1-Co1-O5M	178.89(11)
Co3-O2R	2.106(3)	O3R-Co1-O5M	88.81(11)
Co3-O1M	2.125(3)	O2-Co2-O4	80.30(10)
Co3-O4M	2.103(3)	O2-Co2-O1R	169.65(10)
Co4-O1	2.085(3)	O4-Co2-O1R	91.07(11)
Co4-O3	2.052(3)	O2-Co2-O7M	97.65(11)
Co4-O4	2.111(3)	O4-Co2-O7M	102.02(13)
Co4-O4R	2.086(3)	O1R-Co2-O7M	89.68(12)
Co4-O6M	2.117(3)	O2-Co2-O2M	91.67(11)

Table 2.6 continued.

O4-Co2-O2M	167.28(10)	O1-Co4-O4R	96.88(11)
O1R-Co2-O2M	95.80(12)	O3-Co4-O4	84.22(10)
O7M-Co2-O2M	88.75(14)	O1-Co4-O4	81.07(10)
O2-Co2-O3	82.09(10)	O4R-Co4-O4	100.51(10)
O4-Co2-O3	83.20(10)	O3-Co4-O6M	89.41(11)
O1R-Co2-O3	91.29(10)	O1-Co4-O6M	168.01(10)
O7M-Co2-O3	174.68(13)	O4R-Co4-O6M	92.95(11)
O2M-Co2-O3	85.95(11)	O4-Co4-O6M	90.42(11)
O3-Co3-O4M	168.36(11)	O3-Co4-N4R	113.80(10)
O3-Co3-O2R	91.46(11)	O1-Co4-N4R	98.34(11)
O4M-Co3-O2R	98.27(11)	O4R-Co4-N4R	61.38(11)
O3-Co3-O1	80.80(11)	O4-Co4-N4R	161.78(11)
O4M-Co3-O1	88.59(11)	O6M-Co4-N4R	92.38(11)
O2R-Co3-O1	168.48(10)	Co4-O1-Co1	99.04(10)
O3-Co3-O2	82.71(11)	Co4-O1-Co3	97.09(10)
O4M-Co3-O2	91.09(11)	Co1-O1-Co3	95.79(10)
O2R-Co3-O2	88.82(10)	Co1-O2-Co2	100.20(10)
O1-Co3-O2	81.78(10)	Co1-O2-Co3	97.26(10)
O3-Co3-O1M	97.48(11)	Co2-O2-Co3	96.44(10)
O4M-Co3-O1M	89.13(12)	Co3-O3-Co4	100.16(11)
O2R-Co3-O1M	88.75(11)	Co3-O3-Co2	97.44(11)
O1-Co3-O1M	100.65(10)	Co4-O3-Co2	95.78(11)
O2-Co3-O1M	177.56(10)	Co2-O4-Co1	98.39(10)
O3-Co4-O1	81.38(10)	Co2-O4-Co4	94.69(10)
O3-Co4-O4R	174.69(10)	Co1-O4-Co4	98.54(10)

2.3.2. Magnetochemistry of 7

The magnetic behaviour of 7 was studied in the temperature range 300-1.8 K in an applied field of 1000 G. The variation of $\chi_m T$ with temperature is shown in Figure 2.12. The value of $\chi_m T$ at 300 K is approximately 12 emu K mol^{-1} which is consistent with four non-interacting S = 3/2 centres [$\chi_m T$ = 10.8 emu k mol^{-1}, g = 2.4]. The value then drops steadily with temperature to a minimum of 3 emu K mol^{-1} at 1.8 K, corresponding to an approximately S = 2 ground state. This represents antiferromagnetic exchange between the Co(II) centres. This type of behaviour is unsurprising given that each cobalt is high spin d^7 and therefore both the t_{2g} and e_g orbitals will be involved in the magnetic interaction, unlike the nickel cubanes which contain d^8 metal centres and therefore have full t_{2g} orbitals. Magnetic studies of other cobalt cubanes have given similar results [57, 58, 61].

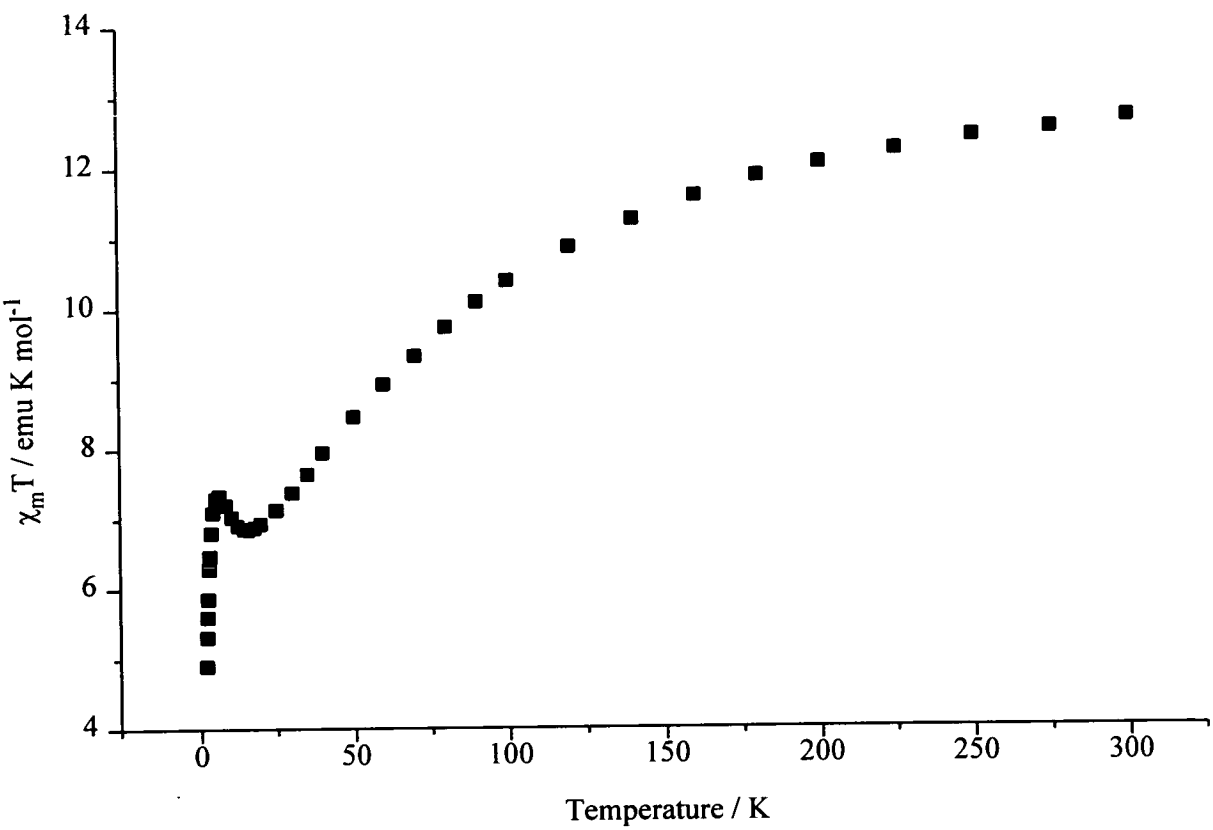

Figure 2.12. The variation of $\chi_m T$ with temperature for 7.

2.3.3. Synthesis and structure of $[Co_{12}(chp)_{18}(OH)_4(\mu_2\text{-}Cl)_2(Hchp)_2(MeOH)_2]$ 8.

Reaction of cobalt chloride with a two fold equivalent of Na(chp) in methanol for three hours at 290 K, followed by evaporation to dryness leads to a paste which may contain **7** amongst other cobalt species. Extended drying *in vacuo* in an attempt to remove any methanol still present, followed by crystallisation from dichloromethane gives purple crystals of $[Co_{12}(chp)_{18}(OH)_4(\mu\text{-}Cl)_2(Hchp)_2(MeOH)_2]$ **8** [Figure 2.13] in 20% yield [71].

8 is a centrosymmetric dodecanuclear species which contains two $[Co_4O_3Cl]^+$ cubes linked by a central eight-membered ring involving four cobalt atoms and four μ-oxygen atoms derived from chp ligands. Co5 and Co5A are each part of a cube and of the eight-membered ring, with Co6 and Co6A the other cobalt atoms within the eight-membered metallocycle. The other three cobalt atoms in the cube are Co2, Co3 and Co4, and both Co2 and Co4 share

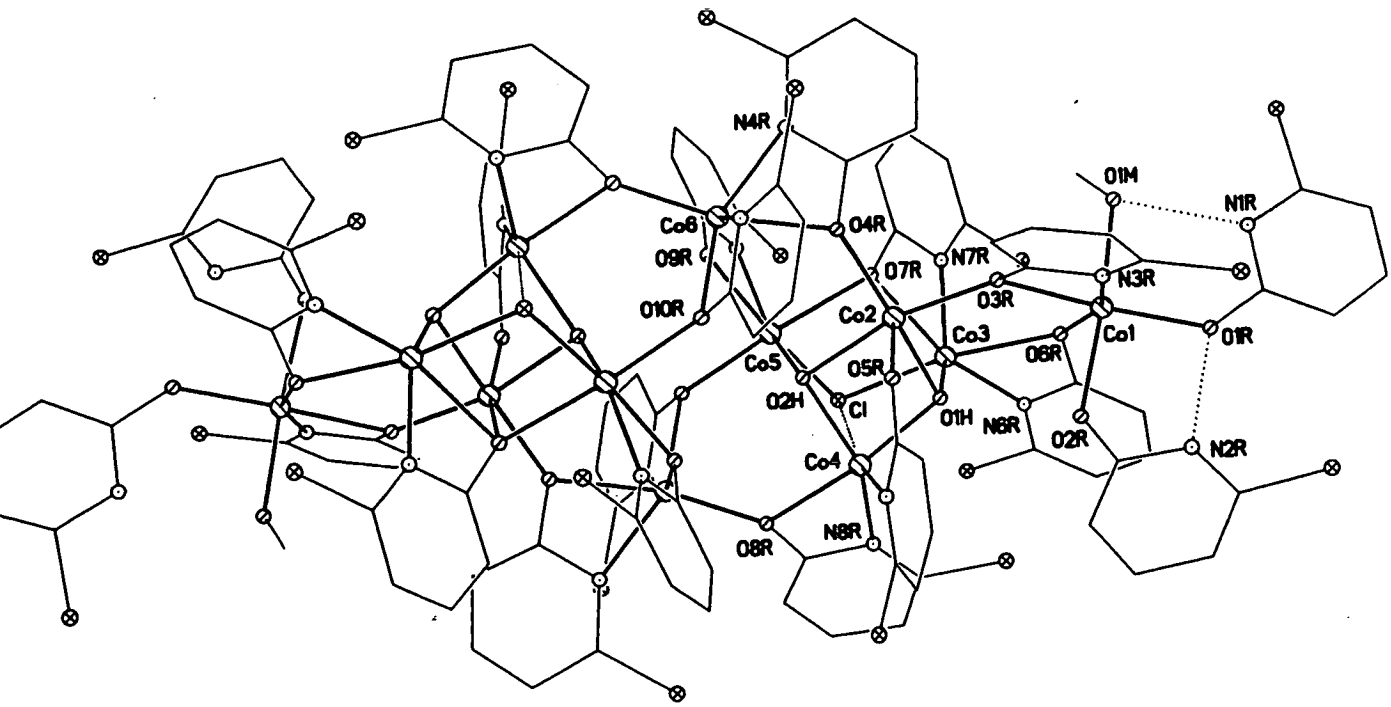

Figure 2.13. The crystal structure of **8**.

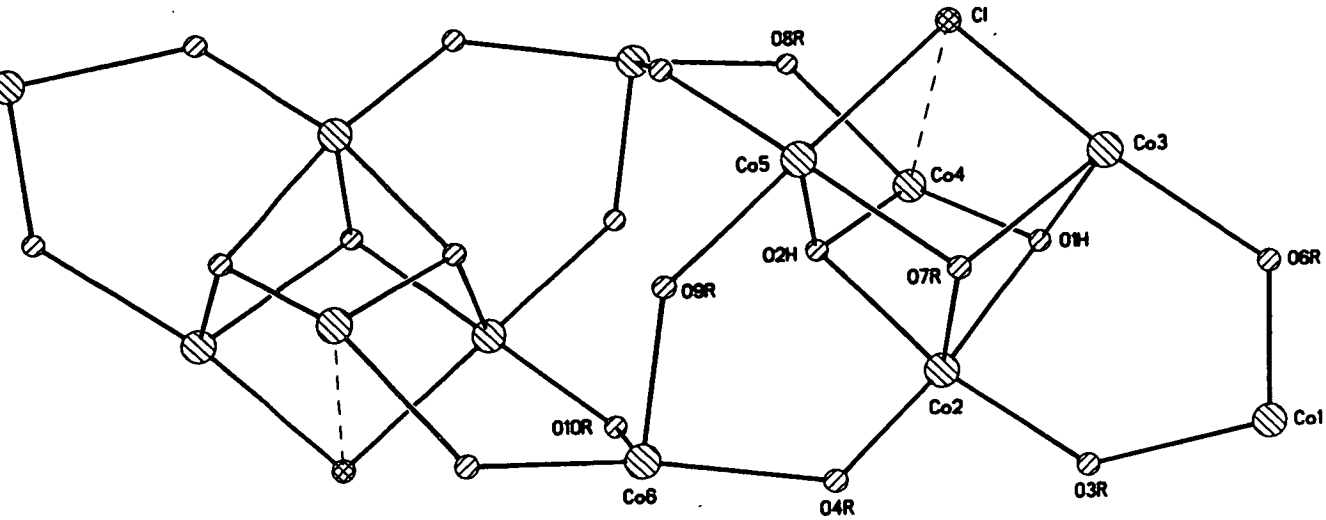

Figure 2.14. The metal polyhedron of **8**.

μ-oxygen atoms with Co6 or Co6A. The non-metal vertices of the cubes are a μ_3-oxygen atom from a chp, two μ_3-hydroxides and a chlorine. The cubes are not ideal as the chlorine group only bridges Co3 and Co5, with a long contact [3.224(11) Å] to Co4. The metal polyhedron is shown in Figure 2.14.

Co4 is the only metal in **8** which is not formally six-coordinate; the vacant site is blocked by the distant chloride group.The shortest Co...Co distance is 2.970(10) Å between Co2 and Co5. The final unique cobalt site [Co1] is at the periphery of the molecule, attached to the cube by two μ-oxygen atoms shared with Co2 and Co3. This bridging is identical to that between Co6 and the cube. The coordination of Co1 is completed by the only residual methanol, which suggests that synthesis of a larger oligomer involving cubes should be possible if total desolvation could be achieved. The chp ligands show four different binding modes. Mononucleating, through their exocyclic oxygen atom only [for example O1R-Co1].

Binucleating, binding to one cobalt [Co4] through the ring nitrogen and to a different cobalt [Co2] through the exocyclic oxygen. Chelating, binding to one cobalt through the ring nitrogen and exocyclic oxygen [N4R, O4R-Co6] with the oxygen atom also bridging to another cobalt [Co2], thus being a μ_2-oxygen. Trinucleating, chelating to one cobalt [Co3] with the oxygen bridging to a further two cobalts [Co2 and Co5], thus being a μ_3-oxygen.

The wide range of bonding modes is reflected in the bond lengths and angles in **8**. The Co...O(chp) lengths range between 2.010-2.390(11) Å while the Co...N(chp) bonds all fall between 2.052-2.181(11) Å. All the cobalt atoms have extremely distorted octahedral geometries with *cis* angles ranging from a low of 60.1(4)° [the bite angle of the chp] to a high of 111.0(4)° caused by the presence of the μ_2-bridging chlorides, and *trans* angles that fall as low as 133.3(5)° due to the presence of trinucleating hydroxide ligands [for example N7R-Co3-O1H]. Selected bond lengths and angles are given in Table 2.7.

Table 2.7. Selected bond lengths (Å) and angles (°) for **8**.

Co1-O6R	2.025(10)	Co3-N6R	2.052(11)
Co1-O2R	2.043(11)	Co3-N7R	2.072(11)
Co1-O1M	2.135(12)	Co3-O6R	2.328(11)
Co1-O1R	2.150(11)	Co3-Cl	2.374(11)
Co1-N3R	2.155(12)	Co3-O7R	2.390(11)
Co1-O3R	2.212(12)	Co4-O1H	2.000(11)
Co2-O5R	2.046(11)	Co4-O2H	2.010(11)
Co2-O3R	2.048(11)	Co4-N8R	2.061(11)
Co2-O4R	2.069(11)	Co4-N5R	2.118(11)
Co2-O2H	2.113(11)	Co4-O8R	2.237(11)
Co2-O1H	2.116(11)	Co5-O2H	1.987(10)
Co2-O6R	2.186(10)	Co5-O10RA	2.080(11)
Co3-O1H	2.002(11)	Co5-N9R	2.102(11)

Table 2.7 continued

Co5-O9R	2.216(11)	O4R-Co2-O2H	96.2(4)
Co5-O7R	2.245(11)	O5R-Co2-O1H	93.2(4)
Co5-Cl	2.400(5)	O3R-Co2-O1H	87.8(4)
Co6-O8RA	2.010(11)	O4R-Co2-O1H	167.4(4)
Co6-O9R	2.060(11)	O2H-Co2-O1H	78.6(4)
Co6-N4R	2.140(11)	O5R-Co2-O7R	164.5(4)
Co6-O10R	2.156(11)	O3R-Co2-O7R	102.9(4)
Co6-N10R	2.181(11)	O4R-Co2-O7R	84.5(4)
Co6-O4R	2.215(11)	O2H-Co2-O7R	79.2(4)
O6R-Co1-O2R	105.2(5)	O1H-Co2-O7R	83.3(4)
O6R-Co1-O1M	93.0(4)	O1H-Co3-N6R	105.4(5)
O2R-Co1-O1M	94.6(4)	O1H-Co3-N7R	133.3(4)
O6R-Co1-O1R	85.0(4)	N6R-Co3-N7R	109.2(5)
O2R-Co1-O1R	90.0(4)	O1H-Co3-O6R	82.6(4)
O1M-Co1-O1R	175.4(4)	N6R-Co3-O6R	60.1(4)
O6R-Co1-N3R	157.3(4)	N7R-Co3-O6R	88.2(5)
O2R-Co1-N3R	97.1(5)	O1H-Co3-Cl	94.7(3)
O1M-Co1-N3R	89.8(5)	N6R-Co3-Cl	111.0(3)
O1R-Co1-N3R	90.5(5)	N7R-Co3-Cl	101.2(4)
O6R-Co1-O3R	96.5(5)	O6R-Co3-Cl	169.1(3)
O2R-Co1-O3R	158.0(4)	O1H-Co3-O7R	80.7(4)
O1M-Co1-O3R	87.7(4)	N6R-Co3-O7R	165.7(4)
O1R-Co1-O3R	88.4(4)	N7R-Co3-O7R	59.3(4)
N3R-Co1-O3R	61.0(4)	O6R-Co3-O7R	108.9(4)
O5R-Co2-O3R	92.0(5)	Cl-Co3-O7R	80.9(3)
O5R-Co2-O4R	97.8(4)	O1H-Co4-O2H	83.9(5)
O3R-Co2-O4R	97.8(5)	O1H-Co4-N8R	106.6(5)
O5R-Co2-O2H	85.3(4)	O2H-Co4-N8R	141.2(5)
O3R-Co2-O2H	166.0(4)	O1H-Co4-N5R	99.9(5)

Table 2.7 continued

O2H-Co4-N5R	104.2(4)	N4R-Co6-O10R	148.8(4)
N8R-Co4-N5R	110.3(5)	O8RA-Co6-N10R	101.1(5)
O1H-Co4-O8R	150.8(5)	O9R-Co6-N10R	157.5(5)
O2H-Co4-O8R	91.5(4)	O4R-Co6-N10R	96.5(5)
N8R-Co4-O8R	60.9(4)	O10R-Co6-N10R	61.5(4)
N5R-Co4-O8R	109.2(4)	O8RA-Co6-O4R	168.1(5)
O2H-Co5-O10RA	94.2(4)	O9R-Co6-O4R	92.3(4)
O2H-Co5-N9R	150.1(5)	O4R-Co6-O4R	61.2(4)
O10RA-Co5-N9R	98.5(4)	O10R-Co6-O4R	91.6(4)
O2H-Co5-O9R	92.3(4)	N10R-Co6-O4R	79.9(4)
O10RA-Co5-O9R	88.3(4)	Co3-Cl-Co5	94.4(2)
N9R-Co5-9OR	61.3(4)	Co4-O1H-Co3	118.8(5)
O2H-Co5-O7R	80.5(4)	Co4-OH-Co2	92.4(4)
O10RA-Co5-O7R	174.5(4)	Co3-O1H-Co2	103.5(5)
N9R-Co5-O7R	86.9(4)	Co5-O2H-Co4	117.9(5)
O9R-Co5-O7R	93.3(5)	Co5-O2H-Co2	104.8(5)
O2H-Co5-Cl	95.3(3)	Co4-O2H-Co2	92.2(4)
O10RA-Co5Cl-	95.7(3)	Co2-O3R-Co1	132.3(5)
N9R-Co5-Cl	110.1(4)	Co2-O4R-Co6	128.2(5)
O9R-Co5-Cl	171.1(3)	Co1-O6R-Co3	128.0(5)
O7R-Co5-Cl	83.4(3)	Co2-O7R-Co3	89.8(4)
O8RA-Co6-O9R	90.9(4)	Co5-O7R-Co3	98.1(4)
O8RA-Co6-N4R	106.9(5)	Co6A-O8R-Co4	125.5(5)
O9R-Co6-N4R	98.1(5)	Co6-O9R-Co5	129.0(5)
O8RA-Co6-O10R	99.3(5)	Co5A-O10R-Co6	123.9(5)
O9R-Co6-O10R	98.1(4)		

2.3.4. Magnetochemistry of 8.

The magnetic behaviour of **8** was studied in the 300-1.8 K temperature range in an applied field of 1000 G. The variation of the product $\chi_m T$ with temperature is shown in Figure 2.15. The value of $\chi_m T$ at 300 K is approximately 37 emu K mol^{-1} which is consistent with twelve non-interacting S = 3/2 centres [$\chi_m T$ = 35.2 emu K mol^{-1}, g = 2.5]. The value of $\chi_m T$ then drops steadily with temperature to a minimum of 7.5 emu K mol^{-1} at 2 K. This value corresponds to an approximately S = 3 state. This is an example of antiferromagnetic coupling between the Co(II) centres.

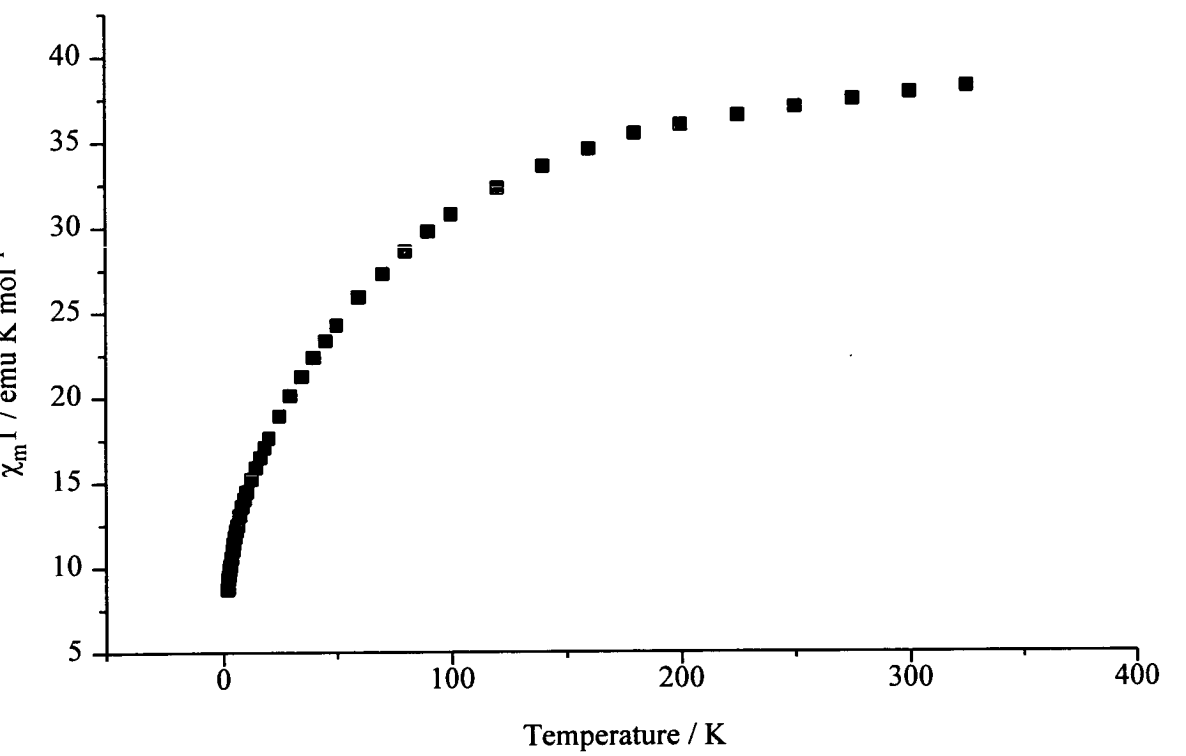

Figure 2.15. The variation of $\chi_m T$ with temperature for **8.**

2.3.5. Synthesis and structure of $[Co_{10}(OH)_4(chp)_{16}(MeCN)_2]$ 9.

Reaction of cobalt chloride with two equivalents of Na(chp) in ethyl acetate for a minimum of 24 hours, followed by evaporation to dryness leads to a paste which can be crystallised from acetonitrile to give $[Co_{10}(OH)_4(chp)_{16}(MeCN)_2]$ **9** [Figure 2.16] after three days.

The structure of **9** is closely related to that of **8**. **9** is a centrosymmetric structure which contains two "cubes" linked by a central eight-membered ring containing four cobalt and four μ_2-oxygen atoms derived from chp ligands. Co2 and Co2A are each part of a cube and of the eight-membered ring, with Co5 and Co5A the other cobalt atoms in the ring. The cubes are best described as $[Co_3O_4]^{2-}$ units with the oxygen vertices of the cube derived from two μ_3-hydroxides,and two μ_2-oxygens from chp ligands. The 'missing' cobalt vertex [Co1, Co1A]

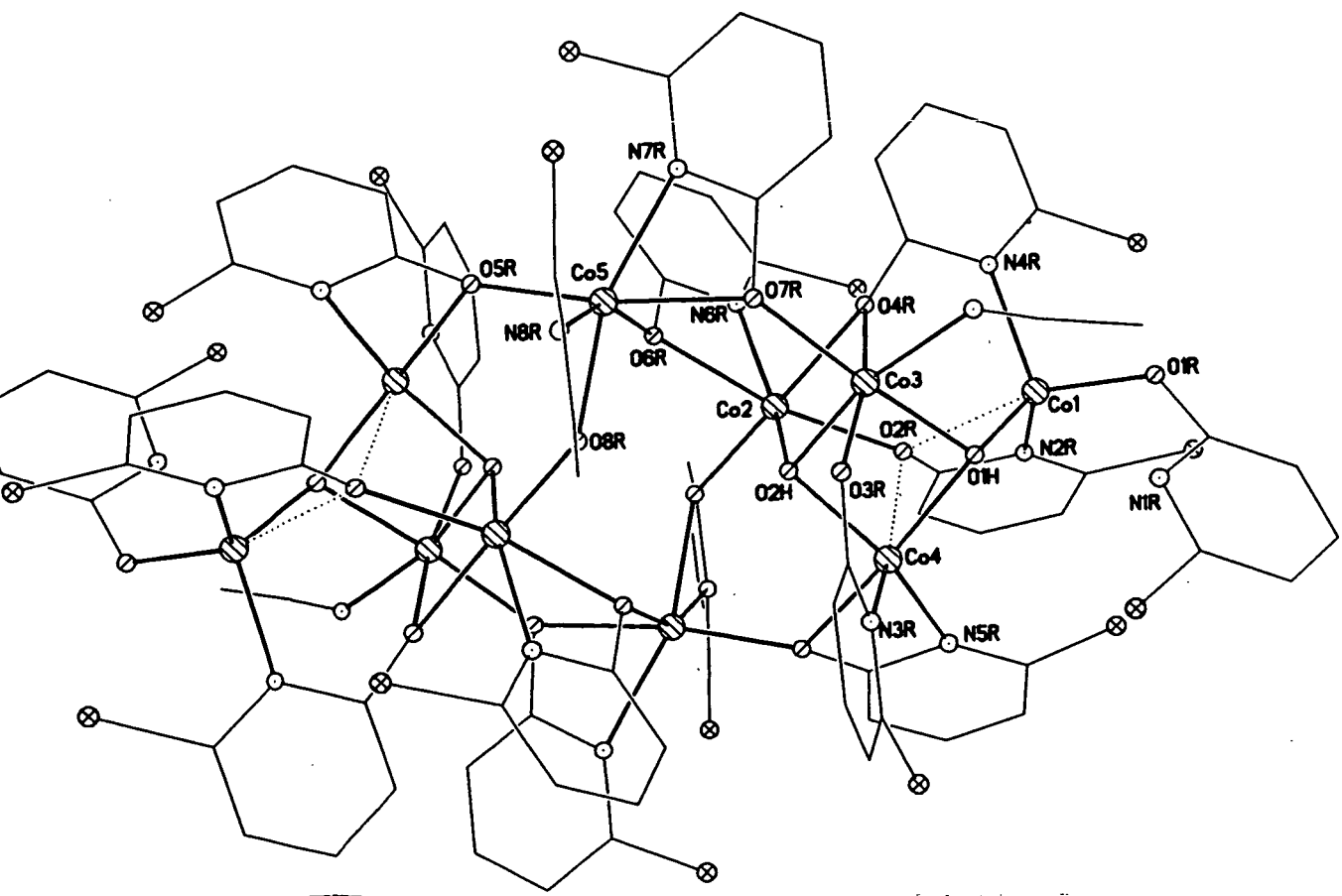

Figure 2.16. The crystal structure of **9**.

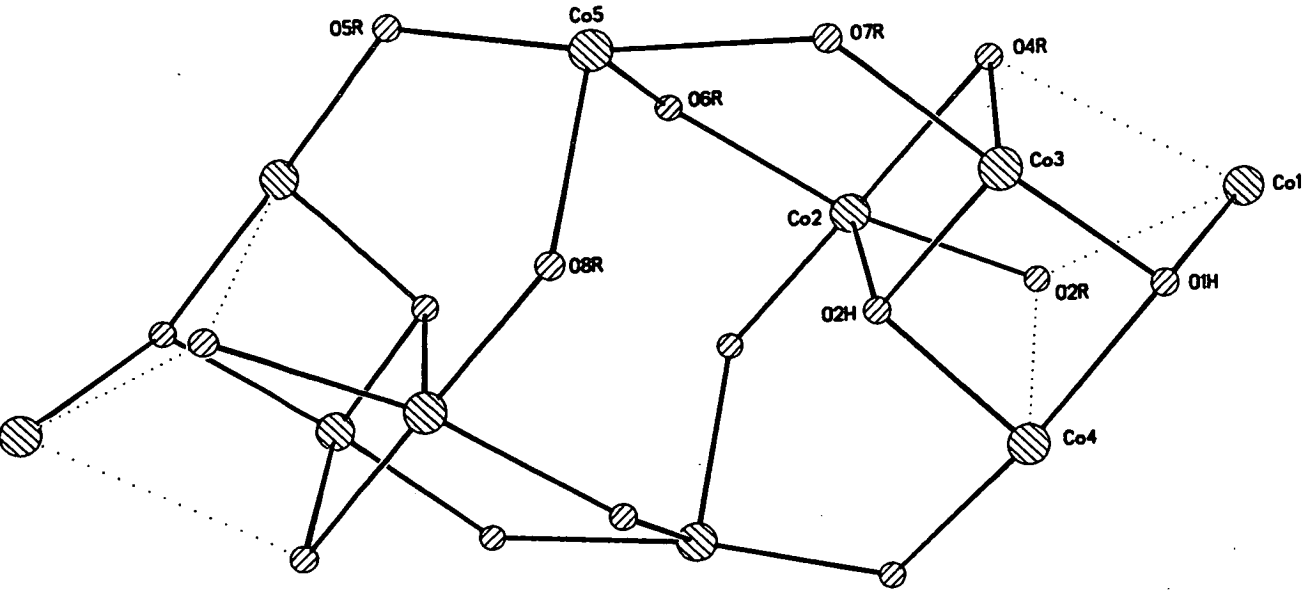

Figure 2.17. The metal polyhedron in 9.

has been displaced from the regular corner of the 'cube' and is attached to the 'cube' *via* one μ_3-hydroxide and the trinucleating chp ligands which provide three of the oxygen vertices of the cube. Co1 and Co1A are four coordinate with their geometries completed by a mono-nucleating chp ligand. All other cobalts are six coordinate and have distorted octahedral geometries. Co4 is formally five coordinate but has a longer contact to a chp-derived oxygen atom [Co4...O2R, 2.890(3) Å].The metal polyhedron is shown in Figure 2.17. The closest Co...Co contact is 2.943(3) Å between Co 3 and Co 4. Selected bond lengths and angles are given in Table 2.8.

Again the chp ligands demonstrate a variety of coordinating modes. Mononucleating, attached to the metal centre through the exocyclic oxygen atom alone [for example to Co1]. Binucleating, bound to one cobalt [Co4] through the ring nitrogen and to another [Co3] through the exocyclic oxygen atom. Chelating to one cobalt [Co5] with the oxygen atom bridging to a second metal centre [Co3]. Trinucleating, bound to one cobalt [Co1] through the

ring nitrogen with the oxygen atom bridging between two different cobalt centres [Co2, Co3].

Again the variety of bonding modes is reflected in the range of bond lengths and angles in **9**, with the Co.-O(chp) bond lengths ranging between 1.907-2.318(3) Å and the Co-N(chp) bonds ranging between 2.078-2.368(3) Å. The crystal quality of **9** was poor and has resulted in the collection of a poor crystallographic data set and an unsatisfactory final structure solution. Therefore the quoted bond lengths and angles are somewhat dubious. However the connectivity is clearly established. Better quality crystals are currently being synthesised.

2.3.6. Magnetochemistry of 9.

The magnetic behaviour of **9** was studied in the temperature range 300 - 1.8 K in an applied field of 1000 G. The variation of $\chi_m T$ with temperature is shown in Figure 2.18. The room temperature value of approximately 26 emu K mol^{-1} is consistent with ten non-interacting S = 3/2 Co(II) centres [$\chi_m T$ = 27 emu K mol^{-1}, g = 2.4]. The value of $\chi_m T$ then drops steadily with temperature giving a minimum of approximately 2.0 emu K mol^{-1} at 1.8 K, indicating strong antiferromagnetic coupling between the metal centres with an S = 1 ground state.

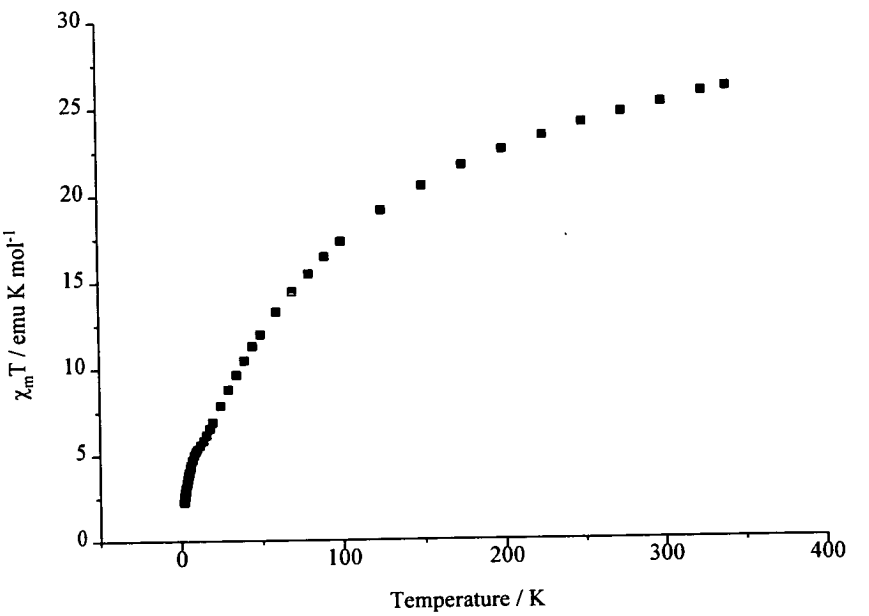

Figure 2.18. The variation of $\chi_m T$ with temperature for **9**.

Table 2.8. Selected bond lengths (Å) and angles (°) for **9**.

Co1-O1H	2.142(12)	O1H-Co1-N4R	115.8(4)
Co1-O1R	1.907(12)	O1R-Co1-N2R	116.8(5)
Co1-N2R	2.102(11)	O1R-Co1-N4R	105.9(4)
Co1-O4R	2.143(11)	N2R-Co1-N4R	102.1(4)
Co2-O2H	2.036(11)	O2H-Co2-O2R	89.0(4)
Co2-O2R	2.173(11)	O2H-Co2-O4R	80.3(4)
Co2-O4R	2.326(11)	O2H-Co2-N6R	152.4(4)
Co2-N6R	2.099(11)	O2H-Co2O6R	94.6(4)
Co2-O6R	2.223(11)	O2H-Co2-O8RA	94.0(4)
Co2-O8RA	2.005(11)	O2R-Co2-O4R	80.7(4)
Co3-O1H	2.113(11)	O2R-Co2-N6R	111.8(4)
Co3-O2H	2.093(11)	O2R-Co2-O6R	169.4(5)
Co3-N1A1	2.092(12)	O2R-Co2-O8RA	102.75(15)
Co3-O3R	2.131(12)	O4R-Co2-N6R	85.3(4)
Co3-O4R	2.193(12)	O4R-Co2-O6R	90.0(4)
Co3-O7R	2.062(12)	O4R-Co2-O8RA	173.3(4)
Co4-O1H	2.038(13)	N6R-Co2-O6R	61.9(4)
Co4-O2H	1.984(12)	N6R-Co2-O8RA	98.6(4)
Co4-N3R	2.315(12)	O6R-Co2-O8RA	87.1(4)
Co4-N5R	2.078(12)	O1H-Co3-O2H	81.2(5)
Co4-O5RA	2.260(12)	O1H-Co3-N1A1	84.7(5)
Co5-O5R	2.087(12)	O1H-Co3-O3R	96.6(5)
Co5-O6R	2.145(12)	O1H-Co3-O4R	87.1(5)
Co5-N7R	2.225(12)	O1H-Co3-O7R	169.8(4)
Co5-O7R	2.318(12)	O2H-Co3-N1A1	165.7(4)
Co5-N8R	2.368(12)	O2H-Co3-O3R	88.8(4)
Co5-O8R	2.213(11)	O2H-Co3-O4R	82.3(4)
O1H-Co1-O1R	98.4(11)	O2H-Co3-O7R	96.0(4)
O1H-Co1-N2R	117.9(10)	N1A1-Co3-O3R	90.8(4)

Table 2.8 continued

N1A1-Co3-O4R	99.1(5)	O6R-Co5-O7R	92.6(5)
N1A1-Co3-O7R	98.2(5)	O6R-Co5-N8R	155.5(4)
O3R-Co3-O4R	169.7(5)	O6R-Co5-O8R	99.2(4)
O3R-Co3-O7R	93.2(5)	N7R-Co5-O7R	61.5(5)
O1H-Co4-O2H	85.7(5)	N7R-Co5-N8R	101.4(5)
O1H-Co4-N3R	99.8(5)	N7R-Co5-O8R	148.9(5)
O1H-Co4-N5R	109.7(5)	O7R-Co5-N8R	81.8(5)
O1H-Co4-O5RA	157.4(5)	O7R-Co5-O8R	91.1(5)
O2H-Co4-N3R	98.5(5)	N8R-Co5-O8R	57.4(5)
O2H-Co4-N5R	140.3(5)	Co1-O1H-Co3	115.0(5)
O2H-Co4-O5RA	90.7(4)	Co1-O1H-Co4	119.1(5)
N3R-Co4-N5R	113.6(5)	Co3-O1H-Co4	90.3(5)
N3R-Co4-O5RA	102.8(5)	Co2-O4R-Co3	92.6(5)
N5R-Co4-O5RA	60.8(5)	Co2-O2HCo3	104.7(5)
O5R-Co5-O6R	93.0(5)	Co2-O2H-Co4	114.5(5)
O5R-Co5-N7R	110.2(5)	Co3-O2H-Co4	92.4(5)
O5R-Co5-O7R	170.5(5)	Co4-O5RA-Co5A	125.8(5)
O5R-Co5-N8R	96.1(5)	Co2-O8RA-Co5A	126.9(5)
O5R-Co5-O8R	95.5(5)	Co3-O7R-Co5	130.1(5)
O6R-Co5-N7R	96.7(5)	Co3-O6R-Co5	128.0(5)

2.3.7. Synthesis and structure of $[Co_2Na_2(chp)_6(H_2O)]_n$ 10 and $[Co_2Na_2(chp)_6]_n$ 11.

Anhydrous cobalt chloride was stirred in methanol with a two fold equivalent of Na(chp) for 24 hours. The paste produced from the removal of the solvent was dried *in vacuo* and crystallised from acetonitrile to give the heterobimetallic polymer $[Co_2Na_2(chp)_6(H_2O)]$ **10** after 24 hours[66]. **10** [Figure 2.19] is isostructural with the nickel polymer **5**. The metal-ligand bonds in **10** are slightly longer than in **5**, for example the Co-O bonds average 2.123(3) Å in **10** whereas the Ni-O bonds in **5** average 2.096(3) Å. Other than this there are no significant differences between the two structures.

If the previous reaction is repeated in the presence of sodium formate then the polymer $[Co_2Na_2(chp)_6]_n$ **11** is produced upon crystallisation from ethyl acetate after one week. **11** [Figure 2.20] is obviously closely related to **10**, the only difference being the absence of the water molecule which bridges the two sodium atoms. Thus the sodium atoms are now four coordinate with a longer contact [3.073(4) Å] to a chlorine atom of a chelating chp ligand. The metal atoms in **11** also show more distortion from regular octahedral geometries with the *cis* angles around the cobalt centres in the range 61.5-119.7(2)° compared to 63.4-103.9(2)° and 62.1-104.2(3)° for **5** and **10** respectively. Selected bond lengths and angles for **10** and **11** are given in Tables 2.9 and 2.10. This apart there are no further significant structural differences.

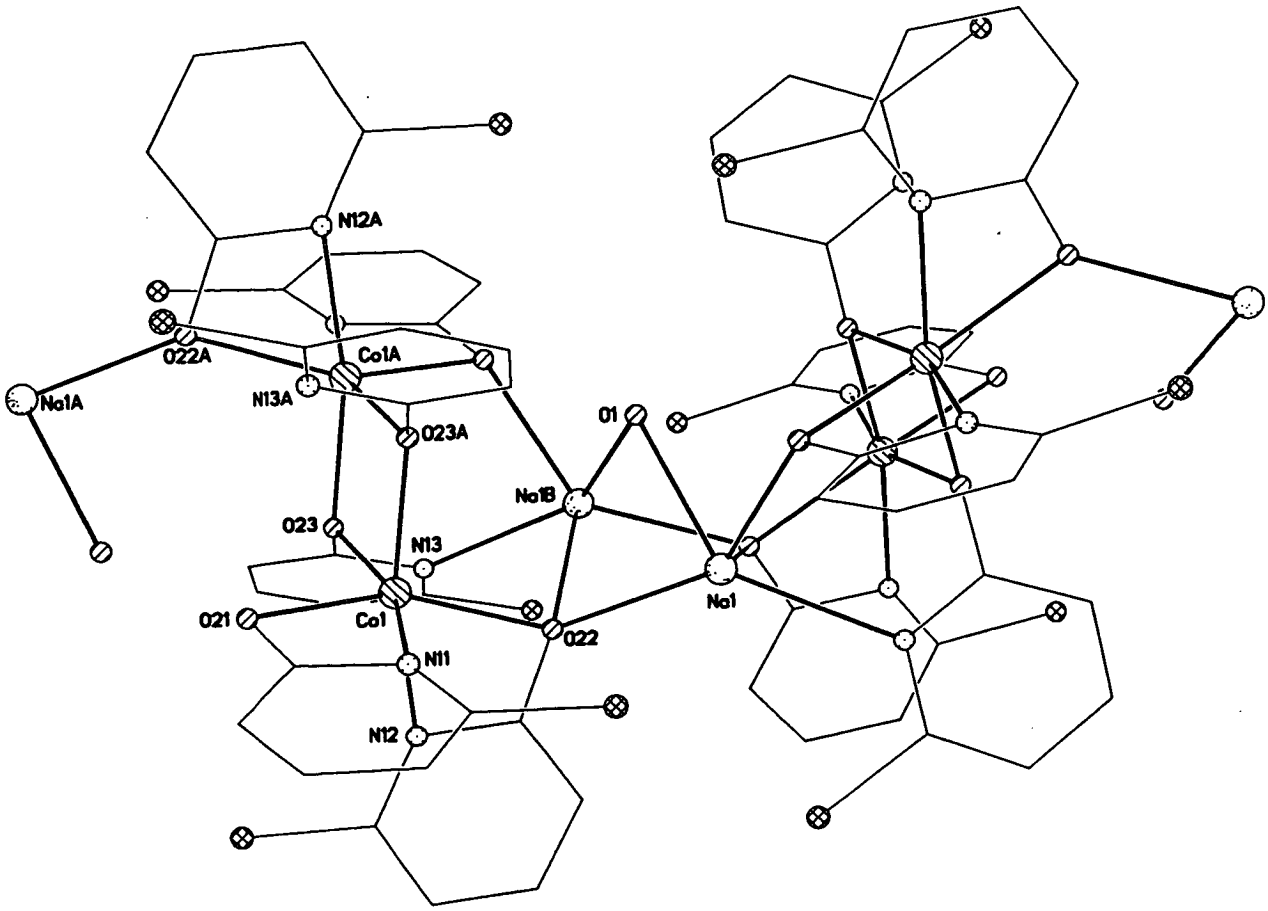

Figure 2.19. The crystal structure of **10.**

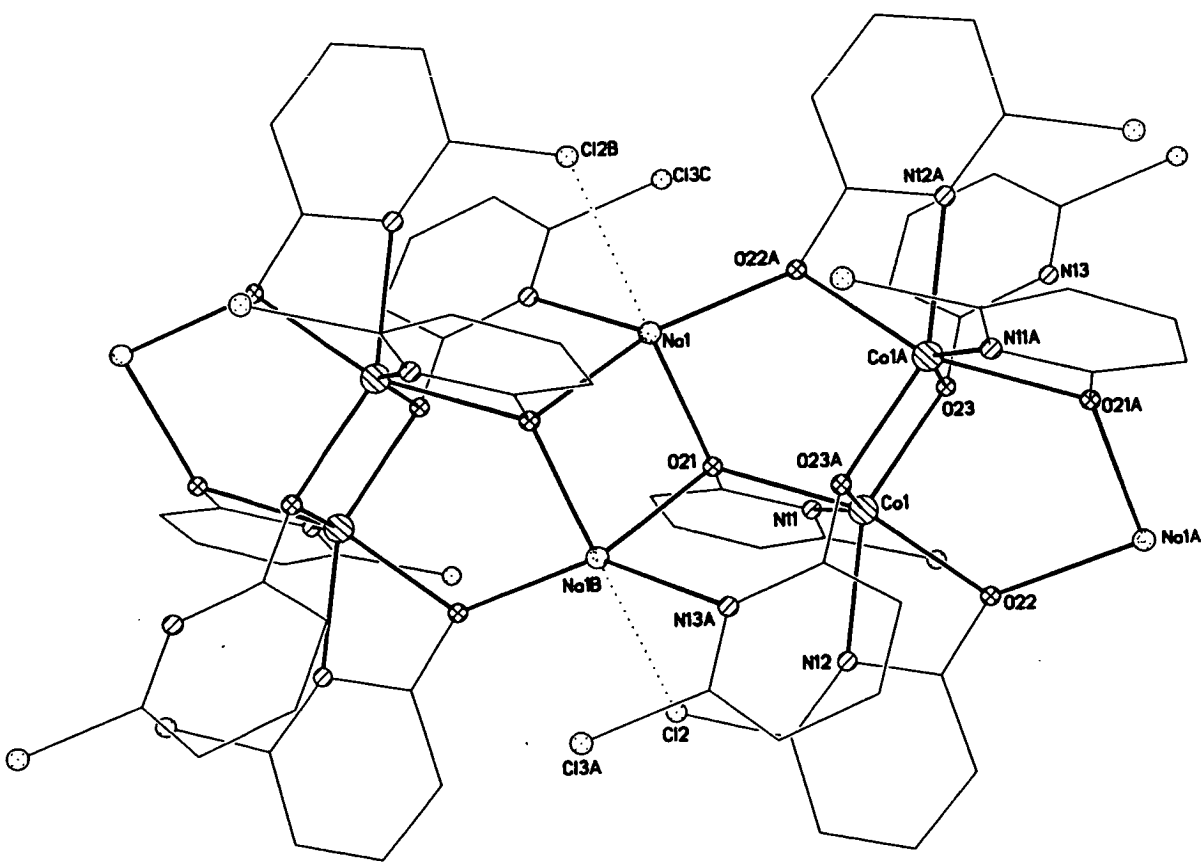

Figure 2.20. The crystal structure of **11.**

2.3.8. Magnetochemistry of 10 and 11.

The magnetic behaviour of both **10** and **11** was studied in the temperature range 300 - 1.8 K in an applied field of 1000 G. The variation of $\chi_m T$ with temperature is shown in Figure 2.21. The behaviour of the two compounds is identical. The room temperature value of $\chi_m T$ = 7 emu K mol^{-1} is consistent with two non-interacting S = 3/2 centres [$\chi_m T$ = 5.4 emu K mol^{-1}, g = 2.4]. The value then increases to a maximum of 12 emu K mol^{-1} at 10 K indicative of ferromagnetic exchange between the Co(II) centres. Below this temperature the value of $\chi_m T$ falls to 10.5 emu K mol^{-1} at 1.8 K. The 10 K value corresponds to an approximately S = 3 state.

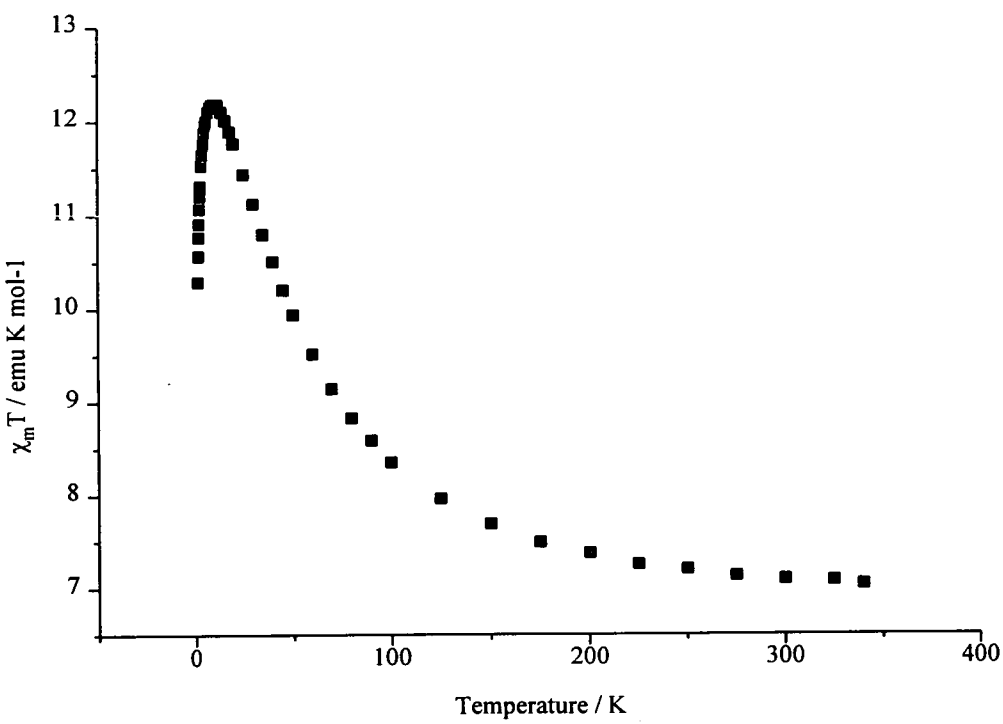

Figure 2.21. The variation of $\chi_m T$ with temperature for **10** and **11**.

There are two previously known cobalt-sodium pyridonate complexes: one polymer $[Co_2Na_2(mhp)_6(Hmhp)(H_2O)]_n$ [66] **12** and a metallocrown $[Na\{Co(mhp)_2\}_6][OAc]$ **13** [53]. The structure of **12** [Figure 2.22] is related to the nickel and cobalt polymers **5**, **10** and **11.** The cobalt sites on **12** are coordinated to two chelating mhp ligands, and two μ_2-oxygen atoms which bridge to a symmetry equivalent cobalt site. Thus $[Co_2(mhp)_6]^{2-}$ can be recognised as a structural feature similar to $[M_2(chp)_6]^{2-}$ in **5**, **10** and **11**. The sodium unit in **12** is different in that each five coordinate sodium site is bound to two μ_2-oxygen donors from mhp ligands chelating to cobalt, the nitrogen donor of an mhp ligand which provides the the oxygen atom which bridges between cobalt centres , a μ_2-oxygen from water and finally a μ_2-oxygen from an Hmhp ligand. This final ligand represents the main difference between **12** and **5**, **10** and **11** with $[Na_2(H_2O)(Hmhp)]^{2+}$ units each bound by two chelating "complex ligands" of formula $[Co_2(mhp)_6]^{2-}$.

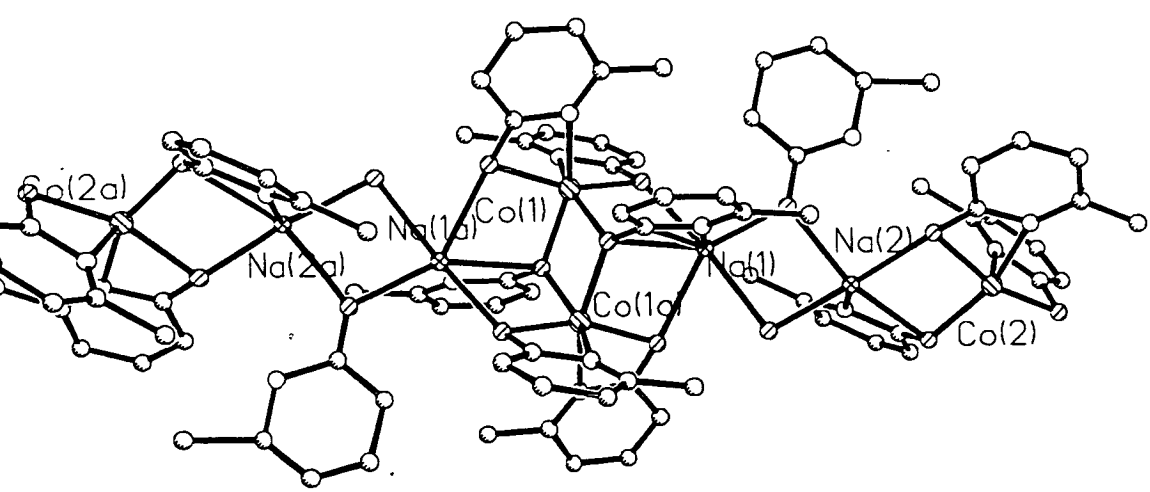

Figure 2.22. The crystal structure of **12**.

Table 2.9 .Selected bond lengths (Å) and angles (°) for **10**.

Co1-O23	2.057(7)	O21-Co1-N11	62.1(3)
Co1-O23A	2.084(7)	O23-Co1-N11	101.7(3)
Co1-N12	2.119(8)	O23A-Co1-O22	104.2(3)
Co1-O21	2.152(7)	N12-Co1-O22	62.2(3)
Co1-N11	2.180(8)	O21-Co1-O22	155.1(3)
Co1-O22	2.197(6)	N11-Co1-O22	97.1(3)
Na1-O22	2.371()	O22-Na1-O1	79.4(2)
Na1-O1	2.372(7)	O22-Na1-O21C	137.6(3)
Na1-O21C	2.377(7)	O1-Na1-O21C	72.4(2)
Na1-O2B	2.439(8)	O22-Na1-O22B	86.0(3)
Na1-N13B	2.513(8)	O1-Na1-O22B	78.0(2)
Na1B-Na1	3.157(8)	O21C-Na1-O22B	117.2(3)
O23-Co1-O23A	79.9(3)	O22-Na1-N13B	136.7(3)
O23-Co1-N12	96.4(3)	O1-Na1-N13B	139.8(2)
O23A-Co1-N12	165.1(3)	O21C-Na1-N13B	82.7(3)
O23-Co1-O21	98.9(3)	O22B-Na1-N13B	86.4(3)
O23A-Co1-O21	93.1(3)	Co1-O22-Na1	128.5(3)
N12-Co1-O21	101.7(3)	Co1-O22-Na1B	102.3(3)
O23-Co1-O21	160.9(3)	Na1-O22-Na1B	82.0(2)
O23A-Co1-N11	98.3(3)	Co1-O23-Co1A	100.1(3)
N12-Co1-N11	89.8(3)		

Table 2.10. Selected bond lengths (Å) and angles (°) for **11**.

Co1-O23	2.045(4)	Co1-O21	2.195(4)
Co1-O23A	2.083(4)	Na1-O22A	2.289(4)
Co1-N11	2.131(4)	Na1-O21	2.327(4)
Co1-N12	2.152(4)	Na1-O21B	2.409(4)
Co1-O22	2.168(4)	Na1-N13C	2.539(4)

Table 2.10 continued

Na1-Cl2B	3.073(3)	N11-Co1-O21	61.5(2)
Na1-Cl3C	3.298(3)	N12-Co1-O21	100.5(2)
O23-Co1-O23A	83.4(2)	O22-Co1-O21	161.36(14)
O23-Co1-N11	104.1(2)	O22A-Na1-O21	99.1(2)
O23A-Co1-N11	150.1(2)	O22A-Na1-O21B	119.2(2)
O23-Co1-N12	152.1(2)	O21-Na1-O21B	95.37(14)
O23A-Co1-N12	98.7(2)	O22A-Na1-N13C	140.6(2)
N11-Co1-N12	88.0(2)	O21-Na1-N13C	96.6(2)
O23-Co1-O22	90.6(2)	O21B-Na1-N13C	94.8(2)
O23A-Co1-O22	88.7(2)	Co1-O21-Na1	117.9(2)
N11-Co1-O22	119.7(2)	Co1-O21-Na1B	109.6(2)
N12-Co1-O22	61.7(2)	Na1-O21-Na1B	84.63(14)
O23-Co1-O21	107.4(2)	Co1-O22-Na1A	125.7(2)
O23A-Co1-O21	88.52(14)	Co1-O23-Co1A	96.6(2)

2.3.9. Synthesis and structure of $[Co_{24}(\mu_3\text{-}OH)_{14}(\mu_2\text{-}OH)(\mu_3\text{-}OMe)_2(\mu_3\text{-}Cl)_2(Cl)_4(mhp)_{22}]$ 14.

Reaction of cobalt (II) chloride with Na(mhp) in methanol for 24 hours at 290 K, followed by evaporation to dryness gave an uncharacterised dark blue paste. Dissolution of this paste in ethyl acetate, followed by filtration, gave dark blue crystals of $[Co_{24}(\mu_3\text{-}OH)_{14}(\mu_2\text{-}OH)_4(\mu_3\text{-}OMe)_2(\mu_3\text{-}Cl)_2(Cl)_4(mhp)_{22}]$ **14** [Figure 2.23] in 20% yield after four days [73].

14, the highest nuclearity complex containing cobalt, has a centrosymmetric structure related to many minerals and to an $[Fe_{17}][Fe_{19}]$ compound reported by Powell and coworkers [36, 37]. It consists of cubic-close packed planes of hydroxide, methoxide or chloride anions bridging cobalt (II) centres. The structure is based on $[Co_3(OH)_4]^{2+}$ cubes with one corner missing, and in some cases with one of the hydroxide vertices occupied by methoxide or chloride groups. The array is therefore held together by OH bridges.

Of the twelve crystallographically independent cobalt sites, five [Co1, Co2, Co3, Co4 and Co5] have a coordination geometry close to a regular octahedron. There are no chelating ligands attached to these metal sites. Three further sites [Co6, Co7 and Co8] have one chelating ligand and four monodentate ligands attached and have more distorted octahedral geometries. Co12 also has one chelating ligand and three further contacts and is probably best described as being based on a distorted tetrahedral geometry [four bonds between 1.971(5) and 2.265(3) Å] with one much longer contact [2.884(5) Å].

The final three distinct sites [Co9, Co10 and Co11] each have two chelating mhp ligands attached, with in each case the bond to the oxygen-donor much longer than the bond to the nitrogen-donor of the group. Two further monodentate ligands lead to a coordination geometry best described as involving four short contacts in a distorted tetrahedral array

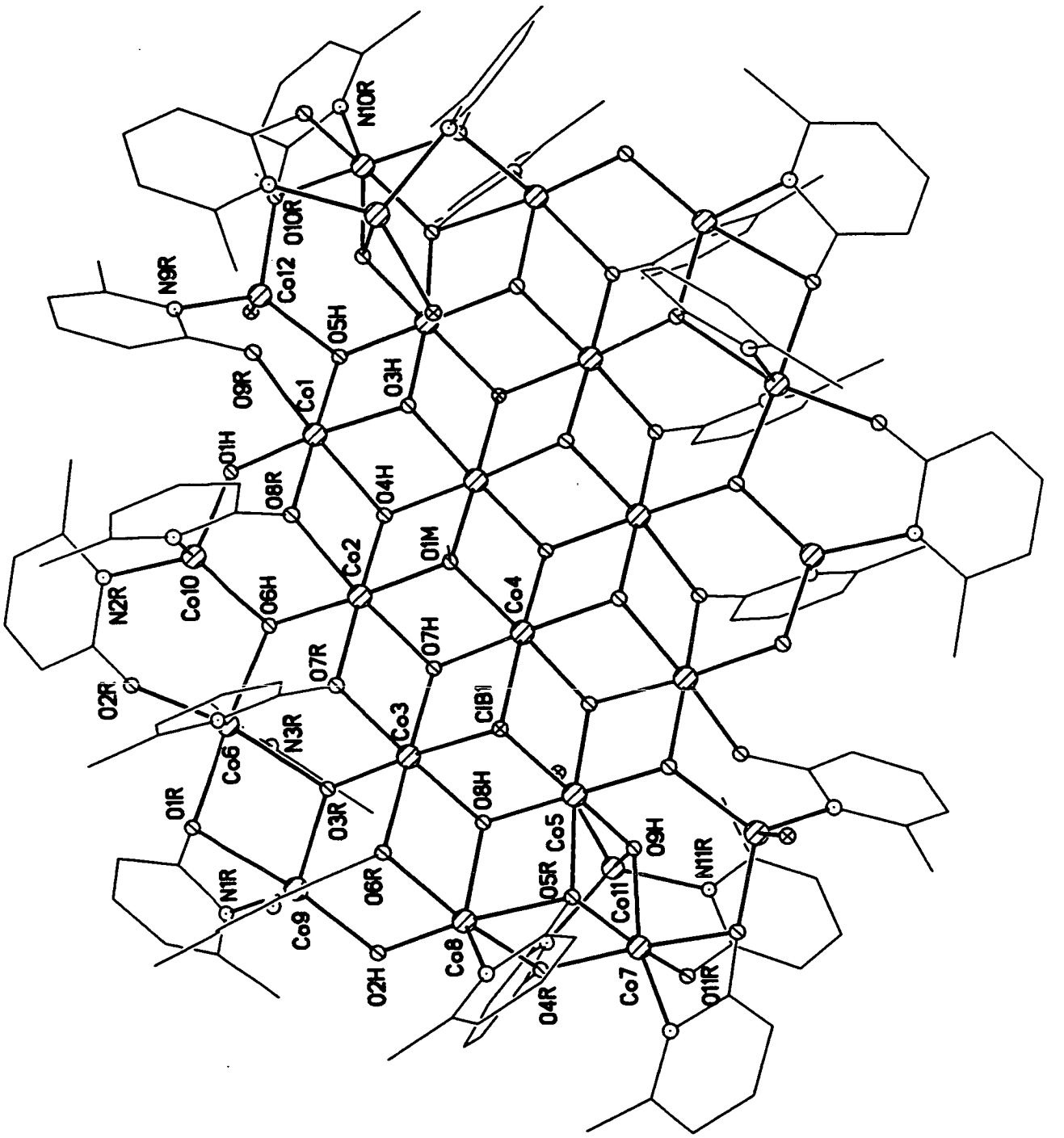

Figure 2.23. The structure of **14** in the crystal.

[1.971-2.282(5) Å] and two longer contacts [2.310-3.022(5) Å]. The shortest Co...Co contact observed in **14** is 3.014(3) Å between Co7 and Co11.

The exterior of the molecule is covered by twenty two pyridonate ligands. These adopt three distinct bonding modes: binucleating, binding to different cobalt atoms through the ring nitrogen and exocyclic oxygen atom [Co6 and Co10]; chelating to one cobalt atom [Co9] and then bridging to a second cobalt atom [Co6] through the oxygen atom. Trinucleating, binding to one cobalt [Co6] through the ring nitrogen only and bridging two further cobalt centres [Co2 and Co3] through the oxygen.

The metal polyhedron is shown in Figure 2.24. The structure can be related to the AX_2 structural type found in CdI_2 or $Mg(OH)_2$. The $[Co_3(OH)_4]^{2+}$ units at the centre of the structure can be regarded as regular cubes with the Co-O-Co angles ranging from 95.3-102.6(2)° whereas with the $[Co_3(OH)_4]^{2+}$ units toward the periphery of the molecule the corner angles of the cubes deviate out to values as large as 118.6(2)°. The corners of the cubes involving chloride are "squashed", falling in the range 77.65-80.24(10)°. Selected bond lengths and angles are given in Table 2.11.

The source of hydroxide in **14** is presumably the ethyl acetate solvent. Ethyl acetate can contain up to 3% by weight of dissolved water . In this synthesis the water content is around 0.1%. Studies which involve varying the amount of water in the solvent are currently underway. Using a solvent with a known propensity for absorbing atmospheric moisture has already been successfully employed to produce large polymetallic complexes [74] and perhaps demonstrates an alternative procedure to arresting the formation of a metal hydroxide in aqueous solution through the use of pH [36, 37].

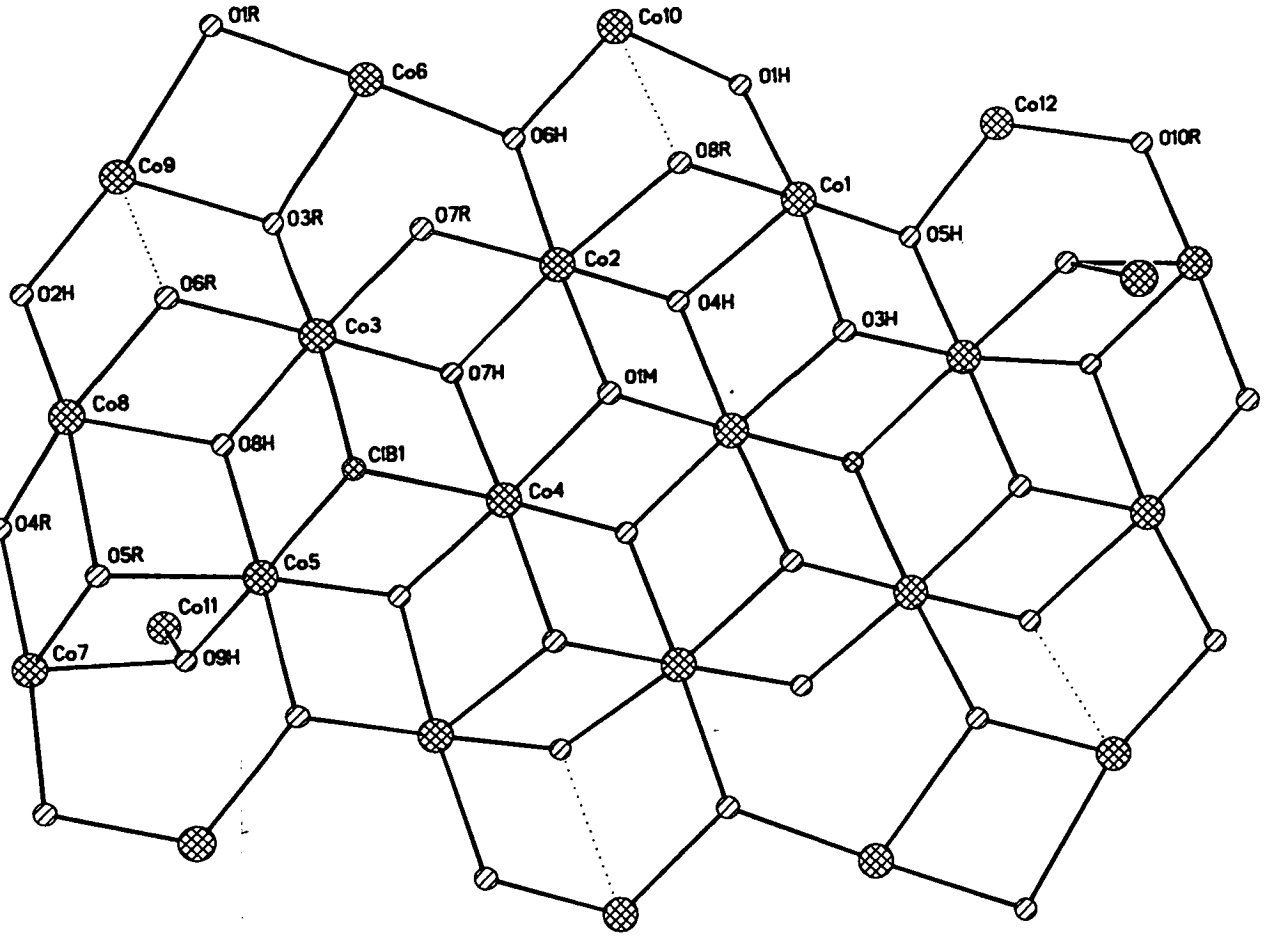

Figure 2.24. The metal polyhedron of **14**.

2.3.10.Magnetochemistry of 14.

The magnetic behaviour of **14** was studied in the 300-1.8 K temperature range in an applied field of 1000 G. The variation of $\chi_m T$ with temperature is shown in Figure 2.25. At room temperature the value of the product $\chi_m T$ is around 63 emu K mol^{-1}. This value corresponds to that for twenty four non-interacting S = 3/2 centres, which would lead to a calculated value of 64.8 emu K mol^{-1} [assuming g = 2.4]. The value of $\chi_m T$ then declines steadily with temperature until 30 K where it increases sharply to a value of 62 emu K mol^{-1} at 8 K. Below this temperature the value falls again, possibly due to intermolecular interactions or zero-field splitting within the ground state. If the 8 K value is due to a non-degenerate spin state it can be estimated that this is approximately an S = 9 state, though further experiments

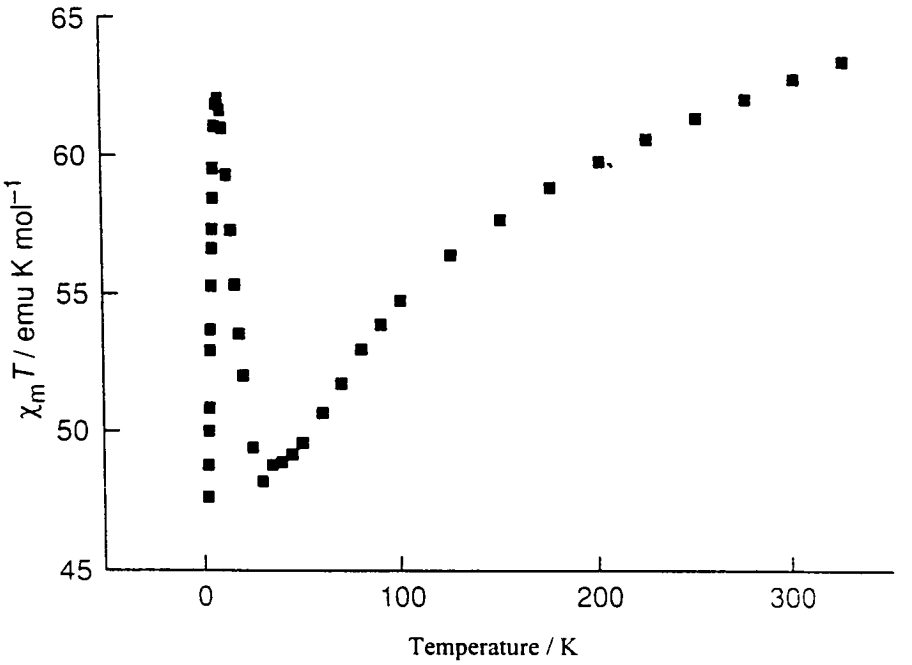

Figure 2.25. The variation of χ_mT with temperature for **14**.

are required to confirm this estimation. However given the structural resemblance between **14** and Powell's $[Fe_{17}][Fe_{19}]$ "crust" a high spin ground state would be unsurprising given that the ground state of the latter is at least S = 33/2.

Plots of the field-cooled and zero-field cooled M/H curves for **14** [where M = magnetisation and H = the applied field; M/H = χ_m if M is linear in H] are shown in Figure 2.26. The difference between the two curves is evident between 5-2 K and provides evidence for a freezing of the spins and may therefore be an indication of superparamagnetic behaviour. Such behaviour has been observed for nanoscale cobalt particles prepared in inverse micelles [75], for a dodecanuclear manganese complex [22, 23] and for a number of iron compounds [40-44]. Further magnetic studies are currently underway to confirm this behaviour.

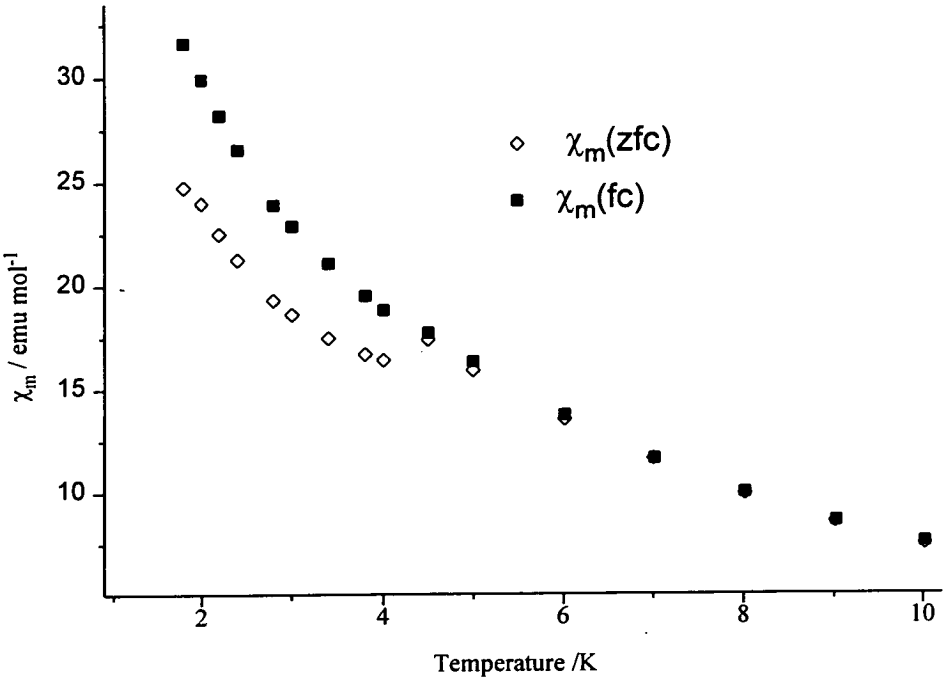

Figure 2.26. Field-cooled (open triangles) and zero-field cooled M/H curves for **14**.

Table 2.11. Selected bond lengths (Å) and angles (°) for **14**.

Co1-O3H	2.051(5)	Co3-O6R	2.070(5)
Co1-O9R	2.119(5)	Co3-O3R	2.139(4)
Co1-O8R	2.120(5)	Co3-Cl1B	2.54(3)
Co1-O5H	2.120(5)	Co4-O3HA	2.031(5)
Co1-O4H	2.168(5)	Co4-O1M	2.054(5)
Co1-O1H	2.194(5)	Co4-O7H	2.093(5)
Co2-O7R	2.058(5)	Co4-O1MA	2.120(5)
Co2-O1M	2.085(5)	Co4-O4HA	2.133(5)
Co2-O4H	2.111(5)	Co4-ClB1	2.603(5)
Co2-O7H	2.117(5)	Co5-O3HA	2.031(5)
Co2-O6H	2.132(5)	Co5-O5R	2.068(5)
Co2-O8R	2.151(5)	Co5-O8H	2.079(5)
Co3-O7H	2.037(5)	Co5-O9H	2.091(5)
Co3-O7R	2.062(5)	Co5-O5H	2.111(5)
Co3-O8H	2.069(5)	Co5-ClB1	2.603(5)

Table 2.11 continued

Co6-O2R	2.019(6)	Co10-O2R	2.799(6)
Co6-O6H	2.086(5)	Co11-O9H	1.971(5)
Co6-O1R	2.097(5)	Co11-N11R	2.035(7)
Co6-N7R	2.178(6)	Co11-N4R	2.050(6)
Co6-N3R	2.246(6)	Co11-ClT1	2.282(3)
Co6-O3R	2.272(5)	Co11-O11R	2.671(5)
Co7-O9H	2.006()5	Co11-O4R	3.022(5)
Co7-O11R	2.035(6)	Co12-O10R	1.971(5)
Co7-O4R	2.071(6)	Co12-O5H	1.984(5)
Co7-N10RA	2.090(5)	Co12-N9R	2.024(5)
Co7-O5R	2.201(5)	Co12-ClT2	2.265(5)
Co7-O10RA	2.213(5)	Co12-O9R	2.884(3)
Co8-O2H	1.997(5)	Co12-O9HA	3.397(5)
Co8-O8H	2.018(5)	O3H-Co1-O9R	93.9(2)
Co8-N5R	2.105(5)	O3H-Co1-O8R	93.9()
Co8-O4R	2.108(5)	O9R-Co1-O8R	96.8(22)
Co8-O6R	2.256(5)	O3H-Co1-O5H	84.3(2)
Co8-O5R	2.376(5)	O9R-Co1-O5H	82.7(2)
Co9-OH	1.974(5)	O8R-Co1-O5H	178.0(2)
Co9-N6R	2.051(7)	O3H-Co1-O4H	80.4(2)
Co9-O3R	2.089(5)	O9R-Co1-O4H	173.5(2)
Co9-N1R	2.097(6)	O8R-Co1-O4H	80.7(2)
Co9-O1R	2.310(5)	O5H-Co1-O4H	99.6(2)
Co9-O6R	2.455(5)	O3H-Co1-O1H	169.7(2)
Co10-O6H	1.992(5)	O9R-Co1-O1H	95.3(2)
Co10-N8R	2.047(6)	O8R-Co1-O1H	89.7(2)
Co10-N2R	2.051(6)	O5H-Co1-O1H	92.2(2)
Co10-O1H	2.084(5)	O4H-Co1-O1H	90.7(2)
Co10-O8R	2.628(5)	O7R-Co2-O1M	99.3(2)

Table 2.11 continued

O7R-Co2-O4H	174.6(2)	O3HA-Co4-O1M	177.3(2)
O1M-Co2-O4H	83.2(2)	O3HA-Co4-O7H	95.7(2)
O7R-Co2-O7H	79.0(2)	O1M-Co4-O7H	82.3(2)
O1M-Co2-O7H	81.0(2)	O3HA-Co4-O1MA	97.4(2)
O4H-Co2-O7H	96.8(2)	O1M-Co4-O1MA	84.7(2)
O7R-Co2-O6H	83.3(2)	O7H-Co4-O1MA	98.7(2)
O1M-Co2-O6H	177.3(2)	O3HA-Co4-O4HA	81.7(2)
O4H-Co2-O6H	94.2(2)	O1M-Co4-O4HA	100.2(2)
O7H-Co2-O6H	100.2(2)	O7H-Co4-O4HA	177.4(2)
O7R-Co2-O8R	103.2(2)	O1MA-Co4-O4HA	81.9(2)
O1M-Co2-O8R	92.6(2)	O3HA-Co4-ClB1	85.5(2)
O4H-Co2-O8R	81.4(2)	O1M-Co4-ClB1	92.6(2)
O7H-Co2-O8R	173.5(2)	O7H-Co4-ClB1	87.9(2)
O6H-Co2-O8R	86.2(2)	O1MA-Co4-ClB1	172.44(14)
O7H-Co3-O7R	80.8(2)	O4H-Co4-ClB1	91.7(2)
O7H-Co3-O8H	98.3(2)	O3HA-Co5-O5R	170.8(2)
O7R-Co3-O8H	175.8(2)	O3HA-Co5-O8H	97.0(2)
O7H-Co3-O6R	176.7(2)	O5R-Co5-O8H	85.3(2)
O7R-Co3-O6R	102.1(2)	O3HA-Co5-O9H	90.5(2)
O8H-Co3-O6R	78.9(2)	O5R-Co5-O9H	80.6(2)
O7H-Co3-O3R	96.9(2)	O8H-Co5-O9H	90.4(2)
O7R-Co3-O3R	90.3(2)	O3HA-Co5-O5HA	85.0(2)
O8H-Co3-O3R	93.9(2)	O5R-Co5-O5HA	93.1(2)
O6R-Co3-O3R	81.7(2)	O8H-Co5-O5HA	177.2(2)
O7H-Co3-ClB1	90.9()	O9H-Co5-O5HA	91.6(2)
O7R-Co3-ClB1	89.2(2)	O3HA-Co5-ClB1	89.4(2)
O8H-Co3-ClB1	86.7(2)	O5R-Co5-ClB1	99.6(2)
O6R-Co3-ClB1	90.7(2)	O8H-Co5-ClB1	88.7(2)
O3R-Co3-ClB1	172.0(2)	O9H-Co5-ClB1	179.12(14)

Table 2.11 continued

O5HA-Co5-ClB1	89.3(2)	N10RA-Co7-O10RA	61.6()2
O2R-Co6-O6H	89.1(2)	O5R-Co7-O10RA	89.0(2)
O2R-Co6-O1R	93.1(2)	O2H-Co8-O8H	107.9(2)
O6H-Co6-O1R	175.8(2)	O2H-Co8-N5R	114.8(2)
O2R-Co6-N7R	96.4(2)	O8H-Co8-N5R	130.7(2)
O6H-Co6-N7R	95.7(2)	O2H-Co8-O4R	100.3(2)
O1R-Co6-N7R	87.6(2)	O8H-Co8-O4R	96.0(2)
O2R-Co6-N3R	103.2(2)	N5R-Co8-O4R	99.3(2)
O6H-Co6-N3R	86.4(2)	O2H-Co8-O6R	81.8(2)
O1R-Co6-N3R	89.6(2)	O8H-Co8-O6R	75.8(2)
N7R-Co6-N3R	160.3(2)	N5R-Co8-O6R	86.9(2)
O2R-Co6-O3R	159.8(2)	O4R-Co8-O6R	171.8(2)
O6H-Co6-O3R	99.8(2)	O2H-Co8-O5R	172.8(2)
O1R-Co6-O3R	77.0(2)	O8H-Co8-O5R	79.0(2)
N7R-Co6-O3R	100.6(2)	N5R-Co8-O5R	59.8(2)
N3R-Co6-O3R	59.8(2)	O4R-Co8-O5R	76.7(2)
O9H-Co7-O11R	90.2(2)	O6R-Co8-O5R	102.1(2)
O9H-Co7-O4R	93.3(2)	O2H-Co9-N6R	101.9(2)
O11R-Co7-O4R	92.8(2)	O2H-Co9-O3R	108.2(2)
O9H-Co7-N10RA	154.2(2)	N6R-Co9-O3R	115.8(2)
O11R-Co7-N10RA	102.4(2)	O2H-Co9-N1R	104.5(2)
O4R-Co7-N10RA	108.2(2)	N6R-Co9-N1R	122.7(2)
O9H-Co7-O5R	97.3(2)	O3R-Co9-N1R	102.8(2)
O11R-Co7-O5R	167.7(2)	O2H-Co9-O1R	164.8(2)
O4R-Co7-O5R	81.5(2)	N6R-Co9-O1R	88.6(2)
N10RA-Co7-O5R	89.8(2)	O3R-Co9-O1R	76.3(2)
O9H-Co7-O10RA	94.6(2)	N1R-Co9-O1R	60.4(2)
O11R-Co7-O10RA	98.3(2)	O2H-Co9-O6R	77.3(2)
O4R-Co7-O10RA	166.3(2)	N6R-Co9-O6R	59.1(2)

Table 2.11 continued

O3R-Co9-O6R	74.1(2)	N11R-Co11-O4R	118.4(2)
N1R-Co9-O6R	176.8(2)	N4R-Co11-O4R	49.6(2)
O1R-Co9-O6R	117.8(2)	ClT1-Co11-O4R	119.72(12)
O6H-Co10-NR	111.9(2)	O11R-Co11-O4R	62.6(2)
O6H-Co10-N2R	113.2(2)	O10R-Co12-O5H	115.1(2)
N8R-Co10-N2R	114.0(2)	O10R-Co12-N9R	99.6(2)
O6H-Co10-O1H	101.9(2)	O5H-Co12-N9R	114.7(2)
N8R-Co10-O1H	113.1(2)	O10R-Co12-ClT2	108.2(2)
N2R-Co10-O1H	101.7(2)	O5H-Co12-ClT2	100.7(2)
O6H-Co10-O8R	77.2(2)	N9R-Co12-ClT2	119.1(2)
N8R-Co10-O8R	56.0(2)	O10R-Co12-O9R	102.9(2)
N2R-Co10-O8R	168.7(2)	O5H-Co12-O9R	67.3(2)
O1H-Co10-O8R	79.5(2)	N9R-Co12-O9R	51.4(2)
O6H-Co10-O2R	71.7(2)	ClT2-Co12-O9R	148.73(12)
N8R-Co10-O2R	103.5(2)	O10R-Co12-O9HA	64.4(2)
N2R-Co10-O2R	52.5(2)	O5H-Co12-O9HA	61.6(2)
O1H-Co10-O2R	142.1(2)	N9R-Co12-O9HA	91.4(2)
O8R-Co10-O2R	131.7(2)	ClT2-Co12-O9HA	149.48(11)
O9H-Co11-N11R	97.4(2)	O9R-Co12-O9HA	51.12(12)
O9H-Co11-N4R	118.7(2)	Co5-ClB1-Co3	80.24(10)
N11R-Co11-N4R	112.9(3)	Co5-ClB1-Co4	79.03(10)
O9H-Co11-ClT1	101.4(2)	Co3-ClB1-Co4	77.65(10)
N11R-Co11-ClT1	121.9(2)	Co4-O1M-Co2	99.5(2)
O4R-Co11-ClT1	104.8(2)	Co2-O1M-Co4A	95.3(2)
O9H-Co11-O11R	74.5(2)	Co2-O1M-Co4A	98.1(2)
N11R-Co11-O11R	56.0(2)	Co10-O1H-Co1	102.3(3)
N4R-Co11-O11R	80.5(2)	Co9-O2H-Co8	110.6(2)
ClT1-Co11-O11R	174.48(13)	Co4A-O3H-Co5A	104.9(2)
O9H-Co11-O4R	69.3(2)	Co4A-O3H-Co1	102.4(2)

Table 2.11 continued

Co5A-O3H-Co1	97.3(2)	Co6-O2R-Co10	84.8(2)
Co2-O4H-Co4A	96.9(2)	Co9-O3R-Co3	107.0(2)
Co2-O4H-Co1	98.8(2)	Co9-O3R-Co6	102.6(2)
Co4A-O4H-Co1	95.4(2)	Co3-O3R-Co6	110.0(2)
Co12-O5H-Co5A	121.1(2)	Co7-O4R-Co8	107.1(2)
Co12-O5H-Co1	112.0(2)	Co7-O4R-Co11	69.74(14)
Co5A-O5H-Co1	92.8(2)	Co8-O4R-Co11	112.2(2)
Co10-O6H-Co6	108.0(2)	Co5-O5R-Co7	97.2(2)
Co10-O6H-Co2	108.1(2)	Co5-O5R-Co8	92.3(2)
Co6-O6H-Co2	118.6(2)	Co7-O5R-Co8	94.4(2)
Co3-O7H-Co4	102.6(2)	Co3-O6R-Co8	98.4(2)
Co3-O7H-Co2	99.5(2)	Co3-O6R-Co9	97.0(2)
Co4-O7H-Co2	97.2(2)	Co8-O6R-Co9	87.6(2)
Co8-O8H-Co3	106.7(2)	Co2-O7R-Co3	100.7(2)
Co8-O8H-Co5	103.3(2)	Co1-O8R-Co2	99.0(2)
Co3-O8H-Co5	101.9(2)	Co1-O8R-Co10	88.5(2)
Co11-O9H-Co7	98.6(2)	Co2-O8R-Co10	88.1(2)
Co11-O9H-Co5	131.1(2)	Co1-O9R-Co12	84.2(2)
Co7-O9H-Co5	102.8(2)	Co12-O10R-Co7A	117.6(2)
Co6-O1R-Co9	101.1(2)	Co7-O11R-Co11	78.4(2)

2.4. Thermolysis Reactions of Nickel and Cobalt Salts.

The thermolysis reactions of the hydroxides and methoxides of nickel and cobalt with 6-chloro-(Hchp) and 6-methyl-2-pyridone (Hmhp) are reported and discussed.

The general reaction scheme is given below:

$$M(OR)_2 + 2Hxhp \rightarrow M(xhp)_2 + 2ROH$$

where R= H, Me, Hxhp= Hchp, Hmhp and M= Ni, Co.

The metal hydroxide / methoxide is heated with Hxhp to the melting point of the ligand (Hxhp) at which point the hydroxide or methoxide becomes protonated producing the alcohol or water which is pumped off under vacuum to a cold trap leaving the melt product $M(xhp)_2$ behind.

This melt product has been crystallised from a number of solvents producing a range of compounds which include two nickel heptamers, cobalt and nickel nonamers and a nickel undecamer. These complexes include the first examples of nickel and cobalt compounds which contain M_4O_6 adamantane units and are also the first examples of vertex- and face-sharing adamantanes.

2.4.1. Synthesis and structure of $[Ni_7(chp)_{12}(MeOH)_6(Cl)_2]$ 15

Reaction of nickel hydroxide with two equivalents of 6-chloro-2-pyridone (Hchp) at 140 °C under nitrogen for two hours produced a green paste which, after drying *in vacuo*, was crystallised from an acetonitrile / methanol mix giving green crystals of $[Ni_7(chp)_{12}(MeOH)_6(Cl)_2]$ **15** [Figure 2.27] in reasonable yield after two days [76].

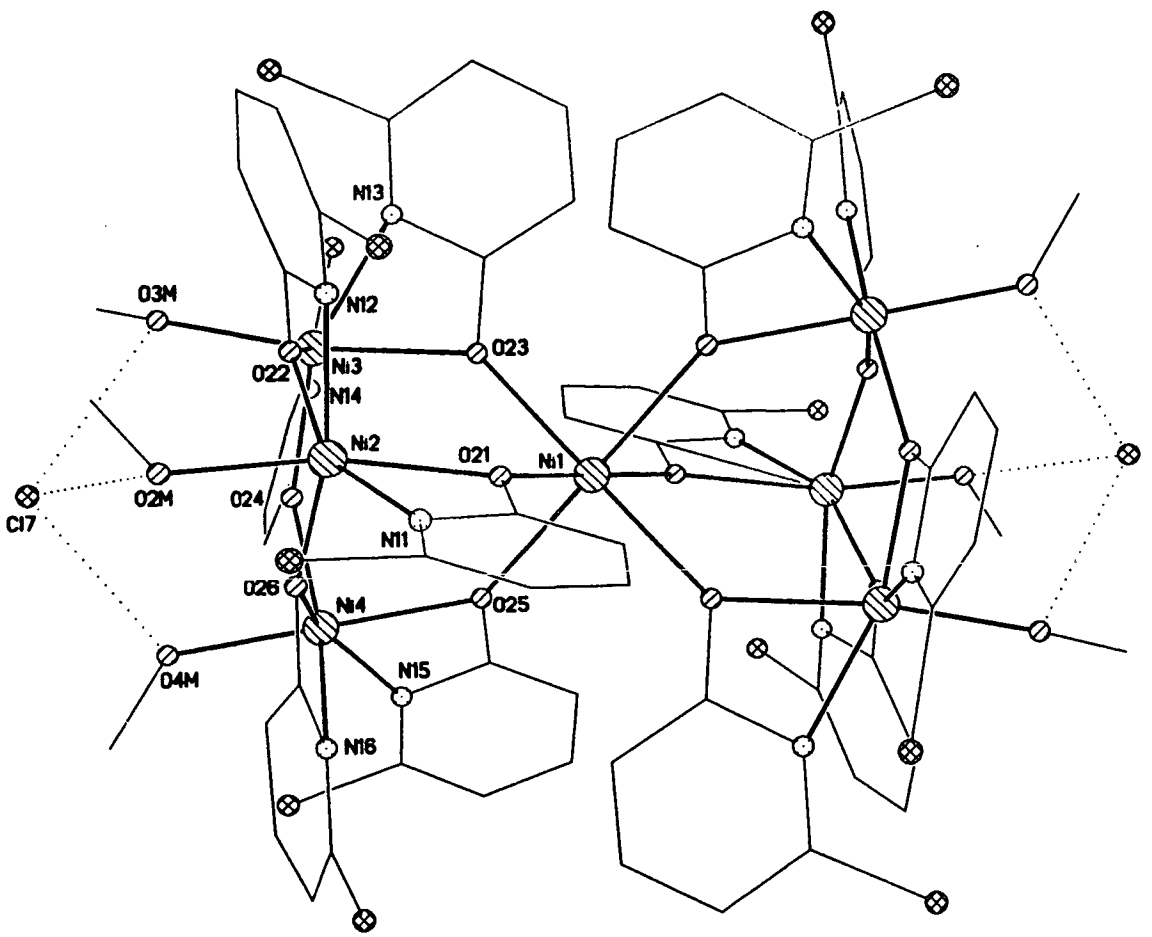

Figure 2.27. The structure of **15** in the crystal.

15 is a heptanuclear complex with the central nickel site [Ni1] lying on a crystallographic inversion centre. This nickel is the shared vertex of two Ni_4O_6 adamantanes with the oxygen atoms provided by binucleating chp ligands, which chelate to the remaining "basal" nickel sites [Ni2, Ni3 and Ni4] in the structure. Each basal site is bound to one further chelating chp and to a bridging oxygen donor from the chp ligand chelating to a neighbouring

nickel. These three chelating chp ligands lie virtually co-planar with the Ni_3-base. Thus chp donors occupy five coordination sites on each basal nickel, with the sixth site occupied by a molecule of methanol in each case. These three terminal methanol ligands form strong hydrogen bonds to chloride ions [average O...Cl, 3.11(3) Å]. The presence of chloride indicates it has been carried through from the nickel chloride used to prepare the nickel hyroxide [experimental section 2.6.13].

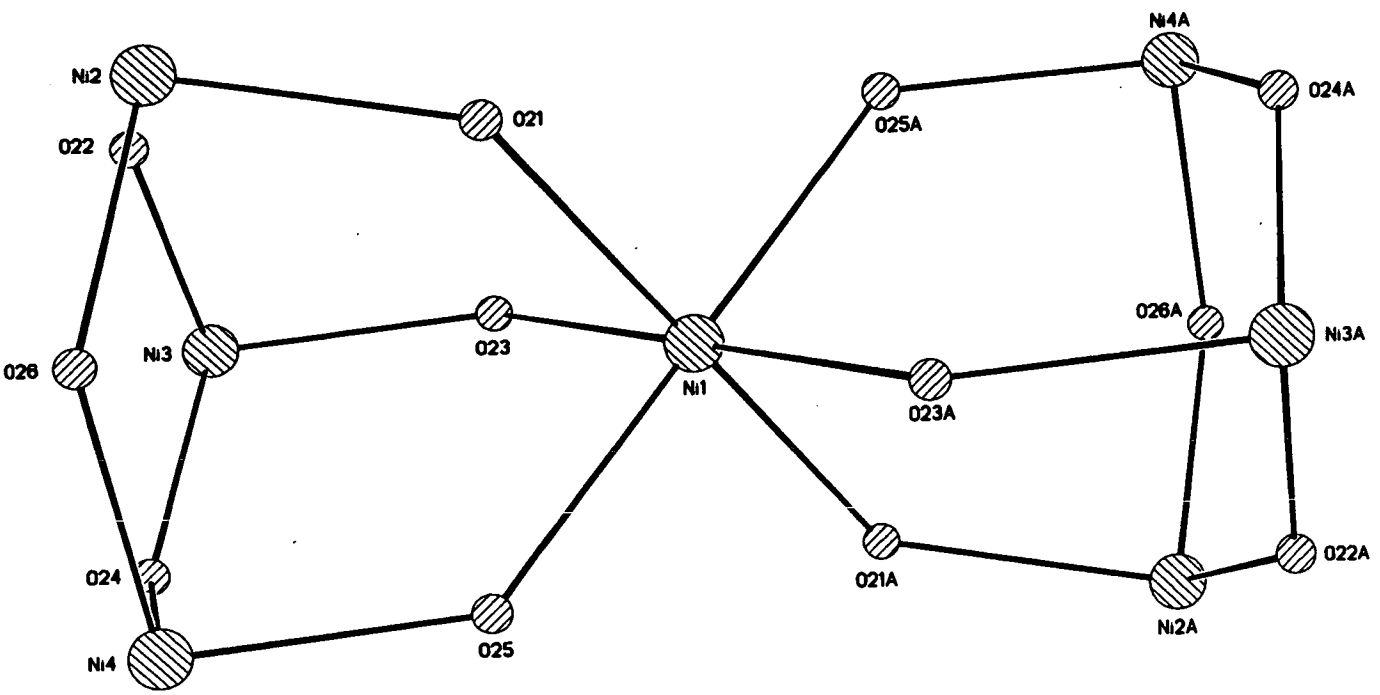

Figure 2.28. The metal polyhedron in **15.**

The chp ligands show only one coordinating mode : chelating one nickel with the exocyclic oxygen atom bridging to a second metal centre. The metal polyhedron showing the two adamantane units is given in Figure 2.28. The central nickel site has a regular octahedral geometry, the three *trans* angles are exactly 180.0(0)° with the *cis* angles varying only between 89.4 and 90.6(2)°. The other nickels have much more distorted octahedral geometries due to the narrow bite angles of the chp ligands [N-Ni-O, 63.2-64.5(3)°]; here the *trans* angles range from 152.6-169.3(3)° and the *cis* angles 63.3-108.5(3)°.

The metal-ligand bond distances vary greatly depending on the metal site. For the central nickel [Ni1] the Ni-O distances are long varying between 2.337-2.369(6) Å. All the other nickel sites have "normal" Ni-O and Ni-N distances [2.018-2.145(7) Å and 2.066-2.105 (8)Å respectively]. The length of the central Ni-O bonds led to the examination that this central site was actually occupied by sodium and not nickel. However crystallographic refinement of the structure with a sodium in place of Ni1 produced physically meaningless results. FAB-mass spectroscopy produced a fragment very close to the molecular ion in mass, and atomic absorption spectroscopy gave the correct analysis for both metals [experimental section 2.6.13]. The closest Ni...Ni contact in **15** is 3.802(3) Å between Ni2 and Ni3. Selected bond lengths and angles are given in Table 2.12.

Table 2.12. Selected bond lengths (Å) and angles (°) for **15.**

Ni1-O21	2.337(7)	Ni3-N14	2.084(9)
Ni1-O21A	2.337(7)	Ni3-O24	2.086(6)
Ni1-O25A	2.338(6)	Ni3-O23	2.145(6)
Ni1-O25	2.338(6)	Ni4-O24	2.018(7)
Ni1-O23	2.369(6)	Ni4-O4M	2.050(7)
Ni1-O23A	2.369(6)	Ni4-O26	2.091(6)
Ni2-O26	2.025(6)	Ni4-N15	2.101(8)
Ni2-N11	2.066(9)	Ni4-N16	2.105(8)
Ni2-O2M	2.084(7)	Ni4-O23	2.120(6)
Ni2-N12	2.087(8)	O21-Ni1-O21A	180.0(0)
Ni2-O22	2.102(7)	O21-Ni1-O25A	89.9(2)
Ni2-O21	2.141(7)	O21A-Ni1-O25A	90.1(2)
Ni3-O22	2.002(7)	O21-Ni1-O25	90.1(2)
Ni3-N13	2.072(8)	O21A-Ni1-O25	89.9(2)
Ni3-O3M	2.075(7)	O25A-Ni1-O25	180.0(0)

Table 2.12 continued

O21-Ni1-O23	89.4(2)	O3M-Ni3-N14	90.6(3)
O21A-Ni1-O23	90.6(2)	O22-Ni3-O24	98.7(3)
O25A-Ni1-O23	90.4(2)	N13-Ni3-O24	153.5(3)
O25-Ni1-O23	89.6(2)	O3M-Ni3-O24	92.5(3)
O21-Ni1-O23A	90.6(2)	N14-Ni3-O24	63.3(3)
O21A-Ni1-O23A	89.4(2)	O22-Ni3-O23	90.3(3)
O25A-Ni1-O23A	89.6(2)	N13-Ni3-O23	64.1(3)
O25-Ni1-O23A	90.4(2)	O3M-Ni3-O23	169.3(3)
O23-Ni1-O23A	180.0(0)	N14-Ni3-O23	98.1(3)
O26-Ni2-N11	102.7(3)	O24-Ni3-O23	96.8(3)
O26-Ni2-O2M	84.0(3)	O24-Ni4-O4M	84.4(3)
N11-Ni2-O2M	105.6(3)	O24-Ni4-O26	96.9(3)
O26-Ni2-N12	158.4(3)	O4M-Ni4-O26	93.0(3)
N11-Ni2-N12	99.0(3)	O24-Ni4-N15	102.7(3)
O2M-Ni2-N12	90.1(3)	O4M-Ni4-N15	107.7(3)
O26-Ni2-O22	95.8(3)	O26-Ni4-N15	152.6(3)
N11-Ni2-O22	156.0(3)	O24-Ni4-N16	159.4(3)
O2M-Ni2-O22	91.4(3)	O4M-Ni4-N16	90.8(3)
N12-Ni2-O22	63.4(3)	O26-Ni4-N16	63.3(3)
O26-Ni2-O21	90.3(3)	N15-Ni4-N16	97.8(3)
N11-Ni2-O21	64.5(3)	O24-Ni4-O25	90.6(3)
O2M-Ni2-O21	167.3(3)	O4M-Ni4-O25	168.4(3)
N12-Ni2-O21	99.2(3)	O26-Ni4-O25	98.(3)
O22-Ni2-O21	100.5(3)	N15-Ni4-O25	63.2(3)
O22-Ni3-N13	99.6(3)	N16-Ni4-O25	97.4(3)
O22-Ni3-O3M	83.2(3)	Ni2-O21-Ni1	131.8(3)
N13-Ni3-O3M	108.5(3)	Ni3-O22-Ni2	135.7(3)
O22-Ni3-N14	160.7(3)	Ni3-O23-Ni1	133.2(3)
N13-Ni3-N14	99.7(3)	Ni4-O24-Ni3	136.2(3)

2.4.2. Magnetochemistry of 15.

The magnetic behaviour of **15** was studied in the temperature range 300-1.8 K in an applied field of 1000 G. The variation of $\chi_m T$ with temperature is given in Figure 2.29. The value of $\chi_m T$ at 300 K is approximately 9 emu K mol^{-1} which is consistent with seven non-interacting S= 1 centres which would give a theoretical value of $\chi_m T$ = 8.5 emu K mol^{-1} [assuming g= 2.2]. The value of $\chi_m T$ then drops steadily with temperature to a minimum of approximately 3.5 emu K mol^{-1} at 2 K, corresponding to an approximately S = 2 ground state. This is an example of antiferromagnetic coupling between the metal centres.

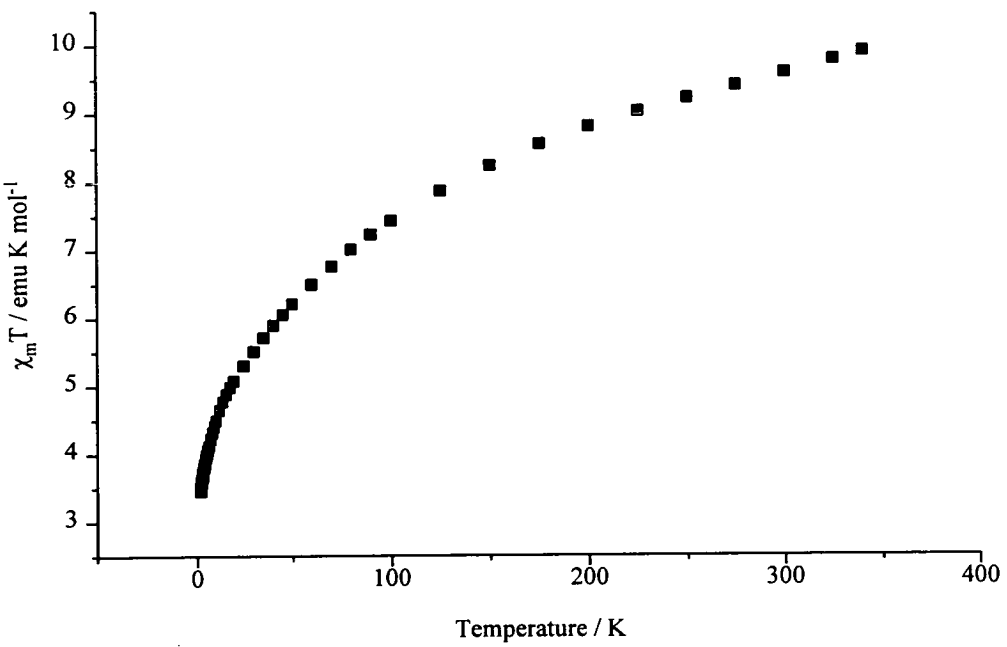

Figure 2.29. The variation of $\chi_m T$ with temperature for **15**.

2.4.3. Synthesis and structure of $[Ni_7(OH)_2(chp)_{12}(MeOH)_6]$ 16.

The procedure used to produce **15** was repeated using nickel methoxide in place of nickel hydroxide. This prodced the related heptamer $[Ni_7(OH)_2(chp)_{12}(MeOH)_6]$ **16** [Figure 2.30] in reasonable yield after two days [76].

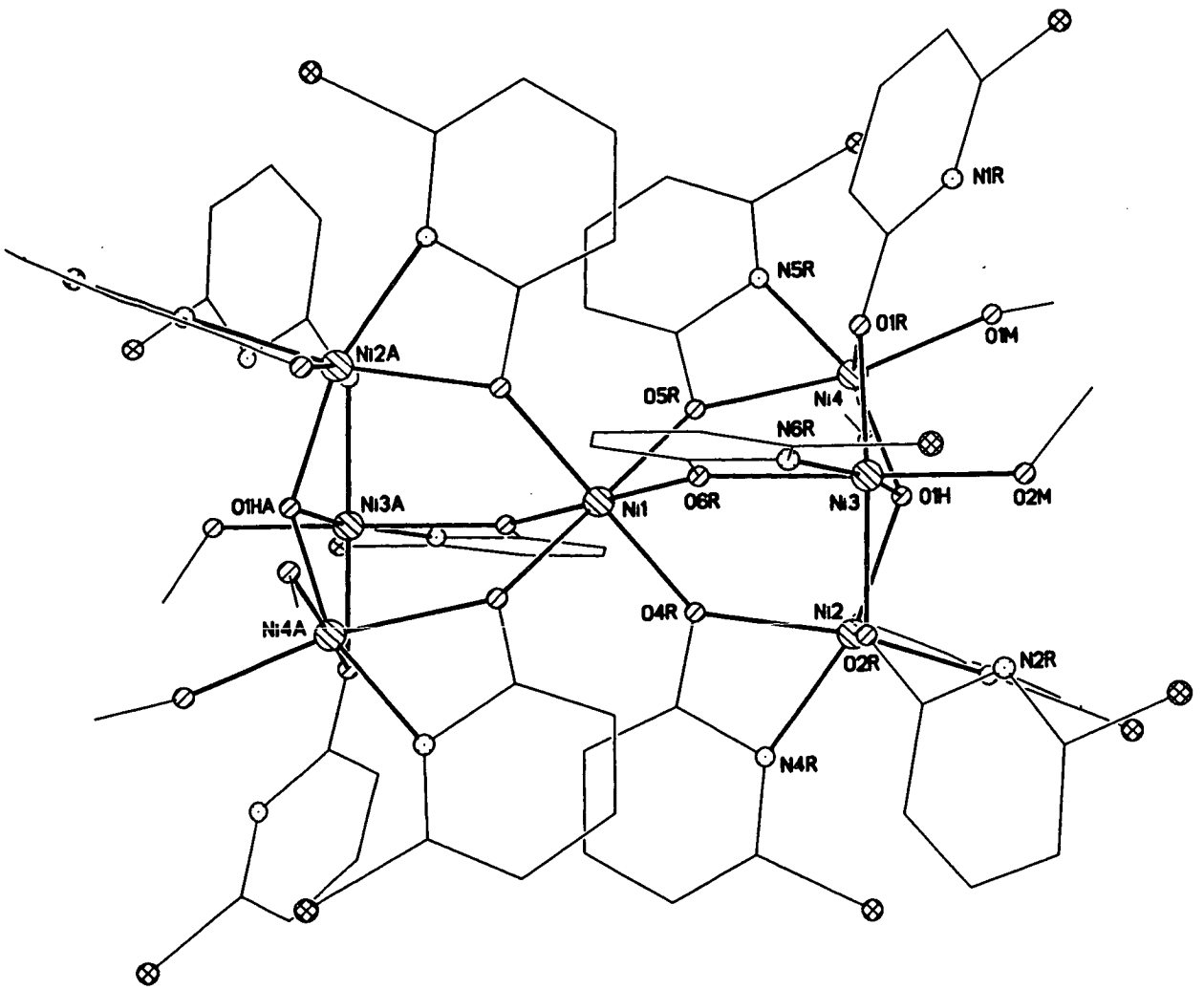

Figure 2.30. The structure of **16** in the crystal.

Again Ni1, the central nickel, is on an inversion centre and bound to six oxygen donors derived from binucleating chp ligands and is the shared vertex of two Ni_4O_6 cages. However in **17** the ideal adamantane cages are distorted by the presence of a μ_3-hydroxide [O1H] linking the three nickel sites [Ni2, Ni3 and Ni4] in the basal plane. These three nickel sites are now disimilar. Ni2 is bound to two chelating chp ligands, the μ_3-hydroxide and to a chp oxygen

which is μ_2-bridging to Ni3 while the ring nitrogen donor forms a hydrogen bond to a methanol ligand. Ni3 is bound to one chelating chp, to the μ_3-hydroxide, to two μ_2-oxygens from chp ligands and to a terminal methanol molecule. Ni4 is bound to one chelating chp ligand, the μ_3-hydroxide, one μ_2-oxygen from a chp and two terminal methanol molecules.

The chp ligands this time show a number of coordinating modes. Purely chelating to only one metal centre [Ni2]. Chelating to one nickel and bridging to one other *via* the exocyclic oxygen atom. Bridging two nickel centres [Ni2 and Ni3] *via* the oxygen atom with the ring nitrogen hydrogen bonded to a terminal methanol ligand [N2R...O2M, 2.631(10) Å]. The metal polyhedron of **16** showing the adamantane units is given in Figure 2.31. Again the central nickel has regular octahedral geometry with the *trans* angles being exactly 180.0(0)° and the *cis* angles ranging between 85.8-94.2(4)°. As with **15** the other nickels have more distorted octahedral geometries due to the chelation of the chp ligands. Ni2-Ni4 have *trans* angles ranging between 157.0-171.0(4)° and *cis* angles 62.5-109.7(5)°.

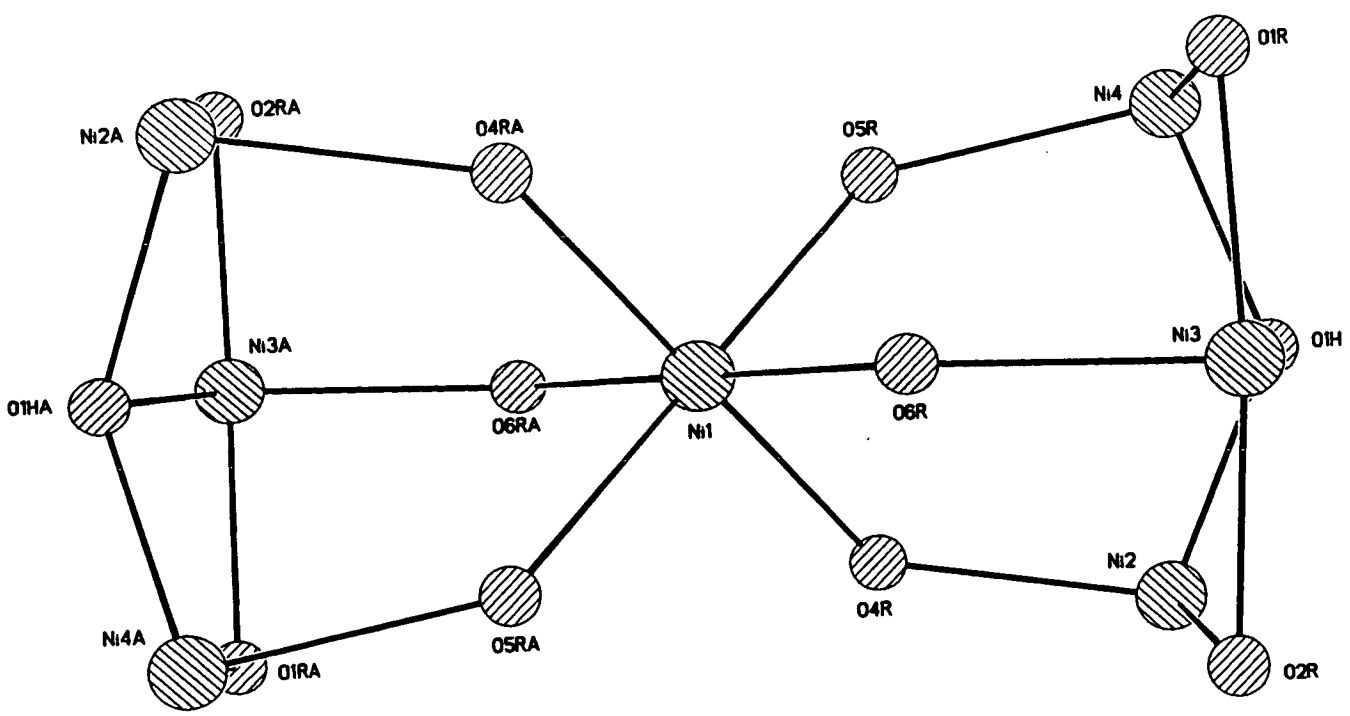

Figure 2.31. The metal polyhedron of **16**.

Unlike **15**, the Ni-O bond lengths in **16** all lie in the range 1.976-2.165(9) Å. The closest Ni...Ni contact is 3.064(1) Å between Ni2 and Ni3. Selected bond lengths and angles are given in Table 2.13.

Table 2.13. Selected bond lengths (Å) and angles (°) for **16**.

Ni1-O6RA	2.025(9)	O6RA-Ni1-O6R	180.00(0)
Ni1-O6R	2.025(9)	O6RA-Ni1-O4RA	85.8(4)
Ni1-O4RA	2.067(9)	O6R-Ni1-O4RA	94.2(4)
Ni1-O4R	2.067(9)	O6RA-Ni1-O4R	94.2(4)
Ni1-O5R	2.114(10)	O6R-Ni1-O4R	85.8(4)
Ni1-O5RA	2.114(10)	O4RA-Ni1-O4R	180.00(0)
Ni2-O1H	2.003(10)	O6RA-Ni1-O5R	94.0(4)
Ni2-N4R	2.050(10)	O6R-Ni1-O5R	86.0(4)
Ni2-N3R	2.116(12)	O4RA-Ni1-O5R	94.0(4)
Ni2-O3R	2.118(11)	O4R-Ni1-O5R	86.0(4)
Ni2-O2R	2.122(10)	O6RA-Ni1-O5RA	86.0(4)
Ni2-O4R	2.123(10)	O6R-Ni1-O5RA	94.0(4)
Ni3-O1H	2.032(10)	O4RA-Ni1-O5RA	86.0(4)
Ni3-O2R	2.081(10)	O4R-Ni1-O5RA	94.0(4)
Ni3-N6R	2.087(10)	O5R-Ni1-O5RA	180.00(0)
Ni3-O1R	2.103(10)	O1H-Ni2-N4R	163.9(5)
Ni3-O6R	2.131(10)	O1H-Ni2-N3R	92.3(5)
Ni3-O2M	2.028(10)	N4R-Ni2-N3R	102.9(5)
Ni4-O1H	1.976(10)	O1H-Ni2-O3R	92.6(5)
Ni4-N5R	2.062(10)	N4R-Ni2-O3R	89.3(4)
Ni4-O1R	2.114(10)	N3R-Ni2-O3R	64.4(5)
Ni4-O5R	2.165(9)	O1H-Ni2-O2R	80.5(5)
Ni4-O1M	2.043(9)	N4R-Ni2-O2R	98.9(5)
Ni4-O3M	2.073(9)	N3R-Ni2-O2R	109.7(5)

Table 2.13 continued

O3R-Ni2-O2R	171.0(4)	O1H-Ni4-O1R	80.1(4)
O1H-Ni2-O4R	99.7(4)	N5R-Ni4-O1R	103.2(4)
N4R-Ni2-O4R	64.2(4)	O1H-Ni4-O5R	97.1(4)
N3R-Ni2-O4R	157.0(4)	N5R-Ni4-O5R	63.1(4)
O3R-Ni2-O4R	95.2(4)	O1R-Ni4-O5R	93.1(4)
O2R-Ni2-O4R	91.7(4)	O1H-Ni4-O1M	93.5(4)
O1H-Ni3-O2R	80.9(4)	O1H-Ni4-O3M	87.7(4)
O1H-Ni3-N6R	165.8(4)	O1M-Ni4-O3M	90.0(4)
O2R-Ni3-N6R	97.0(4)	O1M-Ni4-O1R	86.5(4)
O1H-Ni3-O1R	79.1(4)	O1M-Ni4-N5R	106.5(4)
O2R-Ni3-O1R	158.5(4)	O1M-Ni4-O5R	169.2(4)
N6R-Ni3-O1R	100.6(4)	O3M-Ni4-O1R	167.0(4)
O1H-Ni3-O6R	103.4(4)	O3M-Ni4-N5R	89.8(4)
O2R-Ni3-O6R	90.4(4)	O3M-Ni4-O5R	92.7(4)
N6R-Ni3-O6R	62.5(4)	Ni4-O1H-Ni2	131.1(3)
O1R-Ni3-O6R	86.8(4)	Ni4-O1H-Ni3	101.39(4)
O1H-Ni3-O2M	90.5(4)	Ni4-O1H-Ni3	98.8(4)
O2M-Ni3-O1	97.2(4)	Ni3-O1R-Ni4	94.6(4)
O2M-Ni3-O2R	90.6(4)	Ni3-O2R-Ni2	93.6(4)
O2M-Ni3-N6R	103.6(4)	Ni1-O4R-Ni2	135.7(4)
O2M-Ni3-O6R	166.1(4)	Ni1-O5R-Ni4	135.0(5)
O1H-Ni4-N5R	159.9(5)	Ni1-O6R-Ni3	132.6(5)

2.4.4. Magnetochemistry of 16.

The magnetic behaviour of **16** was studied in the temperature range 300-1.8 K in an applied field of 1000 G. The variation of $\chi_m T$ with temperature is shown in Figure 2.32. The value of $\chi_m T$ at room temperature is approximately 9 emu K mol^{-1} which is consistent

with seven non-interacting S = 1 centres [$\chi_m T$ = 8.5 emu k mol^{-1}, g= 2.2]. As with **15** the value then drops steadily to a minimum of 3 emu K mol^{-1} at 2 K indicating antiferromagnetic coupling between the Ni (II) centres.

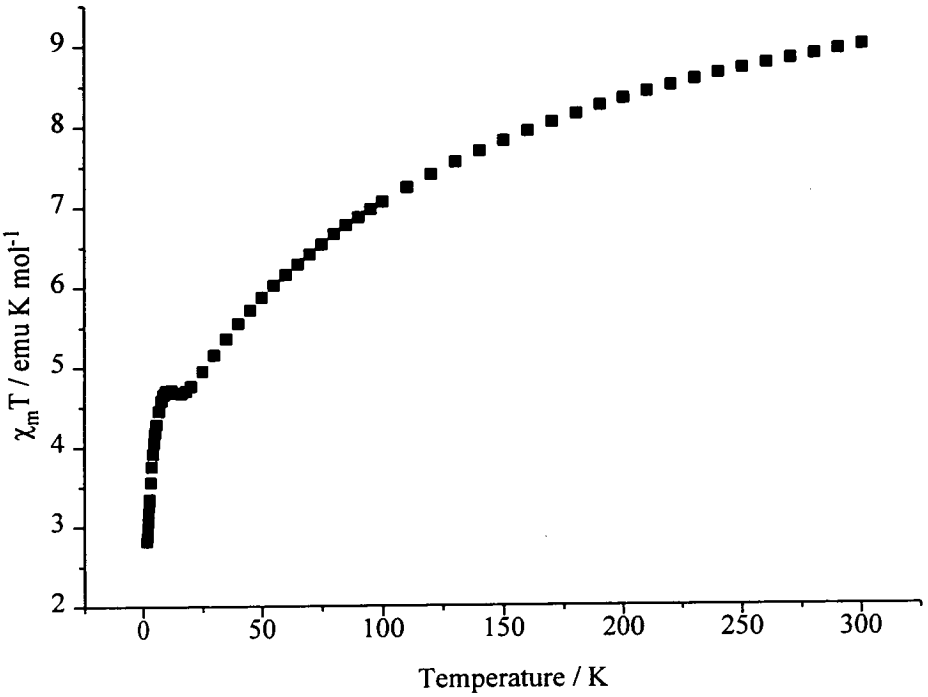

Figure 2.32. The variation of $\chi_m T$ with temperature for **16**.

2.4.5. Synthesis and structure of $[Ni_9(OH)_2(chp)_{16}(MeCN)_2]$ 17.

Given the presence of the terminal methanol molecules in both **15** and **16**, it appeared desirable to the remove the influence of methanol from this chemistry. The reaction which was used to synthesise **15** was repeated and the paste produced from the thermolysis was crystallised from acetonitrile alone. This led to the nonanuclear cage $[Ni_9(OH)_2(chp)_{16}(MeCN)_2]$ **17** [Figure 2.33] in high yield after two days [76].

Again **17** contains a central six coordinate nickel atom [Ni1] which lies on a symmetry element, in this case a two-fold axis. A very similar heptanuclear cage to that in **16** is present with a μ_3-hydroxide ligand bridging the three nickel sites [Ni2, Ni3 and Ni4] within the basal

plane. However the absence of methanol ligands has led to a slightly larger cage, with an additional $[Ni(chp)_3]^-$ unit, containing Ni5, attached to one edge of the triangular base.

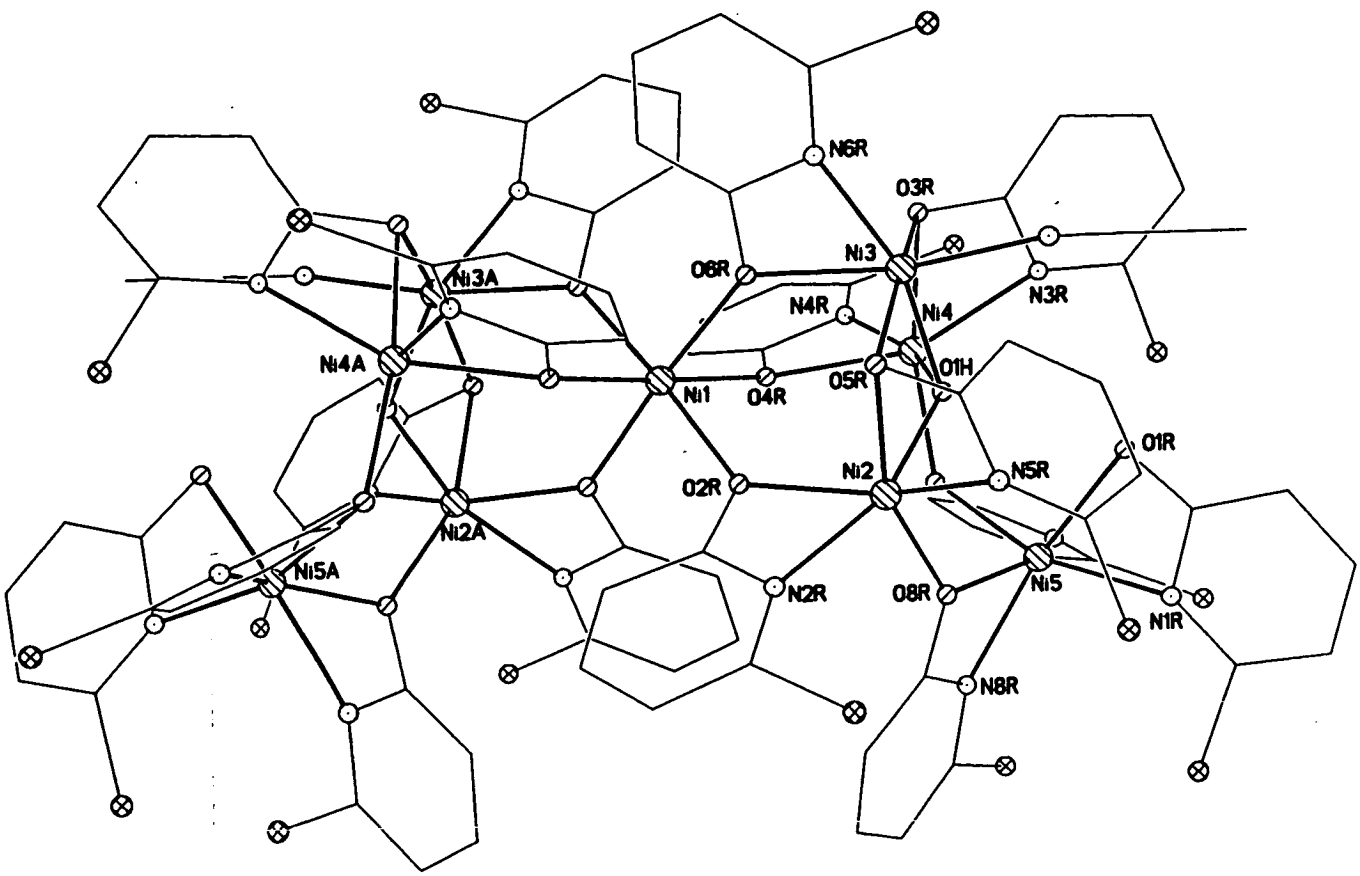

Figure 2.33. The structure of **17** in the crystal.

The three nickel sites in the base are again distinct. Ni2 and Ni4 are identical, bound to two chelating chp ligands, the μ_3-hydroxide and a bridging μ_2-oxygen atom which attaches the $[Ni(chp)_3]^-$ to the cage. Ni3 is unique, bound to one chelating chp ligand, the μ_3-hydroxide, two μ_2-oxygen donors from chp ligands chelating to Ni2 and Ni4 and a terminal acetonitrile ligand. There are two types of chp ligand : chelating to one nickel centre [for example to Ni5] with the exocyclic oxygen atom bridging to one further nickel [Ni2], and chelating [to Ni5] with the oxygen atom hydrogen bonded to the hydroxide on the basal plane [O1R...O1H, 2.722(6) Å]. As with **16** all the Ni-O bond lengths can be regarded as regular as they all fall in the range 2.011-2.198(5) Å, as can the Ni-N bond lengths at 2.053-2.109(5) Å.

Again Ni1 is in a more regular octahedral geometry [*cis* angles, 85.1-95.3(2)°; *trans* angles 175.8-177.7(2)°] than the other nickel atoms [*cis* angles, 62.7-109.4(2)°; *trans* angles, 148.8-169.6(2)°]. The closest Ni...Ni contact is 3.048(5) Å between Ni3 and Ni4. Selected bond lengths and angles are given in Table 2.14.

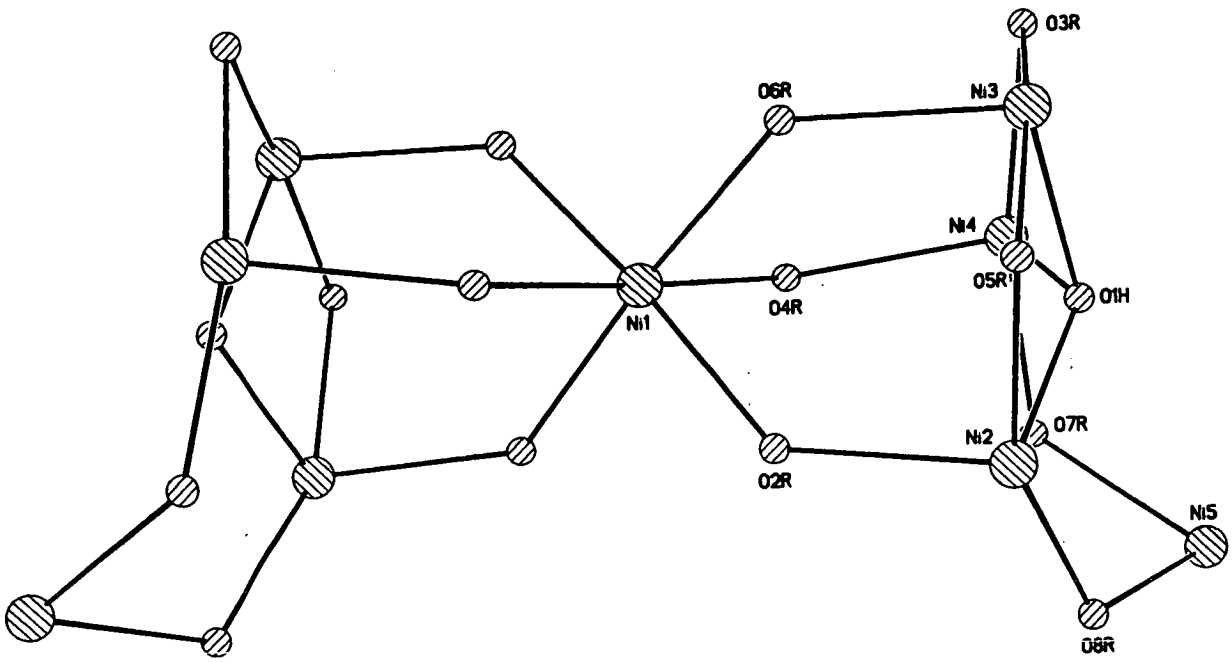

Figure 2.34. The metal polyhedron of **17**.

Table 2.14. Selected bond lengths (Å) and angles (°) for **17**.

Ni1-O4R	2.058(4)	Ni2-N5R	2.080(6)
Ni1-O4RA	2.058(4)	Ni2-N2R	2.094(6)
Ni1-O6R	2.064(5)	Ni2-O2R	2.098(4)
Ni1-O6RA	2.064(5)	Ni2-O5R	2.198(5)
Ni1-O2RA	2.081(5)	Ni3-O1H	2.011(5)
Ni1-O2R	2.081(5)	Ni3-N1E	2.053(6)
Ni2-O1H	2.018(5)	Ni3-N6R	2.054(6)
Ni2-O8R	2.029(5)	Ni3-O5R	2.095(6)

Table 2.14 continued

Ni3-O3R	2.100(5)	O1H-Ni2-O8R	89.2(2)
Ni3-O6R	2.126(5)	O1H-Ni2-N5R	96.4(2)
Ni4-O1H	2.018(5)	O8R-Ni2-N5R	100.7(2)
Ni4-O7R	2.065(5)	O1H-Ni2-N2R	158.7(2)
Ni4-N4R	2.067(6)	O8R-Ni2-N2R	97.6(2)
Ni4-O4R	2.102(4)	N5R-Ni2-N2R	102.0(2)
Ni4-N3R	2.109(6)	O1H-Ni2-O2R	95.3(2)
Ni4-O3R	2.170(5)	O8R-Ni2-O2R	104.2(2)
Ni5-N1R	2.035(6)	N5R-Ni2-O2R	152.6(2)
Ni5-N7R	2.075(6)	N2R-Ni2-O2R	63.5(2)
Ni5-O7R	2.091(5)	O1H-Ni2-O5R	81.0(2)
Ni5-N8R	2.102(7)	O8R-Ni2-O5R	159.2(2)
Ni5-O8R	2.112(5)	N5R-Ni2-O5R	62.7(2)
Ni5-O1R	2.152(5)	N2R-Ni2-O5R	98.1(2)
O4R-Ni1-O4RA	177.7(3)	O2R-Ni2-O5R	94.9(2)
O4R-Ni1-O6R	85.1(2)	O1H-Ni3-N1E	90.5(2)
O4RA-Ni1-O6R	93.4(2)	O1H-Ni3-N6R	162.8(2)
O4R-Ni1-O6RA	93.4(2)	N1E-Ni3-N6R	106.7(2)
O4RA-Ni1-O6RA	85.1(2)	O1H-Ni3-O5R	83.8(2)
O6R-Ni1-O6RA	95.3(3)	N1E-Ni3-O5R	93.5(2)
O4R-Ni1-O2RA	92.3(2)	N6R-Ni3-O5R	95.4(2)
O4RA-Ni1-O2RA	89.3(2)	O1H-Ni3-O3R	83.5(2)
O6R-Ni1-O2RA	175.8(2)	N1E-Ni3-O3R	92.9(2)
O6RA-Ni1-O2RA	88.1(2)	N6R-Ni3-O3R	94.9(2)
O4R-Ni1-O2R	89.3(2)	O5R-Ni3-O3R	165.7(2)
O4RA-Ni1-O2R	92.3(2)	O1H-Ni3-O6R	99.3(2)
O6R-Ni1-O2R	88.1(2)	N1E-Ni3-O6R	169.6(2)
O6RA-Ni1-O2R	175.8(2)	N6R-Ni3-O6R	63.5(2)
O2RA-Ni1-O2R	88.6(2)	O5R-Ni3-O6R	90.9(2)

Table 2.14 continued

O3R-Ni3-O6R	84.9(2)	O7R-Ni5-N8R	95.6(2)
O1H-Ni4-O7R	89.5(2)	N1R-Ni5-O8R	101.7(2)
O1H-Ni4-N4R	162.4(2)	N7R-Ni5-O8R	148.8(2)
O7R-Ni4-N4R	93.8(2)	O7R-Ni5-O8R	93.1(2)
O1H-Ni4-O4R	99.2(2)	N8R-Ni5-O8R	63.2(2)
O7R-Ni4-O4R	90.3(2)	N1R-Ni5-O1R	63.5(2)
N4R-Ni4-O4R	63.5(2)	N7R-Ni5-O1R	106.6(2)
O1H-Ni4-N3R	94.9(2)	O7R-Ni5-O1R	102.3(2)
O7R-Ni4-N3R	109.4(2)	N8R-Ni5-O1R	155.1(2)
N4R-Ni4-N3R	100.3(2)	O8R-Ni5-O1R	98.3(2)
O4R-Ni4-N3R	155.9(2)	Ni3-O1H-Ni4	98.3(2)
O1H-Ni4-O3R	81.5(2)	Ni3-O1H-Ni2	99,8(2)
O7R-Ni4-O3R	167.4(2)	Ni4-O1H-Ni2	135.5(2)
N4R-Ni4-O3R	97.4(2)	Ni1-O2R-Ni2	135.6(2)
O4R-Ni4-O3R	99.8(2)	Ni3-O3R-Ni4	91.1(2)
N3R-Ni4-O3R	63.0(2)	Ni1-O4R-Ni4	130.9(2)
N1R-Ni5-N7R	105.9(3)	Ni3-O5R-Ni2	91.7(2)
N1R-Ni5-O7R	160.6(2)	Ni1-O6R-Ni3	132.4(2)
N7R-Ni5-O7R	63.8(2)	Ni4-O7R-Ni5	115.6(2)
N1R-Ni5-N8R	102.1(3)	Ni2-O8R-Ni5	122.6(3)
N7R-Ni5-N8R	96.8(3)		

2.4.6. Magnetochemistry of 17.

The magnetic behaviour of **17** was examined in the temperature range 300-1.8 K in an applied field of 1000 G. The variation of $\chi_m T$ with temperature is shown in Figure 2.35. The value of $\chi_m T$ at 300 K is approximately 11 emu K mol^{-1} which is consistent with nine non-interacting S= 1 centres [$\chi_m T$= 10.89 emu K mol^{-1}, g = 2.2]. The value then steadily declines

with temperature and reaches a minimum of approximately 3 emu K mol^{-1} at 1.8 K, behaviour consistent with antiferromagnetic coupling between the metal centres.

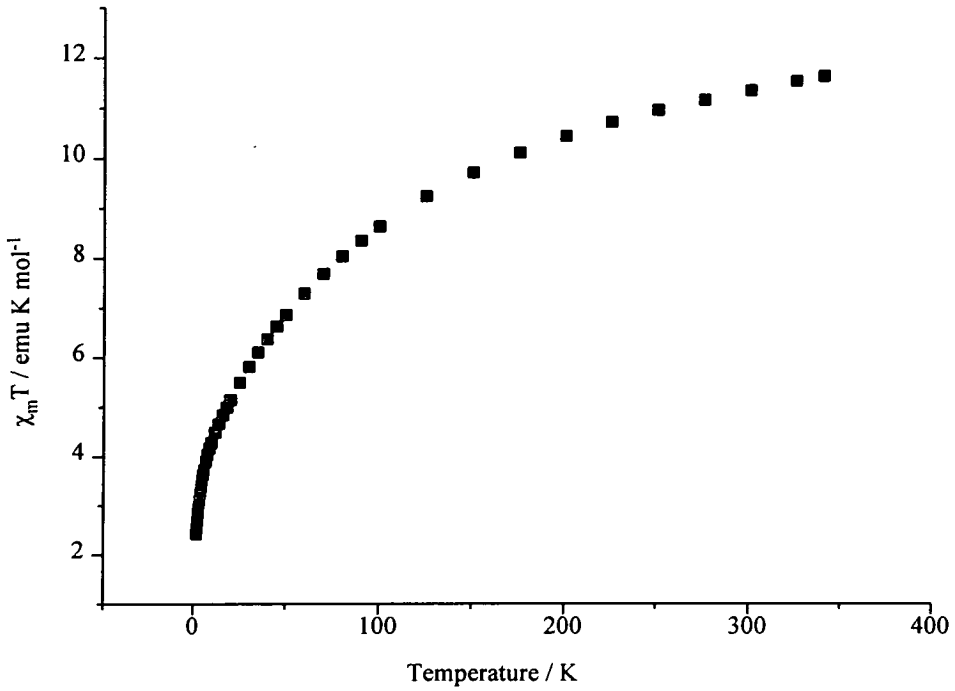

Figure 2.35. The variation of $\chi_m T$ with temperature for **17**

2.4.7. Synthesis and structure of $[Co_9(chp)_{18}]$ 18

Reaction of cobalt methoxide with two equivalents of 6-chloro-2-pyridone (Hchp) at 140 °C under nitrogen for two hours produced a purple "paste" which, after drying *in vacuo*, was crystallised from ethyl acetate to give purple crystals of $[Co_9(chp)_{18}]$ **18** [Figure 2.36] after one week [76]. The homoleptic nonanuclear cage, **18**, has crystallographic D_{3d} symmetry with the central cobalt, [Co1], lying on both a three fold axis (which also passes through Co3) and a two fold axis. The cage is clearly related to the three nickel cages **15-17**, as it contains four adamantane units. Two of the adamantanes share Co1 as a common vertex; two share the basal planes [Co2 and symmetry equivalents] with either Co1 or Co3 providing the fourth vertex. The three crystallographically unique cobalt sites are chemically distinct. Co1 is

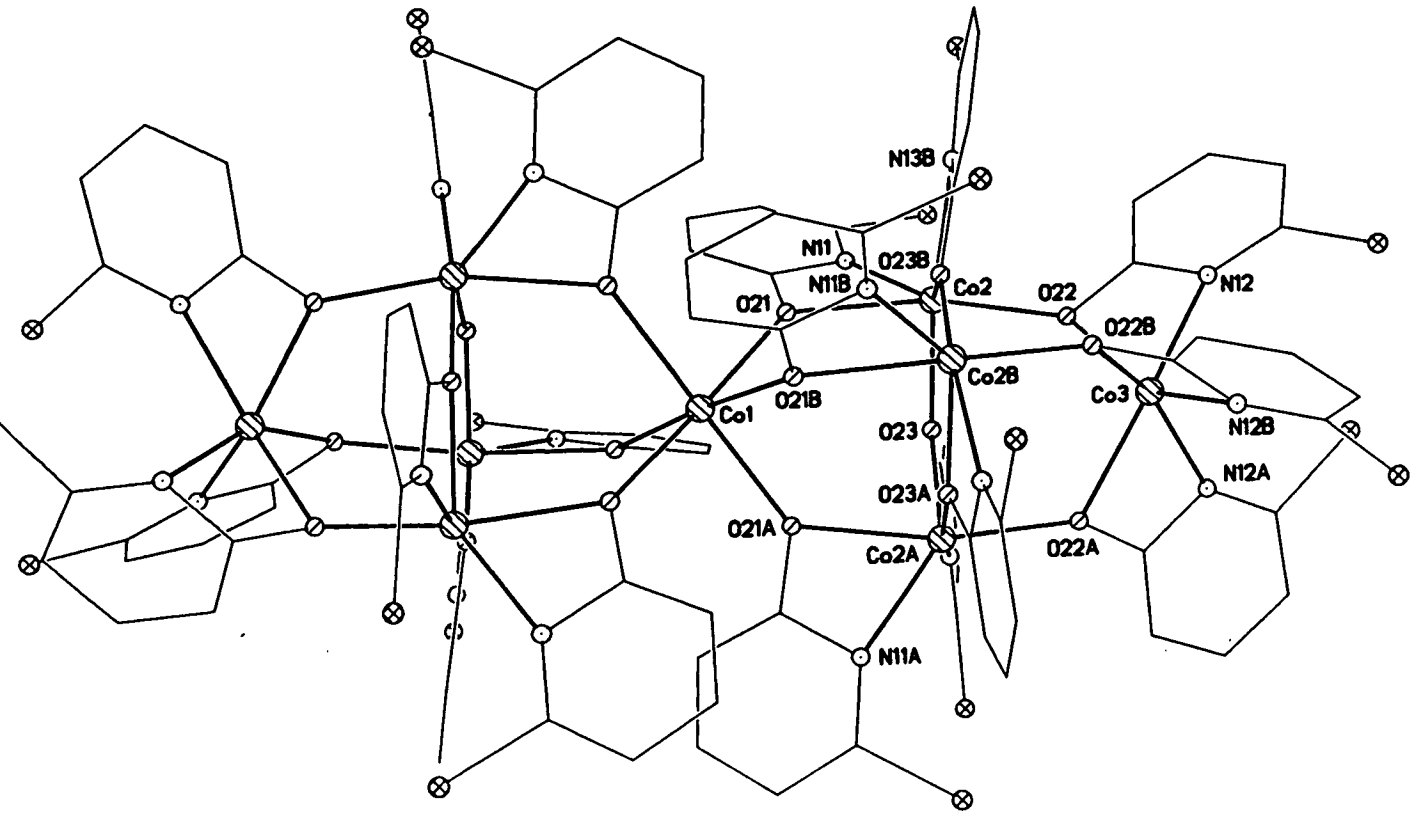

Figure 2.36. The structure of **18** in the crystal.

bound to six oxygen donors in an identical manner to the central metal sites in **15-17**. Co2 is bound to two chelating chp ligands, to two μ_2-oxygen atoms from chp ligands within the basal plane, and to one μ_2-oxygen donor which attaches the Co3 vertex to the cage. Co3 is bound to three chelating chp ligands with a *fac* geometry and with each oxygen donor bridging to the cobalt atoms of the basal plane. Comparing **18** with **15** shows that the three terminal methanol ligands and the hydrogen bonded chloride have been replaced by a $[Co(chp)_3]^-$ moiety, leaving the connectivity of the heptanuclear metal core unchanged. The metal polyhedron is shown in Figure 2.37.

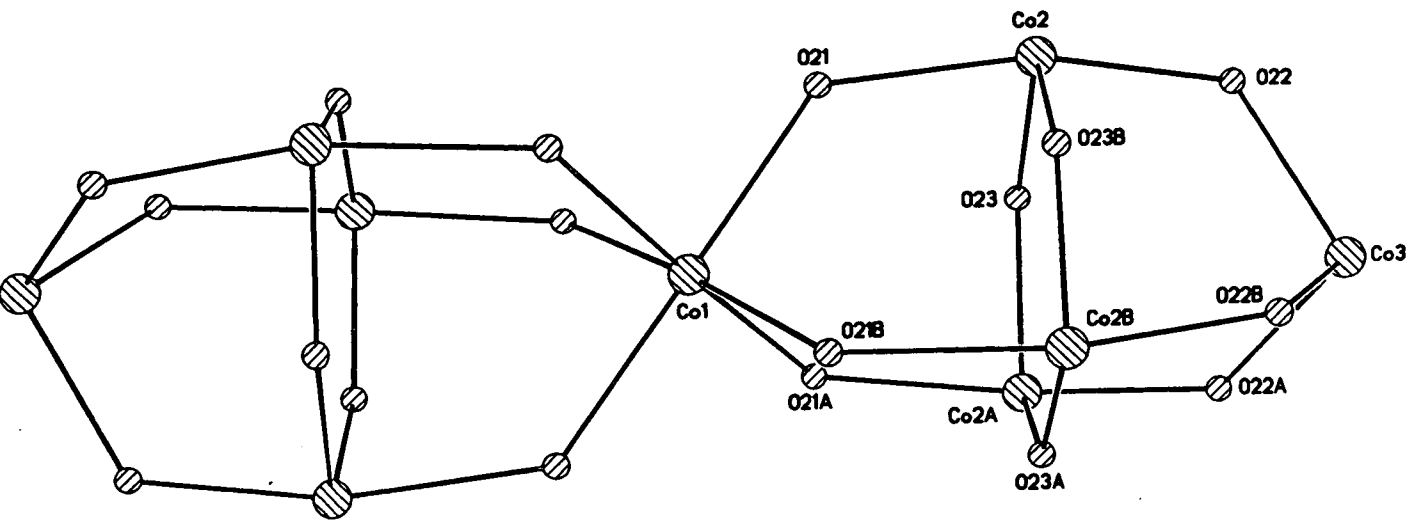

Figure 2.37. The metal polyhedron of **18.**

Like **15** there is only one type of chp ligand; chelating to one metal centre whilst bridging to a second via the exocyclic oxygen atom. The central cobalt, [Co1], has regular octahedral coordination with *trans* angles of 175.6(4)° and *cis* angles of 85.3(3) and 91.6(3)°. The Co1-O bond lengths , like that in **15**, are long at 2.316(3) Å. The other cobalts have more distorted octahedral geometries. For Co2 the distortion is so large, with only two angles approaching a typical *trans* value of *ca* 166° that an octahedral description becomes difficult to maintain and the geometry is therefore better described as irregular. The Co-O and Co-N bond lengths for Co2-Co4 all fall in the range 2.026-2.211(3) and 2.122-2.126(3) Å respectively and can be regarded as "normal". The closest Co...Co contact in **18** is 3.743(6) Å, between Co2 and Co3. Selected bond lengths and angles for **18** are given in Table 2.15.

As with **15** the length of the central Co-O bonds led to the examination that this site was in fact occupied by a sodium. Again replacement of cobalt with sodium in the crystallographic refinement produced physically meaningless results. FAB-mass spectroscopy shows peaks containing five cobalt centres and atomic absorption spectroscopy indicates the total absence of sodium [experimental section 2.6.16.]

The homoleptic chp complex of the heavier group 9 metal rhodium has been reported by Cotton et al [77]. The dimer $[Rh_2(chp)_4]$ contains a rhodium-rhodium single bond. Homoleptic dimers of chromium, molybdenum, tungsten, ruthenium, palladium and copper have all been reported with chp and / or mhp [50]. **18** is an example of the complicated arrays 3d metals will adopt to avoid forming metal-metal bonds.

2.4.8. Magnetochemistry of 18.

The magnetic behaviour of **18** was studied in the temperature range 300-1.8 K in an applied field of 1000 G. The variation of $\chi_m T$ with temperature is shown in Figure 2.38. The room temperature value of $\chi_m T$ is approximately 25 emu K mol^{-1} which is consistent with nine non-interacting S = 3/2 centres [$\chi_m T$ = 24.3 emu K mol^{-1}, g = 2.4]. The value then drops steadily with temperature to give a minimum of approximately 2.5 emu K mol^{-1} at 1.8 K. This is another example of antiferromagnetic exchange between the metal centres. The 1.8 K value corresponds to an approximately S = 1 ground state.

Table 2.15. Seleccted bond lengths (Å) and angles (°) for **18**.

Co1-O21	2.316(6)	O21A-Co1-O21D	91.6(3)
Co1-O21A	2.316(6)	O21A-Co1-O21E	85.3(3)
Co1-O21B	2.316(6)	O21B-Co1-O21C	91.6(3)
Co1-O21C	2.316(6)	O21B-Co1-O21D	85.3(3)
Co1-O21D	2.316(6)	O21B-Co1-O21E	175.6(4)
Co1-O21E	2.316(6)	O21C-Co1-O21D	91.6(3)
Co2-O21	2.111(7)	O21C-Co1-O21E	91.6(3)
Co2-O22	2.037(7)	O21D-Co1-O21E	91.6(3)
Co2-O23	2.026(7)	N11-Co2-O21	61.8(3)
Co2-O23B	2.097(7)	N11-Co2-O22	130.0(3)
Co2-N11	2.122(7)	N11-Co2-N13B	90.6(3)
Co2-N13B	2.245(7)	N11-Co2-O23	102.0(3)
Co3-O22	2.185(7)	N11-Co2-O23B	132.3(3)
Co3-O22A	2.185(7)	O21-Co2-O22	165.3(3)
Co3-O22B	2.185(7)	O21-Co2-N13B	97.5(3)
Co3-N12	2.126(7)	O21-Co2O23	87.1(3)
Co3-N12A	2.126(7)	O21-Co2-O23B	83.1(3)
Co3-N12B	2.126(7)	O22-Co2-N13B	91.5(3)
O21-Co1-O21A	91.6(3)	O22-Co2-O23	81.8(3)
O21-Co1-O21B	91.6(3)	O22-Co2-O23B	91.1(3)
O21-Co1-O21C	85.3(3)	N13B-Co2-O23	167.2(3)
O21-Co1-O21D	175.6(3)	N13B-Co2-O23B	61.5(3)
O21-Co1-O21E	91.6(3)	O23-Co2-O23B	107.6(3)
O21A-Co1-O21B	91.6(3)	Co1-O21-Co2	130.8(3)
O21A-Co1-O21C	175.6(3)	Co2-O22-Co3	124.8(3)

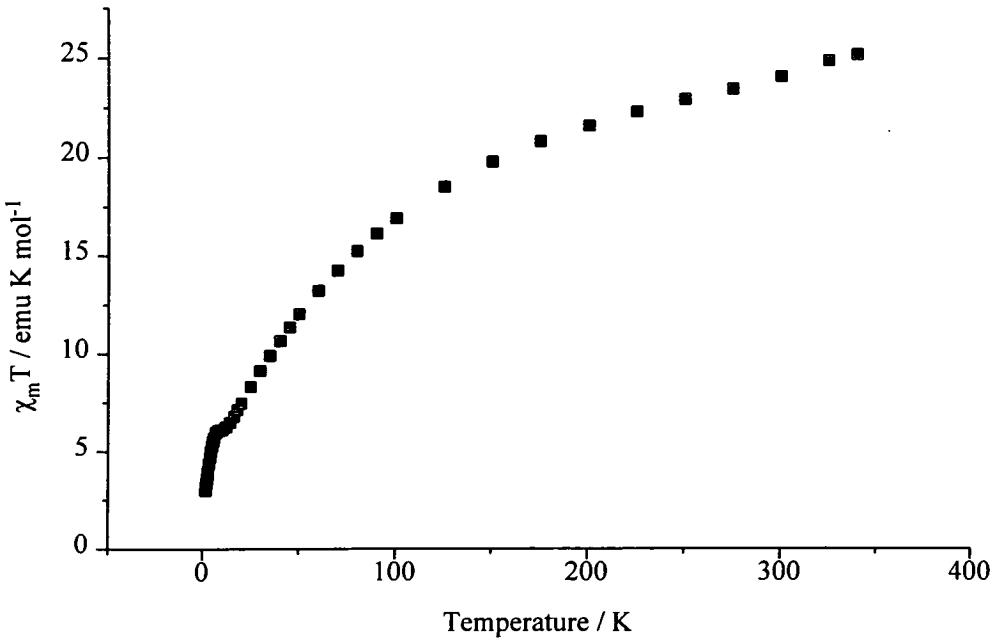

Figure 2.38. The variation of $\chi_m T$ with temperature for **18**.

2.4.9. Synthesis and structure of $[Ni_{11}(OH)_6(mhp)_{15}(Hmhp)(Cl)(H_2O)_2]$ 19.

Reaction of nickel hydroxide with two equivalents of 6-methyl-2-hydroxypyridine (Hmhp) at 160° C under nitrogen for two hours produced a green paste which, after drying *in vacuo*, was crystallised from acetonitrile to give green crystals of $[Ni_{11}(OH)_6(mhp)_{15}(Hmhp)(Cl)(H_2O)_2]$ **19** in high yield after two days [Figure 2.39]. **19** contains a $[Ni_6O_6]^{6+}$ core to which five $[Ni(mhp)_3]^-$ units are linked through either two or three μ_2-oxygen atoms from mhp ligands, capping both the square faces and three of the four rectangular faces of the core. The central nickel-oxygen core is based on two $[Ni_4O_4]^{4+}$ cubes which share a face. This polyhedron is shown in Figure 2.40. It is based on the nickel oxide structure in which each $[Ni_4O_4]$ cube shares each of its six faces with a neighbouring cube. An overlay plot of the core of **19** with Ni(II)O is shown in Figure 2.41. The standard deviation beteen the ideal and observed sites is 0.18%.

All six of the oxygen vertices within the $[Ni_6O_6]^{6+}$ core are derived from either μ_3- or μ_4-hydroxides. There are a number of distinct nickel sites within the core. Ni6 is bound to one

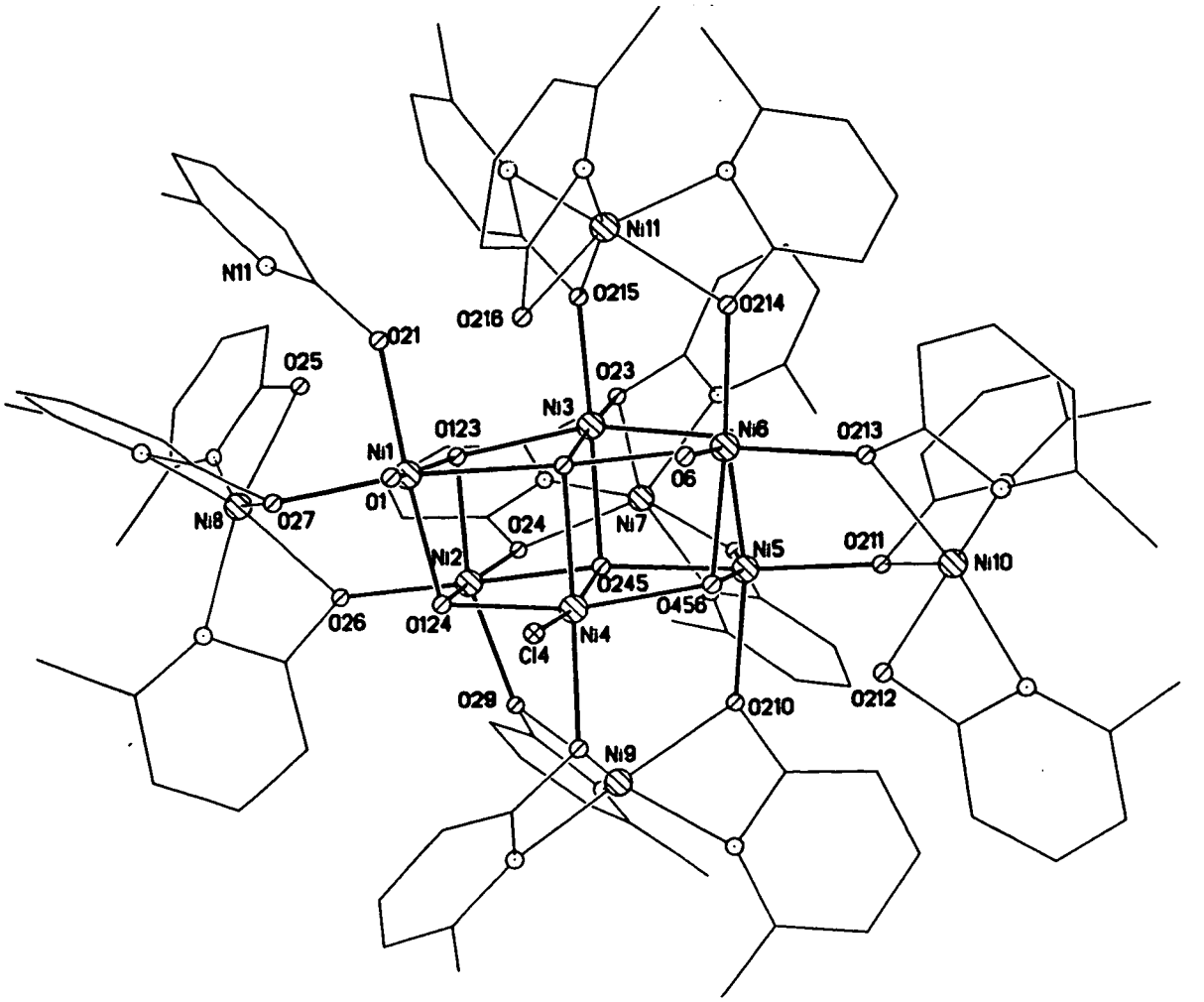

Figure 2.39. The structure of **19** in the crystal.

of the three μ_3-hydroxides which form part of the core [two bonds of 2.005(5) and 2.030(5) Å to O351 and O456 and one longer bond of 2.358(5) Å to O146], to two μ_2-oxygens from mhp's that belong to capping $[Ni(mhp)_3]^-$ units and to a terminal methanol molecule. Ni1 is bound to three μ_3-hydroxides, to one μ_2-oxygen from a capping $[Ni(mhp)_3]^-$ unit, to one mononucleating Hchp ligand and to one terminal methanol molecule. Ni2 and Ni5 are each bound to three μ_3-hydroxides and to three μ_2-oxygens from mhps from the capping $[Ni(mhp)_3]^-$ units. Ni3 is bound to four μ_3-hydroxides and two μ_2-oxygens from mhp ligands. Ni4 is also bound to four μ_3-hydroxides, one μ_2-oxygen from a chp ligand and a chloride. Ni7-Ni11 are part of the $[Ni(mhp)_3]^-$ units which cap the central $[Ni_6O_6]^{6+}$ core. These units either bind to the central core through two μ_2-oxygen atoms [Ni8, Ni10, Ni11] i.e. capping a square

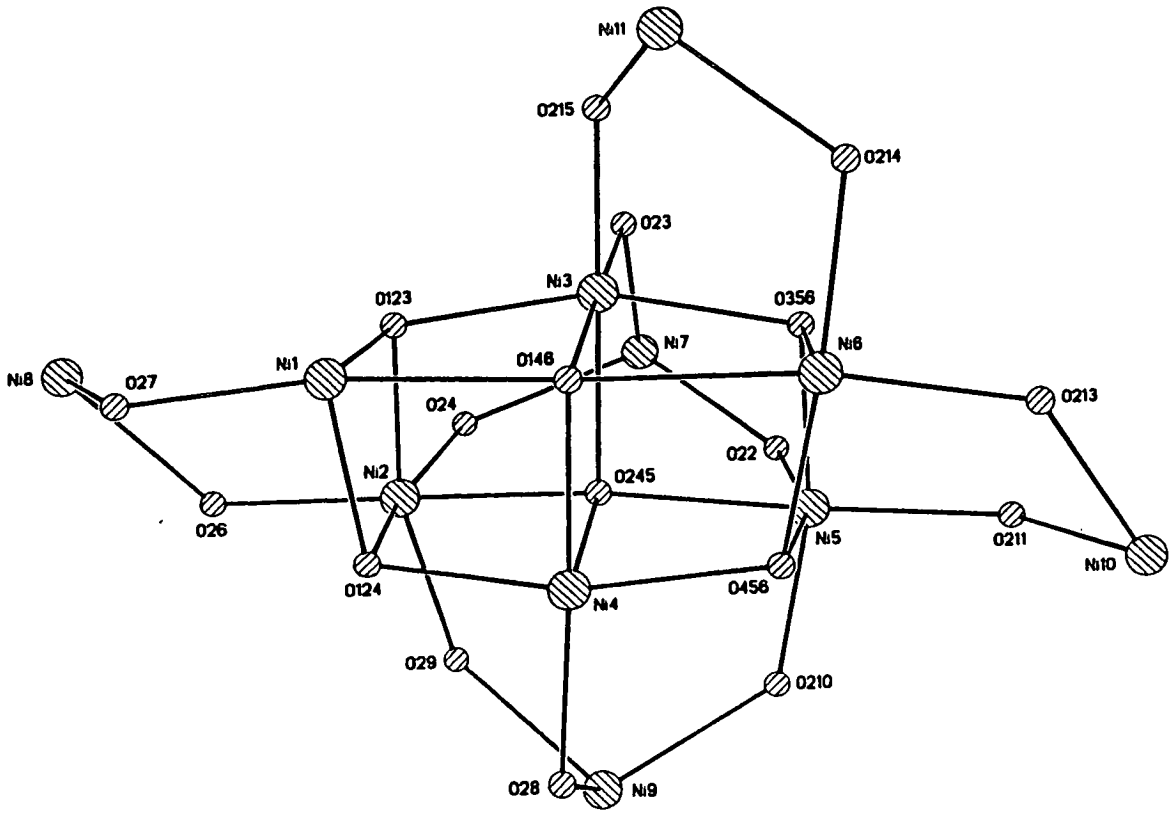

Figure 2.40. The metal polyhedron of **19**.

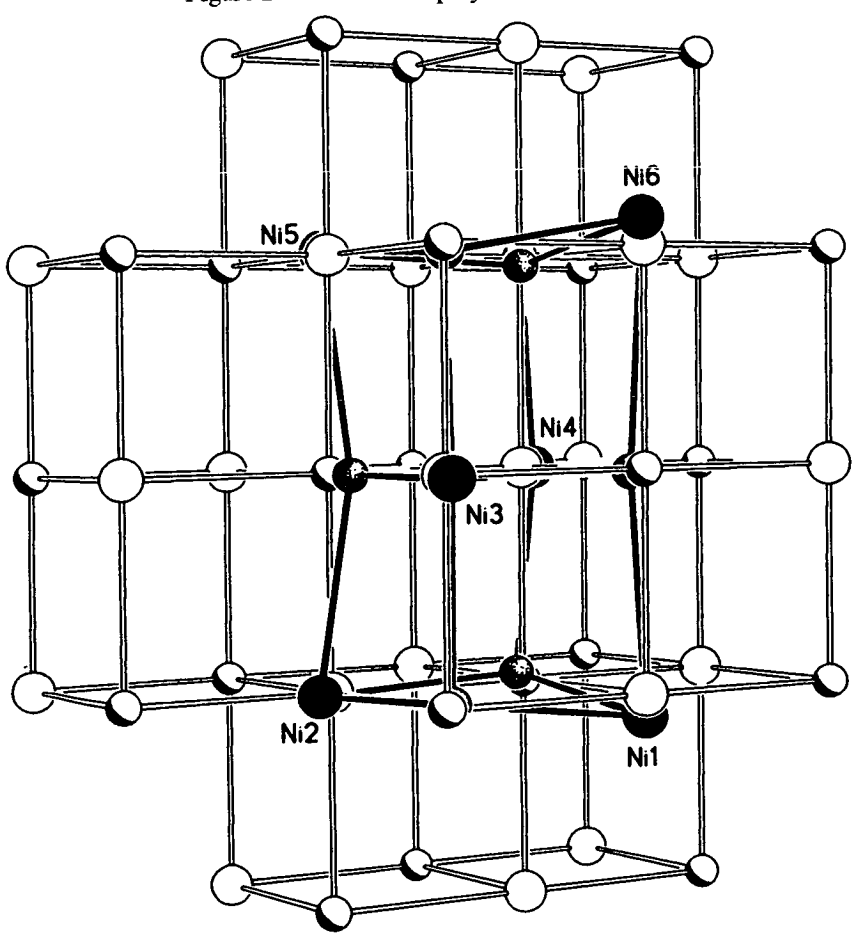

Figure 2.41. An overlay plot of the $[Ni_6O_6]^{6+}$ core of **19** on nickel (II) oxide.

face or 'half' a rectangular face, or through three μ_2-oxygen atoms [Ni7, Ni9] i.e. capping a rectangular face. Each of these $[Ni(mhp)_3]^-$ units has a *fac* geometry.The ligands show three different coordinating modes. Chelating to a nickel with the μ_2-oxygen atom bridging to a nickel in the central core. Purely chelating to a nickel in one of the $[Ni(mhp)_3]^-$ caps, whilst hydrogen bonding to the core of the structure through the exocyclic oxygen atom [for example the oxygen (O216) of the η-mhp attached to Ni11 is hydrogen bonded to two methanol molecules (O1, 2.874(5), O6, 3.035(5) Å), a μ-oxygen from an Hmhp ligand (O21, 2.957(5) Å) and a μ_4-hydroxide (O146, 2.945(5) Å)]. Mononucleating, bridging through the exocyclic oxygen only - the ring nitrogen being protonated.

The nickels which form the caps have a more distorted octahedral geometry than the nickels in the $[Ni_6O_6]^{6+}$ core since they are bound to chelating mhp ligands, with *trans* angles ranging from 148.3-166.5(2)° and *cis* angles between 62.3-111.1(3)°. Within the core itself the *trans* angles are 161.5-177.7(2)° and the *cis* angles 76.5-102.4(2)°. Selected bond lengths and angles are given in Table 2.16.

2.4.10. Magnetochemistry of 19.

The magnetic behaviour of **19** was studied in the temperature range 300- 1.8 K in an applied field of 1000 G. The variation of $\chi_m T$ with temperature is shown in Figure 2.42. The value of $\chi_m T$ at 300 K is approximately 13 emu K mol^{-1} consistent with eleven non-interacting S = 1 centres [$\chi_m T$ = 13.3 emu K mol^{-1}, g = 2.2]. The value then drops steadily with temperature to a mininmum value of approximately 3 emu K mol^{-1} at 1.8 K, corresponding to an approximately S = 2 ground state. This is another example of antiferromagnetic exchange between the Ni (II) centres.

Table 2.16. Bond lengths (Å) and angles (°) for **19**.

Ni1-O123	1.999(5)	Ni5-O245	2.154(7)
Ni1-O124	2.025(5)	Ni6-O356	2.005(6)
Ni1-O21	2.038(5)	Ni6-O213	2.020(7)
Ni1-O27	2.049(5)	Ni6-O456	2.030(5)
Ni1-O1	2.071(5)	Ni6-O214	2.061(5)
Ni1-O146	2.280(5)	Ni6-O6	2.074(5)
Ni2-O123	2.026(5)	Ni6-O146	2.358(5)
Ni2-O26	2.037(5)	Ni7-N14	2.048(7)
Ni2-O24	2.049(5)	Ni7-N13	2.058(6)
Ni2-O124	2.078(5)	Ni7-N12	2.066(7)
Ni2-O29	2.082(5)	Ni7-O23	2.110(6)
Ni2-O245	2.124(5)	Ni7-O22	2.135(6)
Ni3-O23	2.049(5)	Ni7-O24	2.143(5)
Ni3-O146	2.051(5)	Ni8-N15	2.053(7)
Ni3-O215	2.058(5)	Ni8-N16	2.056(7)
Ni3-O123	2.062(5)	Ni8-N17	2.066(7)
Ni3-O356	2.067(5)	Ni8-O27	2.091(6)
Ni3-O245	2.145(5)	Ni8-O25	2.134(6)
Ni4-O456	2.017(5)	Ni8-O26	2.167(6)
Ni4-O124	2.033(5)	Ni9-N110	2.035(6)
Ni4-O28	2.088(5)	Ni9-N19	2.048(7)
Ni4-O146	2.104(5)	Ni9-N18	2.074(7)
Ni4-O245	2.138(5)	Ni9-O28	2.085(5)
Ni4-Cl4	2.418(5)	Ni9-O210	2.119(5)
Ni5-O211	2.034(5)	Ni9-O29	2.153(5)
Ni5-O356	2.050(5)	Ni10-N112	2.059(7)
Ni5-O22	2.055(5)	Ni10-N111	2.076(6)
Ni5-O456	2.056(5)	Ni10-N113	2.079(7)
Ni5-O210	2.067(5)	Ni10-O212	2.084(7)

Table 2.16 continued

Ni10-O213	2.091(7)	O123-Ni2-O29	164.7(2)
Ni10-O211	2.157(5)	O26-Ni2-O29	100.9(2)
Ni11-N116	2.047(7)	O24-Ni2-O29	85.2(2)
Ni11-N115	2.062(7)	O124-Ni2-O29	97.6(2)
Ni11-N114	2.074(6)	O123-Ni2-O245	83.0(2)
Ni11-O214	2.082(5)	O26-Ni2-O245	173.7(2)
Ni11-O215	2.120(5)	O24-Ni2-O245	87.8(2)
Ni11-O216	2.207(6)	O124-Ni2-O245	80.0(2)
O123-Ni1-O124	83.3(2)	O29-Ni2-O245	81.8(2)
O123-Ni1-O21	93.9(2)	O23-Ni3-O146	177.0(2)
O124-Ni1-O21	176.7(2)	O23-Ni3-O215	96.1(2)
O123-Ni1-O27	99.8(2)	O146-Ni3-O215	86.9(2)
O124-Ni1-O27	91.3(2)	O23-Ni3-O123	94.8(2)
O21-Ni1-O27	91.1(2)	O146-Ni3-O123	84.7(2)
O123-Ni1-O1	163.1(2)	O215-Ni3-O123	99.3(2)
O124-Ni1-O1	100.0(2)	O23-Ni3-O356	94.4(2)
O21-Ni1-O1	82.1(2)	O146-Ni3-O356	85.3(2)
O27-Ni1-O1	96.6(2)	O215-Ni3-O356	95.7(2)
O123-Ni1-O146	80.5(2)	O123-Ni3-O356	161.5(2)
O124-Ni1-O146	80.4(2)	O23-Ni3-O245	99.5(2)
O21-Ni1-O146	97.2(2)	O146-Ni3-O245	77.5(2)
O27-Ni1-O146	171.7(2)	O215-Ni3-O245	164.2(2)
O1-Ni1-O146	83.7(2)	O123-Ni3-O245	81.6(2)
O123-Ni2-O26	94.4(2)	O356-Ni3-O245	81.0(2)
O123-Ni2-O24	92.7(2)	O456-Ni4-O124	162.0(2)
O26-Ni2-O24	98.1(2)	O456-Ni4-O28	98.2(2)
O123-Ni2-O124	81.3(2)	O124-Ni4-O28	91.2(2)
O26-Ni2-O124	93.9(2)	O456-Ni4-O146	84.2(2)
O24-Ni2-O124	166.9(2)	O124-Ni4-O146	84.7(2)

Table 2.16 continued

O28-Ni4-O146	172.7(2)	O213-Ni6-O214	91.8(2)
O456-Ni4-O245	82.8(2)	O456-Ni6-O214	174.5(2)
O124-Ni4-O245	80.7(2)	O356-Ni6-O6	165.5(2)
O28-Ni4-O245	96.9(2)	O213-Ni6-O6	94.3(2)
O146-Ni4-O245	76.5(2)	O456-Ni6-O6	95.9(2)
O456-Ni4-Cl4	97.1(2)	O214-Ni6-O6	86.8(2)
O124-Ni4-Cl4	97.8(2)	O356-Ni6-O146	79.0(2)
O28-Ni4-Cl4	92.7(2)	O213-Ni6-O146	170.5(2)
O14-Ni4-Cl4	93.79(15)	O456-Ni6-O146	77.7(2)
O245-Ni4-Cl4	170.29(15)	O214-Ni6-O146	97.7(2)
O211-Ni5-O356	94.9(2)	O6-Ni6-O146	86.7(2)
O211-Ni5-O22	102.4(2)	N14-Ni7-N13	104.7(3)
O356-Ni5-O22	94.0(2)	N14-Ni7-N12	107.8(3)
O211-Ni5-O456	95.3(2)	N13-Ni7-N12	104.1(3)
O356-Ni5-O456	81.8(2)	N14-Ni7-O23	97.8(2)
O22-Ni5-O456	162.2(2)	N13-Ni7-O23	64.0(2)
O211-Ni5-O210	96.7(2)	N12-Ni7-O23	154.0(2)
O356-Ni5-O210	168.0(2)	N14-Ni7-O22	165.4(2)
O22-Ni5-O210	86.5(2)	N13-Ni7-O22	89.1(2)
O456-Ni5-O210	94.1(2)	N12-Ni7-O22	63.2(2)
O211-Ni5-O245	175.2(2)	O23-Ni7-O22	92.5(2)
O356-Ni5-O245	81.2(2)	N14-Ni7-O24	63.0(2)
O22-Ni5-O245	80.7(2)	N13-Ni7-O24	14.3(2)
O456-Ni5-O245	81.5(2)	N12-Ni7-O24	107.5(2)
O210-Ni5-O245	87.1(2)	O23-Ni7-O24	87.8(2)
O356-Ni6-O213	100.2(2)	O22-Ni7-O24	107.3(2)
O356-Ni6-O456	83.6(2)	N15-Ni8-N16	110.7(3)
O213-Ni6-O456	92.7(2)	N15-Ni8-N17	105.0(3)
O356-Ni6-O214	92.6(2)	N16-Ni8-N17	100.2(3)

Table 2.16 continued

N15-Ni8-O27	156.4(3)	N111-Ni10-N113	101.5(3)
N16-Ni8-O27	92.4(3)	N112-Ni10-O212	64.6(2)
N17-Ni8-O27	64.6(3)	N111-Ni10-O212	163.0(3)
N15-Ni8-O25	63.6(3)	N113-N10-O212	95.4(3)
N16-Ni8-O25	164.5(3)	N112-Ni10-O213	156.8(3)
N17-Ni8-O25	95.3(3)	N111-Ni10-O213	90.7(2)
O27-Ni8-O25	95.2(2)	N113-Ni10-O213	64.2(2)
N15-Ni8-O26	103.4(2)	O212-Ni10-O213	96.6(2)
N16-Ni8-O26	63.1(2)	N112-Ni10-O211	108.0(2)
N17-Ni8-O26	150.9(2)	N111-Ni10-O211	62.3(2)
O27-Ni8-O26	91.1(2)	N113-Ni10-O211	149.1(2)
O25-Ni8-O26	103.2(2)	O212-Ni10-O211	102.5(2)
N110-Ni9-N19	106.4(3)	O213-Ni10-O211	88.7(2)
N110-Ni9-N18	105.4(3)	N116-Ni11-N115	107.6(3)
N19-Ni9-N18	105.9(3)	N116-Ni11-N114	109.3(3)
N110-Ni9-O28	99.0(2)	N115-Ni11-N114	99.7(3)
N19-Ni9-O28	154.5(2)	N116-Ni11-O214	101.9(2)
N18-Ni9-O28	64.3(2)	N115-Ni11-O214	149.9(2)
N110-Ni9-O210	64.1(2)	N114-Ni11-O214	64.0(2)
N19-Ni9-O210	101.6(2)	N116-Ni11-O215	160.9(2)
N18-Ni9-O210	152.4(2)	N115-Ni11-O215	63.3(2)
O28-Ni9-O210	91.2(2)	N114-Ni11-O215	89.3(2)
N110-Ni9-O29	166.5(2)	O214-Ni11-O215	90.1(2)
N19-Ni9-O29	63.3(2)	N116-Ni11-O216	63.1(2)
N18-Ni9-O29	86.4(2)	N115-Ni11-O216	106.7(2)
O28-Ni9-O29	91.9(2)	N114-Ni11-O216	153.6(2)
O210-Ni9-O29	108.0(2)	O214-Ni11-O216	91.9(2)
N112-Ni10-N111	111.1(3)	O215-Ni11-O216	102.1(2)
N112-Ni10-N113	102.4(3)	Ni1-O123-Ni2	98.1(2)

Table 2.16 continued

Ni1-O123-Ni3	100.9(2)	Ni6-O356-Ni5	96.4(2)
Ni2-O123-Ni3	99.4(2)	Ni6-O356-Ni3	102(2)
Ni1-O124-Ni4	101.3(2)	Ni5-O356-Ni3	101.2(2)
Ni1-O124-Ni2	95.5(2)	Ni4-O456-Ni6	104.9(2)
Ni4-O124-Ni2	101.4(2)	Ni4-O456-Ni5	100.1(2)
Ni3-O146-Ni4	105.2(2)	Ni6-O456-Ni5	95.4(2)
Ni3-O146-Ni1	92.3(2)	Ni3-O23_Ni7	116.0(2)
Ni4-O146-Ni1	91.3(2)	Ni2-O24-Ni7	128.0(2)
Ni3-O146-Ni6	91.5(2)	Ni2-O26-Ni8	123.3(2)
Ni4-O146-Ni6	91.8(2)	Ni1-O27-Ni8	119.4(2)
Ni1-O146-Ni6	174.4()	Ni9-O28-Ni4	117.1(2)
Ni2-O245-Ni4	96.6(2)	Ni2-O29-Ni9	129.9(2)
Ni2-O245-Ni3	93.8(2)	Ni5-O210-Ni9	127.7(2)
Ni4-O245-Ni3	100.8(2)	Ni5-O211-Ni10	123.9(2)
Ni2-O245-Ni5	164.9(2)	Ni6-O213-Ni10	127.2(2)
Ni4-O245-Ni5	93.4(2)	Ni6-O214-Ni11	121.7(2)
Ni3-O245-Ni5	95.5(2)	Ni3-O215-Ni11	132.1(3)

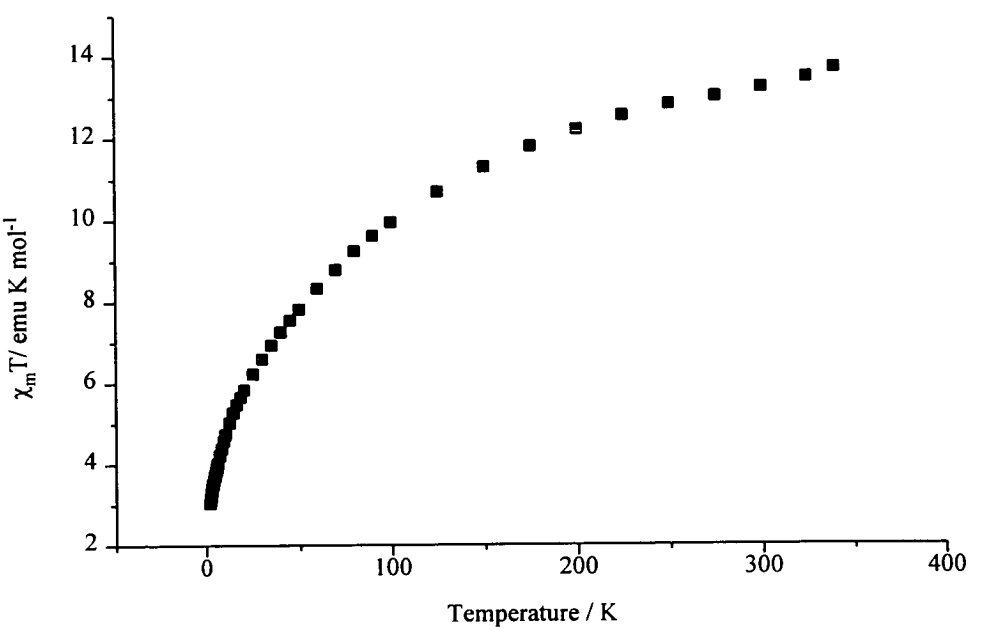

Figure 2.42. The variation of $\chi_m T$ with temperature for **19**.

2.5. Conclusions.

This chapter outlined a number of simple synthetic strategies that can be employed to produce polymetallic nickel and cobalt complexes from metal salts and simple but coordinatively flexible ligands. It also demonstrated the structural importance imparted by the ligand, solvent and metal.

Polymetallic complexes of metals in high oxidation states have been reported which contain as many as 154 metal centres [78]. High nuclearity clusters of low oxidation states rival these species in size, with chalcogenide bridged complexes involving 146 metals structurally characterised [79]. Complexes where the metals are in moderate oxidation states however do not approach these compounds in nuclearity, with the largest reported being an Fe_{20} compound [80]. $[Co_{24}(OH)_{18}(OMe)_2(Cl)_6(mhp)_{22}]$ **14** is the highest nuclearity complex containing cobalt, and consists of cubic-close packed planes of hydroxide, methoxide or chloride anions bridging Co (II) centres. Preliminary magnetic studies indicate the presence of a high spin ground state and the possibility of superparamagnetic behaviour.

Compounds **1-11** and **14** can all be synthesised from the metal chloride and Na(xhp). This is summarised in Table 2.17 below, and illustrates the importance that the ligand, solvent and metal all have in determining the nature of the final product. For example, (A) the effect of the solvent : recrystallisation from dichloromethane rather than acetonitrile produces a cobalt dodecamer [**8**] rather than a heterobimetallic polymer [**10**] from an otherwise identical reaction. In general polar coordinating solvents produce smaller metal clusters than do non-polar non-coordinating solvents - the ligation of solvent molecules such as methanol or acetonitrile to metal centres prevents further oligomerisation. (B) The effect of the ligand : changing chp for mhp produces **6** rather than **3**. The change in structure here is unsurprising given the tautomeric preferences for chp to bind through the oxygen only and for mhp to use

Table 2.17. A summary of the compounds produced from MCl_2 and Na(xhp)

Metal	xhp	Sol A	Sol B	Compound produced
Ni	chp	MeOH	MeOH	$[Ni_4(OMe)_4(chp)_4(MeOH)_7]$ **1**
Ni	bhp	MeOH	MeOH	$[Ni_4(OMe)_4(bhp)_4(MeOH)_7]$ **2**
Co	chp	MeOH	MeOH	$[Co_4(OMe)_4(chp)_4(MeOH)_7]$ **7**
Ni	chp	MeOH	MeCN	$[Ni_2Na_2(chp)_6(H_2O)(MeCN)_4]$ **3**
Ni	chp	MeOH	MeCN	$[Ni_2Na_2(chp)_6(H_2O)_2(MeCN)_4]$ **4**
Ni	chp	MeOH	EtOAc	$[Ni_2Na_2(chp)_6(H_2O)]_n$ **5**
Co	chp	MeOH	MeCN	$[Co_2Na_2(chp)_6(H_2O)]_n$ **10**
Co	chp	MeOH	EtOAc	$[Co_2Na_2(chp)_6]$ **11**
Ni	mhp	MeOH	MeCN/ EtOAc	$[Ni_4Na_4(mhp)_{12}(Hmhp)_2]$ **6**
Co	mhp	MeOH	EtOAc	$[Co_{24}(OH)_{18}(Cl)_6(OMe)_2(mhp)_{22}]$ **14**
Co	chp	MeOH	CH_2Cl_2	$[Co_{12}(OH)_4(chp)_{18}(Hchp)_2(Cl)_2(MeOH)_2]$ **8**
Co	chp	EtOAc	MeCN	$[Co_{10}(OH)_4(chp)_{16}(MeCN)_2]$ **9**

where M = Ni, Co; Sol A = initial solvent; Sol B= crystallisation solvent

both the oxygen and nitrogen atoms. (C) The effect of the metal : replacing nickel with cobalt in an otherwise identical reaction produces a teraicosanuclear species [**14**] rather than a heterobimetallic species [**6**]. Structural differences between nickel and cobalt probably arise from nickels preference for regular octahdral geometry when six-coordinate.

Complexes **15-18** are the first reported nickel and cobalt complexes which contain M_4O_6 adamantane units. They are also the first examples of vertex- and face- sharing adamantanes. Structures featuring a central M_4O_6 core have been reported for the 3d-metals from titanium to iron [81-89] however it remains comparatively rare with only a dozen examples known. Compounds containing this core have never been reported for the later 3d-metals, and only one example exists where adamantane units are linked into higher nuclearity clusters. This

is an iron complex reported by Nair and Hagen [90] in which the two adamantane units share an edge. One of these adamantane complexes, the cobalt nonamer, is a homoleptic complex and perhaps suggests that the synthesis of large polynuclear arrays is not always dependent on the use of either heteroleptic or multifunctional ligand sets.

Another important feature is the structural role played by water. In the vast majority of the complexes reported in this chapter the structures are held together through both bridging pyridonate and hydroxide ligands, with the source of the hydroxides being the use of 'wet' solvents. This is most clearly established in the structure of the cobalt tetraicosahedron, but is a prominent feature throughout this work. The utilisation of 'dry' solvents in anaerobic conditions has previosly been studied in cobalt pyridonate chemistry and has proved to be largely unproductive [51].

2.6. Experimental Section.

All solvents and other reagents were used as obtained. Na(xhp) were synthesised from Hxhp and NaOMe in MeOH. Hbhp was synthesised by a published procedure[91].

2.6.1. $[Ni_4(OMe)_4(chp)_4(MeOH)_7]$.MeOH 1.

1 may be synthesised in a number of ways.

a) $NiCl_2.6H_2O$ (1.000g, 4.21 mmol) and Na(xhp) (1.275g, 8.41 mmol) were stirred in MeOH (30ml) for 24 hours. The resulting solution was filtered and the solvent removed producing a paste which was dried *in vacuo*. Crystallisation of this paste from fresh MeOH (20ml) produces **1** in 80% yield after 24 hours.

b) $Ni(CCl_3COO)_2.4H_2O$ (1.000g, 2.19 mmol) was mixed with Hchp (0.567g, 4.38 mmol) in a Schlenk tube under N_2 and heated to 140°C for 2 hours producing a paste. The trichloroacetic acid and water produced during reaction were pumped off into a cold trap. The paste was then crystallised from MeOH (20ml) producing **1** in 60% yield after 24 hours.

c) $NiCl_2$ (0.500g, 3.86 mmol) and Na(chp) (1.170g, 7.72 mmol) was stirred in MeOH (50ml) for 24 hours, in which time the the colour of the solution turned from yellow to green. This solution was filtered to remove any unreacted $NiCl_2$ and the solvent removed producing a green paste which was crystallised from MeOH (20ml) to give **1** in 50% yield.

CHN, observed (expected); C, 34.0 (34.0); H, 4.61 (4.61); N, 4.96 (4.96) %.

FAB-MS : no significant peaks observed.

2.6.2. $[Ni_4(OMe)_4(bhp)_4(MeOH)_7]$.MeOH 2.

2 may be synthesised in an identical manner to **1**, replacing the pyridonate with the bromine analogue.

CHN, observed (expected); C, 29.2 (29.4); H, 4.02 (4.15); N, 4.20 (4.29) %.

FAB-MS : no significant peaks observed.

2.6.3. $[Ni_2Na_2(chp)_6(MeCN)_4(H_2O)]$ 3.

a) $NiCl_2$ (0.500g, 3.86 mmol) and Na(chp) (1.170, 7.72 mmol) were stirred in MeOH (30 ml) for 24 hours. The solution was filtered and the solvent removed producing a paste, which was dried *in vacuo*. The paste was crystallised from MeCN (20ml) to give crystals of **3** in 75% yield after 2 days.

b) $NiCl_2.6H_2O$ can be used in place of $NiCl_2$ in an identical manner to the above producing **3** in 70% yield.

CHN; observed (expexted); C, 40.6 (40.8); H, 2.9 (2.9); N, 12.1 (12.5) %.

FAB-MS (significant peaks, possible assignments) : m/z 1117, $[Ni_2Na_2(chp)_6(MeCN)_4(H_2O)]^+$; 806, $[Ni_2Na_2(chp)_6]^+$; 655, $[Ni_2Na(chp)_4]^+$; 339, $[NiNa(chp)_2]^+$.

2.6.4. $[Ni_2Na_2(chp)_6(MeCN)_4(H_2O)_2]$ 4.

a) **4** was co-crystallised with **3** when the above reaction was repeated in the presence of 1 mole equivalent of $Na(PhCH_2CO_2)$.

b) $NiCl_2.6H_2O$ may be used in place of $NiCl_2$. Yield for both 10%.

CHN; observed (expected); C, 40.6 (40.5); H, 2.7 (2.9); N, 11.9 (12.4).

FAB-MS : as for **3**.

2.6.5. $[Ni_2Na_2(chp)_6(H_2O)]n$ 5.

$NiCl_2$ (0.250g, 1.3 mmol) and Na(chp) (0.554g, 3.86 mmol) were stirred in MeOH (50 ml) for 24 hours, after which the solution was filtered and the paste produced dried *in vacuo*.

Crystallisation from EtOAc (15 ml) gave green crystals of **5** in 40 % yield.

CHN, observed (expected); C, 37.8 (37.8); H, 2.1 (2.1); N, 8.8 (8.8).

FAB-MS (significant peaks, possible assignments) : m/z 766, $[Ni_2Na_2(chp)_4(H_2O)]^+$; 614, $[NiNa(chp)_4(H_2O)]^+$; 485, $[NiNa(chp)_3(H_2O)]^+$; 444, $[Ni(chp)_3]^+$; 303, $[Na_2(chp)_2]^+$; 280, $[Na(chp)_2]^+$; 210, $[NiNa(chp)_2]^+$; 187, $[Ni(chp)]^+$; 152, $[Na(chp)]^+$.

2.6.6. $[Ni_4Na_4(mhp)_{12}(Hmhp)_2]$ 6.

Na(mhp) (0.506g, 3.86 mmol) was added to a stirred solution of $NiCl_2$ (0.250g, 1.3 mmol) in MeOH (30ml). After 24 hours the green solution was filtered and the filtrate evaporated to dryness under reduced pressure leaving a green paste. Crystallisation of this paste from MeCN (20ml) or EtOAc (20ml) gives crystals of **6** in 70% yield.

CHN, observed (expected); C, 54.6 (54.7); H, 4.6 (4.7); N, 10.5 (10.6).

FAB-MS (significant peaks, possible assignments) : m/z 1843, $[Ni_4Na_4(mhp)_{12}(Hmhp)_2]^+$; 1734, $[Ni_4Na_4(mhp)_{12}(Hmhp)]^+$; 1625, $[Ni_4Na_4(mhp)_{12}]^+$; 1409, $[Ni_4Na_4(mhp)_{10}]^+$; 1326, $[Ni_3Na_3(mhp)_{10}]^+$; 704, $[Ni_2Na_2(mhp)_6]^+$; 596, $[Ni_2Na_2(mhp)_4]^+$; 537 $[NiNa_2(mhp)_4]^+$;429, $[NiNa_2(mhp)_3]^+$; 406, $[NiNa(mhp)_3]^+$; 298, $[NiNa(mhp)_2]^+$.

2.6.7. $[Co_4(OMe)_4(chp)_4(MeOH)_7]$.MeOH 7.

a) $Co(OAc)_2.4H_2O$ (1.000g, 4.02 mmol) and Hchp (1.01g, 8.03 mmol) were mixed in a Schlenk tube and heated to 140°C under N_2 for 2 hours producing a purple paste. The acetic acid and water produced were pumped off into a cold trap. The paste was then added to a solution of MeOH (25 ml) which contained Na(OMe) (0.218g, 4.02 mmol). Crystals of **7** were produced in 90 % yield after 1 day.

b) $CoCl_2.6H_2O$ (1.000g, 4.20 mmol) and Na(chp) (1.274g, 8.40 mmol) were stirred in MeOH (30 ml) for 24 hours. Removal of the solvent produced a purple paste which was dried *in vacuo*. This was then added to a solution of MeOH (25ml) containing Na(OMe) (0.277g, 4.20

mmol) and placed in the fridge at -5°C for 24 hours. Purple crystals of **7** were produced in 30 % yield after 24 hours.

CHN, observed (expected); C, 34.0 (34.0); H, 4.61 (4.61); N, 4.96 (4.96) %.

FAB-MS : no sigificant peaks observed.

2.6.8. $[Co_{12}(OH)_4(chp)_{18}(Hchp)_2(Cl)_2(MeOH)_2]$ 8.

$CoCl_2$ (0.507g, 3.90 mmol) and Na(chp) (1.212g, 8.00 mmol) were stirred in MeOH (30ml) for 3 hours at room temperature. The solution was filtered and the solvent removed producing a purple paste which was dried *in vacuo*. Crystallisation of this paste from CH_2Cl_2 (20ml) gave crystals of **8** in 20 % yield.

CHN, observed (expected); C, 35.6 (35.8); H, 2.10 (2.12); N, 7.95 (8.04) %.

FAB-MS : no significant peaks observed.

2.6.9. $[Co_{10}(OH)_4(chp)_{16}(MeCN)_2]$ 9.

$CoCl_2$ (0.507g, 3.90 mmol) and Na(chp) (1.212g, 8.00 mmol) were stirred in EtOAc (50 ml) for 24 hours before filtration and solvent removal. The resultant purple paste was dried *in vacuo* for several hours. Crystallisation of this paste from MeCN (20 ml) produced purple crystals of **9** in 10 % yield after 3 days.

CHN, observed (expected); C,35.9 (36.0); H, 1.85 (2.07); N, 8.90 (9.01) %.

FAB-MS : no significant peaks observed.

2.6.10. $[Co_2Na_2(chp)_6(H_2O)]_n$ 10.

$CoCl_2$ (0.507, 3.90 mmol) and Na(chp) (1.212g, 8.00 mmol) were stirred in MeOH (50 ml) for 24 hours. The solvent was removed under reduced pressure and the paste dried in vacuo. Recrystallisation of the paste from MeCN (20 ml) produced purple crystals of **10** in 10 % yield

after 4 days.

CHN, observed (expected); C, 37.8 (37.8); H, 2.00 (2.01); N, 8.60 (8.80) %.

FAB-MS (significant peaks, possible assignments) : m/z 766, $[CoNa_2(chp)_5(H_2O)]^+$; 485, $[CoNa(chp)_3(H_2O)]^+$; 280, $[Na(chp)_2]^+$.

2.6.11. $[Co_2Na_2(chp)_6]_n$ 11.

$CoCl_2$ (0.250g, 1.94 mmol) and Na(chp) (0.591g, 3.90 mmol) were stirred in a solution of MeOH (40 ml) that contained one equivalent of $Na(HCO_2)$ (0.135g, 1.94 mmol). After 24 hours the solution was filtered and the solvent removed producing a paste which was dried *in vacuo* for several hours. Crystallisation of the paste from EtOAc (15 ml) produced purple crystals of **11** after one day in 10 % yield.

CHN, observed (expected) ; C, 38.4 (38.5); H, 1.90 (1.93); N, 8.75 (8.98) %.

FAB-MS (significant peaks, possible assignments) : m/z 806, $[Co_2Na_2(chp)_5]^+$; 655, $[Co_2Na(chp)_4]^+$; 504, $[Co_2(chp)_3]$+; 339, $[CoNa(chp)_2]$; 303, $[Na_2(chp)_2]^+$.

2.6.12. $[Co_{24}(OH)_{18}(Cl)_6(OMe)_2(mhp)_{22}]$ 14

$CoCl_2$ (0.500g, 3.88 mmol) and Na(mhp) (1.020g, 7.78 mmol) were stirred in MeOH (40 ml) for 24 hours. The solvent was removed and the blue / purple paste produced dried *in vacuo*. Crystallisation of this paste from EtOAc (25 ml) produced **14** in a maximum of 20 % yield over a period of one week.

CHN, observed (expected); C, 36.7 (36.7); H, 3.50 (3.56); N, 6.98 (7.04) %.

FAB -MS: no significant paks observed.

2.6.13. $[Ni_7(Cl)_2(chp)_{12}(MeOH)_6]$ 15.

$NiCl_2.6H_2O$ (1.000g, 4.21 mmol) was reacted with Na(OH) (0.330g, 8.25 mmol) in H_2O (50

ml) producing a green precipitate of $Ni(OH)_2.2H_2O$ which was filtered and washed with H_2O (5 x 20 ml) and dried *in vacuo*. The resultant $Ni(OH)_2.2H_2O$ was mixed with Hchp (1.065g, 8.22 mmol) and heated to 140°Cunder N_2 in a Schlenk tube for approximately 2 hours, producing a melt. The water produced during the reaction was pumped into a cold trap and any excess Hchp sublimed to a cold finger. The melt was then dissolved in a 1:1 MeOH / MeCN solution (15 ml) producing green crystals of **15** in 30 % yield after 3 days.

CHN, observed (expected); C, 35.6 (35.7); H, 2.50 (2.71); N, 7.40 (7.58); Ni, 17.9 (18.5); Na, 0 (0) %.

FAB-MS (significant peaks, possible assignments) : m/z 2181, $[Ni_7(chp)_{12}(MeOH)_6Cl]^+$; 1921, $[Ni_7(chp)_{11}(MeOH)_3]^+$; 1862, $[Ni_6(chp)_{11}(MeOH)_3]^+$; 1830, $[Ni_6(chp)_{10}(MeOH)_6]^+$; 1734, $[Ni_6(chp)_8(MeOH)_4]^+$; 1605,$[Ni_6(chp)_9(MeOH)_3]^+$; 1509, $[Ni_6(chp)_8(MeOH)_4]^+$; 1477, $[Ni_6(chp)_8(MeOH)_3]^+$; 1413, $[Ni_6(chp)_8(MeOH)]^+$; 1348, $[Ni_6(chp)_7(MeOH)_3]^+$;1284, $[Ni_6(chp)_7(MeOH)]^+$; 1205, $[Ni_3(chp)_8]^+$; 889, $[Ni_2(chp)_6]^+$; 573, $[Ni(chp)_4]^+$; 503, $[Ni_2(chp)_3]^+$; 375, $[Ni_2(chp)_2]^+$.

2.6.14 $[Ni_7(OH)_2(chp)_{12}(MeOH)_6]$ 16.

Synthesis as for **15** using Na(OMe) in place of NaOH, and MeOH in place of H_2O. Crystals grew after 2 days. Yield 25 %.

CHN, observed (expected); C, 36.0 (36.3); H, 2.71 (2.84); N, 7.63 (7.71) %.

FAB-MS (significant peaks, possible assignments) : m/z as for **15** except peak at m/z 2180 assigned as $[Ni_7(OH)_2(chp)_{12}(MeOH)_6]^+$.

2.6.15. $[Ni_9(OH)_2(chp)_{16}(MeCN)_2]$ 17.

Synthesis as for **15** except MeCN (20 ml) alone was used for crystallisation. Crystals grew after one day. Yield 80 %.

CHN, observed (expected); C,37.2 (37.3); H, 2.00 (2.07); N, 9.30 (9.33) %.

FAB-MS (significant peaks, possible assignments) : m/z 2490, $[Ni_9(OH)_2(chp)_{15}]^+$; 2174, $[Ni_8(OH)_2(chp)_{13}]^+$; 1602, $[Ni_7(OH)_2(chp)_9]^+$; 1526, $[Ni_6(OH)(chp)_9]^+$; 1288, $[Ni_4(OH)_4(chp)_8]$+; 1205, $[Ni_3(chp)_8]^+$; 889, $[Ni_2(chp)_6]^+$; 572, $[Ni(chp)_4]^+$.

2.6.16. $[Co_9(chp)_{18}]$ 18.

Synthesis as for **15**, using Co in place of Ni, and crystallisation was from EtOAc (20 ml).

Purple crystals formed after one week. Yield = 14 %.

CHN, observed (expected); C, 37.7 (38.0); H, 1.89 (1.90); N, 8.80 (8.86); Co,18.0 (18.7); Na, 0 (0) %.

FaB-MS (significant peaks, possible assignments) : m/z 1522, $[Co_4(chp)_{10}]^+$; 1323, $[Co_5(chp)_8]^+$; 1264, $[Co_4(chp)_8]^+$; 1195, $[Co_5(chp)_7]^+$; 1136, $[Co_4(chp)_7]^+$; 820, $[Co_3(chp)_5]^+$; 632, $[Co_2(chp)_4]^+$; 573, $[Co(chp)_4]$+; 504, $[Co_2(chp)_3]^+$; 445, $[Co(chp)_3]^+$; 316, $[Co(chp)_2]^+$.

2.6.17. $[Ni_{11}(OH)_6(mhp)_{15}(Hmhp)(Cl)(H_2O)_2]$ 19.

Synthesis as for **16** using Hmhp in place of Hchp. Crystals were grown from MeCN (20 ml) alone after one day in 74 % yield.

CHN, observed (expected); C, 45.2 (45.2); H, 4.01 (4.16); N, 8.70 (8.78) %.

FAB-MS : no significant peaks observed.

CHAPTER 3

NICKEL AND COBALT CARBOXYLATE COMPLEXES OF 6-METHYL-2-PYRIDONE : A FAMILY OF CENTRED-TRICAPPED-TRIGONAL PRISMS AND OTHER DELTAHEDRA.

3.1. Introduction.

This chapter illustrates the synthesis and structure of a number of novel polynuclear nickel and cobalt carboxylate complexes of 6-methyl-2-pyridone. In 1983 Garner and co-workers reported the synthesis of a dodecanuclear species $[Co_{12}(OH)_6(mhp)_{12}(O_2CCH_3)_6]$ **20** whose structure was based on a centred-pentacapped-trigonal prism [Figure 3.1] [54]. It appeared fascinating partly due to the attractiveness of the structure but mainly due to the high nuclearity of the metal array present (the compound is among the highest nuclearity cobalt complexes known with oxygen and nitrogen donors) and the potential it offered for subtle variation. It opened up the possibility of producing and examining the properties of a series of similar compounds if a reliable synthetic strategy could be established. **20** was formed unexpectedly from the thermolysis reaction of cobalt acetate and 6-methyl-2-pyridone (Hmhp) at 120 °C. Interestingly the complex is held together by six central μ_3-hydroxides even though the starting materials and solvents used were all 'dry', again suggesting that the use of 'wet' solvents would be more productive.

This chapter discusses the synthesis, structures and initial magnetic studies of a number of new nickel and cobalt species whose structures are based on centred-tricapped-trigonal prisms which contain either two, one or zero additional caps on the 'upper' and 'lower' triangular faces of the prism. By varying the choice of carboxylate and pyridonate ligands in the reaction scheme the nuclearity and structure of the final product can be changed.

Use of chloroacetate and 6-methyl-2-pyridone produces a nickel dodecamer, similar to the Garner species, which is based on a centred-tricapped-trigonal prism with two additional caps on the 'upper' and 'lower' triangular faces of the prism. Replacement of chloroacetate with acetate produces two nickel undecamers which each contain only one additional cap. One of these undecamers dimerises producing a dimer of hydrogen-bonded undecamers.

All of the trigonal prisms reported in this chapter involve the use of the 6-methyl derivative of 2-pyridone with one exception : use of benzoate with 6-chloro-2-pyridone (Hchp) produces a nickel centred-tricapped-trigonal prism which contains one cap on the 'lower' triangular face and an additional polar-cap on the 'upper' triangular face held in position by hydrogen bonds. Reaction of the methyl derivative produces a benzoate and cobalt centred-tricapped-trigonal prism which contains no additional caps. Use of the more sterically demanding trimethylacetate as the carboxylate invokes a structural change in the polyhedron of the nickel complex produced. It is now based on a fourteen-vertex polyhedron rather than a trigonal prism.

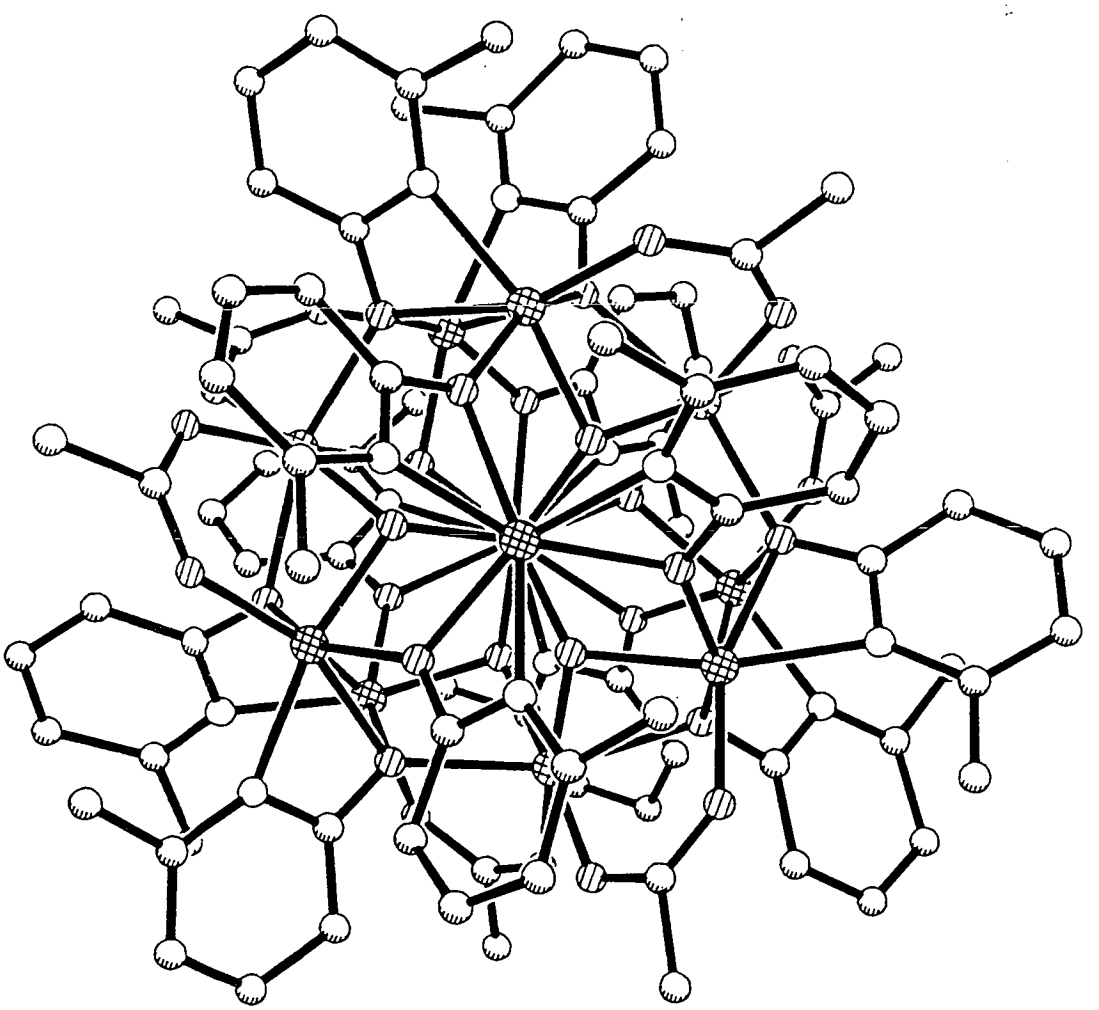

Figure 3.1. The structure of **20** as reported by Garner and co-workers.

3.2.1. Synthesis and structure of $[Ni_{12}(OH)_6(mhp)_{12}(O_2CCH_2Cl)_6]$ 21.

Nickel chloride was stirred in a methanolic solution which contained two equivalents of both Na(mhp) and $Na(O_2CCH_2Cl)$ at 290 K for 24 hours. Removal of the solvent produced a green paste which, after drying *in vacuo*, was crystallised from acetonitrile (or ethyl acetate) to give green crystals of $[Ni_{12}(OH)_6(mhp)_{12}(O_2CCH_2Cl)_6]$ **21** [Figure 3.2] in 50% yield after three days[92].

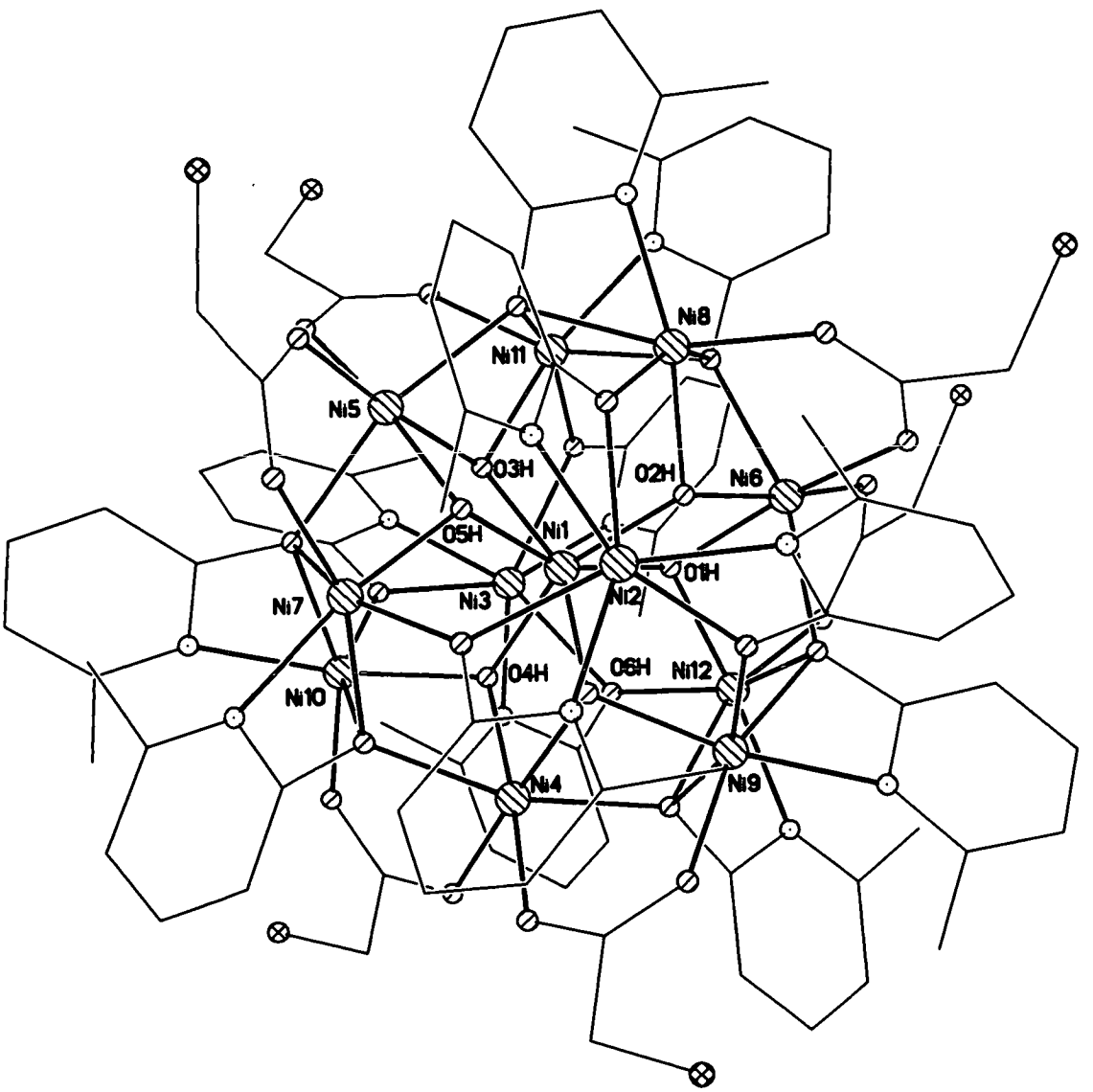

Figure 3.2. The structure of **21** in the crystal.

The central nickel [Ni1] is bound to six μ_3-hydroxides which bridge to the nine further nickels forming the tricapped-trigonal prism. The metal centres at the vertices of the prism [Ni7-Ni12] share one μ_3-hydroxide with Ni1 while the metal atoms capping the square faces of the prism [Ni4-Ni6] share two μ_3-hydroxides with Ni1 forming three Ni_2O_2 rings. The central polyhedron is shown in Figure 3.3 and the centred-tricapped-trigonal prism formed by the metal centres in Figure 3.4.

The exterior of the prism is bridged by six mhp and six chloroacetate ligands. Each mhp ligand binds to one of the nickel atoms at the vertices of the prism through its ring nitrogen and μ_3-bridges through the exocyclic oxygen atom. These three metal atoms attached to the oxygen are the metal vertex to which the nitrogen is bound [i.e. chelating, for example to Ni8], the other vertex which forms a side of the trigonal prism [Ni11] and a metal site which caps one of the square faces of the prism [Ni5]. These six μ_3-oxygen donors thus each occupy the centre of a triangular face bounded by one cap and two vertex-metal atom

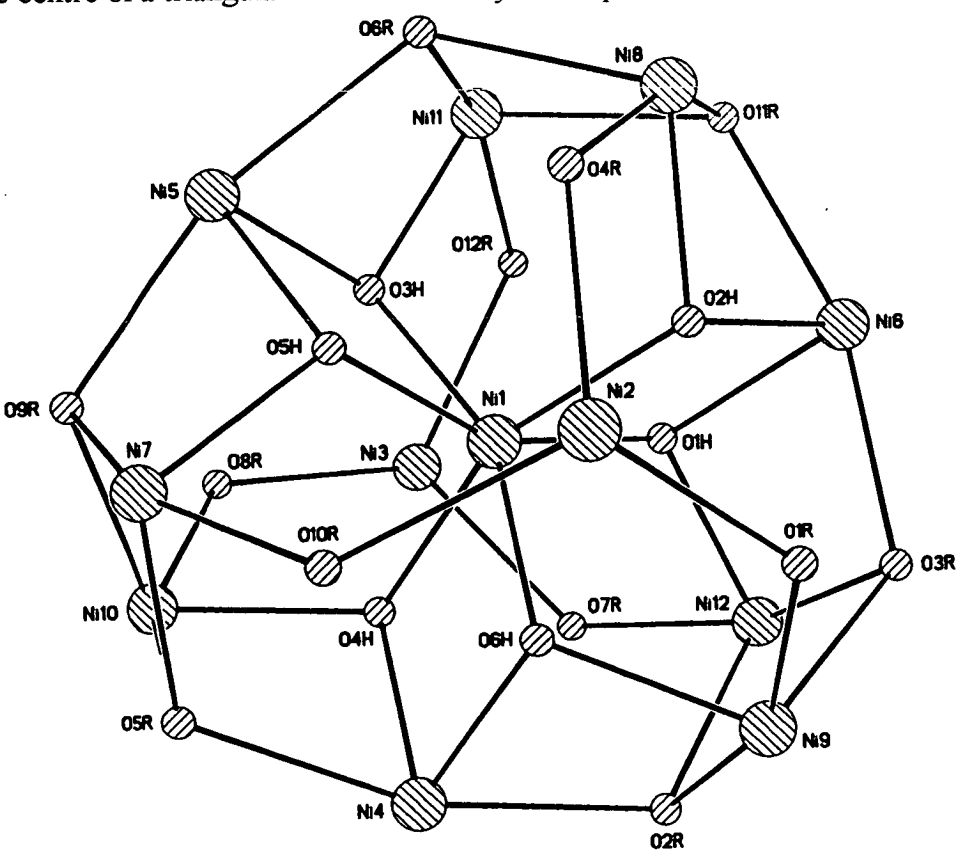

Figure 3.3. The metal polyhedron of **21**.

sites. The chloroacetates bridge in a 1,3-fashion between cap and vertex sites, with each cap attached to two chloroacetate ligands. For example carboxylates bridge between Ni8 and Ni6 and Ni6 and Ni12. The result of these various bridges is to create a central $[Ni_{10}(\mu_3\text{-}OH)_6(\eta^2, \mu_3\text{-}mhp)_6(\eta^2, \mu_2\text{-}O_2CCH_2Cl)_6]^{2+}$ core to which two $[Ni(mhp)_3]^-$ units are attached, one to the 'lower' triangular face and one to the 'upper' triangular face of the prism.

The metal sites are all six coordinate with the central metal [Ni1] bonded exclusively to μ_3-hydroxides. The capping sites [Ni4-Ni6] are bonded to two μ_3-hydroxides, two μ_3-oxygen atoms from mhp ligands and two oxygens derived from chloroacetates. The vertex sites [Ni7-Ni12] are bound to five donors within the central core : one μ_3-hydroxide, two μ_3-oxygen atoms from mhp ligands, one oxygen from a trichloroacetate ligand and one nitrogen donor from an mhp ligand. The final coordination site for these vertex metals is occupied by a μ_2-oxygen atom which attaches the $[Ni(mhp)_3]^-$ units to the triangular faces of the prism.

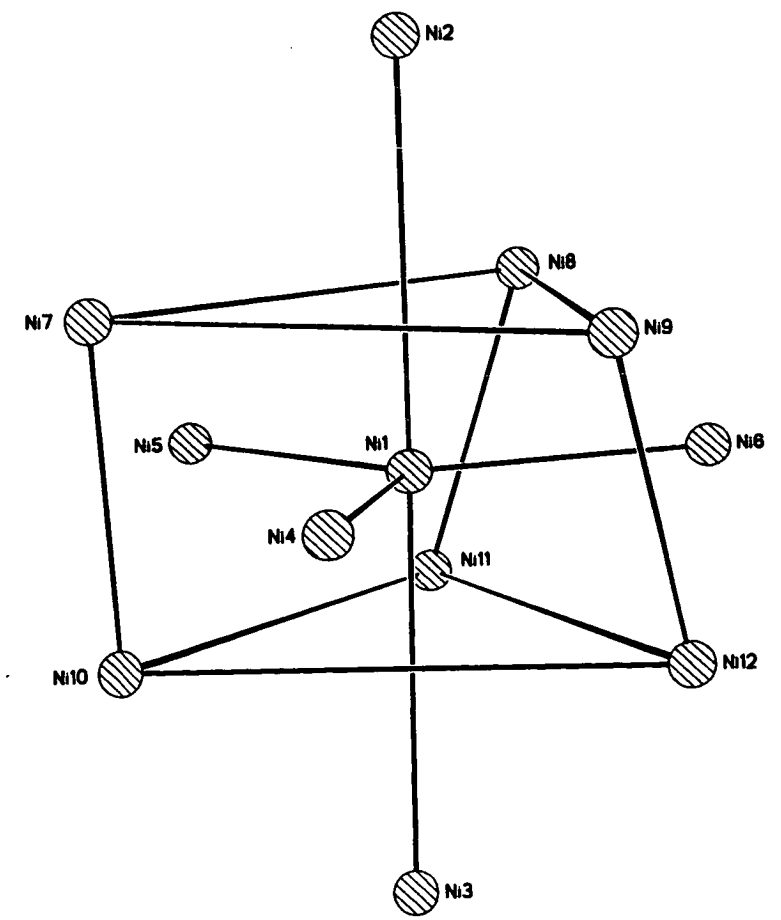

Figure 3.4. The centred-tricapped-trigonal prism in **21**.

The nickels all have distorted octahedral geometries with, in general, the vertex sites [*cis*, 60.6-104.1(2)°; *trans*, 155.8-165.(3)°] and triangular-face-capping sites [*cis*, 61.4-106.4(3)°; *trans*, 157.4-161.9(3)°] in a more distorted arrangement than either the central nickel [*cis*, 79.4-109.8(3)°; *trans*, 157.9-158.4(3)°] or the square-face-capping sites [*cis*, 75.7-97.7(3)°; *trans*, 162.5-173.0(3)°]. The closest Ni...Ni contact is 3.070(3) Å between Ni6 and Ni12. Selected bond lengths and angles are given in Table 3.1. **21** is extremely similar to the Garner species, with chloroacetate replacing acetate and nickel replacing cobalt in the original compound. There are no significant intermolecular interations in **21**.

3.2.2. Magnetochemistry of 21.

The magnetic behaviour of **21** was studied in the temperature range 300-1.8 K in an applied field of 1000 G. The variation of $\chi_m T$ with temperature is shown in Figure 3.5. The room temperature value of the product $\chi_m T$ is approximately 16 emu K mol^{-1} which is consistent with twelve non-interacting S = 1 centres [$\chi_m T$ = 14.5 emu K mol^{-1}, g = 2.2]. The value increases as temperature drops and reaches a maximum of 50 emu K mol^{-1} at 15 K. This value is equivalent to an approximately S = 8 ground state. Below 15 K the value of $\chi_m T$ drops to approximately 37 emu K mol^{-1} possibly due to intermolecular interactions at low temperature.

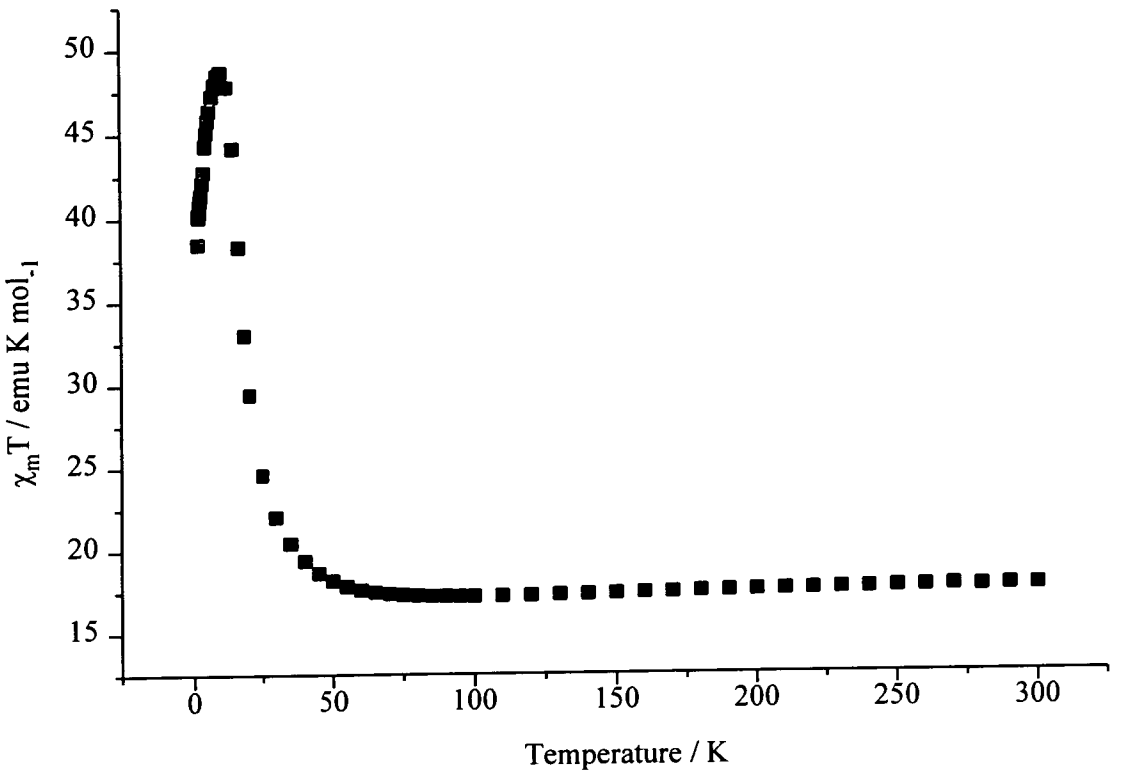

Figure 3.5. The variation of $\chi_m T$ with temperature for **21**.

Table 3.1. Selected bond lengths (Å) and angles (°) for **21**.

Ni1-O5H	2.048(6)	Ni5-O9R	2.137(7)
Ni1-O3H	2.048(6)	Ni6-O2H	2.001(7)
Ni1-O2H	2.049(6)	Ni6-O1H	2.001(7)
Ni1-O6H	2.052(6)	Ni6-O1A2	2.016(7)
Ni1-O4H	2.052(6)	Ni6-O2A5	2.026(7)
Ni1-O1H	2.054(6)	Ni6-O11R	2.098(7)
Ni2-N1R	2.037(10)	Ni6-O3R	2.117(7)
Ni2-N10R	2.048(9)	Ni7-O5H	1.932(6)
Ni2-N4R	2.058(10)	Ni7-O1A4	2.004(7)
Ni2-O10R	2.222(7)	Ni7-N5R	2.041(7)
Ni2-O1R	2.239(8)	Ni7-O10R	2.116(7)
Ni2-O4R	2.246(7)	Ni7-O9R	2.181(7)
Ni3-N12R	2.027(9)	Ni7-O5R	2.290(7)
Ni3-N8R	2.047(9)	Ni8-O2H	1.939(6)
Ni3-N7R	2.054(9)	Ni8-O1A5	2.014(7)
Ni3-O8R	2.215(7)	Ni8-N6R	2.046(8)
Ni3-O7R	2.262(7)	Ni8-O4R	2.146(8)
Ni3-O12R	2.264(7)	Ni8-O11R	2.213(7)
Ni4-O6H	2.004(6)	Ni8-O6R	2.296(7)
Ni4-O4H	2.012(6)	Ni9-O6H	1.939(6)
Ni4-O2A3	2.037(6)	Ni9-O2A1	2.015(7)
Ni4-O1A1	2.039(6)	Ni9-N3R	2.065(9)
Ni4-O5R	2.142(7)	Ni9-O1R	2.123(7)
Ni4-O2R	2.155(7)	Ni9-O2R	2.201(7)
Ni5-O5H	2.006(6)	Ni9-O3R	2.284(7)
Ni5-O3H	2.018(6)	Ni10-O4H	1.940(6)
Ni5-O2A4	2.037(7)	Ni10-O1A3	2.003(6)
Ni5-O1A6	2.047(7)	Ni10-N9R	2.050(7)
Ni5-O6R	2.136(7)	Ni10-O8R	2.119(7)

Table 3.1. continued

Ni10-O5R	2.201(7)	N1R-Ni2-N10R	103.3(3)
Ni10-O9R	2.270(7)	N1R-Ni2-N4R	105.3(3)
Ni11-O3H	1.984(6)	N10R-Ni2-N4R	106.4(3)
Ni11-O2A6	2.022(7)	N1R-Ni2-O10R	160.2(3)
Ni11-N11R	2.049(8)	N10R-Ni2-O10R	62.4(3)
Ni11-O12R	2.145(7)	N4R-Ni2-O10R	92.5(3)
Ni11-O6R	2.177(7)	N1R-Ni2-O1R	62.6(3)
Ni11-O11R	2.308(7)	N10R-Ni2-O1R	93.1(3)
Ni12-O1H	1.944(6)	N4R-Ni2-O1R	159.4(3)
Ni12-O2A2	2.043(7)	O10R-Ni2-O1R	102.7(2)
Ni12-N2R	2.064(8)	N1R-Ni2-O4R	94.9(3)
Ni12-O7R	2.124(7)	N10R-Ni2-O4R	160.5(3)
Ni12-O3R	2.194(7)	N4R-Ni2-O4R	61.4(3)
Ni12-O2R	2.284(7)	O10R-Ni2-O4R	101.4(3)
O5H-Ni1-O3H	79.4(3)	O1R-Ni2-O4R	101.4(3)
O5H-Ni1-O2H	88.0(3)	N12R-Ni3-N8R	103.6(3)
O3H-Ni1-O2H	109.8(2)	N12R-Ni3-N7R	104.6(4)
O5H-Ni1-O6H	88.5(3)	N8R-Ni3-N7R	106.0(4)
O3H-Ni1-O6H	158.1(3)	N12R-Ni3-O8R	157.4(4)
O2H-Ni1-O6H	87.7(2)	N8R-Ni3-O8R	62.8(3)
O5H-Ni1-O4H	108.9(2)	N7R-Ni3-O8R	96.8(3)
O3H-Ni1-O4H	87.1(3)	N12R-Ni3-O7R	92.8(3)
O2H-Ni1-O4H	158.4(3)	N8R-Ni3-O7R	161.9(3)
O6H-Ni1-O4H	79.6(2)	N7R-Ni3-O7R	61.6(3)
O5H-Ni1-O1H	157.9(3)	O8R-Ni3-O7R	103.8(3)
O3H-Ni1-O1H	88.2(3)	N12R-Ni3-O12R	62.3(3)
O2H-Ni1-O1H	79.0(3)	N8R-Ni3-O12R	93.5(3)
O6H-Ni1-O1H	108.6(2)	N7R-Ni3-O12R	158.9(3)
O4H-Ni1-O1H	88.5(2)	O8R-Ni3-O12R	99.0(3)

Table 3.1. continued.

O7R-Ni3-O12R	100.9(3)	O1A6-Ni5-O9R	96.4(3)
O6H-Ni4-O4H	81.7(2)	O6R-Ni5-O9R	162.5(3)
O6H-Ni4-O2A3	171.9(3)	O2H-Ni6-O1H	81.4(2)
O4H-Ni4-O2A3	93.3(3)	O2H-Ni6-O1A2	171.3(3)
O6H-Ni4-O1A1	95.6(3)	O1H-Ni6-O1A2	95.1(3)
O4H-Ni4-O1A1	95.6(3)	O2H-Ni6-O2A5	94.5(3)
O2A3-Ni4-O1A1	172.8(3)	O1H-Ni6-O2A5	170.9(3)
O6H-Ni4-O5R	90.1(3)	O1A2-Ni6-O2A5	90.1(3)
O4H-Ni4-O5R	89.9(3)	O2H-Ni6-O11R	76.7(3)
O2A3-Ni4-O5R	76.5(2)	O1H-Ni6-O11R	90.7(2)
O1A1-Ni4-O5R	97.0(3)	O1A2-Ni6-O11R	95.6(3)
O6H-Ni4-O2R	76.7(4)	O1A5-Ni6-O11R	96.3(3)
O4H-Ni4-O2R	91.1(2)	O2H-Ni6-O3R	89.7(3)
O2A3-Ni4-O2R	97.2(3)	O1H-Ni6-O3R	76.5(3)
O1A1-Ni4-O2R	94.7(3)	O1A2-Ni6-O3R	97.2(3)
O5R-Ni4-O2R	163.0(3)	O2A5-Ni6-O3R	95.5(3)
O5H-Ni5-O3H	81.1(2)	O11R-Ni6-O3R	162.6(3)
O5H-Ni5-O2A4	95.0(2)	O5H-Ni7-O1A4	94.2(3)
O3H-Ni5-O2A4	173.0(3)	O5H-Ni7-N5R	163.5(3)
O5H-Ni5-O1A6	170.8(3)	O1A4-Ni7-N5R	101.5(3)
O3H-Ni5-O1A6	94.4(3)	O5H-Ni7-O10R	83.7(2)
O2A4-NI5-O1A6	90.3(3)	O1A4-Ni7-O10R	95.7(3)
O5H-Ni5-O6R	91.0(3)	N5R-Ni7-O10R	99.5(3)
O3H-Ni5-O6R	76.7(3)	O5H-Ni7-O9R	76.1(3)
O2A4-Ni5-O6R	97.7(3)	O1A4-Ni7-O9R	96.1(3)
O1A6-Ni5-O6R	95.8(3)	N5R-Ni7-O9R	97.0(3)
O5H-Ni5-O9R	75.7(3)	O10R-Ni7-O9R	157.3(3)
O3H-Ni5-O9R	89.9(3)	O5H-Ni7-O5R	103.0(2)
O2A4-Ni5-O9R	94.8(3)	O1A4-Ni7-O5R	160.3(3)

Table 3.1 continued

N5R-Ni7-O5R	60.6(3)	O2A1-Ni9-O3R	160.4(3)
O10R-Ni7-O5R	95.6(3)	N3R-Ni9-O3R	61.5(3)
O9R-Ni7-O5R	79.1(2)	O1R-Ni9-O3R	96.6(3)
O2H-Ni8-O1A5	93.7(3)	O2R-Ni9-O3R	78.6(3)
O2H-Ni8-N6R	163.4(3)	O4H-Ni10-O1A3	94.4(3)
O1A5-Ni8-N6R	101.3(3)	O4H-Ni10-N9R	165.4(3)
O2H-Ni8-O4R	82.7(3)	O1A3-Ni10-N9R	98.8(3)
O1A5-Ni8-O4R	94.4(3)	O4H-Ni10-O8R	81.6(3)
N6R-Ni8-O4R	103.0(3)	O1A3-Ni10-O8R	93.9(3)
O2H-Ni8-O11R	75.2(2)	N9R-Ni10-O8R	103.5(3)
O1A5-Ni8-O11R	96.8(3)	O4H-Ni10-O5R	76.5(3)
N6R-Ni8-O11R	95.8(2)	O1A3-Ni10-O5R	95.6(3)
O4R-Ni8-O11R	155.8(2)	N9R-Ni10-O5R	96.0(2)
O2H-Ni8-O6R	103.0(3)	O8R-Ni10-O5R	156.7(2)
O1A5-Ni8-O6R	159.9(3)	O4H-Ni10-O9R	104.1(2)
N6R-Ni8-O6R	60.9(3)	O1A3-Ni10-O9R	158.8(3)
O4R-Ni8-O6R	98.7(3)	N9R-Ni10-O9R	61.8(3)
O11R-Ni8-O6R	77.1(3)	O8R-Ni10-O9R	98.8(2)
O6H-Ni9-O2A1	94.4(3)	O5R-Ni10-O9R	79.1(2)
O6H-Ni9-N3R	163.9(3)	O3H-Ni11-O2A6	94.5(3)
O2A1-Ni9-N3R	100.9(3)	O3H-Ni11-N11R	164.0(3)
O6H-Ni9-O1R	82.3(3)	O2A6-Ni11-N11R	100.8(3)
O2A1-Ni9-O1R	95.4(3)	O3H-Ni11-O12R	80.7(2)
N3R-Ni9-O1R	101.1(3)	O2A6-Ni11-O12R	93.2(3)
O6H-Ni9-O2R	76.9(3)	N11R-Ni11-O12R	103.0(3)
O2A1-Ni9-O2R	95.9(3)	O3H-Ni11-O6R	77.1(3)
N3R-Ni9-O2R	96.2(3)	O2A6-Ni11-O6R	96.5(3)
O1R-Ni9-O2R	157.1(3)	N11R-Ni11-O6R	96.2(2)
O6H-Ni9-O3R	102.5(3)	O12R-Ni11-O6R	156.4(2)

Table 3.1 continued

O3H-Ni11-O11R	102.89	Ni10-O4H-Ni4	102.9(3)
O2A6-Ni11-O11R	159.8(2)	Ni10-O4H-Ni1	118.3(3)
N11R-Ni11-O11R	61.3(3)	Ni4-O4H-Ni1	99.2(3)
O12R-Ni11-O11R	99.8(3)	Ni7-O5H-Ni5	103.0(3)
O6R-Ni11-O11R	77.6(3)	Ni7-O5H-Ni1	119.4(3)
O1H-Ni12-O2A2	92.8(3)	Ni5-O5H-Ni1	100.0(3)
O1H-Ni12-N2R	163.5(3)	Ni9-O6H-Ni4	102.4(3)
O2A2-Ni12-N2R	101.3(3)	Ni9-O6H-Ni1	119.6(3)
O1H-Ni12-O7R	82.9(3)	Ni4-O6H-Ni1	99.5(3)
O2A2-Ni12-O7R	94.6(3)	Ni9-O1R-Ni2	132.5(3)
N2R-Ni12-O7R	104.1(3)	Ni4-O2R-Ni9	89.7(3)
O1H-Ni12-O3R	75.8(3)	Ni4-O2R-Ni12	122.0(3)
O2A2-Ni12-O3R	97.5(3)	Ni9-O2R-Ni12	100.3(3)
N2R-Ni12-O3R	93.8(3)	Ni6-O3R-Ni12	90.8(3)
O7R-Ni12-O3R	155.9(3)	Ni6-O3R-Ni9	123.3(3)
O1H-Ni12-O2R	103.2(3)	Ni12-O3R-Ni9	100.4(3)
O2A2-Ni12-O2R	162.0(3)	Ni8-O4R-Ni2	132.9(3)
N2R-Ni12-O2R	61.7(3)	Ni4-O5R-Ni10	90.7(3)
O7R-Ni12-O2R	95.5(2)	Ni4-O5R-Ni7	122.5(3)
O3R-Ni12-O2R	78.8(2)	Ni10-O5R-Ni7	99.2(3)
Ni12-O1H-Ni6	102.2(3)	Ni5-O6R-Ni11	90.8(3)
Ni12-O1H-Ni1	119.6(3)	Ni5-O6R-Ni8	120.9(3)
Ni6-O1H-Ni1	99.7(3)	Ni11-O6R-Ni8	102.2(3)
Ni8-O2H-Ni6	102.8(3)	Ni12-O7R-Ni3	134.2(3)
Ni8-O2H-Ni1	119.2(3)	Ni10-O8R-Ni3	133.4(2)
Ni6-O2H-Ni1	99.9(3)	Ni5-O9R-Ni7	91.1(3)
Ni11-O3H-Ni5	101.5(3)	Ni5-O9R-Ni10	121.8(3)
Ni11-O3H-Ni1	118.5(3)	Ni7-O9R-Ni10	100.5(3)
Ni5-O3H-Ni1	99.6(3)	Ni7-O10R-Ni2	132.6(3)

Table 3.1 continued

Ni6-O11R-Ni8	91.1(3)	Ni8-O11R-Ni11	100.8(3)
Ni6-O11R-Ni11	122.4(3)	Ni11-O12R-Ni3	135.6(3)

3.2.3. Synthesis and structure of $[Ni_{11}(OH)_6(chp)_9(O_2CPh)_6(EtOH)_3]^+[Ni(chp)_3]^-$ 22.

Reaction of nickel chloride with two equivalents of both Na(chp) and $Na(O_2CPh)$ in ethanol for 24 hours produced a green paste which was dried *in vacuo*. Crystallisation of this paste from dichloromethane produced green crystals of $[Ni_{11}(OH)_6(chp)_9(O_2CPh)_6(EtOH)_3]^+$ $[Ni(chp)_3]^-$ **22** [Figure 3.6] in approximately 15% yield after four days [93]. **22** consists of two metal-containing fragments, an undecanuclear monocation fragment related to **21** and a

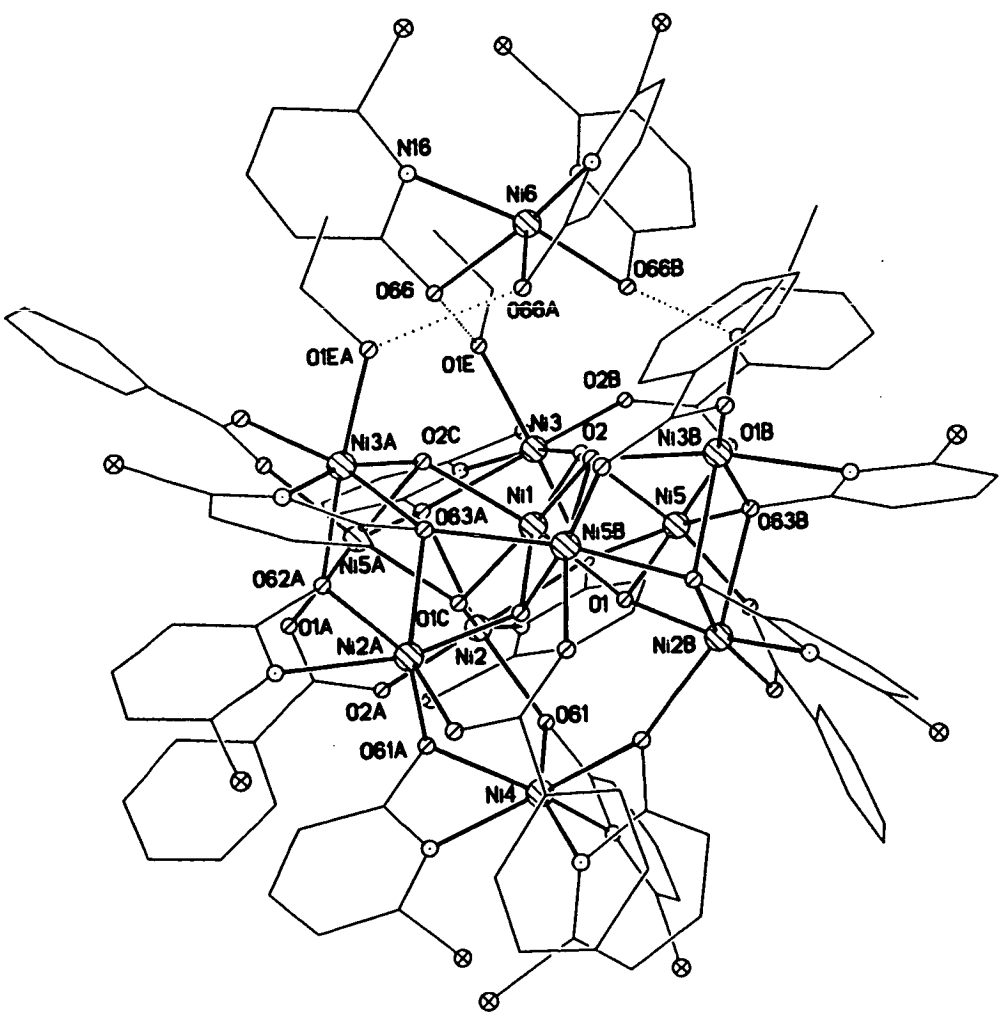

Figure 3.6. The structure of **22** in the crystal.

mononuclear $[Ni(chp)_3]^-$ monoanion which is strongly hydrogen bonded to the larger fragment. **22** is the only centred-tricapped-trigonal prism containing chp ligands and crystallises with a crystallographic C_3 axis coincident with the trigonal axis of the cage. The structure of **22** is extremely similar to that of **20** and **21** and includes the same central $[Ni_{10}(\mu_3\text{-}OH)(\eta^2, \mu_3\text{-}chp)_6(\eta^2, \mu_2\text{-}O_2CPh)_6]^{2+}$ core. Again the central nickel [Ni1] in the core is bound to six μ_3-hydroxides which further bridge to the nine metal atoms which form the tricapped-trigonal prism [the vertex sites Ni2, Ni3 and symmetry equivalents, and the square-face caps Ni5 and symmetry equivalents]. The outside of this prism is covered by six chp and six benzoate ligands which adopt identical bonding modes to the mhp and carboxylate ligands binding the metal core in **20** and **21**. The three $[Ni(chp)_3]^-$ caps on the square faces of the prism [Ni5, Ni5A,Ni5B] are attached to the vertex sites *via* two benzoate ligands, which again bridge in a 1, 3-fashion, and a μ_3-oxygen atom derived from a trinucleating chp ligand. The metal-oxygen polyhedron is shown in Figure 3.7 and the polar-capped centred-trigonal prism in Figure 3.8.

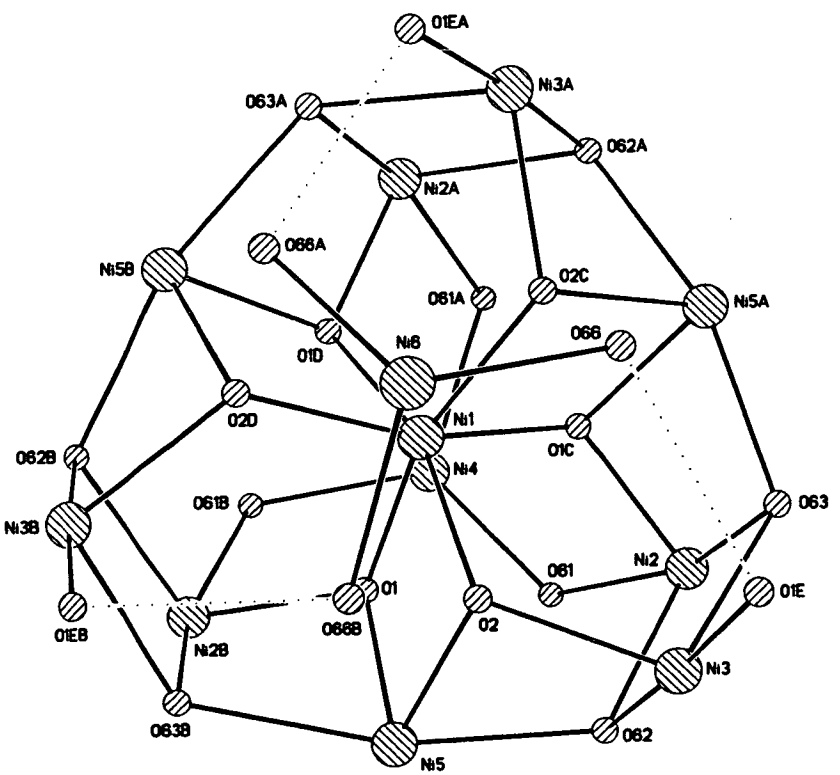

Figure 3.7. The metal-oxygen polyhedron in **22**.

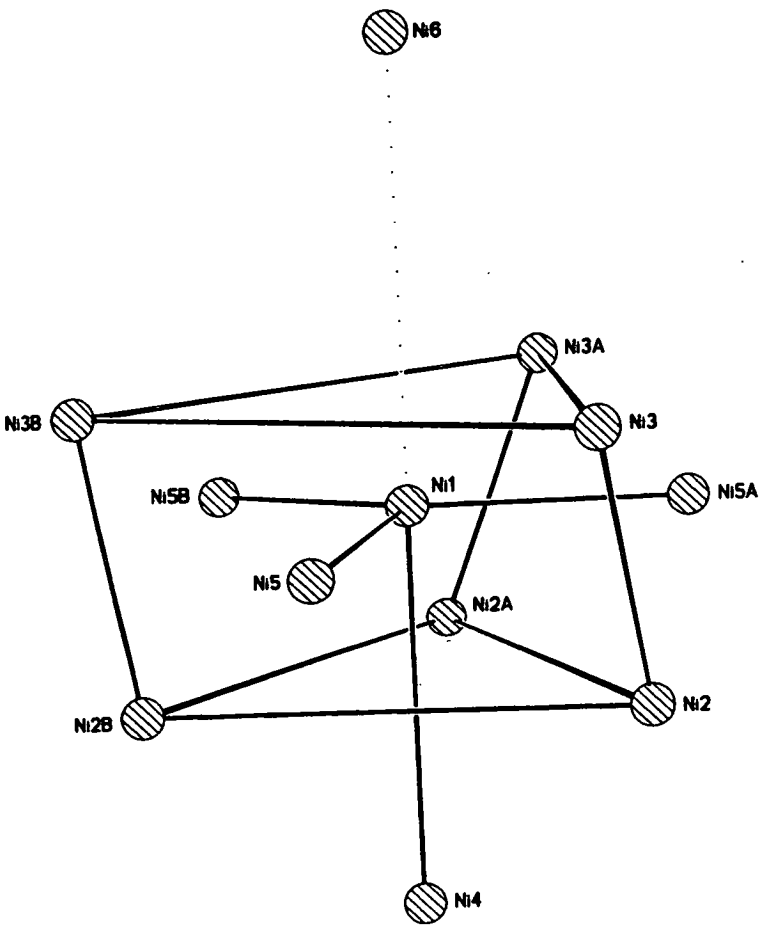

Figure 3.8. The polar-capped centred-trigonal prism formed by the metal centres in **22**.

The significant difference between the structure of **22** and that of **20** and **21** is in the coordination of the nickel vertex sites. Again these metal atoms have similar coordination in five of the six sites, i.e. one μ_3-hydroxide, two μ_3-oxygens from pyridonate ligands, one oxygen from a carboxylate and one nitrogen donor from a pyridonate. The sixth coordination site is where the structural variation in the cages takes place. In both **20** and **21** this site on each of the six metal centres was occupied by a μ_2-oxygen from a pyridonate ligand which attached an $[M(mhp)_3]^-$ unit (M = Co, Ni) to the central $[M_{10}(\mu_3\text{-}OH)(\eta^2, \mu_3\text{-}mhp)_6(\eta^2, \mu_2\text{-}O_2CR)_6]^{2+}$ (R = CH_3, CH_2Cl) core. For **22** in the 'lower' triangular face, which comprises Ni2 and symmetry equivalents, this is again true with three μ_2-oxygens from chp ligands ligating a $[Ni(chp)_3]^-$ unit. However on the 'upper' triangular face these nickel sites are occupied by three molecules of ethanol (carried forward from the first step of the synthesis) and thus have

displaced the $[Ni(chp)_3]^-$ cap. This cap is now strongly hydrogen bonded to the ethanol molecules [O...O, 2.602(10) Å]. The displaced cap has a similar geometry to the attached $[Ni(chp)_3]^-$ fragment on the 'lower' triangular face and to the $[Ni(mhp)_3]^-$ caps present in **20** and **21**.

The nickels have similarly distorted octahedral geometries with the *cis* angles ranging between 61.6-103.5(3)° and the *trans* angles 157.7-176.2(3)°. The Ni...O and Ni...N bond lengths are 1.950-2.254(6) Å and 2.043-2.137(3) Å respectively. The closest Ni...Ni contact is 3.061(6) Å between Ni3 and Ni5. Selected bond lengths and angles are given in Table 3.2. Like **20** the compound lies on a crystallographically-imposed trigonal axis. However **22** is unique in that it crystallises in the polar space group R3c. Refinement of the Flack enantiopole parameter [0.35(6)] indicates that around 65% of the molecules are alligned in one direction and 35% in a second orientation. Although tri- [94-97], tetra- [98-102], penta- [103, 104], and hexanuclear [105, 106] coordination complexes have been crystallised in polar space groups, it is a rare occurrence for higher nuclearity species [107,108]. There are no further significant intemolecular interactions in **22**.

3.2.4. Magnetochemistry of 22.

The magnetic behaviour of **22** was studied in the temperature range 300-1.8 K in an applied field of 1000 G. The variation of $\chi_m T$ with temperature is shown in Figure 3.9. The room temperature value of $\chi_m T$ is approximately 15 emu K mol^{-1} which is consistent with eleven non-interacting S = 1 Ni(II) centres [$\chi_m T$ = 13.3 emu K mol^{-1}, g = 2.2]. The value then decreases steadily with temperature, indicative of antiferromagnetic exchange between the metal centres, giving a minimum of approximately 2 emu K mol^{-1} at 1.8 K. This value corresponds to an approximately S = 1 ground state.

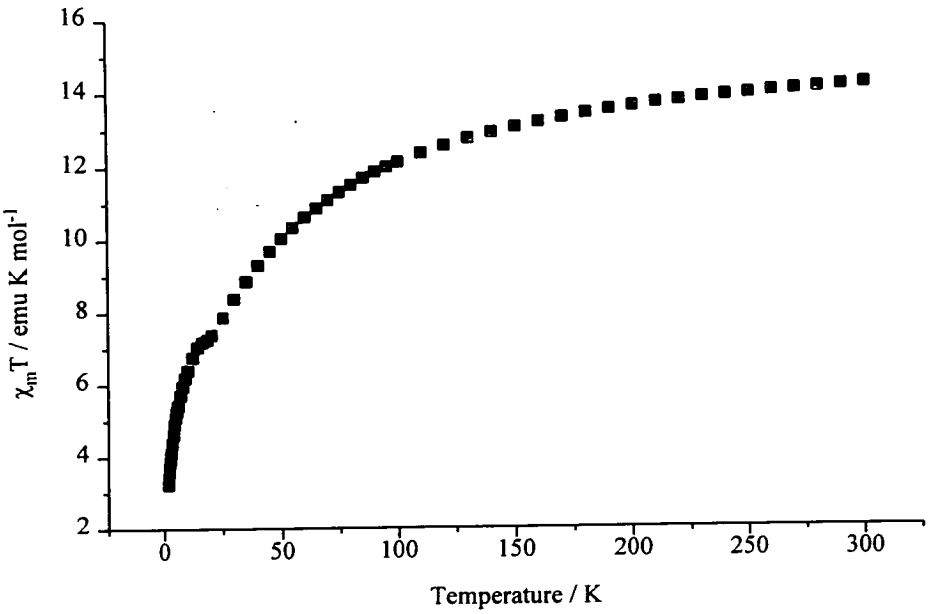

Figure 3.9. The variation of $\chi_m T$ with temprature for **22**.

Table 3.2. Selected bond lengths (Å) and angles (°) for **22**.

Ni1-O1	2.057(6)	Ni4-N11	2.043(8)
Ni1-O1A	2.057(6)	Ni4-N11A	2.043(8)
Ni1-O1B	2.057(6)	Ni4-N11B	2.043(7)
Ni1-O2	2.075(6)	Ni4-O61	2.188(7)
Ni1-O2A	2.075(6)	Ni4-O61A	2.188(6)
Ni1-O2B	2.075(6)	Ni4-O61B	2.188(7)
Ni2-O1A	1.950(6)	Ni5-O1	1.993(6)
Ni2-O2A	1.968(6)	Ni5-O1B	1.993(6)
Ni2-N12	2.071(8)	Ni5-O1A	2.047(7)
Ni2-O61	2.115(6)	Ni5-O2	2.078(6)
Ni2-O62	2.209(7)	Ni5-O63A	2.154(6)
Ni2-O63	2.25496)	Ni5-O62	2.164(6)
Ni3-O2	1.993(6)	Ni6-N16	2.075(8)
Ni3-O2B	2.011(7)	Ni6-N16A	2.075(9)
Ni3-O1E	2.044(7)	Ni6-N16B	2.075(9)
Ni3-O62	2.132(7)	Ni6-O66	2.106(7)
Ni3-N13	2.137(7)	Ni6-O66A	2.106(7)
Ni3-O63	2.190(6)	Ni6-O66B	2.106(7)

Table 3.2. continued.

O1-Ni1-O1A	83.6(3)	O62-Ni3-N13	94.9(3)
O1-Ni1-O2A	103.2(2)	O2-Ni3-O63	99.3(3)
O1-Ni1-O2	81.5(2)	O2B-Ni3-O63	162.4(3)
O1A-Ni1-O2	162.8(2)	O1E-Ni3-O63	90.9(3)
O1B-Ni2-O2A	96.5(3)	O62-Ni3-O63	85.7(2)
O1B-Ni2-N12	162.7(3)	N13-Ni3-O63	62.1(3)
O2A-Ni2-N12	100.3(2)	N11-Ni4 N11A	102.4(3)
O1B-Ni2-O61	85.3(3)	N11A-Ni4-O61	159.0(3)
O2A-Ni2-O61	94.0(3)	N11-Ni4-O61A	95.4(3)
N12-Ni2-O61	97.9(3)	N11-Ni4-O61	62.5(3)
O1B-Ni2-O62	101.5(2)	O61-Ni4-O61A	102.7(3)
O2A-Ni2-O62	161.6(3)	O1-Ni5-O1B	174.2(3)
N12-Ni2-O62	61.6(3)	O1-Ni5-O1A	94.6(3)
O61-Ni2-O62	91.8(3)	O1B-Ni5-O1A	88.7(3)
O2-Ni3-O2B	97.7(3)	O1-Ni5-O2	82.9(2)
O2-Ni3-O1E	99.3(3)	O1B-Ni5-O2	94.9(3)
O2B-Ni3-O1E	90.8(3)	O1A-Ni5-O2	166.2(3)
O2-Ni3-O62	79.6(3)	O1-Ni5-O63A	76.4(3)
O2B-Ni3-O62	92.9(3)	O1B-Ni5-O63A	98.7(3)
O1E-Ni3-O62	176.2(3)	O1A-Ni5-O63A	94.5(3)
O2-Ni3-N13	161.1(3)	O2-Ni5-O63A	98.1(3)
O2B-Ni3-N13	100.7(3)	O1-Ni5-O62	87.1(3)
O1E-Ni3-N13	85.1(3)	O1B-Ni5-O62	97.7(3)
O1B-Ni2-O63	74.8(3)	O1A-Ni5-O62	89.4(3)
O2A-Ni2-O63	98.2(3)	O2-Ni5-O62	77.0(3)
N12-Ni2-O63	98.1(3)	O63A-Ni5-O62	163.2(3)
O61-Ni2-O63	157.7(3)	Ni2A-O1-Ni5	103.1(3)
O62-Ni2-O63	82.4(2)	Ni2A-O1-Ni1	123.5(3)
Ni5-O1-Ni1	99.1(3)	Ni3-O62-Ni2	97.3(2)

Ni3-O2-Ni1	122.9(3)	Ni5-O62-Ni2	125.0(3)
Ni3-O2-Ni5	97.5(2)	Ni5A-O63-Ni3	129.6(3)
N1-O2-Ni5	95.8(2)	Ni5A-O63-Ni2	88.9(2)
Ni2-O61-Ni4	131.0(3)	Ni3-O63-Ni2	94.3(3)
Ni3-O62-Ni5	90.9(2)		

3.2.5. Synthesis and structure of $[Ni_{11}(OH)_6(mhp)_9(O_2CMe)_6(H_2O)_3]_2[CO_3]$ 23 and $[Ni_{11}(OH)_6(mhp)_9(O_2CMe)_7(Hmhp)_2]$ 24.

Reaction of two equivalents of Na(mhp) with nickel acetate in tetrahydrofuran for 24 hours produced a green paste which was dried *in vacuo*. Crystallisation of this paste from dichloromethane gave green crystals of $[Ni_{11}(OH)_6(mhp)_9(O_2CMe)_6(H_2O)_3]_2[CO_3]$ **23** [Figure 3.10] after approximately one week [55].

23 is an undecanuclear cage related to **20-22** and again contains the the same central $[Ni_{10}(\mu_3\text{-}OH)_6(\eta^2, \mu_3\text{-}mhp)_6(\eta^2, \mu_2\text{-}O_2CMe)_6]^{2+}$ core but has only one additional $[Ni(mhp)_3]^-$ cap attached to the 'lower' triangular face of the centred-tricapped-trigonal prism. Ni1 is again at the centre of the structure and is bound to six μ_3-hydroxides shared with nine further nickel sites : the vertex sites [Ni2, Ni4, Ni5, Ni6, Ni9, Ni10] share one of these hydroxides and the nickel caps on the square faces of the prism [Ni3, Ni7, Ni8] share two, forming Ni_2O_2 rings. The pyridonate and carboxylate bridges attached to the core again adopt identical bonding modes to **20-22**.

Like **22** the 'lower' triangular face is ligated to a $[Ni(mhp)_3]^-$ unit : the oxygen of each pyridonate μ_2-bridging to one nickel vertex site. The significant structural change in **23** again occurs in the 'upper' triangular face. In **22** the sixth coordination site on each nickel was occupied by a molecule of ethanol. In this case these three sites are occupied by three molecules of water. This creates a very hydrophilic face for the cage and in the crystal two

molecules of **23** interact *via* six hydrogen bonds [O...O, 2.565-2.896(12) Å] to produce a dimer of undecanuclear cages [Figure 3.11]. The tricapped-trigonal prism formed by the metal centres is shown in Figure 3.13.

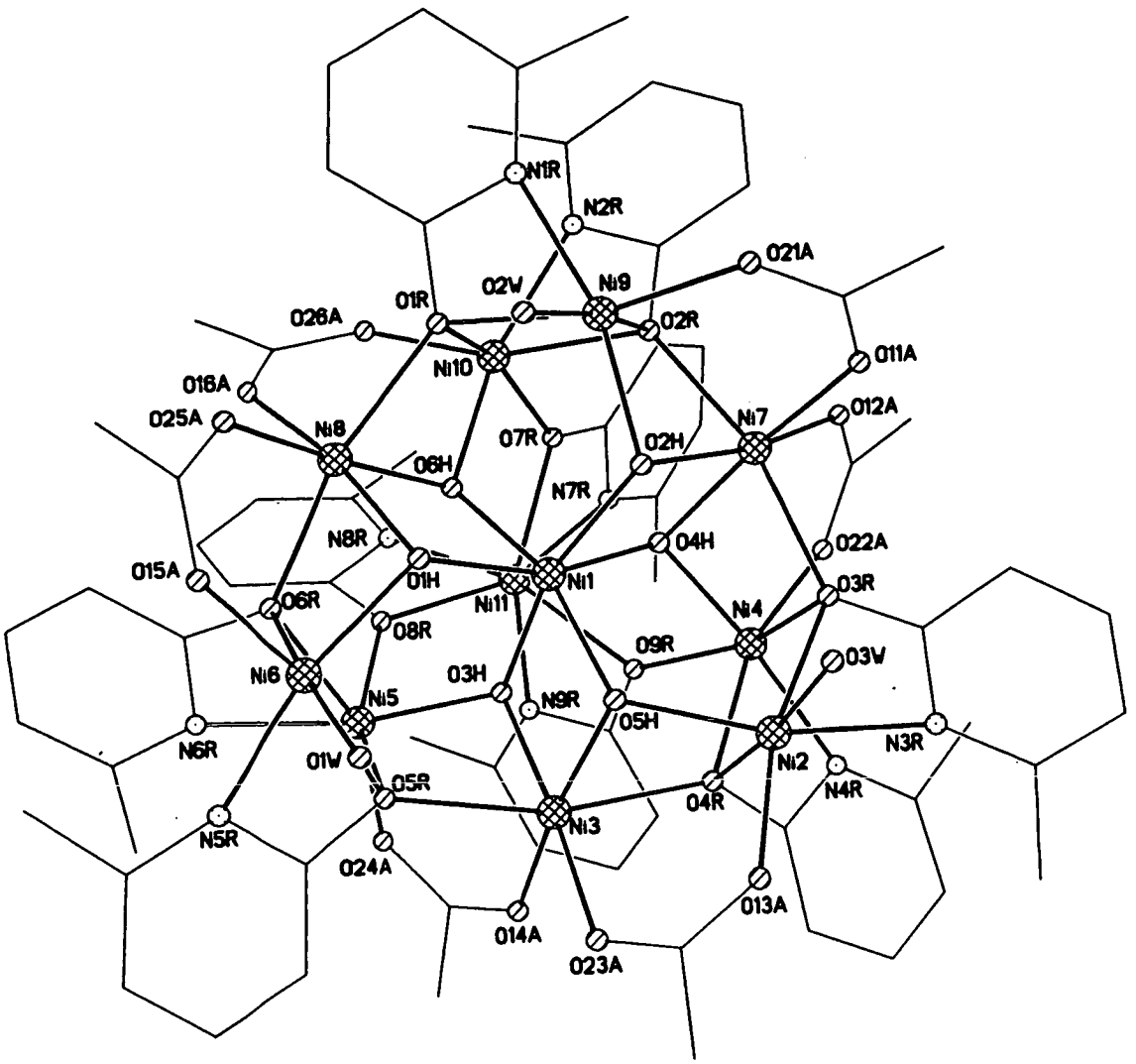

Figure 3.10. The structure of **23** in the crystal.

The nickels have similarly distorted environments to the metal centres in **20-22**. The closest Ni...Ni contact is 3.062(6) Å between Ni7 and Ni9. Selected bond lengths and angles are given in Table 3.3.

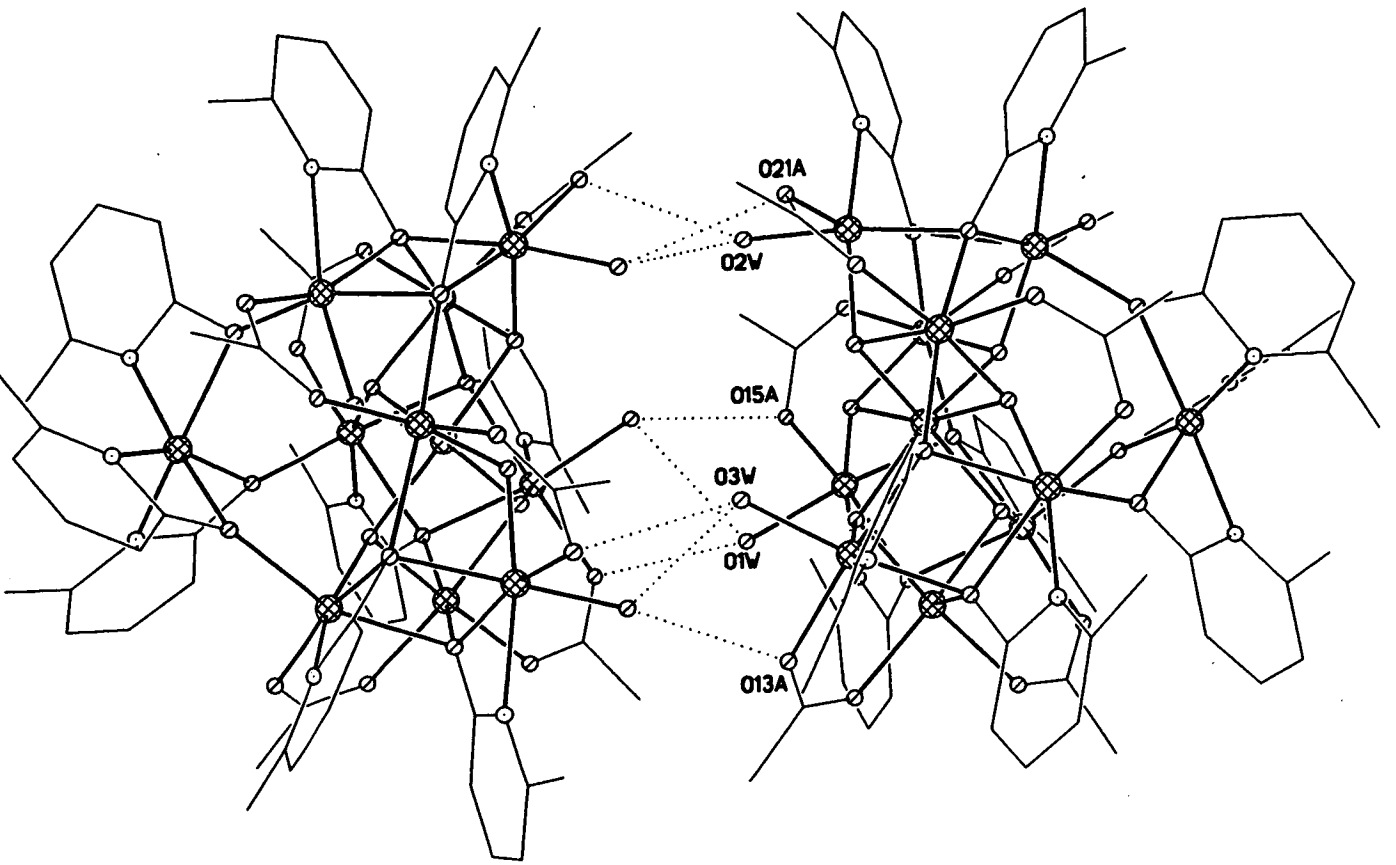

Figure 3.11. The dimer of hydrogen-bonded undecamers formed by **23**.

The reaction which produced **23** was repeated with the first stage carried out in methanol rather than tetrahydrofuran and the related undecanulear complex $[Ni_{11}(\mu_3\text{-}OH)_6(mhp)_9(\mu_2\text{-}O_2CMe)_6(Hmhp)_2(O_2CMe)]$ **24** [Figure 3.12] was produced after two weeks. Both **23** and **24** crystallise in very low yield, but are reproducible. The structure of **24** is almost identical to that of **23** and thus again closely related to **20-22**, with the structural change occuring on the sixth coordination site of the three nickel metals on the 'upper' triangular face of the prism. In **23** these sites are occupied by three water molecules; in **24** these sites are occupied by two molecules of Hmhp and one molecule of acetate. Unlike **23** there are no strong intermolecular interactions. Selected bond lengths and angles for **24** are given in Table 3.4.

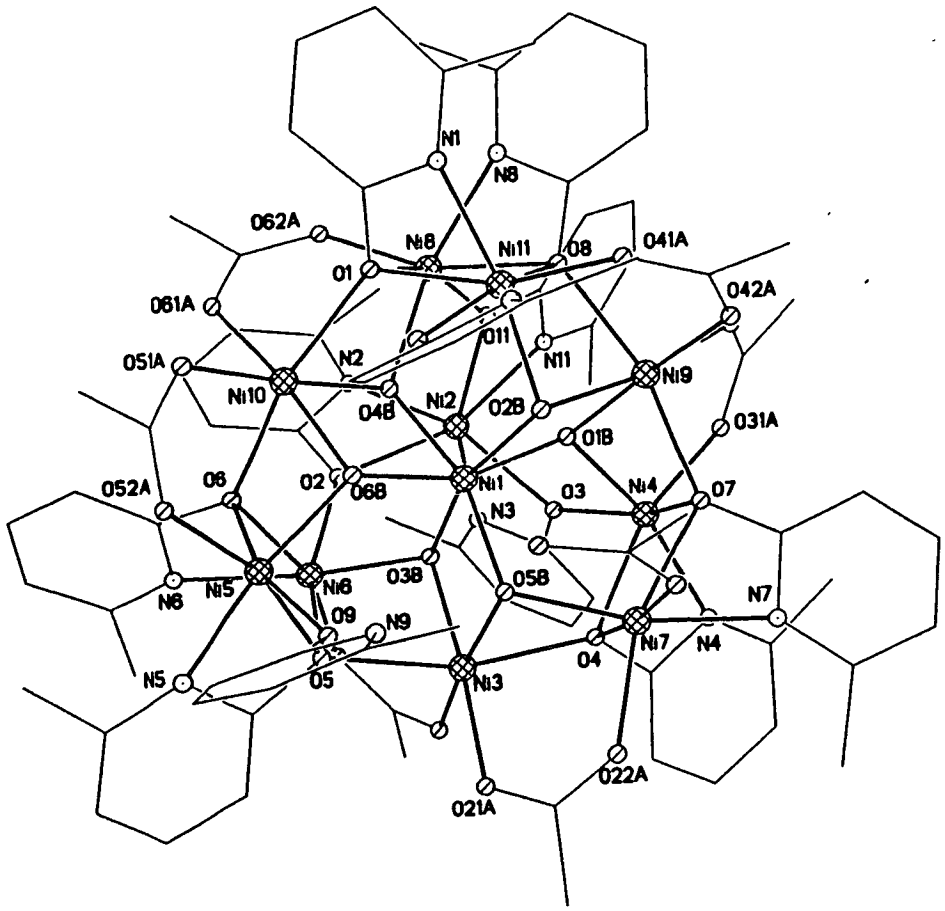

Figure 3.12. The structure of **24** in the crystal.

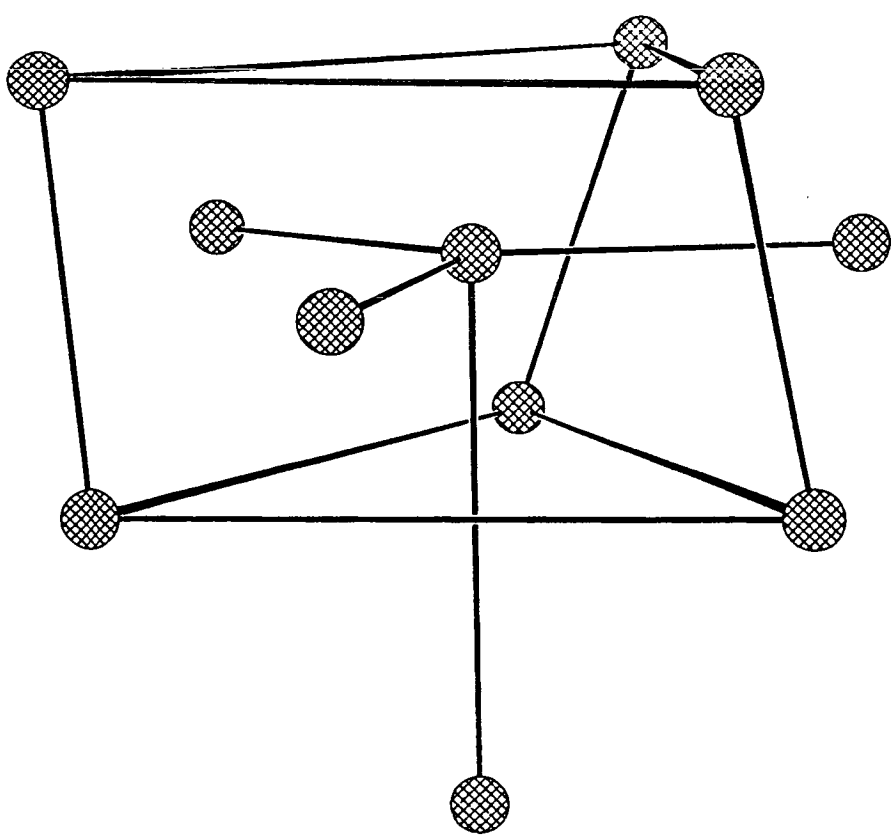

Figure 3.13. The centred-tricapped-trigonal prism common to both **23** and **24**.

Table 3.3. Selected bond lengths (Å) and angles (°) for **23**.

Ni1-O1H	2.096(12)	Ni5-N6R	2.11(2)
Ni1-O2H	2.066(12)	Ni6-O1H	1.994(11)
Ni1-O3H	2.085(12)	Ni6-O15A	2.038(12)
Ni1-O4H	2.057(12)	Ni6-O1W	2.04(2)
Ni1-O5H	2.074(12)	Ni6-O5R	2.209(12)
Ni1-O6H	2.069(12)	Ni6-O6R	2.106(12)
Ni2-O5H	1.994(12)	Ni6-N5R	2.05(2)
Ni2-O3W	2.018(13)	Ni7-O2H	2.087(12)
Ni2-O13A	2.034(13)	Ni7-O4H	1.978(11)
Ni2-O3R	2.225(13)	Ni7-O11A	2.012(13)
Ni2-O4R	2.094(13)	Ni7-O12A	2.013(14)
Ni2-N3R	2.116(14)	Ni7-O2R	2.118(11)
Ni3-O3H	2.009(12)	Ni7-O3R	2.151(11)
Ni3-O5H	2.062(12)	Ni8-O1H	2.074(11)
Ni3-O14A	2.04(2)	Ni8-O6H	1.996(11)
Ni3-O23A	2.022(13)	Ni8-O16A	2.035(120
Ni3-O4R	2.172(12)	Ni8-O25A	2.020(12)
Ni3-O5R	2.198(13)	Ni8-O1R	2.161(12)
Ni4-O4H	1.962(10)	Ni8-O6R	2.130(11)
Ni4-O22A	2.028(14)	Ni9-O2H	1.983(11)
Ni4-O3R	2.173(13)	Ni9-O21A	2.030(13)
Ni4-O4R	2.243(140	Ni9-O2W	2.055(14)
Ni4-O9R	2.095(12)	Ni9-O1R	2.217(12)
Ni4-N4R	2.05(2)	Ni9-O2R	2.1292)
Ni5-O3H	1.935(11)	Ni9-N1R	2.08(2)
Ni5-O24A	1.993(13)	Ni10-O6H	1.964(11)
Ni5-O5R	2.19(2)	Ni10-O26A	1.980(11)
Ni5-O6R	2.247(11)	Ni10-O1R	2.196(11)
Ni5-O8R	2.12(2)	Ni10-O2R	2.240(12)

Table 3.3 continued.

Ni10-O7R	2.148(12)	O5H-Ni2-N3R	162.5(5)
Ni10-N2R	2.078(12)	O3W-Ni2-N3R	82.4(6)
Ni11-O7R	2.225(12)	O13A-Ni2-N3R	104.1(5)
Ni11-O8R	2.209(12)	O4R-Ni2-N3R	98.0(5)
Ni11-O9R	2.218(12)	O5H-Ni2-O3R	100.9(5)
Ni11-N7R	2.01(2)	O3W-Ni2-O3R	89.3(6)
Ni11-N8R	2.02(2)	O13A-Ni2-O3R	165.6(5)
Ni11-N9R	2.04(2)	O4R-Ni2-O3R	84.1(5)
O4H-Ni1-O2H	81.6(5)	N3R-Ni2-O3R	61.6(4)
O4H-Ni1-O6H	85.1(5)	O3H-Ni3-O23A	173.9(5)
O2H-Ni1-O6H	104.3(5)	O3H-Ni3-O14A	94.0(5)
O4H-Ni1-O5H	103.7(5)	O23A-Ni3-O14A	88.3(5)
O2H-Ni1-O5H	91.8(5)	O3H-Ni3-O5H	83.4(5)
O6H-Ni1-O5H	162.8(5)	O23A-Ni3-O5H	95.2(5)
O4H-Ni1-O3H	86.0(5)	O14A-Ni3-O5H	170.2(5)
O2H-Ni1-O3H	164.0(5)	O3H-Ni3-O4R	90.6(5)
O6H-Ni1-O3H	84.6(5)	O23A-Ni3-O4R	94.9(5)
O5H-Ni1-O3H	81.3(5)	O14A-Ni3-O4R	95.1(5)
O4H-Ni1-O1H	162.0(5)	O5H-Ni3-O4R	75.5(5)
O2H-Ni1-O1H	90.4(5)	O3H-Ni3-O5R	74.2(5)
O6H-Ni1-O1H	81.3(4)	O23A-Ni3-O5R	100.1(5)
O5H-Ni1-O1H	92.6(5)	O14A-Ni3-O5R	91.9(5)
O3H-Ni1-O1H	104.3(4)	O5H-Ni3-O5R	96.4(5)
O5H-Ni2-O3W	98.4(4)	O4R-Ni3-O5R	163.6(5)
O5H-Ni2-O13A	93.4(5)	O4H-Ni4-O22A	95.4(6)
O3W-Ni2-O13A	90.9(5)	O4H-Ni4-N4R	163.8(5)
O5H-Ni2-O4R	78.8(5)	O22A-Ni4-N4R	99.3(5)
O3W-Ni2-O4R	172.2(5)	O4H-Ni4-O9R	84.3(5)
O13A-Ni2-O4R	96.5(5)	O22A-Ni4-O9R	94.7(5)

Table 3.3 continued.

N4R-Ni4-O9R	101.3(6)	O15A-Ni6-N5R	104.1(5)
O4H-Ni4-O3R	75.4(5)	O1W-Ni6-N5R	81.8(5)
O22A-Ni4-O3R	96.9(5)	O1H-Ni6-O6R	78.6(5)
N4R-Ni4-O3R	95.8(5)	O15A-Ni6-O6R	97.3(5)
O9R-Ni4-O3R	157.5(4)	O1W-Ni6-O6R	171.0(5)
O4H-Ni4-O4R	102.1(4)	N5R-Ni6-O6R	97.3(5)
O22A-Ni4-O4R	161.5(4)	O1H-Ni6-O5R	100.5(6)
N4R-Ni4-O4R	62.7(5)	O15A-Ni6-O5R	166.9(4)
O9R-Ni4-O4R	93.095)	O1W-Ni6-O5R	85.9(5)
O3R-Ni4-O4R	81.9(5)	N5R-Ni6-O5R	62.8(5)
O3H-Ni5-O24A	96.4(5)	O6R-Ni6-O5R	85.7(5)
O3H-NI5-N6R	164.0(6)	O4H-Ni7-O11A	173.0(5)
O24A-Ni5-N6R	99.4(5)	O4H-Ni7-O12A	96.0(5)
O3H-Ni5-O8R	83.6(5)	O11A-Ni7-O12A	88.4(5)
O24A-Ni5-O8R	96.495)	O4H-Ni7-O2H	82.9(5)
N6R-Ni5-O8R	97.4(6)	O11A-Ni7-O2H	93.7(5)
O3H-Ni5-O5R	75.8(5)	O12A-Ni7-O2H	169.4(5)
O24A-Ni5-O5R	95.3(5)	O4H-Ni7-O2R	89.3(5)
N6R-Ni5-O5R	99.9(6)	O11A-Ni7-O2R	95.9(5)
O8R-Ni5-O5R	157.2(5)	O12A-Ni7-O2R	92.9(5)
O3H-Ni5-O6R	102.8(5)	O2H-Ni7-O2R	76.6(5)
O24A-Ni5-O6R	159.6(5)	O4H-Ni7-O3R	75.6(5)
N6R-Ni5-O6R	61.2(5)	O11A-Ni7-O3R	98.9(5)
O8R-Ni5-O6R	92.6(5)	O12A-Ni7-O3R	91.6(5)
O5R-Ni5-O6R	82.9(5)	O2H-Ni7-O3R	98.3(5)
O1H-Ni6-O15A	92.6(5)	O2R-Ni7-O3R	164.7(5)
O1H-Ni6-O1W	99.6(5)	O6H-Ni8-O25A	172.6(5)
O15A-Ni6-O1W	91.6(5)	O6H-Ni8-O16A	94.9(5)
O1H-Ni6-N5R	163.2(5)	O25A-Ni8-O16A	90.1(5)

Table 3.3 continued.

O6H-Ni8-O1H	83.6(5)	O26A-Ni10-N2R	101.9(5)
O25A-Ni8-O1H	92.4(5)	O6H-Ni10-O7R	83.8(6)
O16A-Ni8-O1H	169.9(5)	O26A-Ni10-O7R	95.3(5)
O6H-Ni8-O6R	88.5(5)	N2R-Ni10-O7R	98.9(5)
O25A-Ni8-O6R	96.6(5)	O6H-Ni10-O1R	75.8(5)
O16A-Ni8-O6R	93.6(5)	O26A-Ni10-O1R	95.8(5)
O1H-Ni8-O6R	76.495)	N2R-Ni10-O1R	97.8(5)
O6H-Ni8-O1R	75.9(5)	O7R-Ni10-O1R	157.5(5)
O25A-Ni8-O1R	98.7(5)	O6H-Ni10-O2R	101.5(5)
O16A-Ni8-O1R	90.6(5)	O26A-Ni10-O2R	161.2(5)
O1H-Ni8-O1R	98.8(6)	N2R-Ni10-O2R	60.6(5)
O6R-Ni8-O1R	164.2(5)	O7R-Ni10-O2R	94.6(5)
O2H-Ni9-O21A	94.0(5)	O1R-Ni10-O2R	80.7(4)
O2H-Ni9-O2W	97.8(5)	N7R-Ni11-N8R	103.3(6)
O21A-Ni9-O2W	91.7(5)	N7R-Ni11-N9R	105.6(6)
O2H-Ni9-N1R	163.0(6)	N8R-Ni11-N9R	104.4(6)
O21A-Ni9-N1R	102.9(5)	N7R-Ni11-O8R	159.4(5)
O2W-Ni9-N1R	83.2(5)	N8R-Ni11-O8R	63.0(6)
O2H-Ni9-O2R	78.9(5)	N9R-Ni11-O8R	93.1(5)
O21A-Ni9-O2R	98.1(5)	N7R-Ni11-O9R	91.8(5)
O2W-Ni9-O2R	169.9(5)	N8R-Ni11-O9R	162.7(5)
N1R-Ni9-O2R	97.1(5)	N9R-Ni11-O9R	62.6(5)
O2H-Ni9-O1R	100.9(5)	O8R-Ni11-O9R	104.6(6)
O21A-Ni9-O1R	165.0(5)	N7R-Ni11-O7R	62.6(5)
O2W-Ni9-O1R	88.2(5)	N8R-Ni11-O7R	93.9(5)
N1R-Ni9-O1R	62.2(5)	N9R-Ni11-O7R	160.4(5)
O2R-Ni9-O1R	83.0(5)	O8R-Ni11-O7R	101.5(5)
O6H-Ni10-O26A	95.5(5)	O9R-Ni11-O7R	100.7(5)
O6H-Ni10-N2R	162.0(5)	Ni6-O1H-Ni8	98.5(5)

Table 3.3 continued.

Ni6-O1H-Ni1	121.2(5)	Ni10-O1R-Ni9	97.0(4)
Ni8-O1H-Ni1	95.7(5)	Ni9-O2R-Ni7	92.7(5)
Ni9-O2H-Ni1	122.8(5)	Ni9-O2R-Ni10	98.7(4)
Ni9-O2H-Ni7	97.5(5)	Ni7-O2R-Ni10	124.0(5)
Ni1-O2H-Ni7	95.7(5)	Ni7-O3R-Ni4	91.2(5)
Ni5-O3H-Ni3	104.8(5)	Ni7-O3R-Ni2	125.7(5)
Ni5-O3H-Ni1	121.3(5)	Ni4-O3R-Ni2	95.9(5)
Ni3-O3H-Ni1	98.2(5)	Ni2-O4R-Ni3	92.8(6)
Ni4-O4H-Ni7	103.3(4)	Ni2-O4R-Ni4	97.6(6)
Ni4-O4H-Ni1	122.4(5)	Ni3-O4R-Ni4	122.8(5)
Ni7O4H-Ni1	99.5(5)	Ni5-O5R-Ni3	90.9(5)
Ni2-O5H-Ni3	99.3(5)	Ni5-O5R-Ni6	94.9(5)
Ni2-O5H-Ni1	122.1(6)	Ni3-O5R-Ni6	128.2(5)
Ni3-O5H-Ni1	96.8(5)	Ni6-O6R-Ni8	93.3(5)
Ni10-O6H-Ni8	103.3(5)	Ni6-O6R-Ni5	96.2(5)
Ni10-O6H-Ni1	121.9(6)	Ni8-O6R-Ni5	124.2(5)
Ni8-O6H-Ni1	99.0(5)	Ni10-O7R-Ni11	131.4(5)
Ni8-O1R-Ni10	90.9(5)	Ni5-O8R-Ni11	130.7(6)
Ni8-O1R-Ni9	124.9(5)	Ni4-O9R-Ni11	132.8(5)

Table 3.4. Selected bond lengths (Å) and angles (°) for **24**.

Ni1-O2B	2.048(7)	Ni2-N3	2.029()9
Ni1-O1B	2.049(7)	Ni2-N11	2.059(9)
Ni1-O3B	2.053(8)	Ni2-O3	2.222(8)
Ni1-O5B	2.062(8)	Ni2-O11	2.230(8)
Ni1-O6B	2.064(8)	Ni2-O2	2.235(8)
Ni1-O4B	2.072(7)	Ni3-O3B	2.013(8)
Ni2-N2	2.021(9)	Ni3-O21A	2.029(8)

Table 3.4 continued

Ni3-O5B	2.033(8)	Ni8-O62A	2.010(8)
Ni3-O72A	2.050(8)	Ni8-N8	2.074(9)
Ni3-O4	2.119(7)	Ni8-O11	2.106(7)
Ni3-O5	2.159(7)	Ni8-O1	2.193(8)
Ni4-O1B	1.960(7)	Ni8-O8	2.276(8)
Ni4-O31A	1.993(8)	Ni9-O1B	1.997(7)
Ni4-N4	2.069(8)	Ni9-O32A	2.039(8)
Ni4-O3	2.153(9)	Ni9-O2B	2.043(7)
Ni4-O7	2.183(8)	Ni9-O42A	2.048(8)
Ni4-O4	2.234(7)	Ni9-O7	2.118(7)
Ni5-O6B	1.972(8)	Ni9-O8	2.156(7)
Ni5-O52A	2.026(8)	Ni10-O4B	1.992(7)
Ni5-O9	2.036(8)	Ni10-O51A	2.008(8)
Ni5-N5	2.077(8)	Ni10-O61A	2.024(8)
Ni5-O6	2.143(8)	Ni10-O6B	2.035(8)
Ni5-O5	2.215(8)	Ni10-O6	2.116(7)
Ni6-O3B	1.939(8)	Ni10-O1	2.131(7)
Ni6-O71A	1.984(8)	Ni11-O2B	1.971(7)
Ni6-N6	2.065(8)	Ni11-O41A	2.043(8)
Ni6-O2	2.109(7)	Ni11-O10	2.050(8)
Ni6-O5	2.196(8)	Ni11-N1	2.072(9)
Ni6-O6	2.266(8)	Ni11-O8	2.128(8)
Ni7-O5B	1.985(8)	Ni11-O1	2.207(8)
Ni7-O22A	2.023(8)	O2B-Ni1-O1B	81.0(3)
Ni7-O11A	2.023(8)	O2B-Ni1-O3B	161.6(3)
Ni7-N7	2.089(9)	O1B-Ni1-O3B	86.6(3)
Ni7-O4	2.203(7)	O2B-Ni1-O5B	89.0(3)
Ni7-O7	2.225(8)	O1B-Ni1-O5B	106.2(3)
Ni8-O4B	1.934(7)	O3B-Ni1-O5B	81.4(3)

Table 3.4 continued

O2B-Ni1-O6B	88.3(3)	O5B-Ni3-O72A	170.2(3)
O1B-Ni1-O6B	159.3(3)	O3B-Ni3-O4	88.1(3)
O3B-Ni1-O6B	107.5(3)	O21A-Ni3-O4	96.5(3)
OB-Ni1-O6B	91.2(3)	O5B-Ni3-O4	77.3(3)
O2B-Ni1-O4B	106.5(3)	O72A-Ni3-O4	93.7(3)
O1B-Ni1-O4B	86.1(3)	O3B-Ni3-O5	75.7(3)
O3B-Ni1-O4B	86.0(3)	O21A-Ni3-O5	99.5(3)
O5B-Ni1-O4B	161.7(3)	O5B-Ni3-O5	94.6(3)
O6B-Ni1-O4B	80.1(3)	O72A-Ni3-O5	93.1(3)
N2-Ni2-N3	105.3(4)	O4-Ni3-O5	162.7(3)
N2-Ni2-N11	104.8(4)	O1B-Ni4-O31A	94.5(3)
N3-Ni2-N11	102.6(4)	O1B-Ni4-N4	163.9(3)
N2-Ni2-O3	161.3(3)	O31A-Ni4-N4	101.3(3)
N3-Ni2-O3	62.6(3)	O1B-Ni4-O3	82.2(3)
N11-Ni2-O3	92.3(3)	O31A-Ni4-O3	93.1(3)
N2-Ni2-O11	94.7(4)	N4-Ni4-O3	99.7(3)
N3-Ni2-O11	157.7(3)	O1B-Ni4-O7	76.4(3)
N11-Ni2-O11	62.1(3)	O31A-Ni4-O7	96.0(3)
O3-Ni2-O11	100.1(3)	N4-Ni4-O7	98.8(3)
N2-Ni2-O2	62.5(3)	O3-Ni4-O7	157.3(3)
N3-Ni2-O2	96.9(4)	O1B-Ni4-O4	102.0(3)
N11-Ni2-O2	159.2(3)	O31A-Ni4-O4	162.6(3)
O3-Ni2-O2	103.1(3)	N4-Ni4-O4	61.9(3)
O11-Ni2-O2	100.9(3)	O3-Ni4-O4	94.4(3)
O3B-Ni3-O21A	175.1(3)	O7-Ni4-O4	82.8(3)
O3B-Ni3-O5B	83.1(3)	O6B-Ni5-O52A	92.9(3)
O21A-Ni3-O5B	96.1(3)	O6B-Ni5-O9	89.0(3)
O3B-Ni3-O72A	92.9(3)	O52A-Ni5-O9	95.1(3)
O21A-Ni3-O72A	88.7(3)	O6B-Ni5-N5	164.4(3)

Table 3.4 continued

O52A-Ni5-N5	101.9(3)	O5B-Ni7-N7	162.4(3)
O9-Ni5-N5	94.3(4)	O22A-Ni7-N7	100.0(3)
O6B-Ni5-O6	77.7(3)	O11A-Ni7-N7	85.9(3)
O52A-Ni5-O6	96.5(3)	O5B-Ni7-O4	76.3(3)
O9-Ni5-O6	162.8(3)	O22A-Ni7-O4	92.9(3)
N5-Ni5-O6	95.7(3)	O11A-Ni7-O4	171.6(3)
O6B-Ni5-O5	102.6(3)	N7-Ni7-O4	94.9(3)
O52A-Ni5-O5	163.7(3)	O5B-Ni7-O7	101.8(3)
O9-Ni5-O5	90.1(3)	O22A-Ni7-O7	160.3(3)
N5-Ni5-O5	62.1(3)	O11A-Ni7-O7	90.6(3)
O6-Ni5-O5	82.3(3)	N7-Ni7-O7	61.5(3)
O3B-Ni6-O71A	94.9(3)	O4-Ni7-O7	82.6(3)
O3B-Ni6-N6	163.6(3)	O4B-Ni8-O62A	95.5(3)
O71A-Ni6-N6	100.5(3)	O4B-Ni8-N8	161.7(3)
O3B-Ni6-O2	82.8(3)	O62A-Ni8-N8	101.7(3)
O71A-Ni6-O2	94.7(3)	O4B-Ni8-O11	84.1(3)
N6-Ni6-O2	101.0(3)	O62A-Ni8-O11	95.6(3)
O3B-Ni6-O5	76.3(3)	N8-Ni8-O11	100.3(3)
O71A-Ni6-O5	98.3(3)	O4B-Ni8-O1	76.0(3)
N6-Ni6-O5	96.1(3)	O62A-Ni8-O1	95.8(3)
O2-Ni6-O5	156.3(3)	N8-Ni8-O1	95.8(3)
O3B-Ni6-O6	102.6(3)	O11-Ni8-O1	157.9(3)
O71A-Ni6-O6	161.3(3)	O4B-Ni8-O8	100.8(3)
N6-Ni6-O6	61.5(3)	O62A-Ni8-O8	161.5(3)
O2-Ni6-O6	93.8(3)	N8-Ni8-O8	61.3(3)
O5-Ni6-O6	80.0(3)	O11-Ni8-O8	94.7(3)
O5B-Ni7-O22A	95.7(3)	O1-Ni8-O8	79.9(3)
O5B-Ni7-O11A	100.6(3)	O1B-Ni9-O32A	95.1(3)
O22A-Ni7-O11A	95.2(3)	O1B-Ni9-O2B	82.3(3)

Table 3.4 continued

O32A-Ni9-O2B	169.2(3)	O2B-Ni11-O10	90.6(3)
O1B-Ni9-O42A	175.0(3)	O41A-Ni11-O10	97.3(3)
O32A-Ni9-O42A	89.1(3)	O2B-Ni11-N1	167.1(3)
O2B-Ni9-O42A	94.1(3)	O41A-Ni11-N1	99.9(3)
O1B-Ni9-O7	77.2(3)	O10-Ni11-N1	91.8(3)
O32A-Ni9-O7	93.8(3)	O2B-Ni11-O8	78.7(3)
O2B-Ni9-O7	95.9(3)	O41A-Ni11-O8	97.6(3)
O42A-Ni9-O7	99.9(3)	O10-Ni11-O8	162.0(3)
O1B-Ni9-O8	87.7(3)	N1-Ni11-O8	95.6(3)
O32A-Ni9-O8	92.9(3)	O2B-Ni11-O1	105.3(3)
O2B-Ni9-O8	76.5(3)	O41A-Ni11-O1	162.1(3)
O42A-Ni9-O8	94.8(3)	O10-Ni11-O1	86.0(3)
O7-Ni9-O8	163.9(3)	N1-Ni11-O1	62.3(3)
O4B-Ni10-O51A	172.7(3)	O8-Ni11-O1	82.9(3)
O4B-Ni10-O61A	95.4(3)	Ni10-O1-Ni11	90.6(3)
O51A-Ni10-O61A	88.6(3)	Ni10-O1-Ni11	121.993)
O4B-Ni10-O6B	82.7(3)	Ni8-O1-Ni11	98.1(3)
O51A-Ni10-O6B	94.4(3)	Ni6-O2-Ni2	132.9(3)
O61A-Ni10-O6B	170.9(3)	Ni4-O3-Ni2	134.7(4)
O4B-Ni10-O6	89.7(3)	Ni3-O4-Ni7	91.2(3)
O51A-Ni10-O6	96.2(3)	Ni3-O4-Ni4	125.9(3)
O61A-Ni10-O6	94.1(3)	Ni7-O4-Ni4	96.6(3)
O6B-Ni10-O6	77.0(3)	Ni3-O5-Ni6	90.5(3)
O4B-Ni10-O1	76.3(3)	Ni3-O5-Ni5	125.1(3)
O51A-Ni10-O1	97.4(3)	Ni6-O5-Ni5	98.4(3)
O61A-Ni10-O1	92.9(3)	Ni10-O6-Ni5	92.1(3)
O6B-Ni10-O1	95.3(3)	Ni10-O6-Ni6	123.3(3)
O6-Ni10-O1	164.9(3)	Ni5-O6-Ni6	98.4(3)
O2B-Ni11-O41A	92.3(3)	Ni9-O7-Ni4	91.1(3)

Table 3.4 continued

Ni9-O7-Ni7	124.4(3)	Ni6-O3B-Ni3	103.0(3)
Ni4-O7-Ni7	97.5(3)	Ni6-O3B-Ni1	120.5(3)
Ni11-O8-Ni9	91.8(3)	Ni3-O3B-Ni1	98.1(4)
Ni9-O8-Ni8	97.9(3)	Ni8-O4B-Ni10	103.1(4)
Ni9-O8-Ni8	124.5(3)	Ni8-O4B-Ni1	121.9(3)
Ni8-O11-Ni2	131.7(3)	Ni10-O4B-Ni1	99.1(3)
Ni4-O1B-Ni9	101.8(3)	Ni7-O5B-Ni3	100.5(3)
Ni4-O1B-Ni1	120.6(4)	Ni7-O5B-Ni1	121.0(4)
Ni9-O1B-Ni1	99.0(3)	Ni3-O5B-Ni1	97.2(3)
Ni11-O2B-Ni9	100.0(3)	Ni5-O6B-Ni10	99.9(3)
Ni11-O2B-Ni1	118.6(4)	Ni5-O6B-Ni1	119.3(4)
Ni9-O2B-Ni1	97.5(3)	Ni10-O6B-Ni1	98.0(3)

3.2.6. Magnetochemistry of 23 and 24.

The magnetic behaviour of **23** and **24** was studied in the temperature range 250-2.0 K. The behaviour of the two compounds is identical. The magnetic behaviour down to 11 K closely resembles the behaviour of a ferrimagnetic system, but below this temperature a rapid decrease in the value of $\chi_m T$ is observed. The data has been modelled on a system in which there are ten interacting nickel (II) ions arranged in a tricapped-trigonal prism with an isolated eleventh nickel (II) ion. The presence of this non-interacting magnetic ion was included in the treatment as an additive term to the magnetic susceptibility assuming a Curie behaviour and a g-factor of 2.2.

The coupling scheme used is shown in Figure 3.14 : one coupling constant (J_1) accounts for the interaction between the central nickel ion and the six nickel ions in the

corners of the prism ; a second constant (J_2) was added for the coupling of the central ion with the three nickels which cap the square faces of the prism; finally, the presence of a coupling between the nine nickel atoms in the outer spherewas included (J_3) according to the structure of the crystal assuming equivalence of all the bridging units. Two fitting procedures were adopted. In the first series of calculations all the data was considered, while in the second only the data from 250 K down the maximum value of $\chi_m T$ was included. These approaches are based on two different assumptions. The first hypothesis considers the overall magnetic behaviour at all temperatures as due only to intra-molecular interactions, while the second procedure assumes that at low temperature some other mechanism prevails in addition to the intra-cluster one. The first procedure yielded a diamagnetic ground state due to antiferromagnetic interactions with J_1 = -9.72(3) cm^{-1}, J_2 = -8.81(4) cm^{-1}, J_3 = -3.68(4) cm^{-1}. In all the calculations the g-factor was maintained for all the Ni(II) ions at 2.2. The calculated curve is shown in Figure 3.15 and the agreement with the experimental behaviour is fair. The second fitting procedure yielded a different set of coupling constants with an alternate ferro-

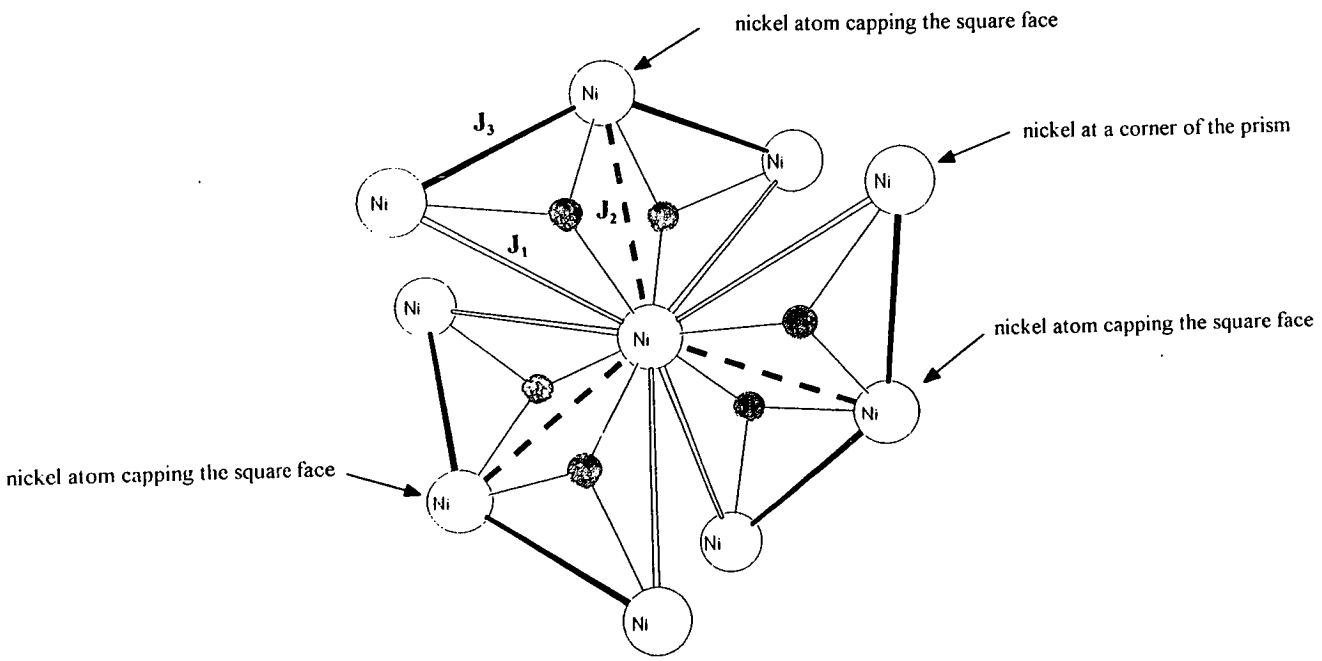

Figure 3.14. The coupling scheme for **23**, **24**.

antiferromagnetic nature : J_1 = 19.54(2) cm^{-1}, J_2 = -53.18(6)cm^{-1}, 1.76(4)cm^{-1}. The calculated ground state has a spin multiplicity S = 4 and the agreement with the experiment is better as shown in Figure 3.15. For this model the low temperature behaviour must be attributed to three different causes : i) saturation effects ; ii) inter-cluster interactions ; iii) zero-field splitting. Saturation effects were ruled out by repeating the measurements at smaller external magnetic fields and no substantial differences in the data sets were observed. The second possible cause for the fall in $\chi_m T$ - inter-cluster coupling - seemed consistent with the crystal structures (especially for **23** which forms a dimer of undecanuclear cages). Therefore the susceptibility below 20 K was calculated as due to dimers of S = 4 units using a simple Bleaney-Bowers expression but no reasonable fitting was obtained. Even considering dipolar interactions in a mean field approach failed to give good results. The zero-field splitting effects were considered by using their energy levels with their spin multiplicity obtained from the second set of calculations. The data were modelled by including zero-field splitting in two ways : first only for the ground S = 4 state which gave a D value of 6.97(2) cm^{-1} and an excellent fit to the experimental data as shown in Figure 3.16. This substantial D value led to

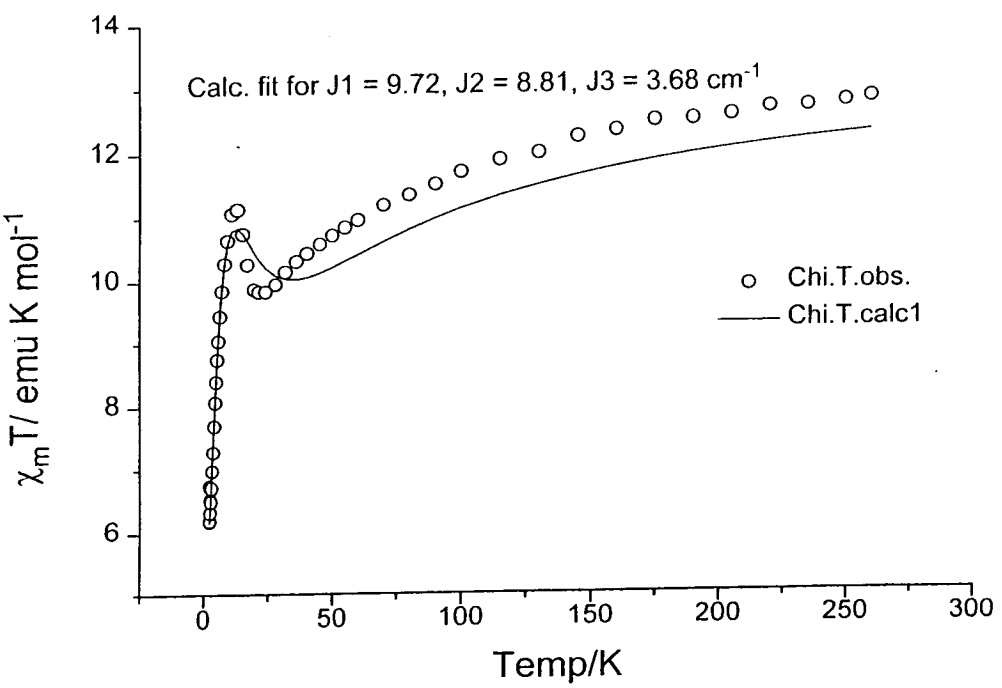

Figure 3.15. The variation of $\chi_m T$ with temperature.

the consideration of a second model in which the splitting of the first excited state (S = 5) was included, however the introduction of the second zero-field splitting parameter did not improve the agreement with the experimental data.

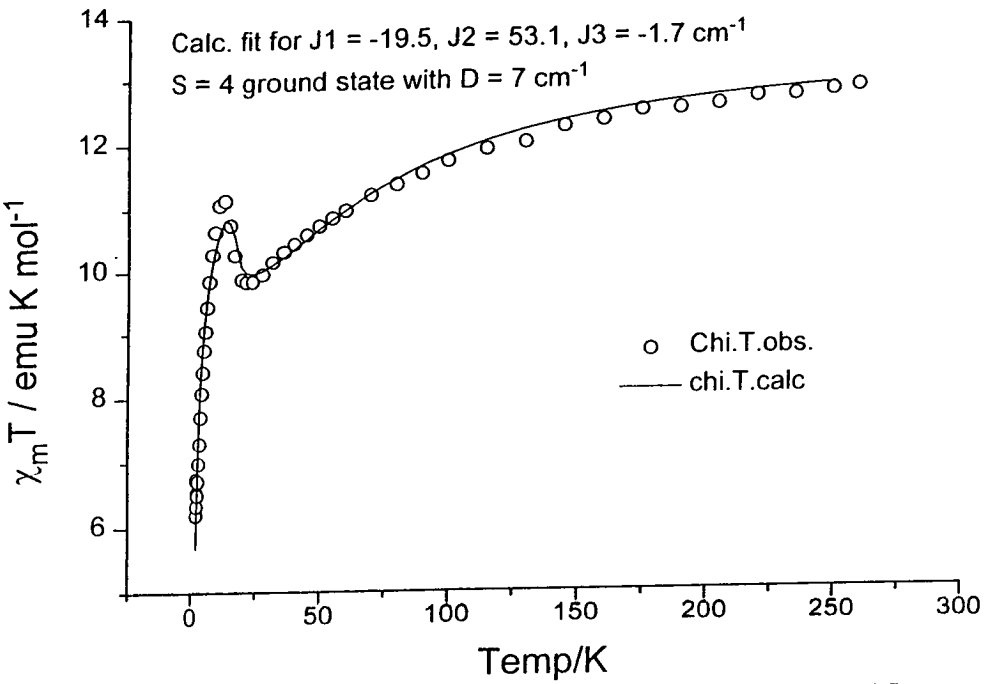

Figure 3.16. The varition of $\chi_m T$ with temperature and its theoretical fit.

3.2.7. Synthesis and structure of $[Co_{10}(\mu_3\text{-}OH)_6(\mu_3\text{-}mhp)_6(O_2CPh)_7Cl(Hmhp)_3(MeCN)]$ 25.

Reaction of cobalt chloride with two equivalents of both Na(mhp) and $Na(O_2CPh)$ in methanol gave a purple solution which, after 24 hours, was evaporated to dryness producing a purple paste. This paste was dried *in vacuo* for 24 hours before being crystallised from acetonitrile to give purple crystals of $[Co_{10}(OH)_6(mhp)_6(O_2CPh)_7(Cl)(Hmhp)_3(MeCN)]$ **25** [Figure 3.17] in moderate yield after four days [93]. The structure of **25** is again based on a centred-tricapped-trigonal prism and is closely related to compounds **20-24**. However whereas each of the previous compounds contained either one or two additional caps on the 'upper' and 'lower' triangular faces of the prism, **25** contains no additional caps.

Again the central core of the complex $[Co_{10}(\mu_3\text{-}OH)_6(\eta^2, \mu_3\text{-}mhp)_6(\eta^2, \mu_2\text{-}O_2CPh)_6]^{2+}$ remains intact with the central cobalt [Co1] attached to the six μ_3-hydroxides which further

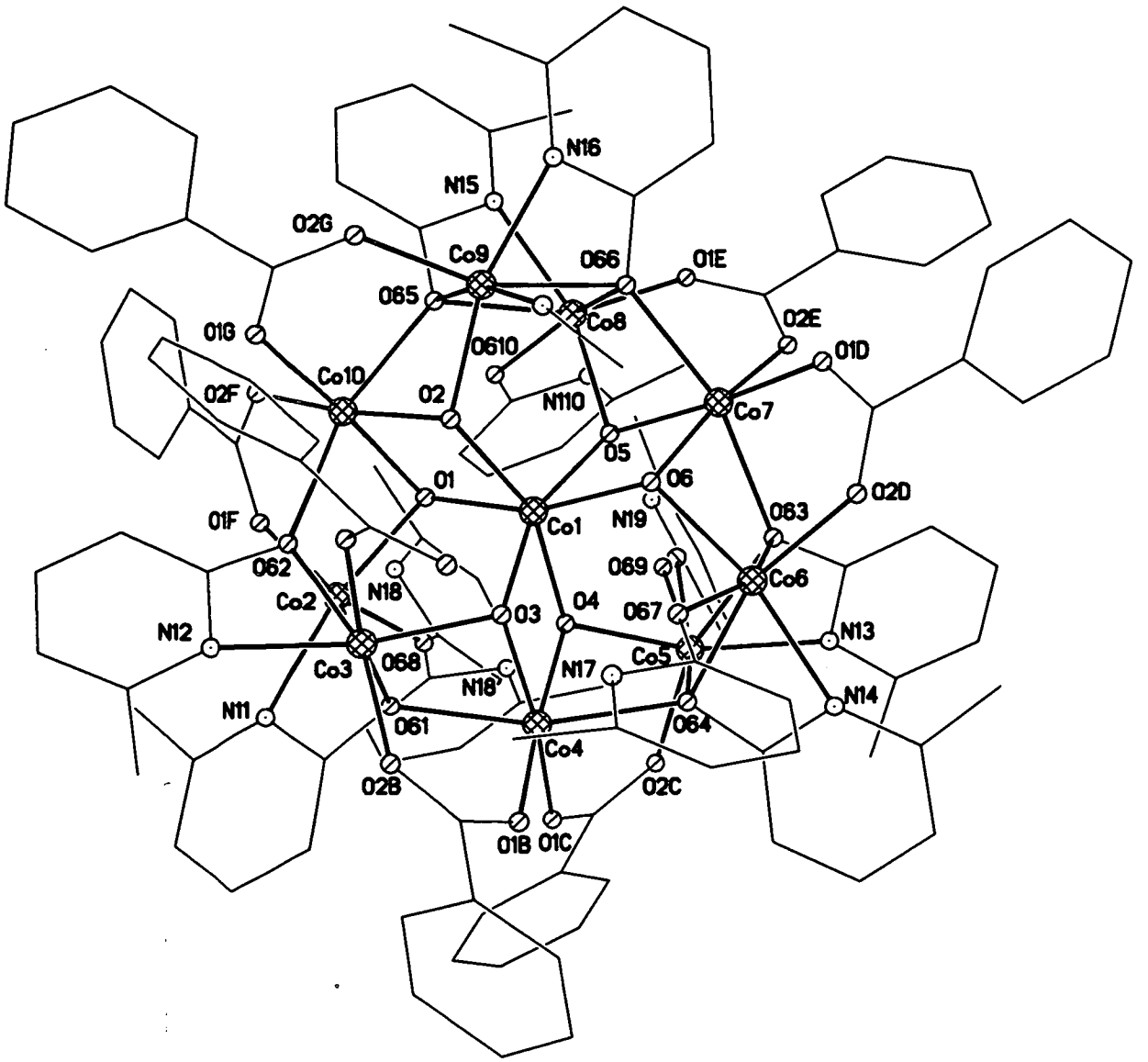

Figure 3.17. The structure of **25** in the crystal.

ligate to the vertex cobalt sites [Co2, Co3, Co5, Co6, Co8, Co9] and to the cobalt atoms capping the square faces of the prism [Co4, Co7, Co10]. The centred-tricapped-trigonal prism formed by the metal centres is shown in Figure 3.18. Again the significant structural difference in **25** comes on the sixth coordination site of the vertex metals. In compounds **22-24** the 'lower' triangular face was capped by a $[Ni(xhp)_3]^-$ moiety but in **25** both triangular faces remain uncapped. Instead these sites are now occupied by one chloride and two Hmhp ligands [on the 'lower' triangular face] and one benzoate and one Hmhp ligand which are strongly hydrogen bonded to each other [N17...O2A, 2.630(7) Å] and one MeCN ligand [on the 'upper' triangular face]. The presence of a larger carboxylate (i.e. benzoate rather than acetate or chloroacetate) and its subsequent intermolecular interactions and steric crowding may be the

reason that further metal fragments [i.e. $Co(mhp)_3^-$ units] are prevented from ligating the triangular faces of the prism. However even though a larger carboxylate has been introduced the coordination geometries around the vertex metal sites [*cis*, 60.1-105.7(5)°; *trans*, 155.2-165.7(3)°] do not appear to be any more distorted than those present in compounds **20-24.** The geometries of the cobalt atoms capping the square faces of the prism are also similar to those in **20-24** : *cis*, 76.6-97.6(3)°; *trans*, 163.5-173.5(3)°. The closest Co...Co distance is 3.065(7) Å between Co9 and Co10. Selected bond lengths and angles for **25** are given in Table 3.5.

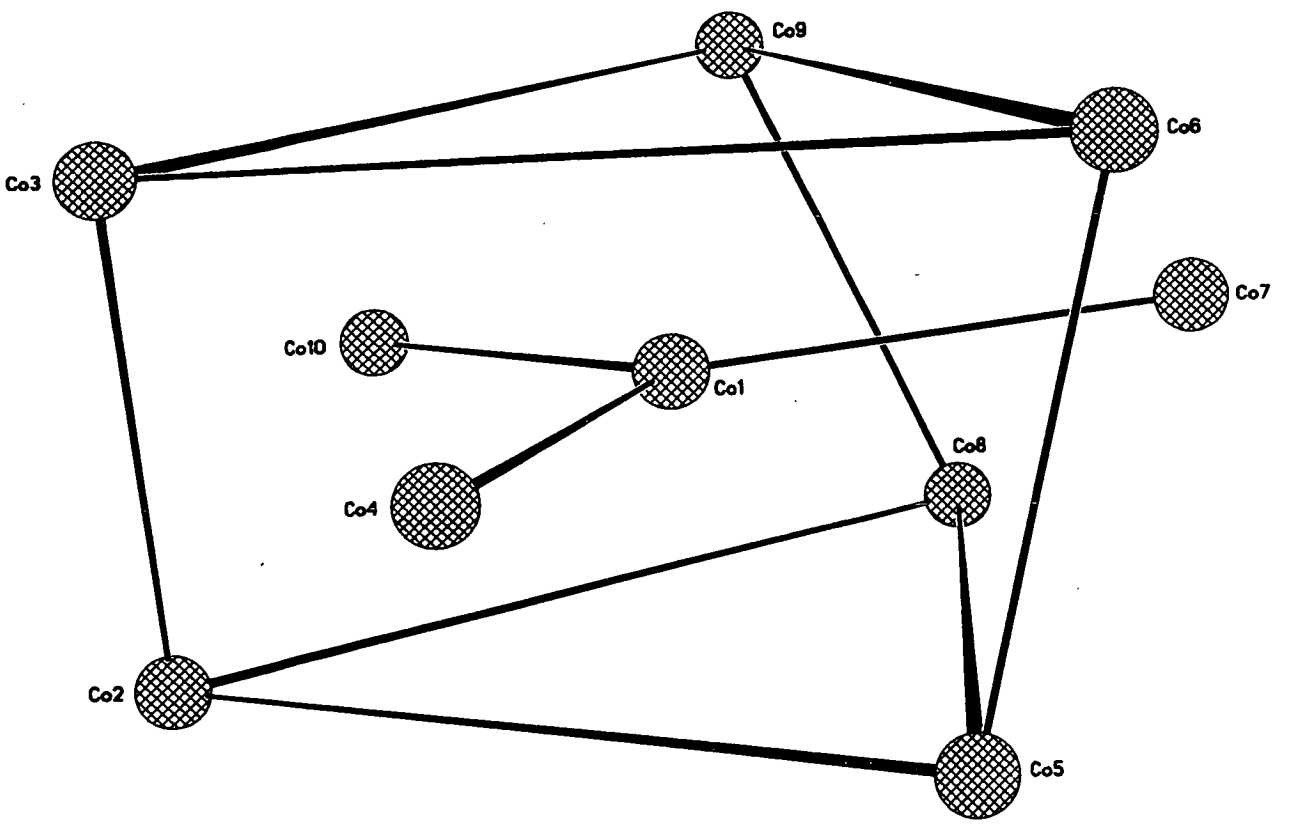

Figure 3.18. The centred-tricapped-trigonal prism formed by **25**.

Table 3.5. Selected bond lengths (Å) and angles (°) for **25**.

Co1-O3	2.080(8)	Co5-Cl9	2.53(2)
Co1-O4	2.080(8)	Co6-O6	2.025(7)
Co1-O1	2.101(8)	Co6-O2D	2.033(7)
Co1-O5	2.107(8)	Co6-O67	2.082(7)
Co1-O2	2.110(8)	Co6-N14	2.154(7)
Co1-O6	2.115(8)	Co6-O63	2.166(7)
Co2-O1	1.993(8)	Co6-O64	2.233(7)
Co2-O1F	2.059(8)	Co7-O2E	2.005(5)
Co2-O68	2.076(8)	Co7-O1D	2.012(7)
Co2-N11	2.110(6)	Co7-O6	2.043(7)
Co2-O62	2.158(8)	Co7-O5	2.053(7)
Co2-O61	2.298(7)	Co7-O63	2.189(7)
Co3-O3	2.012(8)	Co7-O66	2.202(7)
Co3-O1A	2.035(7)	Co8-O5	1.968(8)
Co3-O2B	2.043(7)	Co8-O1E	2.066(7)
Co3-N12	2.136(7)	Co8-O610	2.07(2)
Co3-O61	2.195(7)	Co8-N15	2.101(6)
Co3-O62	2.311(7)	Co8-O66	2.240(8)
Co4-O1C	2.033(7)	Co8-O65	2.316(7)
Co4-O1B	2.045(7)	Co9-O2	1.962(8)
Co4-O3	2.045(7)	Co9-O2G	2.013(8)
Co4-O4	2.052(7)	Co9-N16	2.111(8)
Co4-O61	2.178(7)	Co9-N1S	2.156(12)
Co4-O62	2.193(6)	Co9-O65	2.189(8)
Co5-O4	1.970(7)	Co9-O66	2.317(7)
Co5-O2C	2.051(7)	Co10-O1G	2.026(7)
Co5-N13	2.090(7)	Co10-O2F	2.048(7)
Co5-O69	2.16(2)	Co10-O1	2.051(8)
Co5-O64	2.225(8)	Co10-O2	2.093(8)

Table 3.5. continued

Co10-O62	2.148(8)	O68-Co2-O61	87.9(2)
Co10-O65	2.160(7)	N11-Co2-O61	60.7(2)
O3-Co1-O4	80.693)	O62-Co2-O61	79.3(3)
O3-Co1-O1	110.1(3)	O3-Co3-O1A	93.3(3)
O4-Co1-O1	85.2(3)	O3-Co3-O2B	93.0(2)
O3-Co1-O5	159.3(3)	O1A-Co3-O2B	102.8(2)
O4-Co1-O5	88.8(3)	O3-Co3-N12	163.0(3)
O1-Co1-O5	86.5(3)	O1A-Co3-N12	88.5(3)
O3-Co1-O2	87.7(3)	O2B-Co3-N12	103.0(2)
O4-Co1-O2	158.6(3)	O3-Co3-O61	77.2(3)
O1-Co1-O2	82.0(3)	O1A-Co3-O61	159.6(3)
O5-Co1-O2	107.4(3)	O2B-Co3-O61	95.8(3)
O3-Co1-O6	84.7(3)	N12-Co3-O61	95.5(3)
O4-Co1-O6	107.0(3)	O3-Co3-O62	103.2(3)
O1-Co1-O6	162.6(3)	O1A-Co3-O62	86.5(3)
O5-Co1-O6	81.5(3)	OB2-Co3-O62	160.9(3)
O2-Co1-O6	89.5(3)	N12-Co3-O62	60.1(3)
O1-Co2-O1F	93.2(3)	O61-Co3-O62	78.3(3)
O1-Co2-O68	87.9(3)	O1C-Co4-O1B	92.9(3)
O1F-Co2-O68	98.3(3)	O1C-Co4-O3	169.3(2)
O1-Co2-N11	162.2(3)	O1B-Co4-O3	93.5(2)
O1F-Co2-N11	104.1(3)	O1C-Co4-O4	92.3(2)
O68-Co2-N11	93.7(3)	O1B-Co4-O4	172.5(2)
O1-Co2-O62	78.2(3)	O3-Co4-O4	82.2(3)
O1F-Co2-O62	98.6(3)	O1C-Co4-O61	93.8(2)
O68-Co2-O62	158.7(3)	O1B-Co4-O61	96.3(2)
N11-Co2-O62	94.8(3)	O3-Co4-O61	76.9(2)
O1-Co2-O61	101.7(3)	O4-Co4-O61	88.8(2)
O1F-Co2-O61	164.1(2)	O1C-Co4-O64	94.3(3)

Table 3.5 continued

O1B-Co4-O64	97.6(2)	O67-Co6-N14	99.5(3)
O3-Co4-O64	93.4(3)	O6-Co6-O63	78.1(3)
O4-Co4-O64	76.6(3)	O2D-Co6-O63	95.0(3)
O61-Co4-O64	163.5(3)	O67-Co6-O63	159.1(3)
O4-Co5-O2C	93.5(2)	N14-Co6-O63	94.1(3)
O4-Co5-N13	161.8(2)	O6-Co6-O64	102.3(3)
O2C-Co5-N13	104.6(3)	O2D-Co6-O64	159.3(3)
O4-Co5-O69	85.1(7)	O67-Co6-O64	91.2(3)
O2C-Co5-O69	95.9(7)	N14-Co6-O64	61.1(3)
N13-Co5-O69	94.2(7)	O63-Co6-O64	81.6(3)
O4-Co5-O64	77.5(3)	O2E-Co7-O1D	89.2(3)
O2C-Co5-O64	97.6(2)	O2E-Co7-O6	171.7(3)
N13-Co5-O64	98.4(3)	O1D-Co7-O6	93.4(3)
O69-Co5-O64	158.6(6)	O2E-Co7-O5	93.7(2)
O4-Co5-O63	101.6(3)	O1D-Co7-O5	173.7(3)
O2C-Co5-O63	162.9(2)	O6-Co7-O5	84.6(3)
N13-Co5-O63	60.3(2)	O2E-Co7-O63	94.7(3)
O69-Co5-O63	93.4(7)	O1D-Co7-O63	96.0(3)
O64-Co5-O63	78.1(3)	O6-Co7-O63	77.2(3)
O4-Co5-Cl9	92.1(4)	O5-Co7-O63	89.393)
O2C-Co5-Cl9	95.3(6)	O2E-Co7-O66	95.2(3)
N13-Co5-Cl9	87.7(4)	O1D-Co7-O66	96.9(3)
O64-Co5-Cl9	163.9(5)	O6-Co7-O66	92.4(3)
O63-Co5-Cl9	92.2(5)	O5-Co7-O66	77.3(3)
O6-Co6-O2D	97.0(2)	O63-Co7-O66	163.8(3)
O6-Co6-O67	84.4(3)	O5-Co8-O1E	98.8(2)
O2D-Co6-O67	98.3(2)	O5-Co8-O610	87.3(9)
O6-Co6-N14	162.8(3)	O1E-Co8-O610	105.7(5)
O2D-Co6-N14	99.0(2)	O5-Co8-N15	160.4(3)

Table 3.5 continued

O1E-Co8-N15	100.7(2)	O1G-Co10-O2	94.0(2)
O610-Co8-N15	87.0(9)	O2FCo10-O2	171.8(3)
O5-Co8-O66	78.1(3)	O1-Co10-O2	83.6(3)
O1E-Co8-O66	96.4(3)	O1G-Co10-O62	96.9(2)
O610-Co8-O66	155.2(3)	O2F-Co10-O62	95.8(2)
N15-Co8-O66	100.0(3)	O1-Co10-O62	77.2(3)
O5-Co8-O65	100.4(3)	O2-Co10-O62	91.4(3)
O1E-Co8-O65	159.6(3)	O1G-Co10-O65	95.6(2)
O610-Co8-O65	82.1(3)	O2F-Co10-O65	95.3(3)
N15-Co8-O65	60.2(2)	O1-Co10-O65	89.8(3)
O66-Co8-O65	80.9(3)	O2-Co10-O65	76.9(3)
O2-Co9-O2G	99.2(2)	O62-Co10-O65	163.5(3)
O2-Co9-N16	160.5(3)	Co2-O1-Co10	99.0(3)
O2G-Co9-N16	99.9(3)	Co2-O1-Co1	119.6(3)
O2-Co9-N1S	88.6(3)	Co10-O1-Co1	98.0(4)
O2G-Co9-N1S	92.1(3)	Co9-O2-Co10	98.1(3)
N16-Co9-N1S	94.4(3)	Co9-O2-Co1	122.1(3)
O2-Co9-O65	79.093)	Co10-O2-Co1	96.4(3)
O2G-Co9-O65	96.7(3)	Co3-O3-Co4	100.7(3)
N16-Co9-O65	95.2(3)	Co3-O3-Co1	118.0(3)
N1S-Co9-O65	165.7(3)	Co4-O3-Co1	98.7(3)
O2-Co9-o66	100.5(3)	Co5-O4-Co4	102.0(3)
O2G-Co9-O66	159.6(3)	Co5-O4-Co1	121.2(4)
N16-Co9-O66	60.2(3)	Co4-O4-Co1	98.4(3)
N1S-Co9-O66	93.6(3)	Co8-O5-Co7	100.2(4)
O65-Co9-O66	82.0(3)	Co8-O5-Co1	121.8(3)
O1G-Co10-O2F	89.2(3)	Co7-O5-Co1	96.9(4)
O1G-Co10-O1	173.5(2)	Co6-O6-Co7	99.0(3)
O2F-Co10-O1	94.0(2)	Co6-O6-Co1	120.5(4)

Table 3.5 continued

Co7-O6-Co1	97.0(3)	Co4-O64-Co5	90.1(3)
Co4-O61-Co3	91.2(2)	Co4-O64-Co6	123.3(3)
Co4-O61-Co2	124.5(3)	Co5-O64-Co6	100.3(3)
Co3-O61-Co2	100.2(3)	Co10-O65-Co9	89.6(3)
Co10-O62-Co2	91.2(3)	Co10-O65-Co8	126.8(3)
Co10-O62-Co3	122.9(3)	Co9-O65-Co8	99.1(3)
Co6-O63-Co7	90.6(3)	Co7-O66-Co8	88.0(3)
Co6-O63-Co5	98.9(3)	Co7-O66-Co9	126.7(3)
Co7-O63-Co5	124.2(3)		

3.2.8. Magnetochemistry of 25.

The magnetic behaviour of **25** was studied in the temperature range 300-1.8 K in an applied field of 1000 G. The variation of $\chi_m T$ with temperature is shown in Figure 3.19.

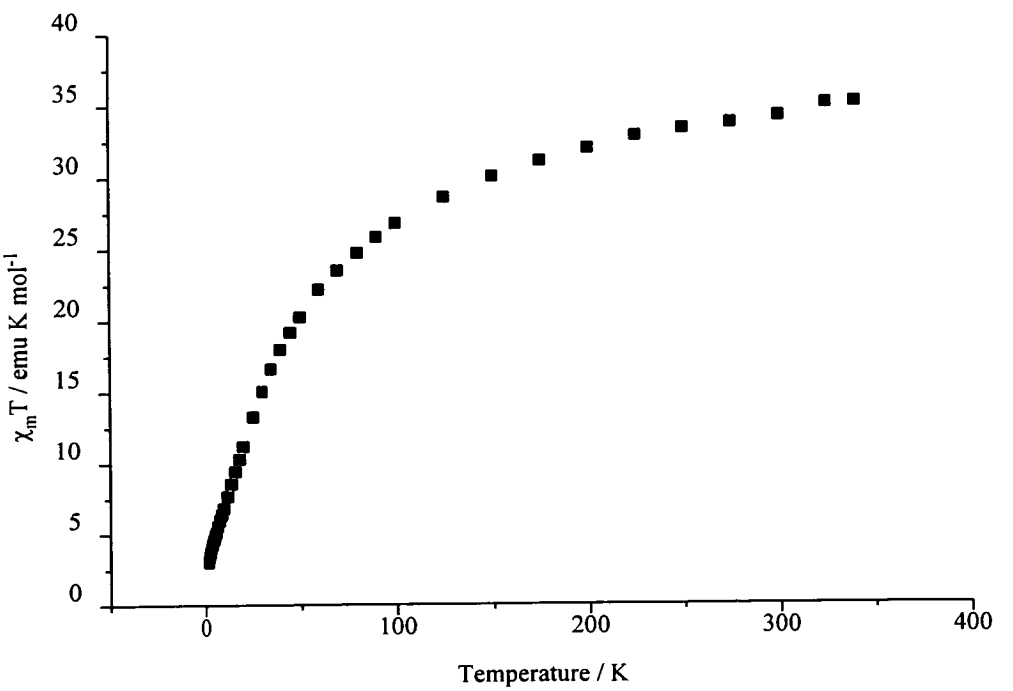

Figure 3.19. The variation of $\chi_m T$ with temperature for **25**.

The room temperature value of $\chi_m T$ is approximately 35 emu K mol^{-1} which is consistant with ten non-interacting Co(II) S = 3/2 centres [$\chi_m T$ = 32 emu K mol^{-1}; g = 2.6]. The value of $\chi_m T$ then drops steadily with temperature to a minimum of approximately 2.0 emu K mol^{-1} at 1.8 K, indicative of antiferromagnetic coupling betwen the metal centres. The 1.8 K value corresponds to a low spin ground state.

3.2.9. Synthesis and structure of $[Ni_{10}(OH)_4(mhp)_{10}(O_2CCMe_3)_6(MeOH)_2]$ 26.

Given that the introduction of benzoate as the carboxylate in the previous reaction produced a centred-tricapped-trigonal prism which contained no caps, due presumably to the size of the ligand, the effect of introducing an even more sterically demanding ligand was investigated. Reaction of nickel chloride with two equivalents of both Na(mhp) and $Na(O_2CCMe_3)$ in methanol produced a paste which was crystallised from acetonitrile to give green crystals of $[Ni_{10}(OH)_4(mhp)_{10}(O_2CCMe_3)_6(MeOH)_2]$ **26** [Figure 3.20] in good yield after two days [92]. Trimethylacetate is a much bulkier ligand than any of the carboxylates discussed earlier and has resulted in a structure which is no longer based on a centred-tricapped-trigonal prism as with **20-25** but instead on a fourteen-vertex deltahedron.

26 crystallises with a two-fold axis passing through Ni1 and Ni2 and is held together by four μ_3-hydroxide ligands , six 1,3-bridging trimethylacetates and ten mhp ligands. The mhp ligands adopt four different coordinating modes : chelating to one nickel [for example Ni6] with the exocyclic oxygen atom bridging to one other nickel centre [Ni3]; chelating to one nickel [Ni5] with the oxygen bridging a total of three nickels [N5, Ni2 and Ni3]; binding to one nickel through the ring nitrogen alone [Ni4] with the oxygen μ_2-bridging two different nickel atoms [Ni1 and Ni6]. Thus the pyridonate ligand shows a much more diverse

coordination chemistry in **26** than it exhibits in the structures of the trigonal prisms. However the binding of the carboxylate (in this case trimethylacetate) is essentially unchanged, bridging in a 1,3 -fashion between the metal centres. The metal polyhedron is shown in Figure 3.21 with the fourteen vertex deltahedron on which it is based in Figure 3.22.

The metal array itself does not describe a complete polyhedron. It is based on a fourteen-vertex cage with five of the 'ideal' vertices missing. Given the absence of so many vertices the overall geometry is surprisingly regular with Ni1 at the centre, Ni3, Ni3A, Ni5 and

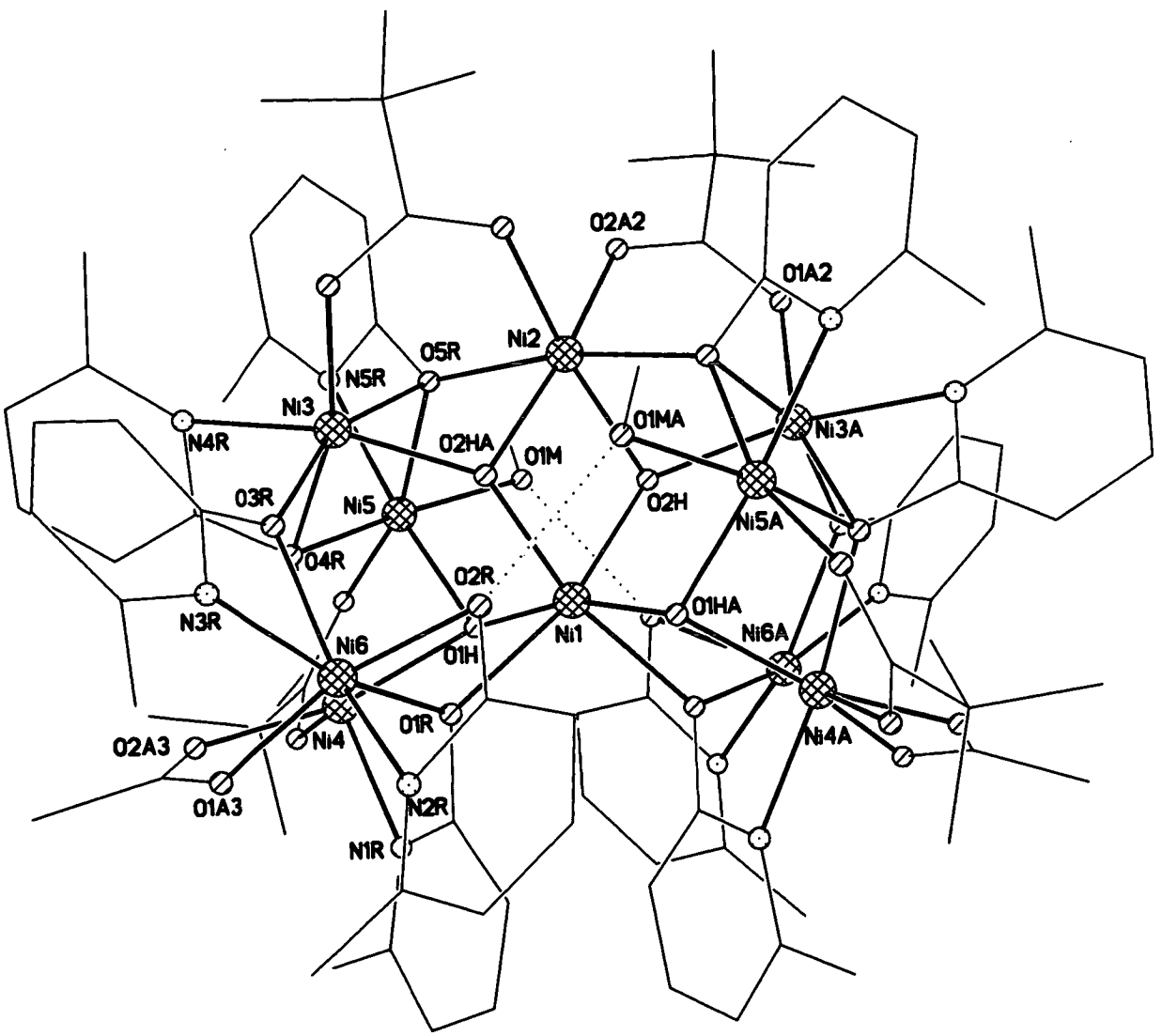

Figure 3.20. The structure of **26** in the crystal.

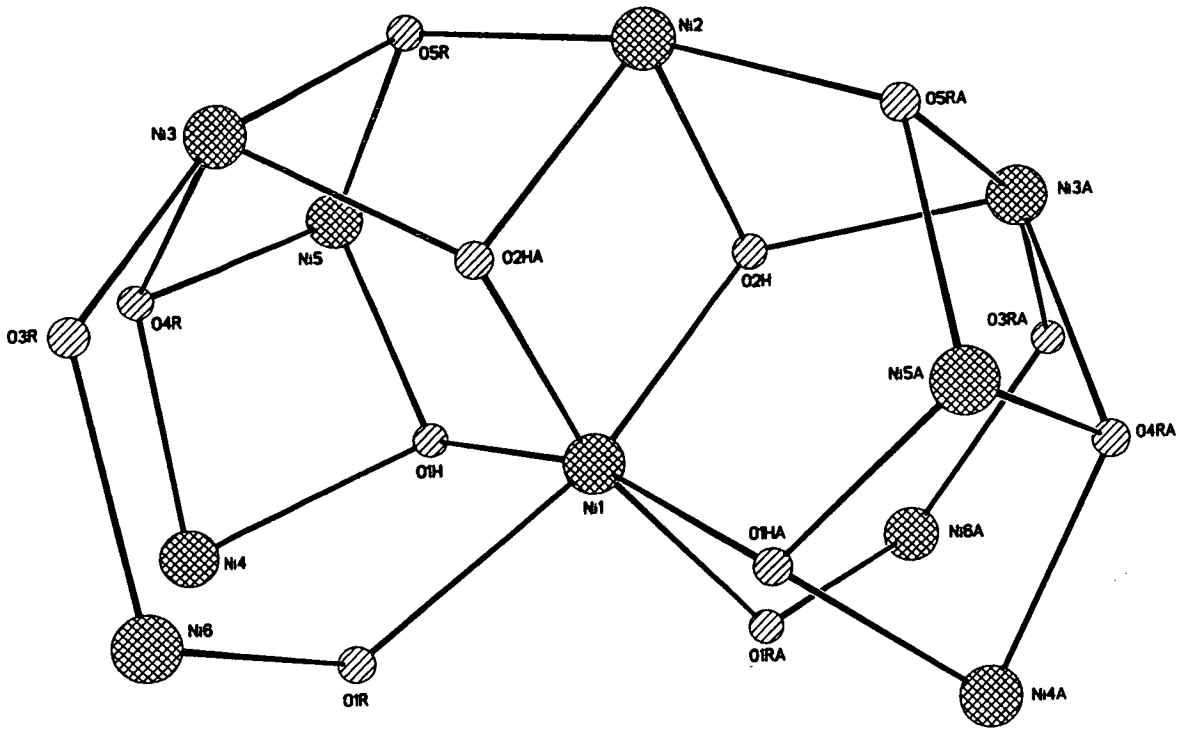

Figure 3.21. The nickel-oxygen polyhedron in **26**.

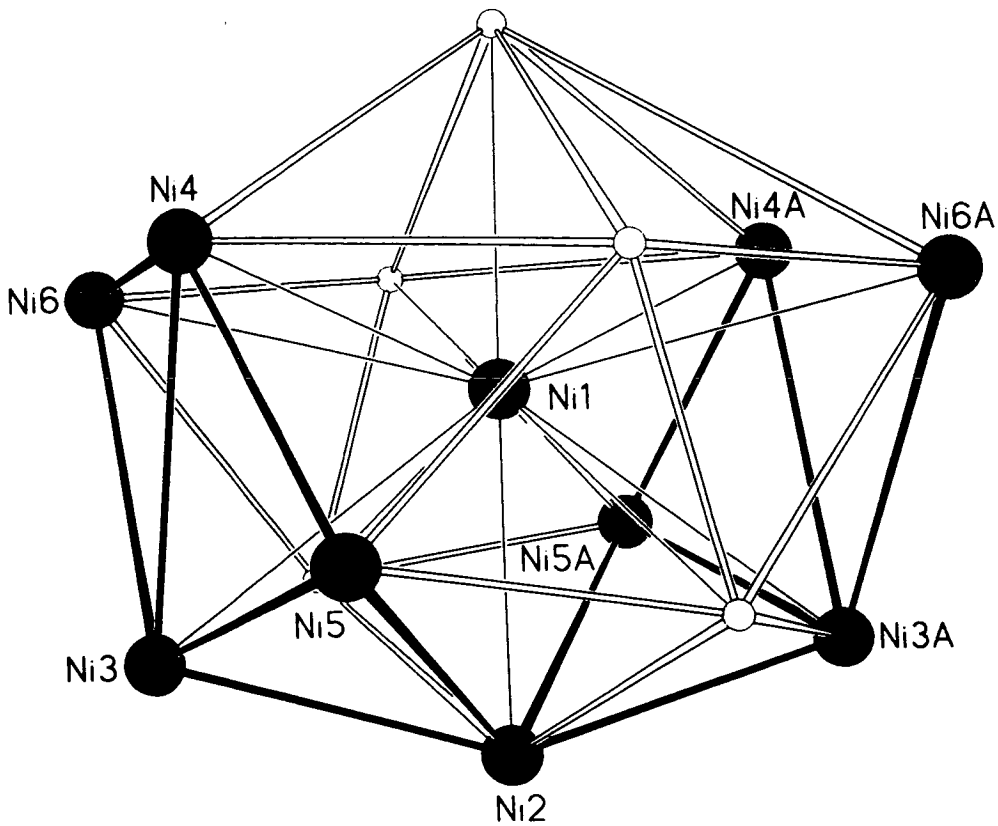

Figure 3.22. The idealised fourteen-vertex polyhedron on which the structure of **26** is based.

and Ni5A occupying four of the vertices of one hexagon and Ni4, Ni4A, Ni6 and Ni6A four of the vertices of the second hexagon. Ni2 caps the former hexagon. All of the nickels have distorted octahedral geometries with the *cis* angles ranging from 62.1-104.9(3)°, and the *trans* angles 153.5-169.6(3) °. Ni4 is formally five-coordinate with its sixth coordination site 'occupied' by O1R [a μ_2-oxygen derived from the mhp ligand which bridges Ni4, Ni1 and Ni6] 2.422(7) Å distant. The closest Ni...Ni. contact is 3.031(7) Å between Ni2 and Ni3. Selected bond lengths and angles are given in Table 3.6.

3.2.10. Magnetochemistry of 26.

The magnetic behaviour of **26** was studied in the temperature range 300-1.8 K in an applied field of 1000 G. The variation of $\chi_m T$ with temperature is shown in Figure 3.23. The room temperature value of $\chi_m T$ is approximately 13 emu K mol^{-1} which is consistent with ten non-interacting S = 1 Ni(II) centres [$\chi_m T$ = 12.1 emu K mol^{-1}; g = 2.2]. The value then drops steadily with temperature giving a minimum value of approximately 2.5 emu K mol^{-1} at 1.8 K, behaviour indicative of antiferromagnetic coupling between the metal centres. The 1.8 K value coresponds to an approximately S = 1 ground state.

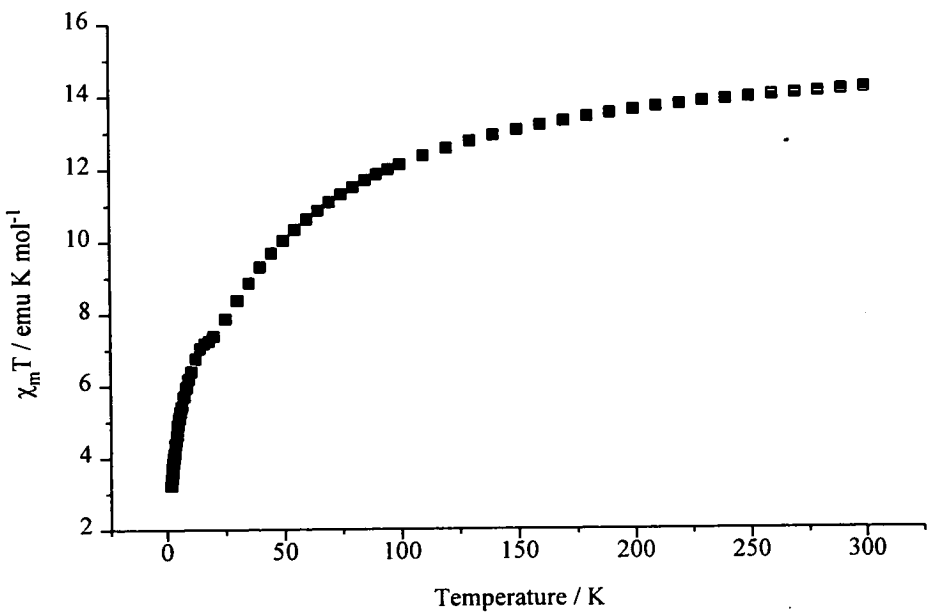

Figure 3.23. The variation of $\chi_m T$ with temperature for **26**.

Table 3.6. Selected bond lengths (Å) and angles (°) for **26**.

Ni1-O1H	2.030(5)	Ni5-O5R	2.168(5)
Ni1-O1HA	2.030(5)	Ni6-O1A3	2.003()5
Ni1-O2H	2.049(5)	Ni6-N2R	2.091(7)
Ni1-O2HA	2.049(5)	Ni6-N3R	2.091(7)
Ni1-O1R	2.267(5)	Ni6-O3R	2.109(5)
Ni1-O1RA	2.267(5)	Ni6-O1R	2.121(5)
Ni2-O2A2	2.018(5)	Ni6-O2R	2.138(5)
Ni2-O2AB	2.018(5)	O1H-Ni1-O1HA	164.9(3)
Ni2-O2HA	2.061(5)	O1H-Ni1-O2H	92.5(2)
Ni2-O2H	2.061(5)	O1HA-Ni1-O2H	98.9(2)
Ni2-O5RA	2.062(5)	O1H-Ni1-O2HA	98.9(2)
Ni2-O5R	2.062(5)	O1HA-Ni1-O2HA	92.5(2)
Ni3-O2HA	1.997(5)	O2H-Ni1-OHA	82.3(2)
Ni3-O1AB	2.006(5)	O1H-Ni1-O1R	82.6(2)
Ni3-O3R	2.007(5)	O1HA-Ni1-O1R	88.3(2)
Ni3-N4R	2.139(5)	O2H-Ni1-O1R	167.1(2)
Ni3-O5R	2.144(5)	O2HA-Ni1-O1R	86.7(2)
Ni3-O4R	2.179(5)	O1H-Ni1-O1RA	88.3(2)
Ni4-O2A3	2.006(5)	O1HA-Ni1-O1RA	82.6(2)
Ni4-O1A1	2.019(5)	O2H-Ni1-O1RA	86.7(2)
Ni4-O4R	2.029(5)	O2HA-Ni1-O1RA	167.1(2)
Ni4-N1R	2.034(5)	O1R-Ni1-O1RA	104.9(3)
Ni4-O1H	2.061(5)	O2A2-Ni2-O2AB	87.1(3)
Ni4-O1R	2.422(7)	O2A2-Ni2-O2HA	168.1(2)
Ni5-O2A1	1.997(6)	O2AB-Ni2-O2HA	96.8(2)
Ni5-O1H	2.031(5)	O2A2-Ni2-O2H	96.8(2)
Ni5-O1M	2.057(5)	O2AB-Ni2-O2H	168.2(2)
Ni5-O4R	2.088(5)	O2HA-Ni2-O2H	81.7(2)
Ni5-N5R	2.090(8)	O2A2-Ni2-O5RA	96.1(3)

Table 3.6 continued

O2AB-Ni2-O5RA	91.4(2)	O2A3-Ni4-O1H	165.9(2)
O2HA-Ni2-O5RA	95.0(2)	O1A1-Ni4-O1H	95.3(2)
O2H-Ni2-O5RA	77.1(2)	O4R-Ni4-O1H	77.2(2)
O2A2-Ni2-O5R	91.4(2)	N1R-Ni4-O1H	101.7(2)
O2AB-Ni2-O5R	96.1(2)	O2A1-Ni5-O1H	95.8(2)
O2HA-Ni2-O5R	77.1(2)	O2A1-Ni5-O1M	91.5(2)
O2H-Ni2-O5R	95.0(2)	O1H-Ni5-O1M	94.5(2)
O5RA-Ni2-O5R	169.6(3)	O2A1-Ni5-O4R	97.2(2)
O2HA-Ni3-O1AB	98.0(2)	O1H-Ni5-O4R	76.6(2)
O2HA-Ni3-O3R	87.3(2)	O1M-Ni5-O4R	168.1(2)
O1AB-Ni3-O3R	98.2(2)	O2A1-Ni5-N5R	99.6(2)
O2HA-Ni3-N4R	162.3(2)	O1H-Ni5-N5R	163.9(3)
O1AB-Ni3-N4R	99.0(2)	O1M-Ni5-N5R	90.0(2)
O3R-Ni3-N4R	94.9(2)	O4R-Ni5-N5R	96.6(2)
O2HA-Ni3-O5R	76.6(2)	O2A1-Ni5-O5R	162.5(2)
O1AB-Ni3-O5R	97.6(2)	O1H-Ni5-O5R	101.4(2)
O3R-Ni3-O5R	158.9(2)	O1M-Ni5-O5R	91.0(2)
N4R-Ni3-O5R	96.5(2)	O4R-Ni5-O5R	83.2(2)
O2HA-Ni3-O4R	100.5(2)	N5R-Ni5-O5R	63.0(2)
O1AB-Ni3-O4R	160.7(2)	O1A3-Ni6-N2R	99.3(2)
O3R-Ni3-O4R	88.0(2)	O1A3-Ni6-N3R	89.1(2)
N4R-Ni3-O4R	62.1(2)	N2R-Ni6-N3R	98.5(2)
O5R-Ni3-O4R	81.7(2)	O1A3-Ni6-O3R	99.0(2)
O2A3-Ni4-O1A1	90.2(2)	N2R-Ni6-O3R	153.5(2)
O2A3-Ni4-O4R	89.4(2)	N3R-Ni6-O3R	62.8(2)
O1A1-Ni4-O4R	95.7(2)	O1A3-Ni6-O1R	93.0(2)
O2A3-Ni4-N1R	89.8(2)	N2R-Ni6-O1R	99.7(2)
O1A1-Ni4-N1R	101.6(2)	N3R-Ni6-O1R	161.1(2)
O4R-Ni4-N1R	162.6(2)	O3R-Ni6-O1R	98.3(2)

Table 3.6 continued

O1A3-Ni6-O2R	162.7(2)	Ni1-O2H-Ni2	98.0(2)
N2R-Ni6-O2R	63.4(2)	Ni6-O1R-Ni1	126.6(2)
N3R-Ni6-O2R	93.5(2)	Ni3-O3R-Ni6	132.3(2)
O3R-Ni6-O2R	97.4(2)	Ni4-O4R-Ni5	95.1(2)
O1R-Ni6-O2R	90.0(2)	Ni4-O4R-Ni3	124.3(2)
Ni1-O1H-Ni5	122.1(2)	Ni5-O4R-Ni3	97.8(2)
Ni1-O1H-Ni4	108.1(2)	Ni2-O5R-Ni3	92.2(2)
Ni5-O1H-Ni4	95.9(2)	Ni2-O5R-Ni5	126.6(2)
Ni3A-O2H-Ni1	127.6(2)	Ni3-O5R-Ni5	96.4(2)
Ni3A-O2H-Ni2	96.6(2)		

Recently two further related structures $[Ni_{10}(OH)_6(mhp)_{6.5}(O_2CCHMe_2)_{6.5}(Hmhp)_3Cl(H_2O)]$ **27** and $[Co_{10}(OH)_6(mhp)_6(O_2CCMe_3)_7Cl(MeCN)_3(H_2O)]$ **28** have been synthesised and structurally characterised [109].

27 is a decanuclear complex based on a centred-tricapped-trigonal prism and is most closely related to the cobalt decamer **25**. The connectivity of the central $[Ni_{10}(\mu_3\text{-}OH)_6(\eta^2, \mu_3\text{-}mhp)_6(\eta^2, \mu_2\text{-}O_2CHMe_2)_6]^{2+}$ core is essentially unaltered from the similar fragments in **20-25**. Like **25** both triangular faces remain uncapped with the three vacant coordination sites on the 'upper' face occupied by one chloride, two oxygen bound Hmhp ligands and on the 'lower' face by a disordered mixture of one water, one Hmhp, a half-occupancy iso-butyrate and a half-occupancy mhp ligand. The metal geometries are similar to those found in **20-25**. The structure of **27** thus seems to support the hypothesis that increasingly bulky carboxylate groups prevent the attachment of the further $[Ni(xhp)_3]^-$ caps to the core structure. The structure of **27** is shown in Figure 3.24.

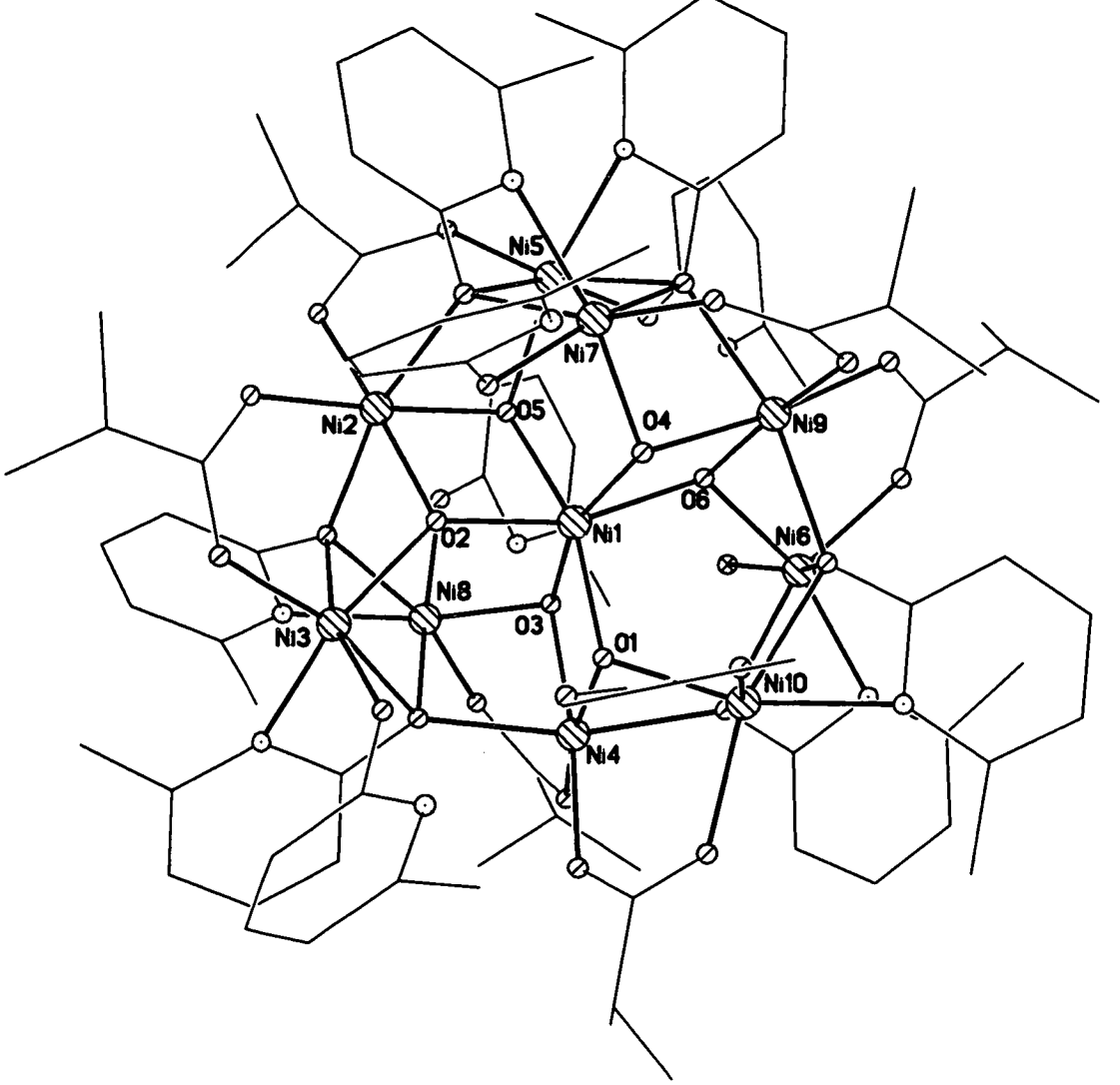

Figure 3.24. The structure of **27** in the crystal.

$[Co_{10}(OH)_6(mhp)_6(O_2CCMe_3)_7Cl(MeCN)_3(H_2O)]$ **28** was synthesised in an identical manner to **26** (replacing nickel with cobalt), the nickel decamer whose structure is based on a fourteen-vertex deltahedron. The structure of **28** however is not based on this deltahedron but on the centred-tricapped-trigonal prisms common to **20-25**. **28** retains the central $[Co_{10}(\mu_3\text{-}OH)_6(\eta^2, \mu_3\text{-}mhp)_6(\eta^2, \mu_2\text{-}O_2CCMe_3)_6]^{2+}$ core with both triangular faces uncapped like **25** and **27**. In this case the three coordination sites on the 'upper' and 'lower' triangular faces are occupied by two acetonitrile and one trimethylacetate molecule and one chloride, one acetonitrile and one water molecule respectively. The structure of **28** is given in Figure 3.25. The reason why **28** should adopt this structure rather than the deltahedron of **26** remains somewhat unclear. It is worth noting that Co9 (a vertex site) in **28** is five coordinate, the only

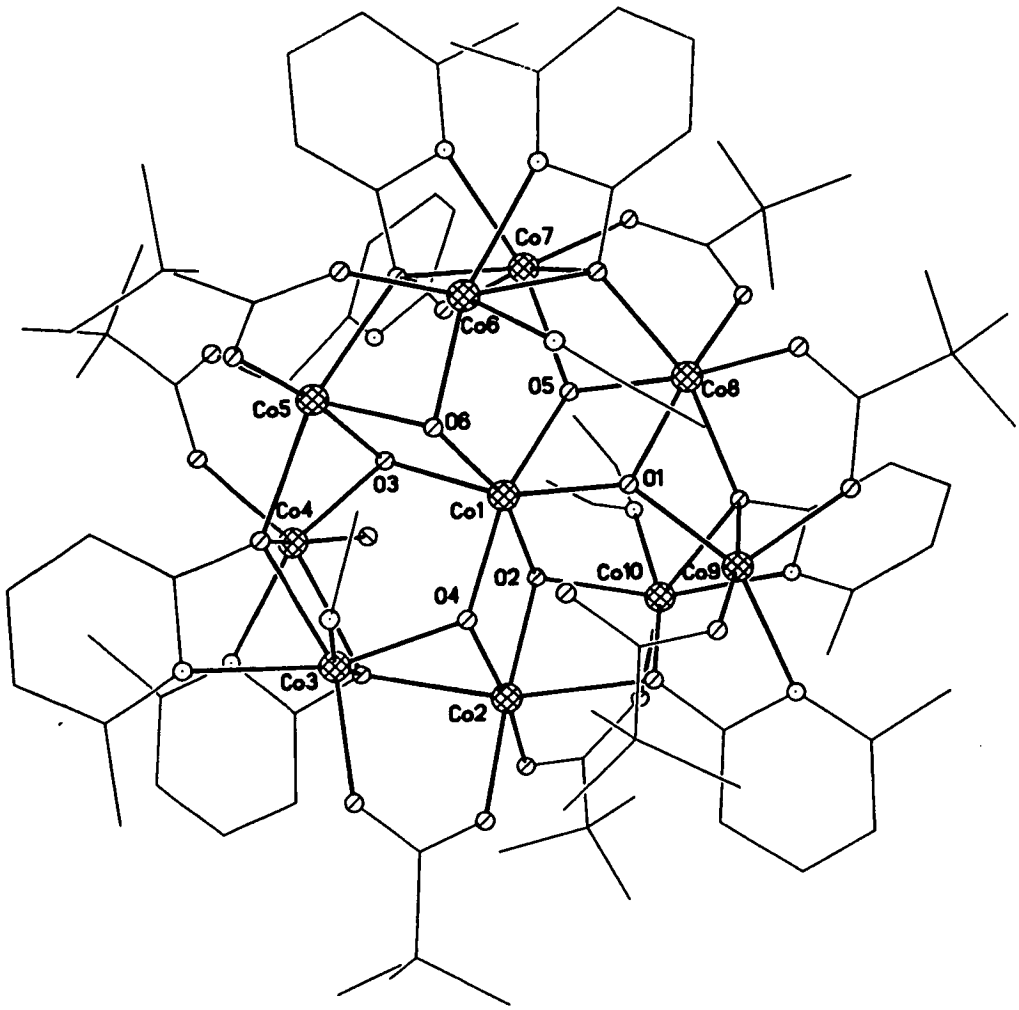

Figure 3.25. The structure of **28** in the crystal.

such metal site in any of the trigonal prisms, with the oxygen donor which should occupy the sixth coordination site 2.515(3) Å distant. This may suggest that the presence of the larger and more sterically demanding trimethylacetate ligand causes considerably more strain in the structure. This however does not explain why the structure of **26** should be so radically altered in comparison. The difference between the two compounds [**26** and **28**] could perhaps be explained by the fact that Ni(II) has a stronger preference for regular geometries when six coordinate than Co(II). However if this was the case then it is likely that the tricapped-trigonal prism in **28** would be more distorted than those seen in the structures that contained smaller carboxylates. In general this appears not to be the case. The *cis* and *trans* angles of the vertex metals in **28** are 59.7-106.6(4)° and 157.9-175.6(4)° respectively and the capping sites 59.6-102.2(5)° and 157.2-171.0(4)°. It is also difficult to dismiss the structure of **26** as "an

exception to the rule" given that it is synthesised in consistently higher yield than any of the trigonal prisms. Therefore whatever factors are involved in the change of structure must be finely balanced. Reactions involving the use of larger carboxylates still, such as di- and triphenylacetate, are currently under investigation with both cobalt and nickel. Initial magnetic studies of **27** and **28** indicate weak antiferromagnetic exchange between the metal centres [109].

3.2.11. Synthesis and structure of $[Ni_6(mhp)_6(PhCOO)_6(PhOOH)_4(H_2O)_6]$.Hmhp 29.

Reaction of two equivalents of Hmhp with nickel benzoate at 160 °C under nitrogen for two hours produced a melt from which the benzoic acid and water produced were pumped-off under reduced pressure and any unreacted Hmhp sublimed to a cold finger. The resultant melt product was crystallised from dichloromethane producing green crystals of $[Ni_6(mhp)_6(PhCOO)_6(PhCOOH)_4(H_2O)_6]$. Hmhp **29** [Figure 3.26] in low yield after four days. **29** is unrelated to the previous complexes discussed in this chapter. **29** crystallises about a two-fold rotation axis and is best described as two equivalent trimers linked together by two μ_3-bridging oxygens derived from two water molecules [O1, O1F]. The central nickel of each 'trimer' [Ni1 and symmetry equivalent] is linked to Ni2 through two 1, 3-bridging benzoates and the μ_3-bridging water molecule. Ni2 is then linked to Ni3, at the periphery of the molecule, through one 1, 3-bridging benzoate, one μ_2-bridging water and a μ_2-bridging oxygen derived from an mhp ligand. The coordination of Ni3 is completed by one mononucleating water molecule and two mononucleating benzoic acid ligands. The coordination of Ni1 is completed by a mononuclating mhp ligand.

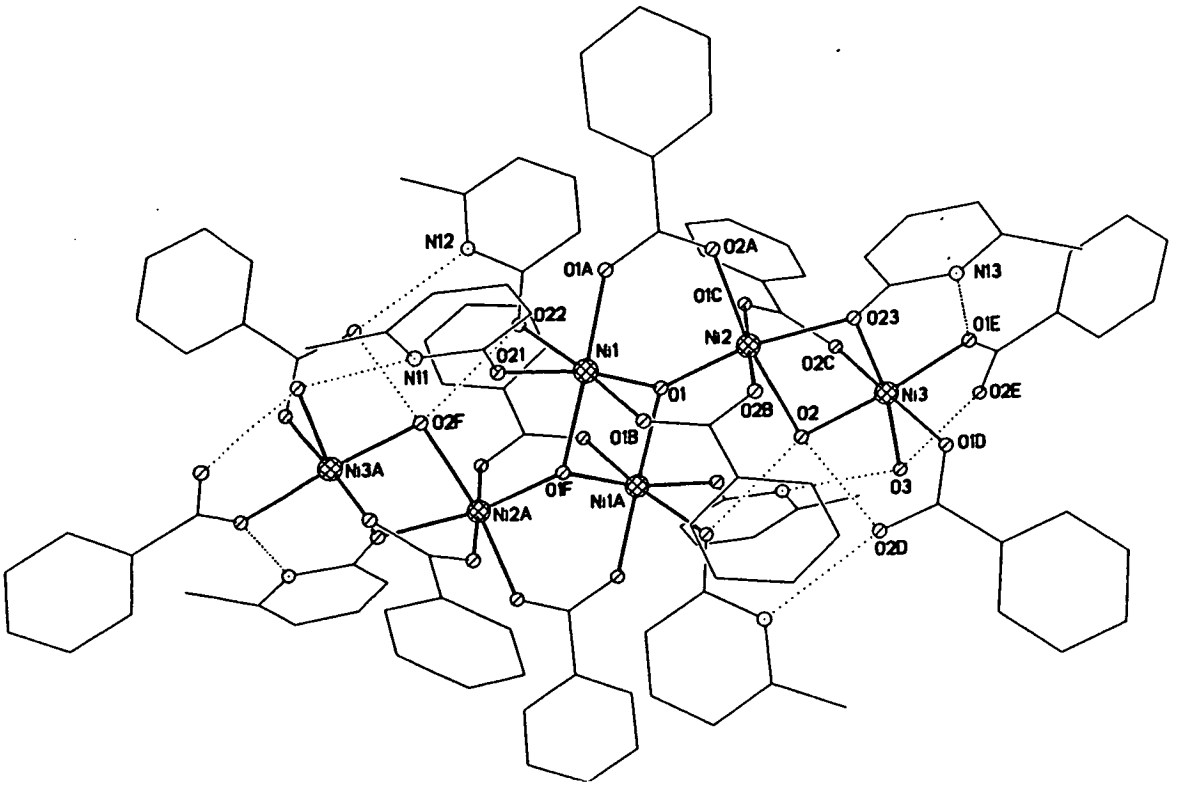

Figure 3.26. The stucture of **29** in the crystal.

The structure of **29** is very unusual and highly unexpected; this is borne out by the coordinating modes (of which there are two) adopted by the mhp ligands. They either bridge two nickel centres through the exocyclic oxygen atom only or are mononucleating, binding to one nickel through the oxygen atom. No mhp ligand in **29** uses its ring nitrogen to coordinate. This type of coordination is rare for mhp and has never been seen before in nickel chemistry, with the only other examples reported being a chromium complex [110], and a series of gold complexes [111]. The benzoate ligands adopt a 1,3-bridging mode while the protonated ligands mononucleate to the peripheral nickel [Ni3].

All of the nickels are six coordinate and have distorted octahedral geometries : the *cis* angles range from 74.86-108.85(12)° and the *trans* angles 162.40-175.59(12)°. The closest Ni...Ni contact is 3.031(7) Å between Ni2 and Ni3. Selected bond lengths and angles are give in Table 3.7. The mhp ligands are all deprotonated which results in an extensively hydrogen bonded structure (particularly at the periphery of the molecule). The ring nitrogen of the μ_2-mhp has a long contact to one of the benzoic acid ligands attached to Ni3 [N13...O1E, 2.947(10) Å] with the second oxygen of the benzoic acid strongly hydrogen bonded to the

terminal water molecule also attached to Ni3 [O2E...O3, 2.353(10) Å]. This water molecule has a further three longer contacts; to an oxygen of a 1, 3-bridging benzoate bound to Ni3 [O3...O2C, 2.797(10) Å]; to the water molecule bridging Ni2 and Ni3 [O3...O2, 2.886(10) Å] and to the ring nitrogen of an mhp ligand bound to Ni1A [O3...N11A, 2.859(10) Å]. The other mononucleating benzoic acid attached to Ni3 is strongly hydrogen bonded to the μ_2-bridging water molecule [O2D...O2, 2.686(10) Å] and to the ring nitrogen of the second mhp ligand attached to Ni1A [O2D...N12A, 2.704(10) Å]. This mhp ligand is hydrogen bonded to the μ_2-water molecule [O22A...O2, 2.700(10) Å] and to the other mhp ligand attached to Ni1A [O22A...O21A, 2.798(10) Å] which in turn is hydrogen bonded to the two benzoate ligands which bridge between Ni1A and Ni2A [O21A...O1AA, 2.700(10) Å; O21A...O1BA, 2.793(10) Å], and to the μ_2-water molecule [O21A...O2, 2.642(10) Å].

The hydrogen bonding in **29** is not however restricted to intramolecular interactions. Between each molecule of **29** exist two molecules of Hmhp which are strongly hydrogen bonded to each other [N14...O24A, 2.622(5) Å] [Figure 3.27]. The exocyclic oxygen atom of each of these pyridones is further hydrogen bonded to the terminal water molecule bound to Ni3 [O24A...O3, 2.734(5) Å].

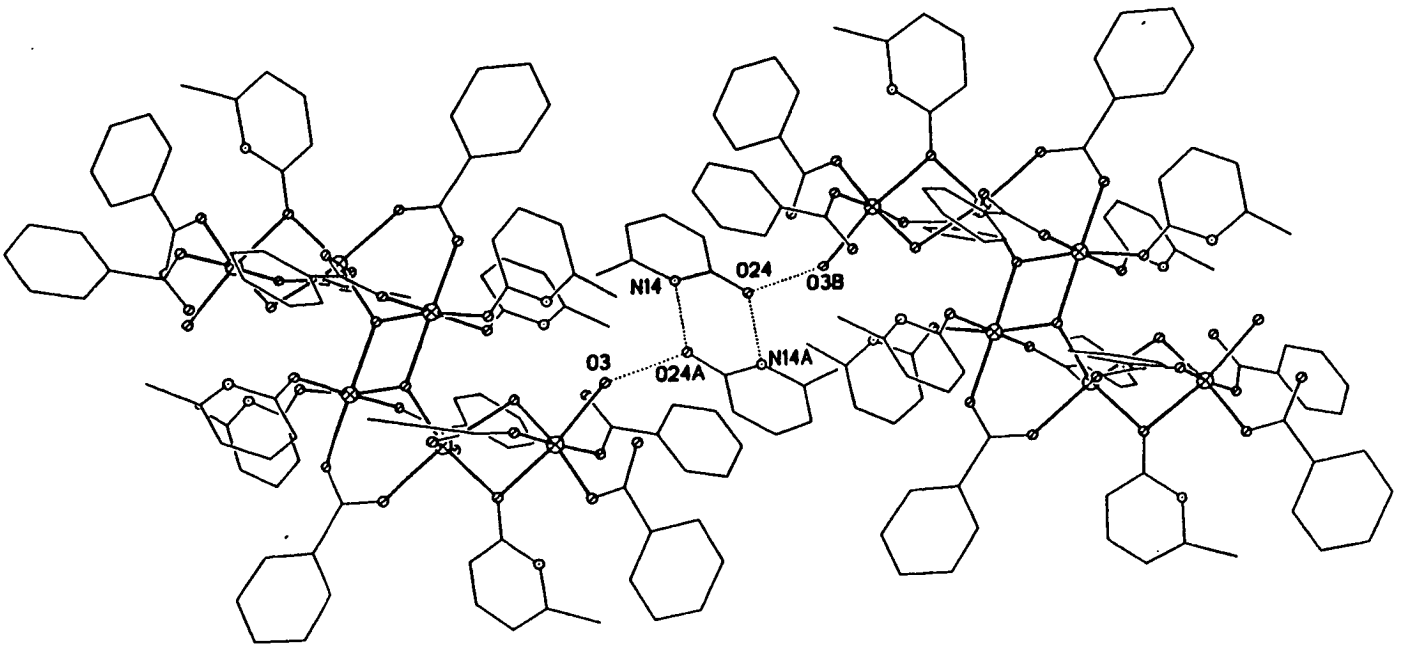

Figure 3.27a. The inter molecular interactions between two molecules of **29**.

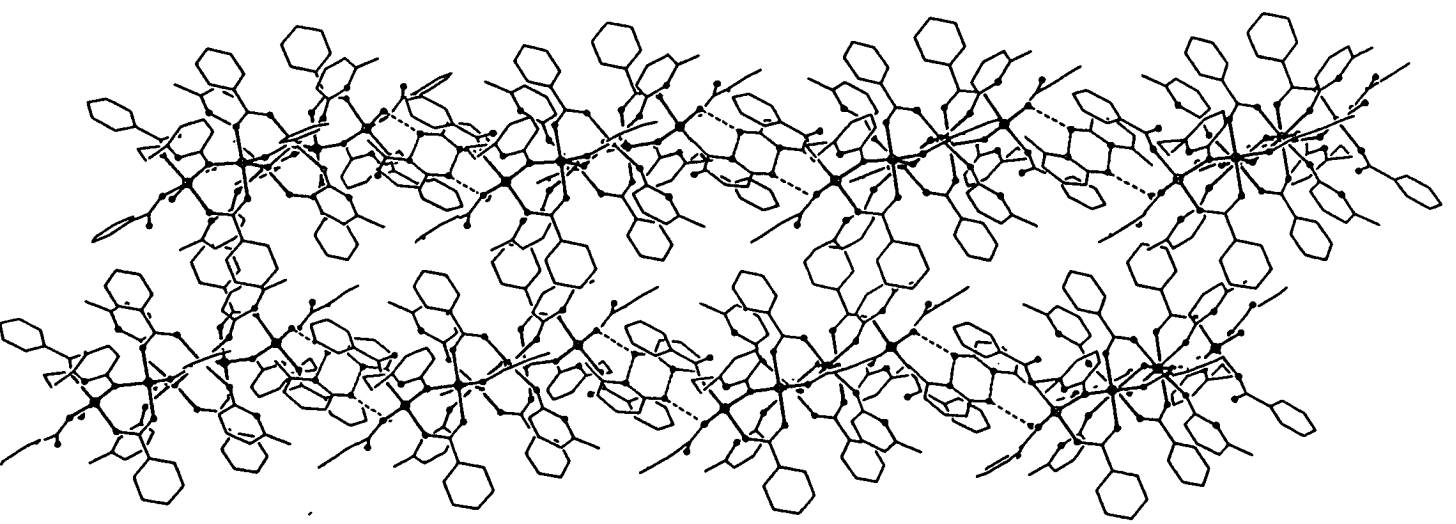

Figure 3.27b. The packing of **29** in the crystal

Table 3.7. Selected bond lengths (Å) and angles (°) for **29**.

Ni1-O1	1.960(3)	O1-Ni1-O1AA	74.86(12)
Ni1-O21	2.013(3)	O21-Ni1-O1AA	93.72(13)
Ni1-O1B	2.028(3)	O1B-Ni1-O1AA	85.91(13)
Ni1-O1A	2.078(3)	O1A-Ni1-O1AA	175.59(12)
Ni1-O22	2.092(3)	O22-Ni1-O1AA	92.78(13)
Ni1-O1AA	2.103(3)	O1-Ni2-O2B	101.60(14)
Ni2-O1	1.929(3)	O1-Ni2-O23	162.40(14)
Ni2-O2B	1.965(3)	O2B-Ni2-O23	86.50(13)
Ni2-O23	2.005(2)	O1-Ni2-O1C	79.18(12)
Ni2-O1C	2.024(3)	O2B-Ni2-O1C	178.33(13)
Ni2-O2A	2.132(3)	O23-Ni2-O1C	92.35(13)
Ni2-O2	2.201(3)	O1-Ni2-O2A	102.44(13)
Ni3-O2	1.865(3)	O2B-Ni2-O2A	90.6(2)
Ni3-O1E	1.890(3)	O23-Ni2-O2A	92.98(14)
Ni3-O1D	2.005(3)	O1C-Ni2-O2A	90.67(14)
Ni3-O2C	2.006(3)	O1-Ni2-O2	86.90(13)
Ni3-O3	2.193(4)	O2B-Ni2-O2	87.93(14)
Ni3-O23	2.198(3)	O23-Ni2-O2	77.72(13)
Ni1A-O1	2.103(3)	O1C-Ni2-O2	90.65(13)
O1-Ni1-O21	168.58(14)	O2A-Ni2-O2	170.65(13)
O1-N1-O21	92.09(13)	O2-Ni3-O1E	172.5(2)
O21-Ni1-O1B	87.42(13)	O2-Ni3-O1D	93.81(13)
O1-Ni1-O1B	108.85(12)	O1E-Ni3-O1D	85.71(13)
O21-Ni1-O1A	82.57(13)	O2-Ni3-O2C	89.24(13)
O1B-Ni1O1A	91.53(14)	O1E-Ni3-O2C	91.87(14)
O1-Ni1-O1A	94.09(13)	O1D-Ni3-O2C	174.48(14)
O21-Ni1-O22	85.92(13)	O2-Ni3-O3	90.31(13)
O1B-Ni1-O22	173.12(11)	O1E-Ni3-O3	97.20(14)
O1A-Ni1-O22	89.34(14)	O1D-Ni3-O3	91.96(14)

Table 3.7 continued

O2C-Ni3-O3	83.41(14)	Ni2-O1-Ni1	104.9(2)
O2-Ni3-O23	80.70(13)	Ni2-O1-Ni1A	131.4(2)
O1E-Ni3-O23	91.80(14)	Ni1-O1-Ni1A	105.14(12)
O1D-Ni3-O23	90.96(15)	Ni3-O3-Ni2	98.21(14)
O2C-Ni3-O23	94.07(14)	Ni2-O23-Ni3	94.17(14)
O3-Ni3-O23	17.72(10)		

3.3. Conclusions.

This chapter outlined the synthesis and structure of a number of novel nickel and cobalt pyridonate complexes whose structures are based on centred-tricapped-trigonal prisms and other deltahedra. The impetus for this work was the publication by Garner and co-workers of a paper describing the the synthesis of the cobalt dodecamer **20** whose structure was that of a pentacapped-trigonal prism. By establishing a reliable synthetic strategy and through subtle variation in the reactants employed the number of additional caps on the 'upper' and 'lower' triangular faces of the prisms can be changed. Use of chloroacetate and mhp produced a nickel dodecamer **21** whose structure is almost identical to the Garner species. Use of chp and benzoate produced a prism which contains a polar cap and can therefore be regarded as an intermediate structure between the parent compounds **20** and **21** and two nickel undecamers **23** and **24** which lack one cap on the 'upper' triangular face. The cobalt complexes of benzoate **25** and trimethylacetate **28** produced structures which lack both caps on the triangular faces.

Perhaps the most significant structural change imparted by the use of increasingly large carboxylate ligands is the change from tricapped-trigonal prism to fourteen-vertex deltahedron. The reason for this dramatic structural change is unclear but is most likely related to a combination of the steric strain placed on the prisms through the use of bulky ligands and

to nickel's preference (compared to cobalt) for a regular octahedral geometry. The cages crystallise in a variety of space groups. A regular centred-tricapped-trigonal prism could have symmetry as high as D_{3d} and although none of the cages have such high symmetry several are disposed about a crystallographic three-fold axis.

Again solvent seems to play a vital role. The reactants used to produce all of these cages [**21-28**] were stirred together for at least three hours (and more regularly twenty four hours) in a solvent (invariably methanol) prior to crystallisation or thermolysis Where mhp is concerned the crystallisation solvent is always acetonitrile (or in one case ethyl acetate) when the preceeding reaction is carried out purely in solution (methanol in every case). When the reaction scheme involves a thermolysis step then only dichloromethane produces the centred-tricapped-trigonal prism. There is only one example of chp producing such a cage [**22**]. This was also crystallised from dichloromethane. The reluctance of compounds containing chp to form these large clusters is unsurprising given their preference to bind metal centres *via* their exocyclic oxygen atom alone. Thus all of these cages [**21-28**] were synthesised from a total of only three crystallisation solvents : acetonitrile, ethyl acetate and dichloromethane. This is summarised in Table 3.8. This all suggests that in order for such structures to form the initial reaction must be carried out in alcohol (i.e.methanol) and the crystallisation in a less polar solvent. The use of bonding, polar solvents in the crystallisation stage does not produce similar species, but instead favours the formation of much smaller metal arrays [55].

The only reaction described in this chapter which did not involve an initial solution step produced an unusual nickel hexamer **29** which is structurally unrelated to any of the other complexes described. It also contains mhp ligands in highly unusual coordinating modes.

Table 3.8. A summary of the nuclearity of the nickel and cobalt carboxylate complexes characterised.

O_2CR	R = Me	CH_2Cl	$CHMe_2$	CMe_3	Ph
Co	12	?	?	10	10
Ni	*11	12	10	10	*6
Solvent	toluene/ *CH_2Cl_2	MeCN and/ or EtOAc	MeCN	MeCN	MeCN/ *CH_2Cl_2

3.4. Experimental Section.

3.4.1. $[Ni_{12}(OH)_6(mhp)_{12}(O_2CCH_2Cl)_6]$ 21.

$NiCl_2.6H_2O$ (1.000g, 4.21 mmol), Na(mhp) (1.104g, 8.41 mmol) and $Na(O_2CPh)$ (1.212g, 8.42 mmol) were stirred in MeOH (40 ml) for 24 hours. Removal of the solvent produced a paste which was dried *in vacuo* for several hours. Crystallisation of this paste from MeCN (20 ml) produced green crystals of **21** in 50% yield after 3 days. Alternatively EtOAc (25 ml) may be used as the crystallisation solvent, giving a yield of 35%.

CHN, observed (expexted); C, 37.7 (37.8); H, 3.20 (3.38); N, 6.25 (6.30) %.

FAB-MS : no significant peaks observed.

3.4.2. $[Ni_{11}(OH)_6(chp)_9(O_2CPh)_6(EtOH)_3][Ni(chp)_3]$ 22.

$NiCl_2.6H_2O$ (1.000g, 4.21 mmol), Na(chp) (1.276, 8.42 mmol) and $Na(O_2CPh)$ (1.212g, 8.42 mmol) were stirred in EtOH (50 ml) for 24 hours. Removal of the solvent produced a green paste which was dried *in vacuo* for several hours. Crystallisation of this paste from CH_2Cl_2 (20 ml) produced green crystals of **22** in 15% after 4 days.

CHN, observed (expected); C, 40.1 (40.3); H, 2.76 (2.80); N, 5.22 (5.23) %.

FAB-MS : no significant peaks observed.

3.4.3. $[Ni_{11}(OH)_6(mhp)_9(O_2CMe)_6(H_2O)_3]_2[CO_3]$ 23.

$Ni(OAc)_2.4H_2O$ (1.000g, 4.02 mmol) and Na(mhp) (1.054g, 8.04 mmol) were stirred in THF (50 ml) for 24 hours. Removal of the solvent produced a paste which was dried *in vacuo*. The dried paste was then mixed with Hmhp (0.440g, 4.02 mmol) in a Schlenk tube and heated to 160 C under N_2 for 2 hours producing a melt. The acetic acid and water vapour produced during the reaction were pumped-off under vacuum and any excess Hmhp sublimed to a cold finger. The melt product was dissolved in CH_2Cl_2 (25 ml) producing green crystals of **23** in 9% yield after 1 week.

CHN, observed (expected); C, 37.9 (38.1); H, 3.57, (3.89); N, 5.80 (5.84) %.

FAB-MS : no significant peaks obsereved.

3.4.4.$[Ni_{11}(OH)_6(mhp)_9(O_2CMe)_7(Hmhp)_2]$ 24.

Synthesis as for **23** with the first step carried out in MeOH (50 ml) rather than THF.

Yield = 10% after 2 weeks.

CHN, observed (expected); C, 40.6 (40.8); H, 3.73 (3.95); N, 6.49 (6.55) %.

FB-MS : no significant peaks observed.

3.4.5. $[Co_{10}(OH)_6(mhp)_6(O_2CPh)_7(Hmhp)_3Cl(MeCN)]$ 25.

Synthesis as for **21** using Co in place of Ni and $Na(O_2CPh)$ in place of $Na(O_2CCH_2Cl)$.

Yield = 20% after 4 days.

CHN, observed (expected); C, 48.5(48.6); H, 3.71 (3.78); N, 5.40 (5.40) %.

FAB-MS : no significant peaks observed.

3.4.6. $[Ni_{10}(OH)_4(mhp)_{10}(O_2CCMe_3)_6(MeOH)_2]$ 26

Synthesis as for **21** using $Na(O_2CCMe_3)$ in place of $Na(O_2CCH_2Cl)$.

Yield = 42% after 2 days.

CHN, observed (expected); C, 48.9 (48.9); H, 5.20 (5.24); N, 5.40 (5.40) %.

FAB-MS : no significant peaks obsserved.

3.4.7. $[Ni_6(mhp)_6(PhCOO)_6(PhCOOH)_4(H_2O)_6]$.Hmhp 29.

$Ni(PhCOO)_2.4H_2O$ (1.000g, 2.68 mmol) and Hmhp (0.600g, 5.50 mmol) were heated together in a Schlenk tube under N_2 for 2 hours, producing a melt. The benzoic and water liberated during the reaction were removed under reduced pressure and any excess Hmhp sublimed to a cold finger. The melt was dissolved an CH_2Cl_2 (25 ml) giving green crystals of **29** in 10% yield after 4 days.

CHN, observed (expected); C, 55.1 (55.3); H, 3.90 (4.28); N, 3.90(4.03) %.

CHAPTER 4

NICKEL AND COBALT CARBOXYLATE COMPLEXES OF 6-CHLORO-2-PYRIDONE.

4.1. Introduction

This chapter illustrates the synthesis, structure and initial magnetic properties of a number of novel nickel and cobalt carboxylate complexes of 6-chloro-2-pyridone. There are only three previously known examples of such compounds. The first is a series of trimers of general formula $[M_3(O_2CR)_2(xhp)_4(R'OH)_7]$. 2R'OH where M = Ni, Co; R = Me, Ph; xhp = chp, bhp and R' = Me, Et [51, 55, 112] and the second a nickel metallocycle $[Ni_{12}(O_2CMe)_{12}(xhp)_{12}(H_2O)_6(THF)_6]$ where xhp = chp, bhp [113]. The third is an unusual centrosymmetric cobalt dimer $[Co(bhp)(O_2CMe)(4, 4'\text{-}Me_2\text{-}2, 2'\text{-}bpy)]_2$ in which the two metal centres are bridged by a μ_2-oxygen atom derived from a bhp ligand [bhp, the 6-bromo- derivative of 2-pyridone, displays identical chemistry to chp and in all cases the two pyridonates are directly replaceable] with the acetate and dimethylbipyridine ligands chelating to one metal centre [51]. Work on the series of metal trimers and metallocycle mentioned above has been continued and expanded and their synthesis and structure will be discussed in more detail in this chapter - this includes the synthesis of the isostructural cobalt dodecamer. Also discussed is the synthesis and structure of two cobalt heptamers whose structures are loosely based on trigonal prisms and a heterobimetallic complex containing chloroacetate. Introduction of the tetranucleating phthalate ligand has led to the synthesis of two larger assemblies : a cobalt tridecanuclear complex and a nickel - sodium supracage. Use of a different starting material : tetraethylammonium chloride has led to the characterisation of a tetranuclear nickel complex containing benzoate and a hexanuclear nickel complex containing trifluoroacetate.

4.2. Synthesis and structure of $[Ni_3(O_2CCMe_3)_2(chp)_4(MeOH)_6]$ 30 and $[Ni_3(PhCH_2CO_2)_2(chp)_4(MeOH)_6]$. 2MeOH 31.

All of the previously characterised trimers $[M_3(O_2CR)_2(xhp)_4(R'OH)_6]$. 2R'OH where M = Ni, Co; R = Me, Ph; xhp = chp, bhp and R' = Me, Et[51, 55, 112] were synthesised *via* a thermolysis reaction of the metal carboxylate and pyridone under nitrogen which produced a melt which was crystallised from methanol. $[Ni_3(O_2CCMe_3)_2(chp)_4(MeOH)_6]$ **30** and $[Ni_3(PhCH_2CO_2)_2(chp)_4(MeOH)_6]$. 2MeOH **31** can also be formed in this way but were initially synthesised *via* an alternative procedure. Reaction of nickel chloride with two equivalents of both Na(chp) and $Na(O_2CCMe_3)$ in methanol for 24 hours produced a paste which was crystallised from fresh methanol to give green crystals of $[Ni_3(O_2CCMe_3)_2(chp)_4(MeOH)_6]$ **30** [Figure 4.1] in high yield after one day. The structure of **30** is similar to the previously reported trimers but not identical.

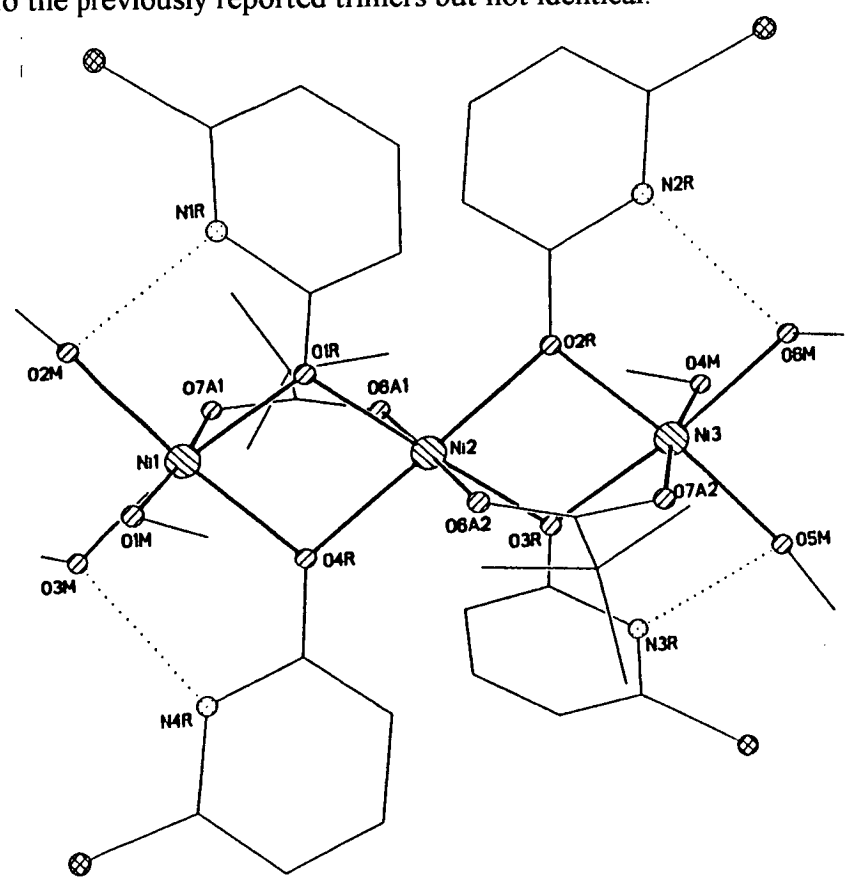

Figure 4.1. The structure of **30** in the crystal.

In all of the previously characterised trimers the central metal atom lies on a crystallographic inversion centre but in **30** this is not the case, each nickel being unique.The central nickel [Ni2] is bridged to the external nickels [Ni1, Ni3] by two μ_2-oxygen atoms from two chp ligands and one 1, 3-bridging trimethylacetate ligand. Ni3 and Ni1 are further ligated by three molecules of methanol, preventing further oligomerisation. All of the metal sites thus have six oxygen-donors in a distorted octahedral array. Ni1, *cis* 83.6-94.1(5)°; *trans*, 171.5-174.2(5)°; Ni2, *cis* 77.2-103.8(5)°; *trans*, 178.1-178.9(5)°; Ni3, *cis* 79.0-95.1(5); *trans*, 171.7-173.1(5)°. The four pyridonate ligands lie in a 'plane' with the two carboxylate ligands *trans* to each other. The Ni...O distances are in the range 1.969-2.122(12)Å. The Ni-O(chp) and Ni-O(O_2CCMe_3) bonds differ in length, with the distances to the central nickel [Ni2] always longer than those to the external nickels [Ni1, Ni3]. For example O1R-Ni1, 2.038(12)Å; O1R-Ni2, 2.096(12)Å and O7A1-Ni1, 1.969(12)Å; O6A1-Ni2, 2.049(12)Å. The variation in bond lengths is a consequence of the strong hydrogen-bonds which exist between the ring nitrogens of the chp ligands and the terminal methanol molecules attached to Ni1 and Ni3. For example N1R...O2M, 2.600(12)Å. This hydrogen-bond has the effect of 'tilting' the pyridonate ligands toward the periphery of the molecule effectively elongating the trimer by 'squashing' down the ends of the molecule.

The Ni...Ni distances of 3.102(12)Å [Ni1...Ni2] and 3.103(12)Å [Ni2...Ni3] are similar to those for the previously reported trimers [av. Ni...Ni, 3.109(3)Å; av. Co...Co, 3.164(3)Å]. Selected bond lengths and angles for **30** are given in Table 4.1.

The main difference between the structure of **30** and those reported previously is the absence of two molecules of alcohol solvate in the crystal. When these are present they participate in strong hydrogen-bonding to one methanol molecule attached to the external metal atoms and to one oxygen of the bridging carboxylates. The packing of **30** [Figure 4.2] is also different, with each trimer hydrogen-bonded to its neighbour *via* two of the three terminal

methanol molecules attached to Ni1 and Ni3 [O4MB...O2MC, 2.829(12)Å; O5MB...O1MC, 2.796(12)Å] creating chains of hydrogen-bonded trimers. In the previously reported trimers the closest intermolecular contacts were between chlorine and nitrogen atoms in neighbouring molecules at 3.467(4)Å and between adjacent chlorine atoms [Cl...Cl, 3.702(3)Å] [112].

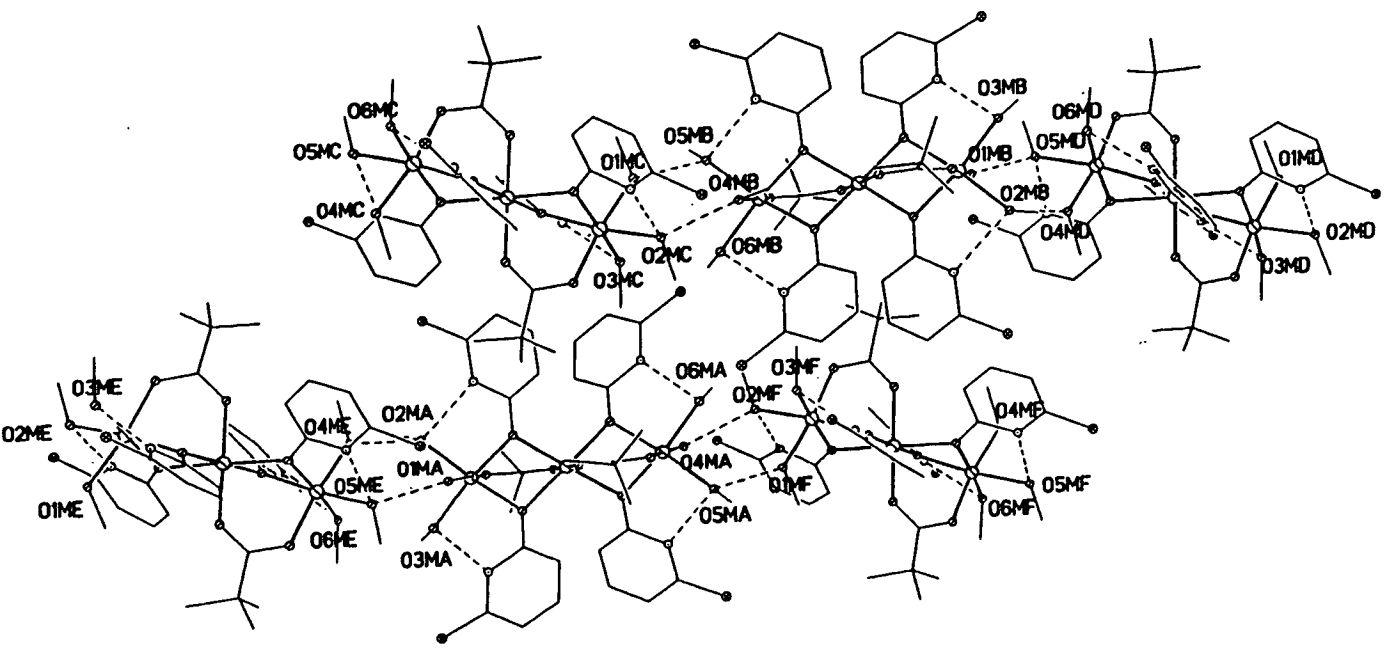

Figure 4.2. The packing of **30** in the crystal.

$[Ni_3(PhCH_2CO_2)_2(chp)_4(MeOH)_6]$. 2MeOH **31** [Figure 4.3] was synthesised by an identical procedure to **30**, replacing trimethylacetate with phenylacetate, but crystallised in much lower yield. The structure of **31** is identical to those reported previously. There are two unique metal sites [Ni1, Ni2] with the central nickel [Ni1] on an inversion centre being bridged to Ni2 by two μ_2-oxygens derived from chp ligands and a 1,3-bridging phenylacetate. The coordination of Ni2 is completed by three molecules of methanol, two of which hydrogen-bond to the ring nitrogens of the chp ligands [O1M...N11, 2.694(7)Å; O2M...N12A,

2.693(7)Å]. The third methanol molecule hydrogen-bonds to a methanol solvent molecule [O3M...O1S, 2.586(7)Å] which in turn has a further hydrogen-bond to one oxygen of the bridging phenylacetate [O1S...O32, 2.714(6)Å]. The Ni...Ni distance in **31** is 3.119(7)Å, again similar to that previously reported. Selected bond lengths and angles are given in Table 4.2. The fact that the introduction of these larger carboxylates has resulted in no significant structural change in the product is unsurprising : the ligands are *trans* to each other and in a different plane to the bridging pyridonates and therefore introduce no steric strain to the molecule.

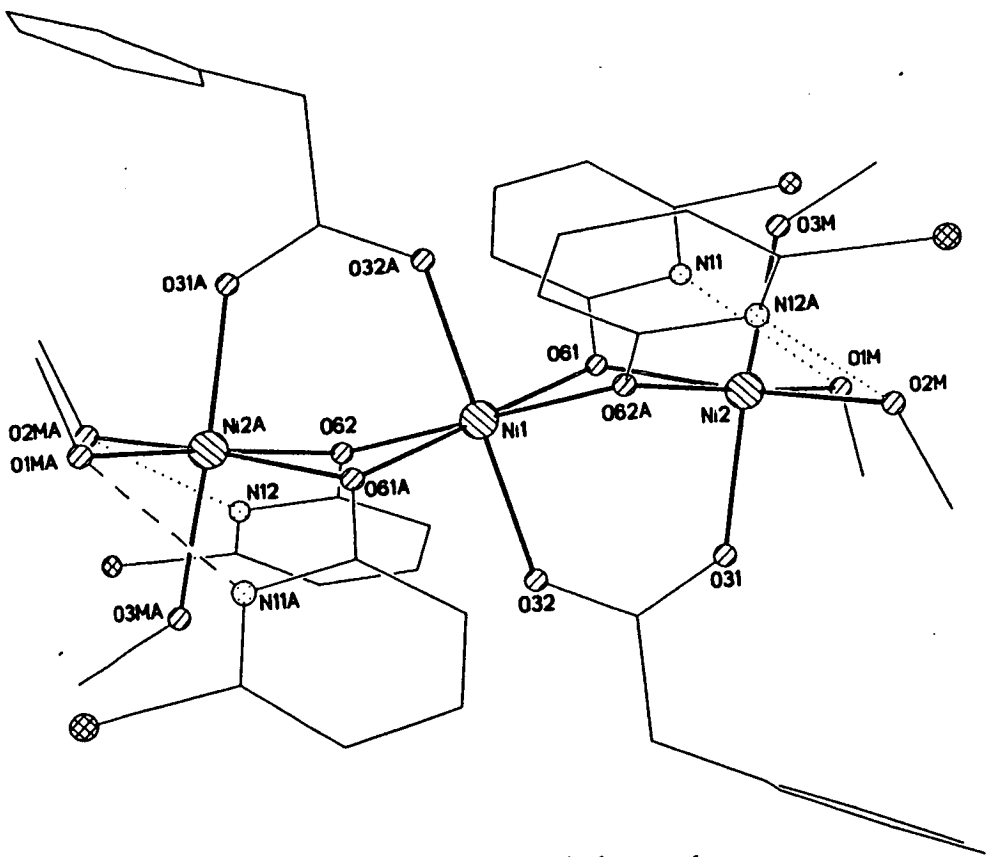

Figure 4.3. The structure of **31** in the crystal.

4.2.1. Magnetochemistry of 30, 31.

The magnetic behaviour of **30** and **31** was studied in the temperature range 300-1.8 K in an applied field of 1000 G. The behaviour of the two compounds is identical. The variation

of the product $\chi_m T$ with temperature is shown in Figure 4.4. The room temperature value of approximately 3.5 emu K mol^{-1} is consistant with three non-interacting Ni(II) S = 1 centres [$\chi_m T$ = 3.63 emu K mol^{-1}, g = 2.2]. The value then drops steadily with temperature giving a minimum value of 1.5 emu K mol^{-1} at 1.8 K, behaviour consistant with antiferromagnetic exchange between the nickel centres. The 1.8 K value corresponds to an approximately S = 1 ground state. This is similar to that reported for all the other nickel pyridonate trimers [55, 112].

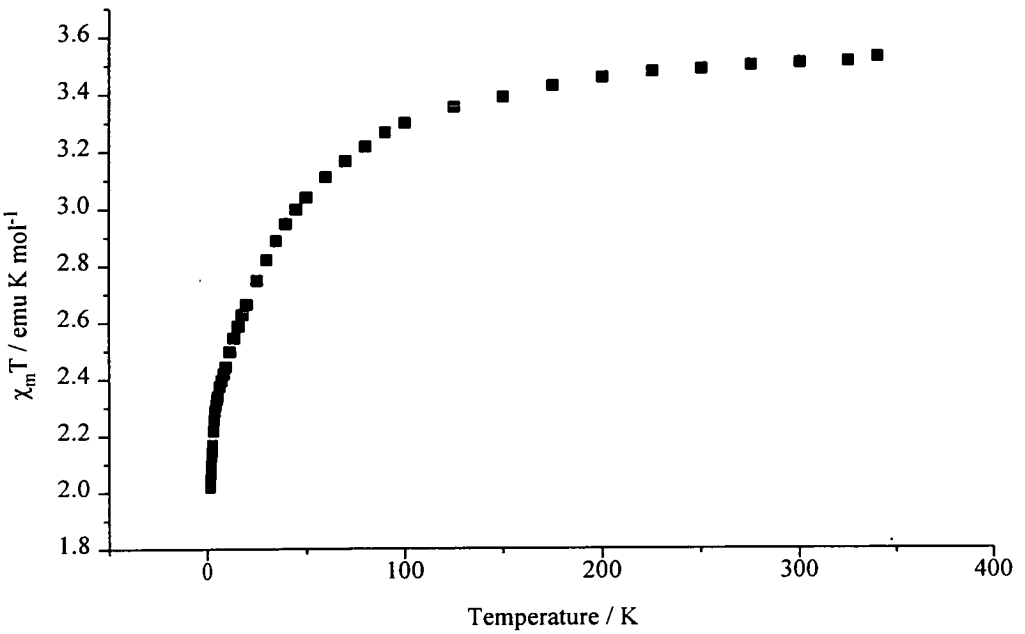

Figure 4.4. The variation of $\chi_m T$ with temperature fo **30** and **31**.

Table 4.1. Selected bond lengths (Å) and angles (°) for **30**.

Ni1-O7A1	1.969(12)	Ni2-O2R	2.065(11)
Ni1-O1R	2.038(12)	Ni2-O1R	2.096(12)
Ni1-O3M	2.058(12)	Ni2-O3R	2.098(12)
Ni1-O4R	2.066(12)	Ni3-O7A2	1.978(12)
Ni1-O1M	2.076(12)	Ni3-O3R	2.038(12)
Ni1-O2M	2.106(12)	Ni3-O2R	2.046(12)
Ni2-O6A2	2.023(12)	Ni3-O6M	2.060(12)
Ni2-O6A1	2.048(12)	Ni3-O4M	2.081(12)
Ni2-O4R	2.058(12)	Ni3-O5M	2.122(12)

Table 4.1 continued

O7A1-Ni1-O1R	93.5(5)	O6A2-Ni2-O3R	90.2(5)
O7A1-Ni1-O3M	91.0(5)	O6A1-Ni2-O3R	90.1(5)
O1R-Ni1-O3M	171.5(5)	O4R-Ni2-O3R	103.8(5)
O7A1-Ni1-O4R	92.8(5)	O2R-Ni2-O3R	77.2(5)
O1R-Ni1-O4R	79.0(5)	O1R-Ni2-O3R	178.1(5)
O3M-Ni1-O4R	93.5(5)	O7A2-Ni3O3R	92.1(5)
O7A1-Ni1-O1M	174.2(5)	O7A2-Ni3-O2R	95.1(5)
O1R-Ni1-O1M	90.2(5)	O3R-Ni3-O2R	79.0(5)
O3M-Ni1-O1M	86.0(5)	O7A2-Ni3-O6M	91.0(5)
O4R-Ni1-O1M	92.3(5)	O3R-Ni3-O6M	173.1(5)
O7A1-Ni1-O2M	91.6(5)	O2R-Ni3-O6M	94.5(5)
O1R-Ni1-O2M	94.1(5)	O7A2-Ni3-O4M	171.8(5)
O3M-Ni1-O2M	93.0(5)	O3R-Ni3-O4M	93.7(5)
O4R-Ni1-O2M	172.0(5)	O2-Ni3-O4M	91.7(5)
O1M-Ni1-O2M	83.6(5)	O6M-Ni3-O4M	83.9()
O6A2-Ni2-O6A1	178.4(5)	O7A2-Ni3-O5M	89.0(5)
O6A2-Ni2-O4R	90.8(5)	O3R-Ni3-O5M	93.7(5)
O6A1-Ni2-O4R	87.6(5)	O2R-Ni3-O5M	171.7(5)
O6A2-Ni2-O2R	89.7(5)	O6M-Ni3-O5M	92.5(5)
O6A1-Ni2-O2R	91.9(5)	O4M-Ni3-O5M	84.8(5)
O4R-Ni2-O2R	178.9(5)	Ni1-O1R-Ni2	97.3(5)
O6A2-Ni2-O1R	88.7(5)	Ni3-O2R-Ni2	98.0(5)
O6A1-Ni2-O1R	91.0(5)	Ni3-O3R-Ni2	97.1(5)
O4R-Ni2-O1R	77.9(5)	Ni2-O4R-Ni11	97.6(5)
O2R-Ni2-O1R	101.1(5)		

Table 4.2. Selected bond lengths (Å) and angles (°) for **31**.

Ni1-O62A	2.060(3)	O32A-Ni1-O61	90.44(11)
Ni1-O62	2.060(3)	O61A-Ni1-O61	180.0(0)
Ni1-O32	2.067(3)	O31-Ni2-O3M	175.64(13)
Ni1-O32A	2.067(3)	O31-Ni2-O2M	91.63(13)
Ni1-O61A	2.090(3)	O3M-Ni2-O2M	84.12(13)
Ni1-O61	2.090(3)	O31-Ni2-O1M	91.94(14)
Ni2-O31	1.995(3)	O3M-Ni2-O1M	87.19(14)
Ni2-O3M	2.032(3)	O2M-Ni2-O1M	91.12(14)
Ni2-O2M	2.068(3)	O31-Ni2-O62A	90.35(13)
Ni2-O1M	2.072(3)	O3M-Ni2-O62A	91.00(13)
Ni2-O62A	2.077(3)	O2M-Ni2-O62A	95.28(13)
Ni2-O61	2.083(3)	O1M-Ni2-O62A	173.14(13)
O62A-Ni1-O62	180.0(0)	O31-Ni2-O61	93.34(13)
O62A-Ni1-O32	89.63(11)	O3M-Ni2-O61	90.99(13)
O62-Ni1-O32	90.37(11)	O2M-Ni2-O61	172.35(14)
O62A-Ni1-O32A	90.37(11)	O1M-Ni2-O61	94.51(13)
O62-Ni1-O32A	89.63(11)	O62A-Ni2-O61	78.89(11)
O32-Ni1-O32A	180.0(0)	Ni2-O61-Ni1	96.71(12)
O62A-Ni1-O61A	100.91(12)	Ni1-O62-Ni2A	97.84(12)
O62-Ni1-O61A	79.09(12)	N11-O1M	2.694(7)
O32-Ni1-O61A	90.44(11)	N12-O2MA	2.693(7)
O32A-Ni1-O61A	89.56(11)	O1S-O32	2.714(7)
O62A-Ni1-O61	79.09(12)	O1S-O3M	2.586(7)
O62-Ni1-O61	100.91(12)	Ni1-Ni2	3.119(7)
O32-Ni1-O61	89.56(11)		

4.2.2. Synthesis and structure of $[Co_{12}(O_2CMe)_{12}(chp)_{12}(H_2O)_6(THF)_6]$ 32.

Hydrated cobalt acetate was placed in a Schlenk tube and dried under vacuum at room temperature for several hours. Two equivalents of 6-chloro-2-pyridone was added and the mixture heated to 130°C under an atmosphere of nitrogen for two hours. The resultant melt was heated under reduced pressure removing the acetic acid formed during the reaction. Any unreacted Hchp was then removed by sublimation to a cold finger. The product was then extracted with tetrahydrofuran and crystallised by slow evaporation to give purple crystals of $[Co_{12}(O_2CMe)_{12}(chp)_{12}(H_2O)_6(THF)_6]$ **32** [Figure 4.5.] in high yield after three days [117]. **32** is isostructural with a nickel metallocycle reported previously [113].

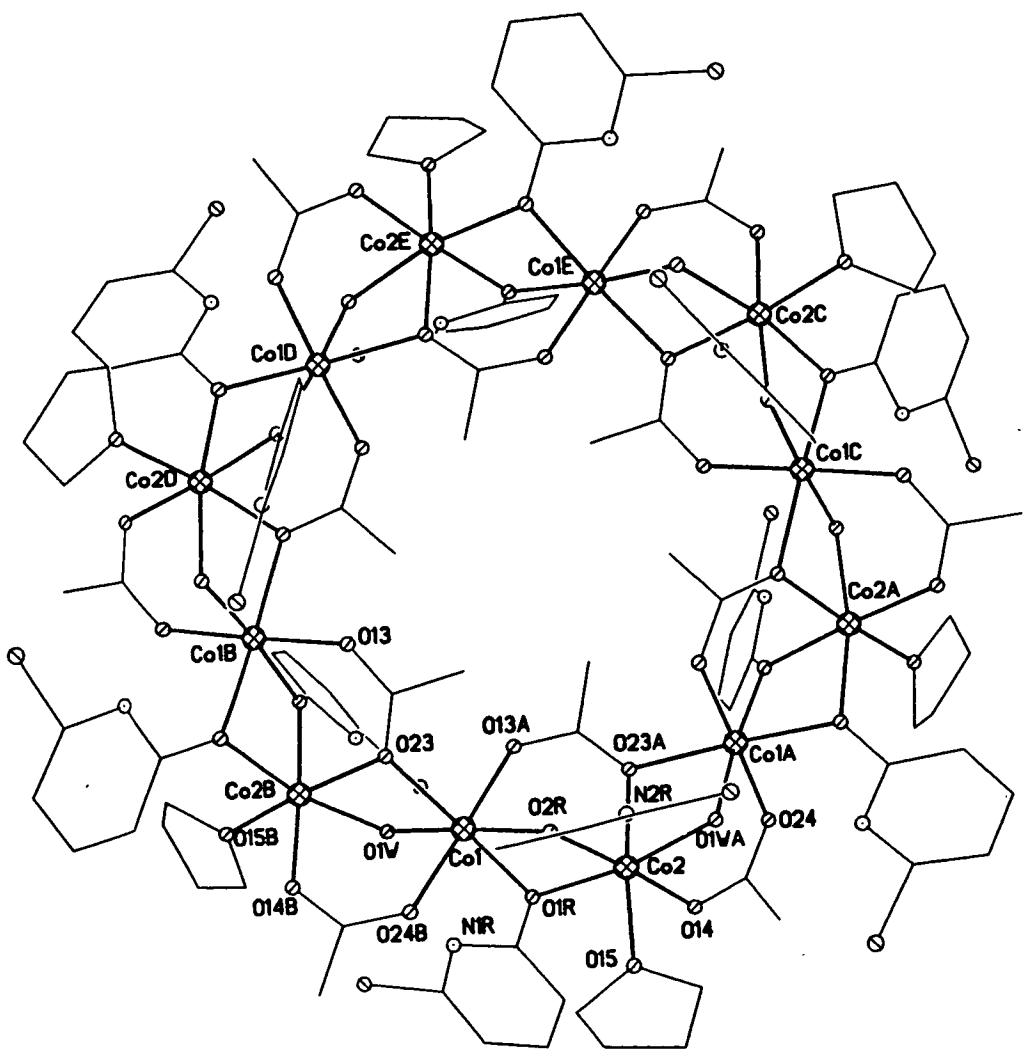

Figure 4.5. The structure of **32** in the crystal.

32 lies on a crystallographic 3 axis with the two cobalt atoms in the asymmetric unit each bound to six oxygen donors. These are derived from four types of ligands. Firstly, there are two oxygens from two different acetate ligands - one of these acetates is outside the metallocycle and bridges adjacent cobalt atoms in a 1,3-fashion. The second acetate lies within the cavity of the metallocycle and is trinucleating, bridging Co1A and Co2 through one oxygen donor and binding to Co1 through the second oxygen donor. Secondly there are two chp ligands which are both μ_2-bridging through the exocyclic oxygen atom. Thirdly, there are water molecules which are μ_2-bridging between the two metal centres and hydrogen-bonded to the deprotonated uncoordinated nitrogen atoms of the chp ligands [O1W...N1R, 2.696(8) Å]. Finally there are terminal THF molecules attached to the Co2 sites. The structure therefore consists of a closed-chain of intersecting $[Co_2O_2]$ rings with each ring additionally bridged by an acetate ligand.

Both metal sites are close to octahedral. Co1 *cis*, 79.2-94.1(3)°; *trans*, 173.1-178.3(3)°; Co2 *cis*, 79.3-99.6(3)°; *trans* 169.1-176.5(3)° with the major distortions being the *cis* angles defined by the two pyridonate oxygen atoms [O1R-Co1-O2R, 79.2(3)°] and the water molecule and the oxygen of the 1,3-bridging acetate [O23-Co1-O1W, 79.2(3)°]. The cobalt-oxygen bond lengths are regular for both unique cobalt atoms with the Co-O(chp) bond lengths in the range 2.082-2.088(7)Å for Co1 and 2.073-2.100(8)Å for Co2. The Co-O(O_2CMe) bond lengths differ from one another quite significantly which is unsurprising given the different coordinating modes they adopt : the acetate outside the metallocycle has two similar bonds to the metal centres [2.036, 2.016(8)Å], whilst the trinucleating acetate within the cavity of the metallocycle has one short bond [2.062(12)Å] and two longer bonds [2.092, 2.130(12)Å] originating from the μ_2-oxygen atom. The Co-O-Co angles in the $[Co_2O_2]$ ring defined by the μ_2-O(H_2O), μ_2-O(chp) μ_2-O(O_2CMe) ligands are 94.8(3)°, 95.3(3)° and 97.2(3)°, and 97.6(3)° respectively. A summary of the bond lengths and angles for **32** is given

in Table 4.3. They are similar to those reported for the nickel dodecamer. The Co...Co distances in **32** are are 3.122(12)Å [Co1...Co2] and 3.176(12)Å [Co1...Co2B] which compare with the Ni...Ni distances of 3.066(7)Å and 3.106(7)Å in the equivalent nickel complex. The variation in the metal...metal contacts is similar to that found in the trinuclear cobalt and nickel complexes discussed earlier, where the metal...metal contacts in the cobalt complexes are always longer than the equivalent distances in the isostructural nickel complexes.

The source of the water in **32** is the THF solvent and is necessary for the structure to form since every second pair of nickel atoms is bridged by a water molecule. Crystallisation of the melt product from dry THF failed to produce **32**. It is also possible that the water came directly from the hydrated cobalt acetate itself, though this is unlikely given the prolonged drying prior to thermolysis.

Recently a number of metal rings have been reported in the literature. Starting with the decanuclear yttrium ring reported by Hubert-Pfalzgraf et al [114] and proceeding via the ferric wheels reported by Holm et al [80], Lippard et al [46] and Winpenny et al [38]. A large metallocycle has also been reported for titanium [115] with the largest metal rings being the giant molybdenum wheels reported by Müller et al [78, 116]. These cyclic structures fall into two broad categories - those which involve monoatomic ligands [78, 80, 116] such as S^{2-} or O^{2-}, and those involving organic ligands. All of the rings involving 3d-metals [46, 113, 115, 117] have involved carboxylate ligands and the metal-metal vectors have been triply-bridged. In the ferric wheels [38, 46] and the nickel and cobalt pyridonate cycles described above, these three bridges have been derived from one carboxylate ligand and two μ_2-oxygen donors from alkoxides or pyridonates : in the titanium octametallocycle two carboxylates and one μ_2-oxygen donor are involved. The presence of mixtures of 1,3-bridging carboxylates and μ_2-oxygen donors spanning the same M...M contact appears to allow these cyclic structures to form in preference to, for example, an equally plausible polymeric structure.

4.2.3. Magnetochemistry of 32.

The magnetic behaviour of the isostructural nickel metallocycle $[Ni_{12}(O_2CMe)_{12}(chp)_{12}(H_2O)_6(THF)_6]$ proved interesting in that ferromagnetic exchange between the Ni (II) centres led to an S = 12 ground state - which is among the largest known for a molecular compound. The magnetic behaviour of **32** was studied in the temperature range 300 - 1.8 K in an applied field of 1000 G, and in comparison to the nickel compound has proved disappointing. The variation of $\chi_m T$ with temperature is shown in Figure 4.6. The room temperature value of $\chi_m T$ = 42 emu K mol^{-1} is consistant with twelve non-interacting Co(II) S = 3/2 centres [$\chi_m T$ = 41 emu K mol^{-1}, g = 2.7]. As the temperature is lowered the value of $\chi_m T$ falls steadily and at the lowest temperature measured had reached 25 emu K mol^{-1}. This behaviour suggests weak antiferromagnetic exchange between the metal centres.

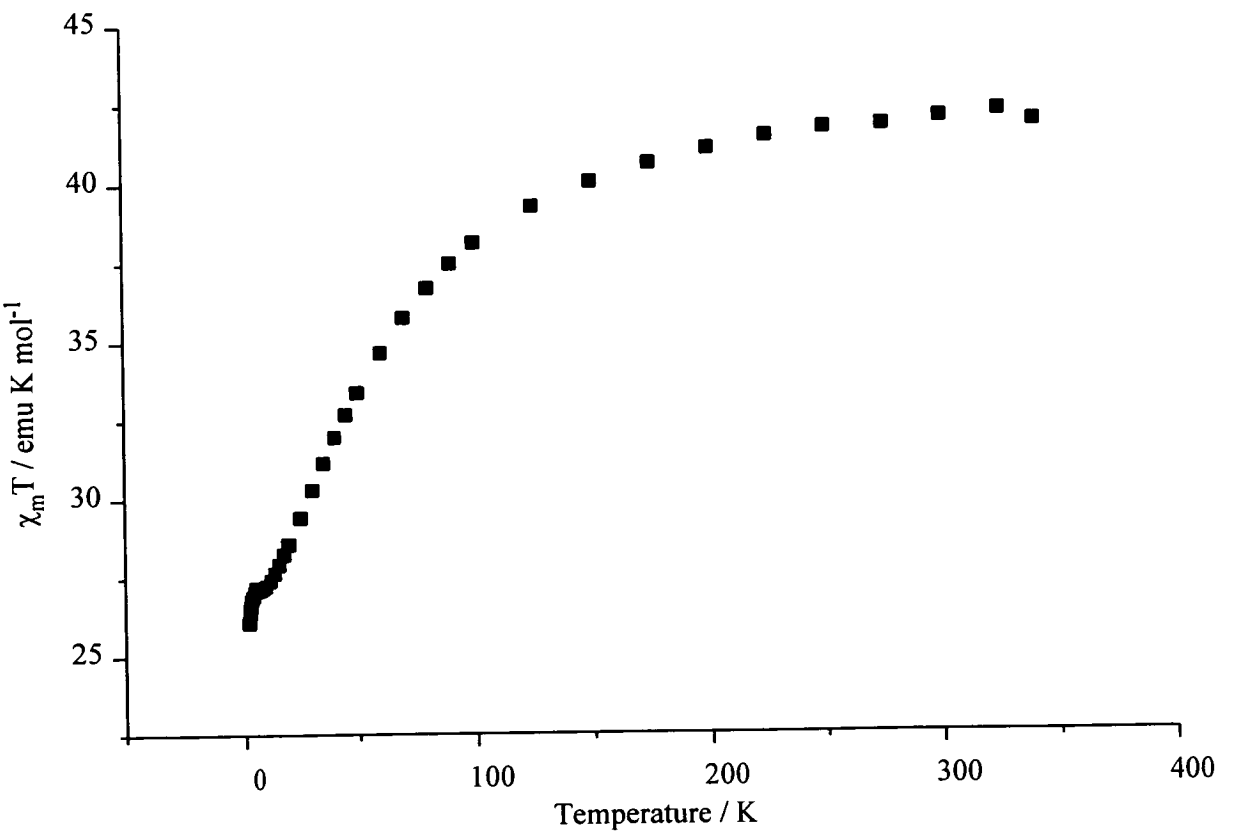

Figure 4.6. The variation of $\chi_m T$ with temperature for **32**.

Table 4.3. Selected bond lengths (Å) and angles (°) for **32**.

Co1-O24B	2.036(8)	O13A-Co1-O1W	89.6(3)
Co1-O13A	2.062(8)	O2R-Co1-O1W	173.2(3)
Co1-O2R	2.082(7)	O1R-Co1-O1W	94.1(3)
Co1-O1R	2.089(7)	O23-Co1-O1W	79.2(3)
Co1-O23	2.130(7)	O14-Co2-O1R	99.6(3)
Co1-O1W	2.151(7)	O14-Co2-O23A	93.3(3)
Co2-O14	2.016(8)	O1R-Co2-O23A	94.8(3)
Co2-O1R	2.073(8)	O14-Co2-O2R	176.5(3)
Co2-O23A	2.092(7)	O1R-Co2-O2R	79.3(3)
Co2-O2R	2.100(7)	O23A-Co2-O2R	90.0(3)
Co2-O15	2.108(8)	O14-Co2-O15	88.6(3)
Co2-O1WA	2.166(7)	O1R-Co2-O15	93.0(3)
O24B-Co1-O13	178.3(3)	O23A-Co2-O15	171.6(3)
O24B-Co1-O2R	92.9(3)	O2R-Co2-O15	88.2(3)
O13A-Co1-O2R	88.7(3)	O14-Co2-O1WA	90.2(3)
O24B-Co1-O1R	90.7(3)	O1R-Co2-O1WA	169.1(3)
O13A-Co1-O1R	90.2(3)	O23-Co2-O1WA	79.7(3)
O2R-Co1-O1R	79.3(3)	O2R-Co2-O1WA	91.3(3)
O24B-Co1-O23	90.6(3)	O15-Co2-O1WA	92.1(3)
O13A-Co1-O23	88.3(3)	Co2-O1R-Co1	97.2(3)
O2R-Co1-O23	107.3(3)	Co1-O2R-Co2	96.5(3)
O1R-Co1-O23	173.1(3)	Co2B-O23-Co1	97.6(3)
O24B-Co1-O1W	88.9(3)	Co1-O1W-Co2B	94.8(3)

4.2.4. Synthesis and structure of $[Co_7(OH)_2(chp)_8(PhCOO)_4(MeCN)]$ 33.

Reaction of cobalt chloride with two equivalents of both Na(chp) and $Na(O_2CPh)$ in methanol for 24 hours produced a paste which was dried *in vacuo* for several hours. Crystallisation of this paste from acetonitrile produced the cobalt heptamer $[Co_7(OH)_2(chp)_8(PhCOO)_4(MeCN)]$ **33** [Figure 4.7] in good yield after two days [71]. The equivalent reaction using Na(mhp) produced the cobalt centred-tricapped-trigonal prism **25**. The polyhedron of metal atoms in **33** is irregular but is loosely based on a trigonal prism capped by Co5 on the 'upper' triangular face. The structure is unrelated to any of the centred-tricapped-trigonal prisms discussed in Chapter 3.

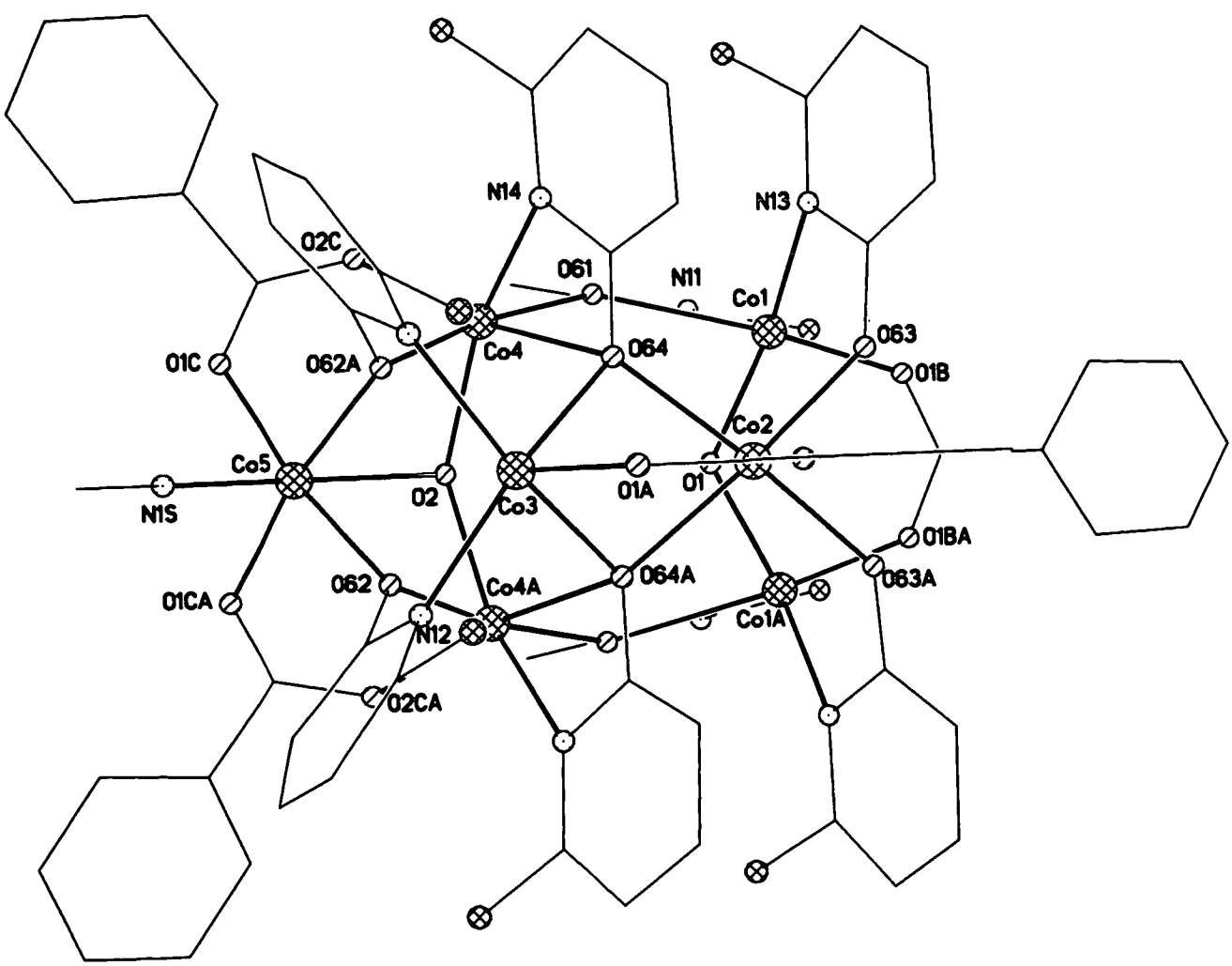

Figure 4.7. The structure of **33** in the crystal.

The cobalts in the 'lower' triangular face [Co1, Co1A and Co2] are bound to a μ_3-hydroxide [O1] with the three edges of the triangle spanned by one 1,3-bridging benzoate and two μ-oxygen atoms derived from chp ligands. The 'upper' triangular face of the prism [Co3, Co4 and Co4A] is bound to the first by two μ_3-oxygen atoms from chp ligands, two μ_2-oxygen atoms from chps and one 1,3-bridging benzoate. The Co3-Co4 and Co3-Co4A edges within this face are bridged by the μ_3-oxygen from the chp ligand and by two further chps which bind to Co3 through the ring nitrogen and to Co4 or Co4A *via* the oxygen atom. These oxygens are themselves μ_2-bridging, binding to the 'capping' cobalt atom [Co5]. This is also attached to Co4 and Co4A by 1,3-bridging benzoates and by the second μ_3-hydroxide group [O2].

Five of the seven cobalt atoms are six-coordinate bound to bridging and chelating benzoates, pyridonates and hydroxides. Co5 is also six-coordinate but the final site is occupied by a molecule of acetonitrile. Co1 is formally five-coordinate with the oxygen atom which should occupy the sixth site [O63] 2.440(3)Å distant. Co3 is five-coordinate with the vacant site pointing toward the centre of the metal polyhedron with a μ_2-oxygen from a bridging pyridonate [O62] 2.429(10)Å distant. The chp ligands adopt three different coordinating modes : trinucleating, chelating to one metal centre through the ring nitrogen and exocyclic oxygen atom with the oxygen bridging to a further two metal sites. Binucleating, chelating to one metal centre with the oxygen atom bridging to a second metal centre and binucleating, binding to one cobalt through the ring nitrogen and to a second cobalt through the exocyclic oxygen. The benzoates all bridge two cobalt atoms in a 1,3-fashion.

The six-coordinate cobalts all have distorted octahedral geometries with the *cis* angles ranging between 58.7-105.5(5)° and the *trans* angles 155.8-167.3(5)°. The cobalt-oxygen and cobalt-nitrogen bonds are all regular : Co-O(OH), 2.008-2.160(12)Å; Co-O(O_2CPh), 2.000-2.047(20)Å; Co-O(chp), 2.008-2.325(12)Å and Co-N(chp), 2.052-2.210(12)Å. The closest

Co...Co contact is 3.098(12)Å between Co5 and Co4. There are no significant intermolecular interactions in **33**. Selected bond lengths are given in Table 4.4.

Table 4.4. Selected bond lengths (Å) and angles (°) for **33**.

Co1-O1B	2.005(13)	Co5-O62A	2.082(12)
Co1-O1	2.008(10)	Co5-O2	2.16(2)
Co1-N13	2.052(12)	Co5-N1S	2.18(3)
Co1-N11	2.070(12)	O1B-Co1-O1	103.8(6)
Co1-O61	2.325(11)	O1B-Co1-N13	103.3(6)
Co2-O2A	2.00(2)	O1-Co1-N13	124.6(6)
Co2-O63	2.078(11)	O1B-Co1-N11	99.8(6)
Co2-O63A	2.078(11)	O1-Co1-N11	104.3(6)
Co2-O1	2.09(2)	N13-Co1-N11	117.3(6)
Co2-O64A	2.159(12)	O1B-Co1-O61	159.2(6)
Co2-O64	2.159(12)	O1-Co1-O61	78.5(6)
Co3-O1A	2.01(2)	N13-Co1-O61	91.6(6)
Co3-O64A	2.209(12)	N11-Co1-O61	60.1(6)
Co3-O64	2.209(12)	O2A-Co2-O63	93.7(5)
Co3-N12	2.210(12)	O2A-Co2-O63A	93.7(5)
Co3-N12A	2.210(12)	O63-Co2-O63A	82.9(5)
Co4-O61	2.008(10)	O2A-Co2-O1	177.9(5)
Co4-O2C	2.047(14)	O63-Co2-O1	84.7(5)
Co4-O2	2.081(7)	O63A-Co2-O1	84.7(5)
Co4-N14	2.087(13)	O2A-Co2-O64A	92.8(5)
Co4-O62A	2.101(13)	O63-Co2-O64A	173.0(5)
Co4-O64	2.380(11)	O63A-Co2-O64A	99.2(5)
Co5-O1CA	2.03(2)	O1-Co2-O64A	88.9(5)
Co5-O1C	2.03(2)	O2A-Co2-O64	92.8(5)
Co5-O62	2.082(11)	O63-Co2-O64	99.2(5)

Table 4.4 continued

O63A-Co2-O64	173.0(5)	O62A-Co4-O64	77.3(4)
O1-Co2-O64	88.9(5)	O1CA-Co5-O1C	98.7(6)
O64A-Co2-O64	77.9(6)	O1CA-Co5-O62	90.7(5)
O1A-Co3-O64A	91.5(5)	O1C-Co5-O62	170.5(5)
O1A-Co3-O64	91.5(5)	O1CA-Co5-O62A	170.5(5)
O64A-Co3-O64	75.8(5)	O1C-Co5-O62A	90.7(5)
O1A-Co3-N12	94.4(5)	O62-Co5-O62A	79.9(5)
O64A-Co3-N12	93.4(5)	O1CA-Co5-O2	98.8(5)
O64-Co3-N12	167.9(5)	O1C-Co5-O2	98.8(5)
O1A-Co3-N12A	94.4(5)	O62-Co5-O2	78.2(5)
O64A-Co3-N12A	167.9(5)	O62A-Co5-O2	78.2(5)
O64-Co3-N12A	93.4(5)	O1CA-Co5-N1S	91.8(7)
N12-Co3-N12A	96.7(5)	O1C-Co5-N1S	91.8(7)
O61-Co4-O2C	100.1(5)	O62-Co5-N1S	89.4(7)
O61-Co4-O2	99.1(5)	O62A-Co5-N1S	89.4(7)
O2C-Co4-O2	95.4(5)	O2-Co5-N1S	163.7(9)
O61-Co4-N14	89.3(5)	Co1-O1-Co1A	115.5(8)
O2C-Co4-N14	105.5(5)	Co1-O1Co2	103.1(6)
O2-Co4-N14	155.8(5)	Co1A-O1-Co2	103.1(6)
O61-Co4-O62A	167.3(5)	Co4A-O2-Co4	135.7(9)
O2C-Co4-O62A	92.6(5)	Co4A-O2-Co5	93.6(5)
O2-Co4-O62A	79.6(5)	Co4-O2-Co2	93.6(5)
N14-Co4-O62A	87.3(5)	Co4-O61-Co1	131.1(5)
O61-Co4-O64	90.4(5)	Co5-O62-Co4A	95.4(5)
O2C-Co4-O64	161.2(5)	Co2-O64-Co3	96.6(4)
O2-Co4-O64	98.3(5)	Co2-O64-Co4	125.2(5)
N14-Co4-O64	58.7(5)	Co3-O64-Co4	99.3(5)

4.2.5. Synthesis and structure of $[Co_7(OH)_2(chp)_8(O_2CCMe_3)_4(Hchp)_{0.69}(MeCN)_{0.31}]$ 34.

Reaction of cobalt chloride with two equivalents of both Na(chp) and $Na(O_2CCMe_3)$ in methanol for 24 hours produced a paste which was dried *in vacuo* for several hours. Crystallisation of this paste from acetonitrile produced the heptametallic species $[Co_7(OH)_2(chp)_8(O_2CCMe_3)_4(Hchp)_{0.69}(MeCN)_{0.31}]$ **34** [Figure 4.8] in moderate yield after four days. The structure of **34** is similar to **33** with trimethylacetate ligands replacing the benzoate ligands. It crystallises in a different space group (triclinic rather than orthorhombic) and now contains seven unique cobalts compared to the five unique metals in **33**. The structure of **34** is again based on a distorted trigonal prism with Co2 capping the 'upper' triangular face. The complex is held together by a mixture of 1,3-bridging trimethylacetates, bi- and trinucleating chp units and μ_3-hydroxides which adopt identical bonding modes to those in **33**.

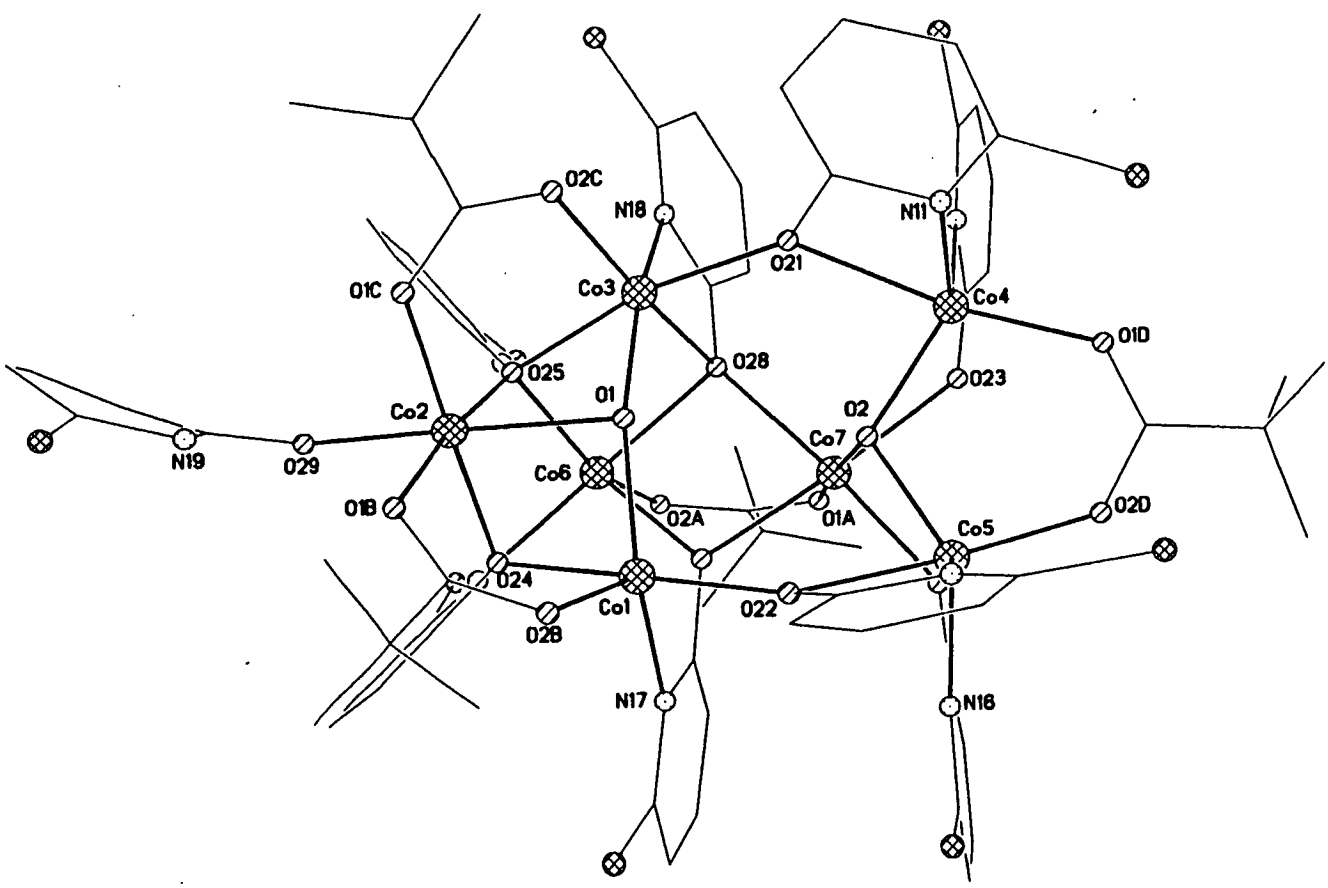

Figure 4.8. The structure of **34** in the crystal.

The main structural difference between **34** and **33** occurs in the coordination of the metal atom which caps the 'upper' triangular face of the trigonal prism. In **33** this metal site is attached to the prism through two 1,3-bridging benzoates, two trinucleating chp ligands and one μ_3-hydroxide. The sixth and final coordination site is occupied by a molecule of acetonitrile. In **34** the cap [Co2] is attached to the 'upper' triangular face in an identical manner through two 1,3-bridging trimethylacetates, two trinucleating chps and one μ_3-hydroxide, but the sixth coordination site is now occupied by a disordered mixture of an Hchp ligand and a molecule of acetonitrile.

Again there are two five-coordinate cobalts in the structure [Co1 and Co4]. The vacant site on Co4 should be occupied by an oxygen [O23] from a chp ligand which is 2.427(10)Å distant. The vacant site on Co1 points to the interior of the cage 2.481(10)Å from O27. The six-coordinate cobalts again have distorted octahedral geometries with the *cis* angles ranging between 59.2-108.7(4)° and the *trans* angles 153.6-178.0(4)°. These distortions are similar to those present in **33**. The cobalt-oxygen and cobalt-nitrogen bonds are also of a similar size : Co-O(OH), 1.992-2.118(9)Å; Co-O(O_2CCMe_3), 1.993-2.045(9)Å; Co-O(chp), 2.027-2.339(8)Å and Co-N(chp), 2.059-2.197(10)Å. The closest Co...Co distance is 3.032(9)Å between Co1 and Co2. Selected bond lengths and angles for **34** are given in Table 4.5. Again there are no significant intermolecular interactions in **34**.

Thus it appears that the introduction of the larger trimethylacetate ligand has had little effect upon the structure of the complex. This is perhaps unsurprising given that there are only four such carboxylates in the structure itself : two attaching the cap to the 'upper' triangular face, one spanning an edge in the 'lower' triangular face and the fourth forming an edge of one of the rectangular faces of the prism joining the 'upper' and 'lower' triangular faces. The carboxylates therefore bridge across the two opposite ends and the side of the molecule, causing minimal steric strain. There are no other cobalt heptamers structurally characterised

containing other carboxylate ligands. Again the presence of bridging hydroxides in both **33** and **34** indicates that the use of 'wet' solvents in the reaction scheme is a necessity.

Table 4.5. Selected bond lengths (Å) and angles (°) for **34**.

Co1-O2B	2.016(11)	Co5-N12	2.090(11)
Co1-O22	2.027(9)	Co5-N16	2.100(12)
Co1-O1	2.047(8)	Co5-O22	2.309(10)
Co1-N17	2.059(11)	Co5-O26	2.362(9)
Co1-O24	2.089(9)	Co6-O2A	2.002(9)
Co2-O1C	2.009(11)	Co6-O27	2.153(8)
Co2-O24	2.028(13)	Co6-N14	2.155(11)
Co2-O1B	2.045(13)	Co6-N15	2.197(10)
Co2-N1S	2.101(9)	Co6-O28	2.208(8)
Co2-O29	2.101(9)	Co6-O25	2.262(8)
Co2-O25	2.101(9)	Co7-O1A	2.017(9)
Co2-O1	2.188(9)	Co7-O26	2.079(9)
Co3-O2C	2.023(9)	Co7-O2	2.096(8)
Co3-O21	2.040(10)	Co7-O23	2.112(8)
Co3-O1	2.060(8)	Co7-O27	2.156(8)
Co3-N18	2.115(9)	Co7-O28	2.159(8)
Co3-O25	2.158(10)	O2B-Co1-O22	97.2(4)
Co3-O28	2.339(11)	O2B-Co1-O1	95.3(4)
Co4-O1D	1.993(12)	O22-Co1-O1	99.5(3)
Co4-O2	2.000(11)	O2B-Co1-N17	113.4(5)
Co4-N11	2.061(10)	O22-Co1-N17	88.6(4)
Co4-N13	2.078(8)	O1-Co1-N17	149.1(4)
Co4-O21	2.298(12)	O2B-Co1-O24	90.4(4)
Co5-O2D	2.000(10)	O22-Co1-O24	171.8(4)
Co5-O2	1.992(8)	O1-Co1-O24	82.7(4)

Table 4.5 continued

N17-Co1-O24	85.6(4)	O1-Co3-O25	79.3(3)
O1C-Co2-O24	178.0(4)	N18-Co3-O25	89.6(3)
O1C-Co2-O1B	90.7(4)	O2C-Co3-O28	162.4(4)
O24-Co2-O1B	91.2(4)	O21-Co3-O28	86.5(3)
O1C-Co2-N1S	89.0(5)	O1-Co3-O28	99.4(3)
O24-Co2-N1S	91.5(4)	N18-Co3-O28	59.7(3)
O1B-Co2-N1S	93.7(4)	O25-Co3-O28	77.4(3)
O1C-Co2-O29	89.0(4)	O1D-Co4-O2	105.3(3)
O24-Co2-O29	91.5(4)	O1D-Co4-N11	100.9(3)
O1B-Co2-O29	93.7(4)	O2-Co4-N11	114.2(4)
O1C-Co2-O25	95.6(4)	O1D-Co4-N13	99.3(3)
O24-Co2-O25	82.5(4)	O2-Co4-N13	126.9(3)
O1B-Co2-O25	173.3(4)	N11-Co4-N13	106.0(5)
N18-Co2-O25	88.8(4)	O1D-Co4-O21	161.7(4)
O29-Co2-O25	88.8(4)	O2-Co4-O21	81.3(4)
O1C-Co2-O1	98.4(4)	N11-Co4-O21	61.1(4)
O24-Co2-O1	80.7(4)	N13-Co4-O21	89.6(5)
O1B-Co2-O1	99.0(4)	O2D-Co5-O2	102.3(5)
N1S-Co2-O1	165.2(4)	O2D-Co5-N12	103.9(4)
O29-Co2-O1	165.2(4)	O2-Co5-N12	110.1(3)
O25-Co2-O1	77.8(4)	O2D-Co5-N16	100.9(3)
O2C-Co3-O21	98.2(4)	O2-Co5-N16	129.3(3)
O2C-Co3-O1	96.5(4)	N12-Co5-N16	107.1(3)
O21-Co3-O1	99.8(4)	O2D-Co5-O22	163.0(3)
O2C-Co3-N18	103.6(4)	O2-Co5-O22	79.6(4)
O21-Co3-N18	85.6(4)	N12-Co5-O22	60.2(3)
O1-Co3-N18	158.3(4)	N16-Co5-O22	90.4(3)
O2C-Co3-O25	98.3(4)	O2D-Co5-O26	84.4(3)
O21-Co3-O25	163.4(4)	O2-Co5-O26	79.1(3)

Table 4.5 continued

N12-Co5-O26	165.5(4)	O26-Co7-O27	95.9(3)
N16-Co5-O26	59.2(4)	O2-Co7-O27	91.6(3)
O22-Co5-O26	112.5(4)	O23-Co7-O27	173.2(3)
O2A-Co6-O27	93.1(4)	O1A-Co7-O28	93.2(3)
O2A-Co6-N14	103.3(3)	O26-Co7-O28	171.3(3)
O27-Co6-N14	92.9(3)	O2-Co7-O28	90.5(3)
O2A-Co6-N15	96.8(3)	O23-Co7-O28	98.1(3)
O27-Co6-N15	165.6(3)	O27-Co7-O28	77.7(3)
N14-Co6-N15	94.8(3)	Co1-O1-Co3	140.6(3)
O2A-Co6-O28	93.3(4)	Co1-O1-Co2	91.4(3)
O27-Co6-O28	76.8(4)	Co1-O1-Co2	92.3(3)
N14-Co6-O28	161.0(4)	Co5-O2-Co4	115.8(3)
N15-Co6-O28	92.3(3)	Co5-O2-Co7	103.2(3)
O2A-Co6-O25	153.6(3)	Co4-O2-Co7	103.5(3)
O27-Co6-O25	108.7(3)	Co3-O21-Co4	132.2(4)
N14-Co6-O25	90.6(4)	Co1-O22-Co5	129.8(4)
N15-Co6-O25	59.2(4)	Co2-O24-Co1	94.8(4)
O28-Co6-O25	78.1(3)	Co2-O25-Co3	92.1(3)
O1A-Co7-O26	93.2(4)	Co2-O25-Co6	117.8(4)
O1A-Co7-O2	173.4(3)	Co3-O25-Co6	101.9(3)
O26-Co7-O2	83.7(3)	Co7-O26-Co5	92.1(3)
O1A-Co7-O23	91.1(3)	Co6-O27-Co7	96.5(3)
O26-Co7-O23	87.7(4)	Co7-O28-Co6	94.8(3)
O2-Co7-O23	83.0(3)	Co7-O28-Co3	123.9(4)
O1A-Co7-O27	94.6(3)	Co6-O28-Co3	98.1(3)

4.2.6. Magnetochemistry of 33 and 34.

The magnetic behaviour of **33** and **34** was studied in the temperature range 300-1.8 K in an applied field of 1000 G. The behaviour of the two compounds is identical. The variation of $\chi_m T$ with temperature is shown in Figure 4.9. The room temperature value of $\chi_m T$ = 18 emu K mol^{-1} is consistant with seven non-interacting S = 3/2 Co(II) centres [$\chi_m T$ = 18.9 emu K mol^{-1}, g = 2.4]. The value then drops with temperature to a minimum of approximately 3 emu K mol^{-1} at 1.8 K. This value corresponds to an approximately S = 1 ground state.

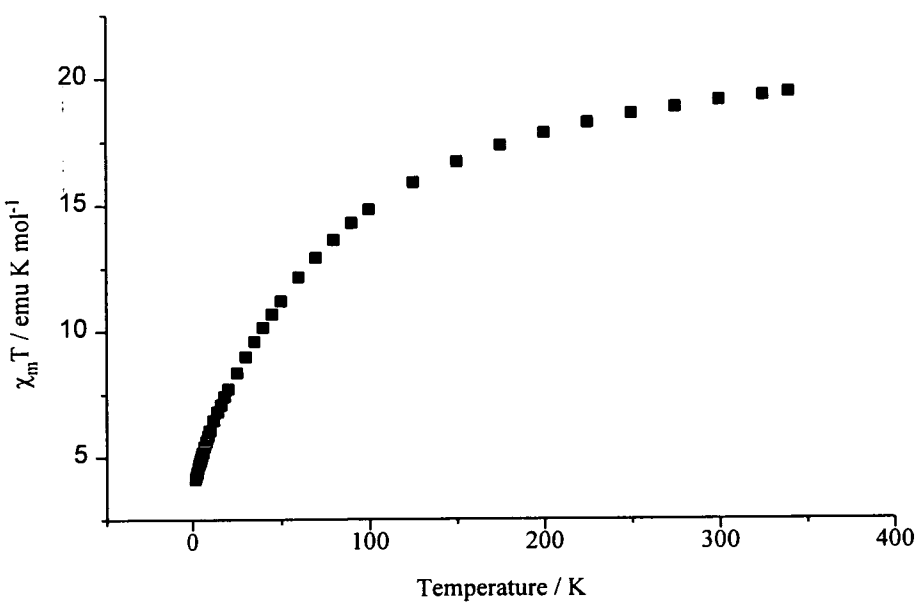

Figure 4.9. The variation of $\chi_m T$ with temperature for **33** and **34.**

4.2.7. Synthesis and structure of $[Ni_{12}Na_4(OH)_2(O_2CCH_2Cl)_8(chp)_8(MeCN)_2]$ 35.

Reaction of nickel chloride with two equivalents of both Na(chp) and $Na(O_2CCH_2Cl)$ in methanol for 24 hours produced a green paste which was dried *in vacuo* for several hours. Crystallisation of this paste from acetonitrile produced green crystals of $[Ni_{12}(OH)_2(O_2CCH_2Cl)_8(chp)_{18}(MeCN)_2]$ **35** [Figure 4.10] in moderate yield after three days.This is the same synthetic procedure used to synthesise the two cobalt heptamers **33** and **34**. The equivalent reaction using the 6-methyl derivative of 2-pyridone produced the dodecanuclear nickel centred-tricapped-trigonal prism **22**. The strucure of **35** is extremely unusual and is unrelated to **33**, **34** or **22**. It's polyhedron [Figure 4.11] does not describe any common structural type.

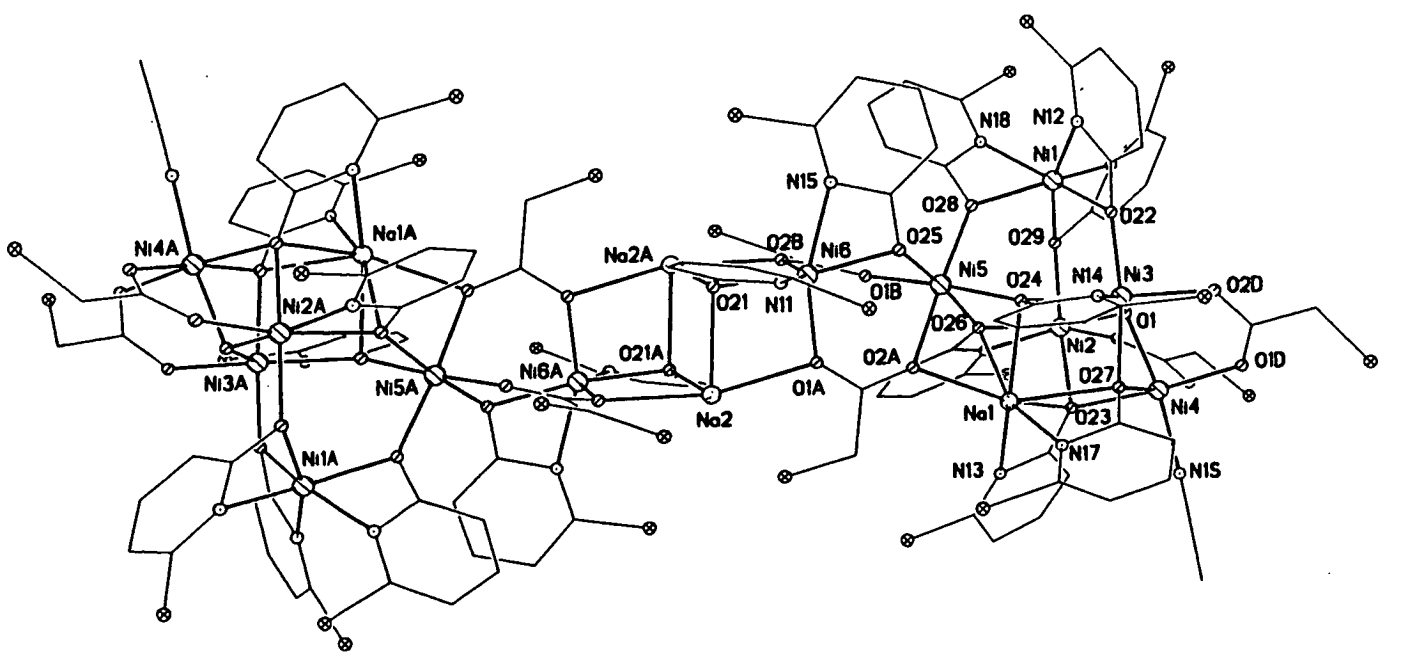

Figure 4.10. The structure of **35** in the crystal.

The structure contains two identical nickel-sodium cages which are linked together by a different central nickel-sodium unit, conaining Ni6, Na2 and symmetry equivalents. This central unit can be regarded as two $[Na_2NiO_4]$ cubes, each missing a vertex, which share the same $[Na_2O_2]$ face. The nickels [Ni6, Ni6A] are six-coordinate, bound to four oxygen and two nitrogen donors in a disordered octahedral array [*cis*, 63.2-110.5(4)°; *trans*, 148.0-168.8 (4)°]. The sodiums [Na2, Na2A] are four-coordinate bound to four oxygen-donors with two longer contacts to chlorine atoms [Na2...Cl1A, 2.964(9)Å; Na2...Cl1C, 3.011(12)Å]. Their geometries are irregular. These central nickel atoms [Ni6, Ni6A] are coordinated to two chelating chp ligands and two molecules of chloroacetate. One of the chp ligands is trinucleating, chelating to Ni6 with the oxygen atom forming a corner of the cube bridging to the two sodium atoms [Na2, Na2a]. The second chp is binucleating, chelating to Ni6 with the exocyclic oxygen atom also bridging to Ni5 which forms part of the peripheral nickel-sodium cage. This nickel-sodium cage is further linked to the central core of the complex *via* two bridging chloroacetates. For both chloroacetate molecules one oxygen of the carboxylate group is binucleating, forming a corner of the central cube by bridging between a nickel and sodium site. However the ligation of the second oxygen atom to the external nickel-sodium cage differs between the two molecules. The first chloroacetate bridges to one further nickel [Ni5] in the external cage thus making the carboxylate trinucleating. The second chloroacetate is also bound to Ni5 but further bridges to Na1 and is thus tetranucleating.

The peripheral nickel sodium fragment in **35** describes an unusual $[Ni_5NaO_9]$ cage which is held together by a blend of bridging hydroxide, pyridonate and chloroacetate ligands. Ni5 is bound to three chelating chp ligands which are all binucleating, each bridging to one further nickel site [Ni2, Ni3 and Ni5] through their exocyclic oxygen atom. These three metal sites [Ni2, Ni3, Ni5] are linked together by two μ_3-oxygen atoms [O24, O26] derived from two trinucleating chps and one μ_3-hydroxide [O1] ligand, forming a six-membered $[Ni_3O_3]$

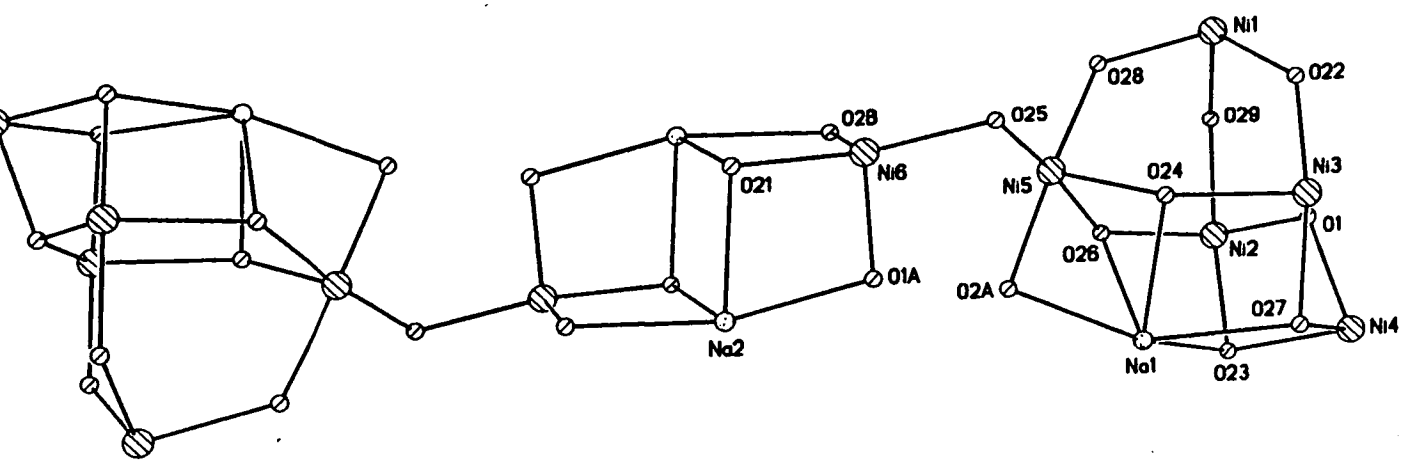

Figure 4.11. The metal polyhedron in **35**.

ring. The oxygens of the two trinucleating chps are also bound to Na1, with the μ_3-hydroxide also ligated to Ni4. Na1 is seven-coordinate with its geometry completed by the chloroacetate which attaches the $[Ni_5NaO_9]$ cage to the central core and two further trinucleating chp ligands which chelate to the sodium through their ring nitrogen and exocyclic oxygen with the oxygen further bridged to two nickel sites : either to Ni2 or Ni3 in the $[Co_3O_3]$ ring and to Ni4 at the 'corner' of the cage. Ni4 is further linked to the $[Ni_3O_3]$ ring by two 1,3-bridging chloroacetate ligands which span the Ni2...Ni4 and Ni4...Ni3 vectors and the μ_3-hydroxide. Its coordination is completed by a molecule of acetonitrile.

The nickel sites within the $[Ni_5NaO_9]$ fragment are all six-coordinate with distorted octahedral geometries. Ni4 and Ni5 are the only metal sites in the cage not ligated by a chelating chp ligand and thus have less distorted geometries [Ni4 *cis*, 79.5-96.5(5)°; *trans*, 171.8-173.0(5)°; Ni5 *cis* 84.6--94.3(5)°; *trans*, 173.5-176.7(5)°] than the other nickel sites

[*cis*, 62.1-110.5(5)°; *trans*, 148.0-168.8(5)°]. Again the geometry of the sodium site [Na1] is best described as irregular. Selected bond lengths and angles for **35** are given in Table 4.6. There are no significant intemolecular interactions in **35**. The reason why **35** adopts such an unusual structure in preference to the capped-trigonal prism common to **33** and **34** is unclear, especially as the syntheses of the three compounds is almost identical. No further nickel complexes containing different carboxylates have been structurally characterised which will be necessary if an acceptable explanation is to be established.

4.2.8. Magnetochemistry of 35.

The magnetic behaviour of **35** was studied in the temperature range 300 - 1.8 K in an applied field of 1000 G. The variation of $\chi_m T$ with temperature is shown in Figure 4.12. The room temperature value of approximately 16 emu K mol^{-1} is consistant with twelve non-interacting Ni(II) S = 1 centres [$\chi_m T$ = 14.5 emu K mol^{-1}, g = 2.2]. The value then drops steadily with temperature giving a minimum of $\chi_m T$ = 4 emu K mol^{-1} at 1.8 K. This value corresponds to an approximately S = 2 ground state.

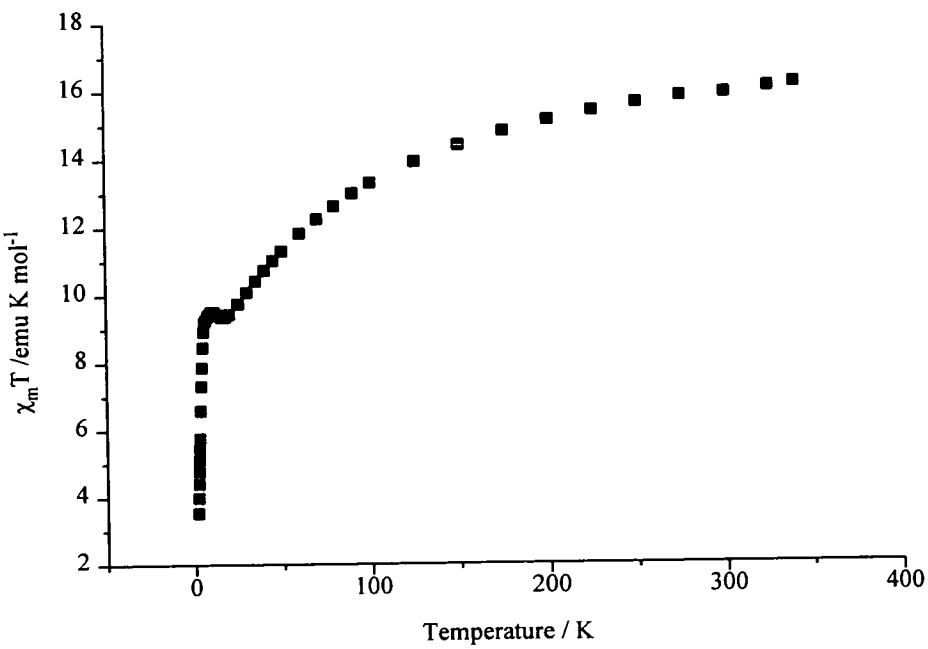

Figure 4.12. The variation of $\chi_m T$ with temperature for **35**.

Table 4.6. Selected bond lengths (Å) and angles (°) for **35**.

Ni1-N18	2.039(10)	Ni5-O26	2.097(8)
Ni1-N19	2.067(10)	Ni6-O2B	2.022(11)
Ni1-N12	2.076(11)	Ni6-O1A	2.032(12)
Ni1-O22	2.112(9)	Ni6-O25	2.051(9)
Ni1-O29	2.121(9)	Ni6-O21	2.059(9)
Ni1-O28	2.124(9)	Ni6-N15	2.140(12)
Ni2-O1C	1.999(9)	Ni6-N11	2.188(11)
Ni2-O1	2.015(9)	Na1-O26	2.412(12)
Ni2-O29	2.042(10)	Na1-O2A	2.419(10)
Ni2-N16	2.066(10)	Na1-O23	2.445(10)
Ni2-O23	2.099(10)	Na1-N17	2.470(13)
Ni2-O26	2.234(8)	Na1-O27	2.498(11)
Ni3-O1	1.982(9)	Na1-O24	2.578(11)
Ni3-O2D	2.015(9)	Na1-N13	2.630(13)
Ni3-O22	2.017(10)	Na2-O21A	2.267(12)
Ni3-N14	2.042(10)	Na2-O1A	2.371(12)
Ni3-O27	2.091(10)	Na2-O2BA	2.435(11)
Ni3-O24	2.245(8)	Na2-O21	2.481(14)
Ni4-O1	2.002(10)	Na2-Cl1A	2.964(9)
Ni4-O2C	2.033(11)	Na2-Cl1?	3.011(15)
Ni4-N1S	2.02(2)	N18-Ni1-N19	102.0(4)
Ni4-O1D	2.069(11)	N18-Ni1-N12	99.1(5)
Ni4-O27	2.086(9)	N19-Ni1-N12	106.3(4)
Ni4-O23	2.098(9)	N18-Ni1-O22	154.4(4)
Ni5-O25	2.034(9)	N19-Ni1-O22	101.0(4)
Ni5-O1B	2.039(9)	N12-Ni1-O22	63.5(4)
Ni5-O28	2.051(9)	N18-Ni1-O29	96.2(4)
Ni5-O24	2.050(9)	N19-Ni1-O29	64.0(4)
Ni5-O2A	2.095(11)	N12-Ni1-O29	163.4(4)

Table 4.6 continued

O22-Ni1-O29	103.9(4)	O22-Ni3-O27	162.8(4)
N18-Ni1-O28	63.6(3)	N14-Ni3-O27	89.8(4)
N19-Ni1-O28	157.8(4)	O1-Ni3-O24	106.2(3)
N12-Ni1-O28	93.2(4)	O2D-Ni3-O24	161.9(4)
O22-Ni1-O28	97.1(4)	O22-Ni3-O24	88.4(4)
O29-Ni1-O28	99.3(3)	N14-Ni3-O24	62.1(3)
O1C-Ni2-O1	91.7(4)	O27-Ni3-O24	87.7(4)
O1C-Ni2-O29	95.0(4)	O1-Ni4-O2C	92.4(4)
O1-Ni2-O29	89.4(4)	O1-Ni4-N1S	172.0(5)
O1C-Ni2-N16	101.8(4)	O2C-Ni4-N1S	91.4(5)
O1-Ni2-N16	163.7(4)	O1-Ni4-O1D	94.9(4)
O29-Ni2-N16	98.4(4)	O2C-Ni4-O1D	91.9(4)
O1C-Ni2-O23	91.7(4)	N1S-Ni4-O1D	92.0(5)
O1-Ni2-O23	79.5(4)	O1-Ni4-O27	79.5(4)
O29-Ni2-O23	167.2(4)	O2C-Ni4-O27	171.8(4)
N16-Ni2-O23	90.9(4)	N1S-Ni4-O27	96.5(5)
O1C-Ni2-O26	163.6(4)	O1D-Ni4-O27	90.2(4)
O1-Ni2-O26	103.7(3)	O1-Ni4-O23	79.8(4)
O29-Ni2-O26	90.7(3)	O2C-Ni4-O23	93.0(4)
N16-Ni2-O26	62.1(3)	N1S-Ni4-O23	92.9(5)
O23-Ni2-O26	85.7(4)	O1D-Ni4-O23	173.0(4)
O1-Ni3-O2D	91.9(4)	O27-Ni4-O23	84.2(4)
O1-Ni3-O22	85.2(4)	O25-Ni5-O1B	91.9(4)
O2D-Ni3-O22	94.9(4)	O25-Ni5-O28	94.1(4)
O1-Ni3-N14	164.9(4)	O1B-Ni5-O28	89.4(4)
O2D-Ni3-N14	99.8(4)	O25-Ni5-O24	94.3(4)
O22-Ni3-N14	103.1(4)	O1B-Ni5-O24	173.5(4)
O1-Ni3-O27	79.8(5)	O28-Ni5-O24	92.2(4)
O2D-Ni3-O27	93.9(4)	O25-Ni5-O2A	88.6(4)

Table 4.6 continued.

O1B-Ni5-O2A	92.4(4)	O2A-Na1-O27	136.7(4)
O28-Ni5-O2A	176.7(4)	O23-Na1-O27	69.2(3)
O24-Ni5-O2A	85.8(4)	N17-Na1-O27	53.7(3)
O25-Ni5-O26	173.8(4)	O26-Na1-O24	68.0(3)
O1B-Ni5-O26	89.0(4)	O2A-Na1-O24	68.7(3)
O28-Ni5-O26	92.1(4)	O23-Na1-O24	111.0(4)
O24-Ni5-O26	84.6(4)	N17-Na1-O24	89.3(4)
O2A-Ni5-O26	85.2(3)	O27-Na1-O24	72.6(3)
O2B-Ni6-O1A	92.8(5)	O26-Na1-N13	90.7(4)
O2B-Ni6-O25	98.2(4)	O2A-Na1-N13	113.8(4)
O1A-Ni6-O25	97.8(4)	O23-Na1-N13	52.6(3)
O2B-Ni6-O21	86.8(4)	N17-Na1-N13	110.6(5)
O1A-Ni6-O21	92.0(4)	O27-Na1-N13	109.5(4)
O25-Ni6-O21	168.8(4)	O24-Na1-N13	157.1(4)
O2B-Ni6-N15	93.1(5)	O21A-Na2-O1A	102.8(4)
O1A-Ni6-N15	160.7(4)	O21A-Na2-O2BA	73.1(4)
O25-Ni6-N15	63.2(3)	O1A-Na2-O2BA	165.3(5)
O21-Ni6-N15	106.7(4)	O21A-Na2-O21	86.4(4)
O2B-Ni6-N11	148.0(4)	O1A-Na2-O21	74.6(4)
O1A-Ni6-N11	96.9(5)	O2BA-Na2-O21	90.9(4)
O25-Ni6-N11	110.5(4)	Ni3-O1-Ni4	98.8(4)
O21-Ni6-N11	62.6(4)	Ni3-O1-Ni2	129.0(4)
N15-Ni6-N11	87.7(5)	Ni4-O1-Ni2	98.8(4)
O26-Na1-O2A	72.0(3)	Ni6-O1A-Na2	98.7(4)
O26-Na1-O23	74.8(3)	Ni5-O2A-Na1	88.8(4)
O2A-Na1-O23	143.8(4)	Ni6-O2B-Na2A	97.8(4)
O26-Na1-N17	156.3(5)	Ni6-O21-Na2A	102.2(4)
O2A-Na1-N17	106.7(4)	Ni6-O21-Na2	94.6(4)
O23-Na1-N17	109.5(4)	Na2A-O21-Na2	93.6(4)

Table 4.6 continued

Ni4-O23-Ni2	93.2(4)	Ni5-O26-Na1	88.5(4)
Ni4-O23-Na1	103.9(4)	Ni2-O26-Na1	94.5(3)
Ni2-O23-Na1	97.1(4)	Ni4-O27-Ni3	92.9(4)
Ni5-O24-Ni3	139.6(4)	Ni4-O27-Na1	102.5(4)
Ni5-O24-Na1	85.2(3)	Ni3-O27-Na1	97.9(4)
Ni3-O24-Na1	91.8(3)	Ni5-O28-Ni1	131.4(4)
Ni5-O25-Ni6	115.3(4)	Ni2-O29-Ni1	123.4(4)
Ni5-O26-Ni2	139.8(4)		

4.2.9. Synthesis and structure of $[Co_{13}(OH)_2(chp)_{20}(phth)_2]$ 36.

Reaction of cobalt chloride with two equivalents of both Na(chp) and Na_2(phth) [phth is the dianion of phthalic acid] in methanol for 24 hours produced a paste which was dried *in vacuo* for several hours. Crystallisation of this paste from dichloromethane produced purple crystals of $[Co_{13}(OH)_2(chp)_{20}(phth)_2]$ **36** [Figure 4.13] after three days [71].

The central cobalt [Co1] lies on an inversion centre and has regular octahedral geometry [*cis*, 74.1-105.9(3)°; *trans*, 180.00(0)°]. It is best regarded as part of two linked Co_7 units and is bound to four μ_2-oxygen atoms derived from chp ligands, all shared with Co4 (and it's symmetry equivalent) and two oxygen atoms from the phthalate ligands. The carboxylate group of which these oxygens are a part, bridges in a 1,3-fashion to Co4. The second carboxylate of the phthalate links to two further cobalt atoms [Co2 and Co3] which both have tetrahedral geometries, bound to two nitrogen and two oxygen donors. The Co2...Co3 vector is further bridged by a μ_3-hydroxide [O1], which also binds to Co4. The chp groups which connect Co1 and Co4 through their oxygen atoms bind to Co2 and Co3 through

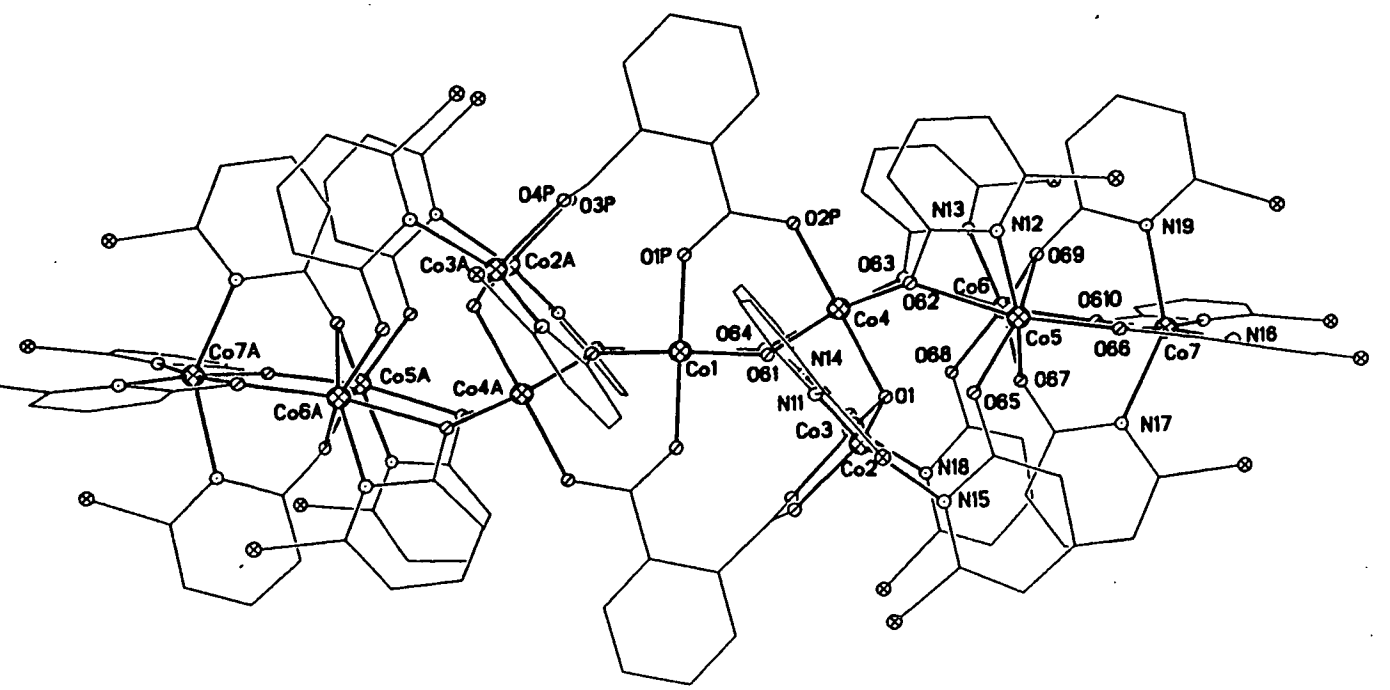

Figure 4.13. The structure of **36** in the crystal.

their nitrogen donors.

The central phthalate-bridged region containing seven cobalt atoms is attached to the remaining cobalt atoms through the bridging chp groups. Co5, Co6 and Co7 are all six-coordinate bound exclusively to nitrogen and oxygen donors derived from chp groups. Co5 and Co6 are bound to five oxygen and one nitrogen atom, while Co7 is bound to four nitrogen and two oxygen donors. The chp ligands adopt three coordinating modes : trinucleating, bound to one cobalt atom through the ring nitrogen [for example Co3] with the oxygen atoms bridging two different metal centres [Co4 and Co1]; binucleating, chelating to one cobalt centre [Co5] with the oxygen atom bound to one further metal [Co4] and binucleating, binding to one cobalt through the ring nitrogen [Co3] with the oxygen atom bound to a

different cobalt [Co6]. The dicarboxylate is tetranucleating bonding to Co1 and Co4A through one carboxylate group and to Co2 and Co3 through the second.

For each metal site [except Co1] at least one chp is chelating therefore the geometries around the meals are distorted from regular octahedral due to the small bite angle of the ligand : the *cis* angles around the six-coordinate cobalt atoms range between 60.5-122.5(3)° and the *trans* angles 145.4-180.0(4)°. The angles around the tetrahedral cobalts [Co2, Co3] range between 100.4-123.9(4)°. The cobalt-oxygen and cobalt-nitrogen bond lengths are all regular : Co-O(phth), 1.972-2.023(9)Å; Co-O(chp), 1.991-2.247(9)Å; Co-N(chp), 2.067-2.214(8)Å and Co-O(OH), 1.986-2.136(9)Å. Selected bond lengths and angles are given in Table 4.7. There are no significant intermolecular interactions in **36**.

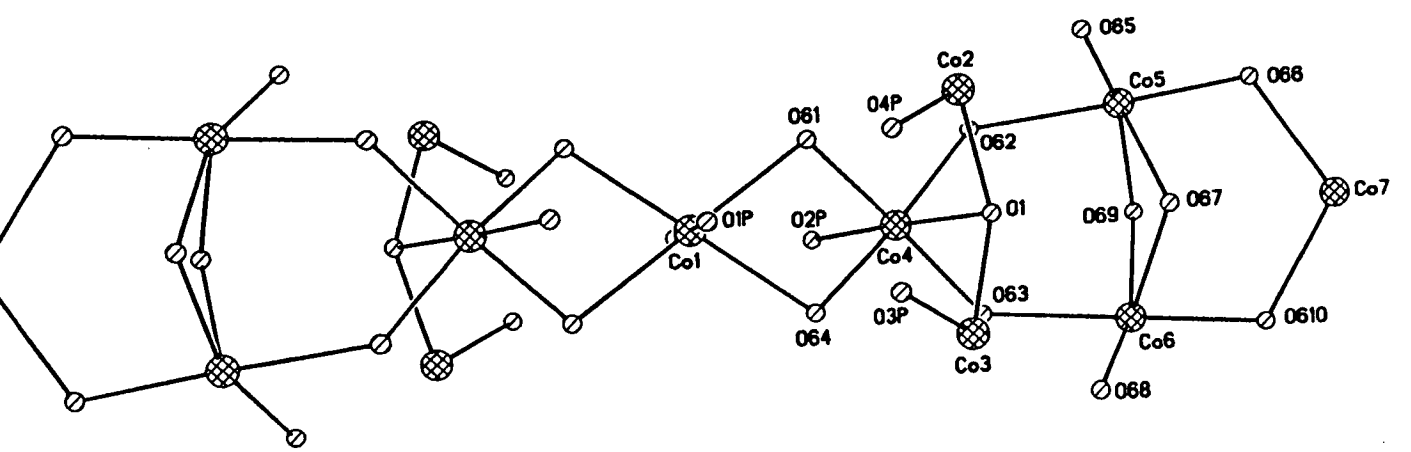

Figure 4.14. The polyhedron of **36**.

4.2.10. Magnetochemistry of 36.

The magnetic behaviour of **36** was studied in the temperature range 300-1.8 K in an applied field of 1000 G. The variation of $\chi_m T$ with temperature is shown in Figure 4.15. The room temperature value of approximately 33 emu K mol^{-1} is consistant with thirteen non-interacting Co(II) S = 3/2 centres [$\chi_m T$ = 35.1 emu K mol-1, g = 2.4]. The value of $\chi_m T$ then drops steadily with temperature giving a minimum value of 5 emu K mol^{-1} at 1.8 K, corresponding to an approximately S = 2 ground state.

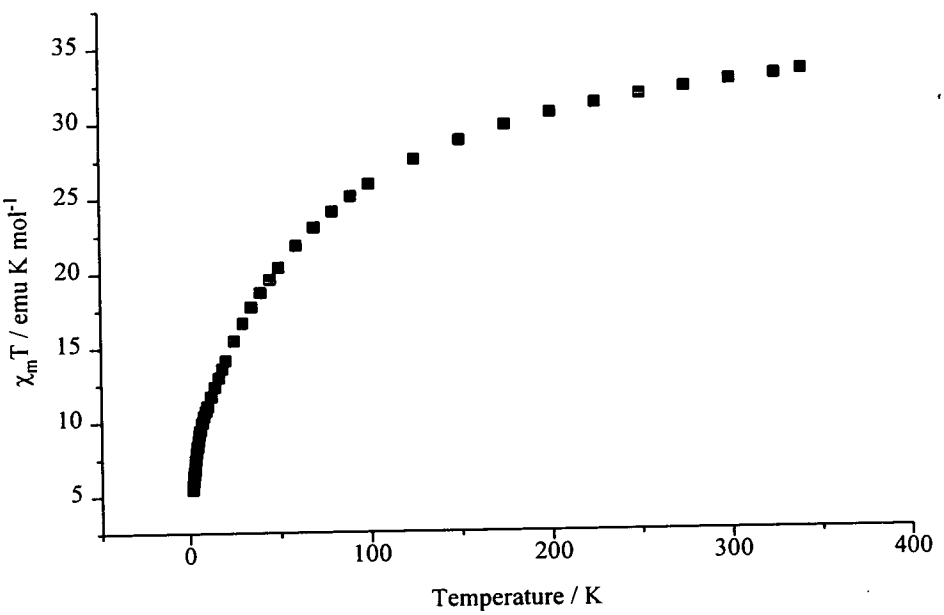

Figure 4.15. The variation of $\chi_m T$ with temperature for **36**.

Table 4.7. Selected bond lengths (Å) and angles (°) for **36**.

Co1-O1P	2.020(9)	Co1-O64A	2.178(7)
Co1-O1PA	2.020(9)	Co2-O4PA	1.972(9)
Co1-O61A	2.136(7)	Co2-O1	2.023(9)
Co1-O61	2.136(7)	Co2-N15	2.078(7)
Co1-O64	2.178(7)	Co2-N11	2.088(8)

Table 4.7 continued

Co3-O1	1.986(9)	O1P-Co1-O61A	90.4(4)
Co3-O3PA	1.987(10)	O1PA-Co1-O61A	89.6(4)
Co3-N14	2.067(8)	O1P-Co1-O61	89.6(4)
Co3-N18	2.082(7)	O1PA-Co1-O61	90.4(4)
Co4-O2P	2.023(10)	O61A-Co1-O61	180.0(0)
Co4-O62	2.035(7)	O1P-Co1-O64	90.5(4)
Co4-O63	2.058(7)	O1PA-Co1-O64	89.5(4)
Co4-O64	2.122(8)	O61A-Co1-O64	105.9(4)
Co4-O1	2.136(9)	O61-Co1-O64	74.1(4)
Co4-O61	2.142(8)	O1P-Co1-O64A	89.5(4)
Co5-O66	1.992(8)	O1PA-Co1-O64A	90.5(4)
Co5-O65	2.018(8)	O61A-Co1-O64A	74.1(4)
Co5-O69	2.088(8)	O61-Co1-O64A	105.9(4)
Co5-N12	2.101(8)	O64-Co1-O64A	180.00(0)
Co5-O67	2.205(9)	O4PA-Co2-o1	100.4(4)
Co5-O62	2.247(8)	O4PA-Co2-N15	102.6(3)
Co6-O610	1.996(7)	O1-Co2-N15	108.0(4)
Co6-O68	2.024(8)	O4PA-Co2-N11	107.9(4)
Co6-O69	2.091(9)	O1-Co2-N11	123.9(4)
Co6-N13	2.145(7)	N15-Co2-N11	111.4(3)
Co6-O63	2.191(7)	O1-Co3-O3PA	100.5(4)
Co6-O67	2.220(7)	O1-Co3-N14	122.8(4)
Co7-N17	2.172(7)	O3PA-Co3-n14	106.5(5)
Co7-N16	2.184(7)	O1-Co3-N18	110.2(4)
Co7-N19	2.188(7)	O3PA-Co3-N18	105.0(3)
Co7-N110	2.214(7)	N14-Co3-N18	109.8(4)
Co7-O610	2.221(7)	O2P-Co4-O62	94.3(4)
Co7-O66	2.225(7)	O2P-Co4-O63	92.6(4)
O1P-Co1-O1PA	180.00(0)	O62-Co4-O63	89.6(4)

Table 4.7 continued

O2P-Co4-O64	92.7(4)	O68-Co6-O69	156.3(3)
O62-Co4-O64	168.6(3)	O610-Co6-N13	111.8(3)
O63-Co4-O64	98.9(3)	O68-Co6-N13	98.0(4)
O2P-Co4-O1	178.0(4)	O69-Co6-N13	94.6(4)
O62-Co4-O1	87.3(3)	O610-Co6-O63	171.5(4)
O63-Co4-O1	86.3(3)	O68-Co6-O63	80.4(4)
O64-Co4-O1	85.9(3)	O69-Co6-O63	88.1(3)
O2P-Co4-O61	94.2(4)	N13-Co6-O63	61.8(3)
O62-Co4-O61	95.5(3)	O610-Co6-O67	82.1(3)
O63-Co4-O61	171.2(4)	O68-Co6-O67	86.8(3)
O64-Co4-O61	75.1(4)	O69-Co6-O67	75.7(3)
O1-Co4-O61	86.8(3)	N13-Co6-O67	163.0(3)
O66-Co5-O65	106.7(4)	O63-Co6-O67	103.3(3)
O66-Co5-O69	87.1(3)	N17-Co7-N16	97.0(5)
O65-Co5-O69	157.9(3)	N17-Co7-N19	145.4(3)
O66-Co5-N12	107.5(3)	N16-Co7-N19	99.1(5)
O65-Co5-N12	104.5(4)	N17-Co7-N110	101.7(4)
O69-Co5-N12	87.0(4)	N16-Co7-N110	122.5(4)
O66-Co5-O67	85.2(3)	N19-Co7-N110	95.1(4)
O65-Co5-O67	87.8(3)	N17-Co7O610	79.8(4)
O69-Co5-O67	76.1(4)	N16-Co7-O610	176.2(4)
N12-Co5-O67	158.5(3)	N19-Co7-O610	82.6(4)
O66-Co5-O62	168.2(3)	N110-Co7-O610	60.5(4)
O65-Co5-O62	81.3(4)	N17-Co7-O66	81.3(4)
O69-Co5-O62	88.1(3)	N16-Co7-O66	60.8(2)
N12-Co5-O62	61.5(2)	N19-Co7-O66	80.3(3)
O67-Co5-O62	104.1(2)	N110-Co7-O66	174.9(4)
O610-Co6-O68	106.7(4)	O610-Co7-O66	116.5(4)
O610-Co6-O69	86.9(3)	Co3-O1-Co2	122.3(4)

Table 4.7 continued

Co3-O1-Co4	103.1(4)	Co4-O64-Co1	98.9(3)
Co2-O1-Co4	101.9(4)	Co5-O66-Co7	114.0(4)
Co1-O61-Co4	99.6(4)	Co5-O67-Co6	96.6(4)
Co4-O62-Co5	125.6(4)	Co6-O69-Co5	104.5(30
Co4-O63-Co6	127.8(4)	Co6-O610-Co7	115.6(3)

4.2.11. Synthesis and structure of $[Ni_{16}Na_6(chp)_4(phth)_{10}(Hphth)_2(OMe)_{10}(OH)_2(MeOH)_{20}]$ 37

Reaction of nickel chloride with two equivalents of both Na(chp) and Na_2(phth) in methanol for three days, followed by filtration, evaporation to dryness and crystallisation from fresh methanol gave green crystals of $[Ni_{16}Na_6(chp)_4(phth)_{10}(Hphth)_2(OMe)_{10}(OH)_2(MeOH)_{20}]$ **37** [Figure 4.16] in low yield after approximately two weeks [118]. **37** is an example of a supracage assembly in which four nickel cubanes are linked through a central sodium octahedron. Such a molecular species , where dissimilar polymetallic fragments (in this case one Na_6 and four Ni_4 cages) are linked into a supracage assembly, appears to be unprecedented. The same reaction in the absence of Na_2(phth) produces the tetranuclear $[Ni_4(OMe)_4(chp)_4(MeOH)_7]$ **1** cage described in Chapter 1. **1** features a similar nickel cube to those present in **37**.

The structure of **37** contains four chemically identical Ni_4 units which are each based on an imperfect $[Ni_4O_4]$ cube. Since the complex lies on a two-fold axis these cubes comprise two crystallographically equivalent pairs. In **1** the cube contained four oxygen vertices derived from μ_3-methoxide groups. In the cubes in **37** two of the oxygen vertices are occupied by μ_3-methoxides and the third by a μ_3-oxygen atom which is derived from either an hydroxide or

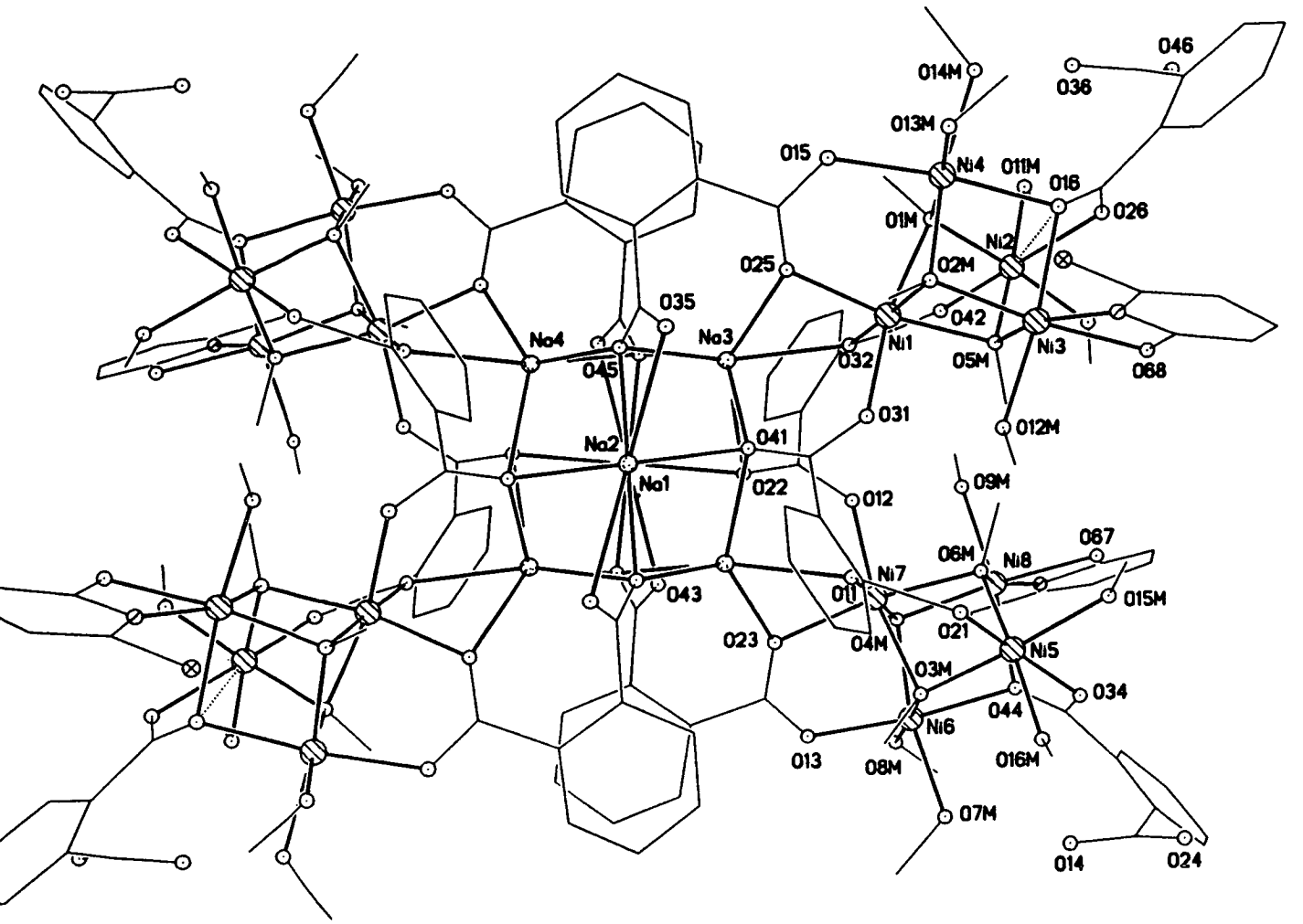

Figure 4.16. The structure of **37** in the crystal.

methoxide group. The fourth vertex is occupied by a μ_2-oxygen atom from a phthalate ligand, hence leaving one N...O edge of the cube unmade [for example Ni2...O16, 3.267(9)Å]. Three of the Ni...Ni vectors are additionally spanned by 1,3-bridging carboxylates derived from phthalates. The nickel sites are all six-coordinate with the geometries distorted from octahedral [*cis*, 63.6-115.9(4)°; *trans* 161.2-178.9(4)°]. The remaining coordination sites on the nickels are occupied by one η^2-chp group and five terminal methanol ligands per Ni_4 cage.

The Ni_4 cages are assembled into a rectangular arrangement through the bridging phthalate groups. The shorter side of the rectangle is bridged by two phthalate groups each of which is attached through both oxygen donors of one carboxylate to one nickel cage and

through one oxygen donor of the second carboxylate to another. The fourth oxygen of this phthalate μ_3-bridges three sodium atoms within the central Na_6 cage. The long edge of the rectangle involves bridging between a Ni_4 unit and the Na_6 cage by one phthalate group and then a further phthalate ligand linking out to the next Ni_4 group. Four of the phthalate groups do not bridge between cages but are attached terminally to the Ni_4 cubes : charge neutrality requires that on average two of these phthalates are protonated in every assembly.

The metal polyhedron is shown in Figure 4.17. The Na_6 cage plays a vital structural role in that all the phthalate bridges interact with this central motif. The cage is surprisingly regular with the sodium polyhedron close to a perfect octahedron : the Na...Na contacts are all in the range 3.59-3.85(2)Å and the Na...Na...Na angles fall within the ranges 58.7-63.8(3)° or 87.8-90.1(3)°, and with each triangular face capped by a μ_3-oxygen atom from a phthalate

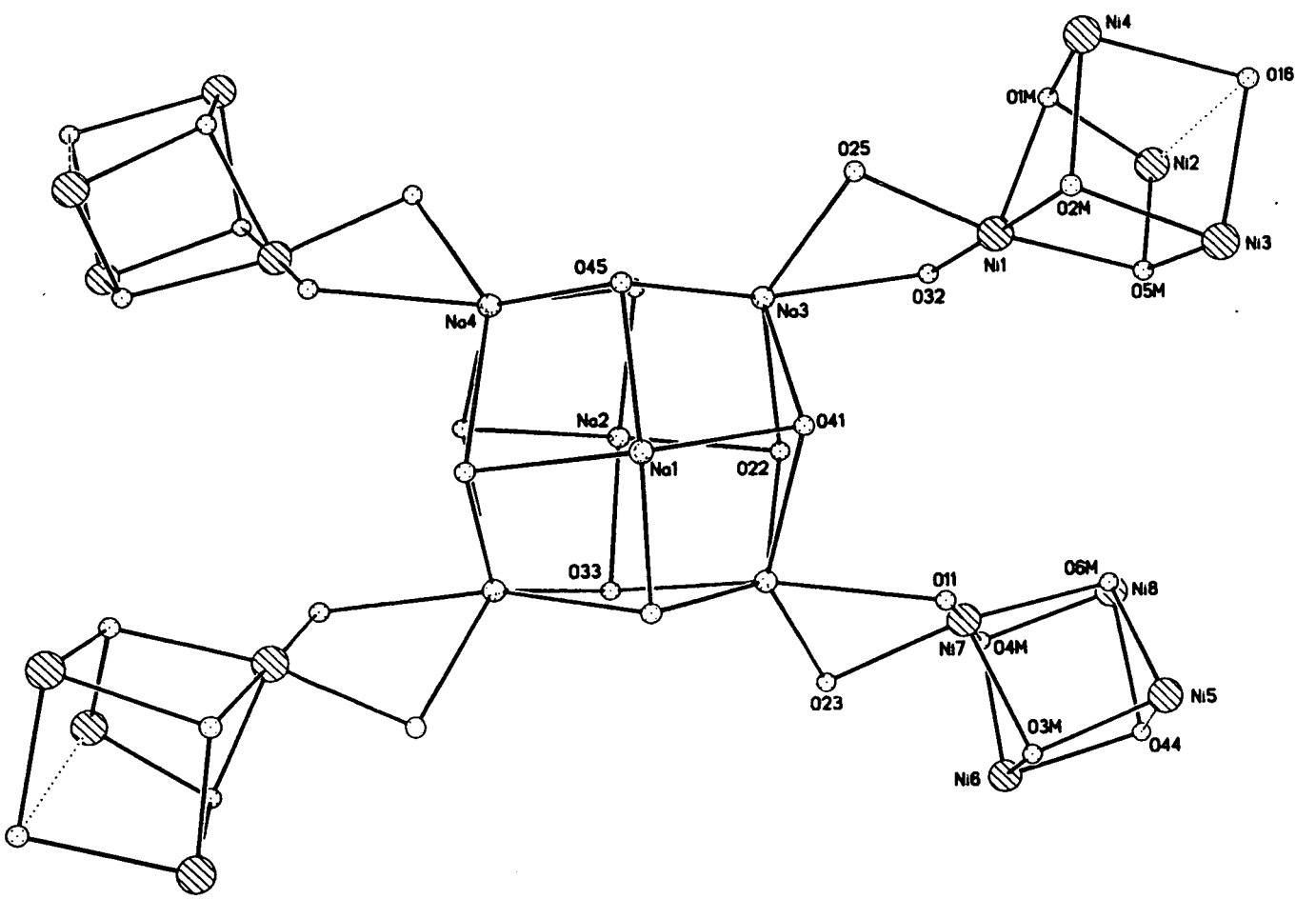

Figure 4.17. The polyhedron in **37**.

group. In each case this oxygen atom is part of a different phthalate group. The Na_6 core therefore provides eight anchoring points about which to assemble the four tetranuclear nickel fragments.

The sodium sites fall into two distinct groups : four [Na3, Na4 and symmetry equivalents] have five short contacts and one long contact to oxygen donors [Na3, 2.252-2.497(13)Å and 2.681(11)Å; Na4, 2.257-2.541(12)Å and 2.671(11)Å], while the sodium atoms on the two-fold axis [Na1, Na2] have four short and two longer bonds to oxygens [Na1, 2.354-2.407(14)Å and 2.707(14)Å; Na2, 2.373-2.497(13)Å and 2.724(13)Å]. These longer bonds are all to the μ_2-oxygens of the phthalate groups. For all the sodium sites the coordination geometries are predictably irregular. The nickel-oxygen and nickel-nitrogen bond lengths are all regular : Ni-O(OMe), 1.993-2.095(10)Å; Ni-O(chp), 2.047-2.052(10)Å; Ni-O(phth), 1.988-2.141(10)Å; Ni-O(MeOH), 2.036-2.095(10)Å and Ni-N(chp), 2.152-2.168 (10)Å. Selected bond lengths and angles are given in Table 4.8.

This type of Na_6 cage is rare, with the only species containing precisely this nuclearity being $[Na_6\{O_2Si(CMe_3)_2\}_6]$ [119]. Octahedral lithium cages are more common [120]. The introduction of the tetranucleating phthalate ligand instead of a binucleating ligand, such as acetate or benzoate, has produced two large polymetallic complexes in **36** and **37**. This suggests that the use of such ligands provides a possible route to even larger metal assemblies. This methodology has already been employed by the Christou group to produce a Mn_{18} cluster [121].

4.2.12. Magnetochemistry of 37.

The magnetic behaviour of **37** was studied in the temperature range 300-1.8 K in an applied field of 1000 G. The variation of $\chi_m T$ with temperature is shown in Figure 4.18. The room temperature value of approximately 19.5 emu K mol^{-1} is consistant with sixteen non-

interacting Ni(II) S = 1 centres [$\chi_m T$ = 19.4 emu K mol^{-1}, g= 2.2]. At lower temperatures $\chi_m T$ rises steadily to a maximum of 22.5 emu K mol^{-1} at 20 K before falling to 18.8 emu K mol^{-1} at the lowest temperature measured. The distances between the nickel cubes suggests that this behaviour must be due to intracube exchange. The magnetic behaviour of these cubes can be related to the Ni-O-Ni angles [65]. In **37** the most obtuse bridging angles are 117.2-124.1(4)° involving Ni2 in one crystallographically independent cage and Ni5 in the second and should lead to the spin at these centres coupling antiferromagnetically with the other spins within the individual cubes - giving an S = 2 ground state for each cube. this suggests that the value of $\chi_m T$ for **37** should fall to approximately 15 emu k mol^{-1} [g = 2.2] at low temperature. The observed behaviour is consistant with this. The maximum in $\chi_m T$ at 20 K is explicable if the lowest spin states (S = 0) are higher in energy and become depopulated, before the higher spin states, as the temperature is lowered.

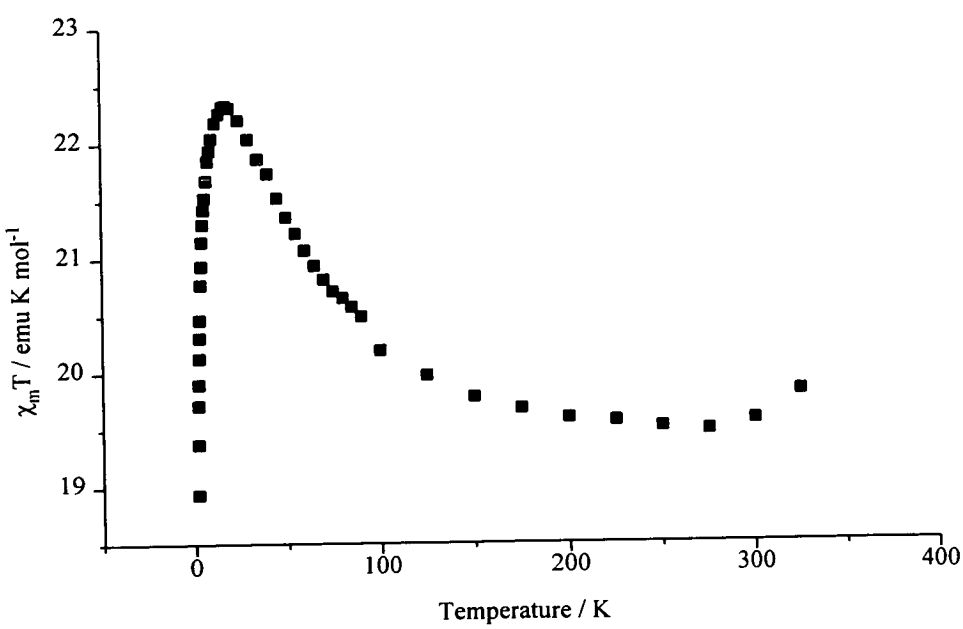

Figure 4.18. The variation of $\chi_m T$ with temperature for **37**.

Table 4.8. Selected bond lengths (Å) and angles (°) for **37**.

Ni1-O32	2.016(9)	Ni5-O15M	2.094(12)
Ni1-O2M	2.031(9)	Ni6-O4M	2.011(7)
Ni1-O5M	2.055(9)	Ni6-O3M	2.030(8)
Ni1-O25	2.056(8)	Ni6-O13	2.035(9)
Ni1-O31	2.077(8)	Ni6-O8M	2.044(10)
Ni1-O1M	2.095(8)	Ni6-O7M	2.048(11)
Ni2-O42	2.028(8)	Ni6-O44	2.141(11)
Ni2-O10M	2.039(9)	Ni7-O11	2.013(9)
Ni2-O1M	2.041(9)	Ni7-O4M	2.037(9)
Ni2-O5M	2.048(8)	Ni7-O12	2.062(8)
Ni2O11M	2.090(9)	Ni7-O6M	2.063(9)
Ni2-O26	2.098(9)	Ni7-O23	2.082(9)
Ni3-O5M	2.030(9)	Ni7-O3M	2.084(8)
Ni3-O2M	2.043(9)	Ni8-O6M	2.027(9)
Ni3-O68	2.052(11)	Ni8-O4M	2.028(8)
Ni3-O12M	2.068(9)	Ni8-O67	2.046(12)
Ni3-O16	2.101(8)	Ni8-O9M	2.072(8)
Ni3-N18	2.152(13)	Ni8-O44	2.126(8)
Ni4-O2M	1.993(8)	Ni8-N17	2.168(14)
Ni4-O13M	2.036(10)	Na1-O33A	2.354(12)
Ni4-O15	2.045(10)	Na1-O33B	2.354(12)
Ni4-O1M	2.075(10)	Na1-O22A	2.407(11)
Ni4-O14M	2.096(9)	Na1-O22B	2.407(11)
Ni4-O16	2.135(10)	Na1-O43B	2.707(14)
Ni5-O21	1.988(10)	Na1-O43A	2.707(14)
Ni5-O34	2.026(10)	Na2-O45	2.373(11)
Ni5-O6M	2.028(9)	Na2-O45C	2.373(11)
Ni5-O16M	2.042(10)	Na2-O41	2.379(12)
Ni5-O3M	2.065(12)	Na2-O41C	2.379(12)

Table 4.8 continued

Na2-O35	2.724(13)	O42-Ni2-O10M	87.7()3
Na2-O35C	2.724(13)	O42-Ni2-O1M	91.1(3)
Na3-O33C	2.252(13)	O10M-Ni2-O1M	174.9(4)
Na3-O41	2.300(12)	O42-Ni2-O5M	94.5(4)
Na3-O32	2.425(10)	O10M-Ni2-O5M	94.4(3)
Na3-O25	2.438(10)	O1M-Ni2-O5M	80.8(3)
Na3-O45	2.497(13)	O42-Ni2-O11M	87.5(3)
Na3-O2	2.681(11)	O10M-Ni2-O11M	90.0(4)
Na4-O45	2.257(13)	O1M-Ni2-O11M	94.9(4)
Na4-O22C	2.326(11)	O5M-Ni2-O11M	175.2(4)
Na4-O11C	2.395(10)	O42-Ni2-O26	166.2(4)
Na4-O23C	2.437(11)	O10M-Ni2-O26	84.4(4)
Na4-O33C	2.541(11)	O1M-Ni2-O26	97.6(4)
Na4-O41C	2.671(11)	O5M-Ni2-O26	97.4(4)
O32-Ni1-O2M	178.4(2)	O11M-Ni2-O26	81.2(4)
O32-Ni1-O5M	97.0(3)	O5M-Ni3-O2M	83.2(3)
O2M-Ni1-O5M	82.9(3)	O5M-Ni3-O68	97.7(4)
O32-Ni1-O25	89.4(4)	O2M-Ni3-O68	174.1(3)
O2M-Ni1-O25	90.5(4)	O5M-Ni3-O12M	88.4(3)
O5M-Ni1-O25	169.7(3)	O2M-Ni3-O12M	92.9(4)
O32-Ni1-O31	93.6(3)	O68-Ni3-O12M	93.0(4)
O2M-Ni1-O31	88.0(3)	O5M-Ni3-O16	97.0(3)
O5M-Ni1-O31	89.6(3)	O2M-Ni3-O16	79.8(3)
O25-Ni1-O31	98.0(3)	O68-Ni3-O16	94.3(4)
O32-Ni1-O1M	92.6(3)	O12M-Ni3-O16	170.3(4)
O2M-Ni1-O1M	85.8(3)	O5M-Ni3-N18	161.2(4)
O5M-Ni1-O1M	79.4(3)	O2M-Ni3-N18	115.6(4)
O25-Ni1-O1M	92.4(3)	O68-Ni3-N18	63.6(5)
O31-Ni1-O1M	167.9(3)	O12M-Ni3-N18	91.2(4)

Table 4.8 continued

O16-Ni3-N18	86.3(4)	O16M-Ni5-O15M	90.5(5)
O2M-Ni4-O13M	93.7(4)	O3M-Ni5-O15M	174.2(4)
O2M-Ni4-O15	92.0(4)	O4M-Ni6-O3M	87.4(3)
O13M-Ni4-O15	86.1(4)	O4M-Ni6-o13	92.8(3)
O2M-Ni4-O1M	87.3(4)	O3M-Ni6-O13	91.0(3)
O13M-Ni4-O1M	177.1(4)	O4M-Ni6-O8M	92.8(4)
O15-Ni4-O1M	91.3(4)	O3M-Ni6-O8M	176.6(4)
O2M-Ni4-O14M	170.1(4)	O13-Ni6-O8M	85.6(4)
O13M-Ni4-O14M	87.0(4)	O4M-Ni6-O7M	169.1(4)
O15-Ni4-O14M	97.9(4)	O3M-Ni6-O7M	91.9(4)
O1M-Ni4-O16	92.4(4)	O13-Ni6-O7M	98.1(4)
O2M-Ni4-O16	80.1(4)	O8M-Ni6-O7M	88.6(4)
O13M-Ni4-O16	91.6(4)	O4M-Ni6-O44	80.2(4)
O15-Ni4-O16	171.6(4)	O3M-Ni6-O44	91.2()
O1M-Ni4-O16	91.2(4)	O13-Ni6-O44	172.6(4)
O14M-Ni4-O16	90.1(4)	O8M-Ni6-O44	92.1(4)
O21-Ni5-O34	166.8(4)	O7M-Ni6-O44	88.9(4)
O21-Ni5-O6M	94.3(3)	O11-Ni7-O4M	178.9(3)
O34-Ni5-O6M	97.3(4)	O11-Ni7-O12	93.2(3)
O21-Ni5-O16M	88.1(3)	O4M-Ni7-O12	88.0(3)
O34-Ni5-O16M	80.9(4)	O11-Ni7-O6M	98.4(3)
O6M-Ni5-O16M	175.2(4)	O4M-Ni7-O6M	81.6(3)
O21-Ni5-O3M	92.7(3)	O12-Ni7-O6M	88.9(3)
O34-Ni5-O3M	95.4(4)	O11-Ni7-O23	87.8(3)
O6M-Ni5-O3M	80.6(4)	O4M-Ni7-O23	92.1(3)
O16M-Ni5-O3M	95.2(4)	O12-Ni7-O23	99.5(3)
O21-Ni5-O15M	88.9(4)	O6M-Ni7-O23	169.3(3)
O34-Ni5-O15M	84.0(4)	O11-Ni7-O3M	93.6(3)
O6M-Ni5-O15M	93.7(4)	O4M-Ni7-O3M	85.3(3)

Table 4.8 continued

O12-Ni7-O3M	167.2(3)	O33B-Na1-O43A	162.3(4)
O6M-Ni7-O3M	79.3(3)	O22A-Na1-O43A	82.7(3)
O23-Ni7-O3M	91.6(2)	O22B-Na1-O43A	115.9(3)
O6M-Ni8-O4M	82.7(3)	O43B-Na1-O43A	136.3(7)
O6M-Ni8-O67	97.4(4)	O45-Na2-O45C	130.8(8)
O4M-Ni8-O67	174.7(4)	O45-Na2-O41	78.1(4)
O6M-Ni8-O9M	87.8(3)	O45C-Na2-O41	81.7(4)
O4M-Ni8-O9M	92.3(3)	O45-Na2-O41C	81.7(4)
O67-Ni8-O9M	93.0(4)	O45C-Na2-O41C	78.1(4)
O6M-Ni8-O44	96.3(3)	O41-Na2-O41C	130.3(8)
O4M-Ni8-O44	80.2(3)	O45-Na2-O35	50.3(4)
O67-Ni8-O44	94.5(4)	O45C-Na2-O35	162.6(4)
O9M-Ni8-O44	170.9(4)	O41-Na2-O35	81.9(3)
O6M-Ni8-N17	161.4(4)	O41C-Na2-O35	117.4(3)
O4M-Ni8-N17	115.9(4)	O45-Na2-O35C	162.6(4)
O67-Ni8-N17	63.9(4)	O45C-Na2-O35C	50.3(4)
O9M-Ni8-N17	92.0(4)	O41-Na2-O35C	117.4(3)
O44-Ni8-N17	86.7(4)	O41C-Na2-O35C	81.9(3)
O33A-Na1-O33B	130.7(8)	O35-Na2-O35C	135.3(6)
O33A-Na1-O22A	79.6(4)	O33C-Na3-O41	129.5(4)
O33B-Na1-O22A	80.4(4)	O33C-Na3-O32	118.3(5)
O33A-Na1-O22B	80.4(4)	O41-Na3-O32	97.1(4)
O33B-Na1-O22B	79.6(4)	O33C-Na3-O25	132.5(4)
O22A-Na1-O22B	130.8(7)	O41-Na3-O25	90.3(4)
O33A-Na1-O43B	162.3(4)	O32-Na3-O25	72.2(3)
O33B-Na1-O43B	50.0(4)	O33C-Na3-o45	82.3(5)
O22A-Na1-O43B	115.9(3)	O41-Na3-O45	77.1(5)
O22B-Na1-O43B	82.7(3)	O32-Na3-O45	155.0(5)
O33A-Na1-O43A	50.0(4)	O25-Na3-O45	83.4(4)

Table 4.8 continued

O33C-Na3-O22	76.6(4)	Ni7-O23-Na4C	90.9(3)
O41-Na3-O22	76.9(4)	Na3C-O33-Na1D	105.7(4)
O32-Na3-O22	78.4(3)	Na3C-O33-Na4C	96.7(5)
O25-Na3-O22	146.2(4)	Na1D-O33-Na4C	96.6(4)
O45-Na3-O22	122.7(4)	Ni1-O25-Na3	90.6(3)
O45-Na4-O22C	130.6(4)	Na4-O45-Na2	103.8(4)
O45-Na4-O11C	120.6(5)	Na4-O45-Na3	97.8(5)
O22C-Na4-O11C	95.3(4)	Na2-O45-Na3	97.0(4)
O45-Na4-O23C	130.9(4)	Ni3-O16-Ni4	96.0(4)
O22C-Na4-O23C	89.9(4)	Ni2-O1M-Ni4	123.3(4)
O11C-Na4-O23C	72.0(4)	Ni2-O1M-Ni1	94.1(3)
O45-Na4-O33C	81.2(4)	Ni4-O1M-Ni1	89.1(3)
O22C-Na4-O33C	77.4(4)	Ni4-O2M-Ni1	93.3(3)
O11C-Na4-O33C	153.4(4)	Ni4-O2M-Ni3	102.4(3)
O23C-Na4-O33C	82.9(4)	Ni1-O2M-Ni3	96.7(4)
O45-Na4-O41C	77.8(4)	Ni6-O3M-Ni5	124.1(4)
O22C-Na4-O41C	76.7(4)	Ni6-O3M-Ni7	90.3(3)
O11C-Na4-O41C	79.7(3)	Ni5-O3M-Ni7	93.2(3)
O23C-Na4-O41C	147.3(4)	Ni6-O4M-Ni8	102.6(4)
O33C-Na4-O41C	121.7(4)	Ni6-O4M-Ni7	92.2(3)
Ni7-O11-Na4C	93.8(4)	Ni8-O4M-Ni7	97.8(3)
Na3-O41-Na2	102.5(4)	Ni3-O5M-Ni2	117.2(4)
Na3-O41-Na4C	101.1(5)	Ni3-O5M-Ni1	96.4(3)
Na2-O41-Na4C	92.2(4)	Ni2-O5M-Ni1	95.1(3)
Na4C-O22-Na1D	101.2(4)	Ni8-O6M-Ni5	118.1(4)
Na4C-O22-Na3	100.1(4)	Ni8-O6M-Ni7	97.1(4)
Na1D-O22-Na3	92.2(3)	Ni5-O6M-Ni7	94.9(3)

4.2.13. Synthesis and structure of $[NEt_4]_2^{2+}[Ni_4(OMe)_2(chp)_4(PhCOO)_4(H_2O)_6]^{2-}$ 38.

Reaction of $[Et_4N]_2[NiCl_4]$ with two equivalents of both Na(chp) and Na(PhCOO) in methanol for 24 hours followed by filtration and evaporation to dryness produced a green paste which was dried *in vacuo* for several days. Crystallisation of this paste from dichloromethane produced green crystals of $[NEt_4]_2^{2+}[Ni_4(OMe)_2(chp)_4(PhCOO)_4(H_2O)_6]^{2-}$ **38** [Figure 4.19] in low yield after one week.

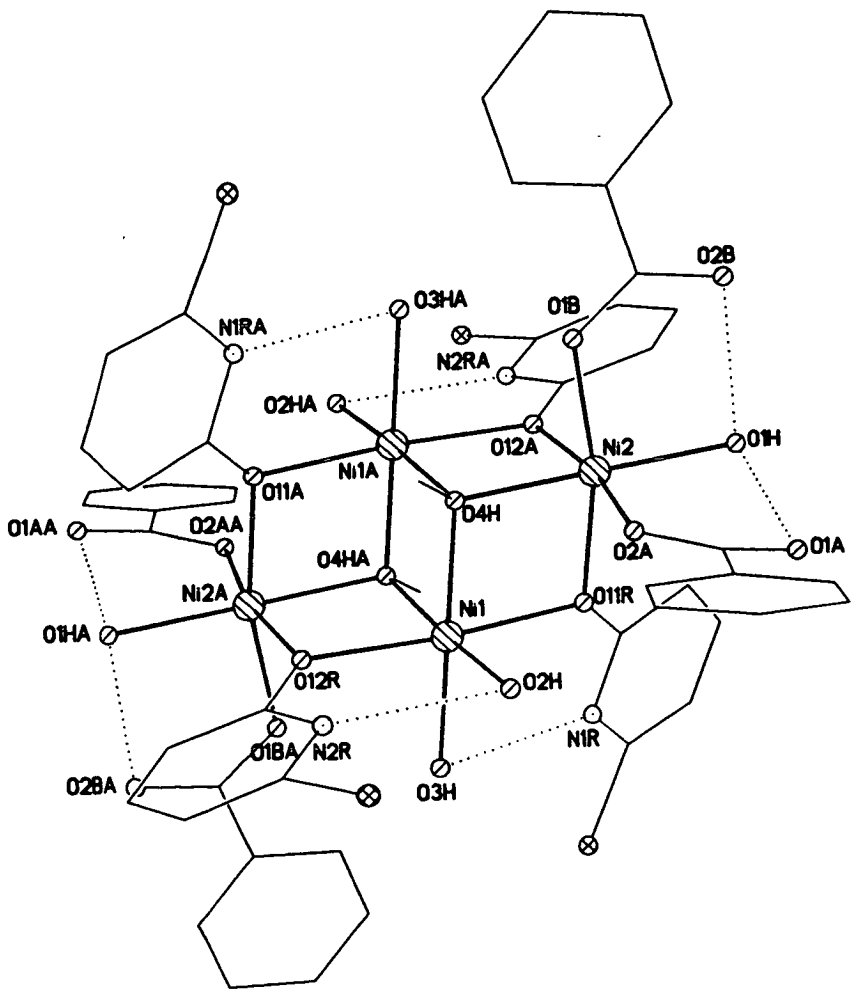

Figure 4.19. The structure of **38** in the crystal.

The structure of **38** consisits of a central nickel-oxygen chair surrounded by bridging pyridonate and terminal benzoate and water ligands. The core of the complex is best described as two $[Ni_3O_4]$ cubes, each of which is missing a vertex, sharing a face. Each cube consists of

three nickel atoms [for example the cube comprising Ni1, Ni2 and Ni1A] and four oxygen atoms [O11R, O4H, O4HA and O12A]. These oxygen atoms are derived from two μ_2-oxygens from chp ligands [O11R, O12A] and two μ_3-methoxides [O4H, O4HA] which, with Ni1 and Ni1A, also form the shared face of the two cubes. There are two unique nickels both of which are six-coordinate. Their geometries are completed by two terminal water molecules [Ni1] and two terminal benzoate ligands and one water molecule [Ni2].

The chp ligands adopt only one coordinating mode, bridging to two metal centres through the exocyclic oxygen atom with the ring nitrogen hydrogen-bonded to one of the terminal water molecules attached to Ni1 [N1R...O3H, 2.685(6)Å; N2R...O2H, 2.684(6)Å]. The two unique benzoate ligands are mononucleating both bound to Ni2 *via* only one oxygen atom of the carboxylate with the second oxygen atom hydrogen-bonded to the terminal water molecule attached to to Ni2 [O2B...O1H, 2.610(6)Å; O1A...O1H, 2.626(6)Å]. Each nickel thus has six oxygen-donors arranged in a distorted octahedral fashion : Ni1 *cis*, 80.80-97.33(14)°; *trans*, 173.91-174.78(14)° and Ni2 *cis*, 80.94-100.22(14)°; *trans*, 167.34-178.76(13)°. The nickel-oxygen bond lengths can all be regarded as regular with Ni-O(OMe), 2.021-2.042(4)Å; Ni-O(chp), 2.091-2.119(4)Å; Ni-O(PhCOO), 2.080-2.082(4)Å and Ni-O(H_2O), 2.062-2.086(4)Å. The closest Ni...Ni contact in **38** is 3.086(6)Å between Ni1 and Ni1A. Selected bond lengths and angles are given in Table 4.9.

The nickel cage in **38** has an overall charge of 2- which is balanced by the presence of two molecules of $[NEt_4]^+$ in the lattice. There are no significant intermolecular interactions. The structure of **38** is unstable - not only does it crystallise in low yield (*ca.* 10%) but the crystals degenerate to an oil after approximately one week if left in solution, or immediately if removed from solution. **38** does not grow from dry solvents or under anaerobic conditions.

Table 4.9. Selected bond lengths (Å) and angles (°) for **38**.

Ni1-O4HA	2.031(4)	O2H-Ni1-O12R	97.33(14)
Ni1-O4H	2.042(3)	O3H-Ni1-O12R	85.48(14)
Ni1-O2H	2.062(4)	O11R-Ni1-O12R	174.59(14)
Ni1-O3H	2.086(3)	O4H-Ni2-O1H	178.76(13)
Ni1-O11R	2.091(3)	O4H-Ni2-O1B	86.58(13)
Ni1-O12R	2.099(3)	O1H-Ni2-O1B	93.42(14)
Ni2-O4H	2.021(3)	O4H-Ni2-O2A	88.67(14)
Ni2-O1H	2.063(3)	O1H-Ni2-O2A	90.08(14)
Ni2-O1B	2.080(3)	O1B-Ni2-O2A	91.5(2)
Ni2-O2A	2.082(4)	O4H-Ni2-O11R	80.94(13)
Ni2-O11R	2.104(3)	O1H-Ni2-O11R	99.10(14)
Ni2-O12RA	2.119(4)	O1B-Ni2-O11R	167.34(13)
O4HA-Ni1-O4H	81.48(14)	O2A-Ni2-O11R	90.34(14)
O4HA-Ni1-O2H	173.91(13)	O4H-Ni2-O12RA	81.02(13)
O4H-Ni1-O2H	92.80(14)	O1H-Ni2-O12RA	100.22(14)
O4HA-Ni1-O3H	93.83(14)	O1B-Ni2-O12RA	89.44(14)
O4H-Ni1-O3H	174.78(14)	O2A-Ni2-O12RA	169.58(13)
O2H-Ni1-O3H	92.0(2)	O11R-Ni2-O12RA	86.58(13)
O4HA-Ni1-O11R	93.89(14)	Ni2-O4H-Ni1A	101.26(14)
O4H-Ni1-O11R	80.80(13)	Ni2-O4H-Ni1	100.75(14)
O2H-Ni1-O11R	87.21(14)	Ni1A-O4H-Ni1	98.52(14)
O3H-Ni1-O11R	97.32(13)	Ni1-O11R-Ni2	96.48(14)
O4HA-Ni1-O12R	81.28(13)	Ni1-O12R-Ni2A	95.97(14)
O4H-Ni1-O12R	96.00(13)		

4.2.14. Synthesis and structure of $[NEt_4]_2^{2+}[Ni_6(OH)_2(chp)_8(CF_3COO)_4(H_2O)_2]^{2-}$ 39.

Reaction of $[EtN_4]_2[NiCl_4]$ with two equivalents of both Na(chp) and $Na(CF_3COO)$ in methanol for 24 hours , followed by fitration and evaporation to dryness, produced a paste which was dried *in vacuo* for 24 hours. Crystallisation of this paste from dichloromethane produced green crystals of $[NEt_4]^{2+}[Ni_6(OH)_2(chp)_8(CF_3COO)_4(H_2O)_2]^{2-}$ **39** [Figure 4.20] in moderate yield after approximately two weeks. The synthesis is identical to that which produced **38**, replacing benzoate with trifluoroacetate.

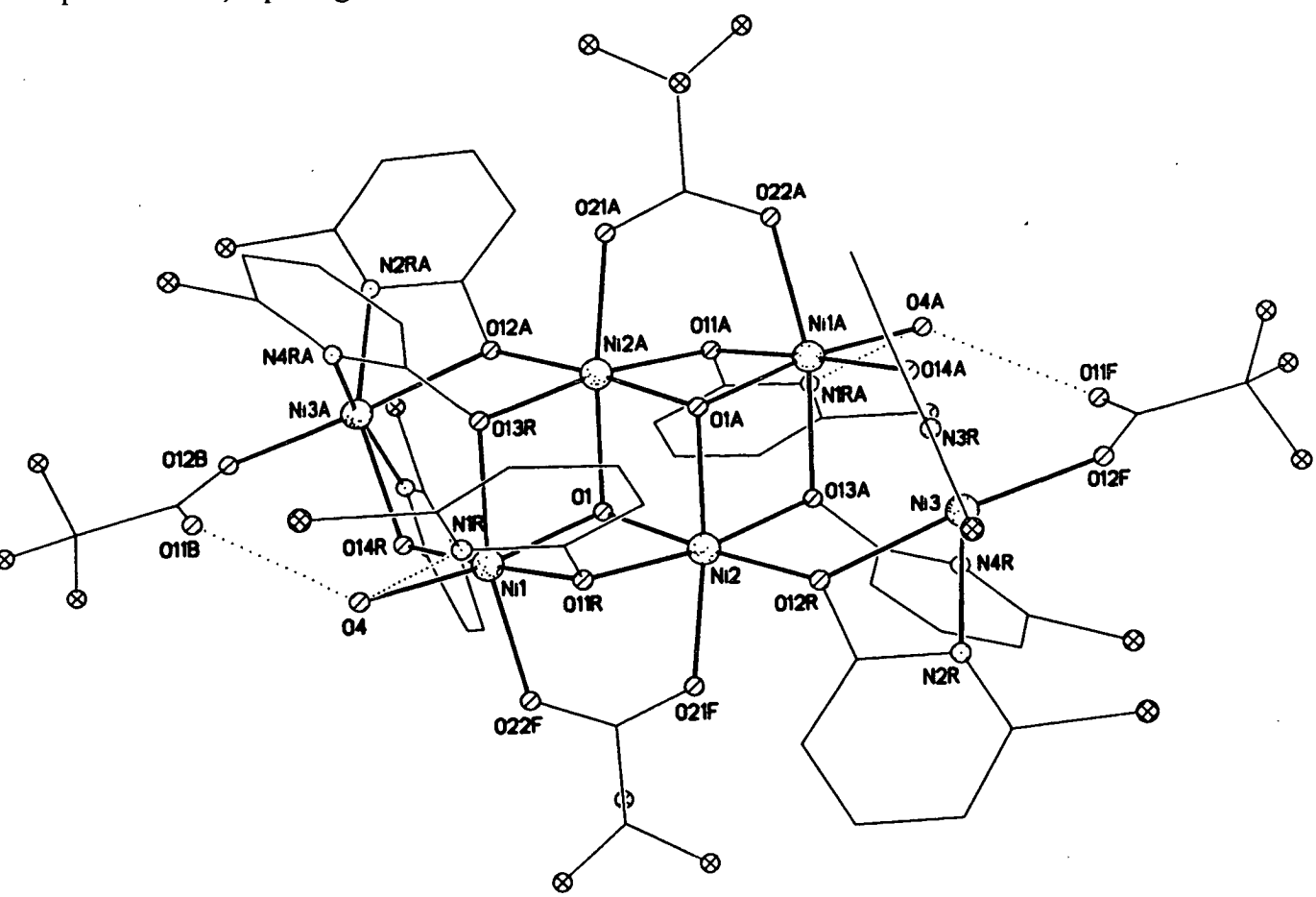

Figure 4.20. The structure of **39** in the crystal.

The structure of **39** is closely related to **38**. Again the central core of the complex consisits of two $[Ni_3O_4]$ cubes, each missing a vertex, sharing a face. Each cube contains three nickel atoms [for example Ni1, Ni2 and Ni2A] and four oxygen atoms [O1, O1A, O11R and

O13R]. These oxygen atoms are derived from two μ_2-oxygens from chp ligands [O11R, O13R] and two μ_3-hydroxides [O1, O1A] which, with Ni2 and Ni2A, also form the shared face of the cubes. These positions were occupied by two μ_3-methoxides in **38**.The Ni1...Ni2 vector in the cube is spanned by a 1,3-bridging trifluoroacetate ligand which ligates to the axial site on both nickel centres. In **38** these axial sites were occupied by a water molecule [Ni1] and a mononucleating carboxylate [Ni2].

The main structural difference between **38** and **39** comes in the ligation to one of the square faces of the cubes in the central core. The face comprising Ni1, Ni2A, O1 and O13R (and symmetry equivalents) is capped by a [Ni(chp)$_3$(CF$_3$COO)] unit containing Ni3A. The cap is bound to the square face *via* three chp ligands. Two of these chps chelate to Ni3 [the capping metal] and bridge to one nickel in the cube through their exocyclic oxygen atom. The third chp ligand provides the oxygen which occupies one of the corners of the cube (i.e. is μ_2-bridging between two nickel vertex sites, for example Ni1-O13R-Ni2A) with the ring nitrogen of the pyridonate [N4RA] ligating to Ni3. In **38** these three sites were occupied by a μ_2-oxygen derived from a chp ligand which provided the corner of the cube and two water molecules. All of the nickel atoms in **39** are six-coordinate, with the geometry of Ni3 and Ni1 completed by a mononucleating trifluoroacetate ligand and a molecule of water respectively.

The chp ligands adopt three different coordinating modes. Trinucleating, binding to one metal centre [Ni3A] through the ring nitrogen whilst μ_2-bridging two others [Ni1, Ni2A] through the oxygen atom. Binucleating, chelating to one metal [Ni3] with the oxygen atom bound to one further nickel [Ni1A or Ni2]. Binucleating, bridging two nickels [Ni1, Ni2] through the oxygen atom with the ring nitrogen hydrogen-bonded to the terminal water molecule attached to Ni1 [N1R...O4, 2.700(4)Å]. The trifluoroacetates adopt two coordinating modes : bridging in a 1,3-fashion [between Ni1 and Ni2] or mononucleating, binding to Ni3 through one oxygen atom of the carboxylate group with the second oxygen

hydrogen-bonded to the terminal water molecule on Ni1A [O11F...O4A, 2.813(4)Å].

In **38** all of the metals were bound to six oxygen-donors. This is also the case for the nickel atoms in **39** which comprise the central face-sharing cubes, but the two capping metals [Ni3, Ni3A] are each bound to three oxygen and three nitrogen-donors. All of the nickels have distorted octahedral geometries, with Ni3 more distorted [*cis*, 62.8-109.9(2)°; *trans*, 151.7-171.5(2)°] than the other nickel sites [Ni1, Ni2 *cis*, 78.8-100.1(2)°; *trans*, 166.8-177.1(2)°]. Ni3 is the only metal centre in **39** which is attached to a chelating chp ligand. The nickel-oxygen and nickel-nitrogen bond lengths are all regular and fall in the range 2.004-2.117(4)Å and 2.117-2.129(4)Å respectively. The closest Ni...Ni contact is 2.969(1)Å between Ni1 and Ni2. Selected bond lengths and angles are given in Table 4.10. Again the 2- charge of the nickel cage is balanced by the presence of two molecules of $[NEt_4]^+$ in the lattice. There are no significant intermolecular interactions in **39**. Unlike **38** , **39** is stable in solution and does not degenerate to an oil.

4.2.15. Magnetochemistry of 39.

The magnetic behaviour of **39** was studied in the temperature range 300-1.8 K in an applied field of 1000 G. The variation of $\chi_m T$ with temperature is shown in Figure 4.21. The room temperature value of approximately 6 emu K mol^{-1} is consistant with six non-interacting Ni(II) S = 1 centres [$\chi_m T$ = 7.3 emu K mol-1, g = 2.2]. The value of $\chi_m T$ remains fairly constant as the temperature is lowered. Below 100 K the value begins to increase and at around 50 K there is a sharp increase in $\chi_m T$ reaching a maximum of approximately 17 emu K mol^{-1} at 10 K, before falling sharply below this temperature to 6 emu K mol^{-1} at the lowest temperature measured. The 10 K value coresponds to an approximately S = 5 ground state.

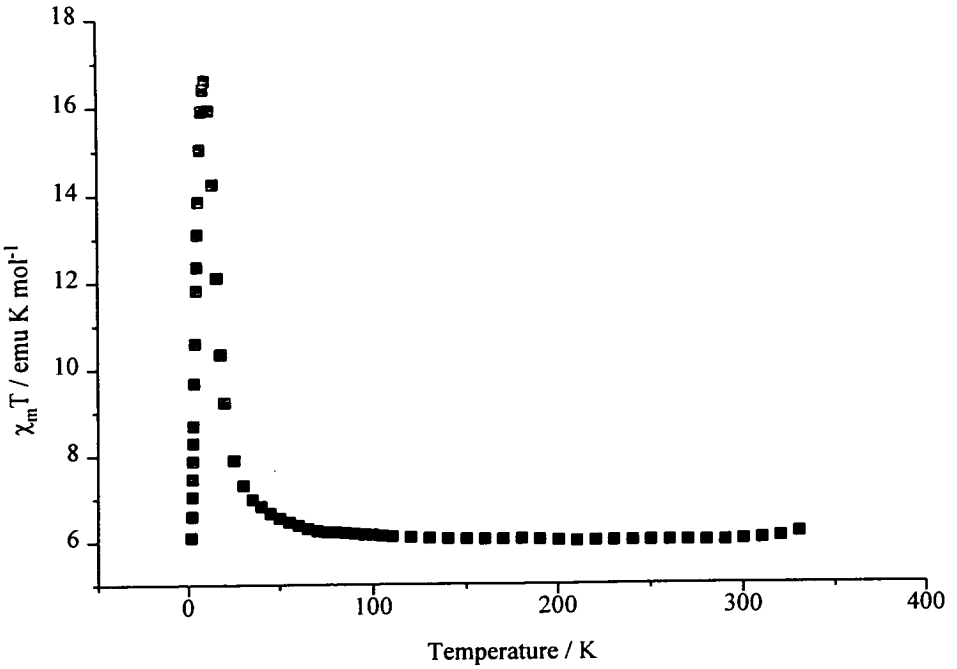

Figure 4.21. The variation of $\chi_m T$ with temperature for **39**.

Table 4.10. Selected bond lengths (Å) and angles (°) for **39**.

Ni1-O1	2.004(4)	Ni3-N3R	2.129(5)
Ni1-O14R	2.018(4)	O1-Ni1-O14R	92.4(2)
Ni1-O4	2.047(4)	O1-Ni1-O4	171.8(2)
Ni1-O22F	2.079(4)	O14R-Ni1-O4	86.0(2)
Ni1-O11R	2.082(4)	O1-Ni1-O22F	90.7(2)
Ni1-O13R	2.108(4)	O14R-Ni1-O22F	97.2(2)
Ni2-O12R	2.020(4)	O4-Ni1-O22F	97.4(2)
Ni2-O1	2.033(4)	O1-Ni1-O11R	86.1(2)
Ni2-O1A	2.034(4)	O14R-Ni1-O11R	177.1(2)
Ni2-O11R	2.068(4)	O4-Ni1-O11R	95.2(2)
Ni2-O21F	2.075(4)	O22F-Ni1-O11R	85.3(2)
Ni2-O13RA	2.083(4)	O1-Ni1-O13R	78.9(2)
Ni3-O12F	2.013(4)	O14R-Ni1-O13R	91.3(2)
Ni3-O14RA	2.098(4)	O4-Ni1-O13R	93.1(2)
Ni3-O12R	2.117(4)	O22F-Ni1-O13R	166.9(2)
Ni3-N2R	2.117(4)	O11R-Ni1-O13R	86.0(2)
Ni3-N4R	2.117(4)	O12R-Ni2-O1	174.0(2)

Table 4.10 continued

O12R-Ni2-O1A	97.9(2)	O14RA-Ni3-N2R	151.7(2)
O1-Ni2-O1A	79.9(2)	O12R-Ni3-N2R	62.8(2)
O12R-Ni2-O11R	100.1(2)	O12F-Ni3-N4R	97.9(2)
O1-Ni2-O11R	85.7(2)	O14RA-Ni3-N4R	103.6(2)
O1A-Ni2-O11R	92.6(2)	O12R-Ni3-N4R	87.4(2)
O12R-Ni2-O21F	92.9(2)	N2R-Ni3-N4R	94.9(2)
O1-Ni2-O21F	89.0(2)	O12F-Ni3-N3R	89.9(2)
O1A-Ni2-O21F	168.8(2)	O14RA-Ni3-N3R	63.0(2)
O11R-Ni2-O21F	88.6(2)	O12R-Ni3-N3R	86.6(2)
O12R-Ni2-O13RA	82.4(2)	N2R-Ni3-N3R	95.0(2)
O1-Ni2-O13RA	91.6(2)	N4R-Ni3-N3R	164.5(2)
O1A-Ni2-O13RA	78.8(2)	Ni1-O1-Ni2	94.7(2)
O11R-Ni2-O13RA	171.3(2)	Ni1-O1-Ni2A	103.6(2)
O21F-Ni2-O13RA	99.7(2)	Ni2-O1-Ni2A	100.1(2)
O12F-Ni3-O14RA	88.8(2)	Ni2-O11R-Ni1	91.4(2)
O12F-Ni3-O12R	171.5(2)	Ni2-O12R-Ni3	123.8(2)
O14RA-Ni3-O12R	96.5(2)	Ni2A-O13R-Ni1	98.4(2)
O12F-Ni3-N2R	109.9(2)	Ni1-O14R-Ni1A	116.7(2)

4.2.16. Synthesis and structure of $[Co_2Na_2(pic)_4(chp)_2(MeOH)]$. 2MeOH 40.

Reaction of cobalt chloride with two equivalents of both Na(chp) and Na(pic) [pic = picolinate] in methanol produced an orange solution after three hours. The solution was filtered and the solvent removed producing a paste which was dried *in vacuo* for several hours. Crystallisation of this paste from fresh methanol produced dark red crystals of $[Co_2Na_2(pic)_4(chp)_2(MeOH)_4]$. 2MeOH **40** [Figure 4.22] after three days.

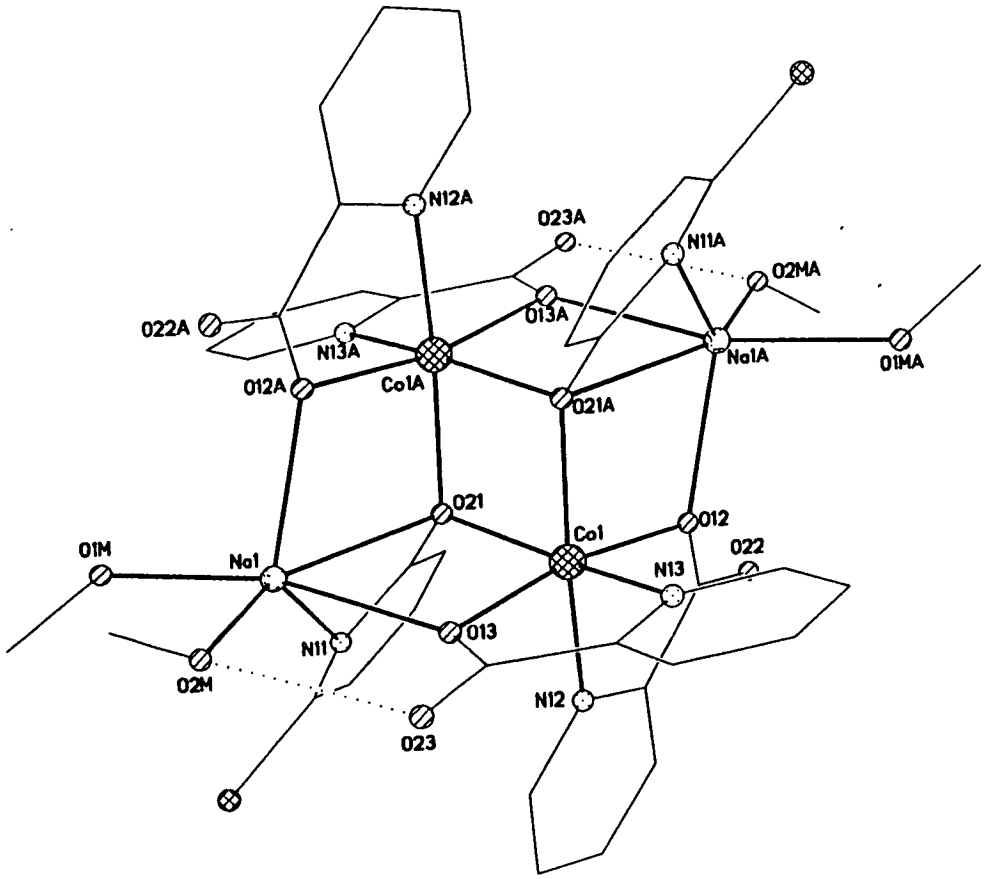

Figure 4.22. The structure of **40** in the crystal.

40 contains a central $[Co_2O_2]$ ring, the oxygens of which belong to two trinucleating chp ligands each of which chelates to a sodium atom on either side of the central Co_2O_2 ring. The coordination of the cobalt atoms is completed by two chelating picolinate ligands which also bridge to the sodium atoms through one of the oxygen atoms of the carboxylate group. The second oxygen in each case remains uncoordinated but forms a hydrogen-bond to either a molecule of methanol solvent [O22... O3M, 2.695(6)Å] or to a methanol molecule attached to the sodium atom [O23...O2M, 2.776(6)Å]. The sodiums are six-coordinate with their geometries completed by another molecule of methanol which is strongly hydrogen-bonded to the methanol solvent [O1M... O3M, 2.740(6)Å].

The cobalt atoms have four oxygen and two nitrogen donors in a distorted octahedral arrangement with the *cis* angles ranging between 78.2-102.0(2)° and the *trans* angles 162.5-169.4(2)°. The sodium atoms have five oxygen donors and one nitrogen donor and their geometries are best described as irregular. The Co-O bond lengths are all in the range 2.060-

2.104(7)Å and the Co-N bonds 2.098-2.103(7)Å. The Na-O and Na-N bonds range 2.343-2.673(6)Å and 2.590(7)Å respectively. The Co...Co distance is 3.237(5)Å with the bridging angle between the two, *via* O21 and symmetry equivalent, being 101.7(2)°. Selected bond lengths and angles are given in Table 4.11.

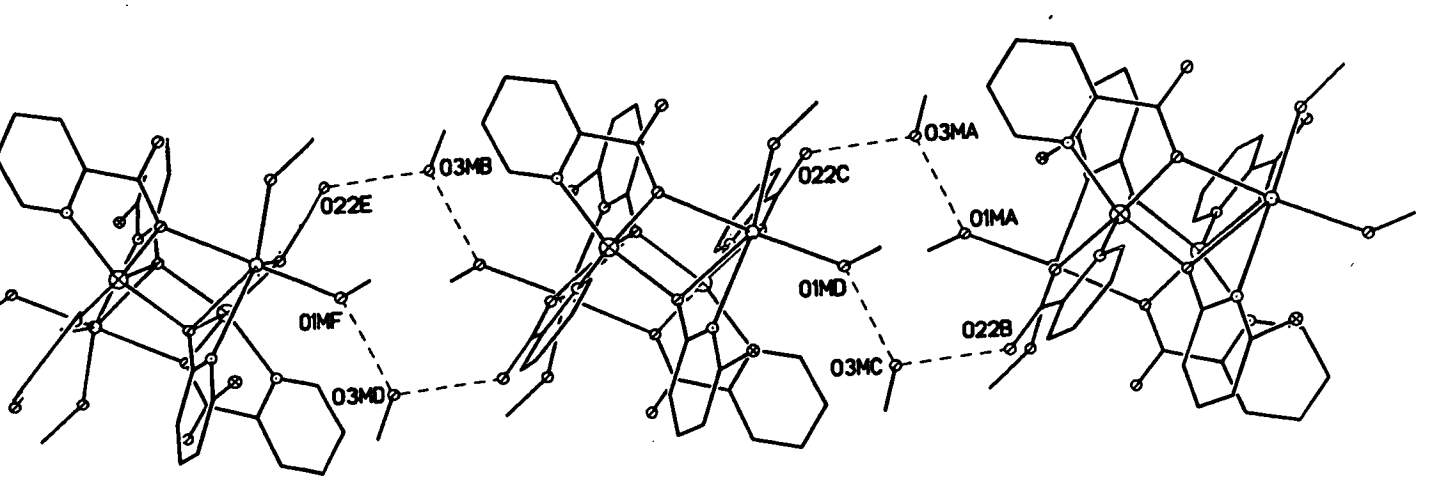

Figure 4.23. The packing in **40**.

The role of the solvent methanol is also significant when looking at the packing of **40** [Figure 4.22]. Between each moleule of **40** there are two methanol molecules. Each of these molecules hydrogen bonds to a terminal methanol on one molecule of **40** [O...O, 2.740(6)Å] and to the uncoordinated oxygen atom of a picolonate on the neighbouring molecule of **40** [O3...O, 2.695(6)Å], thus creating linear chains of **40** in the crystal. The magnetic behaviour of **40** is currently under investigation.

Table 4.11. Selected bond lengths (Å) and angles °() for **40**.

Co1-O13	2.060(5)	O21A-Co1-O21	78.3(2)
Co1-O21A	2.069(6)	O12-Co1-O21	95.2(2)
Co1-O12	2.079(5)	N13-Co1-O21	163.9(2)
Co1-N13	2.098(6)	N12-Co1-O21	92.3(2)
Co1-N12	2.103(7)	O2M-Na1-O1M	93.0(3)
Co1-O21	2.104(5)	O2M-Na1-O12A	111.3(3)
Na1-N11	2.590(7)	O1M-Na1-O12A	96.8(3)
Na1-O21	2.673(6)	O2M-Na1-O13	78.7(2)
Na1-O13	2.433(6)	O1M-Na1-O13	165.4(3)
Na1-O2M	2.343(7)	O12A-Na1-O13	97.4(2)
Na1-O1M	2.353(7)	O2M-Na1-N11	137.0(3)
Na1-O12A	2.359(7)	O1M-Na1-N11	86.9(3)
O13-Co1-O21A	102.0(2)	O12A-Na1-N11	111.4(2)
O13-Co1-O12	169.4(2)	O13-Na1-N11	91.0(2)
O21A-Co1-O12	88.0(2)	O2M-Na1-O21	149.0(2)
O13-Co1-N13	78.4(2)	O1M-Na1-O21	117.9(2)
O21A-Co1-N13	92.5(2)	O12A-Na1-O21	69.5(2)
O12-Co1-N13	97.7(2)	O13-Na1-O21	70.6(2)
O13-Co1-N12	92.6(2)	N11-Na1-O21	50.0(2)
O21A-Co1-N12	162.5(2)	Co1A-O21-Co1	101.7(2)
O12-Co1-N12	78.2(2)	Co1A-O21-Na1	96.3(2)
N13-Co1-N12	99.8(2)	Co1-O21-Na1	94.9(2)
O13-Co1-O21	90.5(2)	Co1-O12-Na1A	106.2(2)

4.3. Conclusions.

This chapter outlined the synthesis and structure of a number of novel nickel and cobalt carboxylate complexes of 6-chloro-2-pyridone. In general the compounds discussed have shown greater structural diversity than was exhibited by the complexes containing 6-methyl-2-pyridone, as discussed in Chapter 3. The reason is that where mhp almost always binds to the metal centres through both nitrogen and oxygen donor atoms (there are only a few examples where this is not the case) the chp ligands have demonstrated a willingness to use either both donor atoms or more regularly the oxygen atom alone.

Thermolysis and solution reactions of metal carboxylates produced two new nickel trimers which belong to a family of compounds of general formula $[M_3(O_2CR)_2(xhp)_4(R'OH)_6]$ and a cobalt metallocycle isostructural with a nickel complex reported previously. Solution reactions have produced two cobalt heptamers whose structures are loosely based on trigonal prisms which contain an additional cap on one of the triangular faces. Attempts to synthesise a similar nickel compound, from an identical procedure , resulted in the characterisation of an unusual heterobimetallic compound of chloroacetate. Introduction of the tetranucleating phthalate ligand produced two large polymetallic complexes : a cobalt tridecamer and a nickel-sodium supracage. The supracage assembly of four nickel cubanes and a sodium octahedron appears to be unprecedented. Use of tetraethylammonium nickel chloride as a starting material produced two related structures : a tetramer and a hexamer whose structures are loosely based around a central core of cubane units.

Again the solvent appears to play a vital structural role, although this is perhaps not as clearly established as in Chapter 2 and Chapter 3. The most obvious example comes from the crystallisation of the melt product of nickel or cobalt acetate with Hchp : methanol produces a trimeric species whereas THF produces a dodecanuclear metallocycle. Interestingly these

metallocycles only form when acetate is the carboxylate. The reason being that the cavity within the metallocycle is not large enough to accomodate any bigger carboxylates. Attempts to synthesise similar compounds from smaller carboxylates such as formate have been unsuccessful. Many of the structures reported also contain ligated solvent molecules.

Like the majority of the complexes reported in this work, water appears to be a vital structural ingredient : all but two of the compounds **30-40** contain hydroxide or water. The source of these hydroxides and waters is either the use of hydrated metal salts or more probably through the use of 'wet' solvents. For example, the prolonged drying of cobalt acetate in the synthesis of the cobalt metallocycle prior to crystallisation from 'wet' THF, agrees with this observation given that the structure of **32** contains six bridging water molecules. All attempts to synthesise **32** from dry THF failed.

Introduction of multifunctional ligands, such as phthalate, appears to increase the nuclearity of the final product in comparison to the use of binucleating carboxylates such as acetate or benzoate. Perhaps more interestingly it opens up the possibility of linking smaller, previously characterised metal fragments, such as cubes, into larger assemblies.

p231 L 1 range between or from

p234 L 2 accommodate

4.4. Experimental Section.

4.4.1. $[Ni_3(O_2CCMe_3)_2(chp)_4(MeOH)_6]$ **30**.

(a) $NiCl_2.6H_2O$ (0.500g, 2.10 mmol), Na(chp) (0.637g, 4.20 mmol) and $Na(O_2CCMe_3)$ (0.521g, 4.20 mmol) were stirred in MeOH (30ml) for 24 hours. The resulting solution was filtered and the solvent removed under reduced pressure, producing a paste. This paste was dried *in vacuo* and added to fresh MeOH (15ml) in an open-topped vial. Green crystals of **30** grew after 24 hours in 70% yield.

(b) $NiCl_2.6H_2O$ (0.500g, 2.10mmol) and $Na(O_2CCMe_3)$ (0.521g, 4.20 mmol) were stirred in MeOH (30ml) for 3 hours. The solution was filtered and the solvent removed under reduced pressure, producing a paste which was dried *in vacuo*. This paste was mixed with Hchp (0.544g, 4.20 mmol) in a Schlenk tube and heated to 130°C under N_2 for 2 hours, producing a melt. The mixture was then heated under reduced pressure for 15 minutes removing the HO_2CCMe_3 and H_2O produced during the reaction. Any unreacted Hchp was sublimed to a cold finger. The product was dissovled in MeOH (15ml) and the solution allowed to stand for 24 hours. Green crystals of **30** grew in 65% yield.

CHN; observed (expected) : C, 39.8 (39.8); H, 4.96 (4.99); N, 5.10 (5.16) %.

FAB-MS (significant peaks, possible assignments) : m/z 1084, $[Ni_3(O_2CCMe_3)_2(chp)_4(MeOH)_6]^+$; 1052, $[Ni_3(O_2CCMe_3)_2(chp)_4(MeOH)_5]^+$; 791, $[Ni_3(chp)_4(O_2CCMe_3)]^+$; 786, $[Ni_3(chp)_4(MeOH)_3]^+$; 764, $[Ni_3(chp)_3(O_2CCMe_3)_2]^+$; 502, $[Ni_2(chp)_3]^+$; 374, $[Ni_2(chp)_2]^+$.

4.4.2. $[Ni_3(PhCH_2CO_2)_2(chp)_4(MeOH)_6]$. 2MeOH **31**

(a) Synthesis as for **30**, replacing $Na(O_2CCMe_3)$ with $Na(PhCH_2CO_2)$. Yield 20%.

(b) Synthesis as for **30**, replacing $Na(O_2CCMe_3)$ with $Na(PhCH_2CO_2)$. Yield 34%.

CHN; observed (expected) : C, 41.3 (41.4); H, 4.10 (4.11); N, 4.55 (4.61) %.

FAB-MS (significant peaks, possible assignments) : m/z 1152, $[Ni_3(PhCH_2CO_2)_2(chp)_4(MeOH)_6]^+$; 960, $[Ni_3(chp)_4(PhCH_2CO_2)_2]^+$; 825, $[Ni_3(chp)_4(PhCH_2CO_2)]^+$; 697, $[Ni_3(chp)_3(PhCH_2CO_2)]^+$; 502, $[Ni_2(chp)_3]^+$; 374, $[Ni_2(chp)_2]^+$.

4.4.3. $[Co_{12}(chp)_{12}(O_2CMe)_{12}(H_2O)_6(THF)_6]$ **32.**

$Co(O_2CMe)_2.4H_2O$ (1.000g, 4.02 mmol) was dried *in vacuo* for 3 hours. Hchp (1.042g, 8.04 mmol) was added and the mixture heated to 130°C under an atmosphere of N_2 for 2 hours. The melt which formed was then heated for 15 minutes under reduced pressure. Unreacted Hchp was sublimed to a cold finger. The melt product was then dissolved in THF (25ml) and crystallised by slow evaporation giving purple crystals of **32** in 42% yield after 3 days.

CHN; observed (expected) : C, 37.2 (37.3); H, 3.02 (3.11); N, 4.78 (4.83) %.

FAB-MS (significant peaks, possible assignments) : m/z 1569, $[Co_6(chp)_6(O_2CMe)_6(H_2O)_5]^+$; 1499, $[Co_5(chp)_7(O_2CMe)_4(THF)]^+$; 1456, $[Co_7(chp)_6(O_2CMe)_4(H_2O)_2]^+$; 1378, $[Co_5(chp)_5(O_2CMe)_4(THF)_3]^+$; 935, $[Co_5(chp)_3(O_2CMe)_4(H_2O)]^+$; 758, $[Co_4(chp)_3(O_2CMe)_2(H_2O)]^+$; 452, $[Co_2(chp)_2(O_2CMe)(H_2O)]^+$; 442, $[Co_3(chp)(O_2CMe)_2(H_2O)]^+$; 375, $[Co_2(chp)_2]^+$.

4.4.4. $[Co_7(OH)_2(chp)_8(PhCOO)_4(MeCN)]$ **33.**

(a) $CoCl_2$ (0.500g, 3.9 mmol) was reacted with Na(chp) (1.182g, 7.8 mmol) and $Na(O_2CPh)$ (1.123g, 7.8 mmol) in MeOH (50ml) for 24 hours before filtration and evaporation to dryness. The resulting purple residue was dried *in vacuo* and extracted with MeCN (25ml). Purple crystals of **33** grew in 2 days in 52% yield.

(b) Synthesis as for (a) using $CoCl_2.6H_2O$ (0.928g, 3.9 mmol) in place of $CoCl_2$. Yield 60%.

CHN; observed (expected); C, 41.7 (42.0); H, 2.30 (2.45); N, 6.25 (6.30) %.

FAB-MS (significant peaks, possible assignments) : m/z 1651, $[Co_6(OH)_2(chp)_5(PhCOO)_2]^+$; 1121, $[Co_4(chp)_5(PhCOO)_2]^+$; 805, $[Co_3(chp)_3(PhCOO)_2]^+$; 496, $[Co_2(chp)_2(PhCOO)]^+$; 375,

$[Co_2(chp)_2]^+$.

4.4.5. $[Co_7(OH)_2(chp)_8(O_2CCMe_3)_4(Hchp)_{0.69}(MeCN)_{0.31}]$ **34.**

(a) Synthesis as for **33** replacing $Na(O_2CPh)$ with $Na(O_2CCMe_3)$ (0.967g, 7.8 mmol). Yield 23%.

(b) Synthesis as for **33** using $CoCl_{2.6}H_2O$ (0.928g, 3.9 mmol). Yield 26%.

CHN; observed (expected) : C, 38.7 (38.8); H, 3.24 (3.39); N, 6.49 (6.56) %.

FAB-MS (significant peaks, possible assignments) : m/z 994, $[Co_3(chp)_4(O_2CCMe_3)_3]^+$; 678, $[Co_2(chp)_2(O_2CCMe_3)_3]^+$; 375, $[Co_2(chp)_2]^+$.

4.4.6. $[Ni_{12}Na_4(O_2CCH_2Cl)_8(chp)_{18}(OH)_2(MeCN)_2]$ **35.**

Synthesis as for **33** using $NiCl_2.6H_2O$ (0.927g, 3.9 mmol). Yield 50%.

CHN; observed (expected) : C, 32.6 (32.6); H, 1.95 (1.96); N, 7.00 (7.05) %.

FAB-MS : no significant peaks observed.

4.4.7. $[Co_{13}(chp)_{20}(phth)_2(OH)_2]$ **36.**

Synthesis as for **33** replacing $Na(O_2CPh)$ with $Na_2(phth)$ (1.280g, 7.9 mmol) and crystallising from CH_2Cl_2 (20ml). Yield 15%.

CHN; observed (expected) : C, 37.6 (37.6); H, 1.80 (1.89); N, 7.49 (7.57) %

FAB-MS : no significant peaks observed.

4.3.8. $[Ni_{16}Na_6(chp)_4(phth)_{10}(Hphth)_2(OMe)_{10}(OH)_2(MeOH)_{20}]$ **37.**

$NiCl_2.6H_2O$ (1.000g, 4.21 mmol), Na(chp) (1.276g, 8.42 mmol) and $Na_2(phth)$ (1.381g, 8.42 mmol) were stirred in MeOH (40ml) for 24 hours. The solution was then filtered and evaporated to dryness. The paste was dried *in vacuo* for several hours and then added to fresh

MeOH (25ml) producing crystals of **37** in 10% yield after 2 weeks.

CHN; observed (expected) : C, 38.1 (38.5); H, 3.60 (3.83); N, 1.20 (1.23) %.

FAB-MS : no significant peaks observed.

4.3.9. $[Et_4N]_2[Ni_4(OMe)_2(PhCOO)_4(chp)_4(H_2O)_6]$ **38.**

$[Et_4N]_2NiCl_4$ was obtained by reacting $NiCl_2.6H_2O$ (1.000g, 4.21 mmol) with Et_4NCl (1.389g, 8.42 mmol) in MeOH (50ml) for 2 hours. The resulting blue solution was filtered and the solvent removed producing $[Et_4N]_2NiCl_4$ which was dried *in vacuo* for several hours. Yield 100%. $[Et_4N]_2NiCl_4$ (1.000g, 2.17 mmol), Na(chp) (0.658g, 4.34 mmol) and $Na(O_2CPh)$ (0.625g, 4.34 mmol) were stirred in methanol for 24 hours. The solvent was removed producing an oil which was dried *in vacuo* for several days, and then dissolved in CH_2Cl_2 (15ml) and allowed to stand. Green crystals of **38** grew after one week. The crystals degenerate to an oil rapidly when out of solution. No CHN or mass spectrum was obtained.

4.3.10. $[Et_4N]_2[Ni_6(OH)_2(chp)_8(CF_3COO)_4(H_2O)]$ **39.**

$[Et_4N]_2NiCl_4$ (1.00g, 2.17 mmol), Na(chp) (0.658g, 4.34 mmol) and $Na(CF_3COO)$ (0.590g, 4.34 mmol) was stirred in MeOH (35ml) for 24 hours . The solution was filtered and evaporated to dryness. The resultant paste was dried *in vacuo* for 24 hours and extracted with CH_2Cl_2 (20ml) giving crystals of **39** in 20% yield after 8 days.

CHN; observed (expected) : C, 35.3 (35.5); H, 3.13 (3.24); N, 6.40 (6.47) %.

4.3.11. $[Co_2Na_2(pic)_4(chp)_2]$ **40.**

Reaction of $CoCl_2.6H_2O$ (0.500g, 2.1 mmol) with Na(chp) (0.637g, 4.2 mmol) and Na(pic) (0.609g, 4.2 mmol) in MeOH (30ml) for 3 hours, followed by filtration and evaporation to dryness produced a paste which was dried *in vacuo* for several hours. Crystallisation of this

paste from MeOH (15ml) produced 40 in 15% yield after one day.

CHN; observed (expected) : C, 44.7(44.9); H, 2.39(2.42); N, 9.20 (9.24) %.

CHAPTER 5

HETEROMETALLIC COMPLEXES OF PYRIDONATE LIGANDS : HIGH NUCLEARITY COBALT-COPPER AND NICKEL-COPPER COORDINATION COMPLEXES AND A SERIES OF NICKEL- AND COBALT-LANTHANIDE COMPOUNDS.

5.1. Introduction.

This chapter outlines the synthesis and structure of a number of mixed-metal complexes of 6-chloro- and 6-methyl-2-pyridone. The chapter is divided into two parts. The first describes the synthesis and characterisation of three heterobimetallic complexes of 3d-metals which were formed from 'one-pot' thermolysis reactions of the metal carboxylates and the protonated pyridone ligand : reaction of cobalt and copper acetate with 6-chloro-2-pyridone at 130°C produced the nonanuclear species $[Co_7Cu_2(OH)_2(chp)_{10}(O_2CMe)_6]$ whilst the reaction of either cobalt or nickel benzoate with copper benzoate at 160°C produced two octanuclear compounds of formula $[M_6Cu_2(OH)_4(mhp)_2(O_2CPh)_{10}(Hmhp)_4(H_2O)_2]$ (M = Co, Ni). The second part of the chapter involves the formation of heterometallic complexes containing both d- and f-block elements. These compounds were synthesised by first isolating a 3d-metal-pyridonate complex and then further reacting with a lanthanide salt. This has produced a family of cobalt compounds of formula $[NEt_4]_2[Co_2Ln_x(OH)_y(chp)_z(NO_3)_5]$ (x = 2, 1; y = 1, 0; z = 6, 5) and a tetranuclear nickel complex $[Ni_2Er_2(chp)_6(NO_3)_4(MeCN)_2]$.

High nuclearity cobalt-copper and nickel-copper coordination complexes.

There are no previously reported heterobimetallic 3d-metal complexes which are stabilised by bridging pyridonate ligands, but there are two examples for the heavier transition metals. The first is $[MoW(mhp)_4]$ [122] which contains a short Mo-W bond of 2.091(1)Å and is isomorphous with the homometallic complexes $[M_2(mhp)_4]$ (M = Mo, W), [123] and the second is an unusual linear tetramer $[Mo_2(php)_4Pd_2Cl_4]$ (php = 6-diphenylphosphino-2-pyridone) [124, 125]. Pyridonate ligands have been used to bridge between 3d and s- and p-block elements : for example copper being linked to barium using 2-pyridone [126], and to magnesium through 6-

chloro-2-pyridone [127]. Although a number of di- and trinuclear cobalt-copper and nickel-copper species are known [128-130] higher nuclearity species are limited and thus far have only been found with copper (I) [131-133]. A polymer containing both cobalt and copper in the 2+ oxidation state has also been reported [134]. The first section of this chapter reports molecular octa- and nonanuclear species containing copper (II) and either cobalt (II) or nickel (II) centres.

5.2.1. Synthesis and structure of $[Co_7Cu_2(OH)_2(chp)_{10}(O_2CMe)_6]$ 41.

Cobalt acetate and copper acetate were intimately mixed with Hchp in a 1 : 1 : 4 mole ratio and fused at 130°C under an atmosphere of nitrogen. After one hour the acetic acid formed was removed by heating under reduced pressure and the resultant paste was extracted with dichloromethane and filtered. Purple crystals of $[Co_7Cu_2(OH)_2(chp)_{10}(O_2CMe)_6]$ **41** [Figure 5.1] were formed in high yield after three days [135].

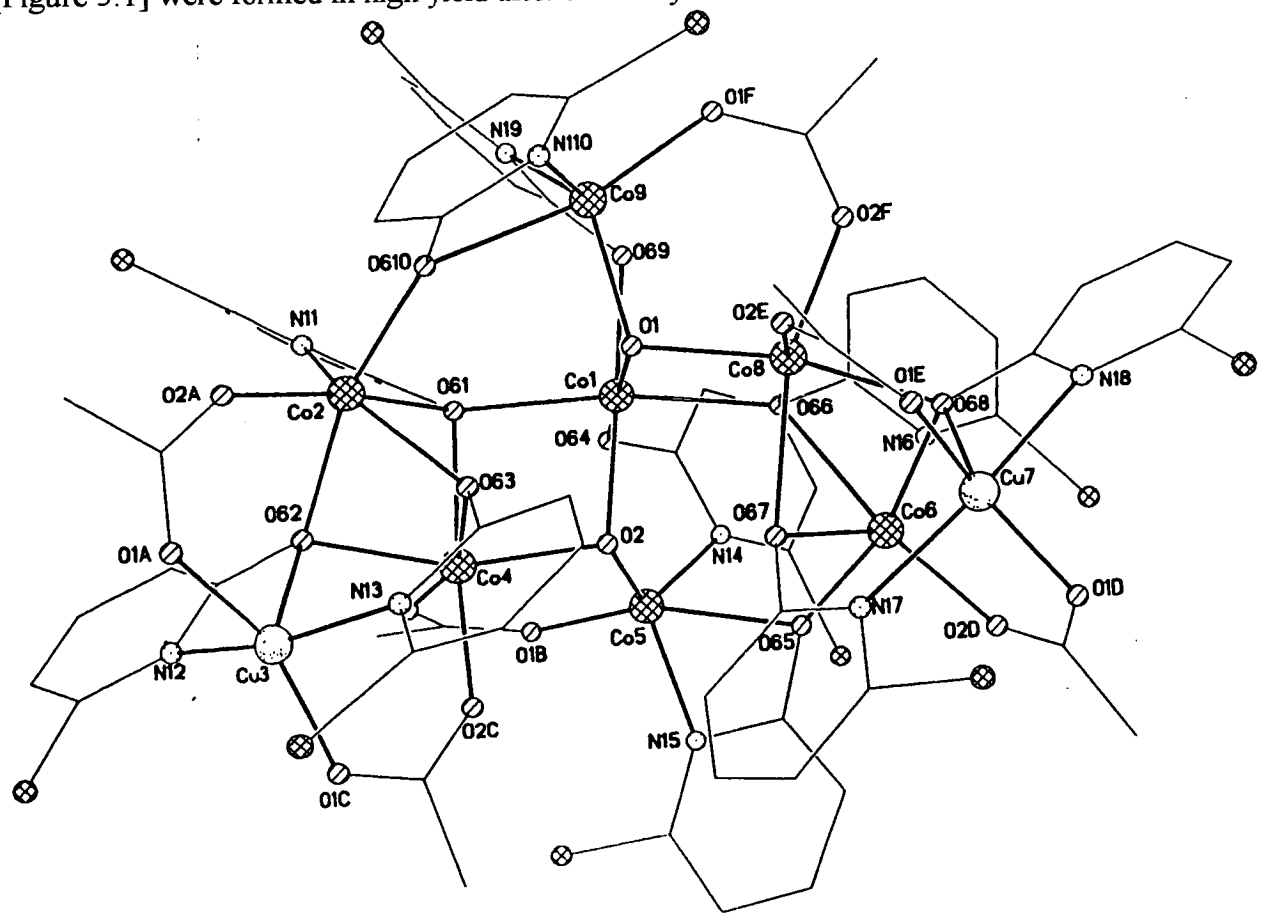

Figure 5.1. The structure of **41** in the crystal.

41 is a nonametallic species containing seven cobalt and two copper atoms. These coordination sites were assigned to the differing metals based on structure refinement and on elemental analysis by atomic absorption spectroscopy [experimental section 5.5.1]. The elemental analysis indicates a $[Co_7Cu_2]$ core and X-ray refinement leads to consistent displacement parameters for the metal sites only if they are assigned as shown in Figure 5.1. The cobalt sites are a mixture of five six-coordinate, each with a geometry based on a distorted octahedron [Co1, 2, 6, 8; *cis*, 60.3-115.1(3)°; *trans*, 137.7-178.3(3)°], and two five-coordinate sites [Co5 and Co9] whose geometries are loosely based on trigonal bipyramids. The remaining two sites are also five coordinate with extremely distorted geometries typical of copper (II). Refining all five-coordinate sites as copper atoms leads to a marked increase in the displacement parameters for M5 and M9 only. All of the five-coordinate sites are bound to two nitrogen and three oxygen donors. For the cobalt sites these are derived from two chps, an acetate and an hydroxide. For the copper sites they are derived from two chps and two acetates. Co2 and Co6 are bound to one nitrogen and five oxygen atoms and the three remaining cobalt sites [Co1, Co4 and Co8] are bound exclusively to oxygen donors.

The polyhedron [Figure 5.2.] defined by the metal sites is extremely irregular. The cobalt sites can be described as belonging to four oxygen-centred cobalt triangles with Co1 a vertex of all four triangles. Thus Co1, Co2, Co4 and Co1, Co6, Co8 form triangles about μ_3-oxygen atoms derived from chp ligands. Co1, Co4, Co5 and Co1, Co8, Co9 describe triangles about μ_3-hydroxides. This array of seven cobalt atoms is far from planar, with Co2, Co4, Co6 and Co8 within one plane and Co1, Co5 and Co9 considerably above this plane. The two copper atoms are also part of these oxygen centred triangles; Cu3, Co2, Co4 and Cu7, Co6, Co8 each define triangles about μ_3-oxygen atoms from chp ligands. The copper atoms lie below the plane of Co2, Co4, Co6 and Co8.

The chp ligands adopt three coordinating modes. Trinucleating, chelating to one metal

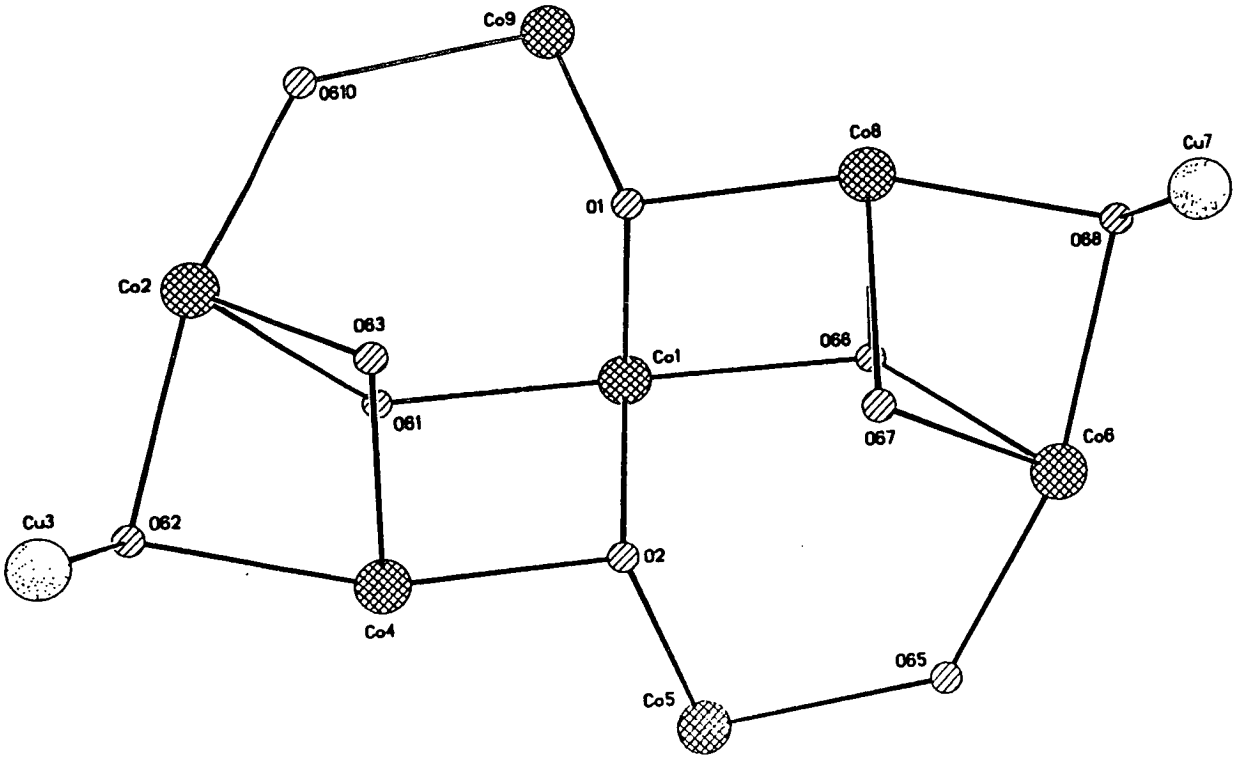

Figure 5.2. The polyhedron of **41**.

centre [Co2, Co6, Cu3 and Cu7] with the exocyclic oxygen atom also providing the central μ_3-bridge in four of the six metal triangles. Binucleating, chelating to one metal centre [Co5 and Co9] with the exocyclic oxygen atom also bound to one other metal [Co6 and Co2]. Binucleatng, binding to one metal [Co9, Co5] through the ring nitrogen with the oxygen atom binding to a second metal centre [Co1] with a long contact to the first metal centre [O69... Co9, 2.562(7)Å and O64...Co5, 2.515(7)Å]. The six acetate ligands present in the structure span the edges of the oxygen-centred triangles, bridging to the metal atoms in a 1,3-fashion [for example Co2...Cu3 and Co8...Co9].

The metal-oxygen and metal-nitrogen bond lengths are: Co-O(OH), 2.007-2.107(6)Å; Co-O(O_2CMe), 1.922-2.032(6)Å; Co-N(chp), 1.981-2.100(8)Å; Cu-O(O_2CMe), 1.922-1.940(6)Å and Cu-N(chp), 1.981-2.016(6)Å. The Co-O(chp) and Cu-O(chp) distances fall into two categories. Two of the cobalts [Co1, Co4] have regular bond lengths [2.019-2.260(6)Å] while the other metals [Co2-Co3, Co5-Co9, Cu3, Cu7] have four or five regular bond lengths and one longer bond [1.977-2.260(6) and 2.314-2.426(7)Å] The closest Co...Co distance is 3.000(6)Å between Co2 and Co4 and the closest Co...Cu distance is 3.495(8)Å

between Co8 and Cu7. Selected bond lengths and angles are given in Table 5.1. There are no significant intermolecular interactions in **41**. Attempts to synthesise the nickel analogue of **41** have so far been unsuccessful.

Table 5.1. Selected bond lengths (Å) and angles (°) for **41**.

Co1-O69	2.019(6)	Co5-O2	2.014(6)
Co1-O64	2.023(7)	Co5-N14	2.055(8)
Co1-O2	2.103(6)	Co5-N15	2.06(9)
Co1-O1	2.107(6)	Co5-O65	2.339(7)
Co1-O66	2.179(6)	Co6-O65	1.977(6)
Co1-O61	2.190(6)	Co6-O2D	1.998(7)
Co2-O610	1.991(6)	Co6-N16	2.100(8)
Co2-O2A	2.004(7)	Co6-O67	2.131(6)
Co2-N11	2.095(9)	Co6-O68	2.175(6)
Co2-O63	2.126(6)	Co6-O66	2.314(6)
Co2-O62	2.159(6)	Cu7-O1E	1.922(7)
Co2-O61	2.307(6)	Cu7-O1D	1.927(7)
Cu3-O1A	1.938(6)	Cu7-N17	1.999(7)
Cu3-O1C	1.940(6)	Cu7-N18	2.016(7)
Cu3-N13	1.981(7)	Cu7-O68	2.412(6)
Cu3-N12	2.003(8)	Co8-O2E	1.991(7)
Cu3-O62	2.426(7)	Co8-O1	2.010(6)
Co4-O2	2.013(6)	Co8-O2F	2.032(6)
Co4-O2C	2.015(7)	Co8-O68	2.072(6)
Co4-O2B	2.020(7)	Co8-O66	2.177(6)
Co4-O62	2.095(7)	Co8-O67	2.346(6)
Co4-O61	2.185(6)	Co9-O1F	1.976(7)
Co4-O63	2.260(6)	Co9-O1	2.007(6)
Co5-O1B	1.974(7)	Co9-N19	2.072(6)

Table 5.1 continued

Co9-N110	2.098(8)	O63-Co2-O62	77.5(2)
Co9-O610	2.368(8)	N11-Co2-O61	60.3(3)
O69-Co1-O64	94.4(3)	O63-Co2-O61	78.4(2)
O69-Co1-O2	178.3(3)	O62-Co2-O61	77.5(2)
O64-Co1-O2	86.7(3)	O1A-Cu3-O1C	154.7(3)
O69-Co1-O1	86.3(2)	O1A-Cu3-N13	91.9(3)
O64-Co1-O1	178.1(3)	O1C-Cu3-N13	92.4(3)
O2-Co1-O1	92.6(2)	O1A-Cu3-N12	90.0(3)
O69-Co1-O66	94.7(2)	O1C-Cu3-N12	92.3(3)
O64-Co1-O66	98.2(2)	N13-Cu3-N12	164.5(3)
O2-Co1-O66	86.5(2)	O1A-Cu3-O62	100.5(3)
O1-Co1-O66	80.0(2)	O1C-Cu3-O62	102.3(3)
O69-Co1-O1	98.5(3)	N13-Cu3-O62	105.5(2)
O64-Co1-O61	94.6(3)	N12-Cu3-O62	59.5(2)
O2-Co1-O61	80.1(2)	O2-Co4-O2C	95.0(3)
O1-Co1-O61	87.0(2)	O2-Co4-O2B	102.0(3)
O66-Co1-O61	160.9(2)	O2C-Co4-O2B	95.1(3)
O610-Co2-O2A	99.6(3)	O2-Co4-O62	161.9(3)
O610-Co2-N11	98.6(3)	O2C-Co4-O62	100.0(2)
O2A-Co2-N11	112.0()3	O2B-Co4-O62	87.0(2)
O610-Co2O63	91.1(2)	O2-Co4-O61	82.2(2)
O2A-Co2-O63	106.6(2)	O2C-Co4-O61	171.8(3)
N11-Co2-O63	137.7(2)	O2B-Co4-O61	93.1(3)
O610-Co2-O62	165.7(3)	O62-Co4-O61	81.6(2)
O2A-Co2-O62	91.9(3)	O2-Co4-O63	92.9(3)
N11-Co2-O62	84.7(2)	O2C-Co4-O63	94.3(2)
O610-Co2-O61	92.0(2)	O2B-Co4-O63	161.7(2)
O2A-Co2-O61	167.1(2)	O62-Co4-O63	75.9(3)

Table 5.1 continued

O61-Co4-O63	78.2(2)	O1D-Cu7-N17	90.6(3)
O1B-Co5-O2	109.5(3)	O1E-Cu7-N18	94.8(3)
O1B-Co5-N14	96.2(3)	O1D-Cu7-N18	88.7(3)
O2-Co5-N14	122.7(3)	N17-Cu7-N18	165.1(3)
O1B-Co5-N15	103.6(3)	O1E-Cu7-O68	104.6(3)
O2-Co5-N15	105.8(3)	O1D-Cu7-O68	96.9(3)
N14-Co5-N15	116.8(3)	N17-Cu7-O68	105.7(3)
O1B-Co5-O65	162.0(3)	N18-Cu7-O68	59.6(3)
O2-Co5-O65	83.5(3)	O2E-Co8-O1	93.4(3)
N14-Co5-O65	86.5(3)	O2E-Co8-O2F	95.3(3)
N15-Co5-O65	59.9(3)	O1-Co8-O2F	102.2(3)
O65-Co6-O2D	98.6(3)	O2E-Co8-O68	100.6(3)
O65-Co6-N16	98.9(3)	O1-Co8-O68	162.4(3)
O2D-Co6-N16	115.1(3)	O2F-Co8-O68	87.2(3)
O65-Co6-O67	90.7(2)	O2E-Co8-O66	172.5(3)
O2D-Co6-O67	103.2(3)	O1-Co8-O66	82.2(3)
N16-Co6-O67	138.3(3)	O2F-Co8-O66	91.7(3)
O65-Co6-O68	164.4(3)	O68-Co8-O66	82.7(3)
O2D-Co6-O68	94.3(3)	O2E-Co8-O67	96.3(3)
N16-Co6-O68	83.2(3)	O1-Co8-O67	92.7(3)
O67-Co6-O68	77.9(2)	O2F-Co8-O67	160.5(3)
O65-Co6-O66	90.3(2)	O68-Co8-O67	75.3(3)
O2D-Co6-O66	170.6(2)	O66-Co8-O67	77.8(3)
N16-Co6-O66	60.2(3)	O1F-Co9-O1	110.0(3)
O67-Co6-O66	79.4(2)	O1F-Co9-N19	94.8(3)
O68-Co6-O66	77.3(2)	O1-Co9-N19	121.1(3)
O1E-Cu7-O1D	156.9(3)	O1F-Co9-N110	104.9(3)
O1E-Cu7-N17	91.6(3)	O1-Co9-N110	104.4(3)

Table 5.1 continued

N19-Co9-N110	119.9(3)	Co4-O62-Co2	89.7(2)
O1F-Co9-O610	162.3(3)	Co4-O62-Cu3	101.3(3)
O1-Co9-O610	83.3(2)	Co2-O62-Cu3	100.5(2)
N19-Co9-O610	87.7(3)	Co2-O63-Co4	86.3(2)
N110-Co9-O610	59.2(3)	Co6-O65-Co5	130.2(3)
Co9-O1-Co8	111.7(3)	Co8-O66-Co1	95.1(2)
Co9-O1-Co1	104.2(3)	Co8-O66-Co6	84.1(2)
Co8-O1-Co1	102.6(3)	Co1-O66-Co6	133.0(3)
Co4-O2-Co5	113.0(3)	Co6-O67-Co8	84.4(2)
Co4-O2-Co1	102.8(3)	Co8-O68-Co6	90.3(2)
Co5-O2-Co1	102.4(3)	Co8-O68-Cu7	102.2(2)
Co4-O61-Co1	94.7(2)	Co6-O68-Cu7	100.3(2)
Co4-O61-Co2	83.8(2)	Co2-O610-Co9	129.2(3)
Co1-O61-Co2	132.3(3)		

5.2.2. Magnetochemistry of 41.

The magnetic behaviour of **42** was studied in the temperature range 300-1.8 K in an applied field of 1000 G. The variation of the product $\chi_m T$ with temperature is shown in Figure 5.3. The room temperature value of approximately 19 emu K mol^{-1} is consistent with a [Co_7Cu_2] core in which the metal centres are not interacting [$\chi_m T$ = 18.9 emu K mol^{-1}; g_{Co} = 2.35 and g_{Cu} = 2.10]. The value of $\chi_m T$ drops steadily with temperature giving a minimum of approximately 2 emu K mol^{-1} at 1.8 K, indicative of antiferromagnetic exchange between the metal centres. The 1.8 K value is equivalent to an approximately S = 1 ground state.

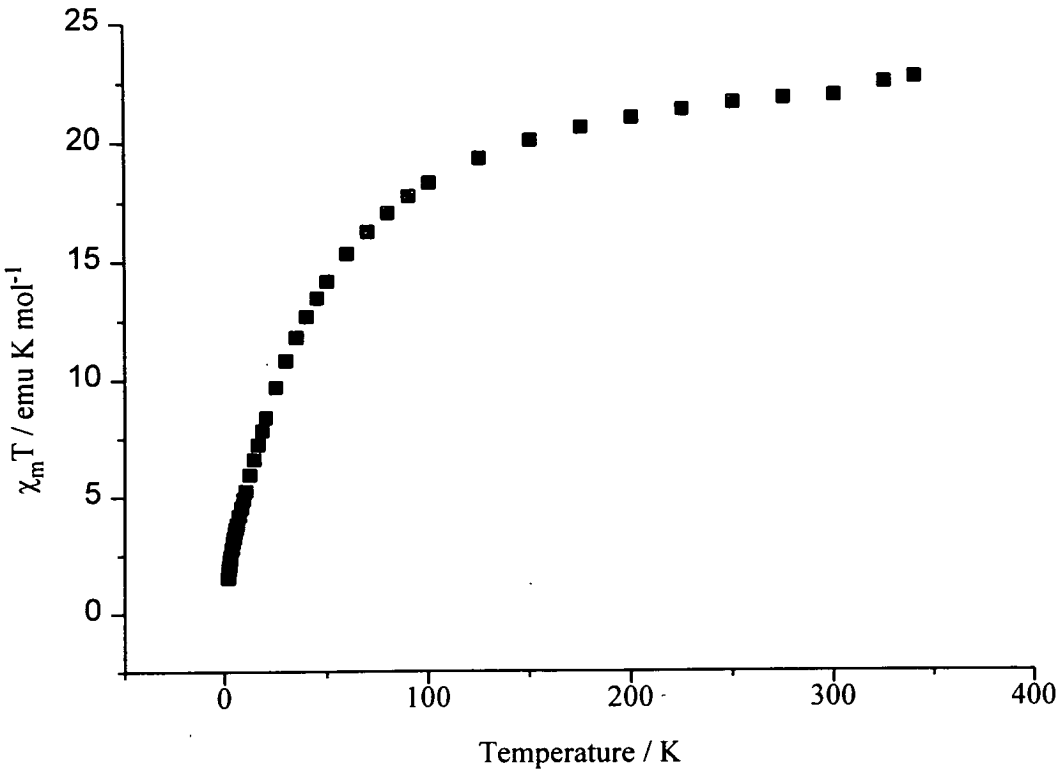

Figure 5.3. The variation of $\chi_m T$ with temperature for **41**.

5.2.3. Synthesis and structure of $[M_6Cu_2(OH)_4(mhp)_2(O_2CPh)_{10}(Hmhp)_4(H_2O)_2]$ (M = Co, 42; M = Ni, 43).

Reaction of copper benzoate with nickel or cobalt benzoate and two equivalents of 6-methyl-2-pyridone at 160°C for two hours under nitrogen produced a paste which was heated under reduced pressure for a further twenty minutes. Extraction of this product in dichloromethane produced the isostructural octanuclear complexes $[M_6Cu_2(OH)_4(mhp)_2(O_2CPh)_{10}(Hmhp)_4(H_2O)_2]$ M = Co, **42**; Ni, **43** [135]. The yield of the cobalt derivative **42** is low (10%) in comparison to the nickel derivative **43** (25%). The structure of **42** is shown in Figure 5.4.

42 contains structural features which are similar to **41**. Again the structure is dominated by oxygen-centred metal triangles : the midpoint of the complex is a bitriangular unit sharing one edge, with Co2 and Co2A in the common edge and Co3 or its symmetry

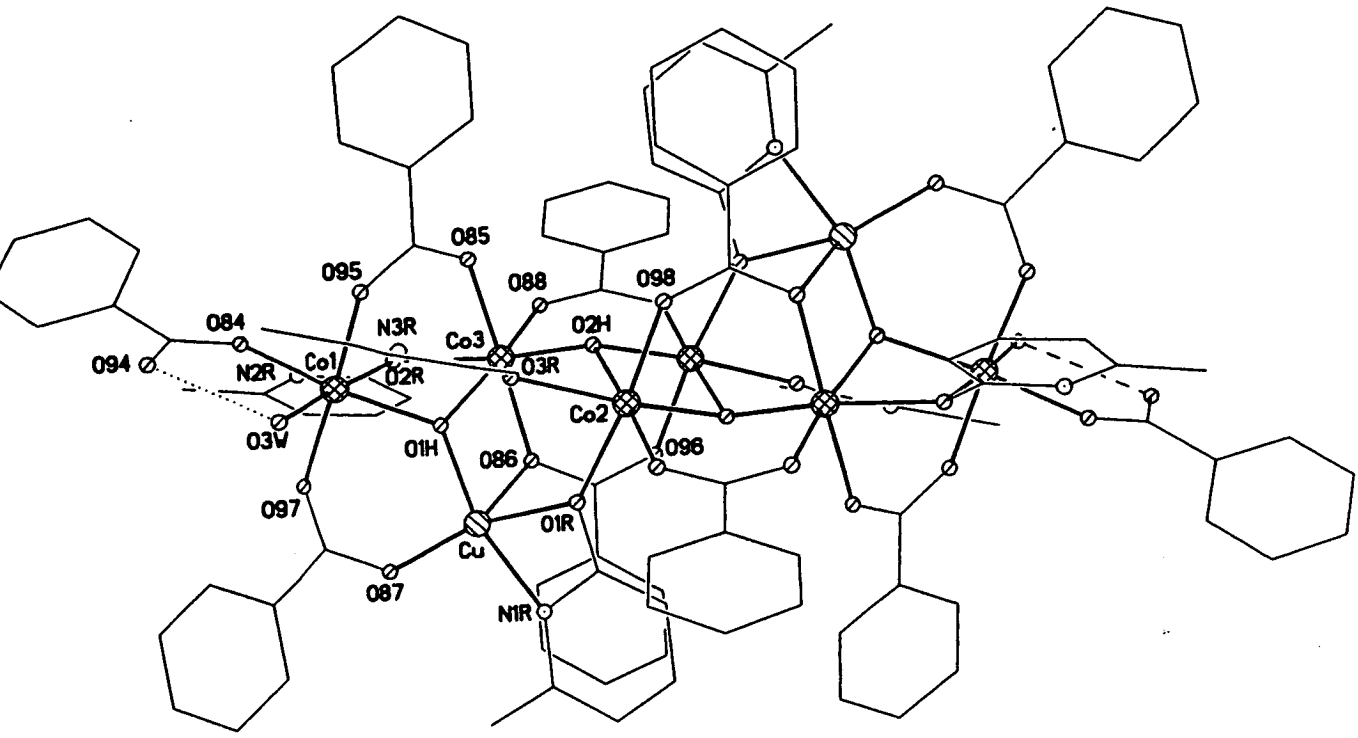

Figure 5.4. The structure of **42** in the crystal.

equivalent completing the triangles. Co3 and Co3A are present in the other crystallographically unique triangle made up of Co3, Co1 and Cu. At the centre of each triangle is a μ_3-hydroxide. The three unique cobalt sites are all bound to an octahedral array of oxygen donors [*cis*, 78.37-99.22(14)°; *trans*, 164.91-177.80(14)°] while the copper site is bound to four oxygen donors and one nitrogen donor, with irregular geometry. Like **41** the assignment of the metal sites was made on the basis of both X-ray refinement and atomic absorption spectroscopy [experimental section 5.5.2].

Unlike **41** the bridging of **42** is dominated more by the benzoate ligands than the pyridonates. Three of the benzoates within the asymmetric unit bridge in a 1,3-fashion [for example between Co1 and Co3]; one is trinucleating bridging Co2A, Co3 and Cu, and the

final unique benzoate is monodentate - bound to Co1 through only one oxygen atom of the carboxylate group, with its second oxygen atom strongly hydrogen-bonded to the terminal water molecule also attached to Co1 [O94R...O3W, 2.655(7)Å]. There is only one mhp ligand in the asymmetric unit : it chelates to Cu1 through its ring nitrogen and exocyclic oxygen atom with the oxygen further bridged to one cobalt centre [Co2]. Also present are two molecules of Hmhp which both coordinate through their exocyclic oxygen alone, although even here variety is found as one Hmhp bridges between Co1 and Co3, with its ring nitrogen having a long contact to an oxygen of the terminally bound benzoate [N2R...O84, 2.717(4)Å], while the second Hmhp is terminally bound to Co2, with the oxygen having a further long contact to the μ_3-bridging hydroxide [O3R..O1H, 2.719(4)Å]. The ring nitrogen of this pyridone is not involved in any hydrogen-bonding. The cobalt-oxygen bond lengths are all regular : Co-O(OH), 2.019-2.097(3)Å; Co-O(O_2CPh), 2.045-2.145(4)Å; Co-O(mhp), 2.114-2.193(4)Å and Co-O(H_2O), 2.135(4)Å, as are the copper bond lengths : Cu-O(OH), 1.917(3)Å; Cu-O(O_2CPh), 1.924-2.396(3)Å; Cu-O(mhp), 2.027(3)Å and Cu-N(mhp) 2.030(4)Å. The closest

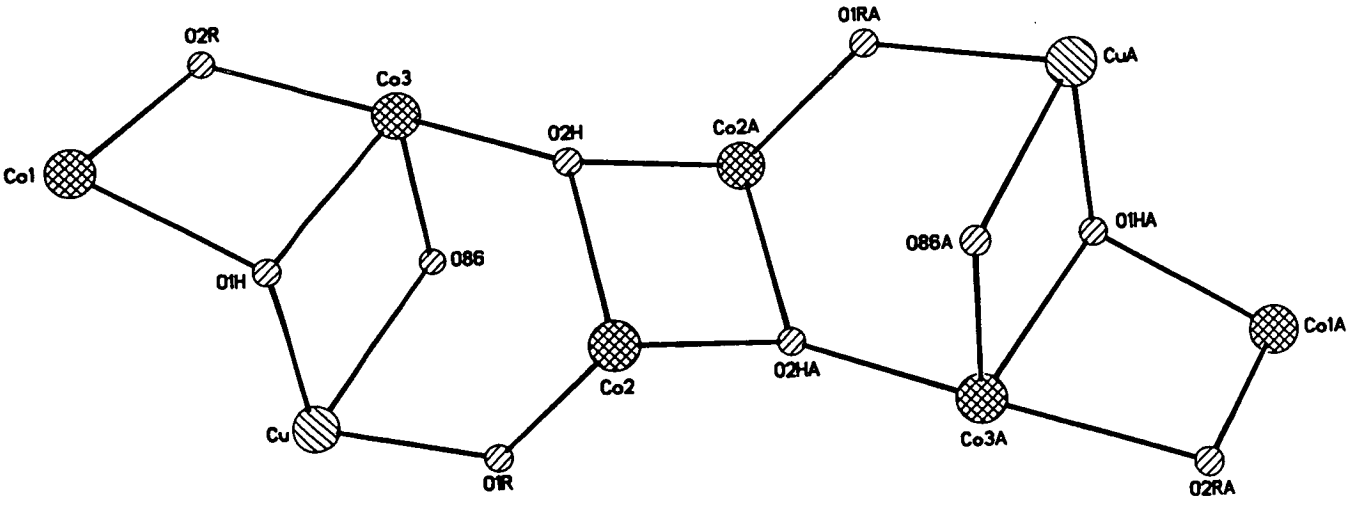

Figure 5.5. The polyhedron of **42**.

Co...Co distance is 3.132(5)Å between Co2 and Co2A with the closest Co...Cu distance of 3.214(5)Å being between Cu and Co3.

In the isostructural nickel complex **43** [Figure 5.6] the nickel-oxygen bonds are always shorter than the equivalent bonds in **42** :Ni-O(OH), 1.952-2.080(6)Å; Ni-O(O_2CPh), 1.965-2.081(6)Å; Ni-O(mhp), 2.055-2.143(6)Å and Ni-O(H_2O), 2.068(6)Å. This is also true with the copper bonds : Cu-O(OH), 1.875(4); Cu-O(O_2CPh), 1.883-2.436(6)Å; Cu-O(mhp), 1.972(5)Å and Cu-N(mhp), 1.975(5)Å. This shortening in the bond lengths is also reflected in the metal...metal distances, with the Ni2...Ni2A contact being 3.085(6)Å and the Cu...Ni3 contact being 3.165(5)Å. Selected bond lengths and angles for both **42** and **43** are given in Table 5.2. The reason for the higher percentage yield of the nickel analogue over the cobalt compound is unclear. There are no significant intermolecular interactions in either **42** or **43**.

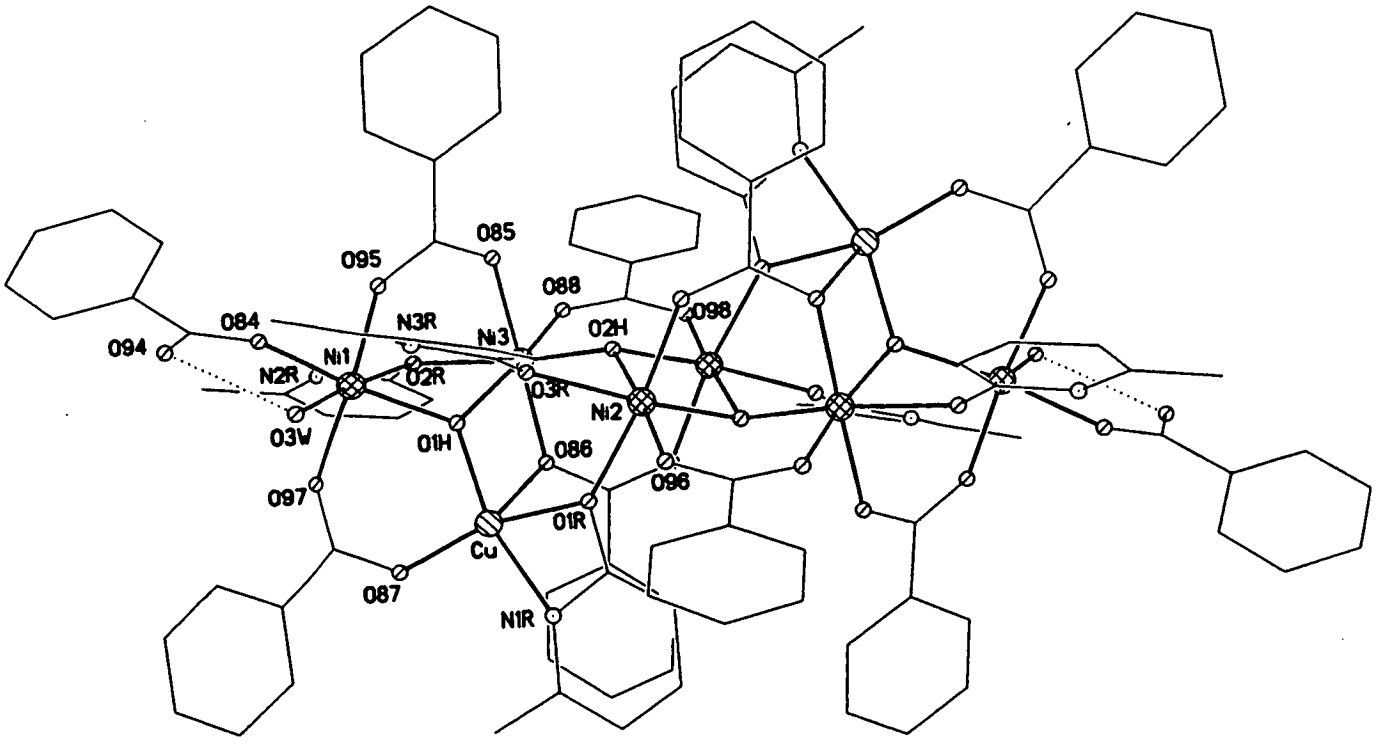

Figure 5.6. The structure of **43** in the crystal.

Table 5.2. Selected bond lengths (Å) and angles (°) for **42** and **43**. M = Co, Ni.

	42	**43**		**42**	**43**
Cu-O1H	1.917(3)	1.875(5)	O1H-M1-O97	93.12(14)	94.4(2)
Cu-O87	1.924(4)	1.883(5)	O84-M1-O97	87.9(2)	87.1(2)
Cu-O1R	2.027(3)	1.972(5)	O95-M1-O97	175.0(2)	174.1(2)
Cu-N1R	2.030(4)	1.975(6)	O1H-M1-O3W	98.80(14)	98.3(2)
Cu-O86	2.395(4)	2.436(6)	O84-M1-O3W	92.97(15)	92.5(2)
M1-O1H	2.019(3)	1.952(5)	O95-M1-O3W	83.26(15)	84.3(2)
M1-O84	2.045(4)	1.965(5)	O97-M1-O3W	92.1(2)	91.1(2)
M1-O95	2.070(4)	2.018(6)	O1H-M1-O2R	79.17(14)	78.2(2)
M1-O97	2.072(4)	2.038(6)	O84-M1-O2R	89.09(14)	91.0(2)
M1-O3W	2.135(4)	2.068(5)	O95-M1-O2R	97.50(15)	96.6(2)
M1-O2R	2.193(4)	2.143(6)	O97-M1-O2R	8725(15)	88.3(2)
M2-O98A	2.054(4)	1.982(6)	O3W-M1-O2R	177.8(2)	176.4(2)
M2-O2HA	2.068(3)	2.007(5)	O98A-M2-O2HA	99.22(14)	102.1(2)
M2-O96A	2.076(4)	2.029(5)	O98A-M2-O96A	91.35(15)	176.7(2)
M2-O2H	2.097(3)	2.031(5)	O2HA-M2-O96A	95.36(14)	80.3(2)
M2-O1R	2.114(4)	2.067(5)	O98A-M2-O2H	177.4(2)	91.7(2)
M2-O3R	2.163(4)	2.129(5)	O2HA-M2-O2H	82.48(14)	94.3(2)
M3-O2H	2.034(3)	1.964(5)	O96A-M2-O2H	90.44(14)	90.4(2)
M3-O88	2.055(4)	2.029(6)	O98A-M2-O1R	89.10(15)	88.7(2)
M3-O1H	2.119(4)	2.055(5)	O2HA-M2-O1R	91.19(13)	92.5(2)
M3-O2R	2.135(4)	2.062(5)	O96A-M2-O1R	173.28(13)	88.9(2)
M3-O86	2.142(4)	2.080(6)	O2H-M2-O1R	89.90(13)	172.9(2)
M3-O85	2.145(4)	2.081(5)	O98A-M2-O3R	92.29(14)	88.7(2)
O2H-M2A	2.068(3)	2.007(5)	O2HA-M2-O3R	168.46(13)	169.2(2)
O1H-M1-O84	168.2(2)	169.1(2)	O96A-M2-O3R	85.19(14)	88.9(2)
O1H-M1-O95	89.5(2)	89.9(2)	O2H-M2-O3R	85.99(14)	85.5(2)
O84-M1-O95	90.5(2)	89.4(2)	O1R-M2-O3R	88.10(13)	87.5(2)

Table 5.2 continued

	42	43		42	43
O2H-M3-O88	98.70(14)	97.0(2)	O1H-M3-O85	92.00(14)	92.6(2)
O2H-M3-O1H	93.30(13)	94.4(2)	O2R-M3-O85	86.07(14)	87.8(2)
O88-M3-O1H	167.64(14)	168.3(2)	O86-M3-O85	173.78(14)	176.0(2)
O2H-M3-O2R	164.91(14)	166.3(2)	Cu-O1H-M1	127.0(2)	125.3(3)
O88-M3-O2R	90.53(14)	91.8(2)	Cu-O1H-M3	105.5(2)	106.3(3)
O1H-M3-O2R	78.37(13)	77.5(2)	M1-O1H-M3	99.44(14)	100.1(3)
O2H-M3-O86	96.03(14)	97.2(2)	M3-O2H-M2A	111.5(2)	112.4(3)
O88-M3-O86	93.4(2)	92.2(2)	M3-O2H-M2	130.2(2)	129.0(3)
O1H-M3-O86	82.35(14)	83.8(2)	M2A-O2H-M2	97.52(14)	99.7(2)
O2R-M3-O86	95.30(14)	93.0(2)	Cu-O1R-M2	133.4(2)	134.7(3)
O2H-M3-O85	81.63(14)	81.4(2)	M3-O2R-M1	93.72(14)	94.9(2)
O88-M3-O85	92.64(15)	91.7(2)	M3-O86-Cu	90.03(14)	89.1(2)

5.2.4. Magnetochemistry of 43.

The magnetic behaviour of **43** was studied in the temperature range 300-1.8 K in an applied field of 1000 G. The variation of $\chi_m T$ with temperature is shown in Figure 5.7. The room temperature value of approximately 9 emu K mol^{-1} is consistent with a $[Ni_6Cu_2]$ core containing non-interacting metal centres [$\chi_m T$ = 8.40 emu K mol^{-1}, g_{Ni} = 2.25 and g_{Cu} = 2.10]. The value of $\chi_m T$ then drops steadily with temperature giving a minimum of approximately 2 emu K mol^{-1} at 1.8 K, behaviour indicative of antiferromagnetic exchange between the metal centres. The 1.8 K value is equivalent to an approximately S = 1 ground state. Magnetic studies of **42** are currently under investigation.

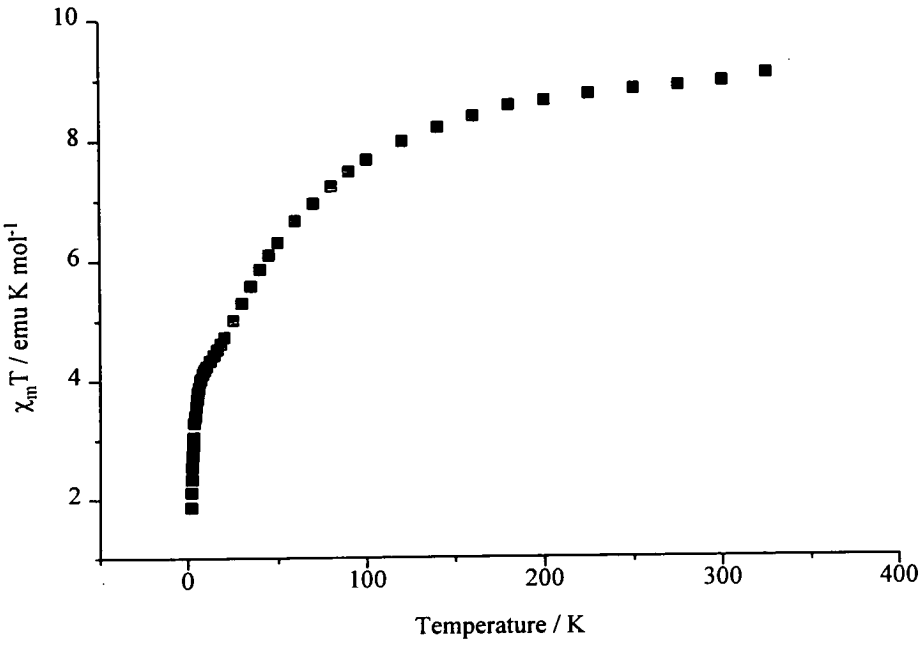

Figure 5.7. The variation of $\chi_m T$ with temperaure for **43**.

In the three compounds **41-43** the ratio of the metals in the reaction mixture does not appear to effect the reaction product. In all cases a side-product of the reaction appears to be homometallic copper pyridonate complexes; for **41** it is the known complex $[Cu_2(chp)_4]$ [136] and for **42** and **43** it is most likely to be $[Cu_2(mhp)_4]$. The side-products observed explain the lower copper : cobalt ratio in the structurally characterised complexes than in the substrates. Attempts to synthesise similar mixed-metal complexes containing different carboxylates, all resulted in the formation of these copper dimers, while any nickel-copper or cobalt-copper species that did form remained in solution and hence remain uncharacterised.

5.2.5. Heterometallic complexes containing d- and f-block elements.

The coupling of lanthanides with other metals was inspired by the discovery of high-temperature superconducting oxides which contained copper and mixtures of other s-, p- and f-block elements [137]. As a result there has been extensive investigation into the synthesis and characterisation of heterometallic complexes containing 3d and 4f elements (particularly copper and gadolinium), in the hope that these species would either display unusual physical properties (for example interesting magnetic behaviour) or themselves be precursors to the superconducting mixed-metal oxide compounds[138-151]. However little has been reported on the related interaction between other 3d-4f mixtures and indeed very few structurally characterised complexes are known which contain such combinations of metals [152-159]. Even in the few known cases the oxidation state or coordination geometry of the 3d-metal often renders the magnetic properties of the polymetallic complex uninteresting. For example nickel complexes are known where thiooxalate bridges between nickel and various 4f-elements [160] however in each case the nickel is in a square planar environment and hence is diamagnetic. Recently an elegant heptanuclear nickel-samarium complex, bridged by L-prolinato ligands was reported [161] but the paper did not contain any magnetic measurements.

This section of Chapter 5 discusses the synthesis, structure and initial magnetic properties of a number of novel nickel and cobalt complexes of the lanthanides. The compounds were synthesised *via* preformed nickel / cobalt-pyridonate complexes rather than the 'one-pot' approach discussed earlier.

5.2.6. Synthesis and structure of $[Ni_2Er_2(chp)_6(NO_3)_4(MeCN)_2]$ 44.

Reaction of erbium nitrate with $[Ni_4(OMe)_4(chp)_4(MeOH)_7]$ **1** in acetonitrile gave a blue / green solution from which green crystals of $[Ni_2Er_2(chp)_6(NO_3)_4(MeCN)_2]$ **44** [Figure 5.8] formed in low yield after two weeks [162]. **44** is a centrosymmetric tetramer which contains a central $[Er_2O_2]$ ring bridged to the peripheral nickel atoms through six chp ligands. These six ligands adopt two distinct bonding modes : four chelate to the nickel centre and bridge to the erbium atom through the exocyclic oxygen atom. The two remaining chp groups bind to the nickel through the ring nitrogen alone and provide the oxygen atoms of the central $[Er_2O_2]$ ring and are therefore trinucleating. The metal atoms and the chp oxygen atoms therefore describe two interpenetrating rings : the $[Er_2O_2]$ unit and an eight membered $[Er_2Ni_2O_4]$

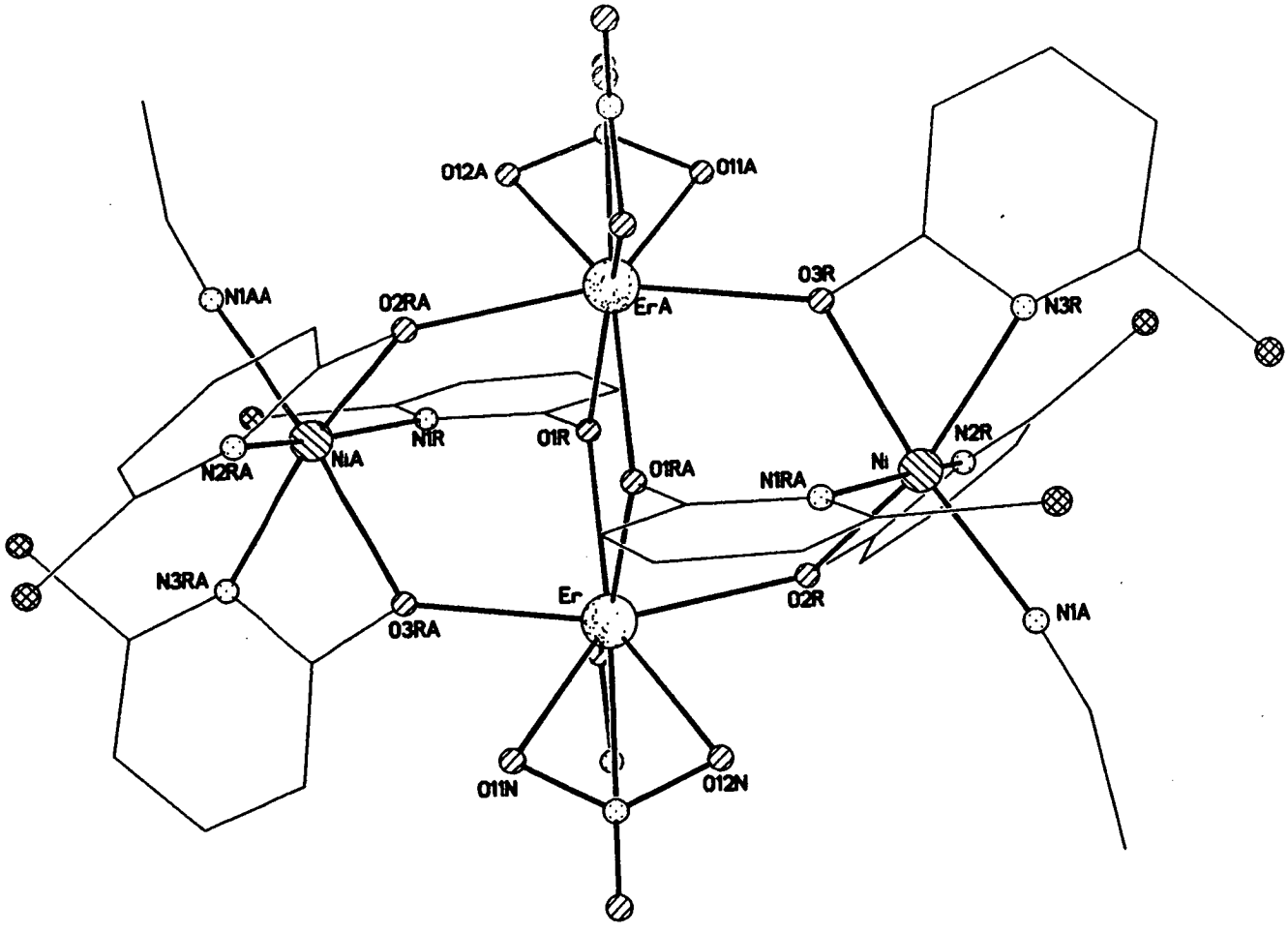

Figure 5.8. The structure of **44** in the crystal.

metallocycle perpendicular to it. The erbium sites are eight coordinate, each bound to four chp oxygen donors and two bidentate nitrate anions. The nickel sites are six-coordinate and have distorted octahedral geometries [*cis*, 61.8-108.8(3)°; *trans*, 151.7-172.2(3)°] comprising three nitrogen and two oxygen-donors derived from chp ligands and one nitrogen atom from an acetonitrile molecule. The distortion away from octahedral is due to the presence of the chelating pyridonate ligands. The erbium-oxygen distances are in the range 2.243-2.347(5)Å [chp] and 2.385-2.427(6)Å [NO_3]. The nickel-oxygen and nickel-nitrogen bond lengths are 2.128-2.207(6)Å and 2.027-2.119(8)Å respectively. The erbium...erbium distance is 3.761(7)Å with the angle between the two, defined by O1R, 109.7(2)°. The nickel...erbium distances range between 3.858-3.878(7)Å. Selected bond lengths and angles are given in Table 5.3. There are no significant intermolecular interactions in **44**. Attempts to synthesise similar complexes containing different lanthanides *via* the same procedure have proved unsuccessful.

5.2.7. Magnetochemistry of 44.

The magnetic behaviour of **44** was studied in the temperature range 300-1.8 K in an applied field of 1000 G. The variation of $\chi_m T$ with temperature is shown in Figure 5.9. The room temperature value of approximately 26 emu K mol^{-1} is consistent with a $[Ni_2Er_2]$ core in which the metals are not interacting [$\chi_m T$ = 25.5 emu K mol^{-1}, g_{Ni} = 2.2 and g_{Er} = 1.2]. The value of $\chi_m T$ declines gradually between 300 and 20 K, where it reaches 22 emu K mol^{-1}. Below 20 K it falls sharply to 13 emu K mol-1 at 2 K, indicating antiferromagnetic exchange between the metal centres.

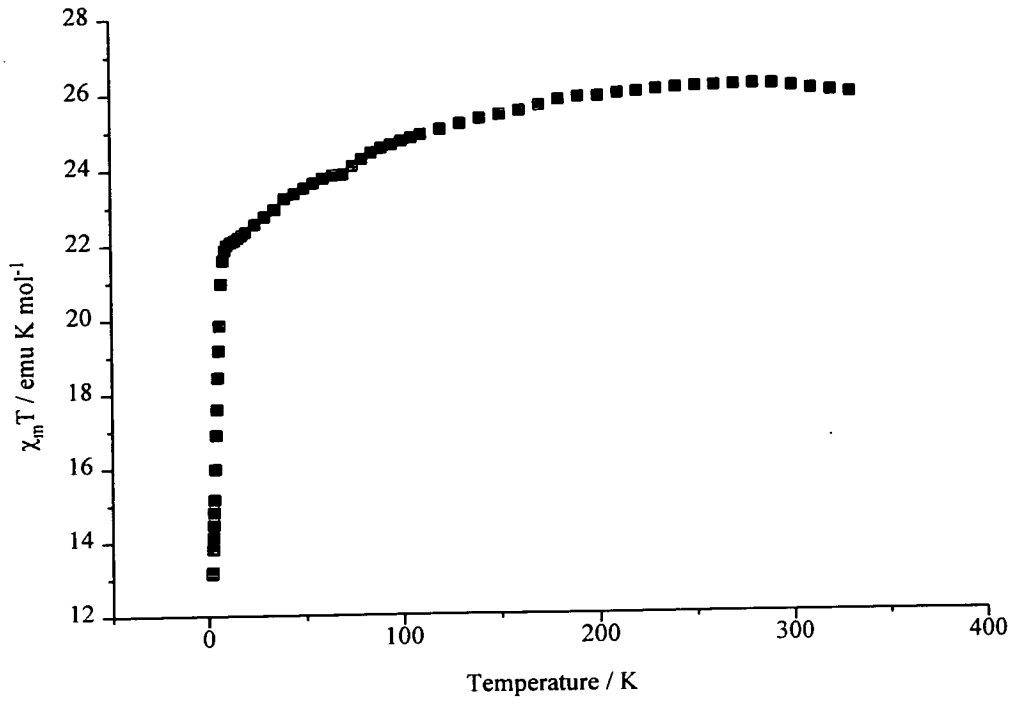

Figure 5.9. The variation of $\chi_m T$ with temperature for **44**.

Table 5.3. Selected bond lengths (Å) and angles (°) for **44**.

Er-O2R	2.243(5)	O2R-Er-O3RA	156.8(2)
Er-O3RA	2.248(5)	O2R-Er-O1RA	80.8(2)
Er-O1RA	2.254(5)	O3RA-Er-O1RA	98.0(2)
Er-O1R	2.347(6)	O2R-Er-O1R	81.2(2)
Er-O11N	2.385(6)	O3RA-Er-O1R	76.7(2)
Er-O12N	2.393(6)	O1RA-Er-O1R	70.3(2)
Er-O22N	2.397(5)	O2R-Er-O11N	128.7(2)
Er-O21N	2.427(5)	O3RA-Er-O11N	74.1(2)
Ni-N1A	2.027(8)	O1RA-Er-O11N	87.3(2)
Ni-N3R	2.084(8)	O1R-Er-O11N	140.0(2)
Ni-N2R	2.101(8)	O2R-Er-O21N	96.2(2)
Ni-N1RA	2.119(7)	O3RA-Er-O21N	93.3(2)
Ni-O3R	2.128(6)	O1RA-Er-O21N	157.6(2)
Ni-O2R	2.207(6)	O1R-Er-O21N	131.5(2)

Table 5.3 continued

O11N-Er-O21N	77.3(2)	N3R-Ni-N2R	95.3(4)
O2R-Er-O22N	87.5(2)	N1A-Ni-N1RA	93.0(3)
O3RA-Er-O22N	81.3(2)	N3R-Ni-N1RA	97.2(3)
O1RA-Er-O22N	147.7(3)	N2R-Ni-N1RA	164.1(3)
O1R-Er-O22N	78.2(2)	N1A-Ni-O3R	172.2(3)
O11N-Er-O22N	122.8(2)	N3R-Ni-O3R	63.5(3)
O21N-Er-O22N	53.3(3)	N2R-Ni-O3R	90.3(3)
O2R-Er-O12N	75.7(2)	N1RA-Ni-O3R	86.7(2)
O3RA-Er-O12N	127.292)	N1A-Ni-O2R	89.6(3)
O1RA-Er-O12N	81.9(2)	N2R-Ni-O2R	151.7(3)
O1R-Er-O12N	146.3(2)	N3R-Ni-O2R	61.8(3)
O11N-Er-O12N	53.2(2)	N1RA-Ni-O2R	103.2(2)
O21N-Er-O12N	75.9(2)	O3R-Ni-O2R	98.1(2)
O22N-Er-O12N	124.3(2)	ErA-O1R-Er	109.7(2)
N1A-Ni-N3R	108.8(3)	Ni-O2R-Er	120.2(2)
N1A-Ni-N2R	92.1(3)	Ni-O3R-ErA	124.8(3)

5.2.8. Synthesis and structure of $[NEt_4]_2[Co_2Yb_2(OH)(chp)_6(NO_3)_5]$ 46.

Reaction of hydrated cobalt chloride with two equivalents of $[NEt_4]Cl$ in methanol produced a blue solution from which $[NEt_4]_2CoCl_4$ was isolated in 100% yield. Reaction of this blue salt with four equivalents of Na(chp) in methanol produced $[NEt_4]_2[Co(chp)_4]$ **45** in 30% yield after extraction with dichloromethane. The salt **45** [Figure 5.10] has been structurally characterised and contains a cobalt (II) centre bound to four oxygen donors with a tetrahedral coordination geometry [102.2-123.8(4)°]. Further reaction of **45** with ytterbium nitrate in a 1:1 mixure of dichloromethane/methanol gave a pink solution.

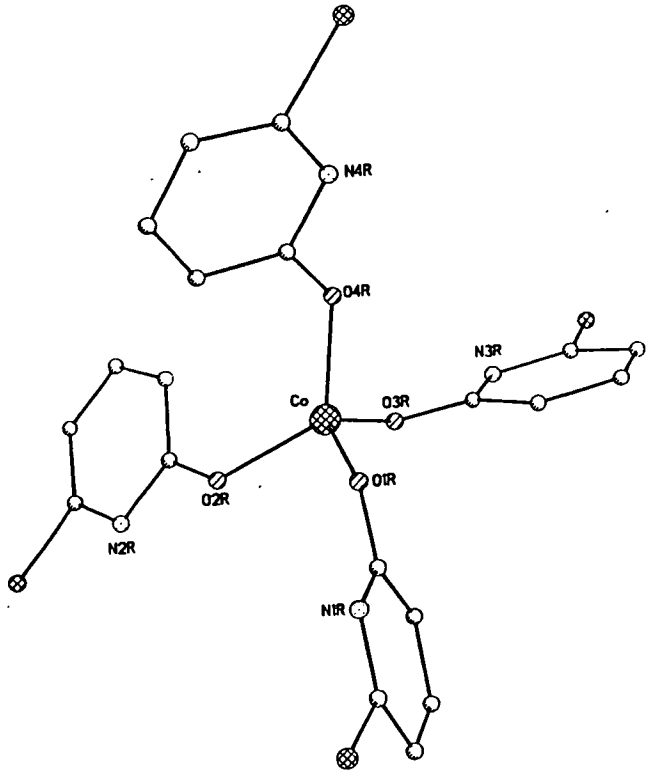

Figure 5.10. The structure of **45** in the crystal. The counter ions have been excluded for clarity. The Co...O distances are in the range 1.935-1.946(8)Å, and the angles around the Co are 102.2-123.8(4)°.

Evaporation to dryness followed by extraction with dichloromethane gave pink crystals of $[NEt_4]_2[Co_2Yb_2(OH)(chp)_6(NO_3)_5]$ **46** [Figure 5.11] in low yield after four days [162]. **46** is a tetrametallic species which contains a central $[Yb_2O_3]$ core bridged to the peripheral cobalt atoms through six chp ligands and one μ_3-hydroxide. The oxygens within the $[Yb_2O_3]$ core are derived from two trinucleating chp ligands and a μ_3-hydroxide. These two chp ligands bridge the two ytterbium atoms through their μ_2-oxygen atom and further bridge to Co1 through their ring nitrogen. The μ_3-hydroxide bridges the two ytterbiums and Co2.

The ytterbium atoms are nine-coordinate bound to three μ_2-oxygen atoms derived from chp groups, the μ_3-hydroxide, two nitrates and a μ-oxygen atom from a binucleating chp. The two cobalt sites are quite distinct. Co2 has a tetrahedral geometry [98.1-117.5°], bound to two nitrogen-donors from chp ligands, and two oxygen-donors : the μ_3-hydroxide and a monodetate nitrate anion. Co2 also has long contacts to the uncoordinated oxygen atom of the nitrate group [Co2...O52N, 2.529(12)Å] and to the two μ-oxygen atoms of the chp ligands

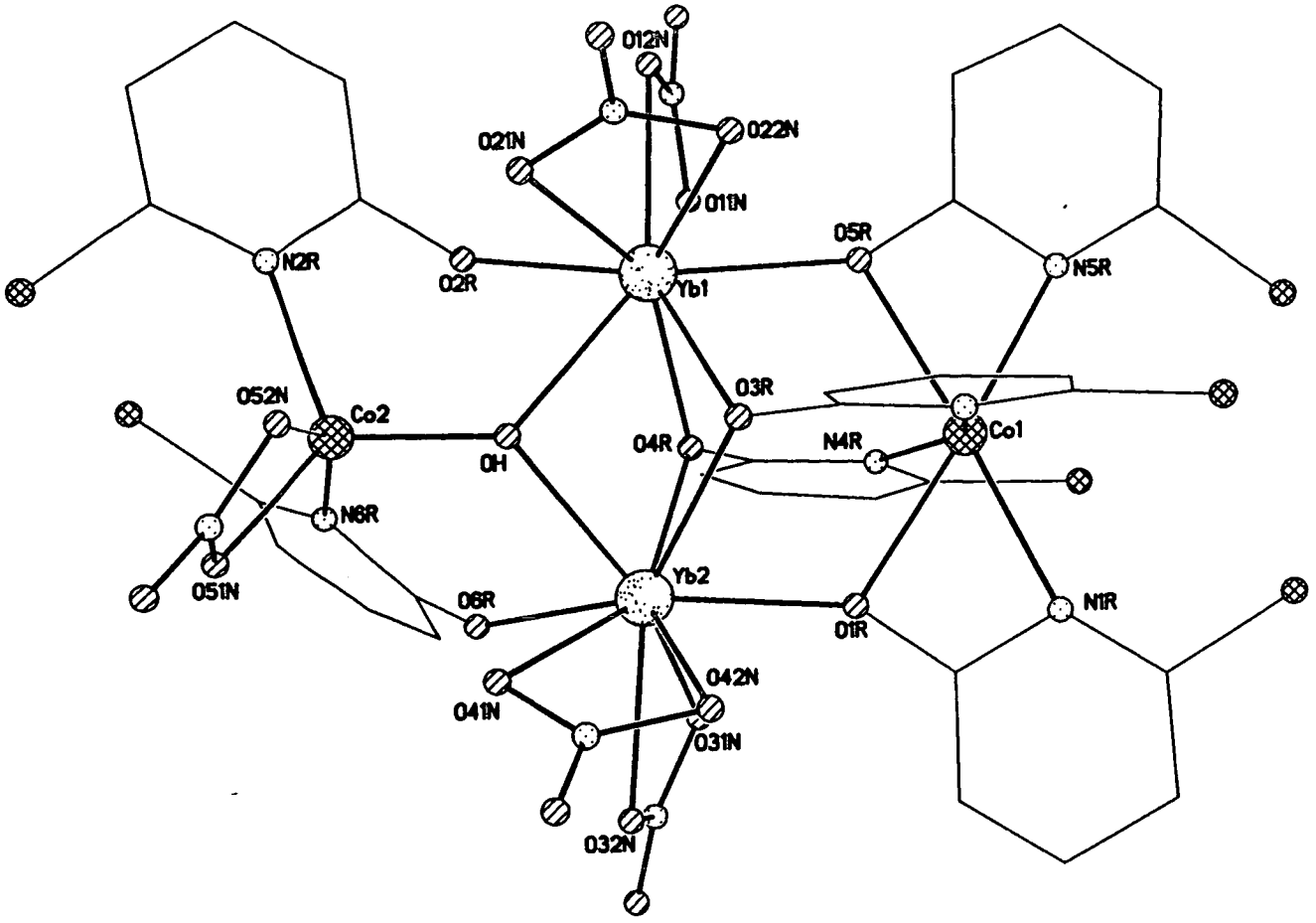

Figure 5.11. The structure of **46** in the crystal.

attached to Co2 [Co2...O2R, 2.614(12)Å; Co2...O6R, 2.779(12)Å]. The second cobalt atom [Co1] is in a distorted octahedral arrangement [*cis*, 61.1-115.1(4)°; *trans*, 152.0-175.8(4)°] binding to both donors of two chelating chp groups and two further nitrogen donors from the pyridonate ligands which supply oxygen donors exclusively to the ytterbium sites. Thus there is one four-coordinate and one six-coordinate cobalt atom within the same structure. The chp ligands in **46** adopt three bonding modes. Binucleating, chelating to one cobalt site through ring nitrogen and exocyclic oxygen atom with the oxygen atom further bridged to one ytterbium atom. Trinucleating, bonding to a cobalt through the ring nitrogen atom while bridging the two ytterbium sites through the oxygen atom. Binucleating, bound to Co2 through the nitrogen donor and ytterbium through the oxygen atom.

The ytterbium-oxygen distances are : 2.231-2.449(11)Å [chp]; 2.287-2.375(11)Å

[OH] and 2.403-2.553(12)Å [NO_3]. The cobalt-oxygen and cobalt-nitrogen bonds are all regular being 1.992-2.230(12)Å and 2.045-2.180(12)Å respectively. The Yb...Yb distance is 3.500(12)Å and the closest Yb...Co distance of 3.741(12)Å is between Co2 and Yb1. Selected bond lengths and angles for **46** are given in Table 5.4. The cage comprising the the four metal centres has an overall 2- charge which is balanced by the presence of two molecules of $[NEt_4]^+$ in the lattice. The closest intermolecular contacts in **46** [Figure 5.12] are between the chlorine atom of a chp group and an oxygen atom of the monodentate nitrate bound to Co2 (the tetrahedral cobalt atom) in one molecule of **46** with two chlorine atoms of chp groups attached to Co1 (the octahedral cobalt atom) in a second molecule of **46** [Cl2A...Cl5C, 3.462(11)Å; O53A...Cl1C, 3.116(11)Å]. The chlorine atom of the second chp group attached to Co2 also has a long contact to a chlorine atom in a chp group attached to a tetrahedral cobalt in a third molecule of **46** [Cl6A...Cl6E, 3.571(12)Å].

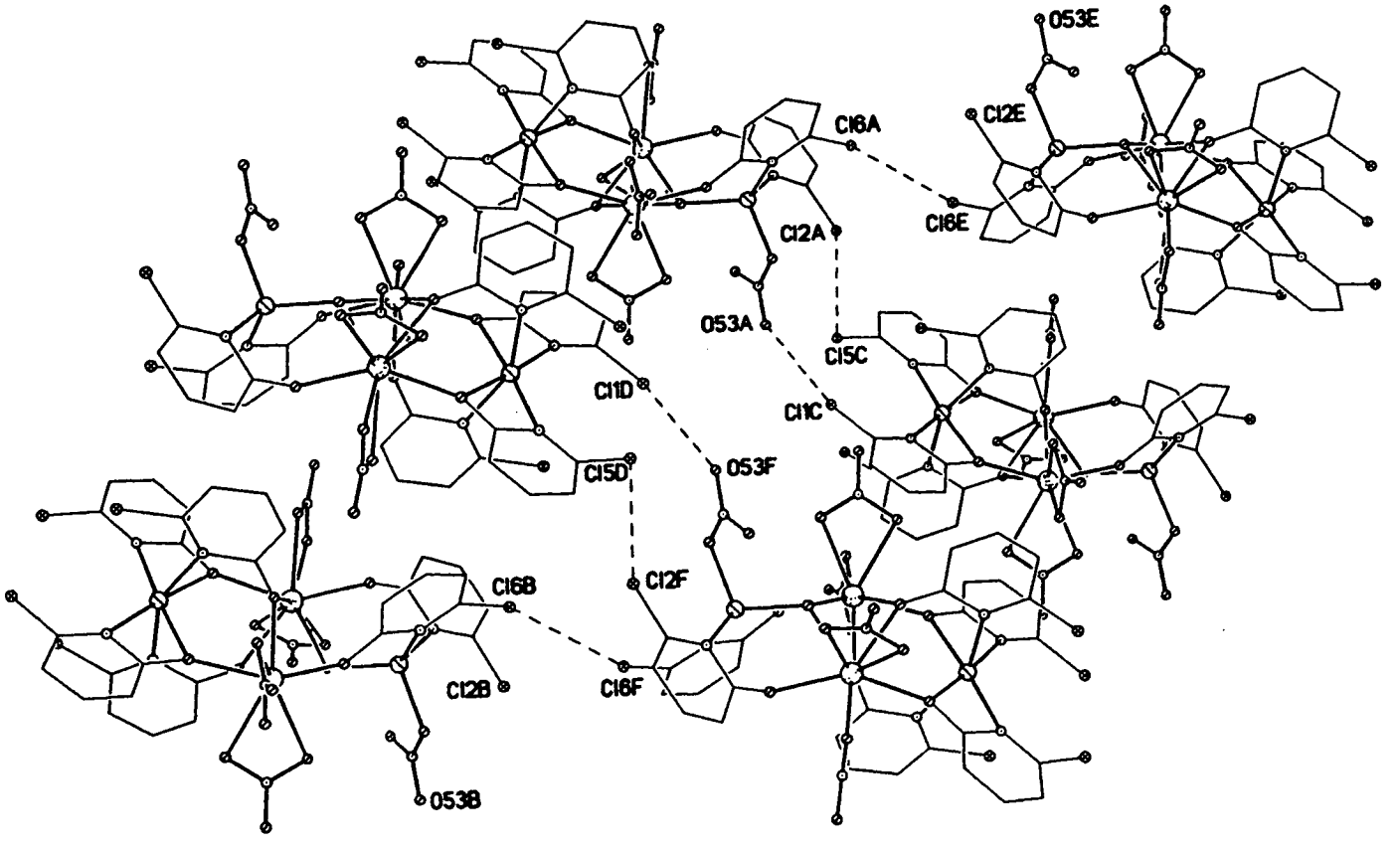

Figure 5.12. The packing of **46** in the crystal.

Table 5.4. Selected bond lengths (Å) and angles (°) for **46**.

Yb1-O2R	2.265(11)	O2R-Yb1-O5R	145.8(4)
Yb1-O5R	2.265(11)	O2R-Yb1-O4R	91.6(4)
Yb1-O4R	2.277(11)	O5R-Yb1-O4R	77.7(4)
Yb1-OH	2.375(10)	O2R-Yb1-OH	71.6(4)
Yb1-O3R	2.400(11)	O5R-Yb1-OH	132.2(4)
Yb1-O12N	2.403(12)	O4R-Yb1-OH	71.8(4)
Yb1-O21N	2.409(11)	O2R-Yb1-O3R	134.6(4)
Yb1-O11N	2.477(11)	O5R-Yb1-O3R	73.7(4)
Yb1-O22N	2.495(12)	O4R-Yb1-O3R	73.9(4)
Yb2-O1R	2.231(10)	OH-Yb1-O3R	63.1(4)
Yb2-O6R	2.239(10)	O2R-Yb1-O12N	78.1(4)
Yb2-O4R	2.276(10)	O5R-Yb1-O12N	85.4(4)
Yb2-OH	2.287(10)	O4R-Yb1-O12N	132.3(4)
Yb2-O32N	2.411(11)	OH-Yb1-O12N	142.0(4)
Yb2-O41N	2.429(13)	O3R-Yb1-O12N	142.4(4)
Yb2-O3R	2.449(10)	O2R-Yb1-O21N	80.2(4)
Yb2-O42N	2.459(12)	O5R-Yb1-O21N	125.4(4)
Yb2-O31N	2.553(12)	O4R-Yb1-O21N	146.6(4)
Co1-N3R	2.131(13)	OH-Yb1-O21N	74.9(4)
Co1-N5R	2.149(13)	O3R-Yb1-O21N	89.0(4)
Co1-N4R	2.172(12)	O12N-Yb1-O21N	77.9(4)
Co1-N1R	2.180(14)	O2R-Yb1-O11N	72.9(4)
Co1-O5R	2.213(11)	O5R-Yb1-O11N	73.2(4)
Co1-O1R	2.230(11)	O4R-Yb1-O11N	78.5(4)
Co2-OH	1.992(10)	OH-Yb1-O11N	132.3(4)
Co2-O51N	2.028(12)	O3R-Yb1-O11N	140.5(4)
Co2-N2R	2.045(14)	O12N-Yb1-O11N	53.9(4)
Co2-N6R	2.052(14)	O21N-Yb1-O11N	128.1(4)

Table 5.4 continued

O2R-Yb1-O22N	126.0(4)	O41N-Yb2-O3R	96.4(4)
O5R-Yb1-O22N	73.9(4)	O1R-Yb2-O41N	76.2(4)
O4R-Yb1-O22N	141.8(4)	O6R-Yb2-O41N	129.8(4)
OH-Yb1-O22N	110.4(4)	O4R-Yb2-O42N	145.9(4)
O3R-Yb1-O22N	74.0(4)	OH-Yb2-O42N	109.5(4)
O12N-Yb1-O22N	70.2(4)	O32N-Yb2-O42N	70.0(4)
O21N-Yb1-O22N	51.5(4)	O41N-Yb2-O42N	52.3(4)
O11N-Yb1-O22N	116.0(4)	O3R-Yb2-O42N	78.3(4)
O1R-Yb2-O6R	140.0(4)	O1R-Yb2-O31N	72.0(4)
O1R-Yb2-O4R	77.8(4)	O6R-Yb2-O31N	69.7(4)
O6R-Yb2-O4R	84.1(4)	O4R-Yb2-O31N	79.5(4)
O1R-Yb2-OH	132.2(4)	OH-Yb2-O31N	136.0(4)
O6R-Yb2-OH	73.5(4)	O32N-Yb2-O31N	52.2(4)
O4R-Yb2-OH	73.4(4)	O41N-Yb2-O31N	122.6(4)
O1R-Yb2-O32N	89.8(4)	O3R-Yb2-O31N	138.3(4)
O6R-Yb2-O32N	76.0(4)	O42N-Yb2-O31N	112.4(4)
O4R-Yb2-O32N	131.5(4)	N3R-Co1-N5R	99.1(5)
OH-Yb2-O32N	137.6(4)	N3R-Co1-N4R	152.0(5)
O1R-Yb2-O41N	128.5(4)	N5R-Co1-N4R	95.5()5
O6R-Yb2-O41N	83.2(4)	N3R-Co1-N1R	95.5(5)
O4R-Yb2-O41N	148.0(4)	N5R-Co1-N1R	122.8(5)
OH-Yb2-O41N	74.9(4)	N4R-Co1-N1R	96.5(5)
O32N-Yb2-O41N	72.9(4)	N3R-Co1-O5R	81.6(4)
O1R-Yb2-O3R	72.0(4)	N5R-Co1-O5R	61.1(4)
O6R-Yb2-O3R	135.4(4)	N4R-Co1-O5R	84.8(4)
O4R-Yb2-O3R	72.9(4)	N1R-Co1-O5R	175.7(4)
OH-Yb2-O3R	63.5(4)	N3R-Co1-O1R	82.2(4)
O32N-Yb2-O3R	146.5(4)	N5R-Co1-O1R	175.8(5)

Table 5.4 continued

N4R-Co1-O1R	81.7(4)	N2R-Co2-N6R	107.8(5)
N1R-Co1-O1R	60.8(4)	Co2-OH-Yb2	122.4(5)
O5R-Co1-O1R	115.4(4)	Co2-OH-Yb1	117.6(5)
OH-Co2-O51N	108.5(5)	Yb2-OH-Yb1	97.3(4)
OH-Co2-N2R	111.2(5)	Co1-O1R-Yb2	119.8(5)
O51N-Co2-N2R	117.5(6)	Yb1-O3R-Yb2	92.4(3)
OH-Co2-N6R	113.3(5)	Yb2-O4R-Yb1	100.4(4)
O51N-Co2-N6R	98.1(5)	Co1-O5R-Yb1	118.0(5)

5.2.9. Synthesis and structure of $[NEt_4]_2[Co_2Dy_2(OH)(chp)_6(NO_3)_5]$ 47 and $[NEt_4]_2[Co_2Gd_2(OH)(chp)_6(NO_3)_5]$ 48.

In an identical procedure to **46** two further heterobimetallic complexes $[NEt_4]_2$ $[Co_2Dy_2(OH)\ (chp)_6(NO_3)_5]$ **47** [Figure 5.13] and $[NEt_4]_2[Co_2Gd_2(OH)(chp)_6(NO_3)_5]$ **48** [Figure 5.14] were synthesised. Their structures are the same as the ytterbium analogue. Selected bond lengths and angles for the two compounds are given in Tables 5.5 and 5.6 respectively. Compound **47** contains a lanthanide [Dy] which is larger than ytterbium and compound **48** contains a lanthanide [Gd] which is larger than dysprosium.This change in the lanthanide is reflected in the lanthanide-oxygen bond lengths present in the three compounds, with the bonds to the ytterbium atom in **46** being the shortest and the bonds to the gadolinium atom in **48** being the longest. For **47** the dysprosium-oxygen distances are : Dy-O(chp), 2.264-2.414(12)Å; Dy-O(OH), 2.370-2.410(10)Å and Dy-O(NO_3), 2.429-2.537(12)Å, and for **48** the gadolinium-oxygen bonds are : Gd-O(chp), 2.26-2.44(6)Å; Gd-O(OH), 2.39-2.48(6)Å and Gd-O(NO_3), 2.41-2.56(2)Å. This trend is also reflected in the metal...metal contacts in **46-48**. In **46** the closest Yb...Yb and Yb...Co distances were 3.500(12)Å and 3.741(12)Å respectively. The equivalent distances in **47** and **48** are 3.568(10)Å [Dy...Dy], 3.698(10)Å

[Dy...Co] and 3.618(9)Å [Gd...Gd] and 3.803(9)Å [Gd...Co].

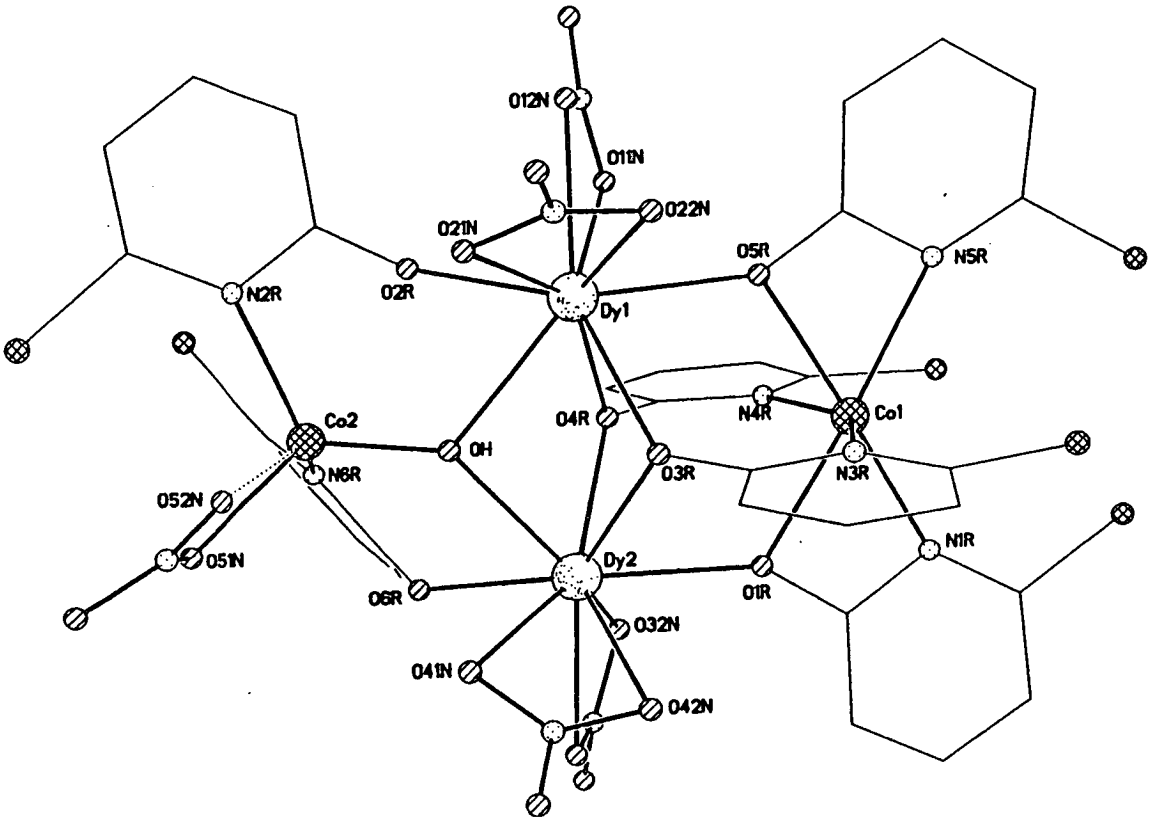

Figure 5.13. The structure of **47** in the crystal.

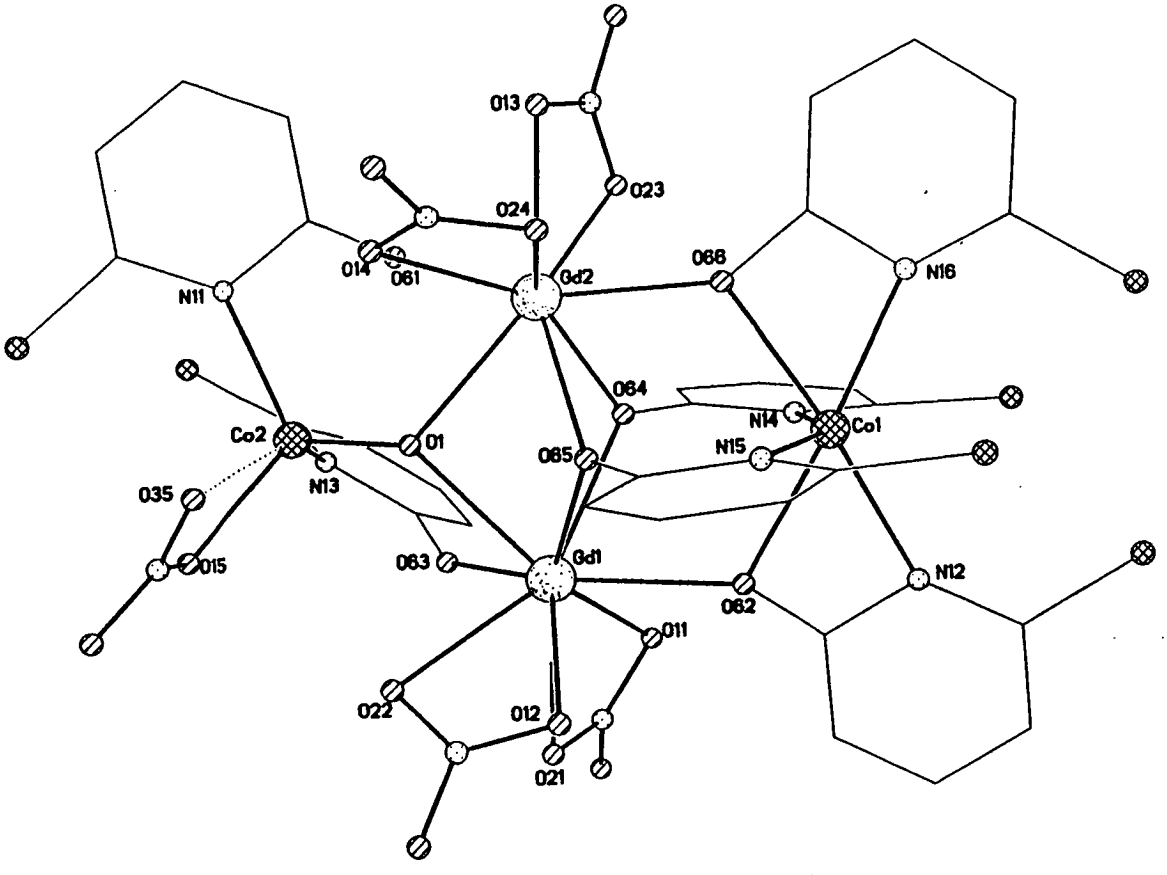

Figure 5.14. The structure of **48** in the crystal.

[The crystal quality of **48** was poor. This has led to a marked increase in the errors associated with the bond lengths, and in particular the bond angles in the structure].

Table 5.5. Selected bond lengths (Å) and angles (°) for **47**.

Dy1-O5R	2.264(11)	Co2-N6R	2.058(15)
Dy1-O2R	2.315(11)	Co2-N2R	2.070(13)
Dy1-O4R	2.325(10)	O5R-Dy1-O2R	143.2(4)
Dy1-OH	2.370(10)	O5R-Dy1-O4R	78.0(3)
Dy1-O3R	2.401(11)	O2R-Dy1-O4R	88.1(4)
Dy1-O21N	2.429(11)	O5R-Dy1-OH	134.6(4)
Dy1-O12N	2.478(10)	O2R-Dy1-OH	69.7(4)
Dy1-O22N	2.491(12)	O4R-Dy1-OH	72.6(4)
Dy1-O11N	2.537(12)	O5R-Dy1-O3R	73.8(4)
Dy2-O1R	2.291(11)	O2R-Dy1-O3R	134.7(4)
Dy2-O6R	2.319(12)	O4R-Dy1-O3R	73.9(4)
Dy2-O4R	2.391(12)	OH-Dy1-O3R	65.3(4)
Dy2-OH	2.410(10)	O5R-Dy1-O21N	125.6(4)
Dy2-O3R	2.414(10)	O2R-Dy1-O21N	82.6(4)
Dy2-O41N	2.433(14)	O4R-Dy1-O21N	148.1(4)
Dy2-O31N	2.469(12)	OH-Dy1-O21N	75.5(4)
Dy2-O42N	2.492(14)	O3R-Dy1-O21N	91.3(4)
Dy2-O32N	2.510(13)	O5R-Dy1-O12N	86.1(4)
Co1-N1R	2.142(14)	O2R-Dy1-O12N	76.6(4)
Co1-N3R	2.17(2)	O4R-Dy1-O12N	129.1(4)
Co1-N4R	2.180(14)	OH-Dy1-O12N	139.3(4)
Co1-N5R	2.203(15)	O3R-Dy1-O12N	145.9(4)
Co1-O1R	2.206(11)	O21N-Dy1-O12N	78.1(4)
Co1-O5R	2.207(10)	O5R-Dy1-O22N	73.8(4)
Co2-OH	1.960(11)	O2R-Dy1-O22N	127.5(4)
Co2-O51N	2.034(13)	O4R-Dy1-O22N	144.4(4)

Table 5.5 continued

OH-Dy1-O22N	113.8(4)	O6R-Dy2-O31N	76.1(4)
O3R-Dy1-O22N	77.6(4)	O4R-Dy2-O31N	130.9(4)
O21N-Dy1-O22N	51.8(4)	OH-Dy2-O31N	140.0(4)
O12N-Dy1-O22N	70.3(4)	O3R-Dy2-O31N	145.9(4)
O5R-Dy1-O11N	72.3(4)	O41N-Dy2-O31N	81.2(5)
O2R-Dy1-O11N	71.5(4)	O1R-Dy2-O42N	76.8(5)
O4R-Dy1-O11N	77.8(4)	O6R-Dy2-O42N	127.7(5)
OH-Dy1-O11N	131.4(4)	O4R-Dy2-O42N	145.2(4)
O3R-Dy1-O11N	139.4(4)	OH-Dy2-O42N	112.9(4)
O21N-Dy1-O11N	126.7(4)	O3R-Dy2-O42N	78.3(4)
O12N-Dy1-O11N	51.3(4)	O41N-Dy2-O42N	51.5(5)
O22N-Dy1-O11N	112.8(4)	O31N-Dy2-O42N	70.0(5)
O1R-Dy2-O6R	141.7(4)	O1R-Dy2-O32N	71.3(4)
O1R-Dy2-O4R	76.2(4)	O6R-Dy2-O32N	71.8(4)
O6R-Dy2-O4R	86.9(4)	O4R-Dy2-O32N	79.0(4)
O1R-Dy2-OH	130.7(4)	OH-Dy2-O32N	133.3(4)
O6R-Dy2-OH	71.8(4)	O3R-Dy2-O32N	137.2(4)
O4R-Dy2-OH	70.8(4)	O41N-Dy2-O32N	131.3(5)
O1R-Dy2-O3R	71.3(4)	O31N-Dy2-O32N	52.1(4)
O6R-Dy2-O3R	135.7(4)	O42N-Dy2-O32N	112.3(5)
O4R-Dy2-O3R	72.5(4)	N1R-Co1-N3R	95.5(6)
OH-Dy2-O3R	64.5(4)	N1R-Co1-N4R	97.7(5)
O1R-Dy2-O41N	127.6(4)	N3R-Co1-N4R	149.6(5)
O6R-Dy2-O41N	85.5(4)	N1R-Co1-N5R	122.9(5)
O4R-Dy2-O41N	143.6(4)	N3R-Co1-N5R	96.1(5)
OH-Dy2-O41N	73.0(4)	N4R-Co1-N5R	99.4(5)
O3R-Dy2-O41N	88.7(5)	N1R-Co1-O1R	61.1(5)
O1R-Dy2-O31N	89.3(4)	N3R-Co1-O1R	78.7(5)

Table 5.5 continued

N4R-Co1-O1R	84.0(5)	OH-Co2-N2R	111.3(5)
N5R-Co1-O1R	173.9(5)	O51N-Co2-N2R	108.6(5)
N1R-Co1-O5R	176.7(5)	N6R-Co2-N2R	111.8(6)
N3R-Co1-O5R	82.4(50	Co2-OH-Dy1	117.0(5)
N4R-Co1-O5R	83.0(5)	Co2-OH-Dy2	119.4(5)
N5R-Co1-O5R	60.0(5)	Dy1-OH-Dy2	96.6(5)
O1R-Co1-O5R	115.8(4)	Co1-O1R-Dy2	120.7(5)
OH-Co2-O51N	115.0(5)	Dy1-O3R-Dy2	95.6(4)
OH-Co2-N6R	114.4(5)	Dy1-O4R-Dy2	98.3(4)
O51N-Co2-N6R	94.7(5)	Co1-O5R-Dy1	118.7(5)

Table 5.6. Selected bond lengths (Å) and angles (°) for **48**.

Gd1-O63	2.35(6)	Gd2-O14	2.47(2)
Gd1-O62	2.41(7)	Gd2-O24	2.54(2)
Gd1-O65	2.43(6)	Co1-N14	2.15(5)
Gd1-O64	2.43(6)	Co1-N16	2.16(5)
Gd1-O12	2.46(2)	Co1-N12	2.17(6)
Gd1-O1	2.48(6)	Co1-O62	2.21(6)
Gd1-O22	2.51(2)	Co1-N15	2.24(5)
Gd1-O21	2.53(2)	Co1-O66	2.26(6)
Gd1-O11	2.56(2)	Co2-O1	1.95(6)
Gd2-O66	2.26(7)	Co2-O15	2.03(2)
Gd2-o64	2.37(6)	Co2-N11	2.11(5)
Gd2-O1	2.39(6)	Co2-N13	2.23(5)
Gd2-O13	2.41(2)	O63-Gd1-O62	142(2)
Gd2-O65	2.42(6)	O63-Gd1-O65	132(2)
Gd2-O61	2.44(2)	O62-Gd1-O65	69(2)
Gd2-O23	2.45(2)	O63-Gd1-O64	82(2)

Table 5.6 continued

O62-Gd1-O64	77(2)	O22-Gd1-O11	120.4(7)
O65-Gd1-O64	70(2)	O64-Gd1-O11	81(2)
O63-Gd1-O12	131(2)	O12-Gd1-O11	107.7(6)
O62-Gd1-O12	75(2)	O21-Gd1-O11	50.4(3)
O65-Gd1-O12	83(2)	O66-Gd2-O64	76(2)
O64-Gd1-O12	147(2)	O66-Gd2-O1	134(2)
O63-Gd1-O1	73(2)	O64-Gd2-O1	76(2)
O62-Gd1-O1	129(2)	O66-Gd2-O13	86(2)
O65-Gd1-O1	63(2)	O64-Gd2-O13	130(2)
O64-Gd1-O1	73(2)	O1-Gd2-O13	140(2)
O12-Gd1-O1	113(2)	O66-Gd2-O65	72(2)
O63-Gd1-O22	86(2)	O64-Gd2-O65	72(2)
O62-Gd1-O22	126(2)	O1-Gd2-O65	64(2)
O65-Gd1-O22	99(2)	O13-Gd2-O65	145(2)
O64-Gd1-O22	150(2)	O66-Gd2-O61	148(2)
O12-Gd1-O22	51.6(4)	O64-Gd2-O61	95(2)
O1-Gd1-O22	77(2)	O1-Gd2-O61	71(2)
O63-Gd1-O21	76(2)	O13-Gd2-O61	77(2)
O62-Gd1-O21	94(2)	O65-Gd2-O61	13592)
O65-Gd1-O21	151(2)	O66-Gd2-O23	75(2)
O64-Gd1-O21	131(2)	O64-Gd2-O23	77(2)
O12-Gd1-O21	68.9(5)	O1-Gd2-O23	132(2)
O1-Gd1-O21	136(2)	O13-Gd2-O23	52.9(4)
O22-Gd1-O21	71.3(5)	O65-Gd2-O23	139(2)
O63-Gd1-O11	70(2)	O61-Gd2-O23	73(2)
O62-Gd1-O11	75(2)	O66-Gd2-O14	12(2)
O65-Gd1-O11	138(2)	O64-Gd2-O14	150(2)
O1-Gd1-O11	137(2)	O1-Gd2-O14	74(2)

Table 5.6 continued

O13-Gd2-O14	76.7(5)	N12-Co1-N15	97(2)
O65-Gd2-O14	94(2)	O62-Co1-N15	81(2)
O61-Gd2-O14	76(2)	N14-Co1-O66	82(2)
O23-Gd2-O14	125.3(7)	N16-Co1-O66	59(3)
O66-Gd2-O24	76(2)	N12-Co1-O66	175(3)
O64-Gd2-O24	141(2)	O62-Co1-O66	117(2)
O1-Gd2-O24	107(2)	N15-Co1-O66	81(2)
O13-Gd2-O24	72.5(5)	O1-Co2-O15	111(2)
O65-Gd2-O24	76(2)	O1-Co2-N11	108(3)
O61-Gd2-O24	123(2)	O15-Co2-N11	117(2)
O23-Gd2-O24	118.4(6)	O1-Co2-N13	121(3)
O14-Gd2-O24	51.1(4)	O15-Co2-N13	96(2)
N14-Co1-N16	97(2)	N11-Co2-N13	104(3)
N14-Co1-N12	97(2)	Co2-O1-Gd2	121(3)
N16-Co1-N12	126(3)	Co2-O1-Gd1	118(3)
N14-Co1-O62	81(2)	Gd2-O1-Gd1	96(2)
N16-Co1-O62	176(3)	Co1-O62-Gd1	118(3)
N12-Co1-O62	58(3)	Gd2-O64-Gd1	98(2)
N14-Co1-N15	147(3)	Gd2-O65-Gd1	97(2)
N16-Co1-N15	98(2)	Co1-O66-Gd2	120(3)

5.2.10. Synthesis and structure of $[NEt_4]_2[CoNd_2(chp)_5(NO_3)_5]$ 49 and $[NEt_4]_2$ $[CoSm_2(chp)_5(NO_3)_5]$ 50.

Reaction of $[NEt_4]_2[Co(chp)_4]$ **45** with neodymium nitrate in a 1:1 methanol / dichloromethane mixture produced a pink solution which was filtered and evaporated to dryness. Extraction with dichloromethane gave pink crystals of $[NEt_4]_2[CoNd_2(chp)_5(NO_3)_5]$

49 [Figure 5.15] in moderate yield after four days. This procedure is identical to that which produced compounds **46-48**. The structure of **49** is similar to these compounds but contains only one cobalt atom as oppose to the two present in **46-48**. **49** contains a $[Nd_2O_3]$ core linked to one cobalt centre *via* four pyridonate ligands. Two of these chp ligands bridge the two neodymium atoms through their exocyclic oxygen atom and bridge to the cobalt centre through their ring nitrogen. The coordination of the cobalt atom is completed by two additional chp ligands which chelate to the cobalt with the exocyclic oxygen atom further bridged to one of the neodymiums. The ligation of this cobalt centre to the lanthanide core is identical to that present in **46-48**. The cobalt thus has four nitrogen and two oxygen-donors, all derived from chp ligands, arranged in a distorted octahedral fashion [*cis*, 60.4-121.6(3)°; *trans*, 147.8-176.5(3)°]. The third chp group, which chelates to one neodymium [Nd] with the oxygen atom further bridged to the second neodymium [NdA], has only 50% occupancy. The second 50% of the time a nitrate group is bound to the neodymium [Nd] through both oxygen

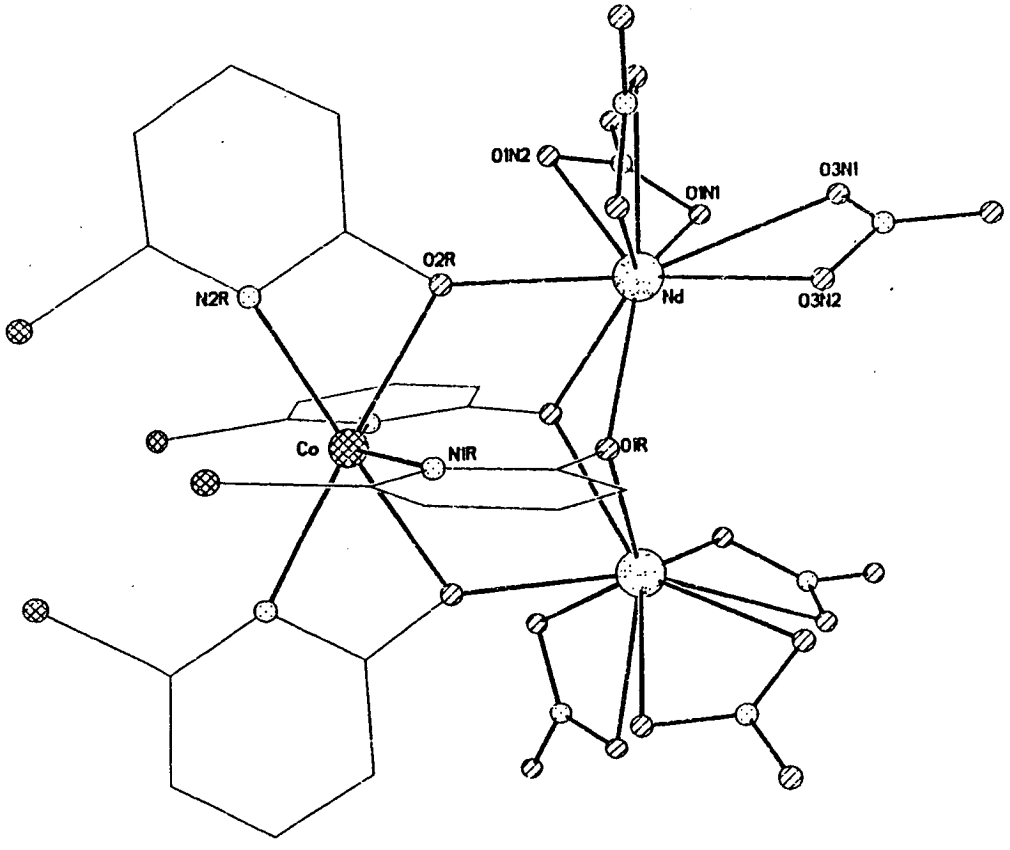

Figure 5.15. The structure of **49** in the crystal.

atoms but does not bind to the second neodymium [NdA]. Thus when the pyridonate ligand is present the two neodymium atoms are distinct : Nd is nine-coordinate with its geometry completed by two further molecules of nitrate, and NdA is ten-coordinate - its geometry completed by three molecules of nitrate. When the nitrate anion rather than the chp group is present the molecule gains symmetry and the two lanthanides become equivalent, both atoms having their coordinations completed by three molecules of nitrate.

The chp ligands adopt three coordinating modes. Trinucleating, chelating to the cobalt and bridging to one neodymium through the exocyclic oxygen atom. Bridging the two neodymium atoms through the oxygen atom and bridging to the cobalt atom through the ring nitrogen, and finally chelating to one neodymium and bridging to the second through the exocyclic oxygen atom. The cobalt-oxygen and cobalt-nitrogen bonds are all regular, being 2.230(6)Å and 2.159-2.179(6)Å respectively. The neodymium-oxygen distances are : 2.338-2.478(7)Å [chp] and 2.552-2.579(7)Å [NO_3] with the Nd...N distance being 2.510(8)Å. The Nd...Nd distance is 3.735(6)Å with the Nd...Co distance 3.956(6)Å in length. These distances are all longer than the equivalent distances in **46-48**, which is unsurprising given that neodymium is a larger lanthanide. Selected bond lengths and angles for **49** are given in Table 5.7.

$[NEt_4]_2[CoSm_2(chp)_5(NO_3)_5]$ **50** was made by an identical procedure to **46-49**. Its structure [Figure 5.16] is analogous to the neodymium complex **49**. Selected bond lengths and angles are given in Table 5.8. However whereas **49** contained a half-occupancy chp ligand and a half-occupancy nitrate ligand, **50** contains only the pyridonate ligand. Thus the two samarium atoms are distinct. Sm1 is ten-coordinate, bound to four μ_2-oxygen atoms derived from bi- and trinucleating chp ligands and three nitrate anions. Sm2 is nine-coordinate bound to three μ_2-oxygens from chp ligands, two nitrates and the chelating pyridonate ligand. The

coordination of the cobalt atom is identical to **49**. Samarium is a smaller lanthanide than neodymium and this is reflected in the bond lengths to the metal site, which in general are smaller than the equivalent distances in **49** : 2.285-2.508(7)Å [chp]; 2.467-2.626(7)Å [NO_3] and 2.542(7)Å [N-chp]. The Sm...Sm distance is 3.682(7)Å with the average Sm...Co distance being 3.804(8)Å. The cobalt-oxygen and cobalt-nitrogen bonds are again regular being 1.917(6)Å and 1.978-2.206(6)Å respectively. There are no significant intermolecular interactions in either **49** or **50**.

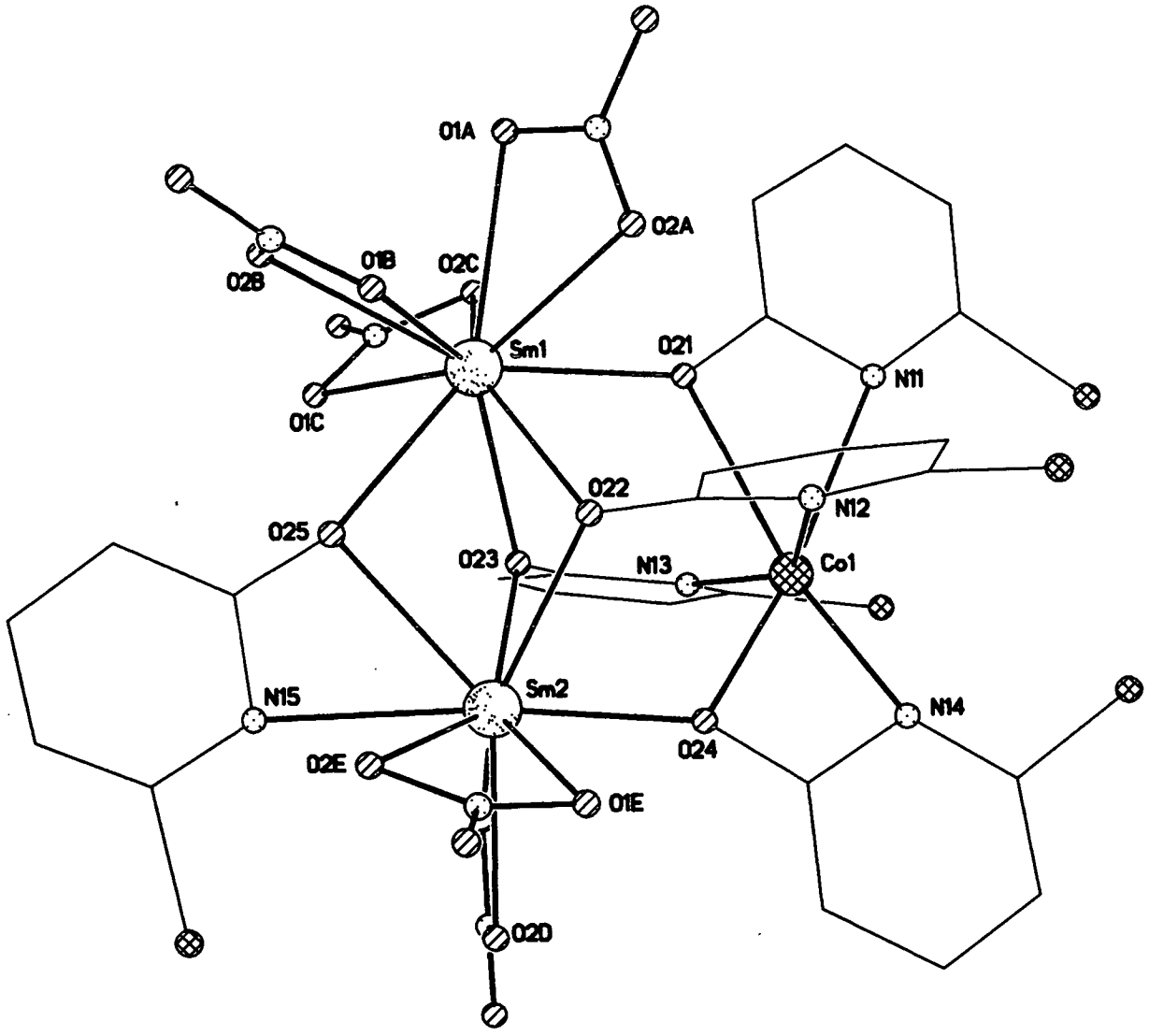

Figure 5.16. The structure of **50** in the crystal.

Table 5.7. Selected bond lengths (Å) and angles (°) for **49**.

Nd-O1R	2.432(7)	O2R-Nd-O1N1	118.9(2)
Nd-O1RA	2.478(7)	O3R-Nd-O1N1	77.9(5)
Nd-O2R	2.338(5)	O1RA-Nd-O1N1	80.3(3)
Nd-O3R	2.382(11)	N3R-Nd-O1N1	79.8(4)
Nd-N3R	2.510(8)	O1R-Nd-O1N2	143.3(2)
Nd-O1N1	2.566(6)	O2R-Nd-O1N2	74.0(2)
Nd-O1N2	2.552(6)	O3R-Nd-O1N2	123.3(5)
Nd-O2N1	2.557(6)	O1RA-Nd-O1N2	82.5(2)
Nd-O2N2	2.557(6)	N3R-Nd-O1N2	120.2(3)
Nd-O3N1	2.579(7)	O1R-Nd-O2N1	75.3(2)
Nd-O3N2	2.576(7)	O2R-Nd-O2N1	74.0(3)
Co-N1R	2.159(6)	O3R-Nd-O2N1	121.8(5)
Co-N1RA	2.159(6)	O1RA-Nd-O2N1	135.8(3)
Co-N2R	2.179(6)	N3R-Nd-O2N1	87.0(4)
Co-N2RA	2.179(6)	O1R-Nd-O2N2	124.3(2)
Co-O2R	2.230(6)	O2R-Nd-O2N2	85.9(3)
Co-O2RA	2.230(6)	O3R-Nd-O2N2	139.9(3)
O1R-Nd-O1RA	69.9(2)	O1RA-Nd-O2N2	149.3(3)
O2R-Nd-O1R	74.6(2)	N3R-Nd-O2N2	86.0(3)
O2R-Nd-O1RA	71.3(2)	O1R-Nd-O3N1	120.6(3)
O3R-Nd-O1R	68.7(4)	O2R-Nd-O3N1	158.6(3)
O3R-Nd-O1RA	68.7(4)	O1RA-Nd-O3N1	126.4(3)
O1R-Nd-N3R	95.3(3)	O1R-Nd-O3N2	77.3(3)
O1RA-Nd-N3R	121.9(2)	O2R-Nd-O3N2	131.9(3)
O2R-Nd-O3R	132.6(3)	O1RA-Nd-O3N2	131.8(3)
O2R-Nd-N3R	160.1(4)	O1N2-Nd-O1N1	49.0(2)
O3R-Nd-N3R	54.0(2)	O2N1-Nd-O2N2	49.2(2)
O1R-Nd-O1N1	141.2(3)	O3N2-Nd-O3N1	48.6(2)

Table 5.7 continued

O2N1-Nd-O1N1	141.7(3)	N1RA-Co-N2R	94.2(4)
O2N2-Nd-O1N1	93.9(3)	N1RA-Co-N2RA	101.4(4)
O1N2-Nd-O2N1	113.1(2)	N2RA-Co-N2R	121.6(3)
O1N2-Nd-O2N2	71.4(3)	N1R-Co-O2R	82.6(3)
O1N2-Nd-O3N2	139.0(3)	N1R-Co-O2RA	81.0(3)
O2N1-Nd-O3N2	61.5(4)	N1RA-Co-O2R	81.0(3)
O2N2-Nd-O3N2	78.8(4)	N1RA-Co-O2RA	82.6(3)
O1N1-Nd-O3N2	107.5(3)	N2R-Co-O2R	60.4(2)
O1N2-Nd-O3N1	95.0(3)	N2R-Co-O2RA	176.5(3)
O2N1-Nd-O3N1	94.5(4)	N2RA-Co-O2R	176.5(3)
O2N2-Nd-O3N1	73.1(4)	N2RA-Co-O2RA	60.4(2)
O1N1-Nd-O3N1	60.2(3)	O2RA-Co-O2R	117.8(3)
N1R-Co-N1RA	147.8(3)	Nd-O1R-NdA	99.0(2)
N1R-Co-N2R	101.4(4)	Co-O2R-Nd	119.9(3)
N1R-Co-N2RA	94.2(4)	Nd-O3R-NdA	99.3(3)

Table 5.8. Selected bond lengths (Å) and angles (°) for **50**.

Sm1-O1A	2.541(7)	Sm2-O2D	2.467(6)
Sm1-O2A	2.626(7)	Sm2-O1E	2.521(7)
Sm1-O1B	2.556(7)	Sm2-O2E	2.486(7)
Sm1-O2B	2.546(8)	Sm2-O22	2.448(7)
Sm1-O1C	2.587(7)	Sm2-O23	2.386(7)
Sm1-O2C	2.535(8)	Sm2-O24	2.285(7)
Sm1-O21	2.377(7)	Sm2-O25	2.487(7)
Sm1-O22	2.423(7)	Sm2-N15	2.542(7)
Sm1-O23	2.508(6)	Co1-N12	2.106(6)
Sm1-O25	2.408(6)	Co1-N13	2.206(6)
Sm2-O1D	2.532(6)	Co1-N14	1.978(6)

Table 5.8 continued

Co1-O24	1.917(6)	O2B-Sm1-O2C	91.1(3)
Co1-N11	1.978(6)	O2B-Sm1-O21	153.7(3)
Co1-O21	1.901(7)	O2B-Sm1-O22	126.1(3)
O1A-Sm1-O2A	49.8(3)	O2B-Sm1-O23	131.1(3)
O1A-Sm1-O1B	74.1(3)	O2B-Sm1-O25	75.8(3)
O1A-Sm1-O2B	69.1(3)	O1C-Sm1-O2C	49.6(2)
O1A-Sm1-O1C	102.6(3)	O1C-Sm1-o21	113.6(2)
O1A-Sm1-O2C	71.5(3)	O1C-Sm1-O22	134.5(2)
O1A-Sm1-O21	85.6(2)	O1C-Sm1-O23	71.7(2)
O1A-Sm1-O22	122.9(2)	O1C-Sm1-O25	74.6(3)
O1A-Sm1-O23	147.3(2)	O2C-Sm1-O21	73.5(4)
O1A-Sm1-O25	142.5(2)	O2CSm1-O22	142.5(4)
O2A-Sm1-O1B	65.1(2)	O2C-Sm1-O23	81.6(3)
O2A-Sm1-O2B	98.9(2)	O2C-Sm1-O25	122.9(2)
O2A-Sm1-O1C	152.3(2)	O21-Sm1-O22	73.6(3)
O2A-Sm1-O2C	109.9(3)	O21-Sm1-O23	68.8(3)
O2A-Sm1-O21	68.0(2)	O21-Sm1-O25	130.5(2)
O2A-Sm1-O22	73.2(3)	O22-Sm1-O23	70.0(2)
O2A-Sm1-O23	129.2(3)	O22-Sm1-O25	69.2(2)
O2A-Sm1-O25	126.9(3)	O23-Sm1-O25	68.6(2)
O1B-Sm1-O2B	49.4(5)	O1D-Sm2-O2D	52.0(2)
O1B-Sm1-O1C	113.7(2)	O1D-Sm2-O1E	125.3(2)
O1B-Sm1-O2C	135.1(3)	O1D-Sm2-O2E	127.3(3)
O1B-Sm1-O21	131.4(2)	O1D-Sm2-O22	140.1(3)
O1B-Sm1-O22	81.3(2)	O1D-Sm2-O23	72.6(3)
O1B-Sm1-O23	138.3(2)	O1D-Sm2-O24	79.7(4)
O1B-Sm1-O25	73.2(2)	O1D-Sm2-N15	76.7(4)
O2B-Sm1-O1C	67.3(3)	O1D-Sm2-O25	114.5(2)

Table 5.8 continued

O2D-Sm2-O1E	76.0(4)	O23-Sm2-O25	69.3(4)
O2D-Sm2-O2E	85.1(2)	O24-Sm2-N15	155.6(3)
O2D-Sm2-O22	150.7(3)	O24-Sm2-O25	135.4(3)
O2D-Sm2-O23	123.7(3)	N15-Sm2-O25	53.0(3)
O2D-Sm2-O24	84.1(3)	N11-Co1-O21	52.4(3)
O2D-Sm2-N15	86.4(3)	N11-Co1-N12	91.3(3)
O2D-Sm2-O25	138.9(3)	N11-Co1-N13	83.3(3)
O1E-Sm2-O2E	50.9(3)	N11-Co1-N14	115.8(4)
O1E-Sm2-O22	79.8(4)	N11-Co1-O24	170.8(4)
O1E-Sm2-O23	146.3(3)	O21-Co1-N12	77.0(3)
O1E-Sm2-O24	79.3(3)	O21-Co1-N13	75.4(3)
O1E-Sm2-N15	120.0(3)	O21-Co1-N14	168.1(3)
O1E-Sm2-O25	115.9(3)	O21-Co1-O24	121.5(3)
O2E-Sm2-O22	92.4(3)	N12-Co1-N13	148.7(3)
O2E-Sm2-O23	145.4(3)	N12-Co1-N14	103.6(3)
O2E-Sm2-O24	130.2(2)	N12-Co1-O24	93.7(3)
O2E-Sm2-N15	71.0(2)	N13-Co1-N14	106.5(3)
O2E-Sm2-O25	76.3(3)	N13-Co1-O24	93.7(3)
O22-Sm2-O23	71.7(3)	N14-Co1-O24	70.4(3)
O22-Sm2-O24	75.3(3)	Co1-O24-Sm2	119.5(2)
O22-Sm2-N15	120.3(2)	Co1-O21-Sm1	129.4(2)
O22-Sm2-O25	67.5(4)	Sm1-O25-Sm2	97.5(3)
O23-Sm2-O24	76.4(4)	Sm1-O22-Sm2	98.2(3)
O23-Sm2-N15	90.4(4)	Sm1-O23-Sm2	97.6(3)

Compounds **46-50** were all synthesised *via* the same procedure. Thus the structural difference observed between compounds **46-48** and **49-50** (i.e. the loss of one cobalt atom) must be a result of the change in size of the lanthanide. The complexes of the smaller lanthanides [Yb, **47**; Dy, **46** and Gd, **48**] contain two cobalt atoms in their structure, while the complexes of the larger lanthanides [Sm, **50** and Nd, **49**] contain only one cobalt in their structure. The lanthanide contraction is also clearly observed with the bonds to the lanthanide centres shortest for ytterbium and largest for neodymium. This trend is also established in the metal...metal contacts observed in **46-50**. This is summarised in Table 5.9. The lanthanides in compounds **46-48** are bound exclusively to oxygen donors and in compounds **49** and **50** they are bound to only one non-oxygen donor, reflecting the lanthanides preference for 'hard' donor atoms.

Table 5.9. A summary of the bond lengths (Å) to the lanthanide centres in **46-50**.

	Yb	**Dy**	**Gd**	**Sm**	**Nd**
O(chp)	2.231-2.449	2.26-2.41	2.26-2.44	2.285-2.508	2.34-2.48
O(OH)	2.287-2.375	2.37-2.41	2.39-2.48	-	-
O(NO3)	2.403-2.553	2.43-2.54	2.35-2.56	2.467-2.626	2.55-2.58
N(chp)	-	-	-	2.54	2.51
Ln...Ln	3.500	3.568	3.618	3.682	3.735
Ln...Co	3.741-3.861	3.698-3.909	3.803-3.972	3.804	3.956
CN	9	9	9	9/10	9/10

CN = coordination number.

5.3. Magnetochemistry of $[NEt_4]_2[Co_2Gd_2(OH)(chp)_6(NO_3)_5]$ 48 and $[NEt_4]_2[CoSm_2(chp)_5(NO_3)_5]$ 50.

Initial magnetic studies of **48** and **50** have been performed in the temperature range 300-1.8 K in an applied field of 1000 G. The room temperature value of χ_mT for **48** [Figure 5.17] is approximately 22 emu K mol^{-1} which is consistent with a $[Co_2Gd_2]$ core in which the metal centres are not interacting [χ_mT = 21.6 emu K mol^{-1}, g_{Co} = 2.5, g_{Gd} = 2.0]. The value of χ_mT remains constant down to approximately 50 K, but below this temperature the value falls reaching 11 emu K mol^{-1} at 2 K. This behaviour is consistent with weak antiferromagnetic exchange between the metal centres. For **50** the room temperature value of χ_mT is approximately 5 emu K mol^{-1} [Figure 5.18] which is consistent with a $[CoSm_2]$ core in which the metals are not interacting [χ_mT = 4.63 emu K mol^{-1}, g_{Co} = 2.4, g_{Sm} = 1.33]. The value of χ_mT drops steadily down to 50 K where it reaches a value of 4.5 emu K mol^{-1}. Below this temperature it drops more sharply to 4.25 emu K mol^{-1} at 20 K and then it rises to sharply to 4.75 emu K mol^{-1} at 10 K. Below 10 K χ_mT drops again to approximately 3.5 emu K mol^{-1} at 1.8 K. This behaviour suggests weak antiferromagnetic exchange between the metal centres. The reason for the increase in χ_mT at 20 K is unclear.

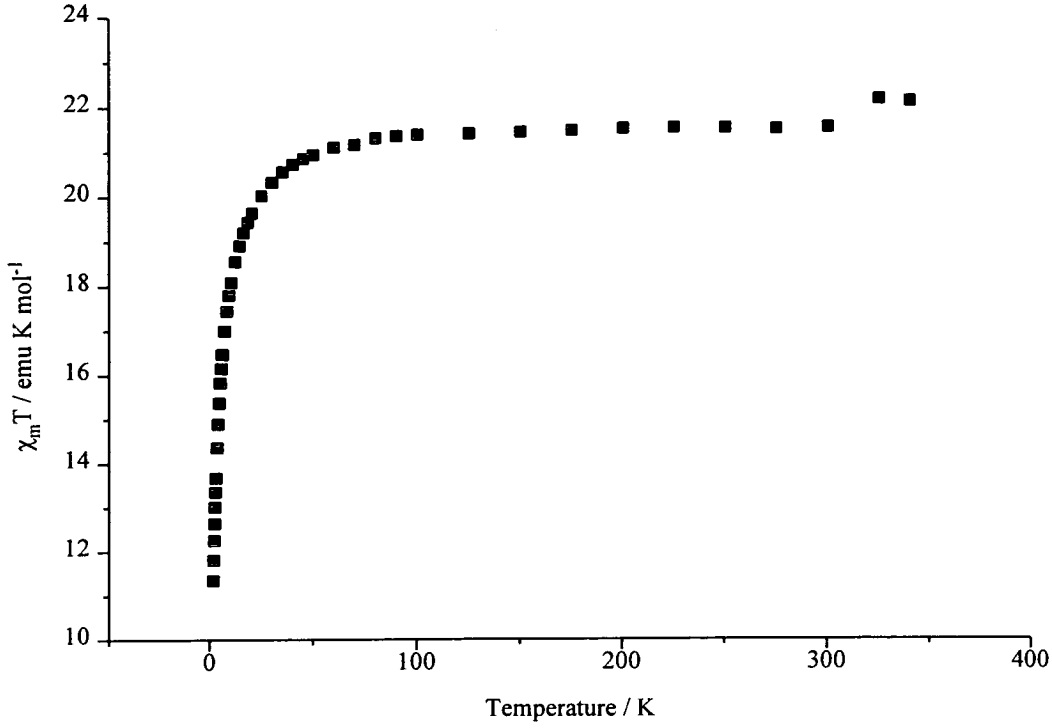

Figure 5.17. The variation of $\chi_m T$ with temperature for **48**.

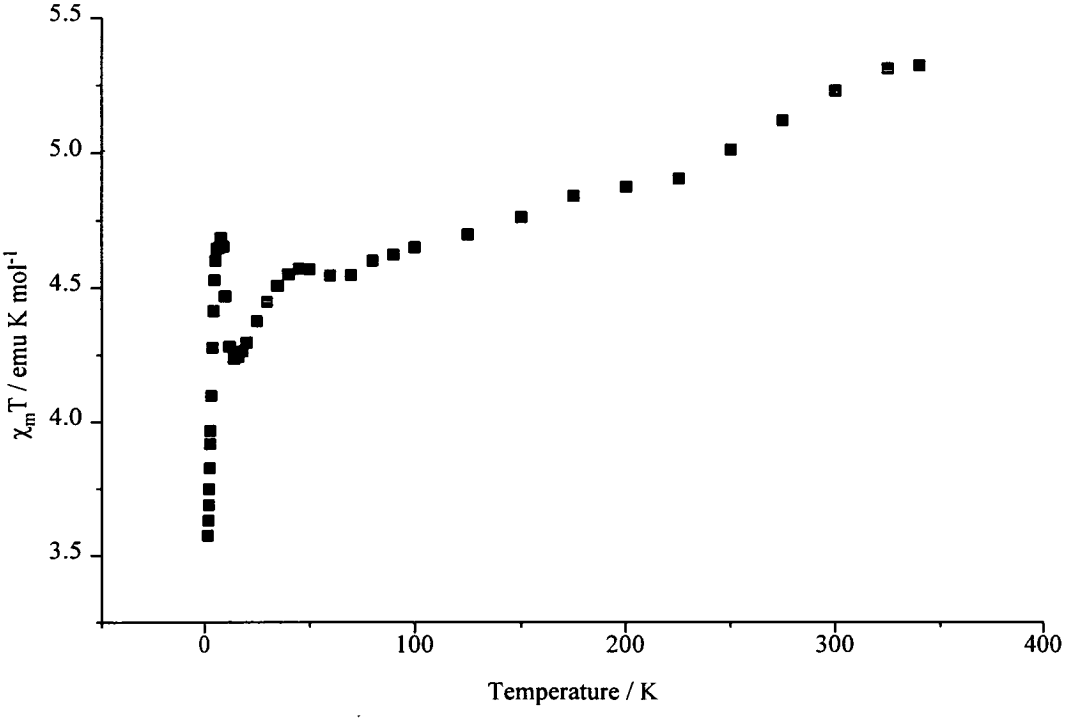

Figure 5.18. The variation of $\chi_m T$ with temperature for **50**.

5.4. Conclusions.

This chapter outlined the synthesis and structure of a number novel heterobimetallic complexes of 6-chloro- and 6-methyl-2-pyridone, using similar synthetic strategies to that employed in the synthesis of homometallic species. These mixed-metal compounds fall into two categories : the first contained mixtures of 3d-metals and the second mixtures of 3d-4f metals. 'One-pot' thermolysis reactions of copper carboxylates produced a nonanuclear cobalt complex of 6-chloro-2-pyridone and two isostructural octanuclear cobalt / nickel complexes of 6-methyl-2-pyridone. These three structures are dominated by oxygen-centred metal triangles. In each case the ratio of the metal atoms in the product does not reflect the ratio of metals in the reaction scheme due to the formation of known homometallic copper-pyridonate side-products. Bonds to the nickel centres are shorter than the equivalent bonds to the cobalt centres. Each of these three compounds contains hydroxide or water molecules within their structures which again emphasises the need for 'wet' solvents.

The synthesis of mixed 3d-4f complexes was carried out *via* preformed nickel and cobalt pyridonate complexes and produced a tetrametallic complex of nickel and erbium and a family of cobalt complexes containing lanthanides from ytterbium to neodymium. This family of compounds illustrates the effects of the lanthanide contraction. The bond lengths to the lanthanide centres, the metal...metal distances and the coordination number of the lanthanide all increase moving from ytterbium to neodymium. The change in size of the lanthanides also invokes a structural change in the product : complexes of the smaller lanthanides [i.e. gadolinium and smaller] contain two cobalt atoms and complexes of the larger lanthanides [i.e. bigger than gadolinium] contain one cobalt atom in their structures. In all of the structures described magnetic studies indicate weak antiferromagnetic exchange between the metal centres.This is in direct contrast with the results obtained for copper-lanthanide species [29, 32].

In particular detailed studies of the magnetic interaction between copper (II) and gadolinium (III) have shown the relationship to be directly ferromagnetic [22].

5.5. Experimental section.

5.5.1. $[Co_7Cu_2(O_2CMe)_6(chp)_{10}(OH)_2]$ **41.**

$Co(O_2CMe)_2.4H_2O$ (1.000 g, 4.02 mmol), $Cu(O_2CMe)_2.H_2O$ (0.802g, 4.02 mmol) and Hchp (2.086g, 16.1 mmol) were mixed together in a Schlenk tube and heated to 130°C under N_2 for 2 hours. The acetic acid and water formed were removed by heating under reduced pressure for 20 minutes at 130 °C. Excess Hchp was sublimed to a cold finger. The resultant paste was dissolved in CH_2Cl_2 (25ml) and allowed to stand. Purple crystals of **41** formed in 60% yield after three days.

CHN, observed (expected) : C, 33.7 (33.6); H, 2.40 (2.50); N, 6.12 (6.32); Co, 18.6 (18.6); Cu, 5.4 (5.7) %.

FAB-MS (significant peaks, possible assignments) : m/z 1480, $[Co_3Cu(O_2CMe)_3(chp)_8(OH)_2]^+$ 1282, $[Co_3Cu(O_2CMe)_4(chp)_6(OH)_2]^+$; 650, $[Co_3Cu(O_2CMe)_2(chp)_2(OH)_2]^+$; 386, $[Co_2Cu(O_2CMe)(chp)(OH)]^+$.

5.5.2. $[Co_6Cu_2(PhCOO)_{10}(mhp)_2(Hmhp)_4(OH)_4(H_2O)_2]$ **42.**

$Co(PhCOO)_2.4H_2O$ (1.000g, 2.68 mmol), $Cu(PhCOO)_2.2H_2O$ (0.915g, 2.68 mmol) and Hmhp (1.625g, 10.7 mmol) were mixed together in a Schlenk tube and heated to 160°C under N_2 for 2 hours. The melt was then heated under reduced pressure for 20 minutes at 130°C. Excess Hmhp was sublimed to a cold finger. Addition of CH_2Cl_2 (25ml) produced brown crystals of **42** in 10% yield after one week.

CHN, observed (expected for **42**. 2Hmhp) : C, 53.1 (53.3); H, 4.03 (3.98); N, 4.26 (4.20); 15.0 (13.3); Cu, 4.51 (4.77) %.

5.5.3. $[Ni_6Cu_2(PhCOO)_{10}(mhp)_2(Hmhp)_4(OH)_4(H_2O)_2]$ **43.**

Synthesis as for **42** using $Ni(PhCOO)_2.4H_2O$ instead of $Co(PhCOO)_2.4H_2O$.

CHN, observed (expected for **43**. Hmhp) : C, 52.6 (52.6); H, 4.03 (3.91); N, 4.12 (3.84); Ni, 14.2 (13.8); Cu, 5.11, (4.97) %.

FAB-MS (significant peaks, possible assignents) : m/z 1132, $[Ni_3Cu(PhCOO)_5(mhp)(OH)_2(Hmhp)(H_2O)_2]^+$; 1023, $[Ni_3Cu(PhCOO)_5(mhp)(OH)_2(H_2O)_2]^+$; 1005, $[Ni_3Cu(PhCOO)_5(mhp)(OH)_2(H_2O)]^+$; 825, $[Ni_2Cu(PhCOO)_4(OH)_2(H_2O)]^+$; 758, $[Ni_3Cu(PhCOO)_4(OH)_2]^+$; 544, $[Ni_2Cu(PhCOO)_3]^+$.

5.5.4. $[Ni_2Er_2(chp)_6(NO_3)_4(MeCN)_2]$ **44.**

$[Ni_4(OMe)_4(chp)_4(MeOH)_7]$ 1 (0.197g, 0.18 mmol) and $Er(NO_3)_3.5H_2O$ (0.08g, 0.18mmol) were mixed in MeCN (15ml) giving a blue / green solution from which green crystals of **44** formed in 10% yield after 2 weeks.

CHN, observed (expected) : C, 24.5 (24.7); H, 1.38 (1.55); N, 10.7 (10.8) %.

5.5.5. $[NEt_4]_2[Co(chp)_4]$ **45.**

$CoCl_2.6H_2O$ (1.000g, 4.2 mmol) and $[Et_4N]Cl$ (1.390g, 8.4 mmol) were stirred in MeOH (30ml) for 2 hours. The solution was filtered and the solvent removed producing a blue solid : $[Et_4N]_2[CoCl_4]$ in 100% yield after drying. $[Et_4N]_2[CoCl_4]$ (1.00g, 2.17 mmol) and Na(chp) (1.315g, 8.68 mmol) were stirred in methanol (30ml) for 3 hours. The solution was filtered, the solvent removed and the paste dried. CH_2Cl_2 (20ml) was added producing blue crystals of

45 in 30% yield after 3 days.

CHN, observed (expected) : C, 51.9 (51.9); H, 6.20 (6.24); N, 10.0 (10.1) %.

5.5.6. $[NEt_4]_2[Co_2Yb_2(OH)(chp)_6(NO_3)_5]$ **46.**

45 (0.250g, 0.3 mmol) and $Yb(NO_3)_3.5H_2O$ (0.135g, 0.3 mmol) were stirred in 1:1 MeOH / CH_2Cl_2 (20ml) for 1 hour, the solution filtered and the solvent removed. Extraction with CH_2Cl_2 (10ml) gave pink crystals of **46** in 18% yield after 4 days.

CHN, observed (expected) : C, 30.5 (30.3); H, 3.46 (3.24); N, 9.70 (9.99) %.

FAB-MS (significant peaks, possible assignments) : m/z 1562, $[Co_2Yb_2(OH)(chp)_6(NO_3)_5]^+$; 1229, $[CoYb_2(chp)_4(NO_3)_5]^+$; 932, $[CoYb(chp)_4(NO_3)_3]^+$.

5.5.7. $[NEt_4]_2[Co_2Dy_2(OH)(chp)_6(NO_3)_5]$ **47.**

Synthesis as for **46** using $Dy(NO_3)_3.5H_2O$.

CHN, observed (expected) : C, 30.2 (30.4); H, 3.12 (3.25); N, 10.0 (10.0) %.

FAB-MS (significant peaks, possible assignments) : m/z 1524, $[Co_2Dy_2(chp)_6(NO_3)_5]^+$; 1146, $[CoDy_2(chp)_4(NO_3)_4]^+$; 898, $[CoDy_2(chp)_4]^+$.

5.5.8. $[NEt_4]_2[Co_2Gd_2(OH)(chp)_6(NO_3)_5]$ **48.**

Synthesis as for **46** using $Gd(NO_3)_3.6H_2O$.

CHN, observed (expected) : C, 30.6 (30.8); H, 3.34 (3.29); N, 9.89 (10.2) %.

FAB-MS (significant peaks, possible assignments) : m/z 1198, $[CoGd_2(chp)_4(NO_3)_5]^+$; 1007, $[CoGd_2(chp)_3(NO_3)_4]^+$; 978, $[CoGd(chp)_4(NO_3)_4]^+$; 888, $[CoGd_2(chp)_4]^+$.

5.5.9. $[NEt_4]_2[CoNd_2(chp)_5(NO_3)_5]$ **49**

Synthesis as for **46** using $Nd(NO_3)_3.6H_2O$.

CHN, observed (expected) : C, 31.4 (31.5); H, 3.37 (3.52); N, 10.7 (10.8) %

FAB-MS (significant peaks, possible assignments) : m/z 1300, $[CoNd_2(chp)_5(NO_3)_5]^+$; 1238, $[CoNd_2(chp)_5(NO_3)_4]^+$; 1176, $[CoNd_2(chp)_5(NO_3)_3]^+$; 1114, $[CoNd_2(chp)_5(NO_3)_2]^+$; 1109; $[CoNd_2(chp)_4(NO_3)_4]^+$.

5.5.10. $[NEt_4]_2[CoSm_2(chp)_5(NO_3)_5]$ **50.**

Synthesis as for **46** using $Sm(NO_3)_3.6H_2O$.

CHN, observed (expected) : C, 31.2 (31.3); H, 3.55 (3.50); N, 10.5 (10.7) %.

FAB-MS (significant peaks, possible assignments) : m/z 1312, $[CoSm_2(chp)_5(NO_3)_5]^+$; 1250, $[CoSm_2(chp)_5(NO_3)_4]^+$; 1188, $[CoSm_2(chp)_5(NO_3)_3]^+$; 1126, $[CoSm_2(chp)_5(NO_3)_2]^+$; 1121, $[CoSm_2(chp)_4(NO_3)_4]^+$; 1064, $[CoSm_2(chp)_5(NO_3)_2]^+$; 1060, $[CoSm_2(chp)_4(NO_3)_3]^+$.

CHAPTER 6

CONCLUSIONS.

The discovery of novel metal polyhedra remains one of the chief goals of synthetic polynuclear chemistry, as new structures may eventually lead to novel properties. In particular if the nature of the product can be controlled and spontaneous self-assembly avoided then the physical properties of the compounds can also be controlled. This would then allow the chemist to design specific compounds with specific properties. However, examples of such designed synthesis are rare. Only recently has interest in polymetallic complexes of metals in moderate oxidation states begun to rival the attention given to high nuclearity species of metals in low or high oxidation states. Such metals may be paramagnetic and therefore the complexes they form may have unusual and exciting magnetic properties. Thus the challenge for the chemist is to synthesise such compounds and examine, understand and manipulate their physical characteristics. This thesis outlined the synthesis, structure and initial magnetic properties of a number of novel polynuclear compounds of nickel and cobalt using a blend of 2-pyridonate and carboxylate ligands. Prior to this study high nuclearity clusters of cobalt and nickel had been little investigated. The structures reported in this work could not have been predicted due to the coordinative flexibility of the ligands and the involvement of both solvent and water. However in order to understand the behaviour of any ligand or set of ligands they must first be tried so that patterns of reactivity and preferred topologies can be recognised. This is necessary before any genuine predictive theories can be established. The derivatives of 2-pyridone employed in this work showed no less than seven different coordinating modes [Figure 6.1]. Terminally bound through the oxygen-donor; chelating through the nitrogen and oxygen; chelating plus 1, 1-bridging through the oxygen; 1, 1-bridging through the oxygen alone; 1, 3-bridging through both the oxygen and nitrogen atoms; chelating plus 1, 1, 1-bridging through the oxygen; 1,1-bridging through the oxygen with the nitrogen bound to a different metal. Where the ring nitrogen is uncoordinated it is usually involved in hydrogen-bonding to another ligand. Frequently several of these different bonding modes

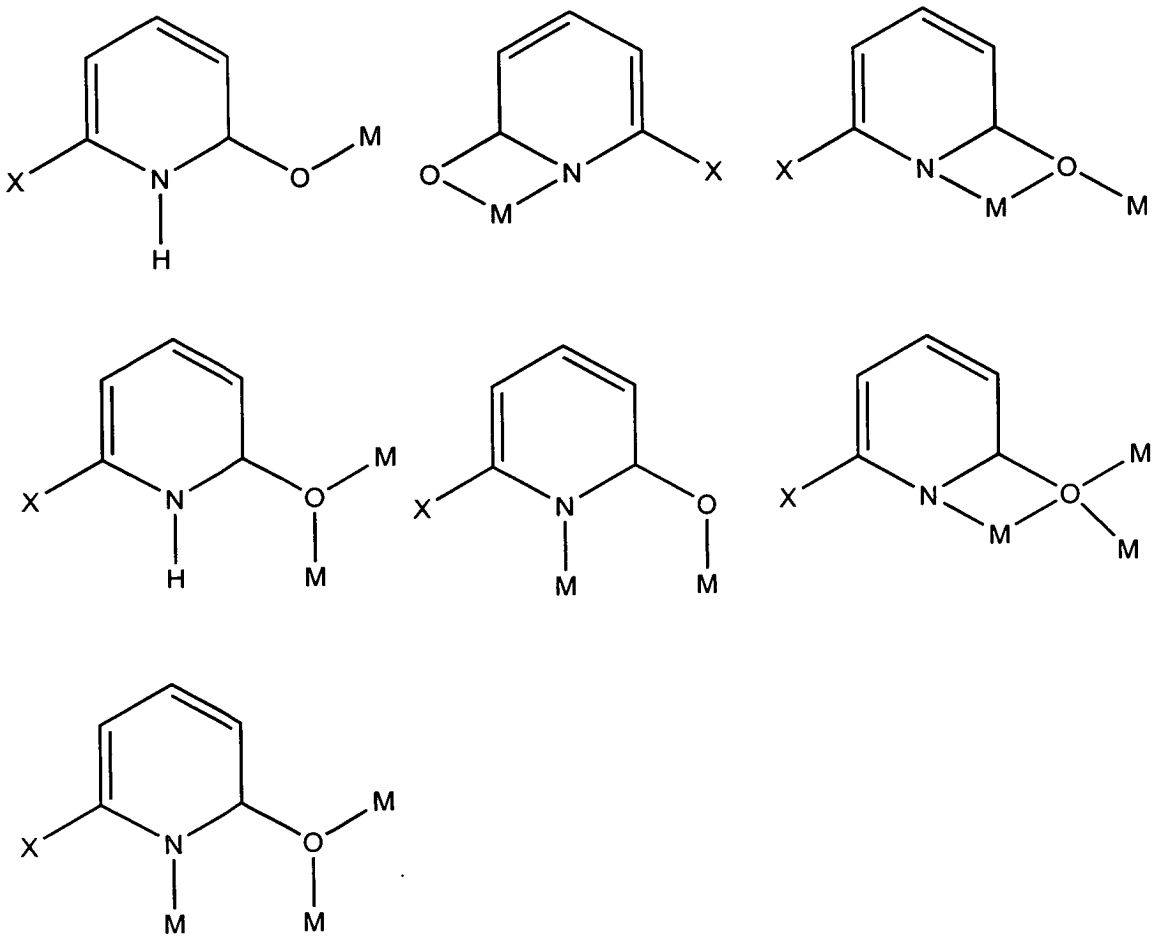

Figure 6.1. The different coordinating modes adopted by the derivatives of 2-pyridone.

appear within the same complex. The carboxylate ligands are more well-behaved and in general act solely as 1, 3-bridges, although occasionally are tri- and tetranucleating. This variety of bonding is seen in complexes containing other 3d-metals but is not observed in complexes of the 4d and 5d-metals, where the 1, 3-bridging mode is almost always the rule.

Solvent and water have also established themselves as vital structural ingredients : all but a few of the compounds discussed in this thesis have contained bridging hydroxides or methoxides and / or coordinated solvent molecules. Previous attempts to form high nuclearity complexes of cobalt and nickel from dry solvents and in the absence of atmospheric moisture have proved wholly unsuccessful. Reactions cannot be carried out using water as the lone solvent (immediate precipitation of the protonated ligands results) and the amount of water which can be 'doped' into other solvents for productive results is unknown. Even where

solvent is not involved in the structure it alone can determine the nature of the final product. This is perhaps most clearly established in Chapter 2 where continual changing of the crystallisation solvent from otherwise identical reaction schemes produced a number of compounds of differing nuclearity and structure, and in Chapter 4 where it meant the difference between producing a trimer [**30**, **31**] or a dodecanuclear metallocycle [**32**]. In general non-coordinating non-polar solvents have appeared to favour the synthesis of higher nuclearity arrays than the coordinating polar solvents.

Unsurprisingly a change in the pyridonate ligand invokes structural change since the two different ligands used favour different tautomeric forms and hence favour different coordinating modes to the metal centres. Perhaps more surprising is the effect observed changing from nickel to cobalt. There is no doubt that there is some structural congruence between the coordination chemistry of these two metals, as the formation of the isostructural trimers and metallocycles demonstrates. However there are also examples where the two metals produce hugely different structures, the most obvious example being between the tetraicosametallic cobalt complex [**14**] and the heterobimetallic complex of nickel and sodium [**6**] discussed in Chapter 2. One explanation may be nickel's preference for regular octahedral geometry when six-coordinate. In almost all of the compounds characterised in this work nickel has been six-coordinate whereas cobalt has demonstrated much more flexibility and has been four-, five- and six-coordinate in a range of distorted geometries.

Thus the structural diversity imparted by metal, ligand and solvent often means that it is difficult to draw practical conclusions about making complexes of a given nuclearity. However this is not the case for certain combinations of ligand and solvent. For example any reaction involving chp and carboxylate will always result in the formation of a trimeric species [**30**, **31**] when crystallised from methanol, and reactions of mhp and carboxylates in acetonitrile or ethyl acetate will produce structures based on centred-tricaped-trigonal prisms

[**21-25**, **27**, **28**]. It should be noted however that only information of the crystalline material is available, while there is no mechanistic information or knowledge of what remains in solution. However despite the difficulties in developing a predictive strategy what is clear is that the methodology employed has led to a wide range of products of massive structural diversity and that routes to high nuclearity species have been clearly established *via* simple synthetic chemistry.

It had been previously thought that in order to form high nuclearity complexes it was necessary to use heteroleptic ligand sets and / or multifunctional ligands. Chapter 2 illustrated routes to such species using only metal salts and pyridonate ligands. The tetraicosametallic **14** is, for example, the largest coordination complex containing cobalt and consists of cubic-close packed planes of hydroxide, methoxide and chloride anions bridging cobalt (II) centres. Its structure is related to many minerals and preliminary magnetic studies indicate a high spin ground state and the possibility of superparamagnetic behaviour. Structures containing adamantane units had never been reported for the later 3d-metals and only one previous example existed where such units had been linked. Simple thermolysis reactions, as described in Chapter 2, produced the first examples of nickel and cobalt compounds containing adamantane units which are also the first examples of vertex- and face-sharing adamantanes [**15-18**]. Complete replacement of methoxide with 6-chloro-2-pyridonate led to a homoleptic nonametallic complex constructed from four adamantane units [**18**]. All other previously reported homoleptic species of pyridonate ligands are dimers. This family of adamantane complexes also introduced the idea that desolvation, or removal of the influence of coordinating solvent ligands, such as methanol, and replacement by non-coordinating solvent allows the formation of higher nuclearity species through the attachment of additional metal fragments to the sites of the displaced solvent molecules.

Introduction of the more rigid carboxylate ligands into a reliable reaction scheme

produced a family of polynuclear cobalt and nickel complexes whose structures are based on centred-tricapped trigonal prisms[**21-25**, **27**, **28**]. By changing the size of the carboxylate ligand and the nature of the pyridonate the number of additional caps on the triangular faces of the prisms can be altered. Eventually the increasing bulk of the carboxylate invokes a structural change in the product [**26**]. Use of the tetranucleating phthalate ligand produced a novel example of a supracage assembly in which four nickel cubanes were linked together through a central sodium octahedron [**37**]. Such a molecular species, where dissimilar polymetallic fragments are linked into a supracage appears to be unprecedented. The cubane or cuboid structural motif is a common one in the chemistry of 6-chloro-2-pyridone [**1**, **2**, **6-9**, **24**] and the idea of oligomerising such cubes *via* desolvation and *via* introduction of rigid linking groups appears to be a valid strategy in the formation of high nuclearity molecules.

The synthetic procedures used in the formation of homometallic species can be extended to produce heterometallic complexes of 3d-metals and of 3d-4f elements: combinations of unlike metal centres have been the subject of recent interest since they may themselves display unusual physical properties or act as precursors to materials such as superconducting oxides.

In general what this thesis has acheived is to produce a number of simple synthetic routes to several high nuclearity complexes, some of which have structures of unprecedented nature; some of which exhibit high spin ground states and interesting magnetic behaviour. Harnessing, explaining and exploiting these two particular features remains the ultimate aim.

References.

1. O. Kahn, Molecular Magnetism, VCH New York.
2. E. Coronado, P. Delhaès, D. Gatteschi and J. S. Miller, Molecular Magnetism : From Molecular Assemblies to the Devices, NATO ASI Series E, Vol. 321.
3. D. Gatteschi, *Adv. Mater.*, 1994, **6**, 635.
4. J. S. Miller and A. J. Epstein, *Angew. Chem., Int. Ed. Engl.*, 1994, **33**, 385.
5. J. S. Miller, A. J . Epstein and W. Reiff, *Chem. Rev.*, 1988, **88**, 201.
6. J. S. Miller, A. J. Epstein and W. Reiff, *Acc. Chem. Res.*, 1988, **21**, 114.
7. P.-M. Allemand, K. C. Khemani, A. Koch, F. Wudl, K. Holczer, S. Donovan, G. Grüner and J. D. Thompson, *Science*, 1991, **253**, 301.
8. O. Khan, *Struct. Bonding* (Berlin) 1987, **68**, 69.
9. O. Khan, Y. Pei, M. Verdaguer, J. P. Renard and J. Sletten, *J. Am. Chem. Soc.*, 1988, **110**, 782.
10. H. O. Stumpf, Y. Pei, L. Ouahab, F. Le Berre, E. Codjori and O. Kahn, *Inorg. Chem.*, 1993, **32**, 782.
11. H. O. Stumpf, Y. Pei, O. Khan, J. Sletten, and J. P. Renard, *J. Am. Chem. Soc.*, 1993, **115**, 6738.
12. H. O. Stumpf, L. Ouahab, Y. Pei, D. Grandjeau and O. Khan, *Science*, 1993, **261**, 447.
13. S. Ferlay, T. Mallah, R. Ouahes, P. Veillet and M. Verdaguer, *Nature*, 1995, **378**, 701.
14. T. Mallah, S. Thiébaut, M. Verdaguer, P. Veillet, *Science*, 1993, **262**, 1554.
15. M.-A. Arrio, P. Sainctavit, C. Cartier dit Moulin, C. Bronder, F. M. F. de Groot, T. Mallah and M. Verdaguer, *J. Phys. Chem.*, 1996, **100**, 4679.

16. T. Mallah, S. Ferlay, C. Auberger, C. Hélary, F. L'Hermite, R. Ouahès, J. Vaissermann, M. Verdaguer and P. Veillet, *Mol. Cryst. Liq. Cryst.*, 1995, **273**, 141.

17. V. Gadet, T. Mallah, I. Castro and M. Verdaguer, *J. Am. Chem. Soc.*, 1992, **114**, 9213.

18. M. Verdaguer, Science, 1996, 272, 698.

19. A. Scuiller, T. Mallah, M. Verdaguer, A. Nivorozkhin, J.-L. Tholence and P. Veillet, *New J. Chem.*, 1996, **20**, 1.

20. A. Caneschi, D. Gatteschi and R. Sessoli, *Acc. Chem. Res.*, 1989, 22, 392.

21. T. Lis, *Acta Crystallogr. Sect. B.*, 1980, **36**, 2042.

22. A. Caneschi, D. Gatteschi and R. Sessoli, *J. Am. Chem. Soc.*, 1991, **113**, 5837.

23. R. Sessoli, D. Gatteschi, A. Caneschi and M. A. Novak, *Nature*, 1993, **365**, 141.

24. J. Friedman, M, Sarachik, J. Tejada and R. Ziolo, *Phys. Rev. Lett.*, 1996, **76**, 3830.

25. L. Thomas, F. Lionti, R. Ballou, D. Gatteschi, R. Sessoli and B. Barbara, *Nature*, 1996, **383**, 145.

26. R. Sessoli, H.-L. Tsai, A. R. Schake, S. Wang, J. B. Vincent, K. Folting, D. Gatteschi, G. Christou and D. N. Hendrickson, *J. Am. Chem. Soc.*, 1993, **115**, 1804.

27. H. J. Eppley, H.-L. Tsai, N. de Vries, K. Folting, G. Christou and D. N. Hendrickson, *J. Am. Chem. Soc.*, 1995, **117**, 301.

28. Y.-G. Wei, S.-W. Zhang, M.-C. Shao and Y.-Q. Tang, *Polyhedron*, 1996, **16**, 1471.

29. H.-L. Tsai, H. J. Eppley, N. de Vries, K. Folting, G. Christou and D. N. Hendrickson, *J. Chem. Soc., Chem. Commun.*, 1994, 1745.

30. D. P. Goldberg, A. Caneschi and S. J. Lippard, *J. Am. Chem. Soc.*, 1993, **115**, 9299.

31. D. P. Goldberg, A. Caneschi, C. D. Delfs, R. Sessoli and S. J. Lippard, *J. Am. Chem. Soc.*, 1995, 117, 5789.

32. A. L. Barra, A. Caneschi, D. Gatteschi and R Sessoli, *J. Am. Chem. Soc.*, 1995, **117**, 8855.

33. A. Caneschi, D. Gatteschi, J. Langier, P. Rey, R. Sessoli and C. Zanchini, *J. Am. Chem. Soc.*, 1993, **115**, 9299.

34. S. M. Gorun and S. J. Lippard, *Inorg. Chem.*, 1991, **30**, 1625.

35. D. M. Kurtz Jnr., *Chem. Rev.*, 1990, **90**, 585.

36. S. L. Heath and A. K. Powell, *Angew. Chem., Int. Ed. Engl.*, 1992, **31**, 191.

37. A. K. Powell, S. L. Heath, D. Gatteschi, L. Pardi, R. Sessoli, G. Spina, F. Del Giallo and F. Pieralli, *J. Am. Chem. Soc.*, 1995, **117**, 2491.

38. C. Benelli, S. Parsons, G. A. Solan and R. E. P. Winpenny, *Angew. Chem., Int. Ed. Engl.*, 1996, **35**, 1825.

39. K. Wieghardt, K. Pohl, I. Jibril and G. Huttner, *Angew. Chem., Int. Ed. Engl.*, 1984, **23**, 77.

40. C. Delfs, D. Gatteschi, L. Pardi, R. Sessoli, K. Wieghardt and D. Hanke, *Inorg. Chem.*, 1993, **32**, 3099.

41. K. L. Taft, G. C. Papaefthymiou and S. J. Lippard, *Science*, 1993, **259**, 1302.

42. K. L. Taft, G. C. Papaefthymiou and S. J. Lippard, *Inorg. Chem.*, 1994, **33**, 1510.

43. W. Micklitz, V. McKee, R. L. Rardin, L. E. Pence, G. C. Papaefthymiou, S. G. Bott and S. J. Lippard, *J. Am. Chem. Soc.*, 1994, **116**, 8061.

44. G. C. Papaefthymiou, *Phys. Rev. B.*, 1992, 10366.

45. K. L. Taft and S. J. Lippard, *J. Am. Chem. Soc.*, 1990, **112**, 9629.

46. K. L. Taft, C. D. Delfs, G. C. Papaefthymiou, S. Foner, D. Gatteschi and S. J. Lippard, *J. Am. Chem. Soc.*, 1994, **116**, 823.

47. A. Caneschi, A. Cornia and S. J. Lippard, *Angew. Chem., Int. Ed. Engl.*, 1995, **34**,

467.

48. A. Katritzky and T. M. Lagowski, *Adv. Heterocycl. Chem.*, 1963, **1**, 312.

49. A. Kvick, *Acta Crystallogr., Sect. B*, 1976, **32**, 220.

50. J. M. Rawson and R. E. P. Winpenny, *Coord. Chem. Rev.*, 1995, **139**, 313.

51. L. M. Gilby, Ph. D. Thesis, The University of Edinburgh, 1994.

52. A. J. Blake, L. M. Gilby and R. E. P. Winpenny, *J. Chem. Soc., Chem. Commun.*, 1992, 1327.

53. S. McConnell, M. Motevalli and P. Thornton, *Polyhedron*, 1995, **14**, 459.

54. W. Clegg, C. D. Garner and M. H. Al-Samman, *Inorg. Chem.*, 1983, **22**, 1534.

55. A. J. Blake, E. K. Brechin, A. Codron, R. O. Gould, C. M. Grant, S. Parsons, J. M. Rawson and R. E. P. Winpenny, *J. Chem. Soc., Chem. Commun.*, 1995, 1983

56. J. A. Bertrand, A .P. Ginsberg, R. I. Kaplan, C. E. Kirkwood, R. L. Martin and R. C. Sherwood, *Inorg. Chem.*, 1971, **10**, 240.

57. J. E. Andrew and A. B. Blake, *J. Chem. Soc., Chem. Commun.*, 1967, 1174.

58. J. E. Andrew and A. B. Blake, *J. Chem. Soc.*, A, 1969, 1456.

59. W. L. Gladfelter, M. W. Lynch, W. P. Schaefer, D. N. Hendrickson and H. B. Gray, *Inorg. Chem.*, 1981, **20**, 2390.

60. P. W. Boyd, R. L. Martin and G. Schwarzenbach, *Aust. J. Chem.*, 1988, **41**, 1449.

61. F. Paap, E. Bouwman, W. L. Dressen, R. A. G. de Graff and J. Reedijk, *J. Chem. Soc., Dalton Trans.*, 1985, 737.

62. A. J. Atkins, A. J. Blake and M. Schröder, *J.Chem. Soc., Chem. Commun.*, 1993, 1662.

63. J. A. Barnes and W. E. Hatfield, *Inorg. Chem.*,1971, **10**, 2355.

64. L. Ballester, E. Coronado, A. Gutierrez, A. Mange, M. F. Perpinan, E. Pinilla and T.

Rico, *Inorg. Chem.*, 1992, **31**, 2053.

65. M. A. Halcrow, J. -S. Sun, J. C. Huffman and G. Christou, *Inorg. Chem.*, 1995, **34**, 4167.

66. E. K. Brechin, L. M. Gilby, S. G. Harris, S. Parsons, and R. E. P. Winpennny, *J. Chem. Soc.*, Dalton Trans., 1997...in press.

67. B. Bogdanovic, C. Kruger and B. Wermeckes, *Angew.Chem., Int.Ed.Engl.*, 1980, **19**, 817.

68. D. C. Bradley, M. B. Hursthouse, A. N. de M. Jelfs and R. L. Short, *Polyhedron*, 1983, **2**, 894.

69. I. G. Dance, R. G. Garbutt and M. L. Scudder, *Inorg. Chem.*,1990, **29** *1571*, .

70. F. Labrize, L. G. Hubert-Pfalzgraf, J. Vaissermann and C. B. Knobbler, *Polyhedron*, 1966, **15**, 577, .

71. E. K. Brechin, S. G. Harris, S. Parsons and R. E. P. Winpenny, *J. Chem. Soc., Chem. Commun.*, 1996, 1439.

72. E. Libby, K. Folting, J. C. Huffman and G. Christou, *J. Am. Chem. Soc.*, 1990, **112**, 5354.

73. E. K. Brechin, S. G. Harris, A. Harrison, S. Parsons, A. G. Whittaker and R. E. P. Winpenny, *J. Chem. Soc., Chem. Commun.*, 1997, 653

74. S.Parsons, G. A. Solan and R. E. P. Winpenny, *J. Chem. Soc., Chem. Commun.*, 1995, 1987.

75. J. P. Chen, C. M. Sorensen, K. J. Klabunder and G. C. Hadjapanayis, *J. Appl. Phys.*, 1994, **78**, 6318.

76. E. K. Brechin, S. G. Harris, S. Parsons and R .E. P. Winpenny, submitted to *Angew. Chem., Int. Ed. Engl.*, 1997.

77. F. A. Cotton and T. R. Felthouse, *Inorg. Chem.*, 1981, **20**, 584.

78. A. Müller, K. Krickenmeyer, J. Meyer, H. Bögge, F. Peters, W. Plass, E. Diemann, S. Dillinger, F. Nonenbruch, M. Randerath and C. Menke, *Angew. Chem., Int. Ed. Engl.*, 1995, **34**, 2122.

79. H Krautscheid, D. Fenske, G. Baum and M. Semmelman, *Angew.Chem., Int. Ed. Engl.*, 1993, **32**, 1303.

80. J. F. You, G. C. Papafethymiou and R. C. Holm, *J. Am. Chem. Soc.*,1992, **114**, 2697.

81. K. Wieghardt, D. Ventur, Y. H. Tsai, C. Kruger., *Inorg. Chim. Acta*, 1985, **99**, L25.

82. L.M. Babcock, V. W. Day, W. G. Klemperer, *J. Chem. Soc., Chem. Commun.*, 1987, 858.

83. F. Bottomley, C. P. Magill and B. Zhao, *Organomet.*, 1990, **9**, 1700.

84. D. Wormsbacher, K. M. Nicholas and A. L. Rheingold, *J. Chem. Soc.,Chem. Commun.*, 1985,721

85. J. Glerup, H. Weihe, P.A. Goodson and D. J. Hodgson, *Inorg. Chim. Acta,* 1993, **212**, 281.

86. K.Wieghardt, U. Bossek, B. Nubber, J. Weiss, J. Bonvoison, M. Corbella, S .E. Vitols and J. J. Girerd, *J. Am. Chem. Soc.*,1988, **110**, 7398.

87. K. S. Hagen, T. D. Westmoreland, W. J. Scott and W. H. Armstrong, *J. Am. Chem. Soc.*,1989, **111**, 1907.

88. B. P. Murch F. C. Bradley, P. D. Boyle, V, Papaefthymiou, L. Que Jr., *J. Am. Chem. Soc.*,1987, **109**, 7993.

89. S. Drueke, K. Wieghardt, B. Nuber, J. Weiss, E. L. Bominaar, A. Sawaryn, H. Winkler and A. X. Trautwein, *Inorg. Chem.*, 1989, **28**, 4477.

90. V. S. Nair and K. S. Hagen, *Inorg. Chem.*, 1992, **31**, 4048.

91. G. R. Newkome, J. Broussard, S. K. Staines and J. D. Sauer, *Synthesis*, 1974, 701.

92. C. Benelli, E. K. Brechin, A. Graham, S. G. Harris,S. Parsons and R. E. P. Winpenny, submitted to *J. Chem. Soc., Dalton Trans.*, 1997.

93. E. K. Brechin, S. Parsons and R. E. P. Winpenny, *J. Chem. Soc., Chem. Commun.*, 1996, 3745.

94. F. B. Hulsbergen, R. W. M. ten Hoedt, G. C. Verschoor, J. Reedijk and A. L. Spek, *J. Chem. Soc., Dalton Trans.*, 1983, 539.

95. J. B. Vincent, H. R. Chang, K. Folting, J. C. Huffman, G. Christou and D. N. Hendrickson, *J. Am. Chem. Soc.*, 1987, 109, 5703.

96. T. Yamagata, K. Tani, Y. Yatsuro and T. Saito, *J. Chem. Soc., Chem. Commun.*,1988, 466.

97. H. Adams, A. Bailey, M. J. S. Dwyer, D. E. Fenton, P. C. Hellier, P. D. Hampstead and J. M. Latour., *J. Chem. Soc., Dalton Trans.*, 1993, 6318.

98. W. H. Armstrong, M. E. Roth and S. J. Lippard, *J. Am. Chem. Soc.*, 1987, **109**, 6318.

99. H. M. Haendler, *Acta Crystallogr.*, Sect. C, 190, **46**, 2054.

100. H. Yang, M. A. Khan and K. M. Nicholas, *J. Chem. Soc., Chem. Commun.*, 1992, 210.

101. S. Teipel, K. Griesar, W. Haase and B. Krebs, *Inorg. Chem.*, 1994, **33**, 4813.

102. N. W. Eilents, J. A. Heppert, M. L. Kennedy and F. Takusagawa, *Inorg. Chem.*, 1994, **33**, 4813.

103. K. J. Stallik and C. O. Quicksall, *Inorg. Chem.*, 1976, **15**, 1577.

104. R. C. Bott, G. Smith, D. S. Sagatys, T. C. W. Mak, D. E. Lynch and C. H. L. Kennard, *Aust. J. Chem.*, 1993, **46**, 105.

105. K. Y. Matsumato, *Bull. Chem. Soc. Jpn*, 1978, **51**, 492.

106. K. Nishikawam, A. Kobayashi and Y. Sasaki, *Bull. Chem. Soc. Jpn*, 1975, **48**, 889.

107. D. Hpu, K. S. Nagen and C. L. Hill, *J. Chem. Soc., Chem. Commun.*, 1993, 426.

108. V. W. Day, T. A Eberspacher, W. G. Klemperer and C. W. Park, J. Am. Chem. Soc., 1993, **115**, 8469.

109. A. Graham, The University of Edinburgh, unpublished results.

110. L. Akhter, W. Clegg, D. Collison and C. D. Garner, *Inorg. Chem.*, 1985, **24**, 1725.

111. F.Bonati, A. Burini, B. R. Pietroni and B. Bovio, *J. Organomet. Chem.*, 1985, **296**, 301.

112. C. M. Grant, Ph. D. Thesis, The University of Edinburgh, 1995.

113. A. J. Blake, C. M. Grant, S. Parsons, J. M. Rawson and R. E. P. Winpenny, *J. Chem. Soc., Chem. Commun.*, 1994, 2363.

114. O. Poncelet, L. G. Hubert-Pfalzgraf, J-C, Daran and R. Astier, *J. Chem. Soc., Chem. Commun.*, 1989, 1846.

115. H. Barrow, D. A. Brown, N. W. Alcock, H.J. Clase and M. G. H. Wallbridge, *J. Chem. Soc., Chem. Commun*, 1995, 1231.

116. A. Müller, K. Krickemeyer, H, Bögge, M. Schmidtmann, F. Peters, C. Menke, and J. Meyer, *Angew. Chem., Int. Ed. Engl.*, 1997, 36, 484.

117. E. K. Brechin, S. G. Harris, S. Parsons and R. E. P. Winpenny, submitted to *J. Chem. Soc., Dalton Trans*, 1997.

118. E. K. Brechin, R. O Gould, S. G Harris, S. Parsons and R. E. P. Winpenny, *J. Am. Chem. Soc.*, 1996, **118**, 11293.

119. S. Schutte, U. Klingelbiel and D. Z. Schmidt-Base, *Naturfosch. B : Chem. Sci.* 1993, **48**, 263.

120. R. A. Jones, S. U. Koschmieder, J. L. Atwood and S. G. J. Bott, *J. Chem. Soc., Chem.*

Commun., 1992, 726.

121. R. C. Squire, S. M. J. Aubin, K. Folting, W. E. Streib, D. N. Hendrickson and G. Christou, *Angew. Chem., Int. Ed. Engl.*, 1995, **34**, 887.

122. F. A. Cotton and B. E. Hanson, *Inorg. Chem.*, 1978, **17**, 3237.

123. F. A. Cotton, P. E. Fanwick, R. H. Niswander and J. C. Sekutowski, *J. Am. Chem. Soc.*, 1980, **100**, 4725.

124. K. Mashima, H, Nakano, T. Mori, H. Takaya and A. Nakamura, *Chem. Lett.*, 1992, 185.

125. K. Mashima, H. Nakano and A. Nakamura, *J. Am. Chem. Soc.*, 1993, **115**, 11632.

126. S. Wang, S. J. Trepanier and M. J. Wagner, *Inorg. Chem.*, 1993, **32**, 833.

127. A. J. Blake, R. O. Gould, C. M. Grant, P. E. Y. Milne, D. Reed and R. E. P. Winpenny, *Angew. Chem., Int. Ed. Engl.*, 1994, **33**, 195.

128. M. Mikuriya, H. Okawa, S. Kida and I. Ueda, *Bull. Chem. Soc. Jpn*, 1978, **51**, 2920.

129. J. Galy, J. Jaud, O. Kahn and P. Tola, *Inorg. Chem.*, 1980, **19**, 2945.

130. U. Thewalt and S. Müller, *Z. Naturforsch. B.*, 1989, **44**, 1206.

131. R. Fuchs and P. Klufers, *J. Organomet. Chem.*, 1992, **424**, 353.

132. H. A. Mirza, J. S. Vittal, R. J. Puddephatt, C. S. Frampton, L. Manojlovic-Muir, W. Xia and R. H. Hill, *Organometallics*, 1993, **12**, 2767.

133. L. M. Englehardt, P. C. Healy, R. M. Shephard, B. W. Skelton and A. H. White, *Inorg. Chem.*, 1988, **23**, 2371.

134. A. Gulbrandsen, J. Sletten, K. Nakatani, Y. Pei and O. Kahn, *Inorg. Chim. Acta*, 1993, **313**, 271.

135. E. K. Brechin, S. G. Harris, S. Parsons and R. E. P. Winpenny, submitted to *J. Chem. Soc., Chem. Commun.*, 1997.

136. A. J. Blake, R. O. Gould, P. E Y. Milne and R. E. P. Winpenny, *J. Chem. Soc., Chem. Commun.*, 1992, 522.

137. G. Bednorz and K. A. Müller, *Z. Phys. B.*, 1986, **64**, 189.

138. A. Bencini, C. Benelli A. Caneschi, R. L. Carlin, A. Dei and D. Gatteschi, *J. Am. Chem. Soc.*, 1990, 29, 1751.

139. C. Benelli, A. Caneschi, D. Gatteschi, O. Guillon and L. Pardi, *Inorg. Chem.*, 1990, **29**, 1751.

140. N. Matsumato, N. Sakamoto, H. Tamaki, H. Okawa and S. Kida, *Chem. Lett.*, 1989, 853.

141. M. Andruh, I. Ramade, E. Codjori, O. Guillon, O. Kahn and J. C. Trombe, *J. Am. Chem. Soc.*, 1993, **115**, 1822.

142. A. J. Blake, R.O Gould, C. M. Grant, P. E. Y. Milne, S. Parsons and R. E. P. Winpenny, *J. Chem. Soc., Dalton Trans.*, 1997, 485.

143. C. Benelli, A. J. Blake, P. E. Y. Milne. J. M. Rawson and R. E. P. Winpenny, *Chem. Eur. J.*, 1995, **1**, 614.

144. J.-P. Costes, F. Dahan, A. Dupuis and J.-P. Laurent, *Inorg. Chem.*, 1996, **35**, 2400.

145. X.-M. Chen, Y.-L. Wu, Y.-X. Tong and X.-Y. Huang, *J. Chem. Soc., Dalton Trans*, 1996, 2443.

146. A. J. Blake, P. E. Y. Milne and R. E. P. Winpenny, *J. Chem. Soc., Dalton Trans,* 1993, 3727.

147. A. J. Blake, V. A. Cherepanov, A. A. Dunlop, C. M. Grant, P. E. Y. Milne, J. M. Rawson and R. E. P. Winpenny, *J. Chem. Soc., Dalton Trans.*, 1994, 2719.

148. D. M. L. Goodgame, D. J. Williams and R. E. P. Winpenny, *Polyhedron*, 1989, **8**, 1531.

149. P. E. Y. Milne, Ph. D. Thesis, The University of Edinburgh, 1993.

150. A. J. Blake, P. E. Y. Milne, P. Thornton and R. E. P. Winpenny, *Angew. Chem., Int. Ed. Engl.*, 1991, **30**, 1139.

151. A. J. Blake, R. O. Gould, P. E. Y. Milne and R. E. P. Winpenny, *J. Chem. Soc., Chem. Commun.*, 1992, 522.

152. A. J. Blake, R. O. Gould, P. E. Y. Milne and R. E. P. Winpenny, *J. Chem. Soc., Chem. Commun.*, 1991, 1453.

153. G. B. Deacon, C. M. Forsyth, W. C. Patalinghug, A. H. White, A. Dietrich and H. Schumann, *Aust, J. Chem.*, 1992, **45**, 567.

154. L. F. Lindoy, H. C. Lip, H. W. Louie, M. G. B. Drew and M. J. Hudson, *J. Chem. Soc., Chem. Commun*, 1977, 77.

155. J. M. Boncella and R. A. Anderen, *J. Chem. Soc., Chem. Commun.*, 1984, 809.

156. W. J. Evans, I. Bloom, J. W. Grate, L. A. Hughes, W. E. Hunter and J. L. Atwood, *Inorg. Chem.*, 1985, **24**, 4620.

157. J. P. White III, H. Deng, E. P. Boyd, J. Galluci and S. G. Shore, *Inorg. Chem.*, 1994, *33*, 1685.

158. D. M. L. Goodgame, S. Menzer, A. T. Ross and D. J. Williams, *J. Chem. Soc., Chem. Commun.*, 1994, 2605.

159. D. Deng, X. Zheng, C. Qian, J. Sun, a. Dormond, D. Baudry and M. Visseaux, *J. Chem. Soc., Dalton Trans.*, 1994, 1665.

160. J.-F. Petit, J. C. Trombe, A. Gleizes and J. Galy, *C. R. Acad. Sci., Ser. 2*, 1987, **304**, 1117.

161. Y. Yukawa, S. Igarashi, A. Yamano and S. Sato, *J. Chem. Soc., Chem. Commun.*, 1997, 711.

162. E. K. Brechin, S. G. Harris, S. Parsons and R. E. P. Winpenny, *J. Chem. Soc., Dalton*

Trans., 1997, 1665.

List of publications.

1. E. K. Brechin, S. G. Harris, S. Parsons and R. E. P. Winpenny, "Vertex- and Face-Sharing Adamantanes : A New Topology in Polymetallic Chemistry." *Angew. Chem., Int. Ed. Engl.*, 1997, in press.
2. E. K. Brechin, S. G. Harris, S. Parsons and R. E. P. Winpenny, "High Nuclearity Cobalt-Copper and Nickel-Copper Coordination Complexes." *J. Chem. Soc., Dalton Trans.*, 1997, in press.
3. E. K. Brechin, S. G. Harris, S. Parsons and R. E. P. Winpenny, "Heterobimetallic Complexes Containing D- and F-Block Elements : Synthesis and Structural Characterisation of Novel Ni-Er and Co-Dy Compounds." *J. Chem. Soc., Dalton Trans.*, 1997, 1665.
4. E. K. Brechin, S. G. Harris, A. Harrison, S. Parsons, A. G. Whittaker and R. E. P. Winpenny, "Synthesis, Structural Characterisation and Preliminary Magnetic Studies of a Tetraicosahedral Cobalt Coordination Complex." *J. Chem. Soc., Chem. Commun.*, 1997, 667.
5. E. K. Brechin, R. O. Gould, S. G. Harris, S. Parsons and R. E. P. Winpenny, "Four Cubes and an Octahedron : A Nickel-Sodium Supracage Assembly." *J. Am. Chem. Soc.*, 1996, **118**, 11293.
6. E. K. Brechin, S. Parsons and R. E. P. Winpenny, "Uncapped and Polar Capped Prisms of Cobalt and Nickel." *J. Chem. Soc., Dalton Trans.*, 1996, 3745.

7. E. K. Brechin, S. G. Harris, S. Parsons and R. E. P. Winpenny, " Desolvating Cubes and Linking Prisms : Routes to High Nuclearty Cobalt Complexes." *J. Chem. Soc., Chem. Commun.*, 1996, 1439.

8. A. J. Blake, E. K. Brechin, A. Codron, R.O Gould, C. M. Grant, S. Parsons, J. M. Rawson and R. E. P. Winpenny, " New Polynuclear Nickel Complexes with a Variety of Pyridonate and Carboxylate Ligands." *J. Chem. Soc. Chem. Commun.*, 1995, 1983.

9. E. K. Brechin, L. M. Gilby, S. G. Harris, S. Parsons and R. E. P. Winpenny, "Heterobimetallic Nickel-Sodium and Cobalt-Sodium Complexes of Pyridonate Ligands." submitted to *J. Chem. Soc., Dalton Trans.*, 1997.

10. E. K. Brechin, S. G. Harris, S. Parsons and R. E. P. Winpenny, "Synthesis, structure and Initial Magnetic Studies of a Cyclic Dodecanuclear Cobalt Complex." submitted to *J. Chem. Soc., Dalton Trans.*, 1997.

11. C. Benelli, E. K. Brechin, A. Graham, S. G. Harris, S. Parsons and R. E. P. Winpenny, "A Family of Polynuclear Cobalt and Nickel Complexes Based on Deltahedra Stabilised by 2-Pyridonate and Carboxylate Ligands." submitted to *J. Chem. Soc., Dalton Trans.*, 1997.

12. E. K. Brechin, A. Graham, S. G. Harris, S. Parsons and R. E. P. Winpenny, "Overcrowding Leads to Prism Reform : New Polyhedra for Polymetallic Cages." submitted to *J. Chem. Soc., Dalton Trans.*, 1997.

13. M. A. Halcrow, L. M. Rodriguez-Martinez, E. K. Brechin, J. E. Davies, I. J. Scowen and M. M°Partlin, "Synthesis, Structure and Magnetism of Homoleptic Complexes of 4-Pyrid-4-yloxy-2, 2, 6, 6,-tetra-methyl-1-Piperidinoxyl ; A New Spin Labelled Pyridine." *J. Chem. Soc. Dalton Trans*, 1997, in press.

Crystallographic Appendix

Table 1. Crystal data and structure refinement for 1.

Identification code	niochp
Empirical formula	C32 H56 Cl4 N4 Ni4 O16
Formula weight	1129.45
Temperature	150(2) K
Wavelength	0.71073 A
Crystal system	TRICLINIC
Space group	P -1
Unit cell dimensions	a = 12.795(6) A alpha = 91.60(4) deg. b = 14.129(7) A beta = 101.20(3) deg. c = 14.191(7) A gamma = 111.81(3) deg.
Volume	2322(2) A^3
Z	2
Density (calculated)	1.615 Mg/m^3
Absorption coefficient	1.894 mm^-1
F(000)	1168
Crystal size	0.55 x 0.35 x 0.20 mm
Theta range for data collection	2.53 to 25.04 deg.
Index ranges	-15<=h<=14, -16<=k<=15, 0<=l<=16
Reflections collected	8746
Independent reflections	6932 [R(int) = 0.0241]
Refinement method	Full-matrix least-squares on F^2
Data / restraints / parameters	6910 / 0 / 554
Goodness-of-fit on F^2	1.058
Final R indices [I>2sigma(I)]	R1 = 0.0355, wR2 = 0.0880
R indices (all data)	R1 = 0.0411, wR2 = 0.0987
Extinction coefficient	0.0001(2)
Largest diff. peak and hole	1.311 and -0.603 e.A^-3

Table 2. Atomic coordinates (x 10^4) and equivalent isotropic displacement parameters (A^2 x 10^3) for 1. U(eq) is defined as one third of the trace of the orthogonalized Uij tensor.

Crystal data and structure refinement for 3. at 220.0(2) K.

Empirical formula	Molecule 1	C38 H32 Cl6 N10 Na2 Ni2 O7
	Molecule 2	C38 H34 Cl6 N10 Na2 Ni2 O8
	= [C76 H66 Cl12 N20 Na4 Ni4 O15]	
Formula weight		2251.69
Wavelength		1.54184 A
Crystal system		Monoclinic
Space group		P2/c
Unit cell dimensions		a = 16.4177(15) A alpha = 90 deg. b = 9.1699(5) A beta = 91.096(11) deg. c = 31.597(2) A gamma = 90 deg.
Volume		4756.0(6) A^3
Z		2
Density (calculated)		1.572 Mg/m^3
Absorption coefficient		4.768 mm^-1
F(000)		2284
Crystal description		Green block
Crystal size		0.27 x 0.16 x 0.10 mm
Theta range for data collection		2.69 to 60.09 deg.
Index ranges		-18<=h<=18, -10<=k<=9, -32<=l<=35
Reflections collected		8871
Independent reflections		6939 [R(int) = 0.1109]
Scan type		omega
Absorption correction		Psi-scans (Tmin= 0.338, Tmax=0.516)
Data / restraints / parameters		6889/0/591 (Full-matrix least-squares on F^2
Goodness-of-fit on F^2		1.051
Conventional R [F>4sigma(F)]		R1 = 0.0532 [4801 data]
R indices (all data)		R1 = 0.0892, wR2 = 0.1263
Final maximum delta/sigma		0.001
Weighting scheme calc w=1/[\s^2^(Fo^2^)+(0.0316P)^2^+8.2341P] where P=(Fo^2^+2Fc^2^)/3		
Largest diff. peak and hole		0.283 and -0.360 e.A^-3

Crystal data and structure refinement for 4 at 220.0(2) K.

Empirical formula	Molecule 1 C38 H32 Cl6 N10 Na2 Ni2 O7 Molecule 2 C38 H34 Cl6 N10 Na2 Ni2 O8 = [C76 H66 Cl12 N20 Na4 Ni4 O15]
Formula weight	2251.69
Wavelength	1.54184 A
Crystal system	Monoclinic
Space group	P2/c
Unit cell dimensions	a = 16.4177(15) A alpha = 90 deg. b = 9.1699(5) A beta = 91.096(11) deg. c = 31.597(2) A gamma = 90 deg.
Volume	4756.0(6) A^3
Z	2
Density (calculated)	1.572 Mg/m^3
Absorption coefficient	4.768 mm^-1
F(000)	2284
Crystal description	Green block
Crystal size	0.27 x 0.16 x 0.10 mm
Theta range for data collection	2.69 to 60.09 deg.
Index ranges	-18<=h<=18, -10<=k<=9, -32<=l<=35
Reflections collected	8871
Independent reflections	6939 [R(int) = 0.1109]
Scan type	omega
Absorption correction	Psi-scans (Tmin= 0.338, Tmax=0.516)
Data / restraints / parameters	6889/0/591 (Full-matrix least-squares on F
Goodness-of-fit on F^2	1.051
Conventional R [F>4sigma(F)]	R1 = 0.0532 [4801 data]
R indices (all data)	R1 = 0.0892, wR2 = 0.1263
Final maximum delta/sigma	0.001
Weighting scheme calc w=1/[\s^2^(Fo^2^)+(0.0316P)^2^+8.2341P] where P=(Fo^2^+2Fc^2^)/3	
Largest diff. peak and hole	0.283 and -0.360 e.A^-3

Crystal data and structure refinement for 5 at 220(2) K.

Empirical formula	C30 H20 Cl6 N6 Na2 Ni2 O7
Formula weight	952.62
Wavelength	1.54184 A
Crystal system	Monoclinic
Space group	C2/c
Unit cell dimensions	a = 21.407(6) A alpha = 90 deg. b = 11.860(3) A beta = 91.04(2) deg. c = 13.912(2) A gamma = 90 deg.
Volume	3531.5(14) A^3
Number of reflections for cell	20 (10 < theta < 22 deg.)
Z	4
Density (calculated)	1.792 Mg/m^3
Absorption coefficient	6.243 mm^-1
F(000)	1912
Crystal description	green block
Crystal size	0.35 x 0.27 x 0.02 mm
Theta range for data collection	4.13 to 59.95 deg.
Index ranges	-24<=h<=24, -13<=k<=13, -1<=l<=15
Reflections collected	4501
Independent reflections	2584 [R(int) = 0.0562]
Scan type	omega-2theta
Absorption correction	Difabs (Tmin= 0.462, Tmax=1.323)
Data / restraints / parameters	2579/56/243 (Full-matrix least-squares on F
Goodness-of-fit on F^2	0.958
Conventional R [F>4sigma(F)]	R1 = 0.0515 [1414 data]
R indices (all data)	R1 = 0.1164, wR2 = 0.1091
Final maximum delta/sigma	-0.012
Weighting scheme calc w=1/[\s^2^(Fo^2^)+(0.0358P)^2^+0.0000P] where P=(Fo^2^+2Fc^2^)/3	
Largest diff. peak and hole	0.303 and -0.293 e.A^-3

Crystal data and structure refinement for 6 at 150.0(2) K.

Empirical formula	C84 H86 N14 Na4 Ni4 O14
Formula weight	1842.47
Wavelength	1.54184 A
Crystal system	Triclinic
Space group	P-1
Unit cell dimensions	a = 10.818(4) A alpha = 109.90(2) deg. b = 14.336(5) A beta = 100.46(2) deg. c = 16.281(6) A gamma = 107.50(2) deg.
Volume	2147.8(13) A^3
Z	1
Density (calculated)	1.424 Mg/m^3
Absorption coefficient	1.764 mm^-1
F(000)	956
Crystal description	Green plate
Crystal size	0.39 x 0.35 x 0.12 mm
Theta range for data collection	3.04 to 59.99 deg.
Index ranges	-12<=h<=11, -16<=k<=13, -14<=l<=18
Reflections collected	6659
Independent reflections	6251 [R(int) = 0.0659]
Scan type	Omega-theta
Absorption correction	DIFABS (Tmin= 0.368, Tmax=1.000)
Data / restraints / parameters	6244/0/541 (Full-matrix least-squares on F^2
Goodness-of-fit on F^2	1.010
Conventional R [F>4sigma(F)]	R1 = 0.0509 [4721 data]
R indices (all data)	R1 = 0.0732, wR2 = 0.1444
Final maximum delta/sigma	-0.001
Weighting scheme calc w=1/[\s^2^(Fo^2^)+(0.0962P)^2^+0.0000P] where P=(Fo^2^+2Fc^2^)/3	
Largest diff. peak and hole	0.403 and -0.443 e.A^-3

Crystal data and structure refinement for 7 at 150(2) K.

Empirical formula	C32 H56 Cl4 Co4 N4 O16
Formula weight	1130.33
Wavelength	0.71073 A
Crystal system	Triclinic
Space group	P-1
Unit cell dimensions	a = 12.892(4) A alpha = 91.35(2) deg. b = 14.235(5) A beta = 112.00(2) deg. c = 14.244(5) A gamma = 101.43(2) deg.
Volume	2361.8(14) A^3
Z	2
Density (calculated)	1.589 Mg/m^3
Absorption coefficient	1.673 mm^-1
F(000)	1160
Crystal description	Red block
Crystal size	0.78 x 0.62 x 0.54 mm
Theta range for data collection	2.52 to 25.03 deg.
Index ranges	-15<=h<=13, -16<=k<=16, 0<=l<=16
Reflections collected	9498
Independent reflections	8321 [R(int) = 0.0397]
Scan type	omega-theta
Absorption correction	Psi-scans (Tmin= 0.383, Tmax=0.486)
Data / restraints / parameters	8310/0/541 (Full-matrix least-squares on F^
Goodness-of-fit on F^2	1.028
Conventional R [F>4sigma(F)]	R1 = 0.0424 [6511 data]
R indices (all data)	R1 = 0.0626, wR2 = 0.1103
Final maximum delta/sigma	0.001
Weighting scheme calc w=1/[\s^2^(Fo^2^)+(0.0544P)^2^+3.0846P] where P=(Fo^2^+2Fc^2^)/3	
Largest diff. peak and hole	1.023 and -0.567 e.A^-3

Crystal data and structure refinement for 8 at 150.0(2) K.

Empirical formula	C108 H94 Cl34 Co12 N20 O30
Formula weight	4064.49
Wavelength	0.71073 A
Crystal system	Monoclinic
Space group	P21/n
Unit cell dimensions	a = 18.286(4) A alpha = 90 deg. b = 16.294(4) A beta = 108.41(2) deg. c = 26.609(6) A gamma = 90 deg.
Volume	7522(3) A^3
Z	2
Density (calculated)	1.794 Mg/m^3
Absorption coefficient	1.963 mm^-1
F(000)	4048
Crystal description	Purple tablet
Crystal size	0.43 x 0.27 x 0.16 mm
Theta range for data collection	2.56 to 22.54 deg.
Index ranges	-19<=h<=18, 0<=k<=17, 0<=l<=28
Reflections collected	11590
Independent reflections	9861 [R(int) = 0.1299]
Scan type	Omega
Data / restraints / parameters	9823/837/688 (Full-matrix least-squares on
Goodness-of-fit on F^2	0.997
Conventional R [F>4sigma(F)]	R1 = 0.0926 [4061 data]
R indices (all data)	R1 = 0.2344, wR2 = 0.2292
Final maximum delta/sigma	-0.031
Weighting scheme calc w=1/[\s^2^(Fo^2^)+(0.0700P)^2^+0.0000P] where P=(Fo^2^+2Fc^2^)/3	
Largest diff. peak and hole	0.721 and -0.809 e.A^-3

Crystal data and structure refinement for 10 at 220(2) K.

Empirical formula	C30 H20 Cl6 Co2 N6 Na2 O7
Formula weight	953.06
Wavelength	1.54184 A
Crystal system	Monoclinic
Space group	C2/c
Unit cell dimensions	a = 21.590(13) A alpha = 90 deg. b = 11.916(9) A beta = 91.37(6) deg. c = 13.879(10) A gamma = 90 deg.
Volume	3570(4) A^3
Z	4
Density (calculated)	1.773 Mg/m^3
Absorption coefficient	12.147 mm^-1
F(000)	1904
Crystal description	Pink plate developed in (001)
Crystal size	0.35 x 0.27 x 0.02 mm
Theta range for data collection	4.10 to 54.96 deg.
Index ranges	-22<=h<=22, 0<=k<=12, 0<=l<=14
Reflections collected	2185
Independent reflections	2185 [R(int) = 0.0000]
Scan type	omega
Absorption correction	Integration (Tmin= 0.0919, Tmax=0.5274)
Data / restraints / parameters	2150/259/244 (Full-matrix least-squares on
Goodness-of-fit on F^2	1.127
Conventional R [F>4sigma(F)]	R1 = 0.0775 [1563 data]
R indices (all data)	R1 = 0.1174, wR2 = 0.2167
Extinction coefficient	0.00021(5)
Final maximum delta/sigma	0.000
Weighting scheme calc w=1/[\s^2^(Fo^2^)+(0.0847P)^2^+53.1420P] where P=(Fo^2^+2Fc^2^)/3	
Largest diff. peak and hole	0.572 and -1.256 e.A^-3

Crystal data and structure refinement for 11

Identification code	cosnat
Empirical formula	C15 H9 Cl3 Co N3 Na O3
Formula weight	467.52
Temperature	220(2) K
Wavelength	0.71073 A
Crystal system	Triclinic
Space group	P-1
Unit cell dimensions	a = 7.261(2) A alpha = 112.204(10) deg. b = 11.316(2) A beta = 93.119(14) deg. c = 12.105(3) A gamma = 105.192(13) deg.
Volume, Z	875.5(3) A^3, 2
Density (calculated)	1.773 Mg/m^3
Absorption coefficient	1.484 mm^-1
F(000)	466
Crystal size	0.35 x 0.18 x 0.08 mm
Theta range for data collection	2.95 to 25.04 deg.
Limiting indices	-8<=h<=8, -13<=k<=12, 0<=l<=14
Reflections collected	3702
Independent reflections	3100 [R(int) = 0.0878]
Absorption correction	None
Refinement method	Full-matrix least-squares on F^2
Data / restraints / parameters	3100 / 0 / 235
Goodness-of-fit on F^2	0.981
Final R indices [I>2sigma(I)]	R1 = 0.0538, wR2 = 0.1019
R indices (all data)	R1 = 0.1090, wR2 = 0.1196
Largest diff. peak and hole	0.529 and -0.613 e.A^-3

Crystal data and structure refinement for 14 . at 220.0(2) K.

Empirical formula	complex	C134 H156 C16 Co24 N22 O42
	solvent	C 4 H 8 O 2
Formula weight		4461.93
Wavelength		0.71073 A
Crystal system		Triclinic
Space group		P-1
Unit cell dimensions		a = 15.459(6) A alpha = 76.43(3) deg. b = 18.619(8) A beta = 70.04(2) deg. c = 21.402(9) A gamma = 72.70(2) deg.
Volume		5467(4) A^3
Z		1
Density (calculated)		1.355 Mg/m^3
Absorption coefficient		1.900 mm^-1
F(000)		2248
Crystal description		Mauve block
Crystal size		0.51 x 0.47 x 0.39 mm
Theta range for data collection		2.63 to 22.52 deg.
Index ranges		-15<=h<=16, -19<=k<=20, 0<=l<=23
Reflections collected		18237
Independent reflections		14255 [R(int) = 0.0234]
Scan type		Omega-theta
Absorption correction		Psi-scans (Tmin= 0.929, Tmax=1.000)
Data / restraints / parameters		14234/999/1065 (Full-matrix least-squares o
Goodness-of-fit on F^2		0.952
Conventional R [F>4sigma(F)]		R1 = 0.0572 [8683 data]
R indices (all data)		R1 = 0.1018, wR2 = 0.1726
Final maximum delta/sigma		0.071
Weighting scheme calc w=1/[\s^2^(Fo^2^)+(0.0813P)^2^+0.0000P] where P=(Fo^2^+2Fc^2^)/3		
Largest diff. peak and hole		0.564 and -0.602 e.A^-3

Crystal data and structure refinement for 15 at 220(2) K.

Empirical formula	C71.40 H65.10 Cl14 N13.70 Ni7 O18
Formula weight	2310.34
Wavelength	1.54184 A
Crystal system	Triclinic
Space group	P-1
Unit cell dimensions	a = 13.706(7) A alpha = 60.68(5) deg. b = 15.216(9) A beta = 67.15(4) deg. c = 15.431(8) A gamma = 69.33(4) deg.
Volume	2532(2) A^3
Number of reflections for cell	30 (9.5 < theta < 29.5 deg.)
Z	1
Density (calculated)	1.515 Mg/m^3
Absorption coefficient	5.331 mm^-1
F(000)	1167
Crystal description	Green column
Crystal size	0.51 x 0.19 x 0.16 mm
Theta range for data collection	3.40 to 60.01 deg.
Index ranges	-13<=h<=15, -14<=k<=17, -10<=l<=17
Reflections collected	7376
Independent reflections	7376 [R(int) = 0.0000]
Scan type	omega
Absorption correction	SHELXA (Tmin= 0.165, Tmax=0.637)
Data / restraints / parameters	7366/0/529 (Full-matrix least-squares on F
Goodness-of-fit on F^2	0.958
Conventional R [F>4sigma(F)]	R1 = 0.0890 [4284 data]
R indices (all data)	R1 = 0.1378, wR2 = 0.2729
Final maximum delta/sigma	0.073
Weighting scheme calc w=1/[\s^2^(Fo^2^)+(0.1707P)^2^+0.0000P] where P=(Fo^2^+2Fc^2^)/3	
Largest diff. peak and hole	0.984 and -1.437 e.A^-3

Crystal data and structure refinement for 16 at 220.0(2) K.

Empirical formula	C66 H62 Cl12 N12 Ni7 O20
Formula weight	2179.65
Wavelength	0.71073 A
Crystal system	Monoclinic
Space group	P21/n
Unit cell dimensions	a = 12.502(4) A alpha = 90 deg. b = 19.917(6) A beta = 106.23(2) deg. c = 17.601(4) A gamma = 90 deg.
Volume	4208(2) A^3
Z	2
Density (calculated)	1.720 Mg/m^3
Absorption coefficient	1.987 mm^-1
F(000)	2204
Crystal description	Green block
Crystal size	0.31 x 0.27 x 0.19 mm
Theta range for data collection	2.55 to 22.56 deg.
Index ranges	-13<=h<=12, 0<=k<=21, 0<=l<=18
Reflections collected	8087
Independent reflections	5516 [R(int) = 0.13, XPREP]
Scan type	Omega-theta(5-30) / LP(28-45 deg.)
Absorption correction	Psi-scans (Tmin= 0.594, Tmax=0.413)
Data / restraints / parameters	5474/8/535 (Full-matrix least-squares on F^
Goodness-of-fit on F^2	1.032
Conventional R [F>4sigma(F)]	R1 = 0.0827 [2899 data]
R indices (all data)	R1 = 0.1756, wR2 = 0.2220
Final maximum delta/sigma	-0.004
Weighting scheme calc w=1/[\s^2^(Fo^2^)+(0.0780P)^2^+0.0000P] where P=(Fo^2^+2Fc^2^)/3	
Largest diff. peak and hole	0.612 and -0.899 e.A^-3

Crystal data and structure refinement for 17 at 220.0(2) K.

Empirical formula	C84 H56 Cl16 N18 Ni9 O18
Formula weight	2701.06
Wavelength	1.54184 A
Crystal system	Monoclinic
Space group	C2/c
Unit cell dimensions	a = 31.570(3) A alpha = 90 deg. b = 12.784(2) A beta = 101.160(10) deg. c = 25.371(3) A gamma = 90 deg.
Volume	10046(2) A^3
Z	4
Density (calculated)	1.786 Mg/m^3
Absorption coefficient	6.325 mm^-1
F(000)	5416
Crystal description	Green wedge
Crystal size	0.23 x 0.16 x 0.16 mm
Theta range for data collection	2.85 to 60.13 deg.
Index ranges	-35<=h<=34, -14<=k<=14, -13<=l<=28
Reflections collected	9367
Independent reflections	7286 [R(int) = 0.0693]
Scan type	Omega-theta scans
Absorption correction	Psi-scans (Tmin= 0.193, Tmax=0.343)
Data / restraints / parameters	7213/0/655 (Full-matrix least-squares on F^2
Goodness-of-fit on F^2	1.020
Conventional R [F>4sigma(F)]	R1 = 0.0602 [4810 data]
R indices (all data)	R1 = 0.1042, wR2 = 0.1524
Final maximum delta/sigma	0.002
Weighting scheme calc w=1/[\s^2^(Fo^2^)+(0.0357P)^2^+70.9774P] where P=(Fo^2^+2Fc^2^)/3	
Largest diff. peak and hole	0.496 and -0.504 e.A^-3

Crystal data and structure refinement for 18 : 220(2) K.

Empirical formula	C102 H78 Cl18 Co9 N18 O24
Formula weight	3108.29
Wavelength	1.54184 A
Crystal system	Rhombohedral
Space group	R-3c
Unit cell dimensions	a = 18.298(2) A alpha = 90 deg. b = 18.298(2) A beta = 90 deg. c = 67.570(8) A gamma = 120 deg.
Volume	19593(4) A^3
Z	6
Density (calculated)	1.581 Mg/m^3
Absorption coefficient	12.695 mm^-1
F(000)	9342
Crystal description	Purple tablet
Crystal size	0.16 x 0.16 x 0.04 mm
Theta range for data collection	3.08 to 60.08 deg.
Index ranges	-17<=h<=16, 0<=k<=20, 0<=l<=71
Reflections collected	3952
Independent reflections	2763 [R(int) = 0.0842]
Scan type	omega with learnt profile
Absorption correction	Difabs (Tmin= 0.176, Tmax=0.604)
Data / restraints / parameters	2729/305/285 (Full-matrix least-squares on
Goodness-of-fit on F^2	1.043
Conventional R [F>4sigma(F)]	R1 = 0.0771 [1404 data]
R indices (all data)	R1 = 0.1633, wR2 = 0.2496
Final maximum delta/sigma	0.000
Weighting scheme calc w=1/[\s^2^(Fo^2^)+(0.0903P)^2^+160.8840P] where P=(Fo^2^+2Fc^2^)/3	
Largest diff. peak and hole	0.700 and -1.317 e.A^-3

Crystal data and structure refinement for 19 at 220(2) K.

Empirical formula	C108 H122 Cl N22 Ni11 O24
Formula weight	2793.54
Wavelength	1.54184 A
Crystal system	Triclinic
Space group	P-1
Unit cell dimensions	a = 13.750(5) A alpha = 100.88(3) deg. b = 15.365(4) A beta = 90.56(4) deg. c = 30.695(9) A gamma = 107.72(2) deg.
Volume	6051(3) A^3
Number of reflections for cell	38 (20 < theta < 22 deg.)
Z	2
Density (calculated)	1.533 Mg/m^3
Absorption coefficient	2.628 mm^-1
F(000)	2882
Crystal description	Green plate developed in (101)
Crystal size	0.39 x 0.27 x 0.04 mm
Theta range for data collection	2.94 to 60.12 deg.
Index ranges	-15<=h<=14, -16<=k<=15, -31<=l<=34
Reflections collected	15641
Independent reflections	14715 [R(int) = 0.0603]
Scan type	omega with learnt profile
Absorption correction	Psi-scans (Tmin= 0.214, Tmax=0.833)
Data / restraints / parameters	14501/9/1504 (Full-matrix-block least-squar
Goodness-of-fit on F^2	1.025
Conventional R [F>4sigma(F)]	R1 = 0.0669 [10093 data]
R indices (all data)	R1 = 0.1053, wR2 = 0.1890 17.15.
Final maximum delta/sigma	0.007
Weighting scheme calc w=1/[\s^2^(Fo^2^)+(0.0743P)^2^+14.1306P] where P=(Fo^2^+2Fc^2^)/3	
Largest diff. peak and hole	0.606 and -0.572 e.A^-3

. Crystal data and structure refinement for 21 at 220.0(2) K.

Empirical formula	C85.72 H93.44 C16 N12 Ni12 O30.86
Formula weight	2702.78
Wavelength	0.71073 A
Crystal system	Monoclinic
Space group	P21/n
Unit cell dimensions	a = 28.278(7) A alpha = 90 deg. b = 15.118(5) A beta = 114.62(2) deg. c = 28.708(8) A gamma = 90 deg.
Volume	11157(6) A^3
Z	4
Density (calculated)	1.609 Mg/m^3
Absorption coefficient	2.194 mm^-1
F(000)	5507
Crystal description	Green block
Crystal size	0.39 x 0.35 x 0.31 mm
Theta range for data collection	2.53 to 21.06 deg.
Index ranges	-28<=h<=25, 0<=k<=15, 0<=l<=28
Reflections collected	13944
Independent reflections	12037 [R(int) = 0.0846]
Scan type	Omega-theta
Absorption correction	Psi-scans (Tmin= 0.336, Tmax=0.256)
Data / restraints / parameters	12033/179/1305 (Full-matrix-block least-squa
Goodness-of-fit on F^2	1.051
Conventional R [F>4sigma(F)]	R1 = 0.0609 [7845 data]
R indices (all data)	R1 = 0.0997, wR2 = 0.1678
Final maximum delta/sigma	-0.019
Weighting scheme calc w=1/[\s^2^(Fo^2^)+(0.0770P)^2^+8.1877P] where P=(Fo^2^+2Fc^2^)/3	
Largest diff. peak and hole	0.781 and -0.518 e.A^-3

Crystal data and structure refinement for 22 at 150(2) K.

Empirical formula	C113 H101 Cl14 N12 Ni12 O34
Formula weight	3371.88
Wavelength	1.54184 A
Crystal system	Rhombohedral
Space group	R3c
Unit cell dimensions	a = 16.279(3) A alpha = 90 deg. b = 16.279(3) A beta = 90 deg. c = 85.61(3) A gamma = 120 deg.
Volume	19647(8) A^3
Z	6
Density (calculated)	1.710 Mg/m^3
Absorption coefficient	5.104 mm^-1
F(000)	10254
Crystal description	Green block
Crystal size	0.46 x 0.39 x 0.35 mm
Theta range for data collection	3.10 to 60.02 deg.
Index ranges	-15<=h<=15, -18<=k<=18, -94<=l<=94
Reflections collected	8039
Independent reflections	3543 [R(int) = 0.0521]
Scan type	omega
Absorption correction	Psi-scan (Tmin= 0.410, Tmax=0.574)
Data / restraints / parameters	3542/7/560 (Full-matrix least-squares on F^2
Goodness-of-fit on F^2	1.078
Conventional R [F>4sigma(F)]	R1 = 0.0491 [3355 data]
R indices (all data)	R1 = 0.0530, wR2 = 0.1399
Absolute structure parameter	0.35(6)
Final maximum delta/sigma	-0.019
Weighting scheme calc w=1/[\s^2^(Fo^2^)+(0.0864P)^2^+128.2114P] where P=(Fo^2^+2Fc^2^)/3	
Largest diff. peak and hole	0.756 and -0.583 e.A^-3

Identification code	nimptf
Empirical formula	C68.50 H89 N9 Ni11 O34
Formula weight	2228.30
Temperature	150(2) K
Wavelength	0.71073 A
Crystal system	monoclinic
Space group	C2/c
Unit cell dimensions	a = 39.931(13) A alpha = 90 deg. b = 25.516(10) A beta = 120.2(3) deg. c = 22.43(2) A gamma = 90 deg.
Volume	19751(17) A^3
Z	8
Density (calculated)	1.499 Mg/m^3
Absorption coefficient	2.122 mm^-1
F(000)	9144
Crystal size	0.50 x 0.20 x 0.14 mm
Theta range for data collection	2.51 to 22.51 deg.
Index ranges	-42<=h<=37, 0<=k<=27, 0<=l<=24
Reflections collected	13013
Independent reflections	12879 [R(int) = 0.2985]
Refinement method	Full-matrix least-squares on F^2
Data / restraints / parameters	12813 / 4 / 1089
Goodness-of-fit on F^2	1.010
Final R indices [I>2sigma(I)]	R1 = 0.0937, wR2 = 0.2132
R indices (all data)	R1 = 0.2039, wR2 = 0.2866
Largest diff. peak and hole	1.311 and -0.833 e.A^-3

Table 2. Atomic coordinates (x 10^4) and equivalent isotropic displacement parameters (A^2 x 10^3) for 1. U(eq) is defined as one third of the trace of the orthogonalized Uij tensor.

Identification code	ni3mhp
Empirical formula	C35 H60 Cl2 N4 Ni3 O14
Formula weight	1007.90
Temperature	150(2) K
Wavelength	0.71073 A
Crystal system, space group	Triclinic, P-1
Unit cell dimensions	a = 15.223(3) A alpha = 78.39(3) deg. b = 16.362(3) A beta = 83.27(3) deg. c = 24.052(5) A gamma = 72.30(3) deg.
Volume	5580.4(19) A^3
Z, Calculated density	8, 2.399 Mg/m^3
Absorption coefficient	2.299 mm^-1
F(000)	4224
Crystal size	0.51 x 0.23 x 0.16 mm
Theta range for data collection	2.58 to 22.53 deg.
Index ranges	-16<=h<=16, -17<=k<=17, -1<=l<=25
Reflections collected / unique	15206 / 14566 [R(int) = 0.0879]
Completeness to theta = 22.53	99.4%
Absorption correction	None
Max. and min. transmission	0.7099 and 0.3868
Refinement method	Full-matrix least-squares on F^2
Data / restraints / parameters	14566 / 1125 / 660
Goodness-of-fit on F^2	0.860
Final R index [I>2sigma(I)]	R1 = 0.0855, [for 10249 data]
R indices (all data)	R1 = 0.1259, wR2 = 0.2642
Largest diff. peak and hole	1.627 and -1.733 e.A^-3

Crystal data and structure refinement for 25 at 150(2) K.

Empirical formula	C108 H105.50 Cl Co10 N11.50 O29
Formula weight	2653.29
Wavelength	0.71073 A
Crystal system	Triclinic
Space group	P-1
Unit cell dimensions	a = 15.995(9) A alpha = 88.84(3) deg. b = 16.176(7) A beta = 85.33(4) deg. c = 25.275(14) A gamma = 61.21(3) deg.
Volume	5711(5) A^3
Z	2
Density (calculated)	1.543 Mg/m^3
Absorption coefficient	1.515 mm^-1
F(000)	2706
Crystal description	Pink plate developed in [001]
Crystal size	0.47 x 0.39 x 0.04 mm
Theta range for data collection	2.52 to 20.00 deg.
Index ranges	-15<=h<=15, -15<=k<=15, 0<=l<=24
Reflections collected	9858
Independent reflections	9655 [R(int) = 0.1559]
Scan type	omega
Absorption correction	Psi-scan (Tmin= 0.549, Tmax=1.000)
Data / restraints / parameters	9600/2508/1429 (Full-matrix-block least-squ
Goodness-of-fit on F^2	1.045
Conventional R [F>4sigma(F)]	R1 = 0.0698 [6038 data]
R indices (all data)	R1 = 0.1299, wR2 = 0.1871
Final maximum delta/sigma	-0.031
Weighting scheme calc w=1/[\s^2^(Fo^2^)+(0.0712P)^2^+35.2113P] where P=(Fo^2^+2Fc^2^)/3	
Largest diff. peak and hole	0.837 and -0.550 e.A^-3

Crystal data and structure refinement for 26 at 220.0(2) K.

Empirical formula	C93 H129.48 N10 Ni10 O28.48
Formula weight	2430.33
Wavelength	1.54184 A
Crystal system	Rhombohedral
Space group	R-3c
Unit cell dimensions	a = 52.372(10) A alpha = 90 deg. b = 52.372(10) A beta = 90 deg. c = 21.805(6) A gamma = 120 deg.
Volume	51795(20) A^3
Z	18
Density (calculated)	1.402 Mg/m^3
Absorption coefficient	2.309 mm^-1
F(000)	22776
Crystal description	Green block
Crystal size	0.39 x 0.35 x 0.31 mm
Theta range for data collection	5.88 to 60.17 deg.
Index ranges	-32<=h<=50, 0<=k<=50, 0<=l<=24
Reflections collected	12734
Independent reflections	8106 [R(int) = 0.0808]
Scan type	Omega
Absorption correction	Psi-scans (Tmin= 0.264, Tmax=0.508)
Data / restraints / parameters	8102/154/661 (Full-matrix least-squares on F
Goodness-of-fit on F^2	0.999
Conventional R [F>4sigma(F)]	R1 = 0.0675 [4819 data]
R indices (all data)	R1 = 0.1196, wR2 = 0.2027
Final maximum delta/sigma	-0.010
Weighting scheme calc w=1/[\s^2^(Fo^2^)+(0.1022P)^2^+0.0000P] where P=(Fo^2^+2Fc^2^)/3	
Largest diff. peak and hole	0.726 and -0.444 e.A^-3

Crystal data and structure refinement for 29 at 220(2) K.

Empirical formula	C62 H64 Cl6 N4 Ni3 O17
Formula weight	1526.00
Wavelength	1.54184 A
Crystal system	Triclinic
Space group	P-1
Unit cell dimensions	a = 14.205(7) A alpha = 62.98(2) deg. b = 16.893(8) A beta = 62.92(2) deg. c = 18.474(10) A gamma = 67.24(2) deg.
Volume	3425(3) A^3
Number of reflections for cell	30 (20 < theta < 22 deg.)
Z	2
Density (calculated)	1.480 Mg/m^3
Absorption coefficient	3.691 mm^-1
F(000)	1572
Crystal description	Green block
Crystal size	0.54 x 0.31 x 0.23 mm
Theta range for data collection	2.86 to 71.93 deg.
Index ranges	-14<=h<=16, -16<=k<=19, -13<=l<=20
Reflections collected	12714
Independent reflections	10434 [R(int) = 0.0631]
Scan type	omega-theta
Absorption correction	Psi-scans (Tmin= 0.459, Tmax=0.956)
Data / restraints / parameters	10421/1/754 (Full-matrix least-squares on F
Goodness-of-fit on F^2	0.965
Conventional R [F>4sigma(F)]	R1 = 0.0666 [6993 data]
R indices (all data)	R1 = 0.0939, wR2 = 0.2020
Final maximum delta/sigma	0.036
Weighting scheme calc w=1/[\s^2^(Fo^2^)+(0.1355P)^2^+0.0000P] where P=(Fo^2^+2Fc^2^)/3	
Largest diff. peak and hole	0.368 and -0.745 e.A^-3

Crystal data and structure refinement for 30 at 220.0(2) K.

Empirical formula	C36 H54 Cl4 N4 Ni3 O14
Formula weight	1084.76
Wavelength	1.54184 A
Crystal system	Monoclinic
Space group	P21/c
Unit cell dimensions	a = 23.142(8) A alpha = 90 deg. b = 20.769(11) A beta = 111.49(2) deg. c = 22.176(6) A gamma = 90 deg.
Volume	9918(7) A^3
Z	8
Density (calculated)	1.453 Mg/m^3
Absorption coefficient	3.828 mm^-1
F(000)	4496
Crystal description	Green block
Crystal size	0.39 x 0.23 x 0.23 mm
Theta range for data collection	2.96 to 40.04 deg.
Index ranges	0<=h<=19, -17<=k<=0, -18<=l<=17
Reflections collected	7348
Independent reflections	5399 [R(int) = 0.0330]
Scan type	Omega-theta
Data / restraints / parameters	5379/0/463 (Full-matrix least-squares on F^
Goodness-of-fit on F^2	1.046
Conventional R [F>4sigma(F)]	R1 = 0.0984 [4447 data]
R indices (all data)	R1 = 0.1149, wR2 = 0.2684
Final maximum delta/sigma	-0.081
Weighting scheme	calc w=1/[\s^2^(Fo^2^)+(0.0836P)^2^+385.1273P] where P=(Fo^2^+2Fc^2^)/3
Largest diff. peak and hole	0.874 and -0.741 e.A^-3

Crystal data and structure refinement for 31 at 220.0(2) K.

Empirical formula	Complex	C42 H50 N4 O14 Cl4 Ni3
	Solvent	C 2 H 8 O 2
Formula weight		1216.87
Wavelength		1.54184 A
Crystal system		Monoclinic
Space group		P21/c
Unit cell dimensions		a = 14.1797(9) A alpha = 90 deg. b = 14.8484(12) A beta = 117.386(4) deg. c = 14.7041(10) A gamma = 90 deg.
Volume		2748.9(3) A^3
Z		2
Density (calculated)		1.470 Mg/m^3
Absorption coefficient		3.550 mm^-1
F(000)		1260
Crystal description		Light green tablet
Crystal size		0.19 x 0.19 x 0.08 mm
Theta range for data collection		3.51 to 60.01 deg.
Index ranges		-15<=h<=14, 0<=k<=16, 0<=l<=16
Reflections collected		4020
Independent reflections		4020 [R(int) = 0.0000]
Scan type		Omega-theta
Absorption correction		Psi-scans (Tmin= 0.263, Tmax=1.000)
Data / restraints / parameters		3991/0/322 (Full-matrix least-squares on F^
Goodness-of-fit on F^2		1.061
Conventional R [F>4sigma(F)]		R1 = 0.0566 [3213 data]
R indices (all data)		R1 = 0.0724, wR2 = 0.1588
Final maximum delta/sigma		-0.001
Weighting scheme calc w=1/[\s^2^(Fo^2^)+(0.0686P)^2^+6.8676P] where P=(Fo^2^+2Fc^2^)/3		
Largest diff. peak and hole		0.536 and -0.847 e.A^-3

Crystal data and structure refinement for 32 at 220.0(2) K.

Empirical formula	Complex:	C108 H132 Cl12 Co12 N12 O48
	Solvent:	C 36 H 76.44 O11.22
Formula weight	Total:	4187.69
Wavelength		0.71073 A
Crystal system		Rhombohedral
Space group		R-3c
Unit cell dimensions		a = 23.094(3) A alpha = 90 deg. b = 23.094(3) A beta = 90 deg. c = 64.051(18) A gamma = 120 deg.
Volume		29584(10) A^3
Z		6
Density (calculated)	Total:	1.410 Mg/m^3
Absorption coefficient		1.221 mm^-1
F(000)	Total:	12949
Crystal description		Red block
Crystal size		0.27 x 0.19 x 0.13 mm
Theta range for data collection		2.60 to 22.55 deg.
Index ranges		0<=h<=21, 0<=k<=21, 0<=l<=68
Reflections collected		4321
Independent reflections		4321 [R(int) = 0.0000]
Scan type		Omega-2theta
Absorption correction		Psi-scans (Tmin= 0.730, Tmax=0.789)
Data / restraints / parameters		4320/70/318 (Full-matrix least-squares on F^2)
Goodness-of-fit on F^2		0.993
Conventional R [F>4sigma(F)]		R1 = 0.0895 [2182 data]
R indices (all data)		R1 = 0.1659, wR2 = 0.2478
Final maximum delta/sigma		0.063
Weighting scheme calc w=1/[\s^2^(Fo^2^)+(0.1131P)^2^+0.0000P] where P=(Fo^2^+2Fc^2^)/3		
Largest diff. peak and hole		0.563 and -0.685 e.A^-3

Crystal data and structure refinement for 33 at 150(2) K.

Empirical formula	C71 H47 C18 Co7 N9 O19
Formula weight	2026.29
Wavelength	0.71073 A
Crystal system	Orthorhombic
Space group	Pnma
Unit cell dimensions	a = 24.034(8) A alpha = 90 deg. b = 20.018(5) A beta = 90 deg. c = 16.304(4) A gamma = 90 deg.
Volume	7844(4) A^3
Z	4
Density (calculated)	1.716 Mg/m^3
Absorption coefficient	1.792 mm^-1
F(000)	4052
Crystal description	Pink lath
Crystal size	0.49 x 0.23 x 0.12 mm
Theta range for data collection	2.53 to 20.00 deg.
Index ranges	0<=h<=25, -21<=k<=0, 0<=l<=17
Reflections collected	3903
Independent reflections	3788 [R(int) = 0.0467]
Scan type	Omega
Absorption correction	Gaussian (Tmin= 0.656, Tmax=0.793)
Data / restraints / parameters	3776/134/291 (Full-matrix least-squares on
Goodness-of-fit on F^2	1.011
Conventional R [F>4sigma(F)]	R1 = 0.0912 [1725 data]
R indices (all data)	R1 = 0.2060, wR2 = 0.2415
Final maximum delta/sigma	-0.001
Weighting scheme calc w=1/[\s^2^(Fo^2^)+(0.0921P)^2^+0.6878P] where P=(Fo^2^+2Fc^2^)/3	
Largest diff. peak and hole	0.760 and -0.773 e.A^-3

Crystal data and structure refinement for 34 at 220(2) K.

Empirical formula	C69.57 H73.94 Cl8.69 Co7 N11.75 O18.69
Formula weight	2094.30
Wavelength	0.71073 A
Crystal system	Triclinic
Space group	P-1
Unit cell dimensions	a = 14.407(4) A alpha = 90.537(14) deg. b = 14.512(4) A beta = 93.80(2) deg. c = 23.321(6) A gamma = 113.40(2) deg.
Volume	4462(2) A^3
Z	2
Density (calculated)	1.559 Mg/m^3
Absorption coefficient	1.598 mm^-1
F(000)	2120
Crystal description	Purple rod
Crystal size	0.43 x 0.12 x 0.12 mm
Theta range for data collection	2.57 to 22.50 deg.
Index ranges	-15<=h<=14, -14<=k<=14, 0<=l<=23
Reflections collected	10286
Independent reflections	9627 [R(int) = 0.3462]
Scan type	omega
Absorption correction	Psi-scans (Tmin= 0.6994, Tmax=0.7994)
Data / restraints / parameters	9559/93/1022 (Full-matrix least-squares on
Goodness-of-fit on F^2	1.006
Conventional R [F>4sigma(F)]	R1 = 0.0764 [5174 data]
R indices (all data)	R1 = 0.1602, wR2 = 0.1966
Final maximum delta/sigma	-0.022
Weighting scheme calc w=1/[\s^2^(Fo^2^)+(0.0441P)^2^+39.9446P] where P=(Fo^2^+2Fc^2^)/3	
Largest diff. peak and hole	0.752 and -0.631 e.A^-3

Crystal data and structure refinement for 35 at 220(2) K.

Empirical formula	C116.60 H89.90 Cl26 N23.30 Na4 Ni12 O37 [Ni12Na4(OH)2(chp)18(ClOAc)8(MeCN)].3.3MeCN.H2O
Formula weight	4127.60
Wavelength	1.54184 A
Crystal system	Triclinic
Space group	P-1
Unit cell dimensions	a = 13.595(7) A alpha = 98.24(4) deg. b = 14.568(8) A beta = 92.84(3) deg. c = 22.513(11) A gamma = 109.25(4) deg.
Volume	4144(4) A^3
Number of reflections for cell	42 (20 < theta < 27 deg.)
Z	1
Density (calculated)	1.654 Mg/m^3
Absorption coefficient	6.027 mm^-1
F(000)	2071
Crystal description	Green block
Crystal size	0.23 x 0.23 x 0.23 mm
Theta range for data collection	3.26 to 50.00 deg.
Index ranges	-15<=h<=15, -16<=k<=16, -15<=l<=25
Reflections collected	9557
Independent reflections	8506 [R(int) = 0.2578]
Scan type	omega-theta with learnt profile (Clegg)
Absorption correction	Difabs (Tmin= 0.117, Tmax=0.585)
Data / restraints / parameters	8416/1746/1043 (Full-matrix least-squares or
Goodness-of-fit on F^2	1.044
Conventional R [F>4sigma(F)]	R1 = 0.0888 [4865 data]
R indices (all data)	R1 = 0.1590, wR2 = 0.2832
Final maximum delta/sigma	-0.022
Weighting scheme calc w=1/[\s^2^(Fo^2^)+(0.1277P)^2^+40.6241P] where P=(Fo^2^+2Fc^2^)/3	
Largest diff. peak and hole	0.972 and -0.663 e.A^-3

Crystal data and structure refinement for 36 at 150(2) K.

Empirical formula	C119 H76 C126 Co13 N20 O30
Formula weight	3953.79
Wavelength	0.71073 A
Crystal system	Monoclinic
Space group	P2/c
Unit cell dimensions	a = 17.165(5) A alpha = 90 deg. b = 18.243(7) A beta = 96.63(4) deg. c = 26.613(8) A gamma = 90 deg.
Volume	8278(5) A^3
Z	2
Density (calculated)	1.586 Mg/m^3
Absorption coefficient	1.753 mm^-1
F(000)	3926
Crystal description	Purple lath
Crystal size	0.23 x 0.19 x 0.16 mm
Theta range for data collection	2.53 to 22.59 deg.
Index ranges	-18<=h<=18, 0<=k<=19, 0<=l<=28
Reflections collected	11996
Independent reflections	10866 [R(int) = 0.2207]
Scan type	omega with learnt profile
Absorption correction	Psi-scans (Tmin= 0.453, Tmax=0.742)
Data / restraints / parameters	10747/1672/961 (Full-matrix least-squares on
Goodness-of-fit on F^2	1.021
Conventional R [F>4sigma(F)]	R1 = 0.0926 [5657 data]
R indices (all data)	R1 = 0.1881, wR2 = 0.2744
Final maximum delta/sigma	0.018
Weighting scheme calc w=1/[\s^2^(Fo^2^)+(0.0887P)^2^+132.5922P] where P=(Fo^2^+2Fc^2^)/3	
Largest diff. peak and hole	1.315 and -0.840 e.A^-3

Crystal data and structure refinement for 37 at 150.0(2) K.

Empirical formula	C153.12 H214.32 Cl4 N4 Na6 Ni16 O97.04
Formula weight	4882.77
Wavelength	1.54184 A
Crystal system	Monoclinic
Space group	I2
Unit cell dimensions	a = 30.00(2) A alpha = 90 deg. b = 13.163(9) A beta = 108.83(4) deg. c = 30.99(3) A gamma = 90 deg.
Volume	11584(14) A^3
Z	2
Density (calculated)	1.399 Mg/m^3
Absorption coefficient	2.625 mm^-1
F(000)	5035
Crystal description	Green block
Crystal size	0.40 x 0.25 x 0.25 mm
Theta range for data collection	3.01 to 60.04 deg.
Index ranges	-33<=h<=31, 0<=k<=14, 0<=l<=34
Reflections collected	8811
Independent reflections	8811 [R(int) = 0.3205]
Scan type	Omega
Absorption correction	Difabs (Tmin= 0.309, Tmax=1.000)
Data / restraints / parameters	8731/312/1257 (Full-matrix-block least-squar
Goodness-of-fit on F^2	1.039
Conventional R [F>4sigma(F)]	R1 = 0.0917 [5282 data]
R indices (all data)	R1 = 0.1617, wR2 = 0.3282
Absolute structure parameter	0.03(8)
Final maximum delta/sigma	0.052
Weighting scheme calc w=1/[\s^2^(Fo^2^)+(0.1569P)^2^+96.2637P] where P=(Fo^2^+2Fc^2^)/3	
Largest diff. peak and hole	0.843 and -0.650 e.A^-3

Crystal data and structure refinement for **38** at 150(2) K.

Empirical formula	C69 H86 Cl12 N6 Ni4 O20
Formula weight	1979.68
Wavelength	0.71073 A
Crystal system	TRICLINIC
Space group	P -1
Unit cell dimensions	a = 12.464(7) A alpha = 100.17(3) deg. b = 12.867(8) A beta = 113.38(3) deg. c = 15.228(8) A gamma = 96.95(5) deg.
Volume	2157(2) A^3
Z	1
Density (calculated)	1.524 Mg/m^3
Absorption coefficient	1.300 mm^-1
F(000)	1018
Crystal description	? ?
Crystal size	0.60 x 0.23 x 0.16 mm
Theta range for data collection	2.70 to 25.06 deg.
Index ranges	-14<=h<=13, -15<=k<=15, 0<=l<=18
Reflections collected	10034
Independent reflections	7630 [R(int) = 0.0744]
Scan type	?
Data / restraints / parameters	7627/10/541 (Full-matrix least-squares on F^2)
Goodness-of-fit on F^2	1.028
Conventional R [F>4sigma(F)]	R1 = 0.0533 [5019 data]
R indices (all data)	R1 = 0.1004, wR2 = 0.1279
Extinction coefficient	0.0003(4)
Final maximum delta/sigma	0.016
Weighting scheme Calc w=1/[\s^2^(Fo^2^)+(0.0504P)^2^+2.6715P] where P=(Fo^2^+2Fc^2^)/3	
Largest diff. peak and hole	0.747 and -0.905 e.A^-3

Crystal data and structure refinement for **39** : 150(2) K.

Empirical formula	C33.50 H35 C17 F6 N5 Ni3 O10
Formula weight	1205.95
Wavelength	0.71073 A
Crystal system	?
Space group	?
Unit cell dimensions	a = 13.649(4) A alpha = 99.71(2) deg. b = 13.736(4) A beta = 113.75(2) deg. c = 15.344(5) A gamma = 104.886(13) deg.
Volume	2421.3(13) A^3
Z	2
Density (calculated)	1.654 Mg/m^3
Absorption coefficient	1.619 mm^-1
F(000)	1216
Crystal description	? ?
Crystal size	0.76 x 0.42 x 0.23 mm
Theta range for data collection	2.54 to 27.53 deg.
Index ranges	-17<=h<=15, -17<=k<=17, 0<=l<=19
Reflections collected	13586
Independent reflections	11150 [R(int) = 0.0437]
Scan type	?
Data / restraints / parameters	11058/67/648 (Full-matrix least-squares on F^2)
Goodness-of-fit on F^2	1.023
Conventional R [F>4sigma(F)]	R1 = 0.0601 [8539 data]
R indices (all data)	R1 = 0.0857, wR2 = 0.1979
Final maximum delta/sigma	-0.164
Weighting scheme calc w=1/[\s^2^(Fo^2^)+(0.0853P)^2^+7.2455P] where P=(Fo^2^+2Fc^2^)/3	
Largest diff. peak and hole	1.521 and -1.358 e.A^-3

Crystal data and structure refinement for 40 at 220(2) K.

Empirical formula	C40 H46 Cl2 Co2 N6 Na2 O16 [Na2Co2(chp)2(pic)4(MeOH)4].2MeOH
Formula weight	1101.57
Wavelength	0.71073 A
Crystal system	Monoclinic
Space group	P21/n
Unit cell dimensions	a = 12.050(3) A alpha = 90 deg. b = 12.893(4) A beta = 109.49(2) deg. c = 17.077(8) A gamma = 90 deg.
Volume	2501.1(15) A^3
Number of reflections for cell	42 (11 < theta < 14 deg.)
Z	2
Density (calculated)	1.463 Mg/m^3
Absorption coefficient	0.858 mm^-1
F(000)	1132
Crystal description	Red block
Crystal size	0.39 x 0.35 x 0.31 mm
Theta range for data collection	2.52 to 22.52 deg.
Index ranges	-12<=h<=12, 0<=k<=13, 0<=l<=18
Reflections collected	4212
Independent reflections	3195 [R(int) = 0.0677]
Scan type	omega-theta
Absorption correction	Difabs (Tmin= 0.387, Tmax=2.089)
Data / restraints / parameters	3188/1/309 (Full-matrix least-squares on F^
Goodness-of-fit on F^2	1.011
Conventional R [F>4sigma(F)]	R1 = 0.0665 [1897 data]
R indices (all data)	R1 = 0.1342, wR2 = 0.1921
Final maximum delta/sigma	0.004
Weighting scheme calc w=1/[\s^2^(Fo^2^)+(0.0987P)^2^+0.0000P] where P=(Fo^2^+2Fc^2^)/3	
Largest diff. peak and hole	0.374 and -0.438 e.A^-3

Crystal data and structure refinement for 41 at 150(2) K.

Empirical formula	C64 H54.50 Cl14 Co7 Cu2 N10 O25.25
Formula weight	2403.57
Wavelength	0.71073 A
Crystal system	Monoclinic
Space group	P2(1)/n
Unit cell dimensions	a = 14.523(4) A alpha = 90 deg. b = 38.611(14) A beta = 112.20(3) deg. c = 16.826(5) A gamma = 90 deg.
Volume	8736(5) A^3
Z	4
Density (calculated)	1.828 Mg/m^3
Absorption coefficient	2.276 mm^-1
F(000)	4782
Crystal description	Purple lath
Crystal size	0.66 x 0.37 x 0.14 mm
Theta range for data collection	2.53 to 22.55 deg.
Index ranges	-15<=h<=14, 0<=k<=41, 0<=l<=18
Reflections collected	12122
Independent reflections	11440 [R(int) = 0.0339]
Scan type	Omega scans with learnt profile
Absorption correction	Psi-scans (Tmin= 0.266, Tmax=0.471)
Data / restraints / parameters	11382/106/1106 (Full-matrix least-squares o
Goodness-of-fit on F^2	1.027
Conventional R [F>4sigma(F)]	R1 = 0.0625 [8083 data]
R indices (all data)	R1 = 0.0978, wR2 = 0.1699
Final maximum delta/sigma	0.018
Weighting scheme calc w=1/[\s^2^(Fo^2^)+(0.0631P)^2^+62.7040P] where P=(Fo^2^+2Fc^2^)/3	
Largest diff. peak and hole	1.404 and -1.362 e.A^-3

Crystal data and structure refinement for 42 at 150.0(2) K.

Empirical formula		C140.4 H156.8 Co6 Cu2 N8 O45.2
	Complex	C106 H 98 Co6 Cu2 N6 O32
	Solvate	C 34.4 H 58.8 N2 O13.2
Formula weight		2448.56 + 711.64 = 3160.20
Wavelength		0.71073 A
Crystal system		Triclinic
Space group		P-1
Unit cell dimensions		a = 14.633(6) A alpha = 94.95(2) deg. b = 17.143(7) A beta = 111.54(2) deg. c = 18.038(8) A gamma = 114.59(2) deg.
Volume		3671(3) A^3
Z		1
Density (calculated)		1.429 Mg/m^3
Absorption coefficient		1.029 mm^-1
F(000)		1637
Crystal description		Yellow-brown block
Crystal size		0.56 x 0.47 x 0.27 mm
Theta range for data collection		2.51 to 25.02 deg.
Index ranges		-17<=h<=15, -20<=k<=20, 0<=l<=21
Reflections collected		13698
Independent reflections		12913 [R(int) = 0.0567]
Scan type		omega-theta
Absorption correction		Psi-scans (Tmin= 0.278, Tmax=0.545)
Data / restraints / parameters		12890/94/888 (Full-matrix least-squares on F
Goodness-of-fit on F^2		1.031
Conventional R [F>4sigma(F)]		R1 = 0.0638 [9138 data]
R indices (all data)		R1 = 0.0986, wR2 = 0.1747
Final maximum delta/sigma		0.016
Weighting scheme calc w=1/[\s^2^(Fo^2^)+(0.0949P)^2^+6.0231P] where P=(Fo^2^+2Fc^2^)/3		
Largest diff. peak and hole		1.081 and -0.775 e.A^-3

Crystal data and structure refinement for 43 at 150.0(2) K.

Empirical formula	C137.20 H149.80 Cu2 N8 Ni6 O43.60
Formula weight	3087.79
Wavelength	1.54184 A
Crystal system	Triclinic
Space group	P-1
Unit cell dimensions	a = 14.569(9) A alpha = 94.93(3) deg. b = 17.036(10) A beta = 111.27(3) deg. c = 17.394(10) A gamma = 114.53(3) deg.
Volume	3515(4) A^3
Z	1
Density (calculated)	1.459 Mg/m^3
Absorption coefficient	1.894 mm^-1
F(000)	1604
Crystal description	Green lath
Crystal size	0.47 x 0.12 x 0.08 mm
Theta range for data collection	2.84 to 60.00 deg.
Index ranges	-16<=h<=14, -19<=k<=19, -6<=l<=20
Reflections collected	10424
Independent reflections	10199 [R(int) = 0.1378]
Scan type	Omega-theta
Absorption correction	Psi-scans (Tmin= 0.627, Tmax=0.800)
Data / restraints / parameters	10178/336/802 (Full-matrix least-squares on
Goodness-of-fit on F^2	1.018
Conventional R [F>4sigma(F)]	R1 = 0.0814 [6087 data]
R indices (all data)	R1 = 0.1402, wR2 = 0.2472
Final maximum delta/sigma	0.007
Weighting scheme calc w=1/[\s^2^(Fo^2^)+(0.1245P)^2^+10.1060P] where P=(Fo^2^+2Fc^2^)/3	
Largest diff. peak and hole	1.055 and -0.964 e.A^-3

Crystal data and structure refinement for 44 at 150.0(2) K.

Empirical formula		C40.68 H39.38 Cl6 Er2 N12.66 Ni2 O19.34
	Complex	C34 H24 Cl6 Er2 N12 Ni2 O18
	Solvent	C 6.68 H15.38 N 0.66 O 1.34
Formula weight		1679.71
Wavelength		0.71073 A
Crystal system		Monoclinic
Space group		P21/c
Unit cell dimensions		a = 11.482(2) A alpha = 90 deg. b = 18.537(3) A beta = 97.41(2) deg. c = 14.005(3) A gamma = 90 deg.
Volume		2956.0(9) A^3
Z		2
Density (calculated)		1.887 Mg/m^3
Absorption coefficient		3.787 mm^-1
F(000)		1642
Crystal description		Green block
Crystal size		0.39 x 0.31 x 0.27 mm
Theta range for data collection		2.64 to 25.03 deg.
Index ranges		-13<=h<=13, 0<=k<=22, 0<=l<=16
Reflections collected		5906
Independent reflections		5207 [R(int) = 0.0282]
Scan type		Omega-theta
Absorption correction		Psi-scans (Tmin= 0.484, Tmax=0.642)
Data / restraints / parameters		5202/19/375 (Full-matrix least-squares on F
Goodness-of-fit on F^2		1.011
Conventional R [F>4sigma(F)]		R1 = 0.0457 [3862 data]
R indices (all data)		R1 = 0.0727, wR2 = 0.1126
Final maximum delta/sigma		-0.003
Weighting scheme calc w=1/[\s^2^(Fo^2^)+(0.0581P)^2^+7.1986P] where P=(Fo^2^+2Fc^2^)/3		
Largest diff. peak and hole		1.402 and -0.917 e.A^-3

Crystal data and structure refinement for 46 at 220.0(2) K.

Empirical formula	C46 H59 Cl6 Co2 N13 O22 Yb2
Formula weight	1822.70
Wavelength	0.71073 A
Crystal system	Triclinic
Space group	P-1
Unit cell dimensions	a = 13.908(5) A alpha = 77.27(2) deg. b = 14.956(6) A beta = 83.02(2) deg. c = 17.909(8) A gamma = 63.85(2) deg.
Volume	3261(2) A^3
Z	2
Density (calculated)	1.857 Mg/m^3
Absorption coefficient	3.670 mm^-1
F(000)	1796
Crystal description	Pink block
Crystal size	0.31 x 0.23 x 0.16 mm
Theta range for data collection	2.55 to 22.55 deg.
Index ranges	-14<=h<=14, -15<=k<=16, 0<=l<=19
Reflections collected	12508
Independent reflections	8533 [R(int) = 0.1162]
Scan type	Omega-theta
Absorption correction	Psi-scans (Tmin= 0.6948, Tmax=0.9976)
Data / restraints / parameters	8470/50/796 (Full-matrix least-squares on F^
Goodness-of-fit on F^2	1.080
Conventional R [F>4sigma(F)]	R1 = 0.0676 [5722 data]
R indices (all data)	R1 = 0.1120, wR2 = 0.1920
Final maximum delta/sigma	0.010
Weighting scheme calc w=1/[\s^2^(Fo^2^)+(0.0878P)^2^+10.8017P] where P=(Fo^2^+2Fc^2^)/3	
Largest diff. peak and hole	1.570 and -1.146 e.A^-3

Crystal data and structure refinement for 47 at 230.0(2) K.

Empirical formula		C49.46 H65.92 Cl12.92 Co2 Dy2 N13 O22
	Complex	C46 H59 Cl 6 Co2 Dy2 N13 O22
	Solvent	C 3.46 H 6.92 Cl 6.92
Formula weight		2095.47
Wavelength		0.71073 A
Crystal system		Triclinic
Space group		P-1
Unit cell dimensions		a = 14.099(4) A alpha = 83.59(2) deg. b = 14.957(3) A beta = 87.91(2) deg. c = 18.941(5) A gamma = 82.92(2) deg.
Volume		3938.0(17) A^3
Z		2
Density (calculated)		1.767 Mg/m^3
Absorption coefficient		2.801 mm^-1
F(000)		2071
Crystal description		Pink chip
Crystal size		0.51 x 0.23 x 0.16 mm
Theta range for data collection		2.58 to 22.53 deg.
Index ranges		-15<=h<=15, -15<=k<=16, 0<=l<=20
Reflections collected		13110
Independent reflections		10290 [R(int) = 0.1020]
Scan type		Omega-theta
Absorption correction		Psi-scans (Tmin= 0.357, Tmax=0.421)
Data / restraints / parameters		10251/77/856 (Full-matrix least-squares on
Goodness-of-fit on F^2		1.022
Conventional R [F>4sigma(F)]		R1 = 0.0765 [5587 data]
R indices (all data)		R1 = 0.1649, wR2 = 0.1909
Final maximum delta/sigma		0.077
Weighting scheme calc w=1/[\s^2^(Fo^2^)+(0.0783P)^2^+10.9484P] where P=(Fo^2^+2Fc^2^)/3		
Largest diff. peak and hole		1.365 and -0.826 e.A^-3

Crystal data and structure refinement for 48 at 293(2) K.

Empirical formula	C46 H59 C16 Co2 Gd2 N13 O22
Formula weight	1791.12
Wavelength	0.71073 A
Crystal system	Triclinic
Space group	P-1
Unit cell dimensions	a = 13.92(2) A alpha = 75.92(14) deg. b = 14.92(2) A beta = 83.31(12) deg. c = 17.80(3) A gamma = 64.84(12) deg.
Volume	3244(8) A^3
Z	2
Density (calculated)	1.834 Mg/m^3
Absorption coefficient	2.850 mm^-1
F(000)	1772
Crystal description	Pink lump
Crystal size	0.39 x 0.31 x 0.31 mm
Theta range for data collection	2.53 to 15.02 deg.
Index ranges	-9<=h<=10, -10<=k<=10, 0<=l<=12
Reflections collected	2613
Independent reflections	2613 [R(int) = 0.0000]
Scan type	omega-theta
Data / restraints / parameters	2586/36/169 (Full-matrix least-squares on F^
Goodness-of-fit on F^2	1.053
Conventional R [F>4sigma(F)]	R1 = 0.1363 [1033 data]
R indices (all data)	R1 = 0.3002, wR2 = 0.3685
Final maximum delta/sigma	-0.001
Weighting scheme calc w=1/[\s^2^(Fo^2^)+(0.1110P)^2^+116.3812P] where P=(Fo^2^+2Fc^2^)/3	
Largest diff. peak and hole	0.899 and -0.875 e.A^-3